Monoterpenoid production and monoterpenoid resistance mechanisms in *Pseudomonas putida*

Dissertation
zur Erlangung des Doktorgrades
der Naturwissenschaften

vorgelegt beim Fachbereich 15 - Biowissenschaften
der Johann Wolfgang Goethe-Universität
in Frankfurt am Main

von
Florence Miramella Schempp, M.Sc.
geboren in Königstein im Taunus

Frankfurt am Main, 2020

(D30)

vom Fachbereich 15 – Biowissenschaften der

Johann Wolfgang Goethe-Universität als Dissertation angenommen.

Dekan:
Prof. Dr. Sven Klimpel
Goethe-Universität Frankfurt, Institut für Ökologie, Evolution und Diversität

Gutachter:
Prof. Dr. Jens Schrader
DECHEMA-Forschungsinstitut, Industrielle Biotechnologie

Prof. Dr. Eckhard Boles
Goethe-Universität Frankfurt, Institut für Molekulare Biowissenschaften

Datum der Disputation: 02.09.2020

„Die Wahrheit ist objektiv und absolut.
Aber wir können niemals sicher sein, dass wir sie gefunden haben.
Unser Wissen ist immer Vermutungswissen.
Unsere Theorien sind Hypothesen.
Wir prüfen auf Wahrheit, indem wir das Falsche ausscheiden.“
Objective Knowledge, Karl Popper, 1972

Für die Menschen, die ich liebe.

This thesis is based on the following publications and manuscripts:

1. **Schempp FM**, Drummond L, Buchhaupt M, Schrader J. 2018. Microbial Cell Factories for the Production of Terpenoid Flavor and Fragrance Compounds.
   J Agric Food Chem 66:2247–2258. DOI: 10.1021/acs.jafc.7b00473
   → incorporated as Chapter 2

2. **Schempp FM**, Strobel I, Etschmann MMW, Bierwirth E, Schewe H, Schrader J, Buchhaupt M. Identification and characterization of fungal limonene-3-hydroxylases.
   submitted
   → incorporated as Chapter 3

3. **Schempp FM**, Hofmann KE, Mi J, Kirchner F, Meffert A, Schewe H, Schrader J, Buchhaupt M. 2020. Investigation of monoterpenoid resistance mechanisms in *Pseudomonas putida* and their consequences for biotransformations.
   Appl Microbiol Biotechnol DOI: 10.1007/s00253-020-10566-3
   → incorporated as Chapter 4

4. Mi J, Sydow A, **Schempp F**, Becher D, Schewe H, Schrader J, Buchhaupt M. 2016. Investigation of plasmid-induced growth defect in *Pseudomonas putida*.
   J Biotechnol 231:167–173. DOI: 10.1016/j.jbiotec.2016.06.001
   → incorporated as Chapter 6

The publications and manuscript contained in this thesis have been inserted as published by or submitted to the respective journals. The numbering and style of references, tables and figures have not been adapted to this thesis.

Zusammenfassung

Monoterpene und Monoterpenoide[1] bilden eine Unterklasse der Terpen(oid)e und finden eine breite Anwendung als Duft- und Aromastoffe, Arzneimittelbestandteile, in Kosmetika und als Agrochemikalien. Seit einigen Jahren wird aber auch ein möglicher Einsatz als zukünftige Biokraftstoffe diskutiert. Für viele dieser Substanzen birgt die Extraktion aus natürlichen Quellen, wie etwa Pflanzenteilen, jedoch einige Herausforderungen, wie z. B. eine sehr geringe Konzentration im Ausgangsmaterial oder die Tatsache, dass die benötigten Pflanzen immer weniger verfügbar sind. Während für einige Monoterpene und Monoterpenoide inzwischen chemische Herstellungsverfahren entwickelt werden konnten, ist es besonders für strukturell komplexere Moleküle immer noch schwierig oder sogar unmöglich, diese mit wirtschaftlichen Prozessen chemisch zu synthetisieren. Deshalb bietet die biotechnologische Herstellung mit Mikroorganismen eine attraktive Alternative. Diese profitiert vor allem von der häufig sehr ausgeprägten Regio- und Stereoselektivität von enzymatischen Reaktionen. Aufgrund ihrer modularen Architektur eignet sich die Terpenoid-Biosynthese besonders gut für das Konzept der mikrobiellen Zellfabrik: Ein Plattform-Wirtsorganismus, der so entwickelt wurde, dass er eine hohe Produktionsrate der zentralen C_5-Prenyldiphosphat-Vorläufer aufweist, könnte die Herstellung einer breiten Palette von Ziel-Terpenoiden ermöglichen, indem die Biosynthese-Module variiert werden, die die C_5-Bausteine in das Produkt von Interesse umwandeln. Eine der großen Herausforderung bei der Biosynthese einiger Monoterpenoide ist jedoch ihre ausgeprägte Zytotoxizität, welche die Herstellung von Monoterpenen und Monoterpenoiden in Mikroorganismen im Vergleich zu längerkettigeren Terpenen (Sesquiterpene, Diterpene, etc.) erschwert.

Edukt- und Produkttoxizität ist ein häufiges Problem bei der Entwicklung von Mikroorganismen für biotechnologische Anwendungen. Aus diesem Grund ist es essenziell, bei der Entwicklung von mikrobiellen Zellfabriken nicht nur die metabolischen Produktionswege zu optimieren, sondern auch die Stämme toleranter gegenüber toxischen Edukten und Produkten zu machen. Obwohl bereits einige Mikroorganismen isoliert werden konnten, die die Anwesenheit von industriell interessanten, kurzkettigen und aromatischen Kohlenwasserstoffen in ihrem Lebensraum tolerieren können, sind diese jedoch meist aus verschiedenen Gründen nicht als Produktionsstämme einsetzbar. Deshalb ist es wichtig, die Mechanismen, die der Toleranz zugrunde liegen, zu verstehen, um diese auf für industrielle Produktionsprozesse geeignete Stämme übertragen zu können. Solche Mechanismen beinhalten die Expression von Efflux-Pumpen, Hitze-Schock-Proteinen (Chaperone) und Membran-modifizierenden Enzymen sowie die Aktivierung von generellen Stress-Antwort-Systemen.

[1]Nach der IUPAC-Definition werden als (Mono-)Terpene nur Kohlenwasserstoffverbindungen bezeichnet. Alle davon abgeleiteten Derivate fallen unten den Begriff (Mono-)Terpenoide.[346,347]

Das Ziel der vorliegenden Arbeit war es eine biotechnologische Ergänzung zu den auf fossilen Rohstoffen basierenden chemischen Prozessen für die industrielle Monoterpenoid-Produktion zu schaffen. Dafür sollte die Grundlage für die weitere Entwicklung einer mikrobiellen Zellfabrik auf Basis des Bakteriums *Pseudomonas putida* KT2440 generiert werden, die selektiv Monoterpenkohlenwasserstoffe oxygenieren und dafür erneuerbare industrielle Abfallströme als Rohstoff für die Monoterpenoid-Produktion nutzen kann (Abbildung 1). Um das Problem der Produkttoxizität zu überwinden, sollte die inhärente Monoterpenoid-Toleranz einiger lösungsmitteltoleranter *P. putida*-Stämme untersucht und anschließend auf den KT2440-Stamm übertragen werden, mit dem Ziel die Monoterpenoid-Produktion mit diesem Organismus zu unterstützen.

Als Modellsubstanz sollte die Herstellung von (-)-Menthol realisiert werden. (-)-Menthol wurde wegen seiner industriellen Bedeutung als einer der weltweit meist genutzten Duft- und Aromastoff sowie seines Einsatzes als medizinischer Bestandteil ausgewählt, von dem jedes Jahr über 30.000 Tonnen produziert werden.

Ein Ansatz für ein Menthol-Produktionsverfahren aus erneuerbaren Rohstoffen könnte eine biotechnologische(-chemische), zweistufige Umwandlung ausgehend von (+)-Limonen sein (Abbildung 1). (+)-Limonen ist das am häufigsten vorkommende monozyklische Monoterpen in der Natur und entsteht beispielsweise als Nebenprodukt bei der Herstellung von Orangensaft, da es sich im Öl von Zitrusschalen auf 70 - 98 % (v/v) akkumulieren kann.

Der erste Schritt der Umwandlung von (+)-Limonen in (-)-Menthol erfordert ein Enzym mit einer Limonen-3-Hydroxylase-Aktivität (L3H), das eine Hydroxylierung von Limonen spezifisch am dritten Kohlenstoff-Atom katalysiert, sodass (+)-*trans*-Isopiperitenol entsteht. (+)-*trans*-Isopiperitenol kann dann entweder durch eine chemische Hydrierung oder einen weiteren enzymatischen Schritt in (-)-Menthol umgewandelt werden.

Das Dissertationsprojekt gliederte sich in drei Teile. Im ersten Teil sollten Enzyme identifiziert werden, die die beabsichtigte Limonen-3-Hydroxylierungsreaktion katalysieren können, um den ersten Schritt der der zweistufigen Umsetzung von (+)-Limonen in (-)-Menthol zu realisieren. Im zweiten Teil sollte die Toleranz des gewählten *P. putida*-Stamms gegenüber Monoterpenen und deren Monoterpenoid-Derivaten erhöht werden. Im dritten Teil sollten die identifizierten L3H-Enzyme im verbesserten *P. putida* KT2440-Stamm exprimiert werden, um einen geeigneten Ganzzell-Biokatalysator für den ersten Schritt der biotechnologischen Menthol-Produktion ausgehend vom Nebenprodukt der Zitrussaft-Industrie (+)-Limonen zu schaffen.

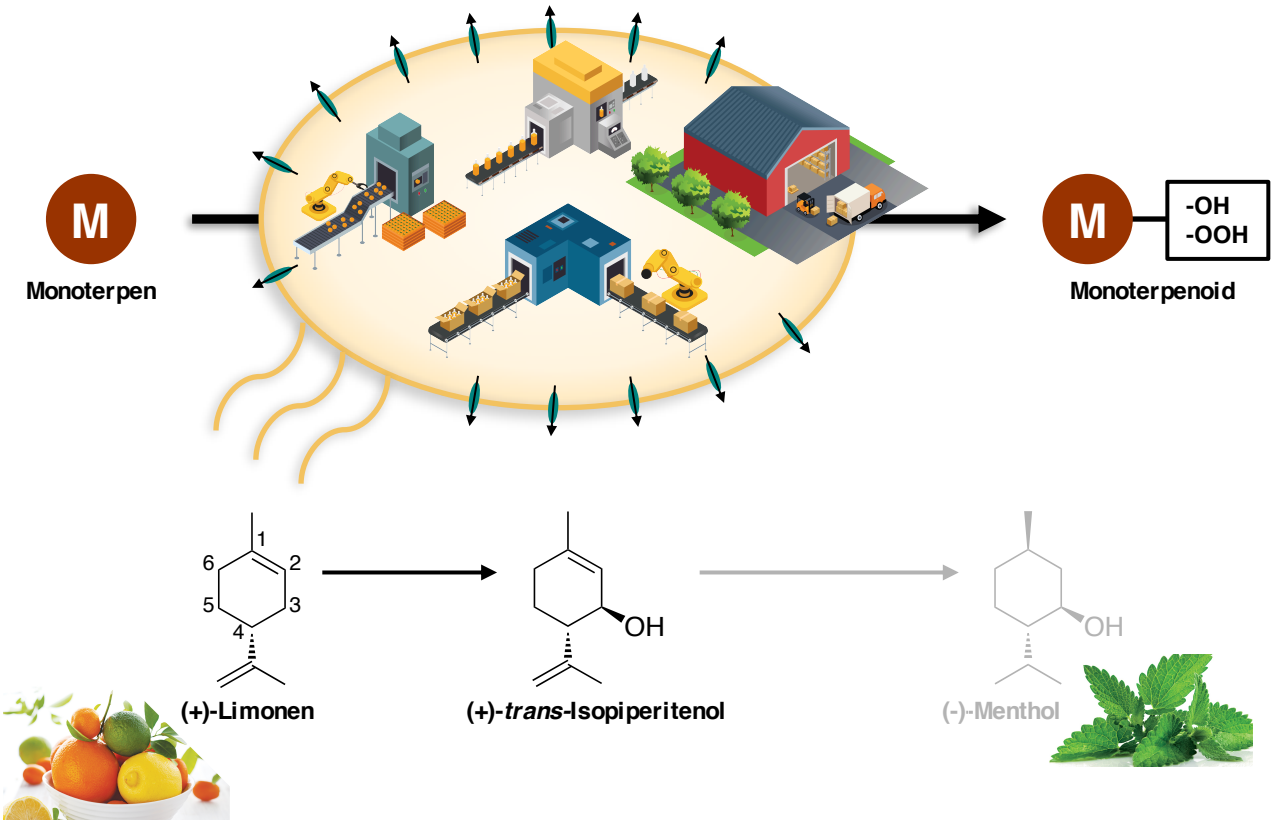

Abbildung 1: Projektübersicht. Das Ziel der Arbeit war es eine Grundlage für die weitere Entwicklung einer Zellfabrik zur Monoterpenoid-Produktion zu schaffen. Da viele Monoterpenoide toxisch für mikrobielle Zellen sind, sollte die Toleranz des ausgewählten Organismus *P. putida* gegenüber diesen Substanzen erhöht werden. Als Modellprozess wurde die Umwandlung von (+)-Limonen, das als Nebenprodukt der Zitrusfrüchte-verarbeitenden Industrie anfällt, in (-)-Menthol gewählt. Dabei sollte im speziellen zunächst der erste Schritt, die *in vivo* Biotransformation von (+)-Limonen in das Zwischenprodukt (+)-*trans*-Isopiperitenol realisiert werden. M: Monoterpen, M-OH: Monoterpen-Alkohol, M-OOH: Monoterpen-Säure.

Teil 1 – Identifizierung und Charakterisierung von pilzlichen Limonen-3-Hydroxylasen

Cytochrom P450 Monooxygenasen (CYPs oder P450s) sind Enzyme, die in der Lage sind, ein Sauerstoffatom unter Normaldruck und bei Raumtemperatur in eine nicht aktivierte C-H-Bindung einzubringen. Dabei können sie beispielsweise Hydroxy-Gruppen erzeugen. Es gibt eine Vielzahl von ganz unterschiedlichen CYPs in allen Domänen des Lebens. Vor allem im Pflanzenreich sind sie sehr weit verbreitet und katalysieren diverse Reaktionen mit hoher Regio- und Stereoselektivität. Während sich die Expression von pflanzlichen CYPs in mikrobiellen Zellfabriken häufig als problematisch erweist, haben diese CYPs jedoch im Erfolgsfall den Vorteil einer oft sehr ausgeprägten Selektivität für die jeweils von ihnen katalysierte Reaktion. Bakterielle CYP-Enzyme, wie beispielsweise P450cam oder BM-3, lassen sich i.d.R. sehr gut in mikrobiellen, vor allem bakteriellen, Zellfabriken exprimieren. Jedoch haben diese ein sehr eingeschränktes Repertoire an Reaktionen, welche von ihnen katalysiert werden können. Während durch Protein-Engineering das Substrat- und

Produktspektrum erweitert werden kann, führt dies jedoch häufig auch dazu, dass die Enzyme weniger spezifisch werden und verschiedenste Nebenprodukte gebildet werden.
Deshalb wurde in der vorliegenden Arbeit versucht, sowohl den Vorteil der hohen Selektivität von eukaryotischen CYPs als auch den der erleichterten Exprimierbarkeit von mikrobiellen CYPs auszunutzen. Dafür sollte als Limonen-3-Hydroxylase ein eukaryotisches Enzym mit hoher Selektivität nicht in einer Pflanze, sondern in einem pilzlichen Mikroorganismus gesucht werden, in der Hoffnung, dass sich dieses dann auch leichter in mikrobiellen Zellfabriken exprimieren lässt als pflanzliche Enzyme.

Aus der Literatur ist bekannt, dass ein bestimmter Pilz, *Hormonema* sp. UOFS Y-0067, (+)-Limonen in *trans*-Isopiperitenol umwandeln kann. Dies spricht dafür, dass dieser Pilz ein oder mehrere Enzyme mit einer Limonen-3-Hydroxylase-Aktivität besitzt. Deshalb wurden weitere Pilze aus der Klasse der Dothideomycetes daraufhin getestet, ob sie ebenfalls diese Reaktion katalysieren können. Dabei zeigte sich, dass auch *Hormonema carpetanum* sowie *Aureobasidium pullulans* mindestens ein L3H-Enzym besitzen müssen. Auf Grundlage des in der NCBI-Datenbank verfügbaren Genoms von *A. pullulans* wurden dann über 50 verschiedene CYP-Gene von *A. pullulans* identifiziert, die potenziell das L3H-Protein codieren könnten. Experimente mit CYP-Inhibitoren hatten zuvor bereits darauf hingewiesen, dass es sich bei dem gesuchten Enzym höchstwahrscheinlich um ein Protein der CYP-Familie handelt. Die verschiedenen CYP-Sequenzen von *A. pullulans* wurden dann im Rahmen dieser Arbeit anhand ihrer Sequenzidentität in Gruppen eingeteilt und aus den verschiedenen Gruppen Kandidaten für einen Funktionstest in *Saccharomyces cerevisiae* ausgewählt. Dabei zeigte sich, dass von 16 getesteten Kandidaten ein Enzym dazu in der Lage war, (+)-Limonen mit einer hohen Regio- und Stereoselektivität in (+)-*trans*-Isopiperitenol umzuwandeln (L3H.Ap = CYP65AH1 von *A. pullulans*). Auf Grundlage der Protein-Sequenz von L3H.Ap wurde dann in Genom-Fragmenten von *H. carpetanum* nach einem ähnlichen Protein gesucht, wodurch auch ein L3H-Enzym aus diesem Pilz identifiziert werden konnte (L3H.Hc = CYP65AH1 von *H. carpetanum*). Da in den durchgeführten Funktionstests mit *S. cerevisiae* L3H.Ap höhere (+)-*trans*-Isopiperitenol-Konzentrationen lieferte als L3H.Hc, wurde im Folgenden das Enzym von *A. pullulans* weiter charakterisiert.
Dafür wurde es in *Pichia pastoris* exprimiert, um eine höher Zellmasse und damit auch Proteinkonzentration zu erhalten. Mit den L3H.Ap-exprimierenden *P. pastoris*-Zellen wurden dann verschiedene Biotransformationsversuche durchgeführt. Dabei zeigte sich, dass das Enzym neben (+)-Limonen auch (-)-Limonen, α- und β-Pinen sowie 3-Caren hydroxylieren kann.

Teil 2 – Entwicklung eines Monoterpenoid-toleranten Produktionsorganismus

Durch den Einsatz von ätherischen Ölen in der Medizin ist schon seit langer Zeit bekannt, dass Monoterpene und ihre Monoterpenoid-Derivate eine toxische Wirkung auf Mikroorganismen haben können. Die genauen Mechanismen, die einige Lösungsmittel-tolerante Bakterien vor diesen Substanzen schützen, wurden jedoch kaum untersucht. Für die Entwicklung von Produktionsstämmen für die biotechnologische Herstellung von Monoterpen(oid)en ist es jedoch unerlässlich zu wissen, ob die allgemeinen Lösungsmittel-Toleranz-Mechanismen von Gram-negativen Bakterien die Zellen auch gegen den toxischen Einfluss von verschiedenen Monoterpenen und ihren Derivaten schützen. Um dies zu untersuchen, wurden mit dem Lösungsmittel-toleranten *P. putida*-Stamm GS1 Untersuchungen durchgeführt, um die Faktoren dann auf industriell nutzbare Produktionsstämme, wie z.B. *P. putida* KT2440, übertragen zu können.

Hierfür wurde in Vorarbeiten eine Mutantenbibliothek von *P. putida* GS1 erstellt und Monoterpenoid-hyperresistente Mutanten daraus selektiert. Die Mutanten wurden dann im Rahmen dieser Arbeit durch Genomsequenzierung, Toxizitätsassays, Deletions- und Komplemenationsexperimente und Expressionslevel-Quantifizierung (qPCRs) weiter charakterisiert. Dabei zeigte sich, dass die verschiedenen getesteten Monoterpene und Monoterpenoide sehr unterschiedliche Toxizitätsniveaus aufweisen und dass eine erhöhte oder verminderte Toleranz gegenüber Monoterpenoiden hauptsächlich auf eine veränderte Expression der Ttg-Efflux-Pumpen zurückzuführen ist. Diese Ergebnisse wurden verwendet, um die Monoterpenoid-Toleranz von *P. putida* KT2440 weiter zu verbessern. Durch das Einbringen einer 10 bp-Deletion im 5‘-UTR-Bereich des *ttgABC*-Operons im Genom von KT2440 konnte eine Überexpression des TtgABC-Efflux-Systems erreicht und dadurch die Monoterpenoid-Toleranz des potenziellen Produktionsorganismus deutlich gesteigert werden.

Teil 3 – Expression von L3H-Enzymen in monoterpenoid-toleranten Bakterien

Nach der Identifizierung von pilzlichen Limonen-3-Hydroxylase-Enzymen und der Entwicklung eines Monoterpenoid-toleranten *P. putida*-Stamms, sollten beide Teile kombiniert werden, um die Grundlage für eine weitere Entwicklung einer mikrobiellen Zellfabrik zu schaffen. Die Expression der Pilzenzyme sollte zunächst in *E. coli* als etabliertem prokaryotischen Expressionsorganismus untersucht und optimiert werden. Anschließend sollte die optimierte Gensequenz in den modifizierten *P. putida*-Stamm überführt werden.

Zu diesem Zweck wurden verschiedene Varianten des L3H.Ap-Gens (CYP65AH1 aus *A. pullulans*) hergestellt. Eine Analyse der Protein-Sequenz hatte zuvor gezeigt, dass es sich bei L3H.Ap um eine CYP der Klasse II handelt. Diese CYPs sind i.d.R. über eine N-terminale Domäne in der Membran des Endoplasmatischen Retikulums (ER) von eukaryotischen Zellen

verankert. Da prokaryotische Zellen jedoch kein ER besitzen, wurden Varianten getestet, die eine Variation der N-terminalen Sequenz aufweisen bzw. bei denen der N-Terminus trunkiert und durch ein 6xHis-Tag ersetzt ist. Darüber hinaus wurde auch eine Codon-Optimierung der Gensequenz getestet.
Neben den verschiedenen Genvarianten wurden auch bei der Durchführung der Protein-Expression unterschiedliche Parameter variiert. So wurden verschiedene Expressionstemperaturen, Expressions-Induktions-Strategien, sowie verschiedene *E. coli*-Stämme verwendet. Einige dieser Bakterien wiesen noch weitere Eigenschaften wie z.B. die Co-Expression von bestimmten Chaperonen auf, um die Produktion von funktionellen Proteinen zu unterstützen. Trotz dieser verschiedenen Ansätze konnte innerhalb dieser Arbeit das pilzliche Enzym von *A. pullulans*, L3H.Ap, jedoch nicht in funktioneller Form in *E. coli* erhalten werden, weshalb auch keine weitere Expression in *P. putida* KT2440 getestet wurde.

Abgesehen von den bereits unternommenen Strategien, könnte noch an weiteren Stellschrauben gedreht werden, um die funktionelle Expression des pilzlichen Gens in prokaryotischen Zellen letztendlich doch noch zu erreichen. Alternativ wäre es eventuell auch möglich das Enzym in den Hefen *P. pastoris* und *S. cerevisiae* zu nutzen, falls z.B. durch geeignete Prozessführung die zytotoxische Wirkung von Monoterpenen und Monoterpenoiden auf die Hefen abgemildert werden könnte.
Des Weiteren zeigen die durchgeführten Toxizitätsassays, dass die Überexpression der Efflux-Pumpen den modifizierten *P. putida*-Stamm nicht nur resistenter gegenüber Isopiperitenol, sondern auch gegenüber anderer Monoterpenoide wie z.B. Verbenon oder α-Terpineol macht. Somit könnte der Monoterpenoid-tolerante *P. putida*-Stamm an sich auch für weitere Monoterpenoid-Biosynthesen genutzt werden, indem dieser mit anderen Terpen-umsetzenden Enzymen kombiniert wird.

Insgesamt konnte in der vorliegenden Arbeit ein weiterer Schritt in Richtung einer möglichen biotechnologischen Produktion von Menthol und anderen Monoterpenoiden getan werden. Bis zur biotechnologischen Monoterpenoid-Produktion im industriellen Maßstab ist es jedoch noch ein langer Weg, sowohl auf wissenschaftlicher als auch auf gesellschaftlicher Ebene.

Abstract

Monoterpenes and their monoterpenoid derivatives form a subclass of terpene(oid)s. They are widely used in medicines/pharmaceuticals, as flavor and fragrance compounds, or in agriculture and are also considered as future biofuels. However, for many of these substances, the extraction from natural sources poses challenges such as occurring at low concentrations in their raw material or because the natural sources are diminishing. Furthermore, many of the structurally more complex terpenoids cannot be chemically synthesized in an economic way. Therefore, microbial production provides an attractive alternative, taking advantage of the often distinct regio- and stereoselectivity of enzymatic reactions. However, monoterpenes and monoterpenoids are challenging products for industrial biotechnology processes due to their pronounced cytotoxicity, which complicates the production in microorganisms compared to longer-chain terpenes (sesquiterpenes, diterpenes, etc.).

The aim of this thesis was to generate a biotechnological complement to fossil-resources-based chemical processes for industrial monoterpenoid production. Therefore, a starting point for the further development of a microbial cell factory based on the microbe *Pseudomonas putida* KT2440 was aimed to be created. This production organism should be able to conduct a whole-cell biocatalysis to selectively oxyfunctionalize monoterpene hydrocarbons using renewable industrial by-products and waste streams as raw material for monoterpenoid production (Figure 1). As a model substance, the production of (-)-menthol should be addressed due to its industrial significance. (-)-Menthol is one of the world's most widely-used flavor and fragrance compounds by volume as well as it being a medical component, having an annual production volume of over 30,000 tons. An approach for (-)-menthol production from renewable resources could be a biotechnological(-chemical) two-step conversion (Figure 1), starting from (+)-limonene, a by-product of the citrus fruit processing industry.

The thesis project was divided into three parts. In the first part, enzymes (limonene-3-hydroxylases) were to be identified that can convert (+)-limonene into the precursor of (-)-menthol, (+)-*trans*-isopiperitenol. To counteract product toxicity, in the second part, the tolerance of the intended production organism *P. putida* KT2440 towards monoterpenes and their monoterpenoid derivatives should be increased. Finally, in the third part, the identified hydroxylase enzymes would be expressed in the improved *P. putida* KT2440 strain to create a whole-cell biocatalyst for the first reaction step of a two-step (-)-menthol production, starting from (+)-limonene.

To achieve these objectives, different genetic/molecular biology and analytical methods were applied. In this way, two cytochrome P450 monooxygenase enzymes from the fungi *Aureobasidium pullulans* and *Hormonema carpetanum* could be identified and successfully

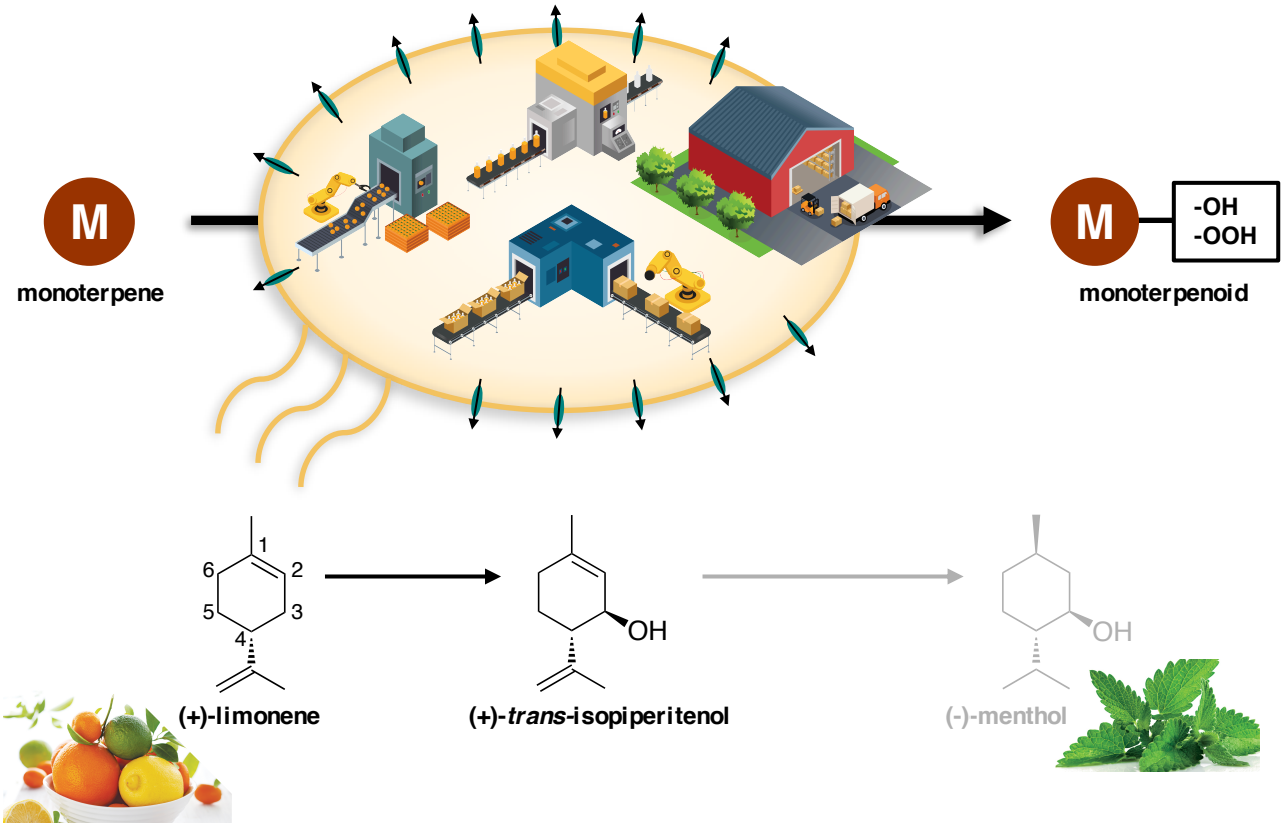

Figure 1: Graphical abstract. Aim of this thesis was to create a starting point for the further development of a cell factory for monoterpenoid production. Since many monoterpenoids are toxic for living cells, the tolerance of the selected host organism *P. putida* towards monoterpenoids should be increased. As model process, the conversion of (+)-limonene, a by-product of the citrus fruit processing industry, into (-)-menthol was chosen. In particular, the first step, the *in vivo* biotransformation of (+)-limonene into the intermediate product (+)-*trans*-isopiperitenol, was to be realized. M: monoterpene, M-OH: monoterpene alcohol, M-OOH: monoterpene acid.

expressed in *Pichia pastoris*, which can catalyze the intended hydroxylation reaction on (+)-limonene with high stereo- and regioselectivity. A further characterization of the enzyme from *A. pullulans* showed that apart from (+)-limonene the protein can also hydroxylate (-)-limonene, α- and β-pinene, as well as 3-carene.

Furthermore, within this thesis, mechanisms of microbial monoterpenoid resistance of *P. putida* could be identified. It was shown that the different monoterpenes and monoterpenoids tested have very different toxicity levels and that mainly the Ttg efflux pumps of *P. putida* GS1 are responsible for the tolerance to many of these compounds. Based on these results, a *P. putida* KT2440 strain with increased resistance to various monoterpenoids, including isopiperitenol, could then be generated, which can be used as a host organism for the further development of monoterpenoid-producing cell factories.

While within the scope of this work the heterologous expression of the fungal gene in prokaryotic cells in a functional form could not be realized despite different approaches, the identified enzymes, the monoterpenoid-tolerant *P. putida* strain and a plasmid developed for heterologous gene expression in *P. putida* provide a good starting point for the further design of a microbial cell factory for biotechnological monoterpenoid production.

Table of contents

Chapter 1 - Introduction

1.1 Monoterpene(oid)s

Terpenes and terpenoids[2] represent one of the largest classes of natural substances with over 80,000 known structures.[1,2] They occur in all kingdoms of life.[2-5] While plants, in particular, are known to produce a wide variety of terpenes and their derivatives with many different ecological, physiological and structural functions, including light-collection pigments, membrane-stabilizing compounds, hormones and other signaling substances, there is also a wealth of different terpenes and terpenoids in the realm of microbes.[6,7]

According to the isoprene rule, established in 1953, all terpenes and terpenoids are composed of isoprene units (C_5).[8] In nature, elongated terpenes are usually formed by head-to-tail condensation of the C_5 unit isopentenyl diphosphate (IPP) with its isomer dimethylallyl diphosphate (DMAPP). Depending on the organism, these C_5 units are provided either by the mevalonate (MVA)[9] or the methylerythritol phosphate pathway (MEP).[10] However, both pathways[3,5] or variants thereof[11,12] may be present in the same organism.

In the last decades, increasing evidence for exceptions of the isoprene rule could be observed. The so-called “non-canonical terpenes” can, for example, be composed of building blocks whose number of carbon atoms is not a multiple of 5.[13–17]

For a more detailed description of the natural synthesis of terpenes and terpenoids, see Chapter 2.

Monoterpenes are lipophilic, volatile, colorless substances that consist of two isoprene units and have a basic scaffold of ten carbon atoms (C_{10}).[18] Starting from the precursor geranyl diphosphate (GPP), which is formed by condensation of IPP with DMAPP, a large number of compounds with linear, mono- or bicyclic backbones and different functional groups can be formed. These include aromatic monoterpenes and oxidized derivatives (monoterpenoids) such as alcohols, aldehydes, ketones, carboxylic acids and esters.[3,6] The introduction of heteroatoms, especially, usually has an effect on the physico-chemical properties of the compounds.[19] In total, the substance class of monoterpenes and monoterpenoids comprises over 1,000 different chemical compounds.[20] Known from many plant families[21], they are responsible for several of the characteristic smells of plants and are found mainly as plant ingredients, such as resins or essential oils of many conifers, citrus fruits and flowers.[4,22] Their biological function is the attraction of pollinators and seed distributors, defense against predators, pathogens and parasites, or the interaction between plants.[4,5,23] Monoterpenes and their derivatives are also present in animals, especially in insects, serving as pheromones or

[2]According to IUPAC definition, terpenes are hydrocarbon compounds. Their (oxygenated) derivatives are referred to as terpenoids.[346,347]

as repellents.[24] In addition, monoterpenes and monoterpenoids occur in fungi and some bacteria, but their biological function in these organisms is much less investigated.[25] It has been shown that fungal volatile organic compounds, including monoterpene(oid)s, interfere with the growth of plants and other fungal species, indicating an inhibitory function of these substances against hosts and competitors.[26,27] In the domain of bacteria, 1,8-cineole and linalool/nerolidol synthases have been identified in *Streptomyces clavuligerus*.[28–30] In addition, different 2-methylisoborneol synthases have been discovered in *Streptomyces coelicolor* and other bacteria.[13,28,31,32] These enzymes produce 2-methylisoborneol, a methylated monoterpenoid which has an earthy and musty smell. Furthermore, monoterpene-emitting cyanobacteria have been reported by Yassaa *et al.* (2008).[33]

Monoterpenes and their derivatives are used as medicinal ingredients, e.g. 1,8-cineole, menthol and verbenone for the treatment of respiratory diseases,[4,6] whilst others are known to have antibacterial, antifungal, antiviral, anti-carcinogenic, antioxidant or anxiolytic (antipanic) activities/effects.[34–37] However, the industrial significance of this substance class is primarily due to their use as flavor and fragrance compounds, agrochemicals and cosmetic ingredients[18] because they often have characteristic odor and taste properties and antimicrobial effects. In addition, the use of monoterpene(oid)s as future biofuels has been discussed.[6,38–40]

Traditionally, terpenes and terpenoids are obtained from the corresponding essential oils.[18] However, for many monoterpene(oid)s, extraction from natural sources poses challenges such as low concentrations in the raw material or steady diminishment of the natural sources. Additionally, extraction from plants often suffers from seasonal and geographical variations in supply and quality which are influenced by factors such as possible crop failures or unfavorable weather conditions. Today, monoterpenes and monoterpenoids can also be produced by chemical synthesis.[1,3] However, chemical synthesis of terpenes is often challenging due to complex, chiral molecular structures and environmentally unfriendly reaction conditions. Therefore, biotechnological production represents an attractive alternative.

Microbial production of substances can take place either as biotransformation or as *de novo* synthesis. *De novo* synthesis means that compounds are produced from comparatively simple precursor molecules (sugars, amino acids, nitrogen salts, minerals, etc.) by (bio-)chemical reactions, usually complex metabolic pathways (Lat. *de novo* = from new/scratch, "total synthesis" in chemistry). In a biotransformation process, precursor molecules are converted into structurally related substances in a few steps, whereby either whole cells, cell extracts or isolated enzymes can be used.[41] However, nowadays, also multistage biotransformation processes have been published, which makes the differentiation between the two forms vaguer.

Biotechnological production by microorganisms or isolated enzymes has the advantage that often inexpensive and renewable raw materials can be used as starting materials. The reactions usually take place under mild process conditions and are highly stereo- and regioselective. In addition, flavoring substances which are biotechnologically produced from natural materials can be labelled as "natural".[3] Moreover, microbial production is less dependent on factors, such as the availability of the specific plant material and climatic and trade policy factors, that can lead to strong fluctuations in the prices of monoterpene(oid)s derived from plants.[6]

Regardless of these advantages, up to now, no biotechnological *de novo* production of monoterpenes and their derivatives has been established on an industrial scale. On a laboratory scale with microbial hosts, the highest reported values for *de novo* production of monoterpenes and monoterpenoids are 3.6 g L^{-1} for limonene (*Escherichia coli*),[42] 2.65 g L^{-1} for sabinene (*E. coli*), 0.18 mg L^{-1} for α-pinene (*Corynebacterium glutamicum*), 11 mg g^{-1} dry cell weight for β-phellandrene (*Synechoscystis* sp.), 505 mg L^{-1} for linalool (*E. coli*), 653 mg L^{-1} for 1,8-cineole (*E. coli*), 1.68 g L^{-1} for geraniol (*Saccharomyces cerevisiae*), and 193 mg L^{-1} for geranic acid (*Pseudomonas putida*).[1,43]

One reason for the so far not established industrial biotechnological *de novo* production lies in the physico-chemical properties of monoterpene(oid)s such as poor water solubility and high volatility combined with pronounced cytotoxicity.[3,4,44] The latter is due to the accumulation of monoterpenes and their derivatives in cell membranes which increases membrane fluidity and disrupts essential functions of the microorganisms.[4,45] To overcome the problem of toxicity, microbial production strains have to be developed that can tolerate higher monoterpene(oid) concentrations.[44] In particular, certain *Pseudomonas putida* strains represent a promising starting point[4] because they inherently show a pronounced tolerance to organic solvents and other toxic substances.[46]

Due to the manifold applications of monoterpenes and their derivatives, and the increasing demand for these substances, the development of new, suitable technologies for monoterpene(oid) production, such as bacterial production strains, is indispensable.[6] For further information on the biotechnological production of terpenes see Chapter 2.

1.1.1 Menthol

Menthol ($C_{10}H_{20}O$, *M* 156.27, 5-methyl-2-(propan-2-yl)-cyclohexan-1-ol) is a monocyclic monoterpene alcohol. It is a waxy, crystalline, colorless substance that is solid at room temperature. Menthol is one of the world's most widely-used flavors and fragrances by volume.[47,48] It occurs naturally in the essential oil of plants of the genus *Mentha* and is

responsible for its typical mint smell and taste. It is the main component of corn mint (*Mentha arvensis)* and peppermint (*Mentha* x *piperita)* oil, but the content may vary due to climatic factors and harvest time.[49–52] Two enantiomeric variants of menthol occur in nature, (+)- and (-)-menthol. (-)-Menthol (1*R*,3*R*,4*S* (= (1*R,*2*S*,5*R*-(-)-5-methyl-2-(1-methyl-ethyl)-cyclohexanol)) is the more abundant isomer and has the classic peppermint smell and taste.[20,53] Since menthol has three asymmetric carbon atoms (chiral centers), diastereomers of menthol exist in nature which are also called "isomeric menthols“: neomenthol, isomenthol and neoisomenthol (Figure 2).[49,53]

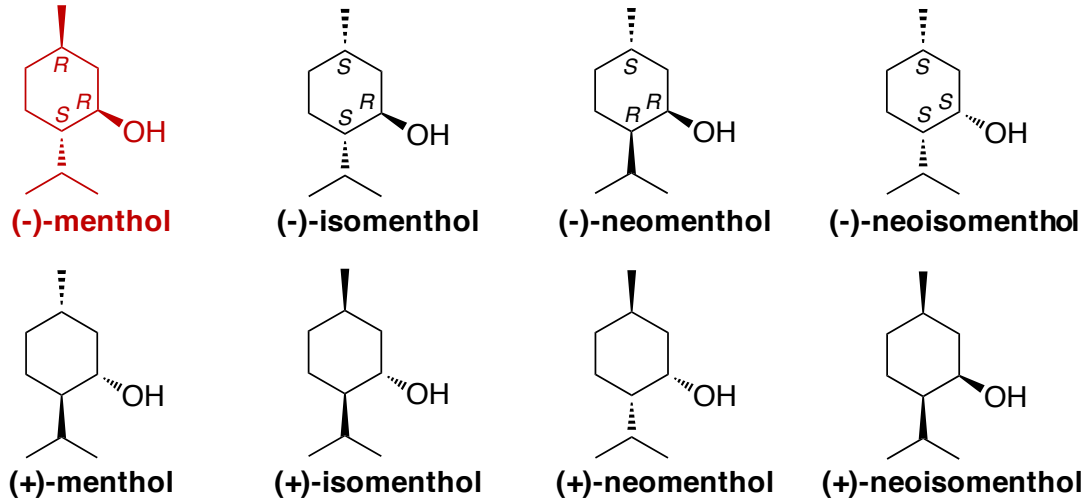

Figure 2: Menthol isomers.

The biosynthesis of menthol has been investigated in detail in the peppermint plant *Mentha* x *piperita*; this takes place in the secretory gland cells of the plant[54,55] in a 7-step process starting from geranyl diphosphate (GPP), the universal monoterpene(oid) precursor (Figure 3).[56,57] GPP is first cyclized to (-)-limonene by a (-)-limonene synthase (LS) enzyme. Subsequently, hydroxylation takes place on carbon atom 3 resulting in (-)-*trans*-isopiperitenol. This selective formation of the *trans* product is catalyzed by certain cytochrome P450 monooxygenases, isoenzymes CYP71D13 (PM17) and CYP71D15 (PM2), acting as limonene-3-hydroxylase enzymes (L3H).[58] (-)-*trans*-Isopiperitenol is then further oxidized to (-)-isopiperitenone by the (-)-*trans*-isopiperitenol dehydrogenase (IPD). (-)-Isopiperitenone reductase (IPR) then hydrogenates the double bond between carbon atom 1 and 2 using NADPH to form (+)-*cis*-isopulegone. Afterwards, isopulegon is converted into (+)-pulegon by isomerization. A further hydrogenation by (+)-pulegone reductase (PR) and a reduction of the carbonyl group by (-)-menthone reductase (MR) result in the product (-)-menthol. During the whole synthesis, three new stereocenters are introduced and two of them are subsequently inverted.[56,57]

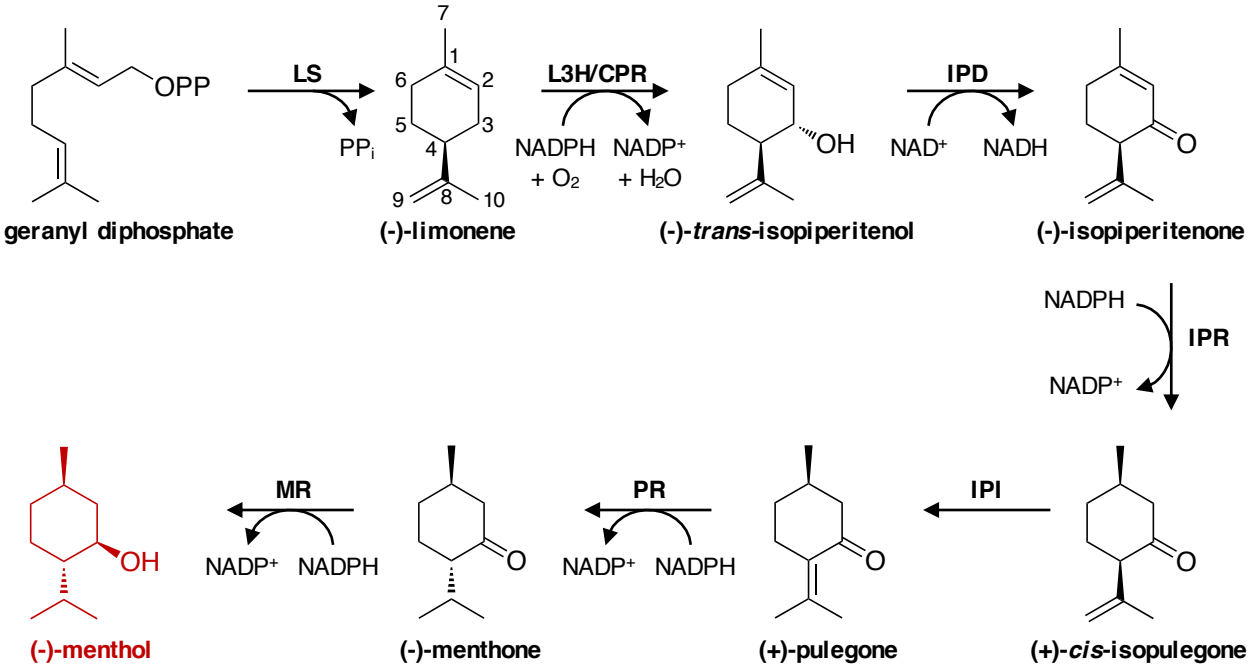

Figure 3: (-)-Menthol biosynthesis pathway in the peppermint plant *Mentha* x *piperita* (according to [56,59,60]). LS: (-)-limonene synthase, PP_i: diphosphate, L3H: (-)-limonene-3-hydroxylase, CPR: cytochrome P450 reductase, IPD: (-)-*trans*-isopiperitenol dehydrogenase, IPR: (-)-isopiperitenone reductase, IPI: (+)-*cis*-isopulegone isomerase, PR: (+)-pulegone reductase, MR: (-)-menthone reductase.

In addition to its mint smell, (-)-menthol also induces a cooling sensation when inhaled, consumed orally or applied to the skin.[48,49,61] This is due to the ability of (-)-menthol to chemically trigger receptors of the transient receptor potential (TRP) superfamily of cation channels (Na^+/Ca^{2+}) which provide a neuronal response to cold temperatures.[62,63] In this sense, it is, so to speak, the counterpart to capsaicin, the chemical responsible for the spiciness of hot chili which stimulates heat sensors even without causing an actual temperature change.[64] Furthermore, (-)-menthol has several biological activities such as its antibacterial, antifungal, anaesthetic, anti-carcinogenic, anti-inflammatory, pain-killing and penetration-enhancing effects, as well as having chemopreventive and immunomodulating actions.[3,48,50,64–69] Since in some applications (-)-menthol displays undesirable properties, derivatives or structurally closely related compounds can be used instead. These so called *cooling agents* have, for example, a lower volatility or display a longer-lasting cooling sensation without any irritating properties.[53,70]

The industrial application of (-)-menthol is very diverse and almost every consumer worldwide uses menthol in everyday life.[47] It is used in cosmetics (shower and shaving products) as well as in care products (toothpaste and mouthwash), but also in perfumery and pharmaceuticals such as cough treatments, nasal decongestants, anti-itch drugs, topical painkillers or to treat

sunburn. Furthermore, it is added to cigarettes, chewing gum, sweets and liqueurs.[53,70,71] Due to its high demand, (-)-menthol is one of the world's most widely used aroma compounds with an annual production volume of over 30,000 metric tons worldwide.[47,48,71] The industrial production of (-)-menthol is still mainly based on plant extraction with about two thirds of the total production volume.[71] Plant-based production takes place by freezing essential oils of corn mint or other mints, resulting in menthol crystals.[49,72] Pure (-)-menthol is obtained by recrystallization from solvents with low boiling points.[53] While several processes exist for the industrial production of (-)-menthol, only chemical synthesis starting from *m*-cresol/thymol (Haarmann-Reimer/Symrise, from 1973), myrcene (Takasago, from 1984), or citral (BASF, from 2012) are of commercial importance (Figure 4).[53,70,71,73]

Biotechnological production of (-)-menthol has been under investigation for many years leading to success on a laboratory scale.[59] However, the technical and economic feasibility of these proof-of-concept approaches has yet to be evaluated and an industrial process has so far not been established.[47]

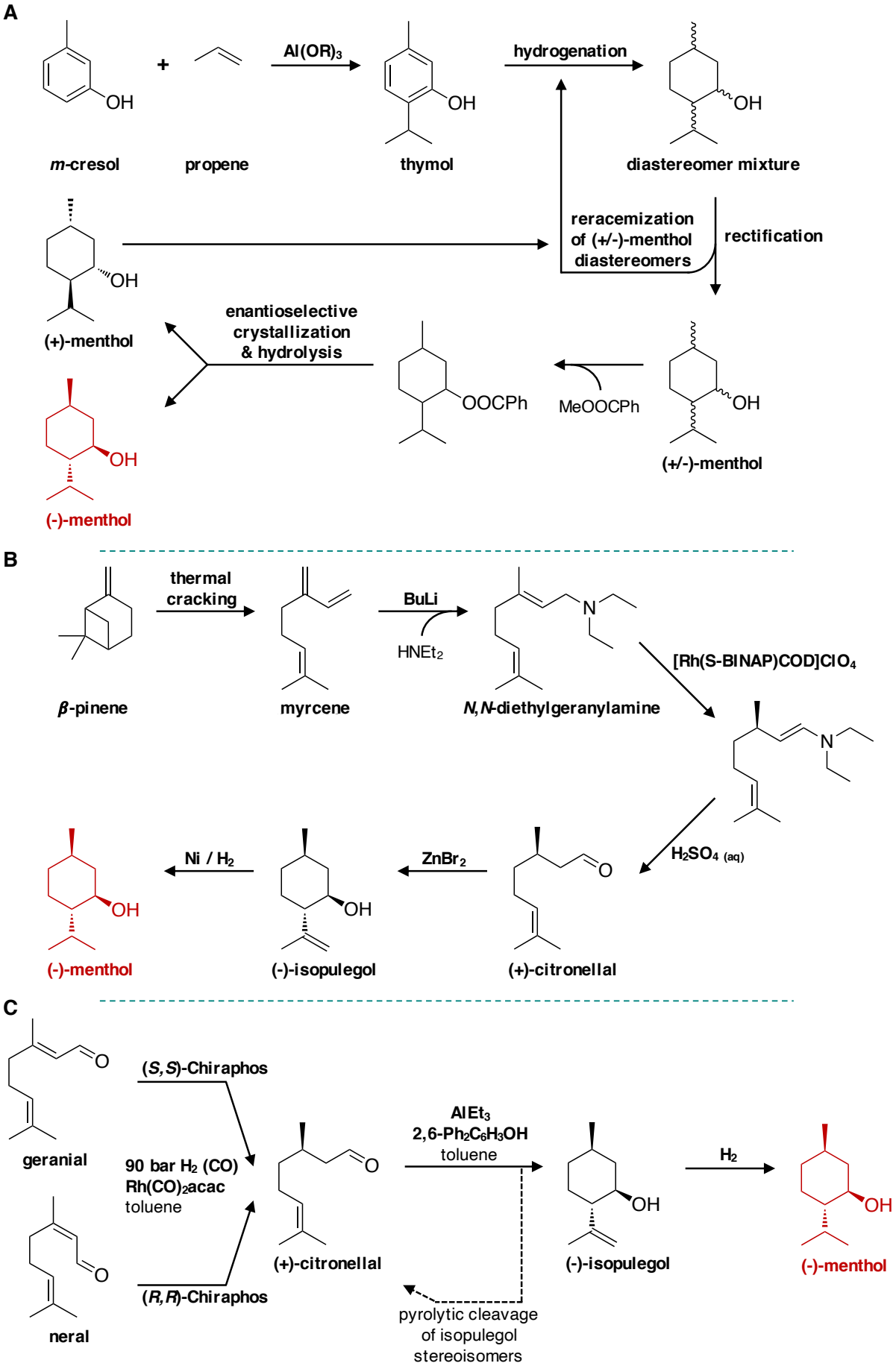

Figure 4: Technical synthesis processes for (-)-menthol production used in industry starting from (A) petrochemical *m*-cresol or renewable resources, (B) β-pinene/myrcene from turpentine or (C) citral (mixture of geranial and neral) (adapted from [3,53,70]).

1.1.2 Cytochrome P450 monooxygenases

Among the many types of terpene modifying enzymes, there is one family often associated with oxidizing reactions. This is the protein family of cytochrome P450 monooxygenases, abbreviated to P450s or CYPs. In their active form, the P450 monooxygenases contain heme as a prosthetic group which is linked to the apoprotein via a conserved cysteine residue.[74,75] Using the central iron atom of heme, they bind and activate molecular oxygen and transfer one oxygen atom to the substrate,[76] giving them the name monooxygenases. When a carbon monoxide molecule is bound in their catalytic site, the enzymes have an absorption maximum at 450 nm, what is accountable for another part of their name, while the P stands for "pigment". Since CYPs are actually not cytochromes in the true sense, "heme-thiolate protein" is also suggested as a name.[77]

For their functionality, CYP enzymes require auxiliary proteins or protein domains which provide the necessary electrons for the CYP reaction. Such reductase proteins, in turn, obtain the reducing equivalents by oxidation of NAD(P)H (Figure 5).[78]

In general, all CYP enzymes can bind and activate atmospheric dioxygen and the following regio- and stereoselective hydroxylation is catalyzed,[75] with R–H representing the substrate:

$$R\text{–}H + O_2 + NAD(P)H + H^+ \rightarrow R\text{–}OH + H_2O + NAD(P)^+$$

In addition, CYP enzymes also catalyze epoxidation, dealkylation, deamination, dehalogenation, dehydrogenation, oxygenation, isomerization and other reactions, such as the further oxidation of hydroxy groups to carbonyl or carboxyl groups, or reductions or rearrangements of oxygenated species.[19,74,75,78–83]

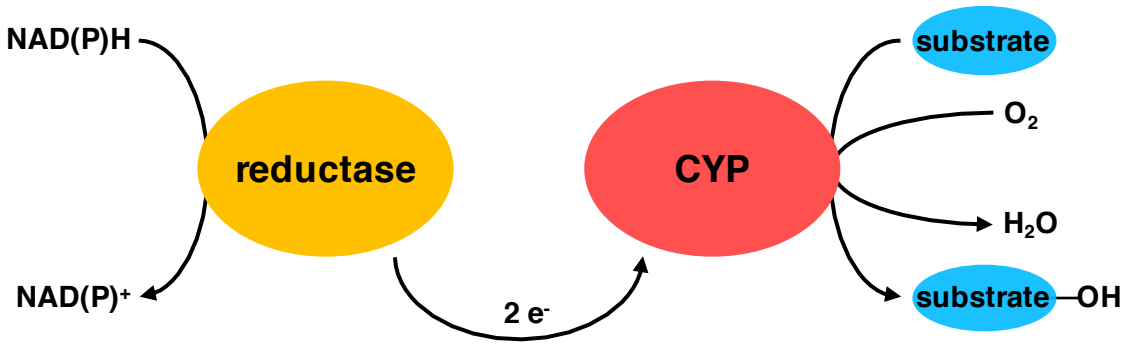

Figure 5: Cytochrome P450 redox chain. Simplified scheme of interaction between cytochrome P450 reductase enzyme and cytochrome P450 monooxygenase (CYP). The reductase takes electrons (e^-) from NAD(P)H and transfers them to a CYP enzyme. In the active center of the CYP the electrons are used to reduce molecular oxygen, and one oxygen atom is transferred to the substrate.

Cytochrome P450s form the largest and functionally most versatile enzyme family in nature;[79] more than 40,000 sequences can be found in the respective databases

today (https://drnelson.uthsc.edu/CytochromeP450.html, https://cyped.biocatnet.de/superfamilies).[70,71] However, only a small number of them have been characterized at the protein or functional level.[75,86,87] CYP proteins occur ubiquitously in all domains of life and catalyze essential reactions in both primary and secondary metabolism.[88] Besides their role in terpenoid biosynthesis to oxygenate the carbon skeletons, they are also involved in carbon source assimilation, in the biosynthesis of physiologically important compounds such as steroids, fatty acids, eicosanoids, vitamins, flavonoids and anthocyanins (floral pigments), the conversion of alkanes and aromatic compounds, and play an essential role in the detoxification and degradation of xenobiotics and other harmful substances.[19,74,78,80,89,90] Therefore, CYPs occur in the human liver for detoxification purposes.[91]

Cytochrome P450 monooxygenase systems are divided into 10 to 13 classes, based on the organization of their redox chains (Figure 6).[81,89,92] The main differences between these classes are whether the proteins are expressed in a soluble form or are membrane-bound and how many individual redox partners are required. In some of these enzymes, the reductase unit forms a fusion protein with the CYP protein domain. Different classes occur depending on the organism. In prokaryotic cells mainly soluble variants are present. Well-studied examples of bacterial CYP enzymes are P450cam from *Pseudomonas putida* and P450-BM3 from *Bacillus megaterium*, belonging to class I or VIII, respectively (Figure 6 A and D). CYP class II enzymes occur most frequently in eukaryotic organisms, including fungi. Unlike bacterial CYPs, the enzymes classified in this group are integral membrane proteins of the endoplasmic reticulum (ER) (Figure 6 B and C).[89,93]

CYP enzymes are characterized by their extremely broad range of protein sequences. They are classified into families according to their primary sequence identity and not, necessarily, according to their specific activity. The nomenclature thus reflects evolutionary relationships of the sequences. In general, CYPs with a protein sequence identity of more than 40 % form members of a family, while a sequence identity of more than 55 % defines members of a subfamily.[77,78] According to the convention, all systematic names for P450 monooxygenases begin with the letters CYP, followed by a number indicating the classification of the enzyme into a family, then a letter for the subfamily and finally a number for each individual protein;[77] following this nomenclature, P450cam is named CYP101A1, for example. Although the primary amino acid sequence identity between different CYPs can be very low, often a higher similarity can be observed in the secondary and tertiary structures.[93,94]

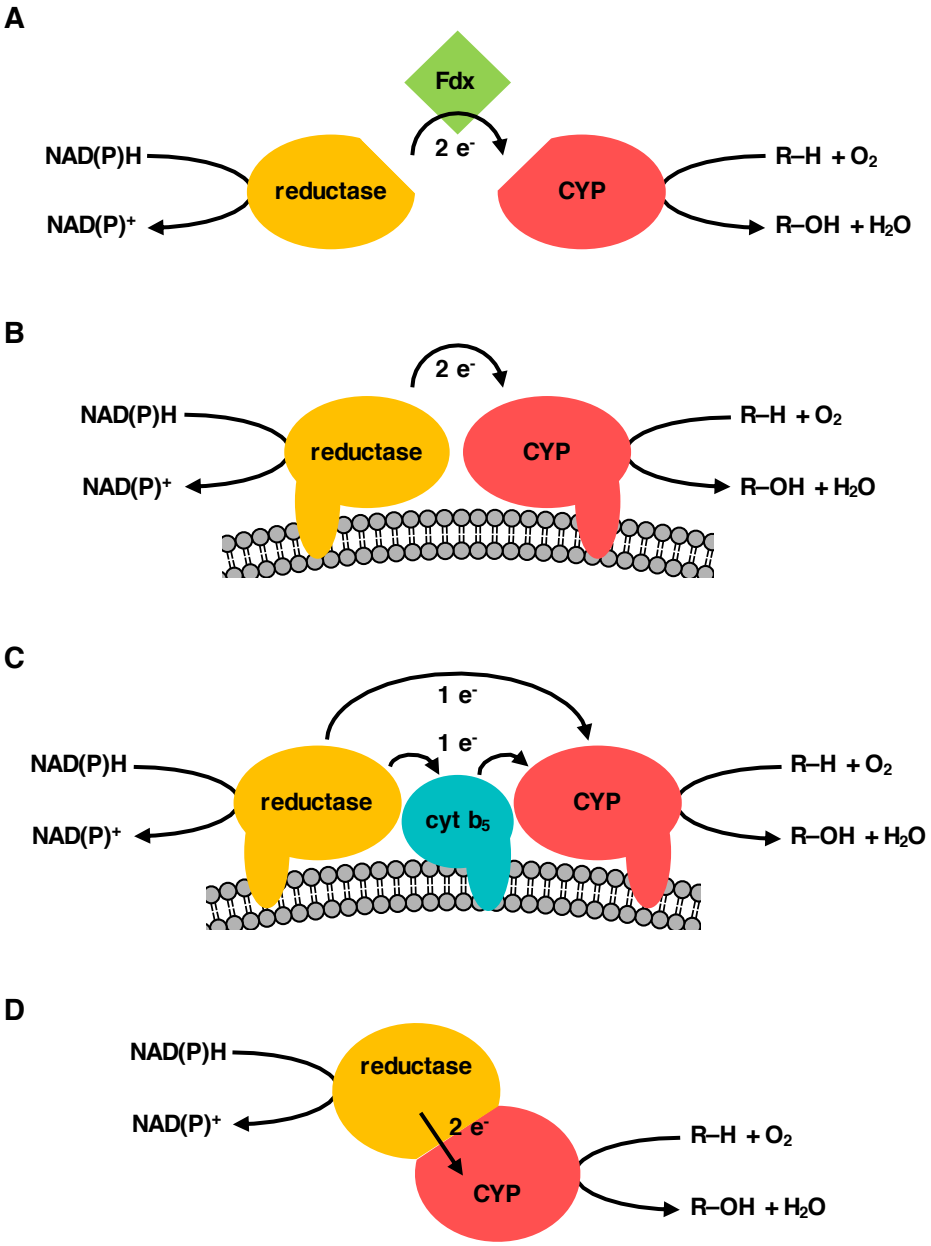

Figure 6: Schematic overview of different cytochrome P450 redox systems.[74,89,92,93,95] (A) Class I: three protein system, CYP and reductase can either be soluble or membrane-bound, electrons (e^-) are transferred from NAD(P)H to ferredoxin (Fdx) by the ferredoxin reductase enzyme and further to the CYP protein, e.g. P450cam (CYP101A1) from *Pseudomonas putida*. (B) and (C) Class II systems: membrane-bound, typical for eukaryotes, composed of cytochrome P450 reductase (CPR) and CYP enzyme or an additional cytochrome b_5 (cyt b_5) as electron transfer protein; in the latter case, the second electron is transferred from the reductase via cytochrome b_5 to the CYP enzyme. (D) Class VIII: one protein fusion system, soluble or membrane-bound systems formed by fusion of CPR-like reductase and CYP domain in a single polypeptide chain, thereby catalytically self-sufficient as monooxygenase, e.g. P450-BM3 (CYP102A1) from *Bacillus megaterium*.

Overall, the superfamily of CYPs accepts a large number of different organic molecules as substrates and catalyzes a wide variety of different reactions.[19,80,82] Due to a multitude of research work, many different CYP enzymes are known today. While some catalyze certain reactions with high substrate and product selectivity,[19,78] others are known to show extreme

versatility acting on a broad range of substrates.[86] However, despite extensive knowledge of a large number of CYP enzymes, it is still difficult to make predictions about certain substrate and product specificities of uncharacterized CYP sequences.[87]

Their ability to catalyze useful reactions, such as the regio- and stereoselective addition of an oxygen atom to non-activated carbon atoms at room temperature under normal pressure, makes CYPs attractive candidates for biotechnological applications in whole-cell biocatalysis.[80] The advantage of using whole-cell biocatalysts is the increased protein stability and efficient cofactor regeneration which is essential for the function of these enzymes.[4,19,74] However, the functional expression of CYP enzymes in microbial hosts is one of the major hurdles when engineering, for instance, terpenoid biosynthesis.[60] This is due to the fact that many natural CYPs are expressed only at low levels in their native environment and exhibit low catalytic activity which is insufficient for biocatalytical processes.[80,96,97] In addition, further limitations have to be overcome including the need for an electron transfer partner and limited electron transfer rate, NAD(P)H requirement, uncoupling of NAD(P)H oxidation and product formation, and often a low substrate solubility.[97] Furthermore, most eukaryotic CYPs are membrane-bound which complicates heterologous expression.[88] Therefore, while in recent years numerous biotechnological conversions have been developed on the basis of CYP enzymes,[74,78] only some have reached the industrial application stage such as the production of hydrocortisone,[80] nootkatone, taxol or artemisinin.[19,95,97–99]

If a CYP enzyme is required to catalyze a specific reaction, one approach is to modify a known enzyme by protein engineering.[19,100] While such an approach can lead to the formation of the desired product, the disadvantage may be a decrease in activity and/or selectivity of the enzyme, resulting in the formation of numerous by-products.[101,102] Furthermore, consideration of the 3D-structure can only be helpful to a limited extent. It has been shown that in many cases the 3D-structure of CYPs with bound substrates do not present the substrate in a position for hydroxylation, but outside of the active site. Before the substrate conversion can take place, a rearrangement of the enzyme is necessary to relocate the substrate to the catalytic center.[97]

Apart from engineering known enzymes to conduct new reactions, another approach is to search in nature's diversity for enzymes that can catalyze the desired reaction natively with a high selectivity. However, this can become akin to the search for a needle in a haystack due to the difficult predictability of substrate selectivity based on protein sequence, and because of the fact that some organisms, such as plants, often encode several hundred CYP enzymes in their genome.[60,87] Even if fitting eukaryotic CYP enzymes are described in literature, they are often difficult to express in microbial hosts, especially if they originate from higher eukaryotes.[95] This may be due to the fact that the ER membrane-bound eukaryotic proteins

lack the appropriate membrane environment in prokaryotic cells or that no suitable reductase can be co-expressed with the respective CYP enzyme.[78] The inherent dependence on a suitable reductase was eliminated by fusing together the naturally separated proteins of the redox chain, thereby creating self-sufficient CYP enzymes.[92] Other studies have established a peroxide shunt pathway, in which H_2O_2 or organic peroxides are used for catalysis instead of O_2 and NAD(P)H. Some CYP enzymes can use such a shunt pathway, which allows them to function without additional electron transport proteins.[80,81,103]

In addition, in recent years many other studies have attempted to improve heterologous expression of CYP enzymes and have provided possible strategies to overcome limitations.[80,86,88,95,97,104] However, no generally applicable guideline has been developed for CYP expression so far, creating the need to develop protocols for each new cytochrome P450 enzyme.[60,88]

1.2 *Pseudomonas putida*

Pseudomonas putida is a Gram-negative, rod-shaped γ-proteobacterium which feeds saprophytically and occurs in various terrestrial and aquatic habitats. The bacteria are found both in the soil and in association with plants, and can also form biofilms.[105,106] *P. putida* strains have a broad spectrum of metabolic activities and can use a variety of organic substances as energy, carbon, nitrogen, phosphate and sulphur sources, making them highly adaptable.[46,107–109]

Bacteria of this species are characterized by a pronounced robustness to extreme environmental conditions such as high temperatures, extreme pH values or the presence of toxic substances.[109,110] They are known to survive in habitats contaminated with organic pollutants and heavy metals, and they are able to degrade and utilize a wide variety of chemicals, including many natural and xenobiotic substances.[107] While most naturally occurring strains of this species can tolerate low concentrations of aromatic hydrocarbons and short-chain alcohols, only a few are able to survive at higher concentrations.[46]

The genome of *Pseudomonas putida* is about 6 Mbp in size and usually consists of only one chromosome;[105] a few subspecies possess an additional autonomously-replicating plasmid, such as *Pseudomonas putida* DOT-T1E.[111] As, nowadays, the complete genome sequences of many strains are available[106,107,112] and numerous techniques for genetic manipulation and gene expression in *Pseudomonas putida* have been developed, this organism is very well genetically accessible.[109,113] These established methods for the genetic engineering of *P. putida* include strategies for deletions and insertions in the genome, using, for example, pEMG-[114] or CRISPR-Cas9-based approaches,[115–117] homologous recombination, or

recombinases and transposons as delivery systems.[118–127] In addition, vector[128,129] and promoter collections[122,124] are available to tune gene expression. Moreover, the use of quantitative omics technologies leads to an ever improving system-wide understanding of cellular processes, which could enable the targeted modification of strains into cell factories for biotechnological applications based on *in silico* models.[109,130,131] Furthermore, *Pseudomonas putida* is easy to cultivate in the laboratory and can also be grown on an industrial scale with high growth rates.[109]

The *P. putida* strain KT2440 was the first Gram-negative soil bacterium to be classified as a safety strain by the *Recombinant DNA Advisory Committee* (RAC), indicating that it is safe to use in a safety level 1 environment.[106,132] Such a certificate is of particular importance for the industrial production with recombinant strains, or their targeted release.

All these properties have contributed to the fact that *Pseudomonas putida* is used in numerous biotechnological processes today. These include the production of secondary metabolites generated natively by the organism and the use of the bacterium as a host for the recombinant biosynthesis of various substances. Among the wide variety of products are fine chemicals, pharmaceuticals and other industrially used substances. These include natural products, such as rhamnolipids, terpenoids, polyketides and non-ribosomal peptides, as well as bio-based polymers, e.g. polyhydroxyalkanoates (PHA), and non-natural chemicals.[109,113]

In some of these processes, the reactants and products have a pronounced cytotoxicity which is a limiting factor for large-scale production. Therefore, the aforementioned natural tolerance of many *Pseudomonas putida* strains to extreme and toxic conditions, compared to other industrial production strains, is of decisive importance.[109,113] Due to these inherent resistances, *Pseudomonas putida* also has great potential for use in bioremediation of toxic waste water and contaminated soils and is currently the subject of ecological and agricultural biotechnological research.[105,109,113]

An example for an especially solvent-tolerant strain is *Pseudomonas putida* GS1 (DSM 12264);[133] this strain was isolated from the sewage sludge of a wastewater treatment plant. However, in comparison to *P. putida* KT2440, *P. putida* GS1, as well as all other *P. putida* strains, belongs to risk group 2 (R2) in Germany. This is due to the fact that these organisms are generally regarded as opportunistic and nosocomial pathogens with a good prognosis; there have been several cases of human infection by *P. putida*, but mainly in immunosuppressed hosts.[134] Only *P. putida* KT2440 has been downrated due to the known absence of virulence factors, exotoxins and cell wall degrading enzymes.[135]

Nevertheless, several biotechnological processes with *P. putida* GS1 have already been described in literature. For instance, it is able to oxidize limonene to perillic acid.[133,136] In

another study, a genetically modified GS1 strain was used as a microbial cell factory for the *de novo* biosynthesis of geranic acid from glycerol.[137] This study as well as subsequent experiments (A. Meffert, unpublished data) also demonstrated that *P. putida* GS1 has a superior geranic acid tolerance compared to microbial production organisms such as *Escherichia coli* and *Bacillus subtilis*. In addition, in 2016 Mi and colleagues described *Pseudomonas*' superior tolerance towards 1,8-cineole compared to *E. coli*.[138]

The resistance of this strain to different monoterpene(oid)s and also the easy genetic accessibility render *Pseudomonas putida* GS1 a promising platform for microbial monoterpenoid production.[137] However, the classification of this and other solvent-tolerant *P. putida* strains in risk group 2 in Germany[135] makes their use in industrial production processes considerably more difficult.

1.3 Solvent tolerance

Solvent tolerance is an important property for microorganisms used in bioremediation systems or for the synthesis of toxic chemicals. While most microbes are highly sensitive to solvents,[139] it has been found that some isolates have the ability to grow in the presence of organic solvents, such as short-chain alcohols and aromatic hydrocarbons, but also other aliphatic, aromatic and heterocyclic substances, for example, monoterpene(oid)s; these include butanol, benzene, toluene, xylene, 1,8-cineole and terpineol.[46,140,141] Among these tolerant organisms are some *Pseudomonas putida* strains such as DOT-T1E, F1, S12 or GS1.[46,133,142,143]

Organic solvents have a toxic effect on microorganisms because they accumulate in the biomembranes.[144,145] This accumulation leads to an increase in membrane fluidity and permeability, resulting in disorganization of the membrane structure and impairment of vital functions. This, in turn, can cause the loss of ions, metabolites, lipids and proteins and the elimination of membrane pH gradients and electronic potentials. In addition, organic solvents denature proteins and cause oxidative damage. The latter is probably due to the interaction of solvents with electron transport systems, resulting in the increased production of hydrogen peroxide and other reactive oxygen species (ROS).[46,146]

It is assumed that toxicity of a particular substance correlates with its hydrophobicity which determines to what extent it accumulates in the cytoplasmic membrane. A measure of hydrophobicity is the logarithm of the octanol-water partition coefficient ($\log P_{ow}$) of the substance.[144] Organic solvents with a $\log P_{ow}$ of between 1.5 and 4 are extremely toxic for microorganisms and other living cells as these are particularly preferentially deposited in biological membranes.[38,139,140,147] For example, commonly used organic solvents such as toluene, hexane or decane have $\log P_{ow}$ values of around 2.8, 3.9 and 6.0, respectively.[148]

Most terpenes and terpenoids have $logP_{ow}$ values of higher than 4 such as sesquiterpene(oid)s (e.g. valencene: 6.5, patchouli: 4.5, santalol: 4.3), diterpene(oid)s (e.g. sclareol: 5.2) and other terpene(oid)s of longer chain length (> 20 carbon atoms), including carotenoids (e.g. astaxanthin: 8.2, retinol: 6.0).[149] Many monoterpenoids, on the other hand, have $logP_{ow}$ values below 3.5 (e.g. menthol: 3.2, isopiperitenol: 2.6, verbenone: 2.1, verbenol: 2.6, α-terpineol: 2.7),[149] which makes them particularly toxic to microorganisms.
However, whether a certain substance has a negative effect on a microorganism is not only related to the inherent toxicity of the substance, but also to the defense system the living organisms have implemented against the specific compound.

Solvent-tolerant *Pseudomonas putida* strains and other Gram-negative bacteria protect themselves against the effects of toxic substances through a multifactorial process. This includes a change in lipid composition of the biomembranes to adjust membrane functionality, the activation of general stress-response systems, increased energy supply and the activation of specific efflux pumps to remove foreign substances from the cells. An interaction of all these factors conveys the high degree of tolerance (Figure 7). These processes are transcriptionally controlled by a number of local and global regulators, for instance, sigma factors regulating extracytoplasmic functions (ECFs), such as one encoded by the gene *rpoT*, as well as by small regulating RNAs (sRNAs).[46,150]

In order to maintain membrane functionality in the presence of organic solvents, the lipid bilayer composition of solvent-tolerant *Pseudomonas putida* strains is altered. Thereby, conversion of *cis*- into *trans*-unsaturated fatty acids serves as a fast response.[145,151] The elongated conformation of the acyl chains in *trans*-unsaturated fatty acids shows a greater similarity to the spatial arrangement of saturated fatty acids compared to *cis*-unsaturated fatty acids.[144] As a result, the conversion leads to a denser membrane packing and, thus, to an increase in melting temperature. This process is catalyzed by a specific *cis-trans* isomerase (Cti).[152] Cti activity is constitutively present in the cells and is located in the periplasm, allowing a rapid response to the presence of toxic solvents.[46,140,152–154] When membrane fluidity is increased, for instance, due to the presence of solvent molecules, Cti can reach its substrate, i.e. the double bonds of unsaturated fatty acids, and thus help to restore membrane rigidity.[154] Since an alteration of the *cis*-to-*trans* ratio in biomembranes can also be observed as a response to other stressors, such as temperature changes, increased salt concentration or heavy metal exposure, this process appears to be a general short-term defense mechanism against harmful environmental conditions. In addition to *cis-trans* isomerization, in the presence of organic solvents cyclopropane fatty acids (CPAs) are formed in

Pseudomonas putida cells. This is achieved by the addition of methyl groups to the double bonds of unsaturated fatty acids by a cyclopropane synthase (Cfa) whose expression is upregulated in *P. putida* in response to solvent stress.[140,150] Moreover, further membrane modifications have been observed in Gram-negative bacteria with solvent exposure. One of these modifications is the change in the composition of different phospholipid head groups which also has an influence on membrane fluidity.[140,150]

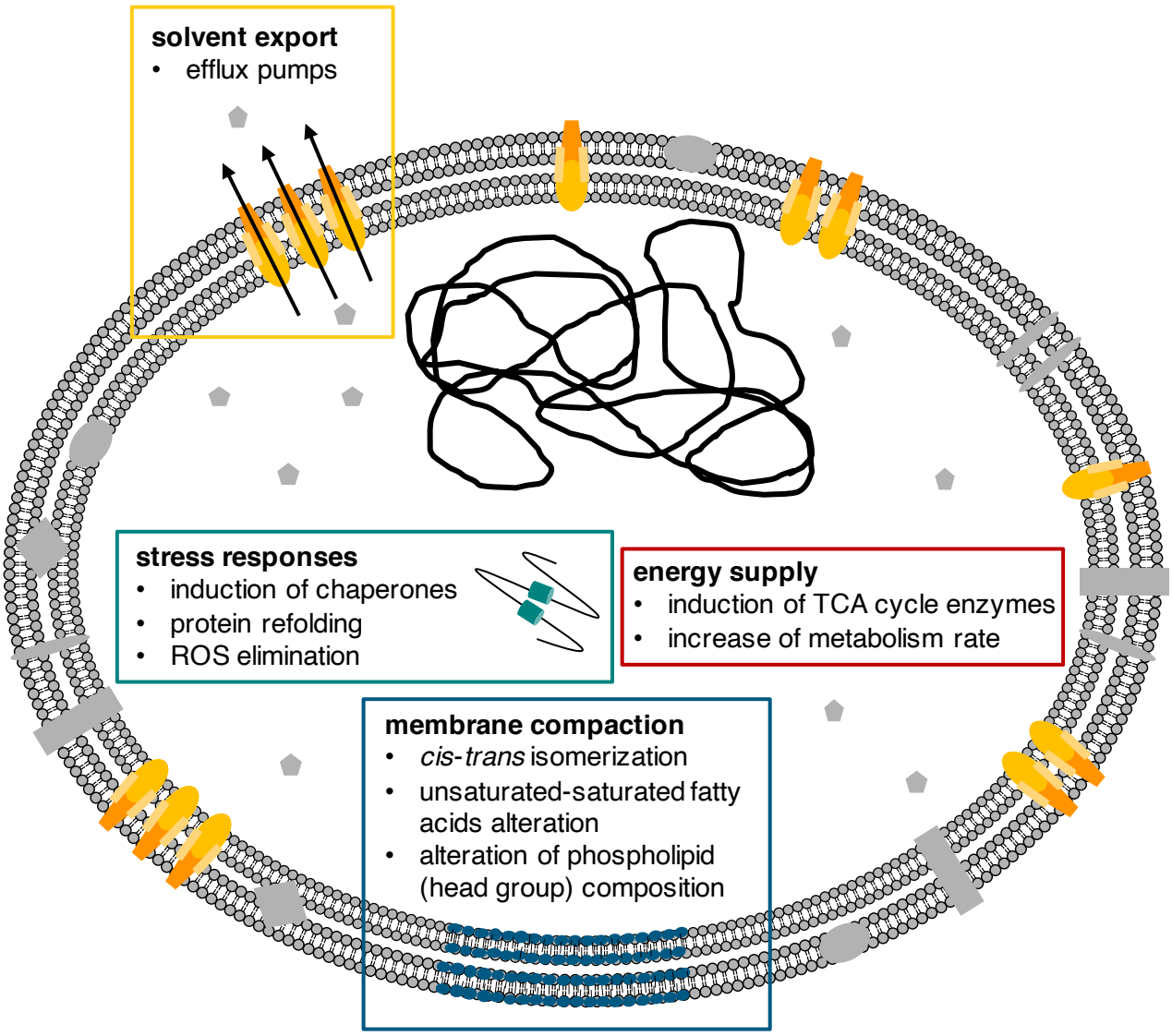

Figure 7: Overview of the main mechanisms considered to be involved in solvent tolerance in *P. putida* (modified from [46]). The multifactorial response system includes solvent export by efflux pumps, chaperone induction for protein refolding, ROS scavenging systems, upregulation of energy metabolism, and membrane compaction. TCA: tricarboxylic acid cycle, ROS: reactive oxygen species.

Since these membrane modifications are not sufficient to prevent the penetration of toxic substances into the cells, additional mechanisms must be involved in the solvent tolerance of *Pseudomonas putida*. Expression of a number of genes has been shown to be upregulated in cells exposed to organic solvents. These genes include DNA repair systems, chaperones to refold solvent-denatured proteins, and the activation of oxygen stress systems to eliminate ROS.[46,150] Apart from the already described mechanisms, active excretion by efflux pumps represents the most efficient protection mechanism against the accumulation of toxic solvents in microbial cells.[46,143,155–157] These are discussed in more detail in the next section (1.3.1 Efflux pumps).

All mechanisms described so far, especially the expression and engine of efflux pumps, require energy. Studies have shown that the growth yield (g biomass per g carbon source) of *Pseudomonas* can be reduced by up to 50 % in the presence of sublethal butanol or toluene concentrations.[46,158,159] Therefore, it is not surprising that solvent-tolerant *P. putida* strains upregulate proteins related to energy metabolism in response to solvent exposure. These include enzymes of the tricarboxylic acid cycle (TCA) and subunits of NADH dehydrogenase and ATP synthase.[158,160] In addition, some strains are able to metabolize small amounts of the solvent for further energy generation.[46,140] Although conversion of the solvents to less toxic substances can also contribute to better bacterial growth in the presence of solvents, this mechanism appears to play a secondary role in solvent resistance, and the development of tolerance to a chemical and the development of its metabolization appear to be independent from each other.[46,140,150]

1.3.1 Efflux pumps

Multidrug resistance (MDR) efflux pumps are membrane transporters that export substances from cells. In pro- and eukaryotes, they represent one of the most effective tolerance mechanisms against toxic chemicals since effective export of these substances prevents them from reaching a lethal concentration inside the cells.[140,161] MDRs catalyze the active export of many structurally and functionally unrelated substances from the cells into the environment. They have an extensive substrate spectrum that ranges from antibiotics and antiseptics to biocides, dyes, detergents, fatty acids, organic solvents, heavy metals and other toxic substances.[46,140,162,163] It is assumed that the selectivity of these systems is determined by physical properties such as charge, hydrophobicity or amphiphilicity. In addition, van der Waals interactions that can be formed between the molecules and the active centers of the proteins, and the flexibility of these binding sites, also contribute to the determination of selectivity.[140] Among the various families of efflux systems, ABC (ATP binding cassette)-efflux

transporters[164] and pumps of the Resistance-Nodulation-Division (RND) family are mainly responsible for the solvent tolerance of many Gram-negative bacteria; such systems allow bacteria to export substances from the cytoplasm and the periplasm to the external medium.[46,150]

An archetypal RND efflux system consists of three components: 1.) a cytoplasmic membrane-integrated export protein that recognizes the substrates and acts as an energy-dependent pump, 2.) a protein in the outer membrane that extends into the periplasm and forms a type of tunnel and 3.) a lipoprotein, also known as membrane fusion protein (MFP), that stabilizes the interaction between the other two elements (Figure 8). All three components are essential for the function of the efflux pumps and the associated genes are usually encoded together in the same operon.[38,46,140] The energy source of the efflux pumps is the proton motive force (PMF) which is generated by a proton concentration gradient across the cytoplasmic membrane.

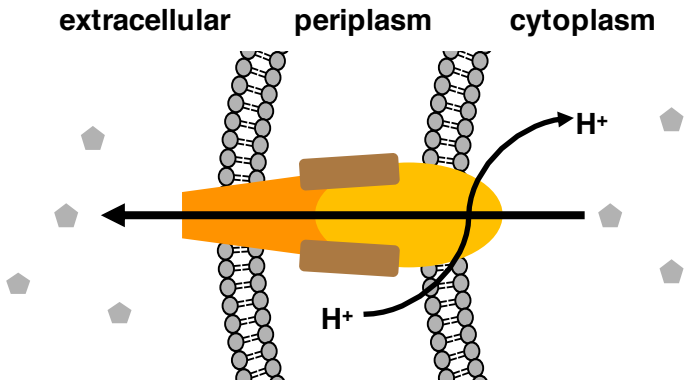

Figure 8: Schematic structure of an RND efflux system (modified from [46]). RND efflux systems typically consist of three components: a cytoplasmic membrane-integrated export protein that recognizes the substrates and acts as an energy-dependent pump (yellow), a protein in the outer membrane that extends into the periplasm and forms a type of tunnel (orange) and a lipoprotein that stabilizes the interaction between the other two components (brown).

In most Gram-negative bacteria, several RND efflux pumps are encoded in the genome; in *Pseudomonas putida* DOT-T1E there are up to 20 different efflux pumps.[150] In *P. putida* several of these systems usually work synergistically together to achieve a high degree of tolerance. Ramos and colleagues identified three RND efflux systems involved in the toluene resistance of *Pseudomonas putida* DOT-T1E which are encoded by the toluene tolerance genes (*ttg*); these efflux pumps are TtgABC, TtgDEF and TtgGHI.[46] While the *ttgABC* and *ttgDEF* operons are chromosomally localized,[40-42] the genes for the TtgGHI efflux system are located on the pGRT1 megaplasmid.[166,167] In these efflux pumps, the TtgB, TtgE and TtgH proteins act as cytoplasmic membrane-integrated transporters, while the proteins TtgC, TtgF and TtgI are located in the outer membrane, and TtgA, TtgD and TtgG represent the membrane

fusion proteins.[140] While the *ttgABC* genes are widespread in the various *Pseudomonas putida* subspecies, the other two operons, *ttgDEF* and *ttgGHI*, appear to be present only in particularly solvent-tolerant strains.[46]

TtgABC has a broad substrate spectrum and is capable of removing various solvents from the cells such as toluene and styrene, but also antibiotics, including ampicillin, carbenicillin, tetracycline, nalidixic acid and chloramphenicol, as well as biocides and dyes and probably even heavy metals.[140,161,168,169] TtgGHI exports solvents such as toluene, styrene, xylene, ethylbenzene and propylbenzene as well as antibiotics, although TtgABC is the main antibiotic efflux transporter.[140,169,170] TtgDEF is also involved in the export of aromatic hydrocarbons such as toluene and styrene, but does not transport antibiotics.[140,166]

When grown under laboratory culture conditions without stressors, the genes for the TtgABC and TtgGHI systems are expressed at high basal levels, so they are responsible for the intrinsic resistance to antibiotics and organic solvents.[46] The addition of aromatic hydrocarbons to the culture medium leads to the increased expression of the *ttgGHI* operon. The transcription of *ttgABC* is slightly increased by the addition of solvents, but strongly by the addition of certain hydrophobic antibiotics or antimicrobial plant compounds. Expression of the *ttgDEF* genes is suppressed without stressors and is only induced by the presence of substrates, such as solvents. Thus, together with the increased expression of the *ttgGHI* operon, the TtgDEF system provides additional, inducible resistance in response to solvent shock.[46,161,165,168–171]

The expression of the Ttg efflux systems is controlled by transcriptional regulators which are partially encoded by adjacent, but divergently transcribed genes (Figure 9).

The *ttgABC* operon is regulated by the TtgR repressor, a TetR-like protein. TtgR binds to a pseudo-palindromic operator sequence at the intersection of the *ttgR* and *ttgABC* promoters and, thus, prevents the expression of *ttgABC* and of its own gene (negative autoregulation).[165,169] In solution, TtgR is present as a dimer. Two of these dimers bind cooperatively to the operator and thereby achieve repression of gene expression. An imperfect palindromic sequence in the operator region of the *ttgABC* operon leads to a low binding affinity of TtgR. In this way, even in the absence of effectors, the TtgABC complex is expressed at a high basal level.[172] The presence of certain substances, e.g. antibiotics or flavonoids, causes a conformational change in the repressor. As a result, the repressor can no longer bind to the *ttgR*/*ttgABC* operator and clears the way for the RNA polymerase, thereby, more TtgABC efflux systems, as well as more TtgR repressor molecules, are produced in the cells. Therefore, the overlapping of the *ttgABC* and *ttgR* promoters not only regulates the amount of efflux pumps produced, but also the amount of TtgR as a function of effector concentration.[46,169,172] This, in turn, leads to a constant down-regulation of *ttgABC* expression and prevents the overexpression of the membrane protein complex.[173]

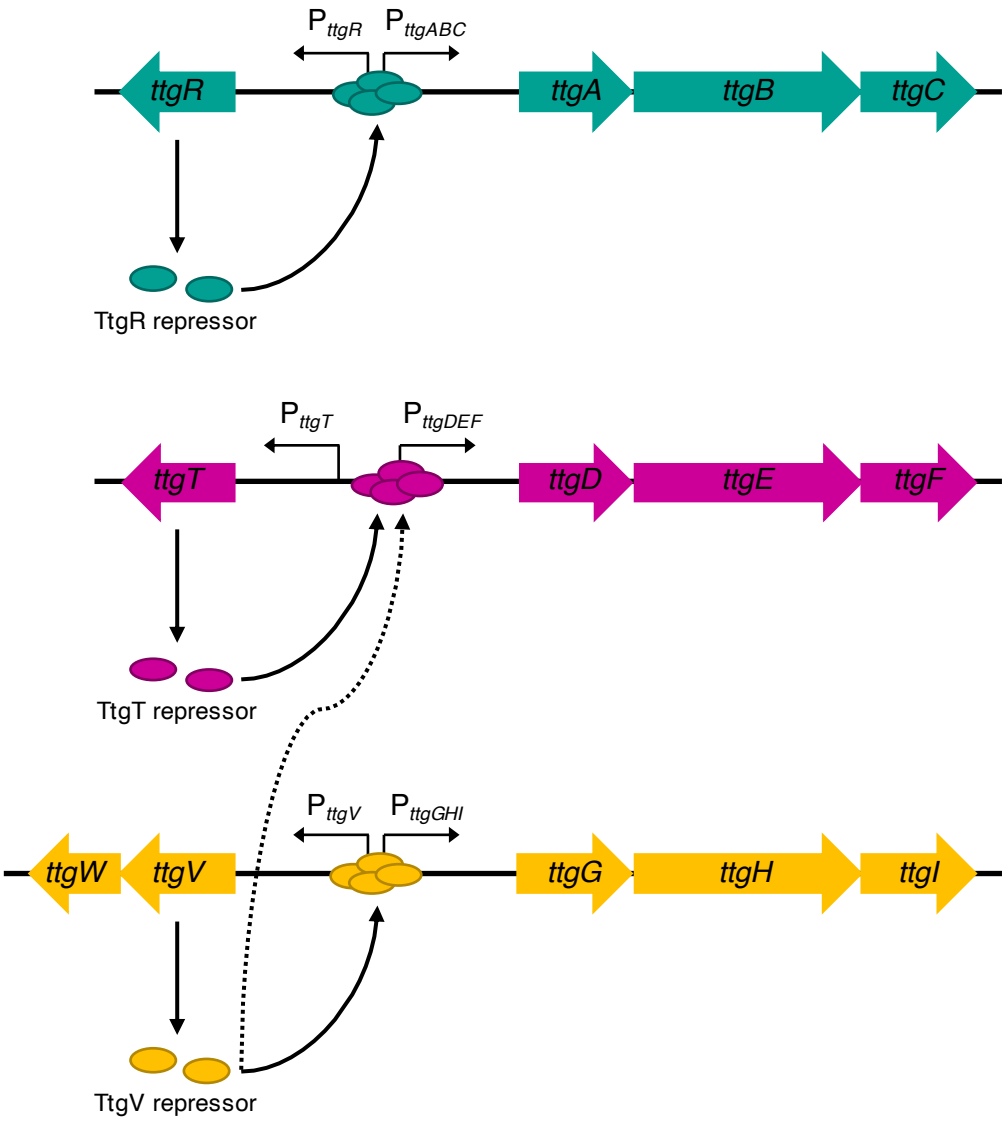

Figure 9: Genomic organization of *ttg* genes (modified from [46] with data from [171]). The TtgABC, TtgDEF and TtgGHI efflux systems are each encoded in one operon in the genome of *Pseudomonas putida* DOT-T1E. The genes for the repressors TtgR, TtgT and TtgV are arranged next to the efflux pump operons but are transcribed divergently. P: promoter.

A similar regulatory principle exists in the expression of the *ttgGHI* operon. Transcription is regulated by the tetrameric repressor TtgV, a member of the isocitrate lyase regulator (IclR) family. TtgV binds a broad spectrum of mono- and bicyclic aromatic substances as effectors. The gene of the TtgV regulator is also located adjacent to the *ttgGHI* genes and is transcribed divergently to them (Figure 9). Also, in this case, the promoter regions of both operons overlap, thus preventing the overexpression of the efflux pump genes. The TtgW protein, which is encoded together with TtgV in one operon, does not appear to have any influence on the expression of *ttgGHI*.[46,161,171]

In strains in which the *ttgGHI*-encoding pGRT1 megaplasmid is present, the expression of the *ttgDEF* operon is also controlled by the TtgV repressor. If the *ttgV* gene is not present, this task is performed by TtgT whose gene is located adjacent to the *ttgDEF* operon (Figure 9). TtgT also belongs to the IclR family and is 63 % identical to TtgV. However, since TtgV has a higher affinity for the operator regions of *ttgDEF* and *ttgGHI* and TtgV is produced in higher concentrations, the regulatory activity of TtgT is only apparent in the absence of the *ttgV* gene. In contrast to the *ttgR* and *ttgV* promoters, the *ttgT* promoter does not overlap with the *ttgDEF* promoter region. *ttgT* is constitutively expressed and transcription does not appear to be induced by the addition of solvents or inhibited by negative autoregulation. TtgT and TtgV show similar, but not identical, effector profiles.[46,171]
Although in cells possessing the *ttgV* gene, the *ttgDEF* and the *ttgGHI* operons are regulated by TtgV, both have different basal expression levels. Fillet *et al.* (2009) showed this effect to result from different binding affinities of the TtgV repressor for the two operator sequences which are only 40 % identical. Thereby, TtgV has a higher affinity for the *ttgDEF* operator and so the expression of the *ttgDEF* operon is repressed more strongly.[174]

In other *Pseudomonas putida* strains, for instance, S12, which do not contain the pGRT1 plasmid, TtgGHI homologous systems such as SrpABC (solvent resistant pump) were found.[155,175] The genes of the *srpABC* operon and the corresponding regulator operon *srpSR* are almost identical to those of the TtgGHI/TtgVW system[140,161,176] and expression is induced by solvents.[177] In *Pseudomonas aeruginosa* similar tolerance mechanisms have been described with the Mex efflux systems,[178–181] whereby, for example, the MexEF pump is involved in the export of butanol and formaldehyde.[46,182]

1.4 Aim of this thesis

Development of a bio-based economy, in which raw materials are recruited from renewable sources, could be a key step to the long-term preservation of our planet. The field of industrial biotechnology can help to provide natural materials in a sustainable way by creating microbial cell factories. While this vision has already become reality for some products, such as the production of insulin with genetically engineered bacteria[183] (see also Chapter 2), for others it is still a long way to an industrial application. Besides low product titers, one of the challenges in the development of microorganisms for industrial bio-production is reactant, intermediate and product toxicity. Therefore, when creating a microbial cell factory, it is essential not only to alter the metabolic pathways to generate the intended products at a high level, but also to enhance the strain's tolerance towards the reactants and products and, thereby, increase overall productivity. This challenge of product toxicity is relevant for monoterpenoid production. In the present work, this difficulty was to be addressed. To generate a biotechnological complement to fossil-resources-based chemical processes for industrial monoterpenoid production, it was aimed to create a starting point for the further development of a microbial cell factory based on the bacterium *Pseudomonas putida* KT2440.[106,184] For this purpose, a whole-cell biocatalysis to selectively oxyfunctionalize monoterpene hydrocarbons was to be developed which can use renewable industrial by-products and waste streams as raw material for monoterpenoid production (Figure 10). Furthermore, the inherent monoterpenoid tolerance of some *P. putida* strains[137] was to be investigated, improved and transferred to the KT2440 strain to aid monoterpenoid production with this organism.

As a model substance, the production of (-)-menthol should be addressed because of its industrial significance as an important flavor and fragrance compound and, also, as a medical component, and because it has an annual production volume of over 30,000 tons (see section 1.1.1 Menthol). One possible approach for (-)-menthol production could be a biotechnological(-chemical) two-step conversion, starting from (+)-limonene (Figure 10). (+)-Limonene is the most abundant monocyclic monoterpene in nature[185] and is produced as a by-product of the citrus industry because it is present in *Citrus* peel oil in concentrations of up to 70 - 98 % (v/v).[53,71] The first step of converting (+)-limonene into (-)-menthol requires an enzyme with a limonene-3-hydroxylase (L3H) activity that specifically catalyzes the hydroxylation of the third carbon atom of (+)-limonene to form (+)-*trans*-isopiperitenol. This can then be transformed further into (-)-menthol via a chemical hydrogenation or by a second enzymatic conversion step. The focus of this thesis was on the development of an *in vivo* process for limonene-3-hydroxylation, while the second step, the hydrogenation from (+)-*trans*-isopiperitenol to (-)-menthol, was not investigated.

In order to develop the described cell factory basis for monoterpene biotransformation, the thesis project was divided into three parts. In the first part, enzymes were to be identified that can catalyze the intended limonene-3-hydroxylation reaction. In the second part, an increase in the tolerance of the selected *P.* putida strain KT2440 towards monoterpenes and their monoterpenoid derivatives should be attempted. In the third part, the identified L3H enzymes were to be expressed in the improved *P. putida* KT2440 strain to create a whole-cell biocatalyst for the first reaction step of a two-step (-)-menthol production, starting from the by-product of citrus fruit processing industry (+)-limonene.

Part 1 – Identification and characterization of limonene-3-hydroxylase enzymes

For implementation of the biotransformation process, suitable enzyme candidates catalyzing the desired reactions have to be identified. It is described in the literature that a limonene-3-hydroxylation reaction can be catalyzed by specific enzymes from *Mentha* plants. In the peppermint plant, *Mentha x piperita*, a native producer of menthol, the second enzyme of the menthol pathway, isoenzymes CYP71D13 (PM17) and CYP71D15 (PM2), can catalyze the limonene-3-hydroxylation with a high regio- and stereoselectivity.[58] Its natural substrate is (-)-limonene but it can also hydroxylate (+)-limonene, the intended biotransformation substrate. However, this plant enzyme is difficult to express in a functional form in microbes for biotechnological purposes.[186,187]

In addition, in the last few years variants of bacterial enzymes have been described which can hydroxylate (+)-limonene to (+)-*trans*-isopiperitenol, but often such engineered enzymes, whether cytochrome P450 monooxygenases or others, catalyze several other side reactions.[102]

Apart from engineering known enzymes to conduct new reactions, another approach is to search in nature's diversity for enzymes that can catalyze the intended reaction natively with high selectivity. This strategy was followed in this work.

While several microorganisms are known to convert limonene into, for instance, α-terpineol, carveol or perilla alcohol,[188,189] only one example of a naturally occurring limonene-3-hydroxylation ability has been published. In 1998, van Dyk and colleagues described that the black yeast-like fungus *Hormonema* sp. UOFS Y-0067 can oxidize (+)-limonene into *trans*-isopiperitenol, with product concentrations of up to 0.5 g L^{-1} (ca. 3 mM, 31 % yield) after 12 h.[190] However, no reproducible production process could be established with the fungus and the authors stated that “it is unlikely that it will ever be possible to base a commercial biotransformation process on an organism like this *Hormonema* sp.”[190] In addition, in this study, the responsible enzyme remained unknown.

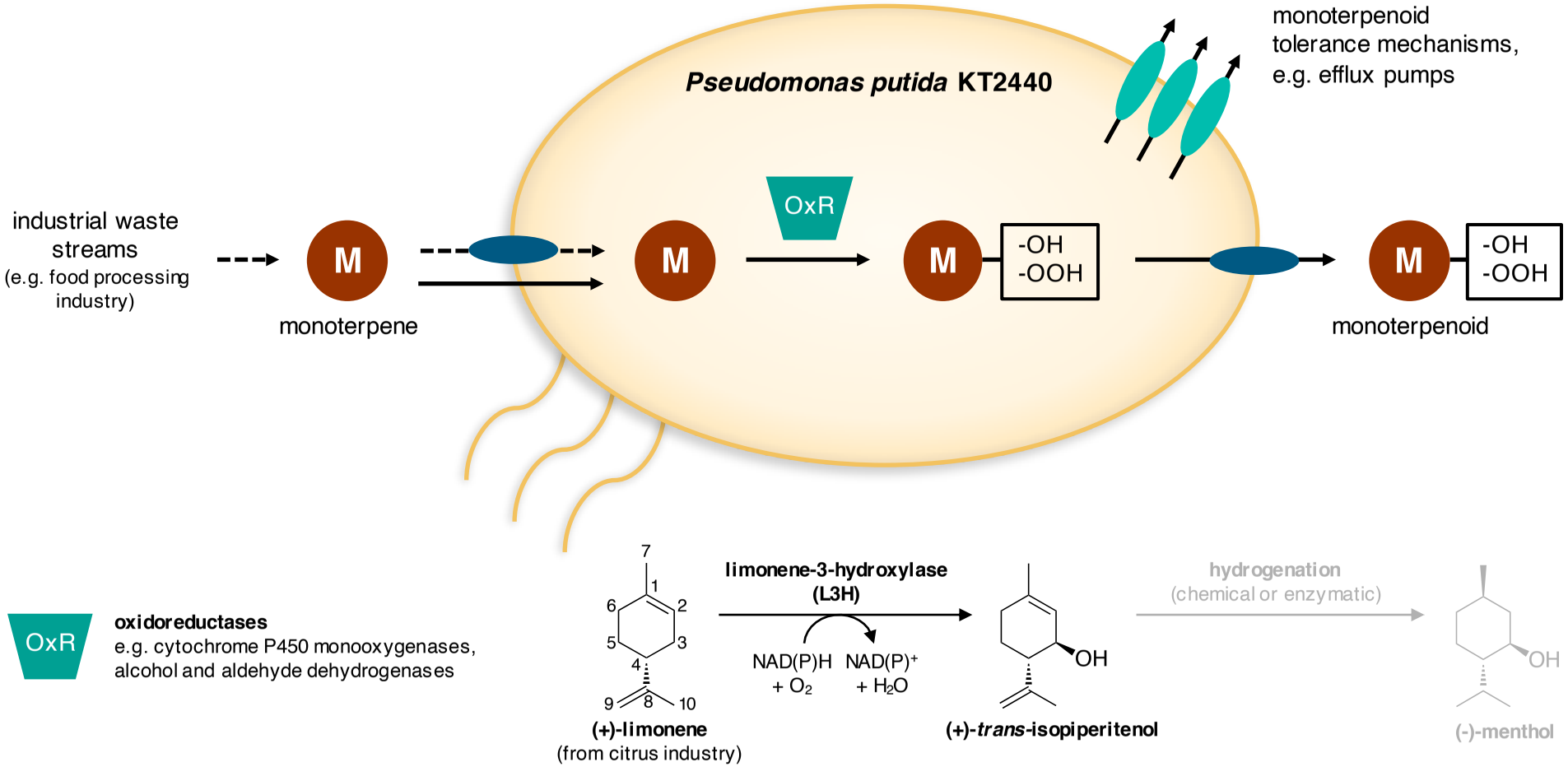

Figure 10: Project overview. The aim of this thesis was to create a starting point for the further development of a cell factory suitable for monoterpenoid production based on the bacterium *Pseudomonas putida* KT2440. Since many monoterpenoids are toxic for living cells, the tolerance of the selected host organism towards monoterpenoids should be increased. As model process, the conversion of (+)-limonene into (-)-menthol was chosen. (+)-Limonene can be obtained as a by-product from citrus processing industry. In particular, the first step, the *in vivo* biotransformation of (+)-limonene into the intermediate product (+)-*trans*-isopiperitenol, was to be realized. M: monoterpene, M-OH: monoterpene alcohol, M-OOH: monoterpene acid.

Based on these findings, apart from *Hormonema* sp. UOFS Y-0067, further *Hormonema* species and other fungi, such as *Aureobasidium pullulans,* were identified that can also catalyze the intended limonene-3-hydroxylation (see Chapter 3). *H. carpetanum* and *A. pullulans* are ubiquitous black yeast-like fungi that can be found on a wide range of plant species, e.g. conifers, apple, grape, cucumber and green beans, without causing any symptoms of disease.[191–193] On the contrary, *A. pullulans* is even used for the biological control of plant diseases.[194–196] In addition, *A. pullulans* has been investigated for other purposes for several years, including the production of enzymes or polysaccharides, especially pullulan, and the degradation of xenobiotic substances.[192,194,197,198]

Several attempts have been undertaken to establish a (+)-*trans*-isopiperitenol production process with *Hormonema carpetanum*, however, although many efforts have been made to optimize cultivation and biotransformation conditions, no reliable production process could be developed (M.M.W. Etschmann, unpublished data). In addition, it was found that limonene and isopiperitenol are toxic for the fungus itself.

Therefore, in the present work, it was aimed to identify the corresponding fungal enzyme for heterologous expression in the intended *P. putida* strain. In former experiments, it was attempted to identify the respective gene by measuring RNA expression alteration after limonene addition (M.M.W. Etschmann, unpublished data). Furthermore, a mutant library of *A. pullulans* was prepared via UV mutagenesis and mutants were screened for increased or decreased limonene-3-hydroxylation activity in order to localize the corresponding gene via the mutation (I. Strobel, unpublished data). However, these attempts were unsuccessful.

Therefore, in this work, potential limonene-3-hydroxylating enzymes should be identified in fungal genomes and categorized into different groups using bioinformatic methods. By combining genetics/molecular biology and analytical techniques, candidate enzymes from these groups should then be tested by heterologous expression in yeast. If positive candidates are identified in this way, they can then be characterized further for later expression in *P. putida.* Since *Aureobasidium pullulans* not only forms hyphae but grows yeast-like in liquid culture medium,[194] the investigations were initiated with this fungus. For procedures and results on this section, see Chapter 3.

Part 2 – Development of a monoterpenoid-tolerant production organism

In order to develop *P. putida* KT2440 into a suitable host for the further development of a cell factory for monoterpenoid production, the natural tolerance of this organism towards monoterpenoids was required to be increased.

The mechanisms underlying the solvent tolerance of some Gram-negative bacteria and *Pseudomonas,* in particular, have already been considered in many studies (see section 1.3

Solvent tolerance). In these cases, however, the investigations mostly referred to substances such as toluene or butanol (summarized, for example, in [46,140]) and less so to monoterpenes and monoterpenoids. Although it has long been known that essential oils and their monoterpenoid components have an antimicrobial effect, it is still largely unknown as to which of the different solvent tolerance mechanisms are mainly responsible for the high monoterpenoid resistance of microorganisms, such as some *Pseudomonas putida* strains. However, for the development of cell factories, it is essential to know the related tolerance mechanisms and their potential specificities. Therefore, in this thesis, it was to be investigated as to which of the general solvent resistance mechanisms contribute to the monoterpenoid tolerance of highly tolerant *P. putida* strains, such as *P. putida* GS1. Subsequently, these mechanisms were to be improved and transferred to the industrially usable production strain *P. putida* KT2440. For procedures and results on this section, see Chapters 4 and 5.

Part 3 – Expression of L3H enzymes in monoterpenoid-tolerant bacteria

Following the identification of fungal limonene-3-hydroxylase enzymes and the development of a *P. putida* strain with improved monoterpenoid-tolerance, both parts would then be combined, to create the basis for the further development of a microbial cell factory for monoterpenoid production. For this purpose, a vector system for heterologous gene expression in *P. putida* was to be developed which does not affect bacterial growth. The expression of the fungal enzymes was to be investigated and optimized initially in *E. coli* as an established prokaryotic expression organism. Subsequently, the optimized gene sequence would be transferred into the tolerance-improved *P. putida* KT2440 strain. For procedures and results on this section, see Chapters 6 and 7.

Chapter 2 - Microbial cell factories for the production of terpenoid flavor and fragrance compounds

Florence M. Schempp, Laura Drummond, Markus Buchhaupt, Jens Schrader

Journal of Agricultural and Food Chemistry, 2018, 66 (10), 2247-2258
DOI: 10.1021/acs.jafc.7b00473

Type: review article
Status: published

Summary:
Terpenoid flavor and fragrance compounds are of great interest to the aroma industry. Microbial production offers alternative, sustainable access to terpenoids independent of natural sources. Genetically modified microorganisms can be used to synthesize terpenes and terpenoids from cheap and renewable resources.
Due to its modular architecture, terpene(oid) biosynthesis is particularly well suited for the concept of a microbial cell factory: a platform host designed for high flux towards the central C_5 prenyl diphosphate precursors allows the production of a wide range of target terpenes and terpenoids by varying the pathway modules that convert the C_5 intermediates into the product of interest.
The following chapter presents terpene(oid) flavor and fragrance compounds marketed or under development by biotech and aroma companies and discusses the specificities of the aroma market. In addition, an overview of the microbial biosynthesis of terpenes and terpenoids is given. Furthermore, key strategies and advances in engineering of microbes to become efficient terpene(oid) producers are described.

Declaration of author contributions to the publication:

Microbial Cell Factories for the Production of Terpenoid Flavor and Fragrance Compounds (Review)

Status: published
Name of journal: Journal of Agricultural and Food Chemistry

Contributing authors: **F. M. Schempp** (Doctoral candidate), L. Drummond, J. Schrader, M. Buchhaupt

What are the contributions of the doctoral candidate and his co-authors?

(1) Concept and design

F. M. Schempp	**35 %**
L. Drummond	20 %
M. Buchhaupt	5 %
J. Schrader	40 %

(2) Conducting tests and experiments

n/a

(3) Compilation of literature and figures

F. M. Schempp	**50 %**	**literature collection and preparation of figures and tables**
L. Drummond	30 %	literature collection and preparation of figures
J. Schrader	20 %	literature collection

(4) Analysis and interpretation of data

F. M. Schempp	**50 %**
L. Drummond	20 %
M. Buchhaupt	5 %
J. Schrader	25 %

(5) Drafting of manuscript

F. M. Schempp	**50 %**
L. Drummond	25 %
M. Buchhaupt	5 %
J. Schrader	20 %

JOURNAL OF AGRICULTURAL AND FOOD CHEMISTRY

Review

pubs.acs.org/JAFC

Microbial Cell Factories for the Production of Terpenoid Flavor and Fragrance Compounds

Florence M. Schempp, Laura Drummond, Markus Buchhaupt, and Jens Schrader*

DECHEMA-Forschungsinstitut, Industrial Biotechnology, Theodor-Heuss-Allee 25, 60486 Frankfurt am Main, Germany

ABSTRACT: Terpenoid flavor and fragrance compounds are of high interest to the aroma industry. Microbial production offers an alternative sustainable access to the desired terpenoids independent of natural sources. Genetically engineered microorganisms can be used to synthesize terpenoids from cheap and renewable resources. Due to its modular architecture, terpenoid biosynthesis is especially well suited for the microbial cell factory concept: a platform host engineered for a high flux toward the central C_5 prenyl diphosphate precursors enables the production of a broad range of target terpenoids just by varying the pathway modules converting the C_5 intermediates to the product of interest. In this review typical terpenoid flavor and fragrance compounds marketed or under development by biotech and aroma companies are given, and the specificities of the aroma market are discussed. The main part of this work focuses on key strategies and recent advances to engineer microbes to become efficient terpenoid producers.

KEYWORDS: *aroma, biotechnology, metabolic engineering, microbial cell factory, terpenoids*

INTRODUCTION

Terpenoids (to improve readability, in this work the term "terpenoid" is used for hydrocarbon terpenes and their oxygen-containing derivatives in contrast to the IUPAC definition) are the largest class of natural products ubiquitously found in all kingdoms of life. They show a broad range of biological functions in intra- and intercellular processes, from cell integrity to energy supply, and also as hormones and mediators of antagonistic and mutualistic interactions among organisms.[1,2] Plants, for instance, produce small volatile terpenoids to attract pollinators or as natural defense chemicals against herbivores or nonvolatile tetraterpenoids (carotenoids) as accessory light-harvesting pigments and protective antioxidants against photodamage. Another example is cholesterol, which is made by animal cells as an important cell membrane component and precursor for steroid biosynthesis. On the basis of the diversity of chemical structures and biological functions of terpenoids, a broad spectrum of commercial applications can be anticipated. Although in some cases the industrial use is still on research and development (R&D) or pilot-scale level, such as the production of terpenoid biofuels, many other products containing terpenoids are already on the market. These products range from pharmaceuticals, such as artemisinin (antimalaria) or taxol (anticancer), to carotenoids as food and feed colorants to monoterpenoids used as natural organic solvents in household cleaners, such as limonene. Valuable properties, such as antiseptic and antibiotic effects, have made terpenoid-rich essential oils universally employed remedies and foodpreservatives from ancient times until today. The most prominent application of terpenoids up to now has been their use as flavors and fragrances, ranging from complex natural extracts and essential oils to chemically synthesized key impact compounds for aroma and scent compositions.

However, many of the structurally more complex terpenoids cannot be chemically synthesized in an economic way. Furthermore, many of these compounds are not extractable from natural sources in a sustainable way anymore, either due to their low concentrations in their raw material or because the natural sources are constantly ceasing. Examples of products from endangered species are the coveted essential oils of agarwood and sandalwood trees.[3−6]

Therefore, microbial production of terpenoids provides an attractive alternative, taking advantage of the often pronounced regio- and stereoselectivity of enzymatic reactions. Two different types can be distinguished: (a) de novo biosynthesis starting from simple carbon sources such as glycerol and (b) biotransformation of a precursor molecule into a structurally related product by a limited number of enzymatic steps with whole cells or isolated enzymes.[4,7] A biotransformation is especially favored if closely related precursor molecules are abundantly available as cheap starting material, for example, limonene or the pinenes.[8,9]

With the advances in biotechnology made in the past decades, new synthetic routes to flavors and fragrances including terpenoids have been developed and are currently in the R&D pipeline of different companies (see Table 1). These approaches rely on the use of engineered microbes to produce flavors and fragrances from renewable resources in defined and reproducible bioprocesses at high yields. Modern -omics technologies together with advanced genetic engineering tools allow fast deciphering of flavor and fragrance biosyntheses and their reassembling as synthetic pathways in tailored production host strains. Because terpenoid biosynthesis relies on a universal metabolic pathway scheme from which the stunning diversity of terpenoids is derived through specific

Special Issue: 11th Wartburg Symposium on Flavor Chemistry and Biology

Received: January 31, 2017
Revised: April 5, 2017
Accepted: April 5, 2017
Published: April 18, 2017

DOI: 10.1021/acs.jafc.7b00473
J. Agric. Food Chem. 2018, 66, 2247−2258

Table 1. Industrial Terpenoid Flavor and Fragrance Compounds Produced by Microbial Cell Factory Approaches, The Corresponding Companies and Their Current Status of Realization

terpenoid/product	odor/taste[113,114]	natural source[114]	microbe	company	current status	comments/references
β-farnesene, other undisclosed terpenoids			yeast	Amyris	marketed	the hydrogenated derivative farnesane is intended to be used as drop-in biofuel; β-farnesene may also be used by the aroma industry as raw material to synthesize other sesquiterpenoid flavors and fragrances; the terpenoid overproducing platform yeast is used to produce an array of so far undisclosed terpenoids for different aroma companies[115]
valencene	orange, citrus	orange peel	yeast	Evolva	marketed	116
			Rhodobacter sphaeroides	Isobionics	marketed	fermentative valencene is also used as precursor for oxidation to nootkatone, which is also marketed[82,117−119]
nootkatone	grapefruit, orange, citrus, bitter	grapefruit oil	*Rhodobacter sphaeroides*	Isobionics	marketed	
			yeast	Evolva	marketed	nootkatone, produced by fermentation of yeast, is offered as a natural flavor and fragrance compound and also as potential natural insect repellent[120]
α- and β-santalol	woody, sweet, warm, balsamic	sandalwood oil: heartwood of *Santalum album*	yeast	Evolva	under development	key compounds of sandalwood oil[121] (also announced to be under development by Isobionics[122])
agarwood compounds (agarwood oil consists of >150 compounds, mostly sesquiterpenoids, chromones, and volatile aromatic compounds[6])	woody, balsamic, leathery, smoky	heartwood of agarwood trees (*Aquilaria* sp. and *Gyrinops* sp.) formed as immune system reaction against wounding and infection with fungi or insects	yeast	Evolva	exploratory phase	123
patchouli oil (major component: patchoulol)	woody, balsamic, camphorous	leaves of *Pogistemon cablin*	yeast	Firmenich	marketed	partnership with Amyris; marketed as "soft, clean version of patchouli without the earthy, leathery and rubbery notes found in the natural oil" under the name Clearwood[124,125] (also announced to be under development by Isobionics[126])
sclareol, precursor to Ambrox	sclareol: sweet, balsamic, mellow, amber, herbal	sclareol: leaves of clary sage (*Salvia sclarea*)	yeast or *E. coli*	Firmenich	marketed	marketed as produced by "white biotechnology coupled with green chemistry"; key is fermentative production of a diterpenoid ambrox precursor, presumably sclareol; production host cannot be stated, presumably either *E. coli* (cf. ref 46) or yeast (cf. ref 127)[128]
	Ambrox: ambergris, sweet, woody, pine, cedar, tea	Ambergris: produced in the digestive system of sperm whales				
stevio glycosides; especially rebaudiosides D and M	sweet	leaves of the plant species *Stevia rebaudiana*	yeast	Cargill	marketed by Cargill as EverSweet	partnership with Evolva; marketed under the name EverSweet as fermentation-based stevia sweeteners with Reb D and M, which improve taste characteristics compared to plant-based stevia sweetener[129]

DOI: 10.1021/acs.jafc.7b00473
J. Agric. Food Chem. 2018, 66, 2247−2258

Journal of Agricultural and Food Chemistry Review

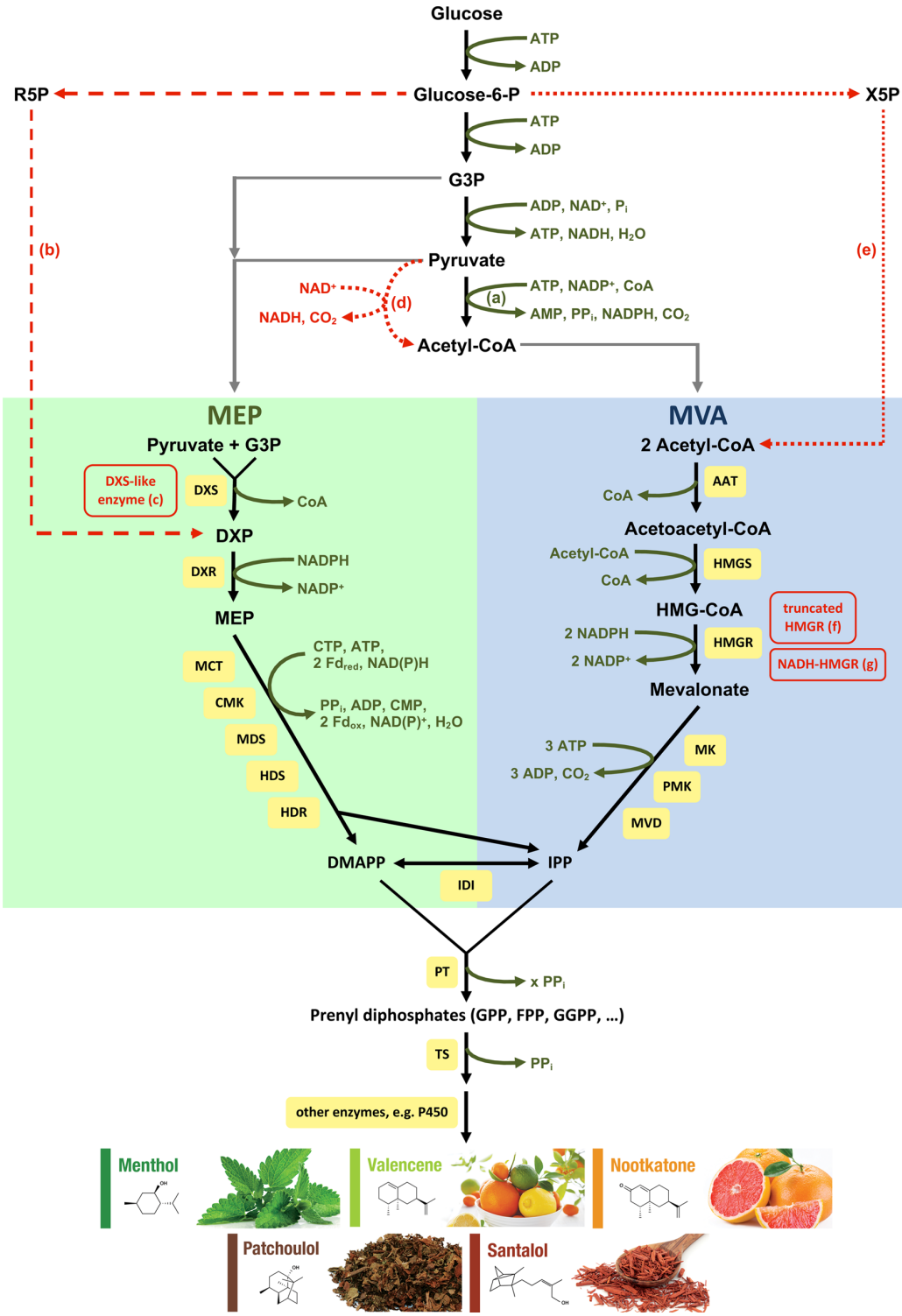

Figure 1. Terpenoid biosynthesis: microbial synthesis of terpenoids via the MVA or MEP pathway starting from glucose (simplified). Black, central metabolic pathways; green, cofactors (stoichiometry only valid for MEP and MVA pathway); yellow boxes, enzymes; red, approaches for engineering flux through MEP and MVA pathway. (a) Native generation of cytosolic acetyl-CoA in *S. cerevisiae* (PDH bypass) (via pyruvate decarboxylase, acetaldehyde dehydrogenase, and acetyl-CoA synthetase); (b) shunt pathway for DXS production by Kirby et al. (via ribulose 5-phosphate converted to DXS by engineered enzymes;[53,54] (c) engineered enzyme catalyzing DXS reaction;[54] (d) shunt to PDH bybass by Meadows et al. (via heterologous aldehyde dehydrogenase (acylating));[51] (e) bypass to central carbon metabolism by Meadows et al. (via pentose phosphate pathway and heterologous phosphoketolase and phosphotransacetylase);[51] (f) Donald et al. and Polakowski et al.;[42,43] (g) cofactor engineered HMGR enzyme[3] (approach also used by Meadows et al.[51]). Metabolites: G3P, D-glyceraldehyde 3-phosphate; R5P, ribulose 5-phosphate; X5P, xylulose 5-phosphate; IPP, isopentenyl diphosphate; DMAPP, dimethylallyl diphosphate; DXP, 1-deoxy-D-xylulose 5-phosphate; MEP, 2-C-methyl-D-erythritol

DOI: 10.1021/acs.jafc.7b00473
J. Agric. Food Chem. 2018, 66, 2247−2258

Figure 1. continued

4-phosphate; HMG-CoA, 3-hydroxy-3-methylglutaryl-CoA; FPP, farnesyl diphosphate; GPP, geranyl diphosphate; GGPP, geranylgeranyl diphosphate. Enzymes: DXS, DXP synthase; DXR, DXP reductoisomerase; MCT, MEP cytidyltransferase; CMK, 4-(cytidine 5-diphospho)-2-*C*-methyl-D-erythritol kinase; MDS, 2-*C*-methyl-D-erythritol 2,4-cyclodiphosphate synthase; HDS, 4-hydroxy-3-methylbut-2-enyl diphosphate synthase; HDR, 4-hydroxy-3-methylbut-2-enyl diphosphate reductase; AAT, acetoacetyl-CoA thiolase; HMGS, HMG-CoA synthase; HMGR, HMG-CoA reductase; MK, mevalonate kinase; PMK, 5-phosphomevalonate kinase; MVD, 5-diphosphomevalonate decarboxylase; IDI, IPP isomerase; PT, prenyltransferases; TS, terpene synthases.

enzymatic functionalization reactions, it represents the ideal scenario for a "microbial cell factory" approach: once a host strain with a high metabolic flux to the terpenoid intermediates has been designed, the introduction of different additional pathway modules gives access to a range of different products based on the same microbial platform technology.

The main scope of this review is to describe key strategies and recent advances to engineer microbes for the de novo production of terpenoid flavor and fragrance compounds. Biotransformation of natural terpenoid precursors, for example, from fruits and vegetables, is another area of intense biotech R&D activities[10,11] but outside the scope of this review . For further information about this topic, the reader is referred to other publications.[4,8,11−15]

SPECIFICS OF THE AROMA MARKET: WHAT DOES IT MEAN FOR BIOTECHNOLOGY?

According to U.S. and European Union (EU) flavor regulations, the use of microorganisms to convert natural raw materials into products leads to aroma compounds that can be described as natural, if these compounds are known to be present as components of natural raw materials.[4] This labeling is especially important to the flavor market because the consumer is willing to pay higher prices for food containing natural ingredients. In contrast, for the fragrance market naturalness plays a minor role, but price dictates the business. However, the consumer's acceptance seems still to be low for added food ingredients produced with genetically engineered microbes. This is despite the fact that the underlying bioprocesses, for example, the conversion of glucose from starch-containing raw material into flavors, is a classical fermentation and the recombinant cells are not present in the product anymore, which is separated from the fermentation broth. In this respect, flavors from engineered microbes are essentially produced by the same principle as are recombinant enzymes used in food processing,[16,17] for example, recombinant chymosin in the dairy industry.[18,19] Thus, sustained information and education based on sound facts is needed in parallel with the development of novel biotechnological processes for aroma compounds to overcome these hurdles built by a negative public perception. In contrast, for scents and odorants, for example, those used in household consumables, public perception may even help in introducing biotechnological processes, which can be positively marketed as being "green", environmentally friendly, and based on renewable resources compared to classical chemical synthesis often starting from fossil raw materials. However, most of the biotechnologically produced fragrance compounds have to be cheap and cost competitive with their chemically synthesized counterparts, because in many typical applications such as their use in household cleaners or detergents, there is no added value because of the "natural" label. In contrast, their natural counterparts used as flavor ingredients usually range up to a factor of 10 in price or even higher.[20] For instance, natural vanillin produced by microbial conversion of natural precursors such as ferulic acid, is sold at a market price of several hundreds of U.S. dollars per kilogram, whereas synthetic vanillin costs only about U.S. $16/kg.[21]

Another characteristic of flavors and fragrances is that the market volume for a single compound is usually low; that is, for most of the target molecules it is rather in the kilogram or at maximum lower tons per year range worldwide. Thus, total costs to install a new biotechnological process for a single aroma compound will easily exceed return on investment for a long time after having established the process. In this respect, the platform idea of microbial cell factories, that is, producing an array of structurally related compounds based on the same microbial technology, as is the case for terpenoids, is especially attractive. As an example, the U.S. company Amyris uses an extensively re-engineered yeast strain to produce β-farnesene and other terpenoids in partnership with aroma companies.[22]

MICROBIAL BIOSYNTHESIS OF TERPENOIDS

The natural synthesis of terpenoids starts with the universal precursors isopentenyl diphosphate (IPP) and dimethylallyl diphosphate (DMAPP), which can be synthesized through two different pathways, the mevalonate pathway (MVA) and the 2-*C*-methyl-D-erythritol-4-phosphate pathway (MEP), also known as the DXP or nonmevalonate pathway. These pathways can be found in distinct organisms, the MVA being present mainly in eukaryotes and archaea and the MEP typically in most bacteria and plant plastids.[23]

The mevalonate pathway starts with the condensation of acetyl-CoA molecules to form 3-hydroxy-3-methylglutaryl-CoA (HMG-CoA) (Figure 1), followed by a reduction step that generates mevalonate. After three more reactions that involve ATP-dependent phosphorylation and a decarboxylation step, IPP is produced, which can then be further isomerized to DMAPP.[24]

The non-mevalonate pathway starts with the condensation of G3P (D-glyceraldehyde-3-phosphate) and pyruvate. The product then undergoes a reductive isomerization reaction to form 2-*C*-methyl-D-erythritol-4-phosphate. After a subsequent coupling with cytidine triphosphate (CTP), a phosphorylation, cyclization, and reductive dehydration, both IPP and DMAPP are formed (Figure 1).[25,26]

Following the generation of the C_5 precursors, one molecule of DMAPP is condensed with one or more molecules of IPP through the action of prenyltransferases, resulting in prenyl diphosphate molecules of various chain lengths.[24] These prenyl diphosphate intermediates are further converted by terpene synthases to form different hydrocarbons and alcohols via ionization of the prenyl diphosphates, rearrangement and often cyclization reactions, and finally deprotonation or water capture.[24] Then, other enzymes, such as cytochrome P450 monooxygenases[11,24,27] but also reductases, dehydrogenases, or various classes of transferases,[28] modify this skeleton to form a broad range of linear or cyclic variants.[29]

DOI: 10.1021/acs.jafc.7b00473
J. Agric. Food Chem. 2018, 66, 2247−2258

Journal of Agricultural and Food Chemistry Review

Scheme 1. Overall Stoichiometry for Synthesizing 1 mol of IPP from Glucose, via Glycolysis and (a) the MEP Pathway (in *E. coli*) or (b) the MVA Pathway (in *S. cerevisiae*) (Adapted from Reference 48)[a]

(a) MEP (*E. coli*)
Glucose + 2 ATP + 3 NADPH + NAD^+ → IPP + CO_2 + 2 ADP + 3 $NADP^+$ + NADH
IPP/Glucose = 0.83 C-mol/C-mol

(b) MVA (*S. cerevisiae*)
1.5 Glucose + 3 ATP + $NADP^+$ + 3 NAD^+ → IPP + 4 CO_2 + 3 AMP + NADPH + 3 NADH
IPP/Glucose = 0.56 C-mol/C-mol

[a]Maximal IPP yields (IPP/glucose) based on carbon stoichiometry.

The resulting terpenoids are classified according to their number of isoprene units (C_5) used: hemiterpenoids (C_5), monoterpenoids (C_{10}), sesquiterpenoids (C_{15}), diterpenoids (C_{20}), sesterterpenoids (C_{25}), triterpenoids (C_{30}), tetraterpenoids (C_{40}), and polyterpenoids with a larger number of isoprene units.[30] In addition, there are substances with mixed origin, such as meroterpenoids, indole diterpenoids, or prenylated aromatic products, that are assembled from a terpenoid and a molecule of another substance class.[31]

METABOLIC ENGINEERING TOWARD INDUSTRIAL PRODUCTION

Metabolic engineering is a process to optimize metabolic pathways and their regulatory networks within a cell for production of a target molecule. The metabolic pathways can be native to the production strain or heterologously introduced.[32] Metabolic engineering has a distinct industrial dimension, because it means not only to combine genes and pathways to produce a product but also to optimize titer, rate/productivity, and yield to develop a cost-effective process.[33,34] For such processes, the production strains usually have to be engineered to maximize the amount of product produced from a given amount of substrate (yield) and the volumetric productivity (also known as "space−time yield"). Therefore, the carbon flux from the educt to the target compound has to be maximized, whereas the drain of carbon into other pathways, including the formation of biomass during the production phase, should be minimized.

In the recent decades, many different ways to engineer microorganisms for industrial production processes have been developed. Common strategies of metabolic engineering, using genetic and protein engineering tools, have been reviewed in many publications.[28,33−39]

In general, for process design, after the selection of a target substance and an appropriate metabolic pathway, a production organism suitable for industrial production and genetic manipulation has to be chosen. After introduction and optimization of the pathway enabling synthesis of the desired product, bioprocess engineering and downstream processing should also be considered.

The generation of efficient terpenoid production strains is currently based on several complementary approaches. Engineering attempts can be carried out at different levels, for example, increasing endogenous precursor supply, changing cofactor requirements, eliminating bottlenecks and competitive reactions, and alleviating toxic effects of intermediates and products and genetic and protein engineering.[28,36,40]

Increasing Endogenous Precursor Supply. Precursor availability in microbes is a key limiting factor for engineering,[41] and modifications of the central carbon metabolism are necessary to redirect the carbon flux to the terpenoid pathway. Attempts to improve terpenoid production by microbes usually rely on maximization of the supply of precursors DMAPP and IPP, formed by one of the two isoprenoid biosynthetic pathways, MVA and MEP. Both pathways are heavily regulated at multiple levels, and there are several possible connections of the isoprenoid pathways to other metabolic routes by delivery and export of carbon precursors.[24]

In *Saccharomyces cerevisiae*, efforts have been made to engineer the MVA pathway. A successful example was the overexpression of a truncated version of 3-hydroxy-3-methylglutaryl-coenzyme A reductase (HMGR1) that did not have feedback inhibition by farnesyl diphosphate (FPP).[42,43] This modified enzyme was, for example, applied to engineer a yeast strain for santalene production, the metabolic precursor of santalol.[44,45]

Introduction of a mevalonate pathway into *Escherichia coli* is widely used to create platform strains for terpenoid production, for example, for the de novo production of sclareol.[46] The introduction of MVA has been more successful than engineering the MEP in *E. coli* so far because it overcomes the native regulation mechanisms of the cell.[47] When the efficiencies of these two pathways are compared, it is possible to find some interesting differences, which could be the source of ideas for the next steps in metabolic engineering of terpenoid production strains. When begun from each particular precursor (acetyl-CoA for the MVA pathway; G3P and pyruvate for the MEP pathway), the stoichiometries of both pathways are virtually the same. However, when the background metabolism of the host is analyzed, some differences are observed regarding the synthesis of precursors. This accounts for the overall energetics of terpenoid production and must be considered in the evaluation of different strategies for engineering microbes and the analysis of pathway efficiency.

When the stoichiometry of the MEP pathway in its natural host, *E. coli*, is analyzed, there is higher carbon efficiency, because only 1 mol of CO_2 is lost per mole of glucose. However, when compared to the MVA pathway in its natural host, *S. cerevisiae*, the former is not as efficient in terms of energetics. The MVA pathway is more energy efficient, because it has a net gain of NADPH and NADH when the central metabolism of the host is taken into account (see Scheme 1). Starting with glucose as carbon source, the production of the substrate acetyl-CoA entails the loss of CO_2, whereas for the production of the substrates G3P and pyruvate, no carbon atoms are lost. The MEP pathway is more efficient in terms of carbon utilization, when the energetics are left aside, because it needs only 1 mol of glucose for the production of 1 mol of IPP, whereas the MVA needs 1.5 mol of glucose per mole of IPP (Scheme 1).

When a heterologous pathway is introduced into an organism, it changes the overall stoichiometry of the reaction from glucose to terpenoid precursors. Studies using in silico models are a helpful tool to calculate the resulting balance between compounds. When engineered strains of the two most widely used organisms are compared, the calculated maximal

DOI: 10.1021/acs.jafc.7b00473
J. Agric. Food Chem. 2018, 66, 2247−2258

IPP yield for *E. coli* bearing both MVA and MEP pathways is higher than for *S. cerevisiae* bearing the same two pathways. This value for *E. coli* is even higher when glycerol is used as carbon source.[48]

An interesting synergistic effect has been found between the MEP and the MVA pathway when both of them were simultaneously engineered in *E. coli* for enhanced isoprene production.[49] The authors demonstrated that a synergistic effect between the MEP pathway and the MVA pathway was responsible for an improvement in isoprene productivity and yield compared to strains overexpressing each pathway separately. This synergy is believed to be a consequence of the complementary nature of these pathways regarding its cofactors, because the synthesis of one IPP molecule from glucose through the MVA pathway has a net gain of NADPH, and this could lead to ATP formation via respiration. The MEP pathway has a high demand for reducing power and ATP. Another reason for this synergic effect would be the reduction of intracellular amounts of downstream metabolites that could cause feedback inhibition.[49]

The mevalonate kinase from MVA is one of the pathway's main bottlenecks because it is subject to inhibition by downstream substrates.[50] The carbon flow through the MEP pathway reduces intracellular amounts of specific metabolites from the terpenoid biosynthesis and thus has a positive effect on lower MVA pathway enzymes.

Therefore, although it is a tough task to indicate which pathway is overall the most efficient one, the concept of synergy, and the engineering of two or more pathways simultaneously, is a new approach for designing terpenoid biosynthesis production processes toward optimal efficiency.

The loss of CO_2 during the production of acetyl-CoA from glucose was elegantly circumvented by Meadows and co-workers[51] through the insertion of two non-native steps on yeast acetyl-CoA metabolism (see also Figure 1). By rerouting the synthesis of acetyl-CoA via xylulose-5-phosphate they were able to avoid a step that entails loss of CO_2, thus making the pathway more carbon efficient. The carbon flux toward terpenoid products is therefore increased; however, the lack of carbon loss through this step comes also with a lack of ATP and NADH production. The addition of an acetaldehyde dehydrogenase balanced this energetic deficiency, avoiding the use of ATP in the PDH (pyruvate dehydrogenase) bypass. This enzyme generates NADH instead of NADPH, a switch of cofactors that is compensatory. The two new bypasses redistribute glucose flux, balancing each other and reducing carbon loss and excess production of NAD(P)H, thus reducing oxygen demand via aerobic respiration. A strain containing four new pathway components showed improvements on farnesene production (21% in yield and 77% in productivity) when compared with the previous generation[52] and reached a remarkable product titer of >130 g/L broth, or 15% by volume.[51] In addition, changes in the metabolism reduced oxygen demand by 75%.

Also with regard to the MEP pathway, a shunt pathway was constructed to generate the first intermediate DXP out of the pentose phosphate ribulose 5-phosphate, for bisabolene production.[53] In this way the loss of one carbon as CO_2, which occurs during the generation of DXP by condensation of pyruvate and G3P, was circumvented. Other studies revealed that enzymes unrelated to isoprenoid biosynthesis, once mutated, can produce pathway intermediates, such as DXP.[54] In these examples for DXP production, the DXP synthase (DXS) reaction is bypassed, which is one of the bottlenecks of the MEP pathway.[55] Thereby, the regulatory mechanisms limiting the activity of the endogenous MEP pathway enzyme can be avoided.

These examples for the MVA and MEP pathways show that shunts and bypasses to the canonical isoprenoid pathways, already existing in nature or synthetically designed, represent a source of potential biotechnological tools to be further addressed in the future.[1]

Instead of redirecting the central carbon metabolism to increase the acetyl-CoA pool in *S. cerevisiae*, it could also be beneficial to use alternative microorganisms whose native metabolism provides a more suitable framework for precursor supply. In contrast to wild type yeasts, in whose cytosol the acetyl-CoA pool is extremely small, some bacterial metabolisms exhibit high flux toward this intermediate. The metabolism of bacteria possessing high polyhydroxybutyrate (PHB) production capabilities, for whose generation acetyl-CoA and acetoacetyl-CoA are early precursors,[56] therefore provides a more suitable starting point for optimization toward isoprenoid production via the MVA pathway. Such microorganisms are, for example, the bacteria *Pseudomonas putida*,[57] *Cupriavidus necator*,[58] or *Methylobacterium extorquens*,[59] in which acetoacetyl-CoA is furthermore an essential intermediate of the anabolic metabolism. As a proof-of-concept, introducing the MVA pathway in *M. extorquens* allowed the production of 1.65 g/L of the sesquiterpenoid hop flavor compound α-humulene from methanol as sole carbon source corresponding to 12% of the maximum theoretical yield.[60]

Another strategy to improve productivity is to divide the bioprocess into a growth phase and a production phase and thereby avoid the allocation of substrate for cell growth. In the growth phase nutrients are employed to build up biomass rapidly, while in the production phase the nutrients are exclusively used for product formation. Therefore, methods to limit growth while allowing production are required.[30] This can be achieved, for example, through carbon or nitrogen restriction.[61]

Alleviating Toxic Effects To Sustain Production Efficiency. Overexpression of the isoprenoid production pathway in microbial hosts can lead to toxicity, metabolic stress,[62] and feedback regulation,[24,63] impairing efficiency and yield. This must be avoided to develop cost-effective production processes. The toxicity results from cytotoxicity or loss of resources needed for cell growth.[29] Hence, to gain a high productivity, in most cases the overexpression of the pathway enzymes is not enough; it is also important to fine-tune the metabolic fluxes. This can be achieved by balancing protein expression and enzyme activities to channel substrate flux and in this way avoid intermediate accumulation.[3,64]

Besides the challenge of creating efficient metabolic processes for terpenoid synthesis, there is the task of circumventing difficulties that arise with the physicochemical properties of terpenoids:[30] hydrophobicity and often pronounced cytotoxicity. With an increased production of terpenoids, in particular oxidized compounds, comes an imposed stress on the cellular machinery.[28] Especially monoterpenoids, but also sesqui- and diterpenoids, can impair cell growth. Therefore, to create economically viable processes, it is essential to control the accumulation of toxic products and thereby avoid negative impacts on cell factory functionality.

Various strategies can be followed to mitigate product toxicity. At the strain level, resilience toward educts and

DOI: 10.1021/acs.jafc.7b00473
J. Agric. Food Chem. 2018, 66, 2247−2258

products can be improved in different ways, engineering inherent or heterologous tolerance mechanisms.[65] Another possibility is to use host organisms that naturally exhibit a pronounced tolerance toward organic solvents, including terpenoids, such as *Bacillus* or *Rhodococcus* strains[66] or *Pseudomonas putida*.[67] Studies have demonstrated that the monoterpenoid resistance of *P. putida* is considerably higher than that of *E. coli* or *S. cerevisiae*,[68,69] which makes it a suitable production strain, especially for monoterpenoids. A first example of *Pseudomonas* monoterpenoid cell factory approach showed the production of antimicrobial geranic acid,[69] used for flavor and fragrance compositions due to its fresh green and woody odor, with glycerol as sole carbon source.

Moreover, the development of flexible induction techniques by dynamic promoters and expression systems that respond to product concentration, cellular parameters, or other environmental queues could further improve the productivity.[33,70] Ideally, the host cell should be able to adjust the pathway activity according to its metabolic status or the concentration of key pathway intermediates or products, with the result that toxic substances never reach inhibitory or lethal levels. An example of such a dynamic promoter can be found for the regulation of FPP production in the isoprenoid biosynthetic pathway of *E. coli*.[71] In addition, dynamic promoters can also increase yield by reducing competitive reactions, without complete loss of resources needed for cell survival, demonstrated for a yeast strain engineered for santalene production.[44] Another option for regulation can be the creation of feedback loops.[72]

In addition, to improve the microbial resilience or to use solvent-tolerant microbes, further optimization can also be done on the bioprocess engineering level. Here, approaches grouped under the term "in situ product removal" (ISPR) can be used for the immediate separation of a product from the biocatalyst. While doing so, the productivity of the process is not only increased by overcoming inhibitory effects but in addition by minimizing product loss due to degradation or uncontrolled evaporation and aiding downstream processing. Several techniques are available. On the basis of the hydrophobicity and volatility of terpenoids, extraction into another phase, hydrophobic adsorption, or evaporation combined with gas phase extraction (stripping) is favorable.[30] Liquid–liquid two-phase cultivation systems were, for example, applied for the production of sclareol,[46] nootkatone,[73] valencene, or patchoulol[74] to trap the product in an organic phase, thus avoiding its evaporative loss. Monoterpenoids tend to be far more toxic than sesquiterpenoids, making the two-phase approach also a technical measure to alleviate product toxicity as has been shown for pinene.[75,76]

Genetic and Protein Engineering. With genetic engineering, gene expression levels and duration can be influenced by multiple parameters, such as promoters, terminators, repressors, transcription factors, gene copy number, codon optimization, small antisense RNAs,[55,77] mRNA secondary structures, or RNA stability.[39] Especially the functional expression of plant proteins, such as cytochrome P450 monooxygenases (P450s), in microbial hosts remains one of the primary challenges during the development of cell factories for terpenoid production.[29] P450s are often the key enzymes in the functionalization of terpene hydrocarbons to the desired flavor and fragrance target compounds. For instance, heterologously expressed P450s are intensively investigated in the context of microbial cell factory approaches as they catalyze the essential oxygenation steps in the respective plants to form, for example, nootkatoone[73,78,79] and santalol.[5,80,81]

Protein engineering is applied to improve catalytic activity, enhance substrate specificity, change regio- or stereospecificity, expand product diversity, change cofactor requirements, increase functional expression/solubility, improve protein–protein interaction, or channel substrate flux. This can be done by (a) evolutionary approaches, (b) rational protein design by directed mutagenesis, (c) de novo generation of enzymes based on computational algorithm and in silico modeling, and (d) co-localization of proteins by creating fusion proteins or utilizing protein, DNA or RNA scaffolds, or cell compartments.[3,28,33]

Protein engineering can be used to develop tailored enzymes and molecularly reprogram key metabolic nodes, as for the MVA/MEP pathway enzymes. Also, the engineering of prenyl transferases, terpenoid synthases, or cytochrome P450 monooxygenases can be favorable.[64]

Terpene synthases, which can be utilized for de novo production of, for example, valencene,[82,83] sclareol,[46,84] or santalene,[85−89] often exhibit a high promiscuity, which results in a broad substrate spectrum.[24] If high purity of the target compound is desired, the synthases have to be engineered toward production of one specific target or at least decreased side-product formation, as was the case for stevioside production by *S. cerevisiae*.[90] However, for synthesis of oils consisting of a compound mixture, such as patchouli oil, the ability of a terpene synthase to produce different terpenoids in a certain ratio can be favorable.[91]

In the case of the bacterial monooxygenases P450cam (*P. putida*) and P450 BM-3 (*B. megaterium*) it was demonstrated that the enzymes can be modified in a way that various terpenoid hydroxylations are carried out by engineered enzyme variants.[3] Furthermore, by recombination of genes, cytochrome P450 fusion proteins with enhanced solubility or protein complexes with improved protein–protein interaction rate, for example, between redox partners, can be achieved.[92] In addition, the fusion of proteins as well as the organization of enzymes in synthetic scaffolds or enclosure of pathways in subcellular compartments can trigger metabolic channeling to minimize losses of intermediate products through degradation or utilization by alternative metabolic routes and help overcome diffusional limitations.[3,28,33,55] Following this approach, fusion proteins of FPP-synthase with patchoulol synthase or α-farnesene synthase have been created.[93,94] The latter study demonstrated that protein fusion can also aid the reduction or elimination of unwanted side reactions. The creation of a synthetic protein scaffold[95] or the introduction in mitochondria was applied to co-localize MVA pathway enzymes.[96] By enclosing production pathways in cell organelles or synthetic cell compartments, the toxic effects of intermediates or products can be prevented.[33,97−99]

Besides engineering proteins to increase their specificity or to couple functional units, altering cofactor requirements can also be beneficial, which is described for the HMG-CoA reductase, a key enzyme in the MVA pathway. Whereas NADPH is used for most anabolic pathways, NADH is produced during catabolism. By engineering a protein to consume NADH instead of NADPH, competition of the product biosynthesis route with other anabolic pathways can be avoided.[3,55]

Microbial Hosts. In addition to optimizing metabolic pathways and flux optimization, the choice of a suitable host strain has to be considered very carefully, because this also determines the success of developing a cost-effective

DOI: 10.1021/acs.jafc.7b00473
J. Agric. Food Chem. 2018, 66, 2247−2258

production process. Ideal host strains should be well characterized with regard to genome sequence and annotation and be easily genetically accessible. In addition, they should be easily cultivated under laboratory conditions and in production scale and grow quickly with simple nutrient demand, especially low-cost feedstocks, because this directly influences production costs.

Although plants are the natural source of terpenoids, engineered microbial platforms are the most convenient and cost-effective approach for large-scale, high-yield production of terpenoids. Two traditional model microorganisms are most commonly used for developing microbial factories, *E. coli* and *S. cerevisiae*, because both organisms are well characterized regarding their physiology, metabolism, and genetics.[33] For instance, *E. coli* has been optimized to produce 1.5 g/L sclareol in high cell density fermentation.[46] *S. cerevisiae* was engineered for, for example, santalene[45,100] or nootkatone production[78,101] and also to synthesize the carotenoid-derived violet-like C_{13} norisoprenoid β-ionone (1 mg/g DCW).[102]

Nevertheless, in relation to the target molecule and the metabolic pathways to be used, alternative host organisms can exhibit genetic and physiological advantages when compared to *E. coli* or *S. cerevisiae*.[11,32] Some microorganisms are able to employ favorable alternative primary metabolism pathways and use different nonglucose carbon sources, or to naturally produce and tolerate large amounts of the desired chemical product, which can be toxic to common production strains, as mentioned above. In particular, the advancing development of -omics technologies and novel metabolic engineering tools for noncoli/nonyeast hosts made alternative organisms available for microbial cell factory design.[33]

Especially for the production of low-cost, high-volume products, an important aspect to tackle is the carbon source used for terpenoid production. Here, organisms that can assimilate low-cost feedstocks are necessary. Moreover, carbon sources such as ethanol and glycerol have great potential for enhancing yield and network flexibility, because, for example, glycerol as source for the MEP shows the highest potential to enhance IPP yields.[48] Besides organisms that can use a wide range of cheap nonsugar carbon sources, for example, the above-mentioned *Methylobacterium extorquens*[103] or the yeast *Yarrowia lipolytica*,[104,105] also bioprocesses with autotrophic microorganisms could become profitable, because these organisms are able to assimilate nonorganic carbon such as atmospheric CO_2.[106] Examples are the photoautotroph cyanobacterium *Synechocystis* sp.,[107] the purple bacterium *Rhodobacter sphaeroides*,[108] or the chemolithoautotrophic organism *Cupriavidus necator*.[58]

Other alternative host organisms for terpenoid production are, for instance, *Bacillus subtilis*[109] or *Corynebacterium glutamicum*, of which the latter has been engineered to synthesize pinene.[75] Furthermore, an engineered strain of the yeast *Pichia pastoris* has demonstrated its potential for the production of nootkatone with a yield of 208 mg/L in a bioreactor.[73]

In addition to the beneficial genetic and physiological properties of these alternative organisms, establishing terpenoid production processes with these unusual hosts—although time-consuming—might be a way to find a gap in the crowded patent landscape. Nonetheless, the genetic tools available for these less known platforms still lag behind those developed for baker's yeast and *E. coli*.[30] Therefore, it could also be an option to transfer useful traits from nonconventional strains, such as tolerance factors,[65,110] to the genetically well tractable platform hosts, depending on the complexity of the factors to be copied.[33]

OUTLOOK

During the past decades, metabolic engineering of microbes has grown to a mature discipline. A special advantage of the cell factory approach is that establishing a platform microbe can deliver a multitude of different target compounds by virtually the same process design, with a change of only the strain variant used for fermentation. Looking at terpenoid flavors and fragrances, engineered baker's yeast is probably the most productive system developed so far with product titers of >130 g/L, as is the case for β-farnesene.[51] The yeast has also the advantage of being an organism generally recognized as safe (GRAS). Sesquiterpene hydrocarbons produced by microbial cell factories may therefore become a more sustainable feedstock for the aroma industry or even substitute for conventional plant-based feedstocks in the future. However, more complex terpenoid structures, which often are the organoleptically preferred targets, require further enzymatic functionalizations, for example, hydroxylations by P450s. Difficult functional expression of plant P450s in microbes and their often low enzyme activities are only two of certainly more reasons why product titers for oxyfunctionalized terpenoids usually lag significantly behind those of their hydrocarbon precursors. With this in mind, the high product titers reported for β-farnesene, obtained after a long and labor intensive work of more than a decade, must not be taken as an easily reachable value for other sought-after terpenoids, such as the santalols. However, the higher market value of the latter compounds will allow bioprocesses to become already economically viable at lower product titers. The synthesis of other interesting terpenoids, for example, the diterpenoid sclareol, an important precursor for (−)-ambrox synthesis, does not require P450s but relies on a two-step reaction cascade by a class II and a class I diterpene synthase.[111] On the basis of the elucidation of the plant biosynthesis, an even more complex pathway would be needed to produce the monoterpenoid (−)-menthol, a "terpenoid blockbuster" sold at more than 30,000 t/a worldwide.[112] In peppermint (*Mentha* × *piperita* L.) (−)-menthol synthesis from GPP requires seven enzymatic steps with (−)-limonene synthase catalyzing the first committed step.[112] This complexity at the metabolic level and also the common cytotoxicity of monoterpenoids against microbes make the development of a (−)-menthol bioprocess a difficult task, although industrial R&D is certainly in progress due to the commercial importance of the product. Nevertheless, the perspectives of microbial cell factories are fascinating. First, they may give the flavor and fragrance industry on-site access to a sustainable and cheap terpenoid feedstock of high quality, which can be refined by existing chemistry to desired products and which are independent of suppliers from countries with climatic and political uncertainties or an endangered biodiversity. Second, the "variation of the same theme" may allow the production of different terpenoid flavors and fragrances with the same biotechnology platform even for niche applications, that is, products with low-volume markets. Finally, combining different terpene synthases and balancing their expression levels or combining oils from differently engineered strain variants may allow the design of highly reproducible "microbial essential oils" that mimic essential oils difficult to access from endangered plants and

DOI: 10.1021/acs.jafc.7b00473
J. Agric. Food Chem. 2018, 66, 2247−2258

may even be used in the future to create novel biotechnological aroma compositions with unique sensory profiles.

AUTHOR INFORMATION

Corresponding Author

*(J.S.) E-mail: schrader@dechema.de. Phone: +49-69-7564-422.

ORCID

Jens Schrader: 0000-0003-2235-6553

Funding

We thank CNPq for supporting L.D. with a scholarship.

Notes

The authors declare no competing financial interest.

ACKNOWLEDGMENTS

We thank Luis Lucchesi for graphic work used in this paper.

ABBREVIATIONS USED

AAT, acetoacetyl-CoA thiolase; ATP, adenosine triphosphate; CMK, 4-(cytidine 5-diphospho)-2-*C*-methyl-D-erythritol kinase; CoA, coenzyme A; CTP, cytidine triphosphate; DCW, dry cell weight; DMAPP, dimethylallyl diphosphate; DMAPP, dimethylallyl diphosphate; DXP, 1-deoxy-D-xylulose 5-phosphate; DXR, DXP reductoisomerase; DXS, DXP synthase; FPP, farnesyl diphosphate; FPP, farnesyl diphosphate; G3P, D-glyceraldehyde 3-phosphate; G3P, D-glyceraldehyde-3-phosphate; GGPP, geranylgeranyl diphosphate; GMO, genetically modified organism; GPP, geranyl diphosphate; HDR, 4-hydroxy-3-methylbut-2-enyl diphosphate reductase; HDS, 4-hydroxy-3-methylbut-2-enyl diphosphate synthase; HMG-CoA, 3-hydroxy-3-methylglutaryl-CoA; HMG-CoA, 3-hydroxy-3-methylglutaryl-CoA; HMGR, HMG-CoA reductase; HMGR1, 3-hydroxy-3-methylglutaryl-coenzyme A reductase; HMGS, HMG-CoA synthase; IDI, IPP isomerase; IPP, isopentenyl diphosphate; IPP, isopentenyl diphosphate; ISPR, in situ product removal; MCT, MEP cytidyltransferase; MDS, 2-*C*-methyl-D-erythritol 2,4-cyclodiphosphate synthase; MEP, 2-*C*-methyl-D-erythritol 4-phosphate; MK, mevalonate kinase; MVA, mevalonate; MVD, 5-diphosphomevalonate decarboxylase; NAD(P)H, nicotinamide adenine dinucleotide (phosphate); P450, cytochrome P450 monooxygenases; PDH, pyruvate dehydrogenase; PHB, polyhydroxybutyrate; PMK, 5-phosphomevalonate kinase; PT, prenyltransferases; R&D, research and development; R5P, ribulose 5-phosphate; TS, terpene synthases; X5P, xylulose 5-phosphate

REFERENCES

(1) Pérez-Gil, J.; Rodríguez-Concepción, M. Metabolic plasticity for isoprenoid biosynthesis in bacteria. *Biochem. J.* **2013**, *452* (1), 19−25.

(2) Gershenzon, J.; Dudareva, N. The function of terpene natural products in the natural world. *Nat. Chem. Biol.* **2007**, *3* (7), 408−414.

(3) Chen, Y.; Zhou, Y. J.; Siewers, V.; Nielsen, J. Enabling technologies to advance microbial isoprenoid production. *Adv. Biochem. Eng./Biotechnol.* **2014**, *148*, 143−160.

(4) *Flavours and Fragrances*, 1st ed.; Berger, R. G., Ed.; Springer-Verlag: Berlin, Germany, 2007.

(5) Diaz-Chavez, M. L.; Moniodis, J.; Madilao, L. L.; Jancsik, S.; Keeling, C. I.; Barbour, E. L.; Ghisalberti, E. L.; Plummer, J. A.; Jones, C. G.; Bohlmann, J. Biosynthesis of sandalwood oil: *Santalum album* CYP76F cytochromes P450 produce santalols and bergamotol. *PLoS One* **2013**, *8* (9), e75053.

(6) Naef, R. The volatile and semi-volatile constituents of agarwood, the infected heartwood of *Aquilaria* species: a review. *Flavour Fragrance J.* **2011**, *26* (2), 73−87.

(7) *Biotechnology of Isoprenoids*; Schrader, J., Bohlmann, J., Eds.; Advances in Biochemical Engineering/Biotechnology; Springer International Publishing: Cham, Germany, 2015; Vol. 148.

(8) Duetz, W. A.; Bouwmeester, H.; Beilen, J. B.; Witholt, B. Biotransformation of limonene by bacteria, fungi, yeasts, and plants. *Appl. Microbiol. Biotechnol.* **2003**, *61* (4), 269−277.

(9) Vespermann, K. A. C.; Paulino, B. N.; Barcelos, M. C. S.; Pessôa, M. G.; Pastore, G. M.; Molina, G. Biotransformation of α- and β-pinene into flavor compounds. *Appl. Microbiol. Biotechnol.* **2017**, *101* (5), 1805−1817.

(10) Bicas, J. L.; Dionísio, A. P.; Pastore, G. M. Bio-oxidation of terpenes: an approach for the flavor industry. *Chem. Rev.* **2009**, *109* (9), 4518−4531.

(11) Janocha, S.; Schmitz, D.; Bernhardt, R. Terpene hydroxylation with microbial cytochrome P450 monooxygenases. *Adv. Biochem. Eng./Biotechnol.* **2015**, *148*, 215−250.

(12) Bicas, J. L.; Dionísio, A. P.; Pastore, G. M. Bio-oxidation of terpenes: an approach for the flavor industry. *Chem. Rev.* **2009**, *109* (9), 4518−4531.

(13) de Carvalho, C. C. C. R.; da Fonseca, M. M. R. Biotransformation of terpenes. *Biotechnol. Adv.* **2006**, *24* (2), 134−142.

(14) Vespermann, K. A. C.; Paulino, B. N.; Barcelos, M. C. S.; Pessôa, M. G.; Pastore, G. M.; Molina, G. Biotransformation of α- and β-pinene into flavor compounds. *Appl. Microbiol. Biotechnol.* **2017**, *101* (5), 1805−1817.

(15) Fraatz, M. A.; Berger, R. G.; Zorn, H. Nootkatone—a biotechnological challenge. *Appl. Microbiol. Biotechnol.* **2009**, *83* (1), 35−41.

(16) Li, S.; Yang, X.; Yang, S.; Zhu, M.; Wang, X. Technology prospecting on enzymes: application, marketing and engineering. *Comput. Struct. Biotechnol. J.* **2012**, *2* (3), e201209017.

(17) Miguel, A. S. M.; Martins-Meyer, T. S.; da Figueiredo Costa, E. V.; Lobo, B. W. P.; Dellamora-Ortiz, G. M. Enzymes in bakery: current and future trends. In *Food Industry*; Muzzalupo, I., Ed.; InTech, 2013; pp 287−231.

(18) Yu, P. L. Production of chymosin for the dairy industry by recombinant DNA technology. *Australas. Biotechnol.* **1994**, *4* (1), 19−23.

(19) Kumar, A.; Grover, S.; Sharma, J.; Batish, V. K. Chymosin and other milk coagulants: sources and biotechnological interventions. *Crit. Rev. Biotechnol.* **2010**, *30* (4), 243−258.

(20) Schrader, J.; Etschmann, M. M. W.; Sell, D.; Hilmer, J.-M.; Rabenhorst, J. Applied biocatalysis for the synthesis of natural flavour compounds − current industrial processes and future prospects. *Biotechnol. Lett.* **2004**, *26* (6), 463−472.

(21) Leffingwell, J.; Leffingwell, D. Flavours & fragrances: recent advances in biotechnology. *Spec. Chem. Mag.* **2015**, *35* (5), 32−34.

(22) Waltz, E. Engineers of scent. *Nat. Biotechnol.* **2015**, *33* (4), 329−332.

(23) Boronat, A.; Rodríguez-Concepción, M. Terpenoid biosynthesis in prokaryotes. *Adv. Biochem. Eng./Biotechnol.* **2014**, *148*, 3−18.

(24) Tholl, D. Biosynthesis and biological functions of terpenoids in plants. *Adv. Biochem. Eng./Biotechnol.* **2015**, *148*, 63−106.

(25) Rodriguez-Concepcion, M. Elucidation of the methylerythritol phosphate pathway for isoprenoid biosynthesis in bacteria and plastids. A metabolic milestone achieved through genomics. *Plant Physiol.* **2002**, *130* (3), 1079−1089.

(26) Rohmer, M.; Rohmer, M. The discovery of a mevalonate-independent pathway for isoprenoid biosynthesis in bacteria, algae and higher plants. *Nat. Prod. Rep.* **1999**, *16* (5), 565−574.

(27) Pateraki, I.; Heskes, A. M.; Hamberger, B. Cytochromes P450 for terpene functionalisation and metabolic engineering. *Adv. Biochem. Eng./Biotechnol.* **2015**, *148*, 107−139.

(28) Kampranis, S. C.; Makris, A. M. Developing a yeast cell factory for the production of terpenoids. *Comput. Struct. Biotechnol. J.* **2012**, *3* (4), e201210006.

DOI: 10.1021/acs.jafc.7b00473
J. Agric. Food Chem. 2018, 66, 2247−2258

(29) Chang, M. C. Y.; Keasling, J. D. Production of isoprenoid pharmaceuticals by engineered microbes. *Nat. Chem. Biol.* **2006**, *2* (12), 674−681.
(30) Schewe, H.; Mirata, M. A.; Schrader, J. Bioprocess engineering for microbial synthesis and conversion of isoprenoids. *Adv. Biochem. Eng./Biotechnol.* **2015**, *148*, 251−286.
(31) Schmidt-Dannert, C. Biosynthesis of terpenoid natural products in fungi. *Adv. Biochem. Eng./Biotechnol.* **2014**, *148*, 19−61.
(32) Zhu, Q.; Jackson, E. N. Metabolic engineering of *Yarrowia lipolytica* for industrial applications. *Curr. Opin. Biotechnol.* **2015**, *36*, 65−72.
(33) Woolston, B. M.; Edgar, S.; Stephanopoulos, G. Metabolic engineering: past and future. *Annu. Rev. Chem. Biomol. Eng.* **2013**, *4* (1), 259−288.
(34) Van Dien, S. From the first drop to the first truckload: commercialization of microbial processes for renewable chemicals. *Curr. Opin. Biotechnol.* **2013**, *24* (6), 1061−1068.
(35) Prather, K. L. J.; Martin, C. H. De novo biosynthetic pathways: rational design of microbial chemical factories. *Curr. Opin. Biotechnol.* **2008**, *19* (5), 468−474.
(36) Lee, J. W.; Na, D.; Park, J. M.; Lee, J.; Choi, S.; Lee, S. Y. Systems metabolic engineering of microorganisms for natural and non-natural chemicals. *Nat. Chem. Biol.* **2012**, *8* (6), 536−546.
(37) Vickers, C. E.; Bongers, M.; Liu, Q.; Delatte, T.; Bouwmeester, H. Metabolic engineering of volatile isoprenoids in plants and microbes. *Plant, Cell Environ.* **2014**, *37* (8), 1753−1775.
(38) Kirby, J.; Keasling, J. D. Biosynthesis of plant isoprenoids: perspectives for microbial engineering. *Annu. Rev. Plant Biol.* **2009**, *60* (1), 335−355.
(39) Immethun, C. M.; Hoynes-O'Connor, A. G.; Balassy, A.; Moon, T. S. Microbial production of isoprenoids enabled by synthetic biology. *Front. Microbiol.* **2013**, *4* (4), 75.
(40) Liu, Y.; Shin, H.; Li, J.; Liu, L. Toward metabolic engineering in the context of system biology and synthetic biology: advances and prospects. *Appl. Microbiol. Biotechnol.* **2015**, *99* (3), 1109−1118.
(41) Vickers, C. E.; Sabri, S. Isoprene. *Adv. Biochem. Eng./Biotechnol.* **2015**, *148*, 289−317.
(42) Polakowski, T.; Stahl, U.; Lang, C. Overexpression of a cytosolic hydroxymethylglutaryl-CoA reductase leads to squalene accumulation in yeast. *Appl. Microbiol. Biotechnol.* **1998**, *49* (1), 66−71.
(43) Donald, K. A. G.; Hampton, R. Y.; Fritz, I. B. Effects of overproduction of the catalytic domain of 3-hydroxy-3-methylglutaryl coenzyme A reductase on squalene synthesis in *Saccharomyces cerevisiae*. *Appl. Environ. Microbiol.* **1997**, *63* (9), 3341−3344.
(44) Scalcinati, G.; Knuf, C.; Partow, S.; Chen, Y.; Maury, J.; Schalk, M.; Daviet, L.; Nielsen, J.; Siewers, V. Dynamic control of gene expression in *Saccharomyces cerevisiae* engineered for the production of plant sesquitepene α-santalene in a fed-batch mode. *Metab. Eng.* **2012**, *14* (2), 91−103.
(45) Scalcinati, G.; Partow, S.; Siewers, V.; Schalk, M.; Daviet, L.; Nielsen, J. Combined metabolic engineering of precursor and co-factor supply to increase α-santalene production by *Saccharomyces cerevisiae*. *Microb. Cell Fact.* **2012**, *11* (1), 117.
(46) Schalk, M.; Pastore, L.; Mirata, M. A.; Khim, S.; Schouwey, M.; Deguerry, F.; Pineda, V.; Rocci, L.; Daviet, L. Toward a biosynthetic route to sclareol and amber odorants. *J. Am. Chem. Soc.* **2012**, *134* (46), 18900−18903.
(47) Zurbriggen, A.; Kirst, H.; Melis, A. Isoprene production via the mevalonic acid pathway in *Escherichia coli* (bacteria). *BioEnergy Res.* **2012**, *5* (4), 814−828.
(48) Gruchattka, E.; Hädicke, O.; Klamt, S.; Schütz, V.; Kayser, O. In silico profiling of *Escherichia coli* and *Saccharomyces cerevisiae* as terpenoid factories. *Microb. Cell Fact.* **2013**, *12* (1), 84.
(49) Yang, C.; Gao, X.; Jiang, Y.; Sun, B.; Gao, F.; Yang, S. Synergy between methylerythritol phosphate pathway and mevalonate pathway for isoprene production in *Escherichia coli*. *Metab. Eng.* **2016**, *37*, 79−91.
(50) Miziorko, H. M. Enzymes of the mevalonate pathway of isoprenoid biosynthesis. *Arch. Biochem. Biophys.* **2011**, *505* (2), 131−143.
(51) Meadows, A. L.; Hawkins, K. M.; Tsegaye, Y.; Antipov, E.; Kim, Y.; Raetz, L.; Dahl, R. H.; Tai, A.; Mahatdejkul-Meadows, T.; Xu, L.; et al. Rewriting yeast central carbon metabolism for industrial isoprenoid production. *Nature* **2016**, *537* (7622), 694−697.
(52) Paddon, C. J.; Westfall, P. J.; Pitera, D. J.; Benjamin, K.; Fisher, K.; McPhee, D.; Leavell, M. D.; Tai, A.; Main, A.; Eng, D.; et al. High-level semi-synthetic production of the potent antimalarial artemisinin. *Nature* **2013**, *496* (7446), 528−532.
(53) Kirby, J.; Nishimoto, M.; Chow, R. W. N.; Baidoo, E. E. K.; Wang, G.; Martin, J.; Schackwitz, W.; Chan, R.; Fortman, J. L.; Keasling, J. D. Enhancing terpene yield from sugars via novel routes to 1-deoxy-D-xylulose 5-phosphate. *Appl. Environ. Microbiol.* **2015**, *81* (1), 130−138.
(54) Perez-Gil, J.; Uros, E. M.; Sauret-Güeto, S.; Lois, L. M.; Kirby, J.; Nishimoto, M.; Baidoo, E. E. K.; Keasling, J. D.; Boronat, A.; Rodriguez-Concepcion, M. Mutations in *Escherichia coli* aceE and ribB genes allow survival of strains defective in the first step of the isoprenoid biosynthesis pathway. *PLoS One* **2012**, *7* (8), e43775.
(55) Kempinski, C.; Jiang, Z.; Bell, S.; Chappell, J. Metabolic engineering of higher plants and algae for isoprenoid production. *Adv. Biochem. Eng./Biotechnol.* **2015**, *148*, 161−199.
(56) Masamune, S.; Walsh, C. T.; Sinskey, A. J.; Peoples, O. P. Poly-(R)-3-hydroxybutyrate (PHB) biosynthesis: mechanistic studies on the biological Claisen condensation catalyzed by β-ketoacyl thiolase. *Pure Appl. Chem.* **1989**, *61* (3), 303−312.
(57) Agrawal, T.; Kotasthane, A. S.; Kushwah, R. Genotypic and phenotypic diversity of polyhydroxybutyrate (PHB) producing *Pseudomonas putida* isolates of Chhattisgarh region and assessment of its phosphate solubilizing ability. *3 Biotech* **2015**, *5*, 45−60.
(58) Garcia-Gonzalez, L.; Mozumder, M. S. I.; Dubreuil, M.; Volcke, E. I. P.; De Wever, H. Sustainable autotrophic production of polyhydroxybutyrate (PHB) from CO_2 using a two-stage cultivation system. *Catal. Today* **2015**, *257* (P2), 237−245.
(59) Korotkova, N.; Chistoserdova, L.; Lidstrom, M. E. Poly-beta-hydroxybutyrate biosynthesis in the facultative methylotroph *Methylobacterium extorquens* AM1: identification and mutation of gap11, gap20, and phaR. *J. Bacteriol.* **2002**, *184* (22), 6174−6181.
(60) Sonntag, F.; Kroner, C.; Lubuta, P.; Peyraud, R.; Horst, A.; Buchhaupt, M.; Schrader, J. Engineering *Methylobacterium extorquens* for de novo synthesis of the sesquiterpenoid α-humulene from methanol. *Metab. Eng.* **2015**, *32*, 82−94.
(61) Tsuruta, H.; Paddon, C. J.; Eng, D.; Lenihan, J. R.; Horning, T.; Anthony, L. C.; Regentin, R.; Keasling, J. D.; Renninger, N. S.; Newman, J. D. High-level production of amorpha-4,11-diene, a precursor of the antimalarial agent artemisinin, in *Escherichia coli*. *PLoS One* **2009**, *4* (2), e4489.
(62) Sivy, T. L.; Fall, R.; Rosenstiel, T. N. Evidence of isoprenoid precursor toxicity in *Bacillus subtilis*. *Biosci., Biotechnol., Biochem.* **2011**, *75* (12), 2376−2383.
(63) Banerjee, A.; Sharkey, T. D. Methylerythritol 4-phosphate (MEP) pathway metabolic regulation. *Nat. Prod. Rep.* **2014**, *31* (8), 1043.
(64) Leonard, E.; Ajikumar, P. K.; Thayer, K.; Xiao, W.-H.; Mo, J. D.; Tidor, B.; Stephanopoulos, G.; Prather, K. L. J. Combining metabolic and protein engineering of a terpenoid biosynthetic pathway for overproduction and selectivity control. *Proc. Natl. Acad. Sci. U. S. A.* **2010**, *107* (31), 13654−13659.
(65) Dunlop, M. J. Engineering microbes for tolerance to next-generation biofuels. *Biotechnol. Biofuels* **2011**, *4*, 32.
(66) *Biology of Rhodococcus*; Alvarez, H. M., Ed.; Microbiology Monographs; Springer: Berlin, Germany, 2010; Vol. 16.
(67) Inoue, A.; Horikoshi, K. A *Pseudomonas* thrives in high concentrations of toluene. *Nature* **1989**, *338* (6212), 264−266.
(68) Inoue, A.; Horikoshi, K. Estimation of solvent-tolerance of bacteria by the solvent parameter log P. *J. Ferment. Bioeng.* **1991**, *71* (3), 194−196.

DOI: 10.1021/acs.jafc.7b00473
J. Agric. Food Chem. 2018, 66, 2247−2258

(69) Mi, J.; Becher, D.; Lubuta, P.; Dany, S.; Tusch, K.; Schewe, H.; Buchhaupt, M.; Schrader, J. De novo production of the monoterpenoid geranic acid by metabolically engineered *Pseudomonas putida*. *Microb. Cell Fact.* **2014**, *13* (1), 170.
(70) George, K. W.; Alonso-Gutierrez, J.; Keasling, J. D.; Lee, T. S. Isoprenoid drugs, biofuels, and chemicals − artemisinin, farnesene, and beyond. *Adv. Biochem. Eng./Biotechnol.* **2015**, *148*, 355−389.
(71) Dahl, R. H.; Zhang, F.; Alonso-Gutierrez, J.; Baidoo, E.; Batth, T. S.; Redding-Johanson, A. M.; Petzold, C. J.; Mukhopadhyay, A.; Lee, T. S.; Adams, P. D.; et al. Engineering dynamic pathway regulation using stress-response promoters. *Nat. Biotechnol.* **2013**, *31* (11), 1039−1046.
(72) Dunlop, M. J.; Keasling, J. D.; Mukhopadhyay, A. A model for improving microbial biofuel production using a synthetic feedback loop. *Syst. Synth. Biol.* **2010**, *4* (2), 95−104.
(73) Wriessnegger, T.; Augustin, P.; Engleder, M.; Leitner, E.; Müller, M.; Kaluzna, I.; Schürmann, M.; Mink, D.; Zellnig, G.; Schwab, H.; et al. Production of the sesquiterpenoid (+)-nootkatone by metabolic engineering of *Pichia pastoris*. *Metab. Eng.* **2014**, *24*, 18−29.
(74) Asadollahi, M. A.; Maury, J.; Møller, K.; Nielsen, K. F.; Schalk, M.; Clark, A.; Nielsen, J. Production of plant sesquiterpenes in *Saccharomyces cerevisiae*: effect of ERG9 repression on sesquiterpene biosynthesis. *Biotechnol. Bioeng.* **2008**, *99* (3), 666−677.
(75) Kang, M.-K.; Eom, J.-H.; Kim, Y.; Um, Y.; Woo, H. M. Biosynthesis of pinene from glucose using metabolically-engineered *Corynebacterium glutamicum*. *Biotechnol. Lett.* **2014**, *36* (10), 2069−2077.
(76) Brennan, T. C. R.; Turner, C. D.; Krömer, J. O.; Nielsen, L. K. Alleviating monoterpene toxicity using a two-phase extractive fermentation for the bioproduction of jet fuel mixtures in *Saccharomyces cerevisiae*. *Biotechnol. Bioeng.* **2012**, *109* (10), 2513−2522.
(77) Schwab, W. Genetic engineering of plants and microbial cells for flavour production. In *Flavours and Fragrances*; Berger, R. G., Ed.; Springer: Berlin, Germany, 2007; pp 615−628.
(78) Cankar, K.; Van Houwelingen, A.; Goedbloed, M.; Renirie, R.; De Jong, R. M.; Bouwmeester, H.; Bosch, D.; Sonke, T.; Beekwilder, J. Valencene oxidase CYP706M1 from Alaska cedar (*Callitropsis nootkatensis*). *FEBS Lett.* **2014**, *588* (6), 1001−1007.
(79) Girhard, M.; Machida, K.; Itoh, M.; Schmid, R. D.; Arisawa, A.; Urlacher, V. B. Regioselective biooxidation of (+)-valencene by recombinant *E. coli* expressing CYP109B1 from *Bacillus subtilis* in a two-liquid-phase system. *Microb. Cell Fact.* **2009**, *8* (1), 36.
(80) Celedon, J. M.; Chiang, A.; Yuen, M. M. S.; Diaz-Chavez, M. L.; Madilao, L. L.; Finnegan, P. M.; Barbour, E. L.; Bohlmann, J. Heartwood-specific transcriptome and metabolite signatures of tropical sandalwood (*Santalum album*) reveal the final step of (Z)-santalol fragrance biosynthesis. *Plant J.* **2016**, *86* (4), 289−299.
(81) Bohlmann, C. J.; Diaz, M. L.; Chavez, M. J. Cytochrome p450 and cytochrome p450 reductase polypeptides, encoding nucleic acid molecules and uses thereof. US20160108374A1, 2016.
(82) Beekwilder, J.; van Houwelingen, A.; Cankar, K.; van Dijk, A. D. J.; de Jong, R. M.; Stoopen, G.; Bouwmeester, H.; Achkar, J.; Sonke, T.; Bosch, D. Valencene synthase from the heartwood of Nootka cypress (*Callitropsis nootkatensis*) for biotechnological production of valencene. *Plant Biotechnol. J.* **2014**, *12* (2), 174−182.
(83) Saran, D.; Park, G. E. Valencene synthase polypeptides, encoding nucleic acid molecules and uses thereof. Patent WO2014150599A1, 2014.
(84) Caniard, A.; Zerbe, P.; Legrand, S.; Cohade, A.; Valot, N.; Magnard, J.-L.; Bohlmann, J.; Legendre, L. Discovery and functional characterization of two diterpene synthases for sclareol biosynthesis in *Salvia sclarea* (L.) and their relevance for perfume manufacture. *BMC Plant Biol.* **2012**, *12* (1), 119.
(85) Jones, C. G.; Moniodis, J.; Zulak, K. G.; Scaffidi, A.; Plummer, J. A.; Ghisalberti, E. L.; Barbour, E. L.; Bohlmann, J. Sandalwood fragrance biosynthesis involves sesquiterpene synthases of both the terpene synthase (TPS)-a and TPS-b subfamilies, including santalene synthases. *J. Biol. Chem.* **2011**, *286* (20), 17445−17454.
(86) Zulak, K.; Jones, C.; Moniodis, J.; Bohlmann, J. Terpene synthases from santalum. US8569025B2, 2013.
(87) Schalk, M. Method for producing alpha-santalene. US20110008836A1, 2011.
(88) Schalk, M. Method for producing beta-santalene. US20110281257A1, 2011.
(89) Srivastava, P. L.; Daramwar, P. P.; Krithika, R.; Pandreka, A.; Shankar, S. S.; Thulasiram, H. V. Functional characterization of novel sesquiterpene synthases from Indian sandalwood, *Santalum album*. *Sci. Rep.* **2015**, *5*, 10095.
(90) Olsson, K.; Carlsen, S.; Semmler, A.; Simón, E.; Mikkelsen, M. D.; Møller, B. L. Microbial production of next-generation stevia sweeteners. *Microb. Cell Fact.* **2016**, *15* (1), 207.
(91) Deguerry, F.; Pastore, L.; Wu, S.; Clark, A.; Chappell, J.; Schalk, M. The diverse sesquiterpene profile of patchouli, *Pogostemon cablin*, is correlated with a limited number of sesquiterpene synthases. *Arch. Biochem. Biophys.* **2006**, *454* (2), 123−136.
(92) Renault, H.; Bassard, J.-E.; Hamberger, B.; Werck-Reichhart, D. Cytochrome P450-mediated metabolic engineering: current progress and future challenges. *Curr. Opin. Plant Biol.* **2014**, *19*, 27−34.
(93) Wang, C.; Yoon, S.-H.; Jang, H.-J.; Chung, Y.-R.; Kim, J.-Y.; Choi, E.-S.; Kim, S.-W. Metabolic engineering of *Escherichia coli* for α-farnesene production. *Metab. Eng.* **2011**, *13* (6), 648−655.
(94) Albertsen, L.; Chen, Y.; Bach, L. S.; Rattleff, S.; Maury, J.; Brix, S.; Nielsen, J.; Mortensen, U. H. Diversion of flux toward sesquiterpene production in *Saccharomyces cerevisiae* by fusion of host and heterologous enzymes. *Appl. Environ. Microbiol.* **2011**, *77* (3), 1033−1040.
(95) Dueber, J. E.; Wu, G. C.; Malmirchegini, G. R.; Moon, T. S.; Petzold, C. J.; Ullal, A. V.; Prather, K. L. J.; Keasling, J. D. Synthetic protein scaffolds provide modular control over metabolic flux. *Nat. Biotechnol.* **2009**, *27* (8), 753.
(96) Lv, X.; Wang, F.; Zhou, P.; Ye, L.; Xie, W.; Xu, H.; Yu, H. Dual regulation of cytoplasmic and mitochondrial acetyl-CoA utilization for improved isoprene production in *Saccharomyces cerevisiae*. *Nat. Commun.* **2016**, *7*, 12851.
(97) Chessher, A.; Breitling, R.; Takano, E. Bacterial microcompartments: biomaterials for synthetic biology-based compartmentalization strategies. *ACS Biomater. Sci. Eng.* **2015**, *1* (6), 345−351.
(98) Zebec, Z.; Wilkes, J.; Jervis, A. J.; Scrutton, N. S.; Takano, E.; Breitling, R. Towards synthesis of monoterpenes and derivatives using synthetic biology. *Curr. Opin. Chem. Biol.* **2016**, *34*, 37−43.
(99) https://terpenosome.wordpress.com (accessed Jan 12, 2017).
(100) Nielsen, J.; Siewers, V.; Chen, Y.; Daviet, L.; Schalk, M. Genetically engineered yeast cells. WO2013102554A1, 2013.
(101) Cankar, K.; van Houwelingen, A.; Bosch, D.; Sonke, T.; Bouwmeester, H.; Beekwilder, J. A chicory cytochrome P450 monooxygenase CYP71AV8 for the oxidation of (+)-valencene. *FEBS Lett.* **2011**, *585* (1), 178−182.
(102) López, J.; Essus, K.; Kim, I.-K.; Pereira, R.; Herzog, J.; Siewers, V.; Nielsen, J.; Agosin, E. Production of β-ionone by combined expression of carotenogenic and plant CCD1 genes in *Saccharomyces cerevisiae*. *Microb. Cell Fact.* **2015**, *14* (1), 84.
(103) Ochsner, A. M.; Sonntag, F.; Buchhaupt, M.; Schrader, J.; Vorholt, J. A. *Methylobacterium extorquens*: methylotrophy and biotechnological applications. *Appl. Microbiol. Biotechnol.* **2015**, *99* (2), 517−534.
(104) Ledesma-Amaro, R.; Nicaud, J.-M. Metabolic engineering for expanding the substrate range of *Yarrowia lipolytica*. *Trends Biotechnol.* **2016**, *34* (10), 798−809.
(105) Liu, H.; Ji, X.; Huang, H. Biotechnological applications of *Yarrowia lipolytica*: past, present and future. *Biotechnol. Adv.* **2015**, *33* (8), 1522−1546.
(106) Nybo, S. E.; Khan, N. E.; Woolston, B. M.; Curtis, W. R. Metabolic engineering in chemolithoautotrophic hosts for the production of fuels and chemicals. *Metab. Eng.* **2015**, *30*, 105−120.
(107) Davies, F. K.; Jinkerson, R. E.; Posewitz, M. C. Toward a photosynthetic microbial platform for terpenoid engineering. *Photosynth. Res.* **2015**, *123* (3), 265−284.

DOI: 10.1021/acs.jafc.7b00473
J. Agric. Food Chem. 2018, 66, 2247−2258

(108) Mackenzie, C.; Eraso, J. M.; Choudhary, M.; Roh, J. H.; Zeng, X.; Bruscella, P.; Puskás, Á.; Kaplan, S. Postgenomic adventures with *Rhodobacter sphaeroides*. *Annu. Rev. Microbiol.* **2007**, *61* (1), 283−307.
(109) Guan, Z.; Xue, D.; Abdallah, I. I.; Dijkshoorn, L.; Setroikromo, R.; Lv, G.; Quax, W. J. Metabolic engineering of *Bacillus subtilis* for terpenoid production. *Appl. Microbiol. Biotechnol.* **2015**, *99* (22), 9395−9406.
(110) Dunlop, M. J.; Dossani, Z. Y.; Szmidt, H. L.; Chu, H. C.; Lee, T. S.; Keasling, J. D.; Hadi, M. Z.; Mukhopadhyay, A. Engineering microbial biofuel tolerance and export using efflux pumps. *Mol. Syst. Biol.* **2011**, *7*, 487.
(111) Zerbe, P.; Bohlmann, J. Enzymes for synthetic biology of ambroxide-related diterpenoid fragrance compounds. *Adv. Biochem. Eng./Biotechnol.* **2015**, *148*, 427−447.
(112) Lange, B. M. Biosynthesis and biotechnology of high-value p-menthane monoterpenes, including menthol, carvone, and limonene. *Adv. Biochem. Eng./Biotechnol.* **2015**, *148*, 319−353.
(113) http://www.thegoodscentscompany.com (accessed Jan 1, 2017).
(114) *Common Fragrance and Flavor Materials: Preparation, Properties and Uses*, 6th ed.; Surburg, H., Panten, J., Eds.; Wiley-VCH, 2016.
(115) http://www.amyris.com (accessed Jan 20, 2017).
(116) http://www.evolva.com/products/valencene (accessed Jan 22, 2017).
(117) http://www.isobionics.com/index-Valencene.html (accessed Jan 22, 2017).
(118) http://www.isobionics.com/index-Nootkatone.html (accessed Jan 22, 2017).
(119) Huembelin, M.; Beekwilder, M. J.; Gerardus, J.; Kierkels, T. *Rhodobacter* for preparing terpenoids. WO2014014339A2, 2014.
(120) http://www.evolva.com/products/nootkatone-2 (accessed Jan 22, 2017).
(121) http://www.evolva.com/products/sandalwood/ (accessed Jan 20, 2017).
(122) http://www.isobionics.com/index-SandalwoodOil.html (accessed Jan 20, 2017).
(123) http://www.evolva.com/products/agarwood/ (accessed Jan 20, 2016).
(124) http://www.firmenich.com (accessed Jan 20, 2017).
(125) Tsuruta, H.; Lenihan, J. R.; Regintin, R. Production of isoprenoids. WO2009042070A2, 2009.
(126) http://www.isobionics.com/index-PatchouliOil.html (accessed Jan 20, 2017).
(127) http://investors.amyris.com/releasedetail.cfm?releaseid=748273 (accessed Jan 22, 2017).
(128) http://www.cosmeticsdesign-europe.com/Formulation-Science/Firmenich-announces-large-scale-production-of-Ambrox-using-White-Biotechnology (accessed Jan 22, 2017).
(129) http://www.evolva.com/personal-care/stevia/www.cargillfoods.com/na/en/products/sweeteners/specialty-sweeteners/eversweet/index.jsp (accessed Jan 22, 2017).

DOI: 10.1021/acs.jafc.7b00473
J. Agric. Food Chem. 2018, 66, 2247−2258

Chapter 3 - Identification of fungal limonene-3-hydroxylases for biotechnological menthol production

Florence M. Schempp, Ingmar Strobel, Maria M. W. Etschmann, Elena Bierwirth, Johannes Panten, Hendrik Schewe, Jens Schrader, Markus Buchhaupt

Type: research article
Status: submitted

Summary:
Many protein engineering strategies have already attempted to produce specific limonene-3-hydroxylases from bacterial cytochrome P450 monooxygenases. However, while these enzymes can be efficiently expressed in bacterial hosts, their selectivity is limited. In nature, a limonene-3-hydroxylation reaction can be catalyzed by an enzyme from the peppermint plant *Mentha* x *piperita*, a native producer of menthol, or from *Mentha spicata*. The only other described occurrence of limonene-3-hydroxylase activity in nature has been detected in a strain of the black yeast-like fungus *Hormonema* sp. in South Africa. However, the responsible enzyme is unknown.
By conducting biotransformation experiments, different other fungi were discovered that can hydroxylate limonene at carbon atom 3. Based on their genome sequences, by performing heterologous gene expression and biotransformation experiments in yeasts, two different fungal CYP proteins could be identified as novel limonene-3-hydroxylase enzymes, one from *Aureobasidium pullulans* and one from *Hormonema carpetanum*. Further characterization of both enzymes showed their potentials but also their limitations for application in biotechnological menthol production. In high-cell density biotransformation experiments with *Pichia pastoris* concentrations of up to 600 µM (+)-*trans*-isopiperitenol, corresponding to 90 mg L^{-1} concentrated yeast cell suspension, could be obtained with high regio- and stereoselectivity. However, apart from *trans*-isopiperitenol also one side product was formed in small quantities (ca. 10 % of total product amount). Thus, further improvements in regard to gene expression and protein engineering to improve regioselectivity are still necessary to make these enzymes usable for biotechnological applications.
In addition to the limonene-3-hydroxylase activity, the newly identified enzyme from *A. pullulans* was found to hydroxylate α- and β-pinene to verbenol and pinocarveol, respectively, as well as 3-carene into different products.

Declaration of author contributions to the manuscript:

Identification of fungal limonene-3-hydroxylases for biotechnological menthol production

Status: submitted

Contributing authors: **F. M. Schempp** (Doctoral candidate), I. Strobel, M. M. W. Etschmann, E. Bierwirth, J. Panten, H. Schewe, J. Schrader, M. Buchhaupt

What are the contributions of the doctoral candidate and his co-authors?

(1) Concept and design

F. M. Schempp	**50 %**
I. Strobel	15 %
M. M. W. Etschmann	15 %
H. Schewe	5 %
J. Schrader	5 %
M. Buchhaupt	10 %

(2) Conducting tests and experiments

F. M. Schempp	**58 %**	**cloning experiments, biotransformation experiments with *A. pullulans*, *S. cerevisiae* and *P. pastoris*, and analytics**
I. Strobel	20 %	biotransformation experiments and analytics with fungi, identification of CYP enzymes in fungal genome
M. M. W. Etschmann	15 %	biotransformation experiments and analytics with fungi, experiments with CYP inhibitors
E. Bierwirth	5 %	cloning experiments
J. Panten	2 %	analysis of selected biotransformation samples

(3) Compilation of data sets and figures

F. M. Schempp	**70 %**	**data collection and preparation of figures and tables**
I. Strobel	15 %	data collection
M. M. W. Etschmann	15 %	data collection

(4) Analysis and interpretation of data

F. M. Schempp	**58 %**	**analysis and interpretation of data**
I. Strobel	10 %	analysis and interpretation of data
M. M. W. Etschmann	10 %	analysis and interpretation of data
J. Panten	2 %	analysis of data
M. Buchhaupt	20 %	analysis and interpretation of data

(5) Drafting of manuscript

F. M. Schempp	**90 %**
M. Buchhaupt	10 %

Identification of fungal limonene-3-hydroxylases for biotechnological menthol production

Author list: Florence M. Schempp[a,b], Ingmar Strobel[a], Maria M. W. Etschmann[a], Elena Bierwirth[b], Johannes Panten[c], Hendrik Schewe[a], Jens Schrader[a], Markus Buchhaupt[a#]

Author's affiliations:
[a]*DECHEMA-Forschungsinstitut, Industrial Biotechnology, Frankfurt am Main, Germany*
[b]*Faculty Biological Sciences, Goethe University Frankfurt, Frankfurt am Main, Germany*
[c]*Symrise AG, S&C Innovations Technology Scouting, Holzminden, Germany*

[#]Address correspondence to Markus Buchhaupt, markus.buchhaupt@dechema.de

Running Head: Identification of fungal limonene-3-hydroxylases

Key words: menthol, fungal enzyme, terpenes, limonene, oxidation, hydroxylation, CYP, P450, biotechnology

Abstract

More than 30,000 tons of menthol are produced every year as a flavor and fragrance compound or as medical component. So far, only extraction from plant material or chemical synthesis is possible. A smart alternative approach for menthol production could be a biotechnological-chemical two-step conversion, starting from (+)-limonene, which is a side product of the citrus processing industry. The first step requires a limonene-3-hydroxylase (L3H) activity that specifically catalyzes hydroxylation of limonene at carbon atom 3. Several protein engineering strategies already attempted to create limonene-3-hydroxylases from bacterial cytochrome P450 monooxygenases (CYPs or P450s), which can be efficiently expressed in bacterial hosts. However, their regiospecificity is rather low, if compared to the highly selective L3H enzymes from the biosynthetic pathway towards menthol in *Mentha* species.

The only naturally occurring limonene-3-hydroxylase activity identified in microorganisms so far, was reported for a strain of the black yeast-like fungus *Hormonema* sp. in South Africa. We discovered different other fungi that can catalyze the intended reaction and identified potential CYP-encoding genes within the genome sequence of one of the strains. Using

heterologous gene expression and biotransformation experiments in yeasts, we were able to identify limonene-3-hydroxylases from *Aureobasidium pullulans* and *Hormonema carpetanum*. Further characterization of both enzymes showed their high stereospecificity and regioselectivity, their potential for limonene-based menthol production and their additional ability to convert α- and β-pinene to verbenol and pinocarveol, respectively.

Importance

(-)-Menthol is an important flavor and fragrance compound and furthermore has medicinal uses. To realize a two-step synthesis starting from renewable (+)-limonene, a regioselective limonene-3-hydroxylase enzyme is necessary.
We identified enzymes from two different fungi, which catalyze this hydroxylation reaction and represent an important module for the development of a biotechnological process for (-)-menthol production from renewable (+)-limonene.

Introduction

(-)-Menthol is a monocyclic monoterpene alcohol with an annual production volume of more than 30,000 tons (1). It is used as a flavor and fragrance compound, as cosmetics additive and as ingredient of pharmaceutical products, e.g. for the treatment of colds or burns (2). Menthol can either be extracted from the essential oil of *Mentha* plants or produced by various chemical processes. The technical synthesis of (-)-menthol is currently carried out using different processes at Symrise/Lanxess (from *m*-cresol), Takasago (from myrcene) and BASF (from citral) (2, 3). However, no biotechnological process for (-)-menthol production has been established so far. Since fossil resources are running out and the product yields from *Mentha* plantations are strongly dependent on changing climatic factors, biotechnological production processes based on renewable raw materials are an attractive alternative. A smart biotechnological menthol synthesis route could be a biotechnological-chemical two-step conversion (4), starting from (+)-limonene (Figure 1). Whereas the stereospecific hydrogenation of *trans*-isopiperitenol could be realized by chemical hydrogenation (4, 5), the conversion of (+)-limonene into *trans*-isopiperitenol requires a hydroxylating enzyme with high stereospecificity and regioselectivity for the carbon 3 position, a limonene-3-hydroxylase (L3H). Therefore, many protein engineering strategies have already attempted to create limonene-3-hydroxylases from bacterial cytochrome P450 monooxygenase (CYPs or P450s) (6-8). However, while these enzymes can be efficiently expressed in bacterial hosts, their regio- and stereoselectivity is limited.

In the peppermint plant *Mentha x piperita,* (-)-menthol is produced from (-)-limonene via a six-step metabolic pathway (9). The first enzyme of this pathway is a selective limonene-3-hydroxylase which is present in two slightly different forms encoded by CYP71D13 (PM17) and CYP71D15 (PM2) (10). As with other enzymes of the menthol pathway (2), several studies have been conducted to express PM17 heterologously in microbial hosts (11, 12), but resulted in rather low productivities.

Besides their occurrence in *Mentha* plants (2, 10, 13), the only other limonene hydroxylase activity with clear selectivity for carbon atom 3 was described for a strain of the black yeast-like fungus *Hormonema* sp. (UOFS Y-0067) (4). The cells were also found to hydroxylate α- and β-pinene. In the respective report, van Dyk and colleagues already suggested the potential use of the fungus for (-)-menthol production from (+)-limonene, but the responsible enzyme remained unknown and the results were not very reproducible. Therefore, they considered it unlikely “that it will ever be possible to base a commercial biotransformation process on an organism like this *Hormonema* sp.”(4)

In order to identify stereo- and regioselective limonene-3-hydroxylases in *Hormonema* or other fungi, we tested different related fungi for the respective conversion. After heterologous expression of many different CYP sequences in yeast, we identified a limonene-3-hydroxylase from *Aureobasidium pullulans* and also from *Hormonema carpetanum*. Subsequently, the enzymes were further characterized in detail regarding substrate and product selectivity.

Results

Hydroxylation capability of different dothideomycetes

In order to investigate if the limonene-3-hydroxylase activity of *Hormonema* sp. UOFS Y-0067 (4) is a common ability in the class of dothideomycetes, several fungi, including different *Hormonema* species, *Sydowia polyspora*, *Rhizosphaera kalkhoffii*, *Aureobasidium pullulans*, *Aureobasidium subglaciale*, *Neofusicoccum parvum*, *Ochroconis constricta* and *Parastagonospora nodorum,* were tested for (+)-limonene hydroxylation capabilities. All *Hormonema* and *Aureobasidium* species, as well as *Sydowia polyspora* and *Rhizosphaera kalkhoffii* were found to convert limonene into *trans*-isopiperitenol (Figure S1, Figure S2). Biotransformation experiments with CYP inhibitor clotrimazole (14) revealed a strong effect on product formation (Figure S3), indicating that the responsible enzyme belongs to the CYP protein family.

In the experiments *A. pullulans* CBS 100280 showed the highest *trans*-isopiperitenol production over time (Figure 2 A). Further analyses confirmed that *A. pullulans* CBS 100280 produces *trans*-isopiperitenol as main product in a limonene biotransformation reaction (Figure 2 B - D). Therefore, and because its genome sequence is available in the NCBI database, this strain was used to search for the respective hydroxylase enzyme.

In order to test if *A. pullulans* CBS 100280 is also able to hydroxylate other monoterpenes, as described by van Dyk and colleagues for *Hormonema* sp. UOFS Y-0067 (4), turpentine oil was added to a biotransformation experiment. Turpentine oil is, for example, produced as waste product during paper production. The oil used in the experiment contained mainly α-pinene, β-pinene, limonene, carene and other terpenoids (Figure S4 A, Figure S5 a). Bioconversion of turpentine oil by *A. pullulans* resulted in a large number of newly formed terpenes. Apart from so far unidentified peaks, among the most abundant products were verbenol and verbenone (Figure S4 B, Figure S5 b).

Identification of fungal limonene-3-hydroxylase enzymes

The genome sequence of *A. pullulans* CBS 100280 (EXF-150) (15), contains 53 genes encoding putative cytochrome P450 monooxygenases. These annotated CYPs from *A. pullulans* were clustered by means of multiple sequence alignment based on their protein sequences (Figure 3). By using the David Nelson's CYP database (16) the individual proteins were assigned into different families based on their protein sequence and named accordingly (Figure 3). Each family assumes characteristic functions, for instance, in regard to conversion and utilization of different metabolites, including those for the transformation of terpenes (CYP52, CYP530 and CYP65) (17).
Of the whole CYPome of *A. pullulans*, 16 sequences were chosen for expression in *Saccharomyces cerevisiae* (Figure 3 – green font, Table S2).

In addition to the potential CYPs, a gene encoding a putative CYP reductase enzyme was identified in the genome of *A. pullulans* (Table S2), by comparing protein sequences of known CYP reductases from other fungi with the genome of *A. pullulans.*

In an initial investigation, *S. cerevisiae* strains harboring the different CYP genes together with the putative CYP reductase were tested in a (+)-limonene biotransformation experiment. One strain led to a clearly increased *trans*-isopiperitenol concentration compared to the background product level of the strain containing the empty vectors (Figure 4, Figure S6). Therefore, we proposed the respective protein CYP65AH1 of *A. pullulans* (Ap) to be a limonene-3-hydroxylase, hereafter referred to as CYP65AH1.Ap or L3H.Ap.

In order to identify further limonene-3-hydroxylase enzymes in the genome of *A. pullulans* and *H. carpetanum*, additional putative CYP genes of both fungi were selected based on the amino acid sequence identity to CYP65AH1.Ap. Thereby, CYP65Z1, CYP65AM4 and CYP65AK1 from *A. pullulans* (Ap) and CYP65AH1 from *H. carpetanum* (Hc) were chosen for further tests (Figure S7 A). The CYP65AH1.Hc gene sequence was identified by analysis of partial genome data of *H. carpetanum* CBS 115712. The amino acid sequence identity between CYP65AH1.Ap (L3H.Ap) and CYP65AZ1.Ap, CYP65AM4.Ap, CYP65AK1.Ap or CYP65AH1.Hc, is about 53 %, 33 %, 41 % and 52 %, respectively. Whereas no limonene conversion could be observed in the biotransformation experiments with CYP65AZ1.Ap, CYP65AM4.Ap and CYP65AK1.Ap (data not shown), *trans*-isopiperitenol could be detected in biotransformation samples with the yeast strain expressing CYP65AH1.Hc (Figure S7 B), further referred to as L3H.Hc.

Further characterization of limonene-3-hydroxylase abilities of L3H.Ap

In order to obtain higher protein amounts to further characterize the limonene-3-hydroxylase enzyme CYP65AH1 of *A. pullulans* (L3H.Ap), we tried to express the protein and several variants in *E. coli*. After all attempts to express the protein in a functional form with *E. coli* failed, we tested expression in the eukaryotic host *Pichia pastoris* (18). For this purpose, two different vector systems were applied. Whereas one of the used vectors is an episomal plasmid with constitutive expression (pBSYA1Z), the pPICZA vector is integrated into the genome of *P. pastoris* and expression of the CYP is induced by methanol addition. As negative control, the cells were transformed with the respective empty expression vector. Furthermore, PM17 from *Mentha x piperita,* codon-optimized for *P. pastoris* (12), was used as a reference.

The experiments showed that with both vector systems higher amounts of *trans*-isopiperitenol were produced from (+)-limonene with L3H.Ap of *A. pullulans* than with PM17 from *Mentha* x *piperita* (Figure 5 A, Figure S8). The maximum *trans*-isopiperitenol concentration obtained in our experiments was around 300 µM (45 mg L^{-1}) in the concentrated yeast cell suspension with constitutive gene expression from the episomal vector.

Apart from *trans*-isopiperitenol, *p*-1,8-menthadien-4-ol could be detected in the limonene biotransformation reactions with L3H.Ap (Figure 5 B - D, Figure S8). However, the peak area of produced *trans*-isopiperitenol is around 10 times larger than the *p*-1,8-menthadien-4-ol peak area. Small *p*-1,8-menthadien-4-ol peaks could be also identified in the limonene biotransformation experiments with *A. pullulans* cultures (Figure 2, retention time (Rt.) 13.4 min) and *S. cerevisiae* cells harboring the fungal L3H enzyme (Figure S6, Rt. 8.2 min).

Further oxidation of the formed *trans*-isopiperitenol or *p*-1,8-menthadien-4-ol was not observed (Figure S8).

When comparing both limonene enantiomers, higher product peaks were obtained with (+)-limonene than with (-)-limonene in a biotransformation experiment with the L3H.Ap-expressing strain (Figure 5 B, Figure S8, Figure S9). PM17 showed an inverse preference (Figure 5 B, Figure S8, Figure S9).
Unexpectedly, when (-)-limonene was used as reactant several different products were formed (Figure S9). However, this could be observed with all strains, harboring the empty vector, L3H.Ap or PM17 from *Mentha* x *piperita,* to a similar extent. The exceptions were *trans*-isopiperitenol, carveol and *p*-1,8-menthadien-4-ol, which slightly differed in the formed quantities between the strains (Figure 5 B).

Alteration of different parameters to optimize the biotransformation process yielded higher *trans*-isopiperitenol amounts and in relation to this reduced side product formation. Beneficial modifications were the alteration of the pH of the biotransformation buffer from 6.0 to 7.4 (Figure S10 A), and increased oxygen supply by upscaling of the reaction vessel (Figure S10 B). With these parameters a maximum concentration of around 600 µM (ca. 90 mg L^{-1} concentrated yeast cell suspension) *trans*-Isopiperitenol could be obtained.

L3H.Ap can hydroxylate α-pinene, β-pinene and 3-carene

To further assess the substrate selectivity of L3H.Ap *in vivo*, other reactants were tested in biotransformation experiments (Table 1). While no products could be detected with γ-terpinene, α-phellandrene, toluene, 1-phenylethanol and 2-phenylethlyalcohol, we observed hydroxylation of 3-carene, α-pinene and β-pinene (Table 1, Figure 6, Figure S11 - Figure S14). The oxygenated monoterpene products were not, or only to a lesser extent, detected in experiments with the empty vector control.

Discussion

In this work, we described two fungal CYP enzymes which can oxidize (+)-limonene at carbon atom 3, resulting in *trans*-isopiperitenol. Based on the protein sequence both enzymes, L3H.Ap and L3H.Hc, belong to the cytochrome P450 monooxygenase family of CYP65, which includes other fungal terpene hydroxylation enzymes described before (17). In contrast to L3H.Ap and L3H.Hc, no limonene hydroxylation activity was detected for CYP65AZ1.Ap, CYP65AM4.Ap and CYP65AK1.Ap as well as all other tested CYP candidate

genes. This could either mean that these enzymes are unable to catalyze the desired reaction or that they are not functionally expressed in the yeast cells under the used conditions. In addition, since CYP enzymes are known to require suitable reductase enzymes for their functionality (19), it is also possible that the CYP reductase provided in the yeast strains is not sufficient. However, for overall CYP activity the redox partners can play a significant role (20). Furthermore, it is described that the type of co-expressed CYP reductase can even influence the product spectrum (21).

The newly discovered limonene-3-hydroxylase from *A. pullulans* shows high stereospecificity and regioselectivity of the catalyzed reaction. Only small amounts (< 10 %) of the side product *p*-1,8-methadien-4-ol were produced from (+)-limonene by *P. pastoris* cells expressing L3H.Ap. Although some P450cam variants with selectivity preference for production of isopiperitenol from (-)-limonene were described (6), the selectivity was lower than that of the fungal enzyme, if (+)-limonene was used as substrate (7). So far, the only highly specific limonene-3-hydroxylase enzymes are known to occur in *Mentha* plants (2, 10, 13). In peppermint, for example, PM17 catalyzes the key hydroxylation during the (-)-menthol biosynthesis pathway. In literature PM17 is described to convert (-)-limonene and (+)-limonene exclusively into the respective *trans*-isopiperitenols (22). However, in experiments with microsomal preparations from the epidermal oil glands (trichomes) of *Mentha* x *piperita* the (-)-isomer was favored by a factor of 2 over the (+)-enantiomer (23). Our results with *P. pastoris* cells indicate that the fungal L3H.Ap enzyme shows a reversed preference, which would be beneficial for the intended process using (+)-limonene from the citrus industry as starting material.
Although the physiological function of the limonene-3-hydroxylases in *A. pullulans*, *H. carpetanum* and other fungi is unclear, one can assume a role in modification/detoxification or utilization of monoterpenes produced by plants, which are colonized by such fungi (24). One would generally expect enzymes with high turnover numbers to carry out respective functions. However, since we did not investigate the protein concentrations in the cells, no conclusions about the differences of catalytic properties and substrate selectivity between the fungal enzymes and the peppermint limonene-3-hydroxylase are possible so far. In addition, as mentioned before, low CYP activity can also be caused by the absence of a suitable reductase enzyme. In order to be able to reliably compare the fungal enzymes with the plant protein, this interaction would also have to be optimized in further experiments.

The yields of *trans*-isopiperitenol produced with *P. pastoris* cells are still low, reaching only up to around 90 mg L^{-1} of product in the concentrated cell suspension after around 24 h.

Higher *trans*-isopiperitenol concentrations have already been reported for biotransformations with yeast cells expressing PM17 from peppermint (12). However, in our setup, using a different strain as well as a different CYP reductase, the *P. pastoris* strain expressing the fungal CYP enzyme L3H.Ap produced higher amounts of (+)-*trans*-isopiperitenol than the respective PM17-expressing strain.

Apart from producing *trans*-isopiperitenol, it was found that L3H.Ap can also hydroxylate α- and β-pinene as well as 3-carene. The reactions delivered verbenol, verbenone, pinocarveol and *p*-1,5-menthadien-8-ol as main products. In the case of α-pinene, the oxidation of verbenol to verbenone might be either caused by L3H activity or by unspecific dehydrogenase activity present in yeast. The production of verbenol and verbenone from α-pinene in the same organism has already been described for bacteria as well as fungi and plant cells (6, 7, 25–28). More knowledge about the three-dimensional properties of the substrate-binding pocket of the CYP enzyme is required to fully understand CYP regioselectivity.

The activity of L3H.Ap on substrates other than limonene is in accordance with the conversion of α- and β-pinene by *Hormonema* sp. (4). However, while van Dyk and colleagues (1998) could also detect verbenol and verbenone as products of the α-pinene biotransformation experiment, β-pinene was converted to pinocamphone and 3-hydroxy-pinocamphone with *Hormonema* sp. (4). In addition to their experiments, oxidation of α- and β-pinene to several products, including verbenol, verbenone and pinocarveol, has been also reported for other fungi (4, 28, 29). Moreover, Chiu and colleagues recently described a CYP enzyme from mountain pine beetle that can hydroxylate α- and β-pinene as well as 3-carene (30). However, for this enzyme of the CYP6 family no activity on limonene isomers was detected. Furthermore, bacterial enzyme variants are known that can use carene, α-pinene or β-pinene as substrates, which are, however, converted into a variety of different products (7).

In this work we described the identification of two fungal limonene-3-hydroxylases that can hydroxylate both limonene enantiomers with high stereospecificity and regioselectivity, but also convert 3-carene, α-pinene and β-pinene. By the use of yeasts expressing the CYP enzymes, novel catalysts for the conversion of (+)-limonene into (+)-*trans*-isopiperitenol could be provided that could become part of a (-)-menthol production process. Further investigations on their catalytic properties as well as optimization of cellular expression will be necessary to assess the full potential of the fungal CYP enzymes for biotechnological terpene conversions.

Materials and methods

Chemicals and media

All chemicals were purchased from Merck KGaA (Germany), previously Sigma-Aldrich (Germany) or Merck Millipore (Germany), or Carl-Roth (Germany) with different purities: (+)-limonene (≥ 99 %), (-)-limonene (≥ 99 %), α-pinene (≥ 98 %), (-)-β-pinene (≥ 99 %), γ-terpinene (≥ 98.5 %), α-phellandrene (≥ 95 %), 3-carene (≥ 98.5 %), 1-phenylethanol (≥ 98 %), 2-phenylethylalcohol (≥ 99 %), (-)-carveol (97 %), (-)-*trans*-pinocarveol (≥ 96 %), (*S*)-*cis*-verbenol (≥ 95 %), (1*S*)-(-)-verbenone (≥ 99 %).
In addition, a 2:1 mixture of (+)-*trans*- and *cis*-isopiperitenol, and turpentine oil was obtained from the company SYMRISE (Germany).

Fungi, except *S. cerevisiae* and *P. pastoris,* were grown in yeast extract/malt extract (YM) medium (3 g L^{-1} yeast extract, 20 g L^{-1} malt extract, 10 g L^{-1} peptone, 10 g L^{-1} glucose) (31). *S. cerevisiae* strains were cultivated in yeast extract peptone (YEP) medium (10 g L^{-1} yeast extract, 20 g L^{-1} peptone) or synthetic complete (SC) medium (6.7 g L^{-1} yeast nitrogen base without amino acids with ammonium sulfate, and amino acid supplements (32)). SC medium pH was adjusted to 6.3 with potassium hydroxide. If needed for selection of plasmids, medium without uracil and L-tryptophan was used. 20 g L^{-1} glucose were added as carbon source.
P. pastoris strains were cultured in YPD, YPDS, BMDY (BMGY with glucose instead of glycerol) or BMMY media according to the *EasySelect™Pichia Expression Kit* manual (Invitrogen) and Weis *et al.* (2004) (33).
E. coli was cultured in lysogeny broth (LB) medium (10 g L^{-1} tryptone, 5 g L^{-1} yeast extract and 5 g L^{-1} NaCl) or terrific broth (TB) medium (24 g L^{-1} yeast extract, 12 g L^{-1} tryptone, 5 g L^{-1} glycerol and 89 mM potassium phosphate buffer).
Antibiotics were added in the following concentrations, if required: ampicillin (Amp) 100 µg mL^{-1}, Zeocin™ (Zeo) 25 - 50 µg mL^{-1} (*E. coli)* or 100 – 500 µg mL^{-1} (*P. pastoris)*.
For solid media 17 - 20 g L^{-1} agar-agar were added.

Investigation of different fungi for limonene-3-hydroxylase activity

All strains tested for limonene-3-hydroxylase activity are listed in Table S1.
Biotransformation experiments with different *Hormonema* species and close relatives (Figure S1) were conducted following a protocol by van Rensburg and colleagues (31). From 20 mL-pre-cultures in 100 mL-Erlenmeyer flasks, 50 mL-main cultures in 300 mL-flasks were inoculated and incubated at 200 rpm (orbit: 2.5 cm) and 20 °C. For biotransformation, 2 g L^{-1} limonene were added to cultures grown for 48 h. To test if the expression of limonene hydroxylating enzymes can be induced by limonene, 100 mg L^{-1} limonene were added 24 h

after inoculation to the respective pre-cultures. After 120 - 144 h of biotransformation, samples of 700 µL were extracted with the same volume of ethyl acetate, containing 50 mg L^{-1} 3-carene as internal standard. Samples were analyzed via GC-FID.
For the biotransformation experiments with *H. carpetanum* under the influence of CYP inhibitor clotrimazole, cells of 48 h old cultures of *H. carpetanum* CBS 115712 were harvested, resuspended in citrate buffer (100 mM, pH 4.5), and limonene as well as different concentrations of clotrimazole (0, 10, 20, 30, 40 µM) were added. After 14 h of biotransformation, samples were taken, extracted with ethyl acetate and analyzed via GC-FID.
In order to test the different dothideomycetes for limonene-3-hydroxylase activities (Figure S2), flasks with 25 ml YM medium were inoculated from a 48 – 86 h old pre-culture and incubated for 48 h at 24 – 27 °C and 120 - 150 rpm (orbit: 2.5 cm). For the biotransformation experiment, 1 g L^{-1} (+)-limonene was added. 700 µL samples were taken from the reactions over a period of 5 - 7 hours (once per hour). Samples were extracted with one volume ethyl acetate and the *trans*-isopiperitenol amount was determined by GC-MS analysis. As negative control YM medium without cells was used.
For biotransformation experiments with turpentine oil, 100 mL YM medium in shake flasks were inoculated with *A. pullulans* CBS 100280 as described above and incubated for 48 h at 27 °C and 140 rpm (orbit: 2.5 cm). Afterwards 170 mg L^{-1} turpentine oil was added. After another 24 and 96 h, the same quantity was added again. 136 h after the first addition of turpentine oil, 5 ml of cell culture was extracted with ½ volume of ethyl acetate and product spectrum analyzed via GC-MS.

Clustering of fungal cytochrome P450 monooxygenase sequences

The protein sequences of all 53 putative CYP enzymes from *A. pullulans* were clustered in a phylogenetic tree with the software *Geneious* (Biomatters Ltd., New Zealand) using default settings (Geneious tree builder, Global alignment, cost matrix: Blosum 62, genetic distance model: Jukes-Cantor, tree built method: neighbor-joining, no outgroup, gap open penalty: 12, gap extension penalty: 3).

Construction of fungal CYP gene expression vectors and yeast strains

All yeast and *E. coli* strains, plasmids and oligonucleotides used in this study are listed in Table S1.
cDNA sequences of selected CYP genes from *A. pullulans* EXF-150 (CBS 100280) were obtained through comparison between gene and protein sequence, stored in the NCBI database (accession numbers see Table S2). For synthesis of template cDNA, *A. pullulans* CBS 100280 cells were inoculated in 25 mL YM medium in a 100 mL shake flask. After

incubation for 24 h at 28 °C and 130 rpm (orbit: 2.5 cm), 100 mg L^{-1} (+)-limonene was added and incubated for further 24 h. Afterwards, cells were harvested, and total RNA isolated with *RNAeasy Plant MiniKit* (Qiagen) according to manufacturer's instructions. cDNA synthesis was performed with *iScript™ Select cDNA Synthesis Kit* (Biorad) using oligo(dT) primers. Afterwards, cDNAs of CYP genes were amplified via PCR. All expression plasmids used in this study were either constructed by the company BioCat GmbH (Germany) or constructed using Gibson isothermal assembly cloning (34, 35). *E. coli* cells were grown at 37 °C. Plasmids were isolated from *E. coli* using the *GeneJET Plasmid Miniprep Kit* (ThermoFisher Scientific).

S. cerevisiae and *P. pastoris* strains were transformed with plasmids according to protocols of Gietz *et al.* (36, 37) or the *EasySelect™Pichia Expression Kit* manual (Invitrogen). Yeast cells were grown at 30 °C on SC selective medium or YPD containing Zeocin™.

Investigation of fungal CYP candidates for limonene-3-hydroxylation in *S. cerevisiae*

For biotransformation experiments with *S. cerevisiae* a protocol based on publications by Emmerstorfer *et al.* was used (12, 38). *S. cerevisiae* CEN-PK2-1C strains, containing different pPK245 and pPK448 expression vectors (see Table S1), were grown on SC medium agar plates for 2 - 3 days. For initial testing of different CYP genes (Figure 4), 5 ml pre-cultures were inoculated and grown over night at 30 °C. Overnight cultures were used to inoculate 50 mL of SC medium in 300 mL Erlenmeyer flasks to an OD_{600} of 0.1 and cells were cultivated for 48 h at 130 rpm (orbit: 2.5 cm) and 30 °C. From these cultures, 150 OD_{600} units were harvested (2,381 x g, 5 min) and resuspended in 350 µL of 50 mM potassium phosphate buffer (pH 7.4). Cell suspensions were then transferred into 2 mL glass vials and 300 mM (+)-limonene stock solution (in DMSO with 1 % Triton® X-100) was added to yield a final limonene concentration of 6 mM. Glass vials were sealed loosely with screw caps and seal tape. Biotransformation was carried out for 16 h at 900 rpm (orbit: 2 - 3 mm) and 30 °C in a tabletop thermo shaker. Terpenoids were extracted with 250 µl of ethyl acetate. After phase separation by centrifugation for 15 min at 2,720 x g, organic layers were analyzed via GC-MS.

Since in these experiments with *S. cerevisiae* it was found that L3H.Ap can work with a native yeast CYP reductase, the putative CYP reductase enzyme from *A. pullulans* was no longer co-expressed from the pPK448 vector backbone in the following experiments with *S. cerevisiae* and *P. pastoris*.

For experiments with *H. carpetanum* CYP65AH1, main cultures were inoculated directly with a pin-head sized colony of yeast from agar plate and incubated for a total of 67 h at 30 °C and 180 rpm (orbit: 2.5 cm). After 48 h, cells were fed with 1 % glucose. From stationary

phase cultures 150 OD_{600} units were harvested and resuspended in 500 µL of 100 mM potassium phosphate buffer. After addition of (+)-limonene to a final concentration of 6 mM, biotransformation reactions were incubated for 25 h at 30 °C and 900 rpm (orbit: 2 – 3 mm). For GC-MS analysis, cell suspensions were extracted with 250 µl methyl *tert*-butyl ether (MTBE) containing 50 µM 3-carene as internal standard. CEN-PK2-1C strains containing the respective empty expression vector were used as negative controls.

Biotransformation experiments with *Pichia pastoris*

An approach modified after Emmerstorfer *et al*. and Weis *et al.* was used (12, 33, 38). *P. pastoris* X-33 strains, containing different pBSYA1Z or pPICZA expression plasmids (see Table S1), were grown on YPD or BMDY medium agar plates containing 100 or 500 µg mL^{-1} Zeocin™ for 2 - 3 days at 30 °C. 25 mL BMDY medium in a 300 mL Erlenmeyer flask was inoculated directly with a pin-head sized colony of *P. pastoris* and incubated for around 24 h at 29 - 30°C and 200 rpm (orbit: 2.5 cm). Afterwards 25 ml BMDY or BMMY medium was added to cultures with pBSYA1Z or pPICZA plasmids, respectively. 24 h later, 1 % glucose was added to strains with pBSYA1Z vectors. Strains with pPICZA plasmids were fed two or three times with 1 % methanol. 150 or 225 OD_{600} units from the 72 - 76 h old cultures were harvested (2,381 x g, 5 min) and resuspended in 375 or 500 µL of 100 mM potassium phosphate buffer (pH 6.0 or 7.4). Cell suspensions were then transferred into 2 mL glass vials and 300 mM (+)- or (-)-limonene stock solution (in DMSO with 1 % of Triton® X-100) was added to yield a final concentration of 6 mM limonene. Glass vials were sealed loosely with screw caps and seal tape. Biotransformation was carried out for 24 h at 900 rpm (orbit: 2 – 3 mm) at 28 - 30°C in a tabletop thermo shaker. Terpenoids were extracted with 250 µL MTBE containing 100 µM 3-carene as internal standard. After phase separation by centrifugation for 15 min at 16,000 x g, organic layers were analyzed via GC-MS.

For experiments in 100 mL reaction vessels, for each biotransformation batch 2250 OD_{600} units were harvested (2,381 x g, 5 min) and resuspended in 5 mL of 100 mM potassium phosphate buffer (pH 6.0). If glucose was added to the biotransformation reaction, 4.25 mL of buffer and 0.75 mL of a 20 % glucose solution were used. The cell suspensions were transferred to 100 mL glass bottles and limonene stock solution was added to a final concentration of 6 mM limonene. The vessels were tightly closed with screw caps and Parafilm®. The glass bottles were incubated for 24.8 h in a cabinet incubator at 30 °C and 250 rpm (orbit: 2.5 cm). Samples of 750 µl were taken at 1.5, 3, 16.5 and 24.8 h and extracted as described for the other *Pichia* samples. Some batches were kept closed throughout the experiment without sampling to make sure that no *trans*-isopiperitenol evaporates.

P. pastoris strains containing the respective empty expression vectors were used as negative controls in all experiments.

To quantify the produced *trans*-isopiperitenol amounts, stock solutions of isopiperitenol (2:1-mixture of *trans* and *cis*) with different concentrations were added to cell suspension aliquots of a *P. pastoris* strain, containing the empty pBSYA1Z vector, and extracted in the same way with MTBE as the biotransformation samples.

For the bioconversion experiments with substrates other than (+)- and (-)-limonene, the different substances (see Table 1) were dissolved in DMSO with 1 % of Triton® X-100 and added to the biotransformation reactions to give a final concentration of 6 mM. Only in the case of isopiperitenol (2:1-mixture of *trans* and *cis*), 0.6 µM were used. Biotransformation samples were extracted as described, but without internal standard.

GC-MS analysis

Extracts from biotransformation experiments with *Hormonema* cultures and related fungi were analyzed using a GC-17A (Shimadzu) system with FID, containing a DB-WAXetr (extended temperature range) column (30 m x 0.25 mm x 0.25 µm, Agilent, former J&W Scientific). Measurements were conducted as follows: helium as carrier gas, split ratio 10, injection at 200 °C with a sample volume of 3 µl and a column flow of 1.2 mL min^{-1}. The column temperature was programmed as follows: 60 °C for 3 minutes, with 10 °C min^{-1} up to 200 °C followed by 3 min at 200 °C.

For GC-MS analysis of other fungi biotransformation samples, except *S. cerevisiae* and *P. pastoris,* a GC-17A QP5050A system (Shimadzu) with a VB-5 column (30 m x 0.25 mm x 0.25 µm, ValcoBond®, Valco Instruments Co. Inc. and VICI AG) or a GCMS-QP2010 SE system (Shimadzu) containing a DB-5 column (30 m x 0.25 mm x 0.25 µm, Agilent) was used. Measurements were conducted as follows: helium as carrier gas, split ratio 10, injection at 250 °C with a sample volume of 1 µl, a column flow of 1.2 mL min^{-1} and a linear velocity of 39.2 cm s^{-1}. The column temperature was programmed as follows: 60 ˚C for 3 min, with 10 °C min^{-1} up to 240 °C followed by 3 min at 240 °C.

Samples of biotransformation experiments with *S. cerevisiae* and *P. pastoris* were analyzed by a GCMS-QP2010 SE (Shimadzu) system containing a DB-5 column (30 m x 0.25 mm x 0.25 µm, Agilent). Measurements were conducted as follows: helium as carrier gas, split ratio 1 or 5, injections at 270 °C, column flow of 0.7 mL min^{-1} and a linear velocity of 30 cm s^{-1}. The column temperature was programmed as follows: 40 °C, 9 °C min^{-1} up to 175 °C followed by 30 ˚C min^{-1} up to 300 °C.

trans-Isopiperitenol, carveol, verbenol, verbenone and pinocarveol were identified by comparison of retention times and mass-spectra with those of chemically synthesized reference substances. *p*-1,8-menthadien-4-ol and *p*-1,5-menthadien-8-ol and other products were identified by comparison of mass-spectra to those of the NIST mass spectral library (v14) or the *MassLib* mass spectral library (Symrise Holzminden, V9.4 0). Identity was assumed if the similarity index was equal to or higher than 90 %. Absolute concentrations of *trans*-isopiperitenol were calculated from chromatogram peak areas by comparison to a calibration curve prepared by measuring a dilution series of isopiperitenol reference substance with known concentrations.

Acknowledgments

This research was supported by funds of the Federal Ministry of Food and Agriculture (BMEL) based on a decision of the Parliament of the Federal Republic of Germany via the Fachagentur Nachwachsende Rohstoffe e.V. (FNR, FKZ 22030615) under ERA-NET, funded from the European Union's Seventh Research Framework Program (ERA IB-2, 6th call, project BioProMo), by funds of the Federal Ministry of Education and Research (BMBF, FKZ 0315810, BioIndustrie2021) and by the LOEWE project AROMAplus of the State of Hessen (Germany).

Author Contributions

F.M.S, I.S., M.M.W.E., H.S., J.S. and M.B designed the research. F.M.S, I.S., M.M.W.E. and E.B. performed the experiments. J.P. contributed reagents and analysis tools. F.M.S, I.S., M.M.W.E., J.P. and M.B. analyzed the data. F.M.S. and M.B. wrote the manuscript with input from all authors.

We declare we have no conflicts of interest regarding the content of this article.

References

1. Kamatou GPP, Vermaak I, Viljoen AM, Lawrence BM. 2013. Menthol: A simple monoterpene with remarkable biological properties. Phytochemistry 96:15–25.
2. Lange BM. 2015. Biosynthesis and Biotechnology of High-Value *p*-Menthane Monoterpenes, Including Menthol, Carvone, and Limonene. Adv Biochem Eng Biotechnol 148:319–353.
3. Schäfer B. 2013. Menthol. Chemie unserer Zeit 47:174–182.
4. van Dyk MS, van Rensburg E, Moleleki N. 1998. Hydroxylation of (+)limonene, (−)alpha-pinene and (−)beta-pinene by a *Hormonema* sp. Biotechnol Lett 20:431–436.
5. van Dyk MS, van Rensburg E, Rensburg IPB, Moleleki N. 1998. Biotransformation of monoterpenoid ketones by yeasts and yeast-like fungi. J Mol Catal B Enzym 5:149–154.
6. Bell SG, Sowden RJ, Wong L-L. 2001. Engineering the haem monooxygenase cytochrome P450cam for monoterpene oxidation. Chem Commun 635–636.
7. Hernandez-Ortega A, Vinaixa M, Zebec Z, Takano E, Scrutton NS. 2018. A Toolbox for Diverse Oxyfunctionalisation of Monoterpenes. Sci Rep 8:14396.
8. Seifert A, Vomund S, Grohmann K, Kriening S, Urlacher VB, Laschat S, Pleiss J. 2009. Rational design of a minimal and highly enriched CYP102A1 mutant library with improved regio-, stereo- and chemoselectivity. ChemBioChem 10:853–861.
9. Croteau RB, Davis EM, Ringer KL, Wildung MR. 2005. (−)-Menthol biosynthesis and molecular genetics. Naturwissenschaften 92:562–577.
10. Lupien S, Karp F, Wildung M, Croteau R. 1999. Regiospecific cytochrome P450 limonene hydroxylases from mint (*Mentha*) species: cDNA isolation, characterization, and functional expression of (-)-4S-limonene-3-hydroxylase and (-)-4S-limonene-6-hydroxylase. Arch Biochem Biophys 368:181–192.
11. Haudenschild C, Schalk M, Karp F, Croteau R. 2000. Functional expression of regiospecific cytochrome P450 limonene hydroxylases from mint (*Mentha* spp.) in *Escherichia coli* and *Saccharomyces cerevisiae*. Arch Biochem Biophys 379:127–136.
12. Emmerstorfer A, Wimmer-Teubenbacher M, Wriessnegger T, Leitner E, Müller M, Kaluzna I, Schürmann M, Mink D, Zellnig G, Schwab H, Pichler H. 2015. Over-expression of ICE2 stabilizes cytochrome P450 reductase in *Saccharomyces cerevisiae* and *Pichia pastoris*. Biotechnol J 10:623–635.
13. Lücker J, Schwab W, Franssen MCR, van der Plas LHW, Bouwmeester HJ, Verhoeven HA. 2004. Metabolic engineering of monoterpene biosynthesis: two-step production of (+)-*trans*-isopiperitenol by tobacco. Plant J 39:135–145.
14. Sheets JJ, Mason JI, Wise CA, Estabrook RW. 1986. Inhibition of rat liver microsomal cytochrome P-450 steroid hydroxylase reactions by imidazole antimycotic agents. Biochem Pharmacol 35:487–91.
15. Gostinčar C, Ohm RA, Kogej T, Sonjak S, Turk M, Zajc J, Zalar P, Grube M, Sun H, Han J, Sharma A, Chiniquy J, Ngan C, Lipzen A, Barry K, Grigoriev I V, Gunde-Cimerman N. 2014. Genome sequencing of four *Aureobasidium pullulans* varieties: biotechnological potential, stress tolerance, and description of new species. BMC Genomics 15:549.
16. Nelson DR. 2009. The cytochrome p450 homepage. Hum Genomics 4:59–65.
17. Kimura M, Tokai T, Takahashi-Ando N, Ohsato S, Fujimura M. 2007. Molecular and genetic studies of *Fusarium trichothecene* biosynthesis: Pathways, genes, and evolution. Biosci Biotechnol Biochem 71:2105–2123.
18. van Wyk N, Kroukamp H, Pretorius I. 2018. The Smell of Synthetic Biology: Engineering Strategies for Aroma Compound Production in Yeast. Fermentation 4:54.
19. Pateraki I, Heskes AM, Hamberger B. 2015. Cytochromes P450 for Terpene Functionalisation and Metabolic Engineering. Adv Biochem Eng Biotechnol 148:107–139.

20. Hussain R, Ahmed M, Khan TA, Akhter Y. 2020. Fungal P450 monooxygenases - the diversity in catalysis and their promising roles in biocontrol activity. Appl Microbiol Biotechnol 104:989–999.
21. Bernhardt R, Urlacher VB. 2014. Cytochromes P450 as promising catalysts for biotechnological application: chances and limitations. Appl Microbiol Biotechnol 98:6185–6203.
22. Wüst M, Little DB, Schalk M, Croteau R. 2001. Hydroxylation of Limonene Enantiomers and Analogs by Recombinant (−)-Limonene 3- and 6-Hydroxylases from Mint (*Mentha*) Species: Evidence for Catalysis within Sterically Constrained Active Sites. Arch Biochem Biophys 387:125–136.
23. Karp F, Mihaliak CA, Harris JL, Croteau R. 1990. Monoterpene biosynthesis: specificity of the hydroxylations of (-)-limonene by enzyme preparations from peppermint (*Mentha piperita*), spearmint (*Mentha spicata*), and perilla (*Perilla frutescens*) leaves. Arch Biochem Biophys 276:219–26.
24. Wang Y, Lim L, Madilao L, Lah L, Bohlmann J, Breuil C. 2014. Gene Discovery for Enzymes Involved in Limonene Modification or Utilization by the Mountain Pine Beetle-Associated Pathogen *Grosmannia clavigera*. Appl Environ Microbiol 80:4566–4576.
25. Bell SG, Chen X, Sowden RJ, Xu F, Williams JN, Wong LL, Rao Z. 2003. Molecular recognition in (+)-α-pinene oxidation by cytochrome P450cam. J Am Chem Soc 125:705–714.
26. Lindmark-Henriksson M, Isaksson D, Sjödin K, Högberg H-E, Vaněk T, Valterová I. 2003. Transformation of α-Pinene Using *Picea abies* Suspension Culture. J Nat Prod 66:337–343.
27. Vanek T, Halík J, Vanková R, Valterová I. 2005. Formation of *trans*-verbenol and verbenone from alpha-pinene catalysed by immobilised *Picea abies* cells. Biosci Biotechnol Biochem 69:321–5.
28. Vespermann KAC, Paulino BN, Barcelos MCS, Pessôa MG, Pastore GM, Molina G. 2017. Biotransformation of α- and β-pinene into flavor compounds. Appl Microbiol Biotechnol 101:1805–1817.
29. Busmann D, Berger RG. 1994. Conversion of myrcene by submerged cultured basidiomycetes. J Biotechnol 37:39–43.
30. Chiu CC, Keeling CI, Bohlmann J. 2019. The cytochrome P450 CYP6DE1 catalyzes the conversion of α-pinene into the mountain pine beetle aggregation pheromone *trans*-verbenol. Sci Rep 9:1477.
31. van Rensburg E, Moleleki N, van der Walt JP, Botes PJ, van Dyk MS. 1997. Biotransformation of (+)limonene and (-)piperitone by yeasts and yeast-like fungi. Biotechnol Lett 19:779–782.
32. Bruder S, Reifenrath M, Thomik T, Boles E, Herzog K. 2016. Parallelised online biomass monitoring in shake flasks enables efficient strain and carbon source dependent growth characterisation of *Saccharomyces cerevisiae*. Microb Cell Fact 15:127.
33. Weis R, Luiten R, Skranc W, Schwab H, Wubbolts M, Glieder A. 2004. Reliable high-throughput screening with *Pichia pastoris* by limiting yeast cell death phenomena. FEMS Yeast Res 5:179–89.
34. Gibson DG, Young L, Chuang R-Y, Venter JC, Hutchison CA, Smith HO. 2009. Enzymatic assembly of DNA molecules up to several hundred kilobases. Nat Methods 6:343–345.
35. Inoue H, Nojima H, Okayama H. 1990. High efficiency transformation of *Escherichia coli* with plasmids. Gene 96:23–8.
36. Gietz RD, Schiestl RH. 2007. High-efficiency yeast transformation using the LiAc/SS carrier DNA/PEG method. Nat Protoc 2:38–41.
37. Gietz RD, Schiestl RH. 2007. Frozen competent yeast cells that can be transformed with high efficiency using the LiAc/SS carrier DNA/PEG method. Nat Protoc 2:1–4.
38. Emmerstorfer-Augustin A, Pichler H. 2016. Production of Aromatic Plant Terpenoids in Recombinant Baker's Yeast, p. 79–89. *In* Fett-Neto, AG (ed.), Biotechnology of Plant Secondary Metabolism. Humana Press, New York.

Tables

Table 1: Overview of tested substrates and detected products of hydroxylation reactions with *P. pastoris* X-33 strain expressing L3H.Ap of *A. pullulans* CBS 100280 (EXF-150). For easier identification, the substances have been numbered in the respective figures (Fig. 2, 5, 6, S6, S8, S9, S11 – S13). These numbers are given in brackets in the table behind the substance names.

Substrate	**Detected products after biotransformation with L3H.Ap in *P. pastoris***
(+)-limonene (**1**)	(+)-*trans*-isopiperitenol (**2**) *p*-1,8-menthadien-4-ol (**3**)
(-)-limonene (**4**)	(-)-*trans*-isopiperitenol (**5**) *p*-1,8-menthadien-4-ol (**3**) carveol (**6**)
isopiperitenol ((+)-*trans*-/*cis*-mixture 2:1)	none
α-pinene (**7**)	verbenol (**8**) verbenone (**9**) further unknown products
β-pinene (**10**)	pinocarveol (**11**) further unknown products
γ-terpinene	none
α-phellandrene	none
3-carene (**12**)	*p*-1,5-menthadien-8-ol (**13**) further unknown products
toluene	none
1-phenylethanol	none
2-phenylethylalcohol	none
DMSO	none

Figures and Legends

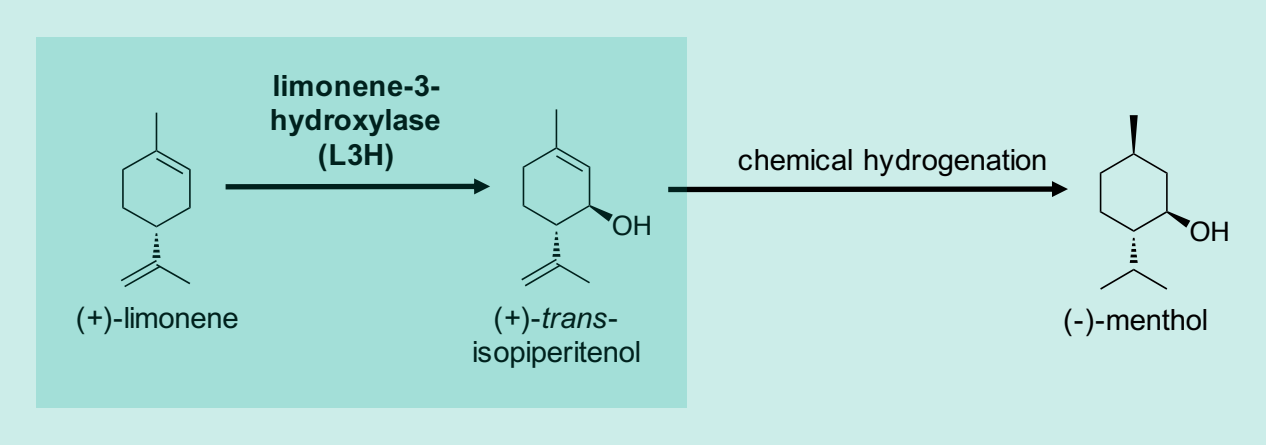

Figure 1: Biotechnological-chemical process for (-)-menthol production, starting from (+)-limonene.

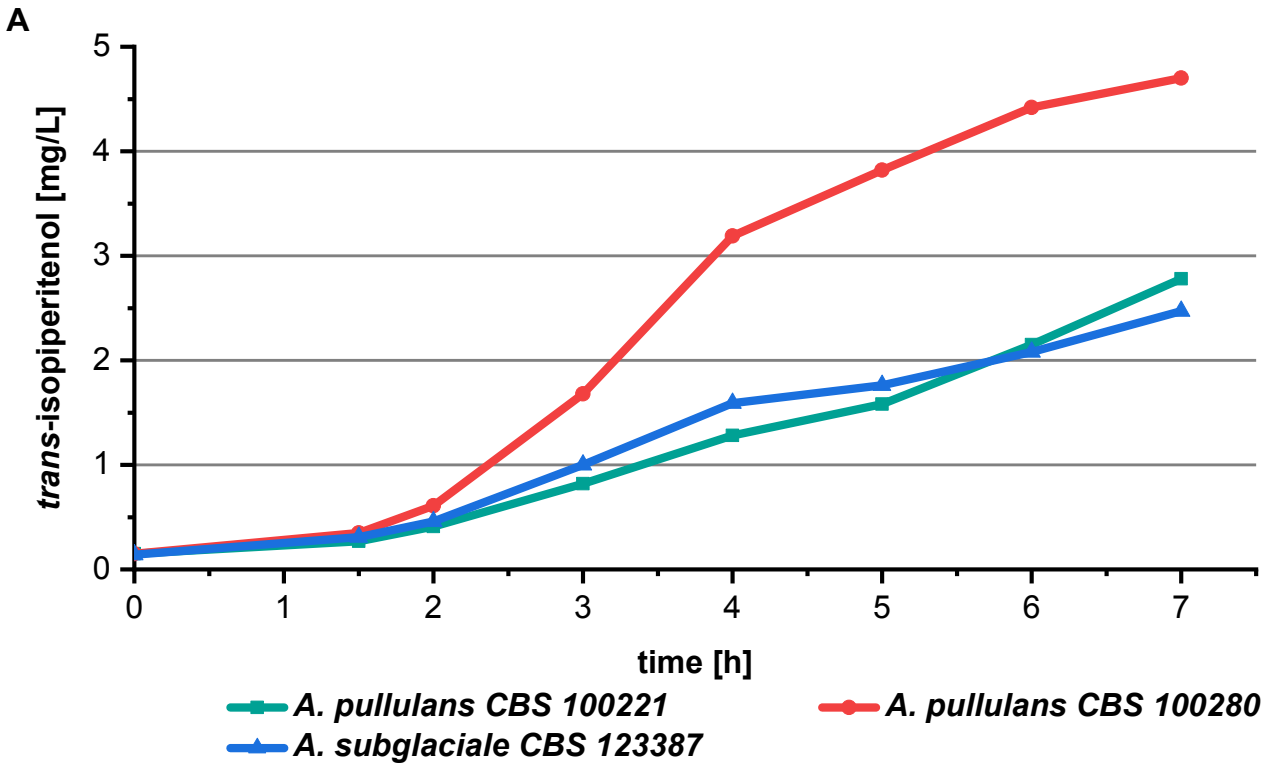
A
trans-isopiperitenol [mg/L]
time [h]
A. pullulans CBS 100221
A. pullulans CBS 100280
A. subglaciale CBS 123387

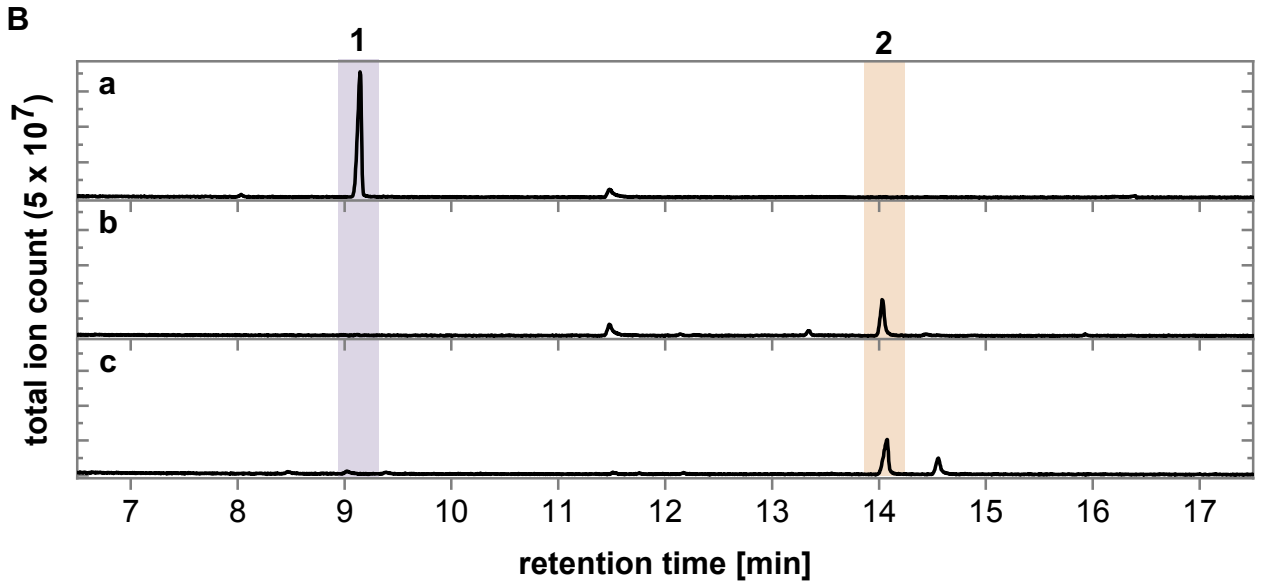
B
1
2
a
b
c
total ion count (5 x 10^7)
retention time [min]

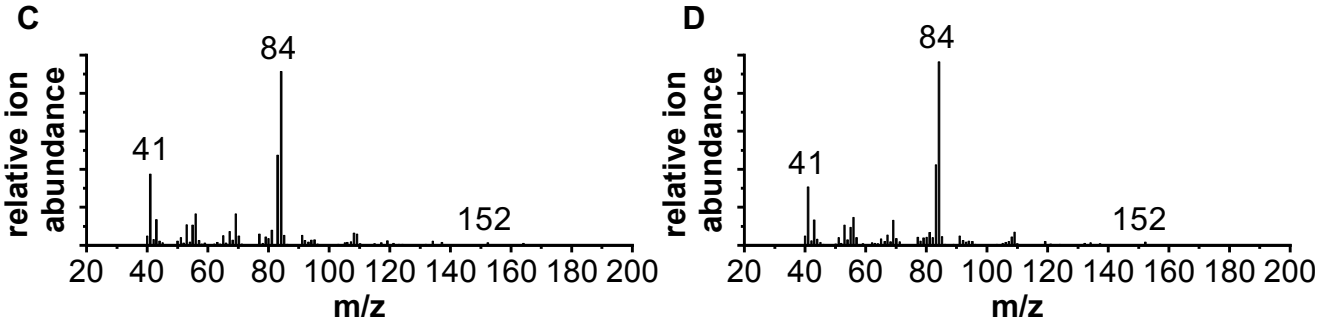
C
D
relative ion abundance
84
41
152
m/z

Figure 2: *trans*-Isopiperitenol production with different *Aureobasidium* species. (A) *trans*-Isopiperitenol production kinetics of different *Aureobasidium* strains. Culture samples of different fungi were taken over a period of 7 hours (once per hour) after addition of 1 g L^{-1} (+)-limonene. Samples were extracted with ethyl acetate and the *trans*-isopiperitenol amount was determined by GC-MS analysis. The data points and error bars represent the mean values and standard deviations of three biological replicates (n = 3). (B) GC-MS analysis of biotransformation of (+)-limonene by *A. pullulans* CBS 100280. Chromatogram of ethyl acetate extract from (a) *A. pullulans* culture after addition of 1 g L^{-1} limonene (t = 0 h) is compared to (b) *A. pullulans* culture 24 h after addition of limonene, and (c) isopiperitenol reference substance (2:1-mixture of (+)-*trans*-/*cis*-isopiperitenol). *trans*-Isopiperitenol (peak 2, retention time (Rt.) 14 min) was identified as the main product of (+)-limonene (peak 1) biotransformation by comparison of retention time and mass-spectrum (C) to those of the isopiperitenol reference substance (D).

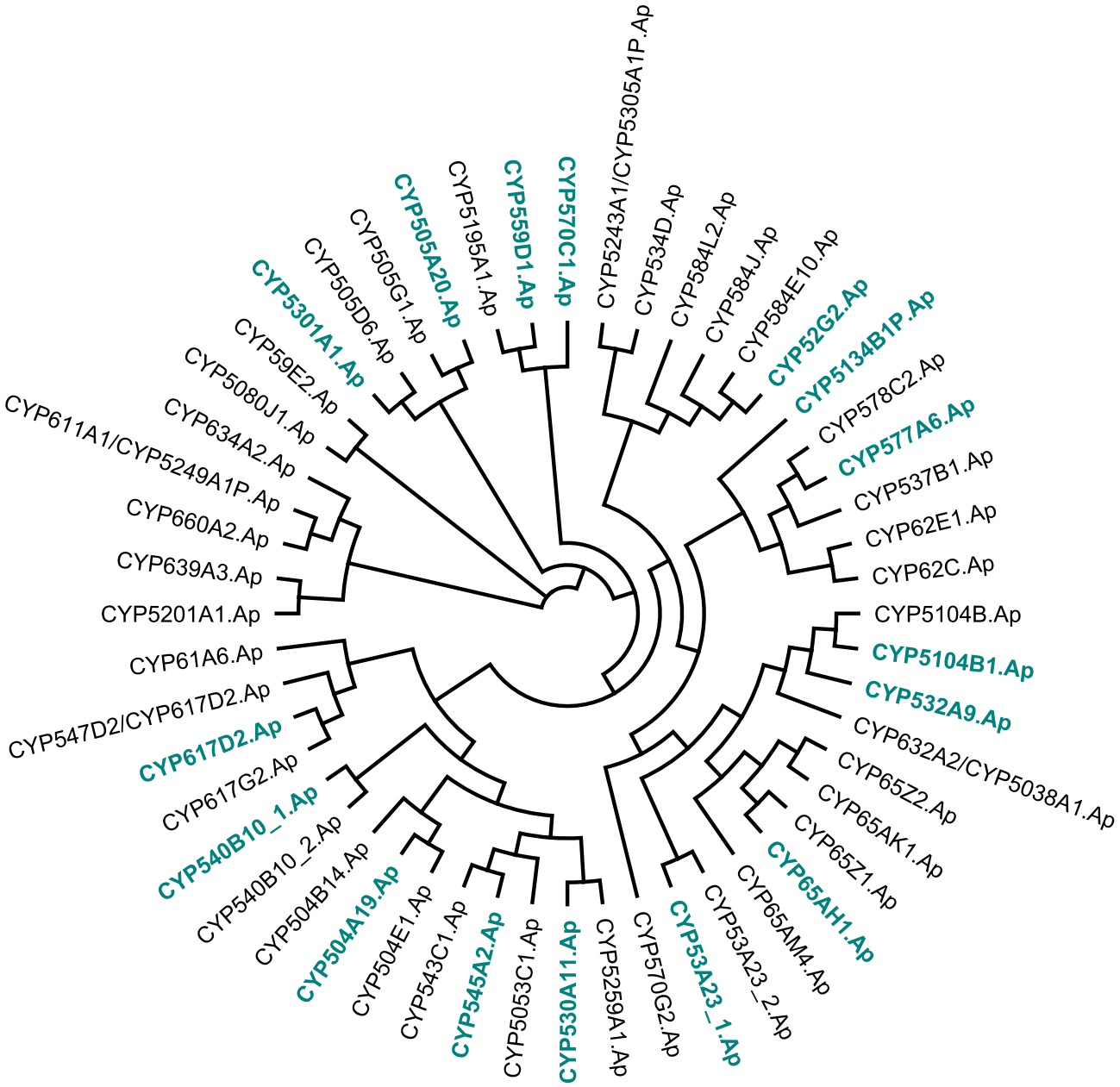

Figure 3: Clustering of cytochrome P450 monooxygenases of *A. pullulans* CBS 100280 (EXF-150). The proteins annotated as cytochrome P450 monooxygenases were analyzed for their amino acid sequence identity and subdivided into protein families. CYP candidate genes chosen for expression in *S. cerevisiae* are marked in green.

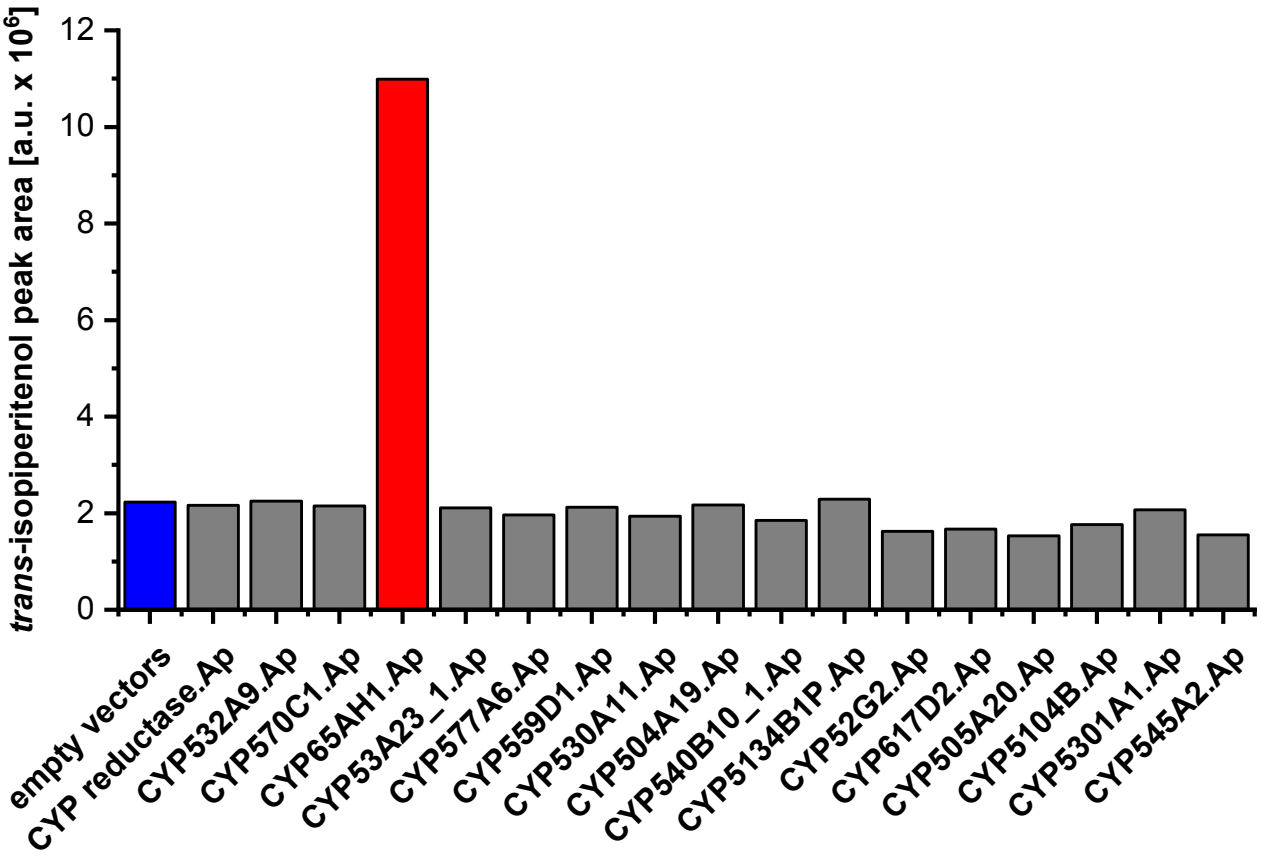

Figure 4: *trans*-Isopiperitenol peak areas achieved in (+)-limonene biotransformation experiment with different *S. cerevisiae* CEN-PK2-1C strains. empty vectors: yeast strain harboring empty pPK245 and pPK448 vectors, CYP reductase.Ap: cells expressing putative CYP reductase gene from *A. pullulans* CBS 100280 (EXF-150) from pPK448 vector, CYP532A9.Ap – CYP545A2.Ap: cells expressing different putative CYPs from *A. pullulans* CBS 100280 (EXF-150) from pPK245 vector together with putative CYP reductase from *A. pullulans* from pPK448 plasmid. *trans*-Isopiperitenol peak areas were determined by GC-MS analysis. (n = 1)

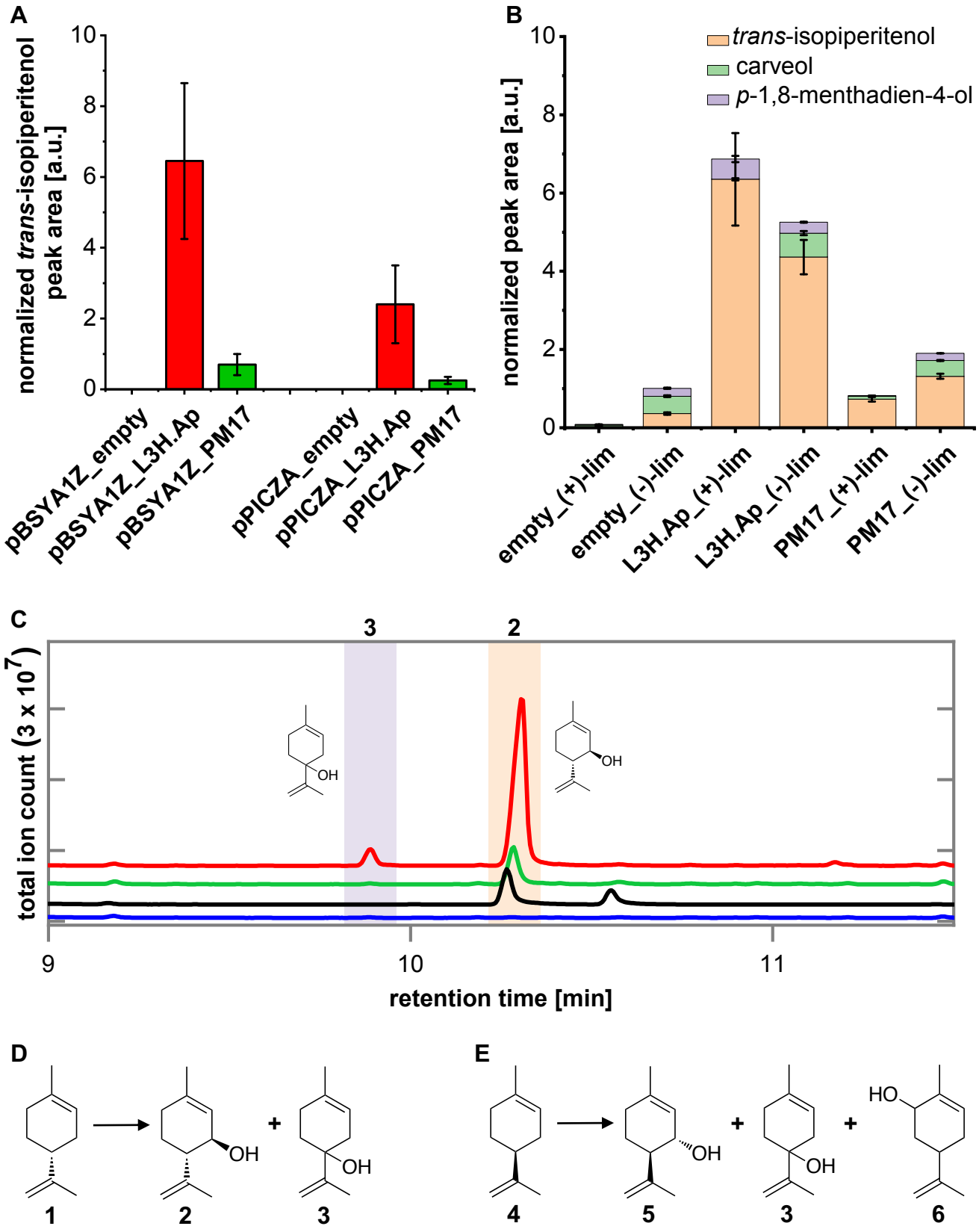
A
normalized trans-isopiperitenol peak area [a.u.]
pBSYA1Z_empty
pBSYA1Z_L3H.Ap
pBSYA1Z_PM17
pPICZA_empty
pPICZA_L3H.Ap
pPICZA_PM17
B
normalized peak area [a.u.]
trans-isopiperitenol
carveol
p-1,8-menthadien-4-ol
empty_(+)-lim
empty_(-)-lim
L3H.Ap_(+)-lim
L3H.Ap_(-)-lim
PM17_(+)-lim
PM17_(-)-lim
C
total ion count (3 x 10^7)
retention time [min]
OH
D
E
HO

Figure 5: Hydroxylation of limonene with *P. pastoris* X-33 strains expressing L3H enzymes. (A) *trans*-Isopiperitenol peak areas achieved in (+)-limonene biotransformation experiment with different *P. pastoris* X-33 strains. pBSYA1Z: episomal, constitutive gene expression, pPICZA: genome integrated, methanol-induced gene expression. empty: *P. pastoris* with empty expression vector, L3H.Ap: with CYP65AH1 of *A. pullulans*, PM17: with limonene-3-hydroxylase enzyme of *Mentha x piperita.* (B) Product peak areas achieved in biotransformation experiment with (+)- or (-)-limonene with *P. pastoris* X-33 strains harboring empty pBSYA1Z plasmid or expressing limonene-3-hydroxylase enzymes from *A. pullulans* (L3H.Ap) or *Mentha* x *piperita* (PM17) from pBSYA1Z backbone. While with (-)-limonene several different products were formed with all strains (see Figure S9), only peak areas of the products that differ in quantity between the tested strains are shown. Chromatograms see Figure 5 C, Figure S8 and Figure S9. In (A) and (B) peak areas were determined by GC-MS analysis, and normalized to the peak are of internal standard (3-carene) and the number of cells corresponding to 150 (A) or 225 (B) OD units. The data points and error bars represent the mean values and standard deviations of six (A: n = 6) or three (B: n = 3) biological replicates. (C) GC-MS analysis of (+)-limonene biotransformation experiment shown in Figure 5 B. Chromatogram of the negative control with the empty pBSYA1Z expression plasmid (blue) is compared to a strain harboring PM17 from *Mentha* x *piperita* (green) or L3H.Ap (red), and isopiperitenol reference substance (2:1-mixture of (+)-*trans*-/*cis*-isopiperitenol) (black). *trans*-Isopiperitenol (peak 2, Rt. 10.3 min) was identified as the main product (> 90 %) of (+)-limonene biotransformation. As side product (< 10 %) *p*-1,8-menthadien-4-ol (peak 3, Rt. 9.8 min) was formed by cells expressing L3H.Ap. (D, E) Reactants and main products of bioconversion reactions catalyzed by L3H.Ap. 1: (+)-limonene, 2: (+)-*trans*-isopiperitenol, 3: *p*-1,8-menthadien-4-ol, 4: (-)-limonene, 5: (-)-*trans*-isopiperitenol, 6: carveol (MS spectrum see Figure S14).

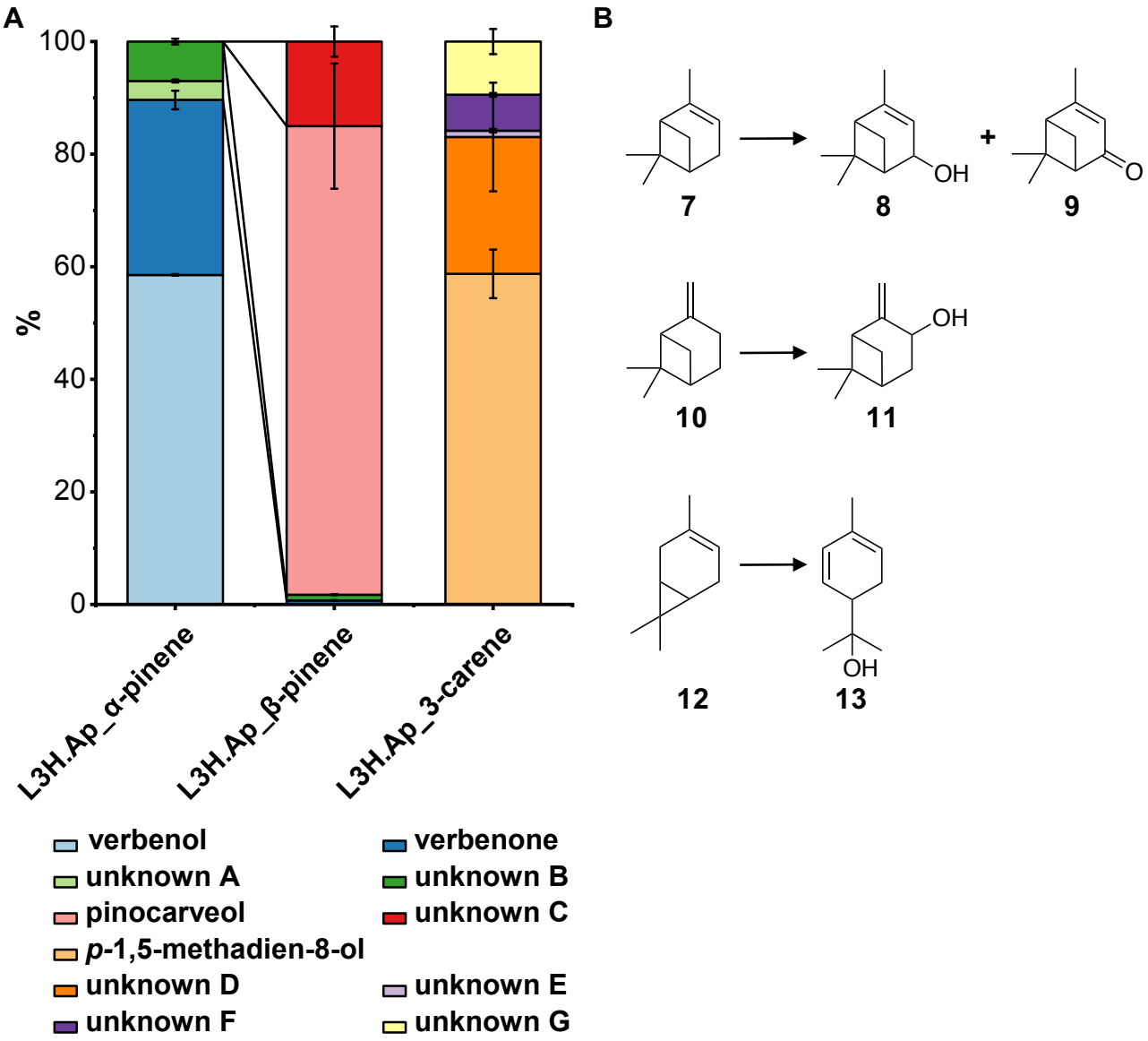

Figure 6: Hydroxylation of monoterpene substrates with *P. pastoris* X-33 expressing L3H.Ap. (A) Relative quantitative composition of products formed in biotransformation experiments of α-pinene, β-pinene or 3-carene with *P. pastoris* X-33 cells expressing L3H.Ap from pBSYA1Z backbone. If possible, products were identified via comparison of retention times and mass-spectra with those of chemically synthesized reference substances, or by comparison of mass-spectra to those of the NIST mass spectral library (v14, MS spectra see Figure S14). Chromatograms see Figure S11 – Figure S13. The data points and error bars represent the mean values and standard deviations of three biological replicates (n = 3). (B) Reactants and main products of bioconversion reactions catalyzed by L3H.Ap. 7: α-pinene, 8: verbenol, 9: verbenone, 10: β-pinene, 11: pinocarveol, 12: 3-carene, 13: *p*-1,5-menthadien-8-ol.

Supplementary tables

Table S1: Fungal and bacterial strains, plasmids and oligonucleotides used in this study.

Strains	Genotype	Resource/Reference
Hormonema dematoides ATCC 201675	wild type	ATCC microbiology collection, USA
Hormonema prunorum CBS 933.72	wild type	Centraalbureau voor Schimmelcultures (CBS-KNAW), Utrecht, Netherlands
Hormonema carpetanum CBS 115712	wild type	CBS-KNAW, Utrecht, Netherlands
Hormonema dematoides ATCC 66687	wild type	ATCC microbiology collection, USA
Hormonema carpetanum CBS 115713	wild type	CBS-KNAW, Utrecht, Netherlands
Sydowia polyspora CBS 116.29	wild type	CBS-KNAW, Utrecht, Netherlands
Hormonema dematoides ATCC 201676	wild type	ATCC microbiology collection, USA
Hormonema prunorum CBS 934.72	wild type	CBS-KNAW, Utrecht, Netherlands
Hormonema dematoides DSM 14201	wild type	Deutsche Sammlung von Mikroorganismen und Zellkulturen (DSMZ), Braunschweig, Germany
Rhizosphaera kalkhoffii ATCC 46388	wild type	ATCC microbiology collection, USA
Hormonema schizolunatum CBS 707.95	wild type	CBS-KNAW, Utrecht, Netherlands
Hormonema schizolunatum CBS 706.95	wild type	CBS-KNAW, Utrecht, Netherlands
Hormonema prunorum CBS 935.72	wild type	CBS-KNAW, Utrecht, Netherlands
Aureobasidium pullulans CBS 100221	wild type	CBS-KNAW, Utrecht, Netherlands
Aureobasidium pullulans CBS 100280 (EXF-150)	wild type	CBS-KNAW, Utrecht, Netherlands (1)
Aureobasidium subglaciale CBS 123387	wild type	CBS-KNAW, Utrecht, Netherlands
Neofusicoccum parvum	wild type	strain collection DECHEMA research institute, Frankfurt a.M., Germany
Ochroconis constricta	wild type	strain collection DECHEMA research institute, Frankfurt a.M., Germany
Parastagonospora nodorum	wild type	strain collection DECHEMA research institute, Frankfurt a.M., Germany
S. cerevisiae CEN-PK2-1C	*MATa his3D1 leu2-3_112 ura3-52 trp1-289; MAL2-8c SUC2*	(2)

P. pastoris X-33	wild type	Invitrogen Corporation (Carlsbad, CA, USA)
E. coli DH5α	*fhuA2* Δ(*argF-lacZ*)U169 *phoA glnV44* Φ80 Δ(*lacZ*)M15 *gyrA96 recA1 relA1 endA1 thi-1 hsdR17*	(3, 4)

Plasmids		**Resource/ Reference**
pPK448	expression plasmid for *S. cerevisiae,* TRP1	(5)
pPK245	expression plasmid for *S. cerevisiae, URA3*	(5)
pPK448_CYP reductase.Ap	expression plasmid with cDNA from putative CYP reductase enzyme from *A. pullulans*	this work
pPK245_CYP532A9.Ap	expression plasmid with CYP532A9.Ap cDNA from *A. pullulans*	this work
pPK245_CYP570C1.Ap	expression plasmid with CYP570C1.Ap cDNA from *A. pullulans*	this work
pPK245_CYP65AH1.Ap	expression plasmid with CYP65AH1.Ap (L3H.Ap) cDNA from *A. pullulans*	this work
pPK245_CYP53A23_1.Ap	expression plasmid with CYP53A23_1.Ap cDNA from *A. pullulans*	this work
pPK245_CYP577A6.Ap	expression plasmid with CYP577A6.Ap cDNA from *A. pullulans*	this work
pPK245_CYP559D1.Ap	expression plasmid with CYP559D1.Ap cDNA from *A. pullulans*	this work
pPK245_CYP530A11.Ap	expression plasmid with CYP530A11.Ap cDNA from *A. pullulans*	this work
pPK245_CYP504A19.Ap	expression plasmid with CYP504A19.Ap cDNA from *A. pullulans*	this work
pPK245_CYP540B10_1.Ap	expression plasmid with CYP540B10_1.Ap cDNA from *A. pullulans*	this work
pPK245_CYP5134B1P.Ap	expression plasmid with CYP5134B1P.Ap cDNA from *A. pullulans*	this work
pPK245_CYP52G2.Ap	expression plasmid with CYP52G2.Ap cDNA from *A. pullulans*	this work
pPK245_CYP617D2.Ap	expression plasmid with CYP617D2.Ap cDNA from *A. pullulans*	this work
pPK245_CYP505A20.Ap	expression plasmid with CYP505A20.Ap cDNA from *A. pullulans*	this work
pPK245_CYP5104B.Ap	expression plasmid with CYP5104B.Ap cDNA from *A. pullulans*	this work
pPK245_CYP5301A1.Ap	expression plasmid with CYP5301A1.Ap cDNA from *A. pullulans*	this work
pPK245_CYP545A2.Ap	expression plasmid with CYP545A2.Ap cDNA from *A. pullulans*	this work
pPK245_CYP65AH1.Hc	expression plasmid with CYP65AH1.Hc (L3H.Hc) cDNA from *H. carpetanum*	this work
pBSYA1Z	expression plasmid for *P. pastoris*, episomal, GAP promoter, Zeocin™ resistance gene (Zeo^R)	Bisy e.U. (Hofstätten/Raab, Austria)

pBSYA1Z_CYP65AH1.Ap	expression plasmid with CYP65AH1.Ap (L3H.Ap) cDNA from *A. pullulans*	this work
pBSYA1Z_CYP65AK1.Ap	expression plasmid with CYP65AK1.Ap cDNA from *A. pullulans*	this work
pBSYA1Z_CYP65AM4.Ap	expression plasmid with CYP65AM4.Ap cDNA from *A. pullulans*	this work
pBSYA1Z_CYP65AZ1.Ap	expression plasmid with CYP65AZ1.Ap cDNA from *A. pullulans*	this work
pBSYA1Z_PM17	expression plasmid with CYP71D13 (PM17) cDNA from *Mentha* x *piperita*, codon-optimized for *P. pastoris* and with FLAG tag (6)	this work
pPICZA	expression plasmid for *P. pastoris*, genome integrated, AOX1 promoter, Zeo^R	Invitrogen Corporation (Carlsbad, CA, USA)
pPICZA_CYP65AH1.Ap	expression plasmid with CYP65AH1.Ap (L3H.Ap) cDNA from *A. pullulans*	this work
pPICZA_PM17	expression plasmid with CYP71D13 (PM17) cDNA from *Mentha* x *piperita*, codon-optimized for *P. pastoris* and with FLAG tag (6)	this work

Oligonucleotides/PCR primers		**Purpose**
P1	TCGAATAAACACACATAAACAAACGAATTCATGGCGCAACTCG ATACTCTC	Cloning of CYP reductase.Ap gene in pPK448 backbone
P2	TATTTAAATGCAAGATTTAAAGTAGGTACCTCATGACCAGACAT CTTCTTGG	
P3	TACAAAAAACACATACATAAACTAGAATTCATGATCATCGGCGA GTTAGTACC	Cloning of CYP532A9.Ap gene in pPK245 backbone
P4	TATTTTTATATAATTATATTAATCTTAGGTACCTTATACAGGAAC CTCGCGAG	
P5	TACAAAAAACACATACATAAACTAGAATTCATGTTCTCGGAGCA AATCACC	Cloning of CYP65AH1.Ap gene in pPK245 backbone
P6	TATTTTTATATAATTATATTAATCTTAGGTACCTCAAGTCGTAGT CTCGAAGGTG	
P7	TACAAAAAACACATACATAAACTAGAATTCATGGGTGTCGTCGA GCTCC	Cloning of CYP53A23_1.Ap gene in pPK245 backbone
P8	TATTTTTATATAATTATATTAATCTTAGGTACCTCAAACATTCCT CCTCTTCATACCAAC	
P9	TACAAAAAACACATACATAAACTAGAATTCATGGATTTTCTGAT CGCCTACTTC	Cloning of CYP559D1.Ap gene in pPK245 backbone
P10	TATTTTTATATAATTATATTAATCTTAGGTACCTTACCACGCGTG CCTG	
P11	TACAAAAAACACATACATAAACTAGAATTCATGTCGCTTCTCTC CTTCTCAC	Cloning of CYP5134B1P.Ap gene in pPK245 backbone
P12	TATTTTTATATAATTATATTAATCTTAGGTACCCTACCAACCTGC CTTCTTCAAAC	
P13	TACAAAAAACACATACATAAACTAGAATTCATGGCGAGCATTCC TGTATTC	Cloning of CYP52G2.Ap gene in pPK245 backbone
P14	TATTTTTATATAATTATATTAATCTTAGGTACCTCAGTGAGAGGC GACATCTT	
P15	TACAAAAAACACATACATAAACTAGAATTCATGGCGTTTGCACG GCTG	Cloning of CYP617D2.Ap gene in pPK245 backbone
P16	TATTTTTATATAATTATATTAATCTTAGGTACCCTAATCTTCTATA CATCTCAAATTAACTAAAACAC	

P17	TCAATTGAACAACTATCAAAACACAATGTTCTCGGAGCAAATCACC	Cloning of CYP65AH1.Ap gene in pBSYA1Z backbone
P18	TTCTGACATCCTCTTGAGCGGCCGCTCAAGTCGTAGTCTCGAAGG	
P19	TCAATTGAACAACTATCAAAACACAATGGACGTCGAACGACTC	Cloning of CYP65AK1.Ap gene in pBSYA1Z backbone
P20	TTCTGACATCCTCTTGAGCGGCCGCTCACCGGACCACTCGTC	
P21	TCAATTGAACAACTATCAAAACACAATGCTGACCTTTGCTTTGTTC	Cloning of CYP65AM4.Ap gene in pBSYA1Z backbone
P22	TTCTGACATCCTCTTGAGCGGCCGCTCAATCTGTCACAGCAGTAAGTTTG	
P23	TCAATTGAACAACTATCAAAACACAATGGCACTTCTCGACAGC	Cloning of CYP65AZ1.Ap gene in pBSYA1Z backbone
P24	TTCTGACATCCTCTTGAGCGGCCGCCTACGCAACACTACCTCTAGC	
P25	TCAATTGAACAACTATCAAAACACAATGGAATTGCAAATCTCTTCTGC	Cloning of PM17 gene in pBSYA1Z backbone
P26	TTCTGACATCCTCTTGAGCGGCCGCTTATTACTTATCGTCGTCATCCTTGT	
P27	AGATCAAAAAACAACTAATTATTCGAAACGATGTTCTCGGAGCAAATCACCAAGG	Cloning of CYP65AH1.Ap gene in pPICZA backbone
P28	CAGATCCTCTTCTGAGATGAGTTTTTGTTCAGTCGTAGTCTCGAAGGTG	
P29	AGATCAAAAAACAACTAATTATTCGAAACGATGGAATTGCAAATCTCTTCTGC	Cloning of PM17 gene in pPICZA backbone
P30	CAGATCCTCTTCTGAGATGAGTTTTTGTTCCTTATCGTCGTCATCCTTGTAATC	

Table S2: Overview of tested genes of *A. pullulans* and *H. carpetanum,* and corresponding identification numbers in NCBI database (https://www.ncbi.nlm.nih.gov)**.**

Assigned name	Fungus	Protein ID (NCBI)	CDS Region in Nucleotide (NCBI)
CYP532A9.Ap	*A. pullulans* CBS 100280 (EXF-150)	KEQ81481.1	KL584991.1 168089-169727 (-)
CYP570C1.Ap	*A. pullulans* CBS 100280 (EXF-150)	KEQ78964.1	KL585011.1 18606-21954 (-)
CYP65AH1.Ap = L3H.Ap	*A. pullulans* CBS 100280 (EXF-150)	KEQ84190.1	KL584983.1 1119615-1121409 (+)
CYP53A23_1.Ap	*A. pullulans* CBS 100280 (EXF-150)	KEQ80869.1	KL584995.1 247821-249405 (-)
CYP577A6.Ap	*A. pullulans* CBS 100280 (EXF-150)	KEQ83870.1	KL584983.1 395652-397327 (-)
CYP559D1.Ap	*A. pullulans* CBS 100280 (EXF-150)	KEQ79812.1	KL585002.1 12910-14340 (+)
CYP530A11.Ap	*A. pullulans* CBS 100280 (EXF-150)	KEQ82851.1	KL584986.1 570068-571752 (+
CYP504A19.Ap	*A. pullulans* CBS 100280 (EXF-150)	KEQ83160.1	KL584985.1 502941-504594 (+)
CYP540B10_1.Ap	*A. pullulans* CBS 100280 (EXF-150)	KEQ83654.1	KL584984.1 923272-925034 (+)
CYP5134B1P.Ap	*A. pullulans* CBS 100280 (EXF-150)	KEQ87691.1	KL584976.1 805063-806956 (+)
CYP52G2.Ap	*A. pullulans* CBS 100280 (EXF-150)	KEQ88534.1	KL584975.1 925132-926791 (+)
CYP617D2.Ap	*A. pullulans* CBS 100280 (EXF-150)	KEQ85574.1	KL584980.1 912796-914541 (-)
CYP505A20.Ap	*A. pullulans* CBS 100280 (EXF-150)	KEQ88047.1	KL584976.1 1655524-1658837 (+)
CYP5104B.Ap	*A. pullulans* CBS 100280 (EXF-150)	KEQ89245.1	KL584974.1 492744-494512 (-)
CYP5301A1.Ap	*A. pullulans* CBS 100280 (EXF-150)	KEQ86419.1	KL584978.1 477404-479028 (+)
CYP545A2.Ap	*A. pullulans* CBS 100280 (EXF-150)	KEQ87624.1	KL584976.1 640968-642710 (+)
CYP65Z1.Ap	*A. pullulans* CBS 100280 (EXF-150)	KEQ82374.1	KL584987.1 17037-18701 (-)
CYP65AK1.Ap	*A. pullulans* CBS 100280 (EXF-150)	KEQ88046.1	KL584976.1 1653162-1654855 (+)
CYP65Z2.Ap	*A. pullulans* CBS 100280 (EXF-150)	KEQ86879.1	KL584977.1 281164-283019 (+)
CYP65AM4.Ap	*A. pullulans* CBS 100280 (EXF-150)	KEQ83455.1	KL584984.1 403111-405055 (-)
CYP reductase.Ap (putative CYP reductase)	*A. pullulans* CBS 100280 (EXF-150)	KEQ88142.1	KL584976.1 1879859-1882002 (+)

CYP65AH1.Hc = L3H.Hc	*Hormonema carpetanum* CBS 115712	Protein sequence: MAQHDITKLLSYAVAIGISYAI AQLTYNVFFHPLRKFPGPLIN AATPFPRLWLYYNGRENLGL AALHKKYGSIVRVAPDELSFI DGAAWKDIYGTAKDINRKDE KFYPVSANGVHSILTANDADH TRMRKALLPAFSDRALRAQE GLLKTYVQWLVTGLRQKQEK GEAIDMVKMYNFTSFDIMSDL SFGEPLGALKNMEATDWMTT IFDMIFYWAFSRIPRHFPIVWA IVDFCIPKSFKDKGLASFNHT VERVNKRLEMETDRPDLVSFI MENNHGSTSVEELHSNADIF MIAGTETTSTLLSGLTCLLLQ NPRVMEKLTAEIRGAFPTVD DITIDTLAALPYLAACINEAFRI YPPVPTAVRRLTNATTGAQV AGHWIPPNTSVGVPQWPAN HSDKNFVDPESFIPERWVAE GTEDYDERFAGDNRQAMQP FSVGKRNCIGKNLAYHEMRLI IAYLFVTFDLNWDNKADADD WLDQKLYILWDKKPLMCKLT PVAA	Gene sequence: ATGGCGCAACACGATATCACCAAGCTGCTCTC TTATGCTGTGGCCATTGGTATCTCATACGCCA TCGCTCAACTCACCTACAATGTGTTCTTCCAC CCTCTCCGCAAGTTTCCCGGGCCTCTTATAAA CGCAGCGACACCTTTCCCTCGTCTCTGGCTCT ACTATAACGGCCGCGAAAACCTGGGACTCGC CGCTCTTCACAAGAAATACGGCAGCATTGTCC GCGTCGCCCCTGACGAACTCAGCTTCATTGAC GGCGCAGCCTGGAAGGATATCTACGGTACCG CAAAGGACATCAATCGCAAGGATGAAAAGTTC TACCCAGTGTCTGCGAATGGAGTCCACAGTAT CCTCACCGCCAACGACGCCGATCACACTCGC ATGAGAAAGGCACTGTTGCCCGCCTTCTCGG ACCGCGCTCTTAGGGCTCAGGAAGGTCTGCT CAAGACATATGTGCAGTGGTTGGTGACCGGA CTGCGACAGAAGCAGGAAAAGGGTGAGGCCA TCGATATGGTCAAGATGTACAACTTCACAAGG TGAGTCTAATGGTGTACGGGAAATGGTAATCC TCCGGAGAGAGAGACCTTCTGGGTGGATTCT GCATGCGCTGTATCCTTATGCTGACGGAAATC ACACTGCAGCTTCGACATCATGTCGGATCTTT CATTCGGCGAGCCTCTCGGGGCGCTCAAGAA CATGGAAGCAACAGACTGGATGACGACCATCT TCGACATGATCTTCTACTGGGCCTTCAGCCGT ATCCCTCGCCACTTCCCCATTGTCTGGGCAAT CGTCGACTTCTGCATCCCCAAGTCATTCAAGG ACAAGGGTCTCGCCTCTTTCAACCACACGGTC GAGCGCGTGAACAAGCGTTTGGAAATGGAGA CCGATCGTCCTGATCTCGTGTCTTTCATCATG GAGAACAACCACGGCAGCACATCGGTCGAAG AGCTGCACTCTAACGCGGACATCTTCATGATT GCTGGAACCGAGACGACCTCGACGCTGCTGA GCGGTCTCACTTGCTTGCTGCTGCAGAACCC GAGAGTCATGGAGAAGCTCACTGCCGAGATC AGAGGTGCTTTCCCGACCGTTGACGACATCAC CATCGATACCCTCGCAGCTCTTCCGGTAAGTG ATTGTCCCACTGCCAGGAGATCCAGAGAGAC ACAGACTGTAAGCTGACATTTACAACTTAGTA CCTCGCCGCTTGCATCAACGAAGCCTTCCGC ATTTATCCTCCCGTCCCAACCGCCGTGCGCC GTCTCACAAACGCCACCACCGGTGCTCAAGTT GCCGGCCACTGGATCCCTCCGAACACAAGCG TCGGCGTTCCCCAATGGCCCGCCAACCACTC GGACAAGAACTTCGTCGACCCCGAAAGCTTCA TCCCCGAGCGCTGGGTCGCCGAGGGCACCG AGGACTACGATGAGCGCTTCGCCGGAGACAA CAGACAAGCGATGCAACCGTTCTCGGTCGGC AAGAGAAACTGCATTGGAAAGAAGTGAGTCTT GCCATTCTTACCCCAGCCGTCATTTCACCCCC CACCCACCCCTTACCCGTCATTCCACGACCAC CCATCTGCGAACCACAAGACCTCATGACTGAC AACATCCGCCTACAGCCTCGCGTACCACGAAA TGCGTCTCATCATCGCCTACCTCTTCGTGACC TTCGATCTCAACTGGGACAACAAGGCAGATGC CGACGACTGGCTGGACCAAAAGCTCTACATC CTGTGGGACAAGAAGCCGCTGATGTGCAAGC TCACCCCCGTCGCCGCCTAG

Supplementary figures

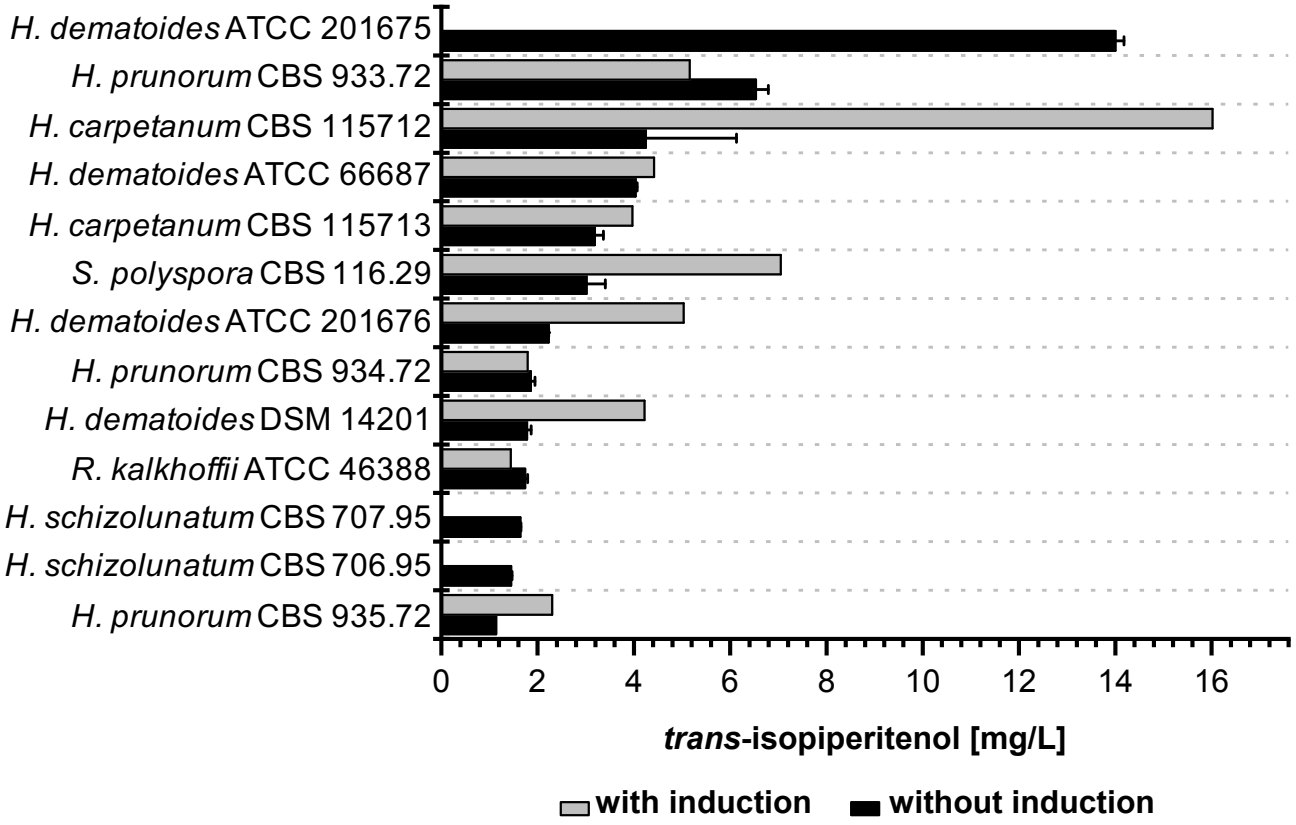

Figure S1: *trans*-Isopiperitenol production with different *Hormonema* species and related fungi. Shown are the maximum product concentrations achieved during biotransformation of (+)-limonene. The substrate was added to the 48-hour old cultures in a concentration of 2 g L^{-1}. The strains were either cultivated without or with 100 mg L^{-1} (+)-limonene during the growth phase before the biotransformation in order to potentially induce gene expression of limonene converting enzymes. The data points and error bars represent the (mean) values (and standard deviations) of one (with induction) or two (without induction) biological replicates. The highest *trans*-isopiperitenol concentration was obtained with cells of *Hormonema carpetanum* CBS 115712 after pre-induction with (+)-limonene.

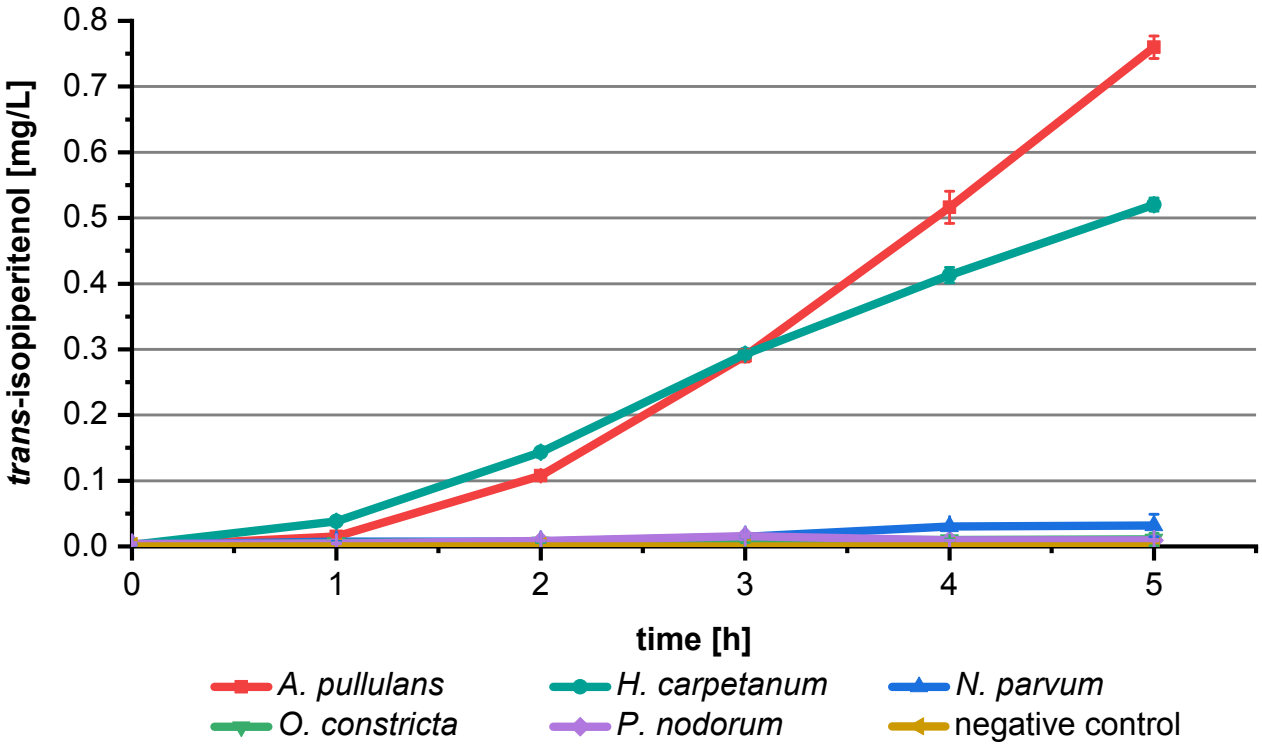

Figure S2: *trans*-Isopiperitenol production over time of different dothideomycetes. Culture samples of different fungi were taken over a period of 5 h (once per hour) after addition of 1 g L^{-1} (+)-limonene. Samples were extracted with ethyl acetate and the *trans*-isopiperitenol amount was determined by GC-MS analysis. Negative control: without cells. Data points and error bars represent the mean values and standard deviations of three biological replicates (n = 3).

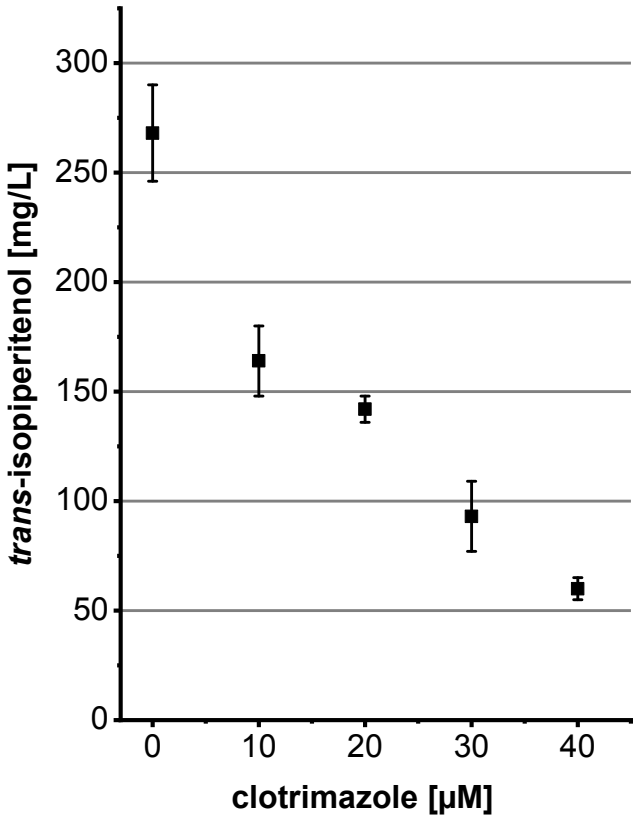

Figure S3: Influence of CYP inhibitor clotrimazole on the formation of *trans*-isopiperitenol in *H. carpetanum* CBS 115712 cultures after (+)-limonene addition. Cells of 48 h old cultures of *H. carpetanum* CBS 115712 were resuspended in citrate buffer (100 mM, pH 4.5) and 2 g L^{-1} limonene and different concentrations of clotrimazole (0, 10, 20, 30, 40 µM) were added. After 14 h of biotransformation, samples were taken, extracted with ethyl acetate and analyzed via GC-FID. Data points and error bars represent the mean values and standard deviations of two biological replicates (n = 2). IC_{50} value of 17 µM for clotrimazole has been described for the inhibition of limonene-3-hydroxylase from *Mentha* x *piperita* (7). In the biotransformation experiments with *H. carpetanum* CBS 115712 the IC_{50} value for clotrimazole was reached at around 20 µM.

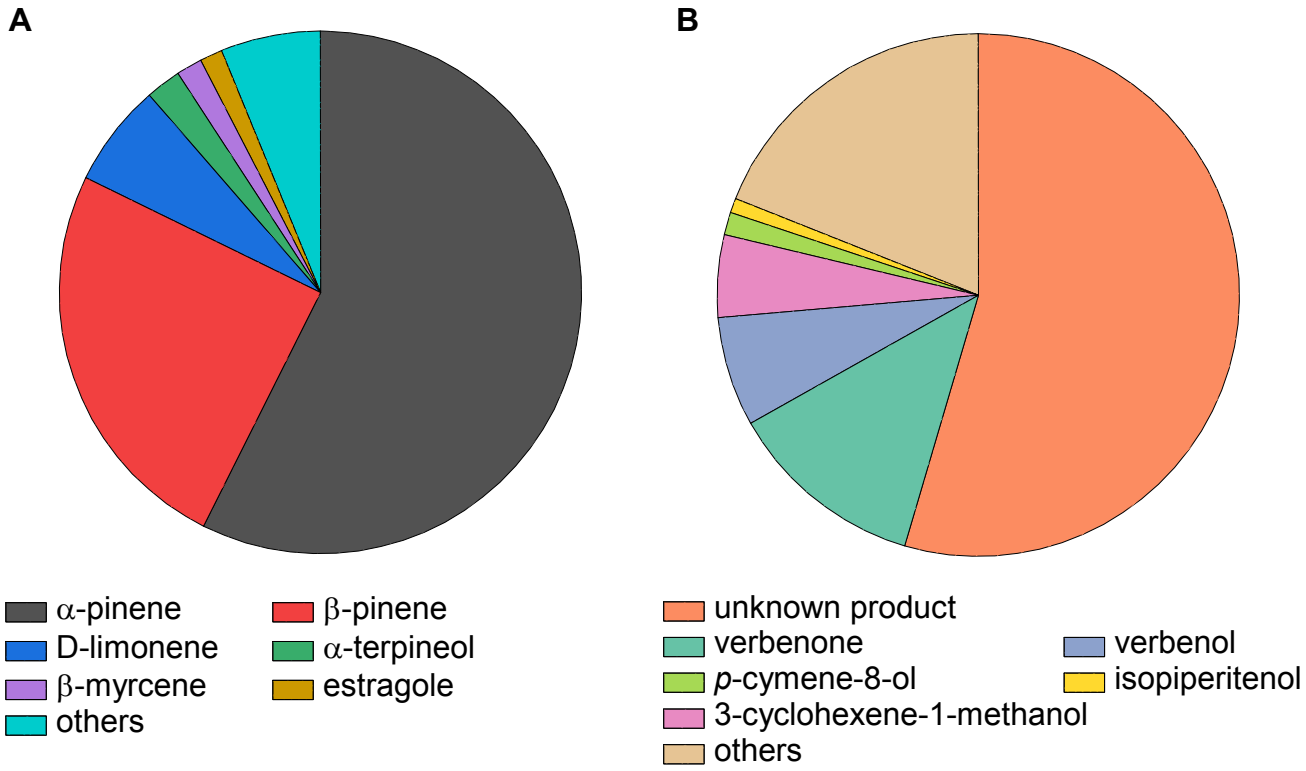

Figure S4: Bioconversion of turpentine oil with *A. pullulans* CBS 100280. (A) Composition of used turpentine oil. (B) Newly formed products after bioconversion of turpentine oil with *A. pullulans* CBS 100280. After 48 h cultivation of *A. pullulans* in YMSA medium, 170 mg L^{-1} turpentine oil was added. The same quantity was added again after another 24 and 48 h. Product spectrum was analyzed 136 h after the first addition of turpentine oil via GC-MS. Obtained peak areas are shown relative to each other in the circle diagram. Peak identification was done by comparison of mass spectra to NIST mass spectral library (v14). Chromatograms see Figure S5.

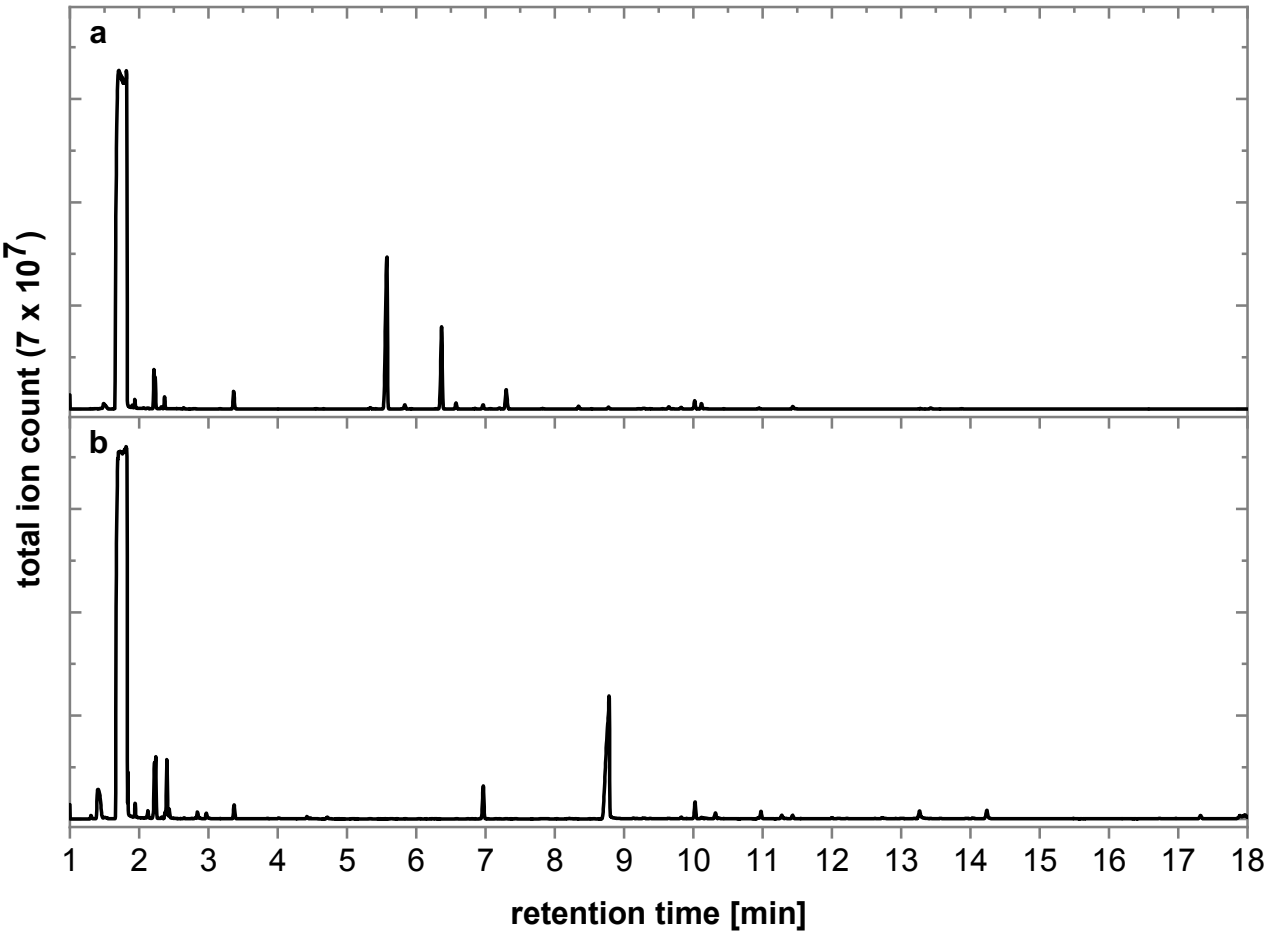

Figure S5: GC-MS analysis of bioconversion of turpentine oil with *A. pullulans* CBS 100280. Chromatogram from (a) composition of used turpentine oil is compared to (b) extract of *A. pullulans* culture after 136 h of biotransformation.

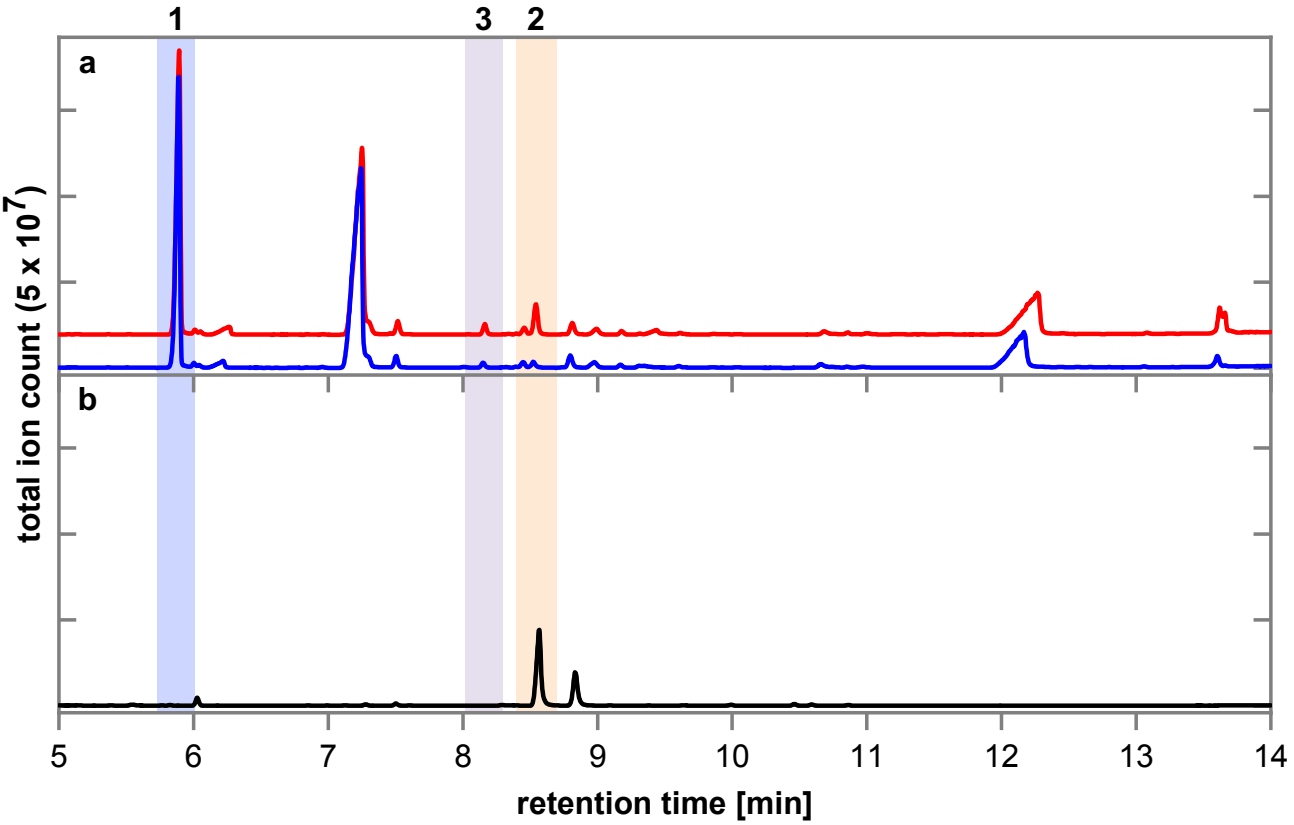

Figure S6: GC-MS analysis of biotransformation of (+)-limonene with different *S. cerevisiae* CEN-PK2-1C strains. Chromatogram from (a) the negative control harboring the empty expression plasmids pPK245 and pPK448 (blue), is compared to a strain expressing L3H.Ap and a putative CYP reductase gene from *A. pullulans* (red), and (b) isopiperitenol reference substance (2:1-mixture of (+)-*trans*-/*cis*-isopiperitenol). Peak 1 is (+)-limonene (Rt. 5.8 min), peak 2 is *trans*-isopiperitenol (Rt. 8.8 min) and peak 3 is *p*-1,8-methadien-4-ol (Rt. 8.2 min).

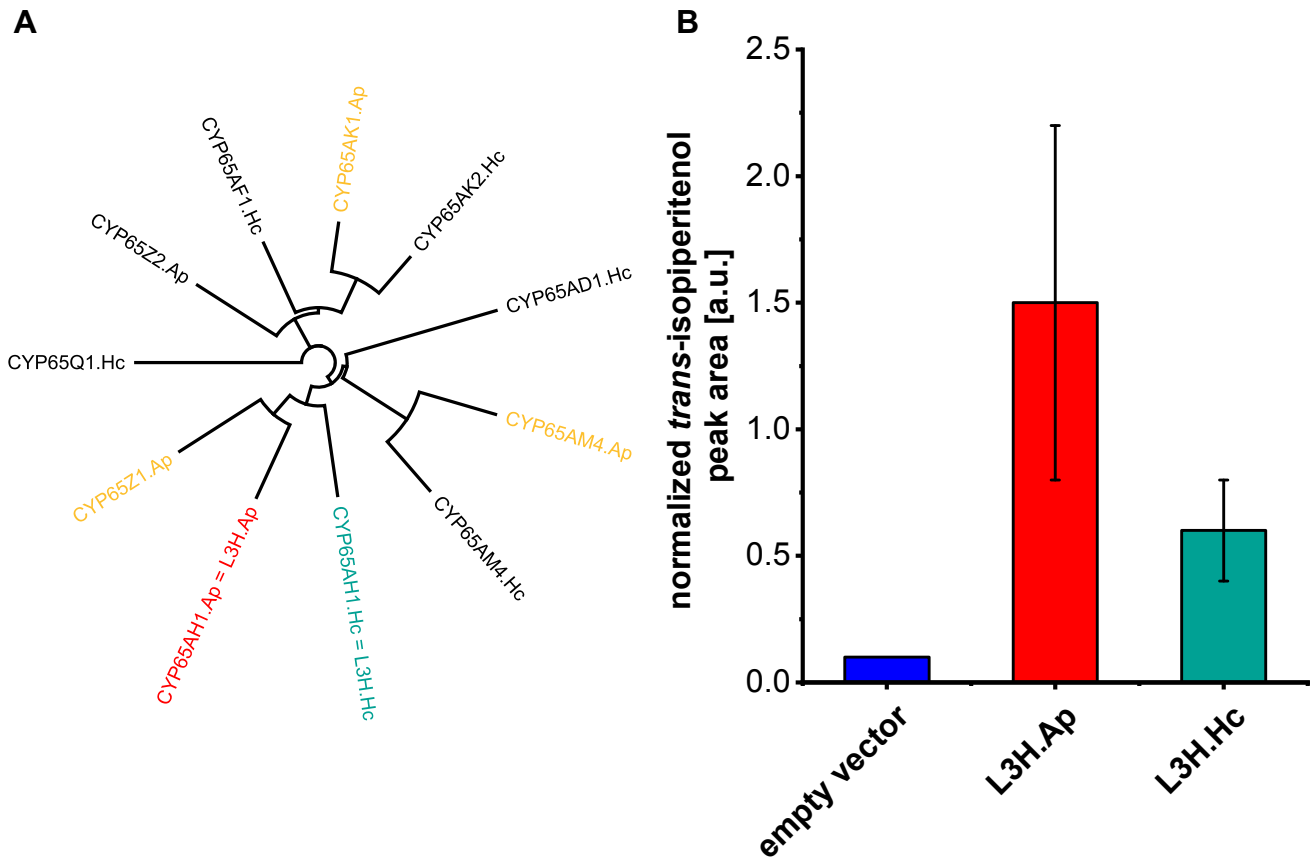

Figure S7: Testing of L3H.Ap homologues for limonene-3-hydroxylase activity. (A) Tree diagram of CYP proteins of the CYP65 family from *A. pullulans* (Ap) and *H. carpetanum* (Hc). Limonene-3-hydroxylase enzymes from *A. pullulans* (L3H.Ap = CYP65AH1.Ap) and *H. carpetanum* (L3H.Hc = CYP65AH1.Hc) as well as other tested CYP candidates from *A. pullulans* are marked in red, green or yellow, respectively. (B) *trans*-isopiperitenol peak areas measured after (+)-limonene biotransformation with different *S. cerevisiae* CEN-PK2-1C strains. empty: *S. cerevisiae* with empty expression vector pPK245, L3H.Ap: with CYP65AH1 of *A. pullulans*, L3H.Hc: with CYP65AH1 of *H. carpetanum*. (+)-*trans*-isopiperitenol peak areas were determined by GC-MS analysis. Data points and error bars represent the mean values and standard deviations of three biological replicates (n = 3).

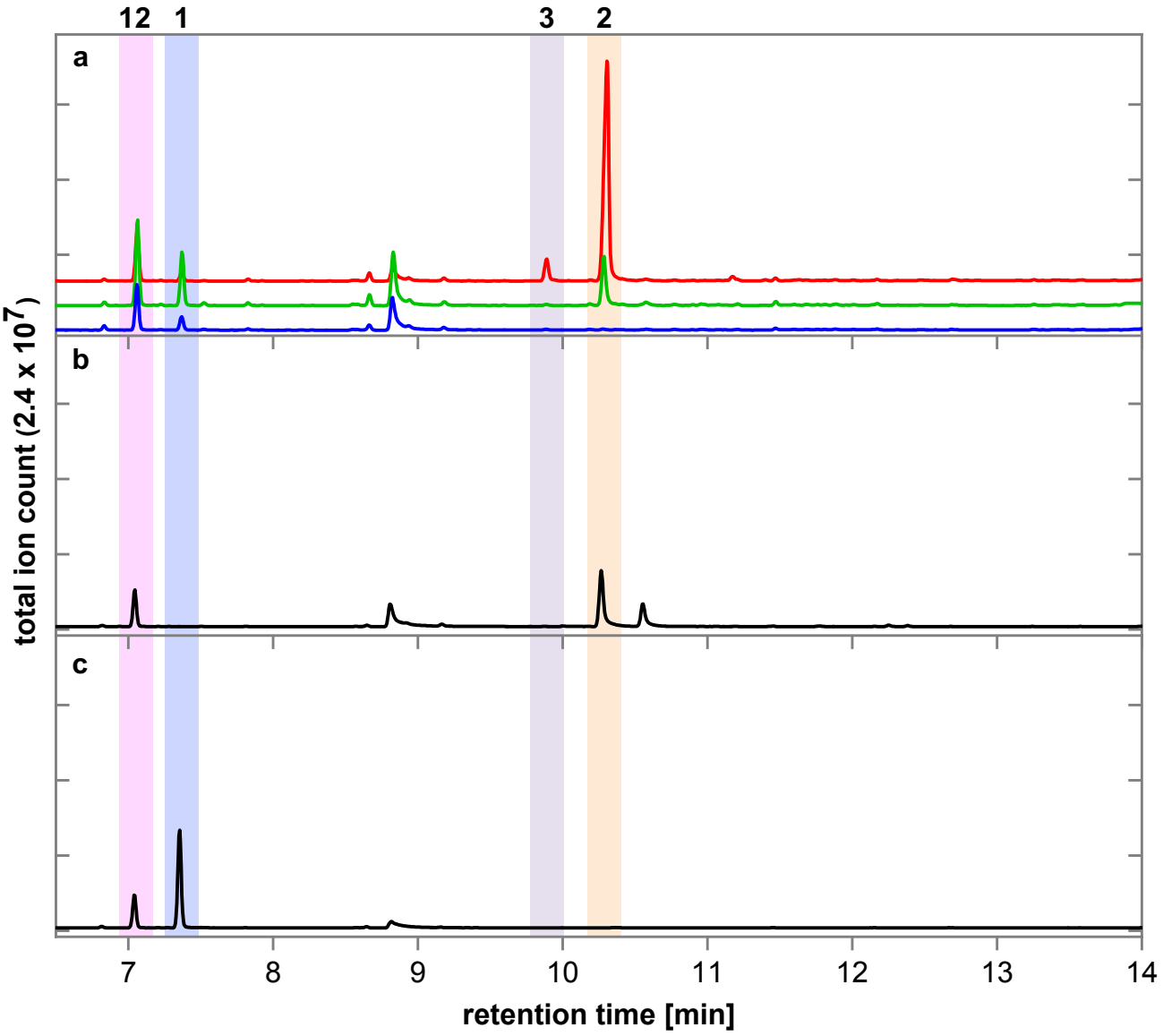

Figure S8: GC-MS analysis of hydroxylation of (+)-limonene with *P. pastoris* strains expressing limonene-3-hydroxylases. Chromatogram from (a) the negative control with the empty expression pBSYA1Z plasmid (blue) is compared to a strain expressing PM17 from *Mentha* x *piperita* (green) or L3H.Ap (red), (b) isopiperitenol reference substance (2:1-mixture of (+)-*trans*-/*cis*-isopiperitenol) extracted from cell culture, and (c) (+)-limonene stock solution used in the experiment. Peak 1 is (+)-limonene (Rt. 7.4 min), peak 2 is *trans*-isopiperitenol (Rt. 10.2 min), peak 3 is *p*-1,8-methadien-4-ol (Rt. 9.8 min) and peak 12 is 3-carene (Rt. 7 min) used as internal standard. While triplicates were used in the experiment, only one chromatogram each is shown here as an example.

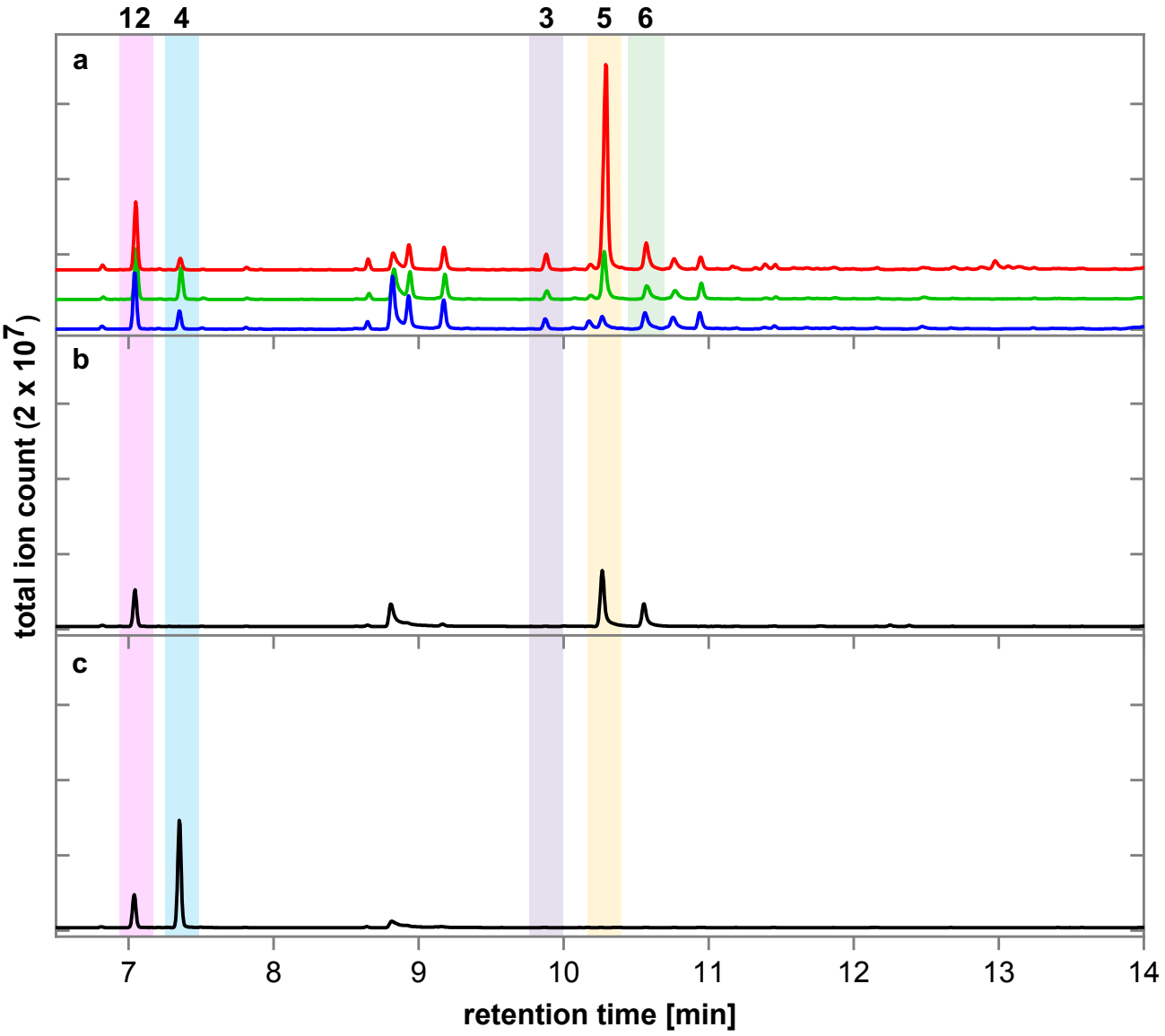

Figure S9: GC-MS analysis of biotransformation of (-)-limonene with *P. pastoris* X-33 strains expressing limonene-3-hydroxylases. Chromatogram from (a) the negative control with the empty expression pBSYA1Z plasmid (blue) is compared to a strain expressing PM17 from *Mentha* x *piperita* (green) or L3H.Ap (red), (b) isopiperitenol reference substance (2:1-mixture of (+)-*trans*-/*cis*-isopiperitenol) extracted from cell culture, and (c) (-)-limonene stock solution used in the experiment. Peak 3 is *p*-1,8-methadien-4-ol (Rt. 9.8 min), peak 4 is (-)-limonene (Rt. 7.4 min), peak 5 is *trans*-isopiperitenol (Rt. 10.2 min (in a (-) and in b (+)), in (a) peak 6 is carveol (Rt. 10.6 min, MS spectrum see Figure S14) and peak 12 is 3-carene (Rt. 7 min) used as internal standard. While triplicates were used in the experiment, only one chromatogram each is shown here as an example.

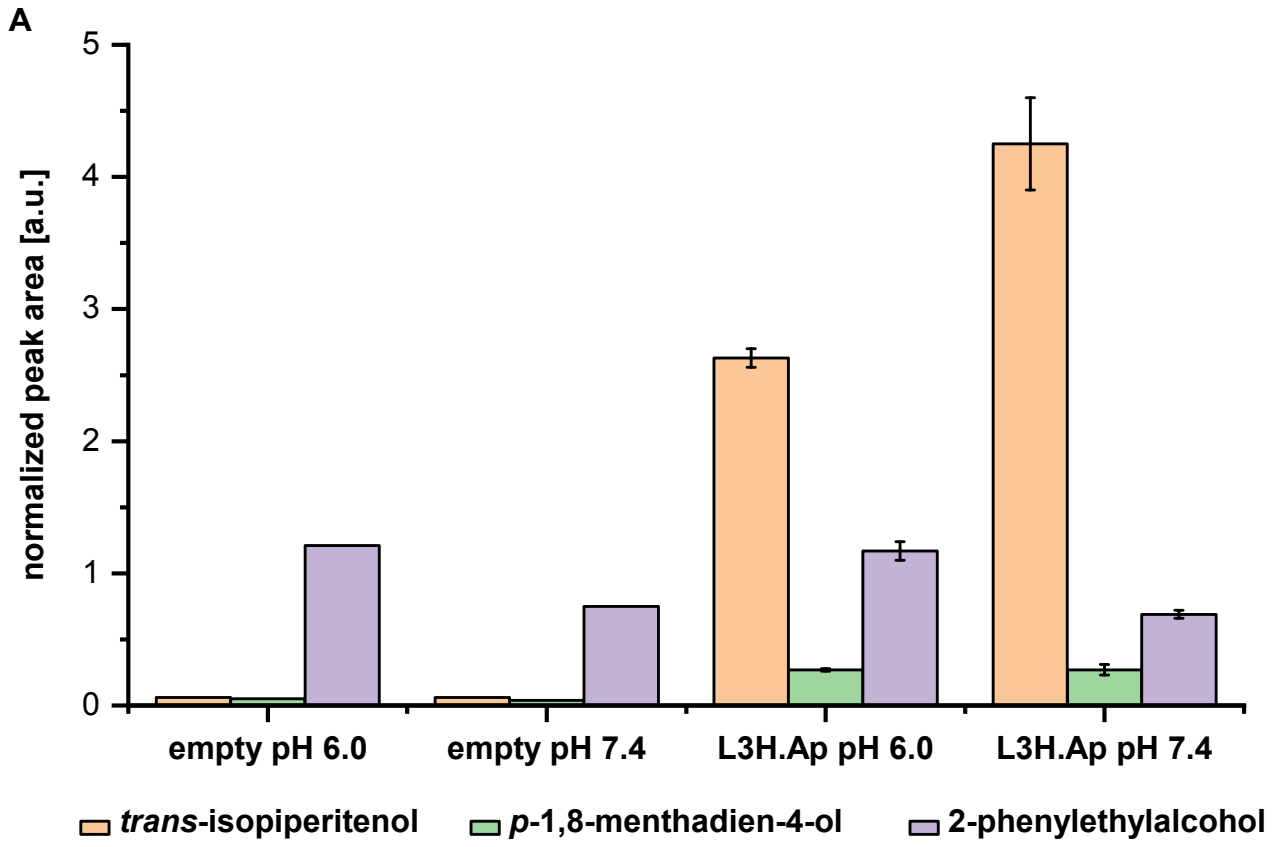
A
normalized peak area [a.u.]
0
1
2
3
4
5
empty pH 6.0
empty pH 7.4
L3H.Ap pH 6.0
L3H.Ap pH 7.4
trans-isopiperitenol
p-1,8-menthadien-4-ol
2-phenylethylalcohol

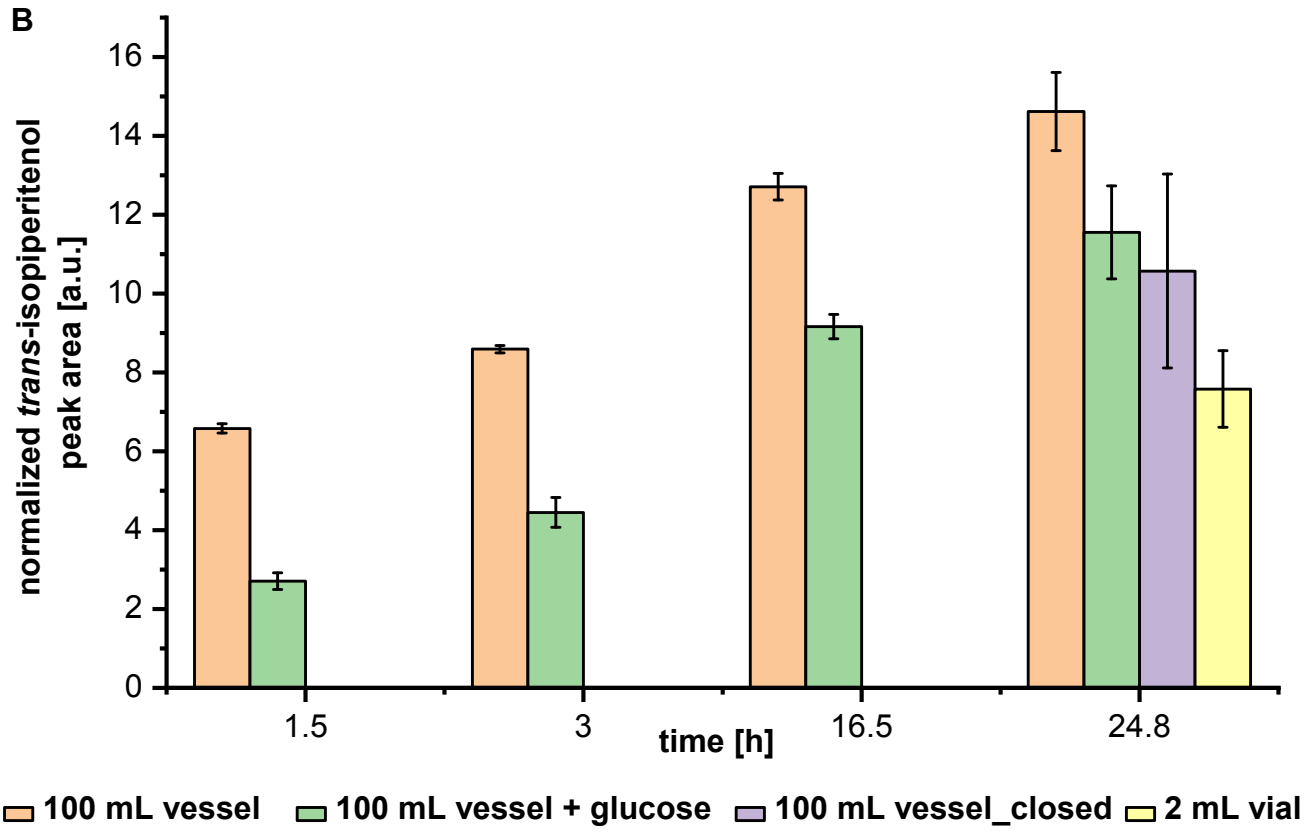
B
normalized trans-isopiperitenol peak area [a.u.]
0
2
4
6
8
10
12
14
16
1.5
3
16.5
24.8
time [h]
100 mL vessel
100 mL vessel + glucose
100 mL vessel_closed
2 mL vial

Figure S10: Product peak areas achieved in (+)-limonene biotransformation experiments with *P. pastoris* X-33 strains expressing limonene-3-hydroxylases under different conditions. Peak areas were determined by GC-MS analysis and normalized to the peak area of the internal standard (3-carene). The data points and error bars represent the mean values and standard deviations of two or three biological replicates (n = 2 - 3). (A) Investigation of the influence of buffer pH on product formation. empty: *P. pastoris* strain with empty pBSYA1Z expression vector, L3H.Ap: strain expressing CYP65AH1 of *A. pullulans* from pBSYA1Z backbone. For biotransformation 100 mM potassium phosphate buffer with pH 6.0 or pH 7.4 was used. Increase of pH value of the biotransformation buffer resulted in higher product peaks and in relation to this reduced side product formation. (B) Investigation of the influence of reaction vessel volume and glucose feeding on product formation. For the experiment a *P. pastoris* strain expressing L3H.Ap from pBSYA1Z backbone was used. Biotransformation was carried out in reaction vessels with a total volume of 100 ml or 2 ml with culture volumes of 7.5 mL or 750 µL, respectively. For "+ glucose" 2 % glucose was added at the beginning of the biotransformation. From "100 mL vessel" and "100 mL vessel + glucose" samples were taken at different time points (1.5, 3, 16.6 and 24.8 h after limonene addition). The reaction vessels of "100 mL_closed" and "2 mL vial" remained closed during the entire experiment and samples were only taken at the end (t = 24.8 h). Upscaling of the biotransformation culture and vessel volume increased product formation and a constant increase of the *trans*-isopiperitenol concentration could be observed over time. In the end of the experiment, a maximum concentration of around 600 µM (ca. 90 mg L^{-1} concentrated yeast cell suspension) *trans*-Isopiperitenol could be obtained. The addition of glucose to the biotransformation buffer to improve cofactor regeneration was not beneficial. When glucose was added, the pH of the biotransformation suspension decreased to under pH 5 during the experiment.

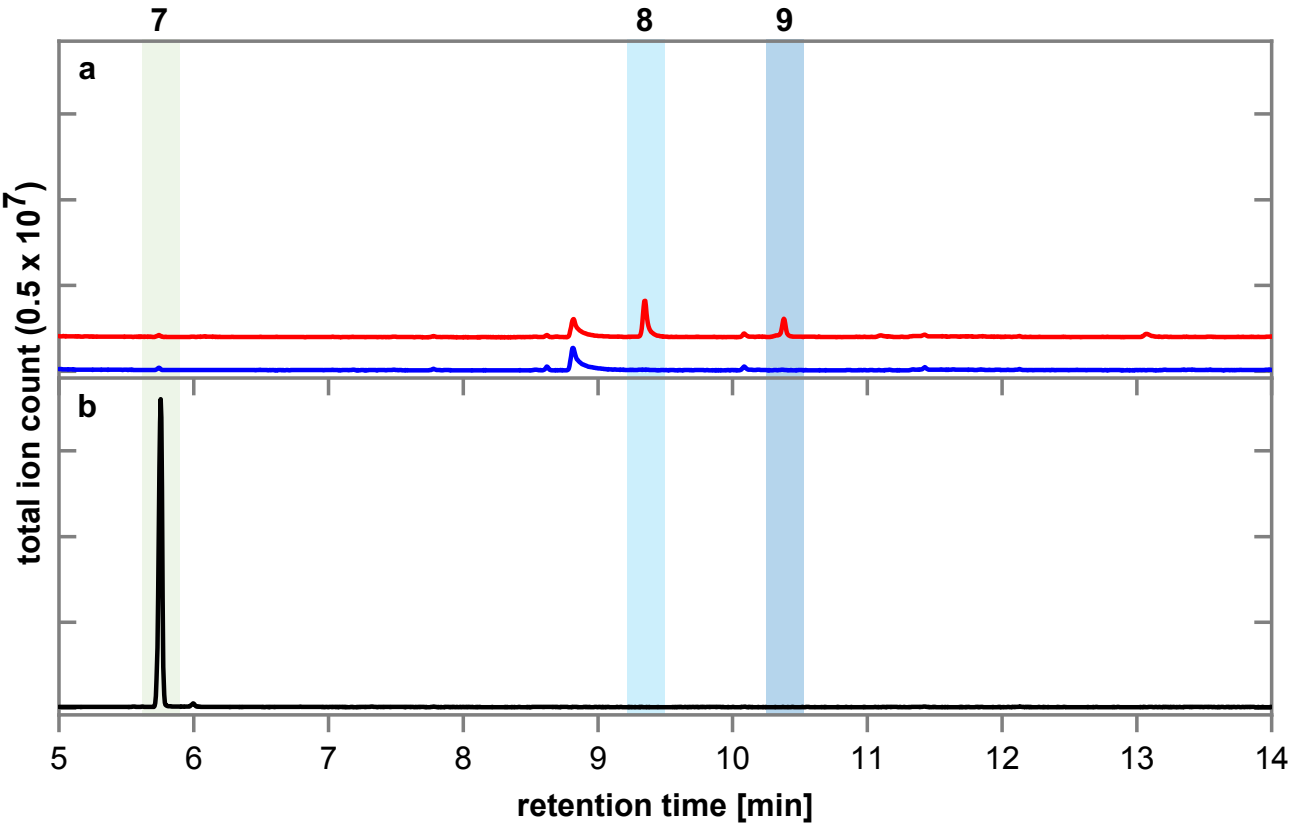

Figure S11: GC-MS analysis of biotransformation of α-pinene with *P. pastoris* X-33 strains expressing limonene-3-hydroxylase. Chromatogram from (a) the negative control with the empty expression pBSYA1Z plasmid (blue) is compared to a strain expressing L3H.Ap (red), and (b) α-pinene stock solution used in the experiment. Peak 7 is α-pinene (Rt. 5.75 min), peak 8 is verbenol (Rt. 9.35 min) and peak 9 is verbenone (Rt. 10.4 min). For MS spectra of product peaks 8 and 9 see Figure S14. While triplicates were used in the experiment, only one chromatogram each is shown here as an example.

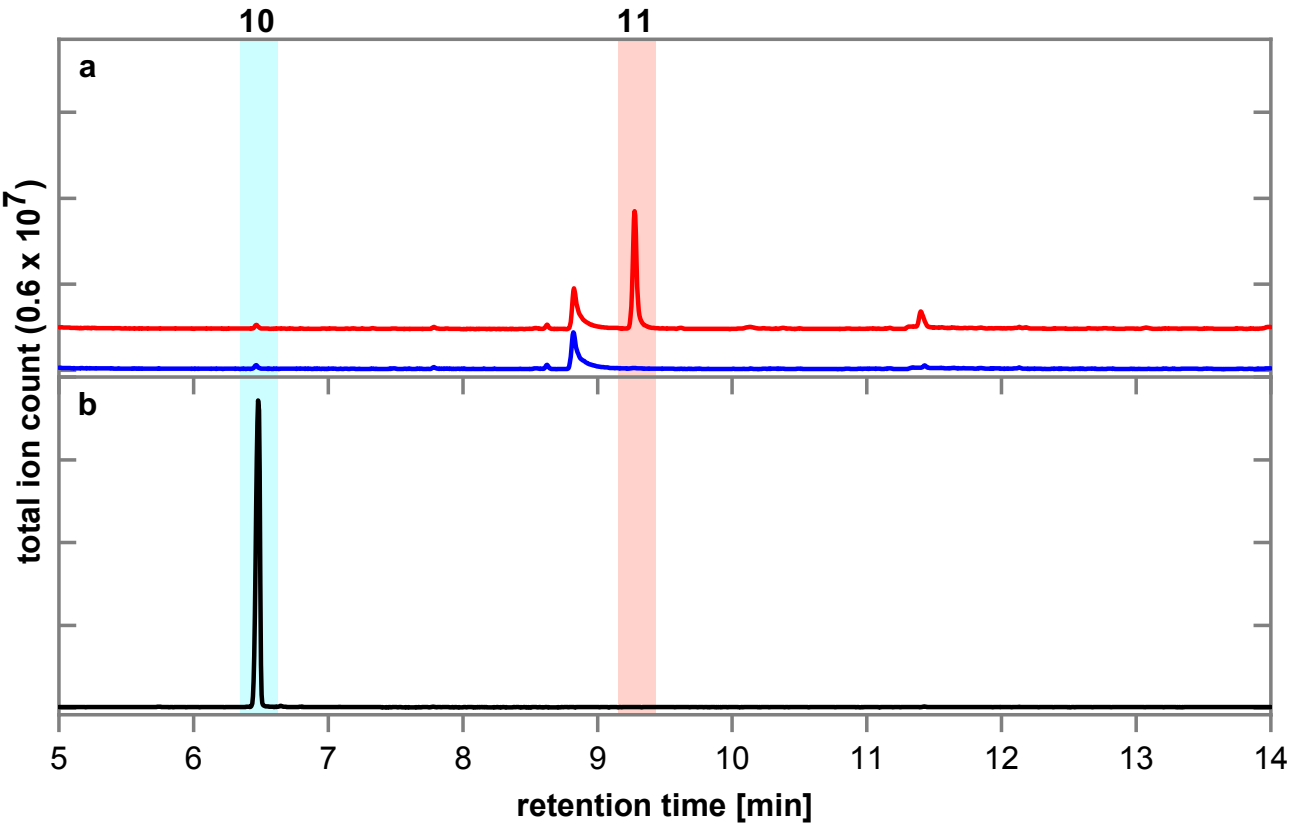

Figure S12: GC-MS analysis of biotransformation of β-pinene with *P. pastoris* X-33 strains expressing limonene-3-hydroxylase. Chromatogram from (a) the negative control with the empty expression pBSYA1Z plasmid (blue) is compared to a strain expressing L3H.Ap (red), and (b) β-pinene stock solution used in the experiment. Peak 10 is β-pinene (Rt. 6.5 min) and peak 11 is pinocarveol (Rt. 9.25 min). For MS spectrum of product peak 11 see Figure S14. While triplicates were used in the experiment, only one chromatogram each is shown here as an example.

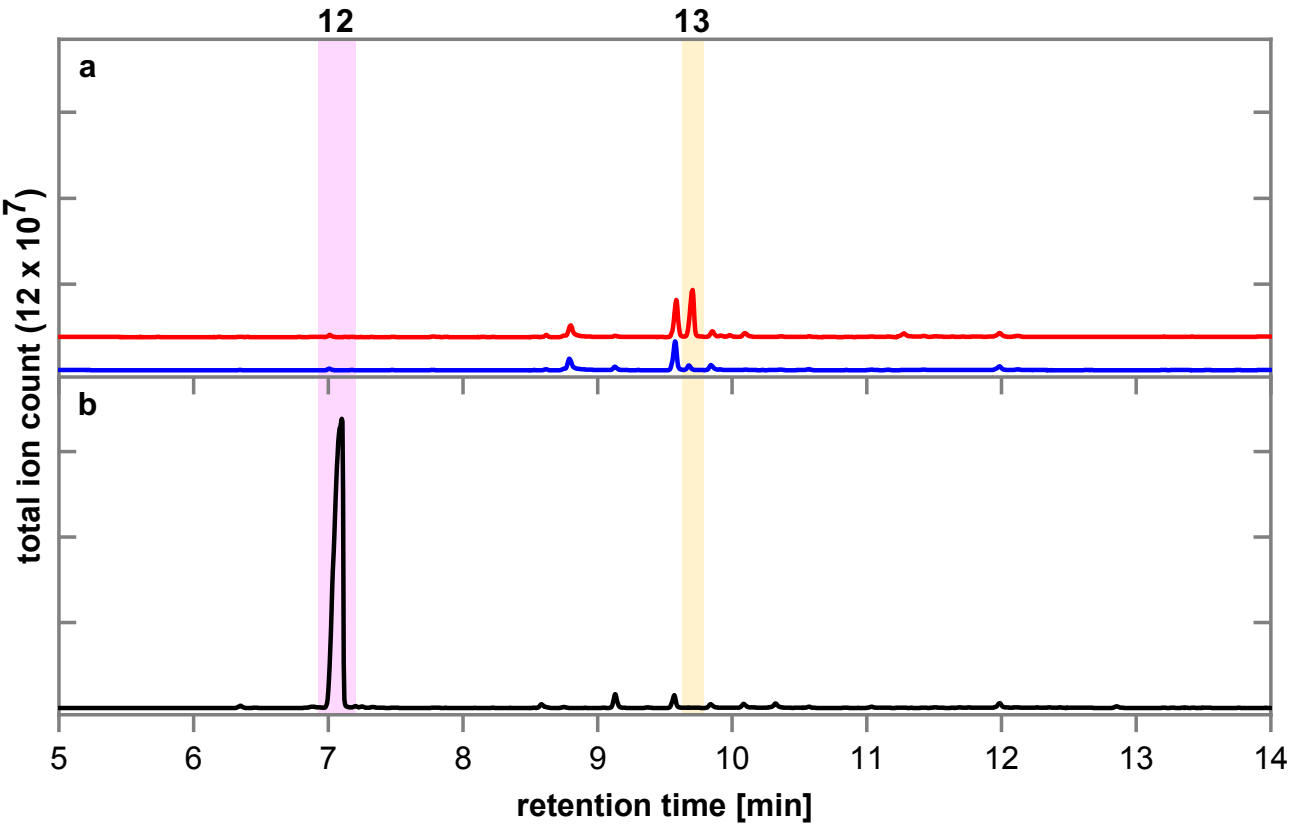

Figure S13: GC-MS analysis of biotransformation of 3-carene with *P. pastoris* X-33 strains expressing limonene-3-hydroxylase. Chromatogram from (a) the negative control with the empty expression pBSYA1Z plasmid (blue) is compared to a strain expressing L3H.Ap (red), and (b) 3-carene stock solution used in the experiment. Peak 12 is 3-carene (Rt. 7.0 min) and peak 13 is *p*-1,5-menthadien-8-ol (Rt. 9.7 min). For MS spectrum of product peak 13 see Figure S14. While triplicates were used in the experiment, only one chromatogram each is shown here as an example.

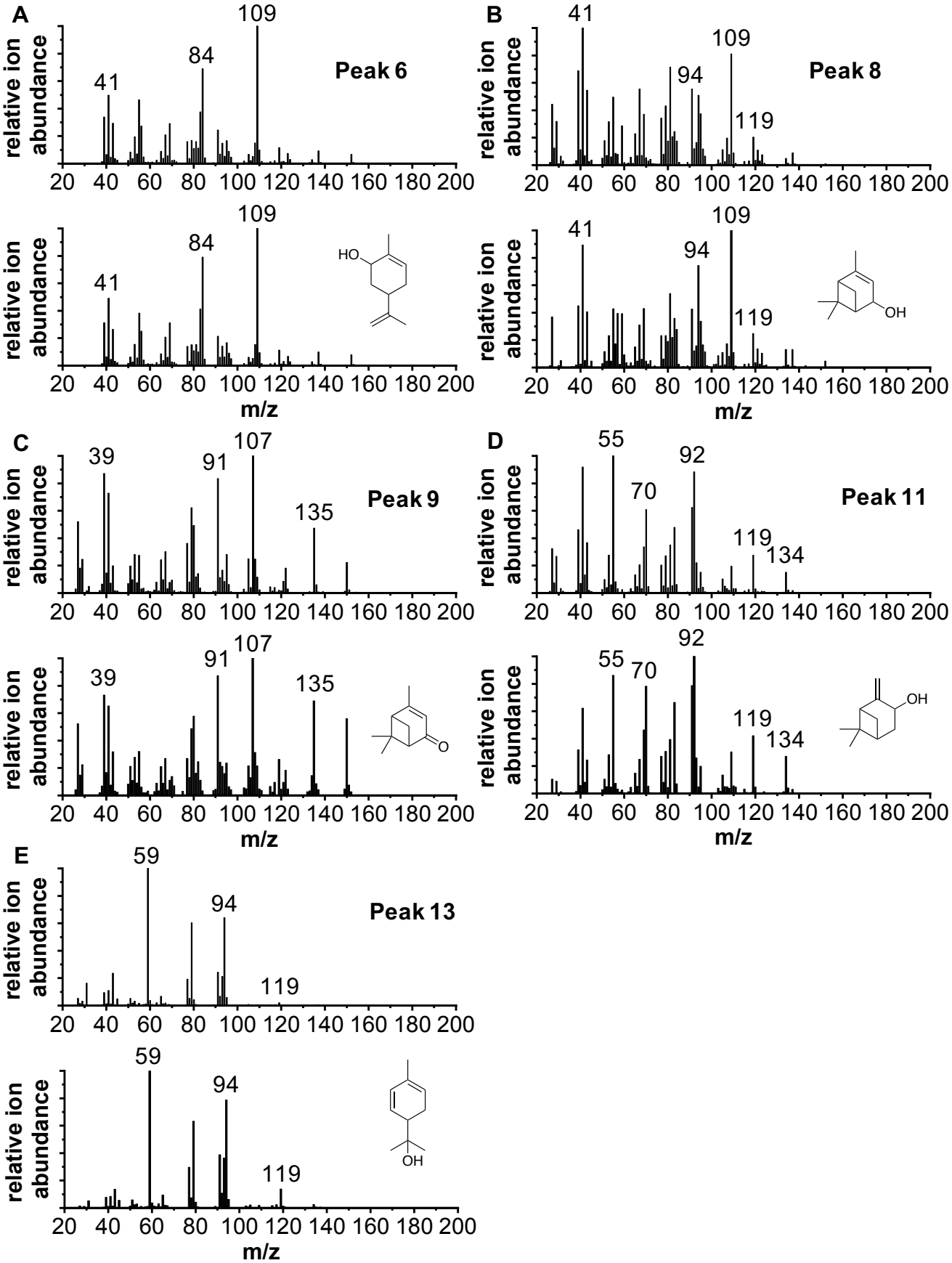

Figure S14: Identification of terpene conversion products. Mass spectra of product peak 6 (A), peak 8 (B), peak 9 (C), peak 11 (D) and peak 13 (E) obtained in biotransformation experiments with *P. pastoris* cells expressing L3H.Ap (above) are compared with those of reference compounds (below). Mass spectra were either obtained by GC-MS analysis of a reference substance or taken from the NIST mass spectral library (v14).

References – Supplementary material

1. Gostinčar C, Ohm RA, Kogej T, Sonjak S, Turk M, Zajc J, Zalar P, Grube M, Sun H, Han J, Sharma A, Chiniquy J, Ngan C, Lipzen A, Barry K, Grigoriev I V, Gunde-Cimerman N. 2014. Genome sequencing of four *Aureobasidium pullulans* varieties: biotechnological potential, stress tolerance, and description of new species. BMC Genomics 15:549.
2. Entian K-D, Kötter P. 2007. Yeast Genetic Strain and Plasmid Collections. Methods Microbiol 36:629–666.
3. Hanahan D. 1985. Techniques for transformation of *E. coli*, p. 109–135. *In* Glover, DM (ed.), DNA cloning: a practical approach. IRL Press, Oxford, United Kingdom.
4. Grant SG, Jessee J, Bloom FR, Hanahan D. 1990. Differential plasmid rescue from transgenic mouse DNAs into *Escherichia coli* methylation-restriction mutants. Proc Natl Acad Sci 87:4645–4649.
5. Entian K-D, Kötter P. 2007. 25 Yeast Genetic Strain and Plasmid Collections. Methods Microbiol 36:629–666.
6. Emmerstorfer A, Wimmer-Teubenbacher M, Wriessnegger T, Leitner E, Müller M, Kaluzna I, Schürmann M, Mink D, Zellnig G, Schwab H, Pichler H. 2015. Over-expression of ICE2 stabilizes cytochrome P450 reductase in *Saccharomyces cerevisiae* and *Pichia pastoris*. Biotechnol J 10:623–635.
7. Karp F, Mihaliak CA, Harris JL, Croteau R. 1990. Monoterpene biosynthesis: specificity of the hydroxylations of (-)-limonene by enzyme preparations from peppermint (*Mentha piperita*), spearmint (*Mentha spicata*), and perilla (*Perilla frutescens*) leaves. Arch Biochem Biophys 276:219–26.

Chapter 4 – Investigation of monoterpenoid resistance mechanisms in *Pseudomonas putida* and their consequences for biotransformations

Florence M. Schempp, Katharina E. Hofmann, Jia Mi, Ferdinand Kirchner, Annika Meffert, Hendrik Schewe, Jens Schrader, Markus Buchhaupt

Applied Microbiology and Biotechnology
DOI: 10.1007/s00253-020-10566-3

Type: research article
Status: published

Summary:
Some subspecies of the bacterium *Pseudomonas putida* show an inherent, extraordinarily high tolerance towards solvents and other organic substances such as monoterpene(oid)s. However, they are classified as biosafety level 2 organism, which makes the use of these bacteria for industrial applications considerably more difficult. In order to utilize the underlying monoterpenoid tolerance mechanisms for the development of cell factories by transferring them to suitable host strains for biotechnological production processes, a detailed knowledge is necessary. In this context, it is essential to know which molecular factors are specifically involved in monoterpenoid tolerance and whether they have particular specificities for certain structural elements and substances. For this purpose, a study was conducted comprising the creation of a mutant library, the selection for monoterpenoid-hypertolerant mutants and further characterization of the mutant strains via genome sequencing, deletion and complementation experiments, gene expression quantification (qPCRs), determination of efflux activity and toxicity assays.
The results showed that increased or decreased tolerance for monoterpenoids is mainly related to the altered expression levels of the efflux systems TtgABC and TtgDEF. In addition, it was found that increased monoterpenoid tolerance can counteract biotransformation ability, indicating the need for a fine-tuned and knowledge-based tolerance improvement for production strain development.
These results can be used to improve further the monoterpenoid tolerance of the intended *P. putida* KT2440 production strain, aiding the efficient monoterpenoid synthesis with this organism.

Declaration of author contributions to the publication:

Investigation of monoterpenoid resistance mechanisms in *Pseudomonas putida* and their consequences for biotransformations

Status: published
Name of journal: Applied Microbiology and Biotechnology

Contributing authors: **F. M. Schempp** (Doctoral candidate), K. E. Hofmann, J. Mi, F. Kirchner, A. Meffert, H. Schewe, J. Schrader, M. Buchhaupt

What are the contributions of the doctoral candidate and his co-authors?

(1) Concept and design

F. M. Schempp	**50 %**
J. Mi	10 %
H. Schewe	5 %
J. Schrader	5 %
M. Buchhaupt	30 %

(2) Conducting tests and experiments

F. M. Schempp	**50 %**	**growth experiments/toxicity assays and analytics, genetic characterization of mutants, cloning experiments, deletion and complementation experiments, qPCRs, biotransformation experiment**
K. E. Hofmann	30 %	growth experiments/toxicity assays, biotransformation experiment
J. Mi	10 %	generation and selection of the mutant library
F. Kirchner	5 %	selection of the mutant library, Splinkerette PCR
A. Meffert	5 %	efflux activity assays

(3) Compilation of data sets and figures

F. M. Schempp	**68 %**	**data collection and preparation of figures and tables**
K. E. Hofmann	25 %	data collection
F. Kirchner	5 %	data collection
A. Meffert	2 %	data collection

(4) Analysis and interpretation of data

F. M. Schempp	**60 %**	**analysis and interpretation of data, statistical analysis**
K. E. Hofmann	10 %	analysis of data
J. Mi	5 %	analysis of data
F. Kirchner	5 %	analysis of data
M. Buchhaupt	20 %	analysis and interpretation of data

(5) Drafting of manuscript

F. M. Schempp	**90 %**
M. Buchhaupt	10 %

Applied Microbiology and Biotechnology
https://doi.org/10.1007/s00253-020-10566-3

APPLIED MICROBIAL AND CELL PHYSIOLOGY

Investigation of monoterpenoid resistance mechanisms in *Pseudomonas putida* and their consequences for biotransformations

Florence Miramella Schempp[1,2] · Katharina Elisabeth Hofmann[1] · Jia Mi[1] · Ferdinand Kirchner[1] · Annika Meffert[1] · Hendrik Schewe[1] · Jens Schrader[1] · Markus Buchhaupt[1]

Received: 20 January 2020 / Revised: 5 March 2020 / Accepted: 20 March 2020

Abstract
Monoterpenoids are widely used in industrial applications, e.g. as active ingredients in pharmaceuticals, in flavor and fragrance compositions, and in agriculture. Severe toxic effects are known for some monoterpenoids making them challenging compounds for biotechnological production processes. Some strains of the bacterium *Pseudomonas putida* show an inherent extraordinarily high tolerance towards solvents including monoterpenoids. An understanding of the underlying factors can help to create suitable strains for monoterpenoids de novo production or conversion. In addition, knowledge about tolerance mechanisms could allow a deeper insight into how bacteria can oppose monoterpenoid containing drugs, like tea tree oil. Within this work, the resistance mechanisms of *P. putida* GS1 were investigated using selected monoterpenoid-hypertolerant mutants. Most of the mutations were found in efflux pump promoter regions or associated transcription factors. Surprisingly, while for the tested monoterpenoid alcohols, ketone, and ether high efflux pump expression increased monoterpenoid tolerance, it reduced the tolerance against geranic acid. However, an increase of geranic acid tolerance could be gained by a mutation in an efflux pump component. It was also found that increased monoterpenoid tolerance can counteract efficient biotransformation ability, indicating the need for a fine-tuned and knowledge-based tolerance improvement for production strain development.

Key points
- *Altered monoterpenoid tolerance mainly related to altered activity of efflux pumps.*
- *Increased tolerance to geranic acid surprisingly caused by decreased export activity.*
- *Reduction of export activity can be beneficial for biotechnological conversions.*

Keywords *Pseudomonas putida* GS1 · Monoterpenes · Monoterpenoids · Resistance · Tolerance · Ttg efflux pumps

Introduction

Monoterpenoids are a class of natural products containing more than 1000 different substances (Breitmaier 2005). All contain a linear, cyclic, or bicyclic C_{10} backbone (Habermehl et al. 2008) forming different hydrocarbons or oxygenated compounds (Berger 2007; Schrader and Bohlmann 2015). In nature, monoterpenoids are ubiquitously present in plants, e.g., in essential oils of coniferous wood, in citrus fruits, and in flowers (Schrader 2010). In industry, monoterpenoids are widely used in pharmaceuticals, flavor and fragrance, and agriculture (Habermehl et al. 2008; Chen et al. 2015). However, for many monoterpenoids, the extraction from natural sources poses challenges low concentration in the raw material or because the natural sources are constantly ceasing. Furthermore, many of the structurally more complex terpenoids cannot be chemically synthesized in an economic way. Therefore, microbial production or conversion processes can provide attractive alternatives, particularly if regioselective or stereoselective reactions are included (Berger 2007; Chen et al. 2015).

Electronic supplementary material The online version of this article (https://doi.org/10.1007/s00253-020-10566-3) contains supplementary material, which is available to authorized users.

✉ Markus Buchhaupt
markus.buchhaupt@dechema.de

[1] DECHEMA-Forschungsinstitut, Industrial Biotechnology, Theodor-Heuss-Allee 25, 60486 Frankfurt am Main, Germany

[2] Faculty Biological Sciences, Goethe University Frankfurt, Max-von-Laue-Str. 9, 60438 Frankfurt am Main, Germany

Published online: 16 April 2020

Monoterpenoids have certain physicochemical characteristics that impede the development of industrial bioprocesses dealing with such compounds as educts and/or products: poor water solubility, high volatility, and distinct cytotoxicity (Trombetta et al. 2005; Berger 2007; Schrader 2010). The latter is related to their accumulation in the cell membrane, leading to an increased membrane fluidity and disturbance of essential cellular functions. In addition, protein denaturation and oxidative damage are caused by incubation of cells with certain monoterpenoids (Andrews et al. 1980; Uribe et al. 1985; Sikkema et al. 1994; Trombetta et al. 2005; Schrader 2010).

It is known that certain microorganisms, among others some strains of *Pseudomonas putida*, can cope with high concentrations of organic solvents (Ramos et al. 2015), including monoterpenoids (Speelmans et al. 1998; Mi et al. 2014). *P. putida* is a gram-negative, saprotrophic soil bacterium (Nelson et al. 2002; Silby et al. 2011) with a diverse catabolism, including the ability to degrade different organic solvents (Timmis 2002; Wu et al. 2011; Ramos et al. 2015). Several *P. putida*-based biotechnological production processes for monoterpenoids have been described, such as the biotransformation of limonene to perillic acid (Speelmans et al. 1998; Mars et al. 2001) or perillyl alcohol (van Beilen et al. 2005; Cornelissen et al. 2011; Cornelissen et al. 2013), the de novo synthesis of geranic acid starting from glycerol (Mi et al. 2014), or the regioselective and stereoselective hydroxylation of 1,8-cineole to (1*R*)-6β-hydroxy-1,8-cineole (Mi et al. 2016).

To further increase the native monoterpenoid tolerance of *P. putida* and to enable the transfer of underlying resistance mechanisms to suitable host strains for biotechnological production processes, the molecular factors of monoterpenoid tolerance and potential specificities for certain structural elements have to be determined. The general solvent tolerance mechanisms in *P. putida* have been studied intensively with a focus on the model compounds toluene or butanol, reviewed previously (Isken and de Bont 1998; Ramos et al. 2002; Ramos et al. 2015). The multifactorial response after solvent exposure involves changes in membrane composition (Pinkart and White 1997; Ramos et al. 1997; Isken and de Bont 1998; Heipieper et al. 2003), activation of a general stress response system, enhanced energy generation (Ramos et al. 2015), and induction of specific efflux pumps that extrude solvents to the medium (Isken and de Bont 1996; Ramos et al. 1997; Kieboom et al. 1998). In *P. putida* DOT-T1E, three RND (resistance-nodulation-division) efflux systems have been identified to be directly involved in solvent tolerance (Ramos et al. 2015). These efflux systems (TtgABC, TtgDEF, and TtgGHI) are encoded by the so-called toluene tolerance genes (Ramos et al. 1998; Mosqueda and Ramos 2000; Duque et al. 2001; Rodríguez-Herva et al. 2007). All three efflux pumps consist of three components: an inner membrane protein (TtgB/E/H), which binds the substrates and acts as the extrusion element, an outer membrane protein that reaches into the periplasmic space to form a channel (TtgC/F/I), and a lipoprotein that plays a role in stabilizing the interaction between the other two elements (TtgA/D/G) (Ramos et al. 2002). The Ttg pump-mediated efflux is energized by the proton motive force across the cytoplasmic membrane (Udaondo et al. 2012; Ramos et al. 2015). Expression of the *ttg* operons is repressed by the transcription factors TtgR, TtgT, and TtgV, which are encoded adjacent to the *ttg* efflux pump operons (Duque et al. 2001; Ramos et al. 2002; Rojas et al. 2003; Teran et al. 2003; Ramos et al. 2005; Krell et al. 2007; Terán et al. 2007; Ramos et al. 2015). In other *Pseudomonas* strains, similar tolerance mechanisms have been described, such as the SrpABC efflux pump in *P. putida* S12 (Isken and de Bont 1996; Kieboom et al. 1998) or the Mex efflux systems in *Pseudomonas aeruginosa* (Poole et al. 1993; Gotoh et al. 1995; Poole et al. 1996). Whether these general solvent resistance mechanisms of *P. putida* also apply to monoterpenes and monoterpenoids remains to be investigated.

In vitro studies by Sikkema et al. (1994) and experiments with *Escherichia coli* by Trombetta et al. (2005) have shown that the toxic effect of monoterpenes and their derivatives is at least partially caused by the incorporation of the substances into the bacterial cell membranes, whereby the function of the membranes is disturbed. In addition, they probably also penetrate the cells and interact with other targets, such as enzymes (Sikkema et al. 1994; Trombetta et al. 2005). With regard to tolerance mechanisms, the MexAB-OprM efflux pump of *P. aeruginosa* was shown to play a decisive role for the tolerance of this species to tea tree oil and its monoterpenoid compounds (Papadopoulos et al. 2008). The Mex efflux systems of *P. aeruginosa* are very similar to the Ttg and Srp efflux pumps of *P. putida* (Ramos et al. 2002). In addition, other studies with *E. coli* revealed that active efflux of monoterpenoids is an important factor for increased tolerance (Dunlop et al. 2011). These studies let us expect an involvement of *P. putida* efflux systems in monoterpenoid tolerance.

To test this hypothesis and to identify and further characterize mechanisms specifically responsible for the natural high tolerance of *P. putida* GS1 towards several monoterpenoids, we selected monoterpenoid-hypertolerant mutants and characterized them via genome sequencing, deletion and complementation experiments, tolerance assays, qPCRs, and efflux activity measurements. Moreover, the impact of increased monoterpenoid tolerance on a biotechnological production process was investigated.

Materials and methods

Chemicals and media

All chemicals were purchased from Sigma-Aldrich (Taufkirchen, Germany), Carl-Roth (Karlsruhe, Germany), or Merck Millipore (Darmstadt, Germany).

Monoterpenoids were acquired with different purities: 1,8-cineole (≥ 99%), citral (≥ 98%), geranic acid (≥ 85%), geraniol (≥ 99%), geranyl acetate (≥ 99%), geranyl formate (≥ 95%), linalool (≥ 97%), myrcene (≥ 95%), α-terpinene (≥ 95%), γ-terpinene (≥ 98.5%), (+)-terpinen-4-ol (≥ 98.5%), (+)-α-terpineol (≥ 97%), α-terpinyl acetate (≥ 97%), and (1*S*)-(−)-verbenone (≥ 99%).

For cultivation of *E. coli* and *P. putida*, lysogeny broth (LB) or terrific broth (TB) medium was used. For solid media, 17 g l^{-1} agar-agar was added. Antibiotics and other supplements were used at the following concentrations, if required: kanamycin (Km) 50 μg ml^{-1}, gentamicin (Gm) 25 μg ml^{-1}, tetracycline (Tet) 50–150 μg ml^{-1}, and L-rhamnose 2 mg ml^{-1}.

Strains, plasmids, and oligonucleotides

All strains, plasmids, and oligonucleotides used in this study are listed in Online Resource Table S1.

P. putida cells were routinely grown at 30 °C and *E. coli* cells at 37 °C. All oligonucleotides were ordered from Sigma-Aldrich (Taufkirchen, Germany).

Strain and plasmid construction

Deletion mutants of *ttgR*, *ttgT*, and 10 nucleotides of *ttgABC*-5′-UTR were obtained following the method published by Martínez-García and de Lorenzo (2011). For this purpose, plasmids pEMG-Δ*ttgR*, pEMG-Δ*ttgT*, and pEMG-Δ10 nt-*ttgABC* were constructed using primer P1–P4, P5–P8, or P9–P12, respectively. The correct deletion was checked by colony PCR and sequencing of the obtained PCR fragments.

Plasmids pMiS4-*ttgR* and pMiS4-*ttgT* were constructed by amplifying the *ttgR* and the *ttgT* genes together with their native promoter regions via PCR using *P. putida* GS1 gDNA as template and primer P13 and P14 or P15 and P16, respectively.

All plasmids used in this study were constructed using Gibson isothermal assembly (Gibson et al. 2009) and chemical competent *E. coli* cells (Inoue et al. 1990). The correct and sequenced plasmids were electroporated into *P. putida* GS1 strains following a protocol by Choi et al. (2006).

Generation of mutant library

Transposon mutagenesis of *P. putida* GS1 was performed following methods published by Klebensberger et al. (2007) and Li et al. (2010). Introduction of plasmid pALMAR-3, harboring a *Himar1 mariner* transposon (Lampe et al. 1999), into *P. putida* GS1 was performed by bi-parental mating with *E. coli* S17-1 λpir as donor. For *E. coli* S17-1 λpir harboring pALMAR-3, 20 ml LB medium containing 30 μg ml^{-1} kanamycin was inoculated with an OD_{600} of 0.1 from an overnight pre-culture. For *P. putida* GS1, 100 ml LB medium was inoculated with an OD_{600} of 0.05. After reaching OD_{600} of 2 or 0.3, respectively, 8 ml of LB culture of the *E. coli* donor strain and 100 ml of the recipient strain *P. putida* GS1 were harvested, washed twice with 8 ml pre-warmed LB medium, and resuspended in 400 μl pre-warmed LB medium each. Subsequently, the cell suspensions were mixed in a 1:1 volume ratio (cell ratio *E. coli* to *P. putida* around 1:2) and placed on LB agar. After incubation for 24 h at 30 °C, the cells were resuspended from the plate with 2 ml 0.9% (*w*/*v*) NaCl solution. One hundred microliter aliquots of the cell suspension were spread on *Pseudomonas* isolation agar plates (King et al. 1954) containing 150 μg ml^{-1} tetracycline to select for *P. putida* transposon mutants. After incubation for 24 h at 30 °C, colonies were washed from the plates with 2 ml LB medium containing 20% glycerol and stored at − 80 °C.

Growth selection of monoterpenoid-hypertolerant mutants

For growth selection under different monoterpenoid stress conditions, both *P. putida* GS1 wildtype (WT) cells and the transposon mutant library were used as a mixture to ensure large cell variety at the starting point. The monoterpenoids were added directly to the bacteria cultures in different, partly increasing concentrations: 1,8-cineole 20, 40, and 60 mM; geranic acid 35 and 90 mM; geraniol 32 and 65 mM; α-terpineol 17.5 mM; and verbenone 35 mM. The cryo stocks were thawed on ice and grown overnight at 30 °C in shake flasks with 20 ml TB medium containing 50 μg ml^{-1} tetracycline.

For the selection of 1,8-cineole-hypertolerant mutants, the preculture was diluted to an OD_{600} of 0.1 with TB medium. The cells were cultivated with the stressor for 24 h at 30 °C in a microbioreactor system (BioLector®) at 1000 rpm using 1.5 ml culture volume in 48-well Flowerplates® (m2p-labs GmbH, Baesweiler, Germany) covered by gas-permeable sealing foil. From the stationary phase culture, new TB cultures were inoculated to an OD_{600} of 0.1 and again cultivated in the microbioreactor system with 1,8-cineole. This procedure was followed for five cultivation steps. After each round, cultures with improved tolerance properties were selected for the next selection round. Each culture was cultivated in triplicates. Only for the first cultivation 50 μg ml^{-1} tetracycline was added to the medium. After cultivation 2, 3, and 4, the cells were spread on LB-agar plates and incubated over night at 30 °C or for 3 days at room temperature. Subsequently, the cells were washed from the agar plates with 3 ml NaCl (0.9%), and 1 ml of the cell suspension was used to inoculate the new culture.

For the selection of geranic acid, geraniol, α-terpineol, and verbenone-hypertolerant mutants 200 μl preculture was transferred into 20 ml TB medium each and the respective stressor

was added. The cultures were incubated in shake flasks for around 24 h at 30 °C. Between five and seven sequential cultivation rounds were conducted for each monoterpenoid. For each further round, the main culture was inoculated to a start OD_{600} of 0.1. Before the last cultivation round for all monoterpenoids, the cells were spread out on LB agar to obtain single colonies for inoculation.

Based on the growth performance of the different mutants in the last cultivation round, for each selection substance one (or in the case of verbenone two) candidate strains were selected for further characterization.

Genetic characterization of monoterpenoid-hypertolerant mutants

In order to determine the genotype of the selected mutant strains, the mutation sites were mapped via splinkerette PCR (Devon et al. 1995; Mikkers et al. 2002) (CR mutant) or genome sequencing (TR, GR, GAR, VR1, VR2 mutant).

For the 1,8-cineole selected mutant (CR), gDNA was extracted using the *GenElute Bacterial Genomic DNA* kit (Sigma-Aldrich, Taufkirchen, Germany). Of total gDNA, 1.5 μg was digested with BamHI. Subsequently, hybridized splinkerette adapter (P17 and P18, 1.2 pmol) was ligated to 300 ng of the DNA fragments using T4-Ligase (NEB, Frankfurt am Main, Germany). Ligation products were isolated using the *DNA Clean & Concentrator™-5* kit (Zymo Research, Freiburg, Germany). Transposon-chromosome junctions were amplified by PCR with a primer specific for the adapter (P19) and a primer specific for the mariner transposon (P20). After purification of the PCR product with the *DNA Clean & Concentrator™-5* kit (Zymo Research, Freiburg, Germany), a second PCR with the first PCR product as template using primer P21 and P22 was conducted. Finally, the obtained PCR product was purified as described before and sequenced.

To localize the transposon integration site, the sequences adjacent to the transposon were mapped to the genome sequence of *P. putida* GS1. The latter was provided by the company GenXPro (Frankfurt am Main, Germany) using the SMRT method and with the annotation software Prokka (v1.11) (Torsten Seemann 2014).

For the genotypic characterization of the mutants GAR, GR, TR, VR1, and VR2, for each strain, 200 ml TB medium was inoculated to an OD_{600} of 0.2 from an overnight culture and incubated at 30 °C and 180 rpm. When cultures reached an OD_{600} between 2.5 and 5, cells were harvested, washed with 20 ml H_2O, and frozen with liquid nitrogen to store at − 80 °C. Genomic DNA preparation and genome sequencing via SBS (*sequencing by synthesis*)-Illumina approach (Illumina, San Diego, USA) was conducted by the company GenXPro (Frankfurt am Main, Germany). Reads obtained from sequencing were mapped against the *P. putida* GS1 genome using the software G*eneious* (Biomatters Ltd., Auckland, New Zealand). In order to reduce errors occurring from the sequencing method, the *P. putida* GS1 WT genome was resequenced in parallel with the Illumina approach.

Monoterpenoid tolerance assays

Pre-cultures of *P. putida* GS1 WT and mutant strains grown in TB medium were used to inoculate TB cultures to an OD_{600} of 0.1, supplemented with appropriate antibiotics if required. The respective monoterpenoid was added directly after inoculation. The concentrations tested for each compound, without consideration of purity, were 1,8-cineole 40, 60, 100, and 200 mM; citral 25 and 100 mM; geranic acid 100 and 200 mM of substance with 85% geranic acid; geraniol 40, 65, and 100 mM; geranyl acetate 25 and 100 mM; geranyl formate 25 and 100 mM; linalool 25 and 100 mM; myrcene 17.5, 35, 60, 100, and 200 mM; α-terpinene 25 and 200 mM; γ-terpinene 17.5, 35, 60, 100, and 200 mM; (+)-terpinen-4-ol 80 mM; (+)-α-terpineol 17.5, 35, and 60 mM; α-terpinyl acetate 25 and 100 mM; (1*S*)-(−)-verbenone 15, 25, and 35 mM.

Cells exposed to the different chemicals were incubated for 48 h at 30 °C in a microbioreactor system (BioLector®) at 1000 rpm and 85% humidity using 1 ml culture volume in 48-well Flowerplates® (m2p-labs GmbH) covered with gas-permeable sealing foil. Biomass formation was monitored via scattered light signal intensity at 620 nm. If the strains contained the pMiS4-eGFP plasmid, growth was monitored additionally via GFP fluorescence signal intensity, using an excitation filter of 488 nm and an emission filter of 520 nm. For induction of GFP expression, L-rhamnose was added to a final concentration of 0.2% (*w*/*v*) directly after inoculation. All growth comparison experiments in Flowerplates® were performed at least in triplicates. Culture samples were distributed randomly on the plate.

For quantification of verbenone concentration in the cell suspensions and in cell-free medium over time, cells were cultivated as described above but with 1.5 ml culture volume. Verbenone (35 mM) was added at inoculation. Samples of 180 μl were taken at time points $t = 0$, 15, 22, 40, and 45 h. To the samples, 20 μl 1 M H_2SO_4 was added and analytes were extracted using 200 μl ethyl acetate. Samples were centrifuged (16,000× *g*, 2 min), and the organic phase was analyzed by GC-MS (GC-17A with QP5050A detector, Shimadzu) with a VB-5 column (30 m × 0.25 mm × 0.25 μm, ValcoBond® (Valco Instruments Co. Inc. and VICI AG)). Measurements were conducted as follows: helium as carrier gas, split ratio 35, injections at 250 °C, and a column flow of 2.6 ml min^{-1}. The column temperature was programmed as follows: 80 °C for 3 min, 7 °C min^{-1} up to 150 °C followed by 150 °C for 2 min. Absolute concentration of verbenone was calculated from chromatogram peak areas by comparison to a calibration curve prepared by measuring a

dilution series of verbenone standard with known concentrations.

RNA extraction, cDNA synthesis, and quantitative polymerase chain reaction

In order to quantify differences in expression of the efflux pump genes between *P. putida* GS1 WT and mutants, total RNA was harvested from growing cultures following a protocol modified from Otto et al. (2019). Therefore, pre-cultures grown in TB medium were used to inoculate TB medium to an OD_{600} of 0.1. Cultures were cultivated at 30 °C and 200 rpm until mid-exponential growth phase (OD_{600} 0.9–1.1). Samples of 1 ml cell suspension were harvested (13,000× *g*, 2 min), resuspended in 800 µl *RNA/DNAShield* solution (Zymo Research Europe GmbH), and stored at − 80 °C until further analysis. RNA was extracted from cells using *Quick RNA™ Miniprep Plus Kit* (Zymo Research Europe GmbH) following manufacturer's instructions including in-column DNase treatment. cDNA was prepared from purified RNA using the *IScript™ gDNA Clear cDNA Synthesis Kit* (Bio-Rad Laboratories, Inc.). The expression levels of different efflux pump genes were analyzed using primers designed by an online Realtime PCR tool (http://www.idtdna.com/scitools/Applications/RealTimePCR). Primers are listed in Table S1 (P23–34). As reference gene, *rpoD* was used and amplified with primers described previously (Franden et al. 2018). Quantitative PCR was performed using *QuantiTec SYBR Green PCR Kit* (Qiagen) on a *PikoReal™ Real-Time PCR* System (Thermo Scientific). The reaction conditions were 15 min at 95 °C, 45× (15 s at 94 °C, 30 s at 60 °C, and 30 s at 72 °C), followed by melting curve analysis (30 s starting at 50 °C, increasing 0.2 °C per cycle, ending at 95 °C). Experiments were performed with biological triplicates. No-template controls were run for every primer pair, and no-RT (reverse transcriptase) controls were run for every RNA sample. Transcript levels of *ttg* genes were estimated by comparing their Ct (cycle threshold) values to the Ct value of the housekeeping gene *rpoD* (Wang and Nomura 2010). Final expression levels were averaged for each mutant strain and normalized to the expression level of the *P. putida* GS1 wild-type strain using the following formula:

$\Delta\Delta Ct = \Delta CtE - \Delta CtC$
with $\Delta CtE = Ct$ (*ttg* gene mutant) − Ct (*rpoD* gene mutant).
and $\Delta CtC = Ct$ (*ttg* gene wild type) − Ct (*rpoD* gene wild type).

Gene expression fold change was calculated as follows:

$$\text{Fold change} = 2^{-\Delta\Delta Ct}.$$

For statistical analysis, Shapiro-Wilk normality test, followed by pairwise comparison using van der Waerden normal score test with Benjamini-Yakutiel *p* value adjustment, was applied on ΔCt values.

Efflux activity assay

Efflux pump activity of *P. putida* wild type and mutants was determined via resazurin accumulation assay described by Vidal-Aroca et al. (2009). Ten milliliter LB medium in 100-ml Erlenmeyer flasks was inoculated from overnight cultures to an OD_{600} of 0.1 and grown at 30 °C and 180 rpm to mid-exponential phase (OD_{600} around 1). Cells were harvested by centrifugation (12,000× *g*, 3 min). The cell pellets were washed two times with 1× PBS buffer and resuspended in PBS + 0.4% glucose. Fluorescence signal was measured with an *Infinite® 200 PRO* microtiter plate reader (Tecan). Experiments were performed with biological triplicates. The slope of the fluorescence increase was averaged for each strain over 50 min of the experiment and compared to the wild-type value. For statistical analysis, Shapiro-Wilk normality test, followed by pairwise comparison using van der Waerden normal score test with Benjamini-Yakutiel *p* value adjustment, was applied on slope mean values of fluorescence measurements.

Biotransformation experiments

An approach modified from Mi et al. (2014) was used. Pre-cultures of *P. putida* GS1 WT and mutant strains grown in TB medium were diluted with TB medium to an OD_{600} of 0.1. Cultures were divided into 1.5 ml aliquots in 48-well Flowerplates® (m2p-labs GmbH, Baesweiler, Germany), and 35 mM geraniol as biotransformation substrate was added directly after inoculation. Cells were incubated for 38 h at 30 °C in a microbioreactor system (BioLector®) at 1000 rpm covered with gas-permeable sealing foil. Biomass formation was monitored via scattered light signal intensity at 620 nm. Geranic acid concentrations at different time points (0, 12, 21, and 38 h) were determined by HPLC analysis. All strains were tested in triplicates, distributed randomly on the plate.

To *P. putida* culture samples of 150 µl, 15 µl 1 M HCl was added and analytes were extracted using 165 µl hexane containing 1 mM thymol as an internal standard. Samples were centrifuged (16,000× *g*, 5 min), and the organic phase was analyzed by HPLC, consisting of a diode array detector and a C18 column (Alltech Alltima, C18, 5 µm, 250 × 4.6 mm; C18 Precolumn, Grace GmbH and Co. KG, Worms, Germany). Substances were separated isocratically using acetonitrile/acidified water (containing 0.05% (*v*/*v*) 3 M phosphoric acid) in a ratio of 45:55 (*v*/*v*) as mobile phase. After

each run, the column was washed with 90:10 mixture of acetonitrile/acidified water.

For statistical analysis, Shapiro-Wilk normality test, followed by pairwise comparison using van der Waerden normal score test with Benjamini-Yakutiel *p* value adjustment, was applied.

Results

Tolerance of *P. putida* GS1 towards monoterpenoids

For the development of microbial monoterpenoid production strains, a deep molecular understanding of the tolerance mechanisms for such compounds represents a prerequisite. As *P. putida* shows strong monoterpenoid tolerance (Inoue and Horikoshi 1991; Speelmans et al. 1998; Mi et al. 2014; Rau et al. 2016) and its organic solvent resistance mechanisms have been extensively studied (Isken and de Bont 1998; Ramos et al. 2015), we chose the *P. putida* strain GS1 (Speelmans et al. 1998) to explore its behavior after exposure to a number of different monoterpenoids (Fig. 1).

The effects of the different compounds on the growth of *P. putida* GS1 were investigated by comparing characteristics of the growth curves from microbioreactor cultivations under the influence of exogenously added chemicals. Cell density was monitored via scattered light signal and GFP fluorescence measurements. Experiments without addition and with different concentrations of monoterpenes and monoterpenoids had previously confirmed that growth curves obtained by scattered light signal measurements and fluorescence measurements are comparable for most of the substances tested (Online Resource Fig. S1–Fig. S4) and that GFP gene expression does not influence the growth of *P. putida*. Only in the case of geranic acid an interference of the substance with the scattered light signal could be observed and the GFP signal was necessary to monitor growth.

Analysis of the resulting data showed that the monoterpenes and monoterpenoids affect growth of *P. putida* GS1 differently (Fig. 2, Online Resource Fig. S2–Fig. S4). The bacterium could cope with the hydrocarbons (myrcene, α-terpinene, γ-terpinene) up to the highest tested concentration of 200 mM and the esterified monoterpenoids (geranyl acetate, geranyl formate, α-terpinyl acetate) up to the highest tested concentration of 100 mM without any apparent effect on its growth. The aldehyde citral, the ether 1,8-cineole, and the alcohols geraniol and linalool caused a slight prolongation of the lag phase when added in concentrations between 100 and 200 mM. However, if geraniol, linalool, or geranyl acetate were added, *P. putida* GS1 reached higher maximal GFP fluorescence intensities compared with cultures without monoterpenoid addition. Addition of 200 mM geranic acid caused a reduction in growth rate and a slightly prolonged lag phase. The most pronounced growth inhibition was observed for the ketone verbenone and the alcohols α-terpineol and terpinen-4-ol, which caused lag phase prolongations of more than 10 h if present in concentrations of 35, 60, and 80 mM, respectively.

Testing different concentrations of the same monoterpenoid revealed a positive correlation between compound concentration and severity of growth inhibition (Online Resource Fig. S1).

Isolation and investigation of monoterpenoid-hypertolerant mutants

In order to investigate the molecular mechanisms of monoterpenoid tolerance in *P. putida* GS1 and their specificities, a mutant library was created by transposon mutagenesis

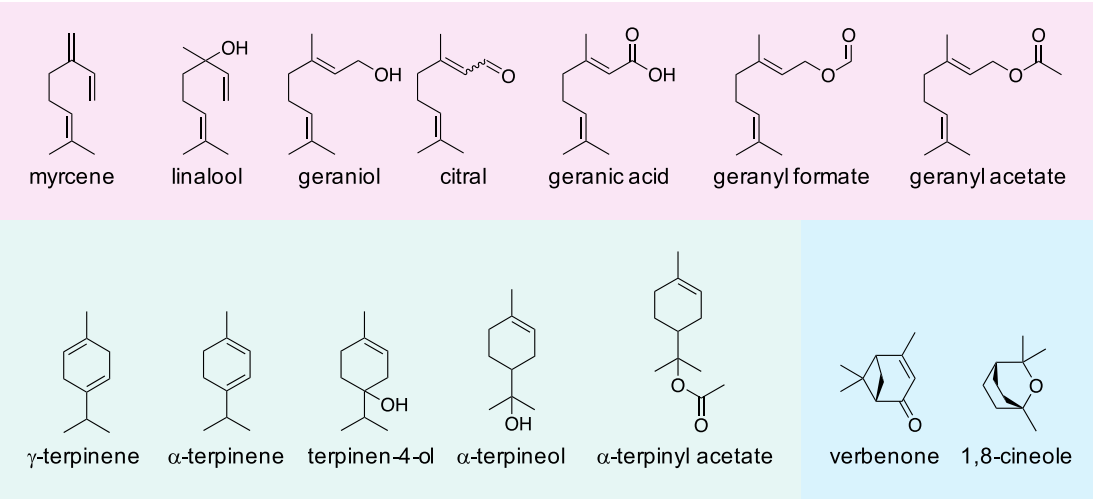

Fig. 1 Chemical structures of monoterpenes and monoterpenoids used in this study. Red: linear, green: monocyclic, blue: bicyclic structures

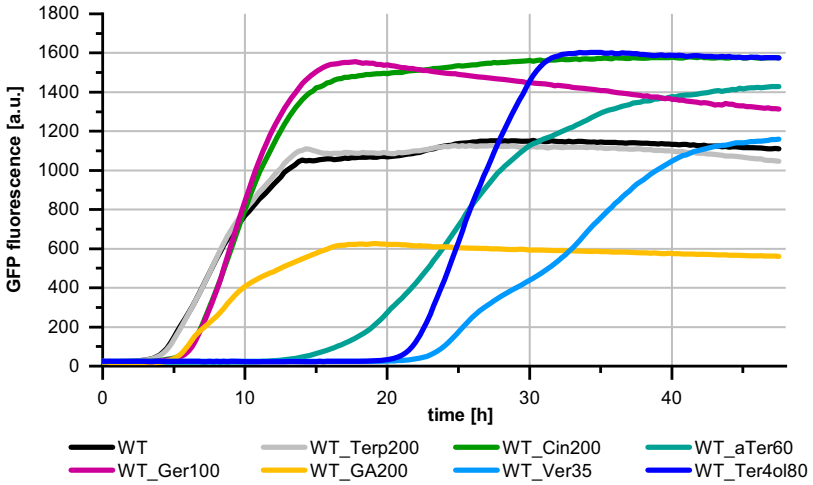

Fig. 2 Growth of *P. putida* GS1 (WT) + pMiS4-eGFP without and in the presence of different monoterpenes and monoterpenoids. Terp200: γ-terpinene (200 mM), Cin200: 1,8-cineole (200 mM), aTer60: α-terpineol (60 mM), Ger100: geraniol (100 mM), GA200: geranic acid (200 mM), Ver35: verbenone (35 mM), Ter4ol80: terpinen-4-ol (80 mM). Tolerance assays were conducted in a microbioreactor system over 48 h. Biomass formation was monitored every 10–15 min via GFP fluorescence signal intensity (excitation filter 488 nm; emission filter 520 nm). The data points represent the mean values of three biological replicates. For variations between the replicates of each strain, see Online Resource Fig. S18

with a *Himar1 mariner* transposon (Lampe et al. 1999; Klebensberger et al. 2007; Li et al. 2010). The mutant library was grown in the presence of one of the toxic compounds 1,8-cineole, geranic acid, geraniol, α-terpineol, or verbenone, and monoterpenoid-hypertolerant mutants were selected. To ensure a large diversity at the starting point, also *P. putida* GS1 wild-type cells were added to the mutant selection process. After testing the phenotypes of several mutants, one representative with improved growth characteristics towards the specific selection monoterpenoid (shorter lag phase and/or increased growth rate) compared with the WT strain was chosen for further studies. The strains were named according to the monoterpenoid used as selective agent: 1,8-cineole-resistant (CR), geranic acid-resistant (GAR), geraniol-resistant (GR), α-terpineol-resistant (TR), and verbenone-resistant (VR1) mutant.

Without the addition of monoterpenoids, the mutants showed similar growth curve characteristics as the wild-type strain (Online Resource Fig. S5). Monoterpenoid tolerance assays in microbioreactor cultivations with 1,8-cineole (200 mM), geraniol (100 mM), α-terpineol (60 mM), terpinen-4-ol (80 mM), or verbenone (35 mM) revealed improved tolerance of the mutant strains CR, GR, TR, and VR1 compared with the wild-type strain (Fig. 3a, Online Resource Fig. S6–Fig. S12). The most profound tolerance phenotypes for these compounds were obtained for the TR and the VR1 mutant. In contrary, when CR, GR, TR, and VR1 were exposed to 200 mM geranic acid, their growth was impaired to a higher extent than that of the wild-type strain (Fig. 3b). The only exception was the GAR mutant, which showed an improved tolerance towards geranic acid compared with the wild-type strain (Fig. 3b). However, the GAR strain was much more sensitive towards all other monoterpenoids tested (Fig. 3a, Online Resource Fig. S6–Fig. S12).

To identify the genotypic characteristics causing the specific monoterpenoid-hypertolerant phenotypes of the mutants, either a splinkerette PCR approach was applied to identify transposon integration sites, or whole genome sequencing. The results are summarized in Fig. 4a, b, Table 1, and Online Resource Table S2. In the CR mutant, the transposon was localized in the *ttgR* gene, the transcriptional regulator of the genes encoding the TtgABC efflux pump. The transposon in the GR mutant was found to be inserted in the *ttgT* gene, the transcriptional regulator repressing transcription of the *ttgDEF* operon. Genome analysis of GAR, TR, and VR1 revealed no mariner transposon sequence but distinct other mutations. In the TR mutant, a 10-nucleotide deletion was identified in the region directly behind the transcription start of the *ttgABC* operon. The deleted region includes the − 35 region of the *ttgR* promoter.

In order to verify the correlation between the identified Ttg-related mutations in the CR, GR, and TR mutant and improved monoterpenoid tolerance, *P. putida* GS1 strains were constructed which contain a deletion of either the *ttgR* or the *ttgT* gene or lack the 10 nucleotides in the region between the *ttgR* and *ttgA* open reading frames according to the respective mutation observed in the TR genome. Monoterpenoid tolerance assays conducted with the constructed deletion mutants Δ*ttgR*, Δ*ttgT*, and $\Delta 10nt_{ttgABC\text{-}5'UTR}$ and the original mutants CR, GR, and TR showed comparable tolerance phenotypes (Online Resource Fig. S13–Fig. S15). When the CR and Δ*ttgR* or the GR and Δ*ttgT* strains were complemented with a plasmid for expression of the *ttgR* or the *ttgT* gene, respectively, the mutant strains showed a similar sensitivity towards

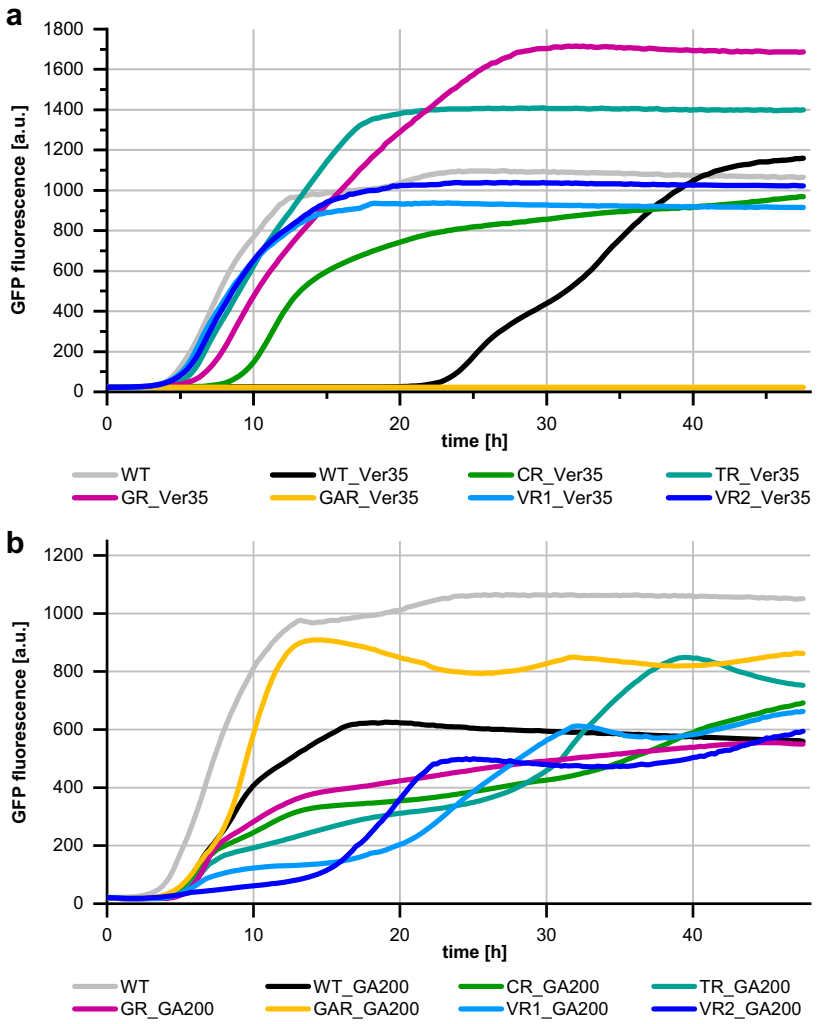

Fig. 3 Growth of *P. putida* GS1 WT and mutants + pMiS4-eGFP in the presence of **a** 35 mM verbenone (Ver35) or **b** 200 mM geranic acid (GA200). Tolerance assays were conducted in a microbioreactor system over 48 h. Biomass formation was monitored every 10–15 min via GFP fluorescence signal intensity (excitation filter 488 nm; emission filter 520 nm). The data points represent the mean values of three biological replicas. For variations between the replicas of each strain, see Online Resource Fig. S24 and Fig. S28

the monoterpenoids as the wild-type strain. These results confirm that deletion of both the *ttgR* and the *ttgT* gene as well as the deletion of 10 bp in the region between the *ttgR* and *ttgA* open reading frames are causal for the observed monoterpenoid-hypertolerant phenotypes of CR, GR, and TR.

Analysis of the genome sequence data obtained for the GAR mutant revealed a deletion of 41 nucleotides in the *ttgA* gene, coding for a subunit of the TtgABC efflux system. The deletion results in a stop codon after nucleotide 207 of the open reading frame.

In the genome of VR1, a variety of different mutations were identified (Online Resource Table S2). Because none of the identified mutations could be directly linked to an increased monoterpenoid tolerance, a second mutant selected in the presence of verbenone (VR2) was investigated. VR2 showed similar tolerance phenotypes in the tolerance assays compared with VR1 (Fig. 3, Online Resource Fig. S6–Fig. S12) and again over 30 different mutations were identified in its genome (Online Resource Table S2). In both strains, a mutation was present in a gene encoding a DNA repair protein (VR1: *mutS*, VR2: *mutL*). In addition, the genomes of both strains contained a mutation in one of the *nuo* genes (VR1: *nuoB*, VR2: *nuoG*), encoding subunits of NADH-quinone oxidoreductase/NADH dehydrogenase, which is part of the respiratory chain.

As the analysis of VR1 and VR2 genome sequences did not reveal indications for efflux pump alterations, we aimed to test a putative detoxification of verbenone by degradation or conversion by these mutants. However, this hypothesis could be disproven by GC-MS analyses. No conversion products were detectable, and verbenone concentration decreased in the VR cultures over time with the same rate as with WT cells and in the medium control without cells (Online Resource Fig. S16).

Quantitative PCR analysis of mRNA levels of *ttg* genes *ttgR*, *ttgA*, *ttgB*, *ttgT*, and *ttgE* showed reduced expression of TtgR and increased production of TtgABC efflux system in the CR mutant (Fig. 4c). In the TR mutant, transcription of the *ttgABC* efflux pump genes were also significantly enhanced.

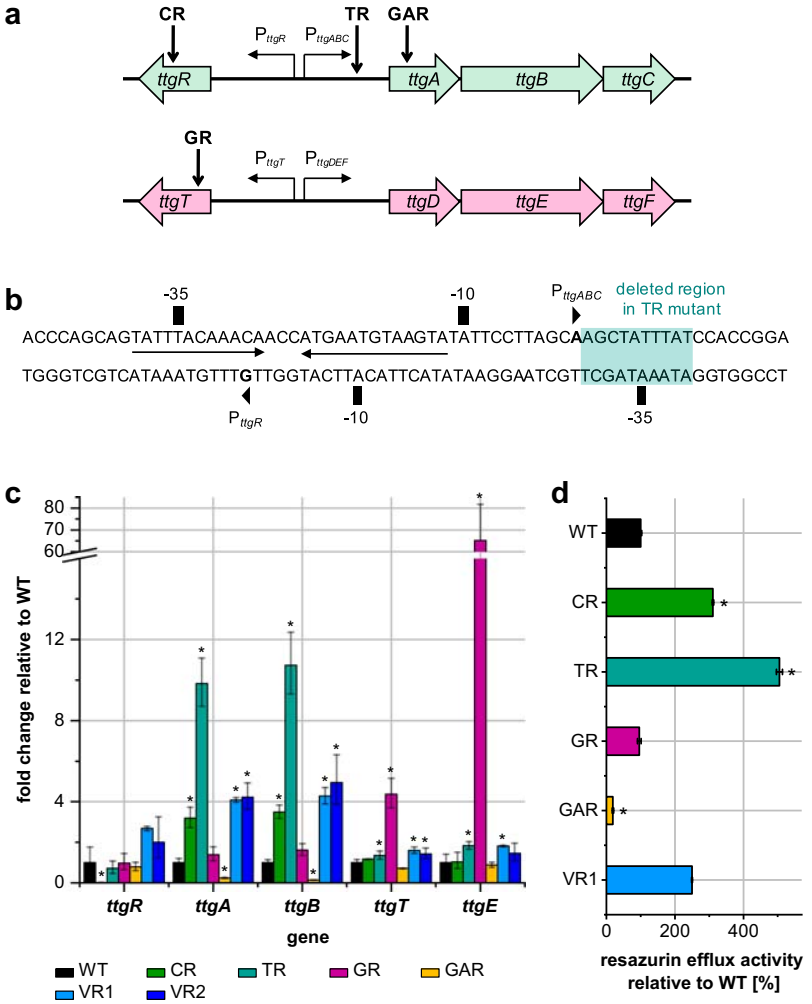

Fig. 4 Further characterization of mutant strains (CR, TR, GR, GAR, VR1, and VR2). **a** Localization of identified mutations in different mutant strains. **b** Nucleotide sequence of the *ttgABC-ttgR* intergenic region. Deleted region in TR mutant is highlighted in green. The putative TtgR palindromic recognition site is indicated by the arrows; *ttgABC* and *ttgR* + 1 (arrowheads), − 10, and − 35 points are marked according to Terán et al. (2003). **c** Relative expression levels of *ttg* genes in mutants compared with *P. putida* GS1 wild type ($2^{-\Delta\Delta Ct}$). **d** Resazurin efflux pump activity of *P. putida* GS1 mutant strains relative to wild type. Slope mean values of fluorescence increase over time of mutant strains normalized to wild type are given. Cells were grown in LB medium until mid-exponential phase and resuspended in PBS buffer with resazurin. Efflux activity was monitored by measuring the fluorescence intensity of resazurin reduction product resorufin (excitation filter 530 nm; emission filter 590 nm). While a slow increase in fluorescence indicates high efflux activity, a high slope shows low efflux activity. In **c** und **d**, results represent the mean values and standard deviations of three biological replicates. The asterisks indicate a significant difference for the mutant strains compared with wild-type GS1 according to van der Waerden normal score test with Benjamini-Yakutiel p value adjustment ($p < 0.05$)

The opposite was the case with the GAR mutant, which showed a decrease of the TtgABC efflux system mRNA levels. In the GR mutant, the expression of the TtgDEF efflux system was increased. VR1 and VR2 also showed an enhanced mRNA quantity of both efflux pump systems compared with the GS1 wild type.

To measure the efflux activity of the different strains, an efflux pump activity assay was performed according to a protocol by Vidal-Aroca and colleagues (2009). The experiments revealed a reduced resazurin efflux activity for the GAR mutant compared with the wild-type strain (Fig. 4d). While no difference in resazurin efflux activity could be measured between the GR mutant and the wild type, an increased efflux was observed for the CR, TR, and VR1 mutant in the experiments.

Geranic acid biotransformation performance of monoterpenoid-hypertolerant strains

For efficient and robust microbial monoterpenoid de novo production or biotransformation processes, both tolerance of the cells towards educts and products, and productivity should be as high as possible, whereby interactions between these parameters are possible. In order to investigate if the altered

Table 1 Mutant strains, selection substances, and identified mutations presumably causing the altered monoterpenoid tolerance phenotypes

Mutant	Selection substance	Mutation responsible for or involved in evolution of hypertolerance phenotype
CR	1,8-Cineole	Transposon insertion in *ttgR* gene (487 nucleotides downstream of start codon)
		ttgR ➔ transcriptional regulator of *ttgABC* operon
TR	α-Terpineol	Deletion of 10 nucleotides in 5′-UTR of *ttgABC* mRNA (directly after $P_{ttgABC}+1$) and −35 region of P_{ttgR}
GR	Geraniol	Transposon insertion in *ttgT* gene (40 nucleotides downstream of start codon)
		ttgT ➔ transcriptional regulator of *ttgDEF* operon
GAR	Geranic acid	Deletion of 41 nucleotides in *ttgA* gene (109 nucleotides downstream of start codon)
		ttgA ➔ subunit of TtgABC efflux system
VR1	Verbenone	• 33 different mutations (16-nucleotide deletion, 32 single nucleotide exchanges)
		• DNA repair protein (*mutS*)
		• Subunit of respiratory chain protein (*nuoB*)
VR2	Verbenone	• 32 different mutations (1 nucleotide deletion, 1 nucleotide insertion, 30 single nucleotide exchanges)
		• DNA repair protein (*mutL*)
		• Subunit of respiratory chain protein (*nuoG*)

monoterpenoid tolerance properties of the mutant strains influence their bioconversion abilities, they were employed for the conversion of geraniol into geranic acid. *P. putida* GS1 has been demonstrated to carry out this biotransformation (Mi et al. 2014). Geraniol (35 mM) was added directly after inoculation of the cultures in the microbioreactor system, and geranic acid concentration was determined at different time points within 38 h (Fig. 5).

In the wild-type culture, a product concentration of 15 mM was reached after 12 h, which increased up to 16 mM until 38 h. Using the TR strain, a geranic acid concentration of 9.5 mM was observed after 38 h. The mutants CR and GR produced geranic acid levels in the range of the wild-type value. Only with the geranic acid mutant GAR, the used geraniol was nearly completely oxidized to 32 mM geranic acid after 38 h. However, the whole conversion took place in the last 14 h of the experiment. This observation was accompanied by the growth curve of GAR. While the wild-type strain and the other mutants started to grow about 5 h after inoculation, cell density of the GAR mutant started to increase after 20 h.

Discussion

It is long known that some essential oils and their monoterpenoid compounds exhibit antimicrobial properties. However, the specific bacterial mechanisms causing the natural tolerance of, e.g., *Pseudomonas putida* strains towards specific monoterpenoids have hardly been explored. A deeper understanding of the underlying factors and the specificities of the mechanisms is crucial for the development of highly efficient and robust microorganisms producing monoterpenoids de novo or via biotransformation.

In the conducted experiments, the different monoterpenes and monoterpenoids affected the growth behavior of *P. putida* GS1 wild type very differently. None of the tested hydrocarbons and esterified monoterpenoids showed an inhibitory effect on cell growth in the concentrations tested. This indicates that no inhibition of cell functions takes place or that the cells can protect themselves against the substances without affecting growth. Addition of the alcohols, aldehyde, ether, ketone, and acid caused a prolongation of the lag phase, but to different extents. These results are in accordance with the general assumption that the toxicity of a particular substance correlates with its hydrophobicity. The hydrophobicity determines to what extent the compound accumulates in the cytoplasmic membrane. A measure of the hydrophobicity is the logarithm of the octanol-water partition coefficient ($\log P_{ow}$) of the respective substance, with values between 1 and 4.5. The lower the $\log P_{ow}$ value, the more toxic the substance is (Inoue and Horikoshi 1989; Sikkema et al. 1994; Ramos et al. 2002; Kabelitz et al. 2003; Dunlop 2011). According to the SciFinder database, the $\log P_{ow}$ value increases as follows: verbenone < terpinen-4-ol < α-terpineol < linalool = 1,8-cineole < geraniol < geranic acid < citral < geranyl formate < α-terpinyl acetate < geranyl acetate < γ-terpinene < α-terpinene.

Apart from the chemical and physical properties that determine the toxicity of the monoterpenes and monoterpenoids, the observed effects also depend on how effectively *P. putida* GS1 can defend itself against the various substances with its inherent mechanisms. While in the genome of *P. putida* DOT-T1E the genes of three different Ttg efflux systems, TtgABC,

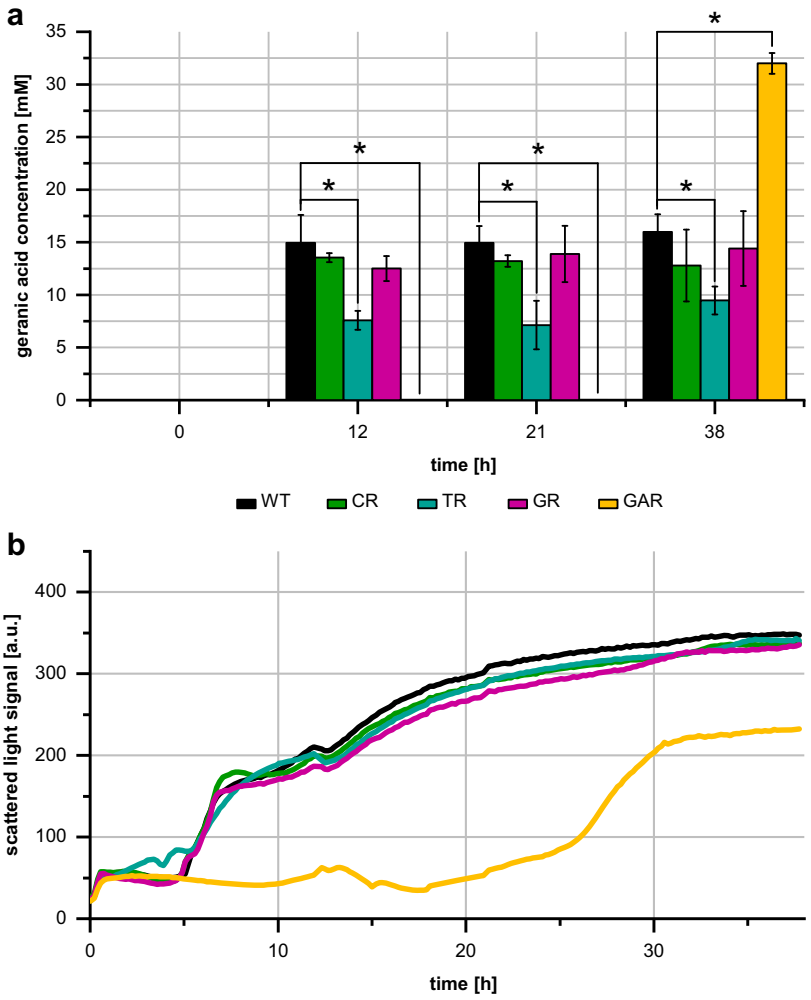

Fig. 5 Geranic acid production (**a**) and growth (**b**) of *P. putida* GS1 WT and mutants (CR, TR, GR, GAR) in a geraniol to geranic acid biotransformation. The experiment was conducted in a microbioreactor system over 38 h. To determine geranic acid concentration, samples were taken at time points $t = 0$, 12, 21, and 38 h and analyzed via HPLC. The data points represent the mean values and standard deviations of three biological replicas. The asterisks indicate a significant difference for the mutant strains as compared with wild-type GS1 according to van der Waerden normal score test with Benjamini-Yakutiel p value adjustment ($p < 0.05$). Biomass formation was monitored every 10–15 min via scattered light signal intensity (absorbance at 620 nm). The data points represent the mean values of three biological replicas. For variations in growth between the replicas of each strain, see Online Resource Fig. S29

TtgDEF and TtgGHI, were found (Segura et al. 2003), the frequently used KT2440 strain contains only the TtgABC system (Nelson et al. 2002). Genome sequencing of the GS1 strain revealed two Ttg efflux systems, TtgABC and TtgDEF, which are very similar to the systems in KT2440 and DOT-T1E (Online Resource Table S3). Some of these systems, such as the TtgABC efflux pump, mediate an intrinsic basal solvent tolerance (Ramos et al. 1998; Rojas et al. 2001). Other mechanisms, such as the expression of the *ttgDEF* operon or an increased TtgABC production, first have to be activated (Mosqueda and Ramos 2000; Rojas et al. 2001; Ramos et al. 2015). This can prolong the lag phase in the presence of toxic compounds, because the cells can only protect themselves effectively against the substances after the genes have been expressed. However, the fact that in the presence of verbenone, α-terpineol and terpinene-4-ol growth is delayed for more than 10 h, is probably not only due to the circumstance that transcription of tolerance mechanisms, such as efflux pumps, first has to be induced. Even with activated efflux pumps, the concentration of the substances in the medium must decrease below a certain value before cell growth is no longer inhibited. Experiments with verbenone showed that the monoterpenoid concentration in the cultures decreases over time (Online Resource Fig. S16) due to evaporation. The concentration reached after about 15 h was ca. 15 mM, which did not cause strong inhibitory effects in previous experiments (Online Resource Fig. S1).

In addition to a prolonged lag phase, the presence of α-terpineol, verbenone, and geranic acid impaired growth rate and in the case of geranic acid growth yield. These effects can be explained by an alteration of cellular processes and metabolic fluxes in the cells, e.g., due to increased membrane permeability or the inhibition of certain proteins (Sikkema et al. 1994). Furthermore, the high energy demand of efflux pump activity can cause a reduced growth yield (Ramos et al. 1997; Isken et al. 1999).

The positive effect of some compounds on the maximal biomass yield of *P. putida* GS1 might be explained by a

metabolization of the monoterpenoids. As described previously, *P. putida* GS1 is not able to utilize geraniol or geranic acid as sole carbon source (Cantwell et al. 1978; Mi et al. 2014), but can oxidize geraniol into geranic acid, thereby forming NADH and $FADH_2$ (Mi et al. 2014) and providing the cells with an additional energy source.

To further elucidate the monoterpenoid tolerance mechanisms in *P. putida* GS1, we isolated and characterized monoterpenoid-hypertolerant mutants. Tolerance assays with selected strains showed different extents of tolerance improvement and different specificities. Genome sequencing, gene expression quantification of *ttg* genes, and efflux activity assays provided further insight into differences between the mutant strains on the cellular level.

In the CR and GR strain, transposon insertion in the *ttgR* or *ttgT* repressor gene, respectively, resulted in a constitutive and increased expression of the corresponding efflux pump proteins TtgABC or TtgDEF (Duque et al. 2001; Terán et al. 2007). Constitutive efflux pump expression can improve solvent tolerance (Fukumori et al. 1998; Duque et al. 2001; Rau et al. 2016) and usually results in a clear reduction of the increased lag phase duration caused by the toxic compound.

The 10-nucleotide deletion in the TR mutant covers the region of the *ttgABC*-5′-UTR directly after the transcription start as well as the −35 region of the *ttgR* promoter (Terán et al. 2003). The hypertolerance phenotype can be a result of increased *ttgABC* mRNA stability or translation rate. Quantitative PCR experiments showed enhanced transcript levels of the *ttgABC* operon in the TR mutant, which fits to increased efflux activity compared with the wild type. This results in improved solvent tolerance (Fukumori et al. 1998; Duque et al. 2001), as shown in the growth experiments with different monoterpenoids.

In the GAR mutant, the deletion in the *ttgA* gene results in a loss of the TtgABC efflux system accompanied by a reduced resazurin efflux activity. The strain showed an increased sensitivity towards the tested monoterpenoid alcohols, 1,8-cineole, and verbenone, indicating that a functional TtgABC efflux system is not only essential for the tolerance towards toluene and different antibiotics (Ramos et al. 1998; Rojas et al. 2001; Martínez-García and de Lorenzo 2011), but also for monoterpenoid resilience of *P. putida* GS1. The relation between an active efflux and improved monoterpenoid tolerance is in accordance with previous findings. Papadopoulos and colleagues reported that in *Pseudomonas aeruginosa,* the MexAB-OprM efflux system plays a decisive role for the strain's tolerance towards monoterpenoids such as terpinen-4-ol, 1,8-cineole, and α-terpineol and that the absence of a pump subunit or the entire pump leads to a higher sensitivity towards different monoterpenoids (Papadopoulos et al. 2008). Also for *E. coli* (Shah et al. 2013) and eukaryotic systems (Wang et al. 2013), a causal connection between the presence of efflux pumps and tolerance to monoterpenes and monoterpenoids has been described. However, the correlation between efflux pump expression and monoterpenoid tolerance does not explain the increased tolerance of the GAR strain towards geranic acid, because in this case, loss of an efflux pump component increased the tolerance. A possible explanation is based on the presumption that the geranic acid import rate might be much higher compared with those of the other compounds. If such a continuous uptake is accompanied by a concomitant energy-demanding efflux (Ramos et al. 2002), a futile cycle would have been created. This hypothesis would also explain the clearly reduced growth rate and yield of the wild-type strain in the presence of geranic acid, caused by an energy-consuming futile cycle. The loss of TtgABC activity in the GAR mutant would thus interrupt the cycle and allow a higher growth rate again.

Analysis of the VR mutant genomes revealed more than 30 mutations each, but none of them was located in an efflux pump operon. Nevertheless, further experiments showed increased transcription of TtgABC and TtgDEF efflux pump systems concomitant with an enhanced resazurin efflux activity compared with the wild type. Which mutations lead to an increased expression of the efflux pump genes is unclear. However, the high number of mutations in both strains can be explained by mutations in *mutS* or *mutL*, respectively, which are known to cause high mutation rates (Acharya et al. 2003; Brandt 2006). The fact that both independent strains represent mutator strains strongly indicates that the selection procedure with verbenone required a multigenic trait to bring up these highly tolerant strains. A comparison of the additional genome changes revealed that both strains have a point mutation in a *nuo* gene (VR1: *nuoB*, VR2: *nuoG*). *NuoB* and *nuoG* encode subunits of NADH-ubiquinone oxidoreductase, which is part of the respiratory chain (Weidner et al. 1993; Camacho Carvajal et al. 2002). *NuoB* and *nuoG* were already found to be upregulated in *P. putida* S12 cells during toluene stress (Wijte et al. 2011). The *nuo* gene mutations in VR1 and VR2 could possibly lead to an increased catabolism to provide more ATP for monoterpenoid export or other tolerance mechanisms.

To test the applicability of such hypertolerant strains in biotechnological processes, geraniol to geranic acid biotransformation experiments were conducted. After 38 h, a geranic acid concentration of around 16 mM could be achieved with the wild-type strain, which corresponds to a product yield of 45% and is in accordance with previous studies (Mi et al. 2014). The experiments with the mutants showed that the different tolerance levels of the mutants, caused by differences in efflux activity, had an impact on the conversion of geraniol into geranic acid. The two extremes were the mutants TR and GAR. For the TR mutant, characterized by a high monoterpenoid tolerance and high level of resazurin efflux activity, geraniol conversion ability was significantly

impaired. In contrast to this, an almost quantitative conversion of geraniol could be achieved with the GAR mutant (product yield 91%). Our explanation for biotransformation performance reduction of the TR strain is an enhanced export of the biotransformation educt geraniol caused by *ttgABC* overexpression. The GAR mutant lacks this efflux pump and therefore presumably has no or strongly reduced geraniol export activity. This can lead to a strong improvement of the reaction yield, since the educt geraniol is available in the cells for bioconversion. The extraordinarily long lag phase, which was caused by the strong reduction or lack of geraniol efflux activity, can be overcome by separation of growth and production phase in a respective process.

In conclusion, our study demonstrates the highly different toxicity levels of certain monoterpenes and monoterpenoids and reveals the Ttg efflux pumps of *P. putida* GS1 to be mainly responsible for tolerance towards many of the tested compounds. The application example furthermore clearly demonstrates that a fine-tuned tailoring of transport and tolerance properties is essential for the design of efficient and robust biotechnological processes.

Acknowledgments We thank the Jenal group (Uni Basel) for providing us with the pALMAR-3 plasmid.

Author contribution F.M.S., J.M., H.S., J.S., and M.B. designed the research. F.M.S., K.E.H., J.M., F.K., and A.M. performed the experiments. F.M.S., K.E.H., J.M., F.K., and M.B. analyzed the data. F.M.S. and M.B. wrote the manuscript with input from all authors.

Funding information Open Access funding provided by Projekt DEAL. This research was supported by funds of the Federal Ministry of Food and Agriculture (BMEL) based on a decision of the Parliament of the Federal Republic of Germany via the Fachagentur Nachwachsende Rohstoffe e.V. (FNR, FKZ 22030615) under ERA-NET, funded from the European Union's Seventh Research Framework Program (ERA IB-2, 6th call, project BioProMo), and by the LOEWE project AROMAplus of the State of Hesse (Germany).

Compliance with ethical standards

Conflict of interest The authors declare that they have no conflict of interest.

Ethical approval This article does not contain any studies with human participants or animals performed by any of the authors.

References

Acharya S, Foster PL, Brooks P, Fishel R (2003) The coordinated functions of the *E. coli* MutS and MutL proteins in mismatch repair. Mol Cell 12:233–246. https://doi.org/10.1016/S1097-2765(03)00219-3

Andrews RE, Parks LW, Spence KD (1980) Some effects of Douglas fir terpenes on certain microorganisms. Appl Environ Microbiol 40: 301–304

Berger RG (ed) (2007) Flavours and Fragrances. Springer-Verlag, Berlin, Heidelberg

Brandt U (2006) Energy converting NADH: quinone oxidoreductase (complex I). Annu Rev Biochem 75:69–92. https://doi.org/10.1146/annurev.biochem.75.103004.142539

Breitmaier E (2005) Terpene, 2. Auflage. WILEY-VCH Verlag GmbH & Co. KGaA, Weinheim. https://doi.org/10.1002/9783527623693

Camacho Carvajal MM, Wijfjes AHM, Mulders IHM, Lugtenberg BJJ, Bloemberg GV (2002) Characterization of NADH dehydrogenases of *Pseudomonas fluorescens* WCS365 and their role in competitive root colonization. Mol Plant-Microbe Interact 15:662–671. https://doi.org/10.1094/MPMI.2002.15.7.662

Cantwell SG, Lau EP, Watt DS, Fall RR (1978) Biodegradation of acyclic isoprenoids by *Pseudomonas* species. J Bacteriol 135:324–333

Chen Y, Zhou YJ, Siewers V, Nielsen J (2015) Enabling technologies to advance microbial isoprenoid production. Adv Biochem Eng Biotechnol 148:143–160. https://doi.org/10.1007/10_2014_284

Choi K-H, Kumar A, Schweizer HP (2006) A 10-min method for preparation of highly electrocompetent *Pseudomonas aeruginosa* cells: application for DNA fragment transfer between chromosomes and plasmid transformation. J Microbiol Methods 64:391–397. https://doi.org/10.1016/j.mimet.2005.06.001

Cornelissen S, Julsing MK, Volmer J, Riechert O, Schmid A, Bühler B (2013) Whole-cell-based CYP153A6-catalyzed (S)-limonene hydroxylation efficiency depends on host background and profits from monoterpene uptake via AlkL. Biotechnol Bioeng 110:1282–1292. https://doi.org/10.1002/bit.24801

Cornelissen S, Liu S, Deshmukh AT, Schmid A, Bühler B (2011) Cell physiology rather than enzyme kinetics can determine the efficiency of cytochrome P450-catalyzed C–H-oxyfunctionalization. J Ind Microbiol Biotechnol 38:1359–1370. https://doi.org/10.1007/s10295-010-0919-y

Devon RS, Porteous DJ, Brookes AJ (1995) Splinkerettes—improved vectorettes for greater efficiency in PCR walking. Nucleic Acids Res 23:1644–1645. https://doi.org/10.1093/nar/23.9.1644

Dunlop MJ (2011) Engineering microbes for tolerance to next-generation biofuels. Biotechnol Biofuels 4:32. https://doi.org/10.1186/1754-6834-4-32

Dunlop MJ, Dossani ZY, Szmidt HL, Chu HC, Lee TS, Keasling JD, Hadi MZ, Mukhopadhyay A (2011) Engineering microbial biofuel tolerance and export using efflux pumps. Mol Syst Biol 7:487–487. https://doi.org/10.1038/msb.2011.21

Duque E, Segura A, Mosqueda G, Ramos JL (2001) Global and cognate regulators control the expression of the organic solvent efflux pumps TtgABC and TtgDEF of *Pseudomonas putida*. Mol Microbiol 39: 1100–1106. https://doi.org/10.1046/j.1365-2958.2001.02310.x

Franden MA, Jayakody LN, Li WJ, Wagner NJ, Cleveland NS, Michener WE, Hauer B, Blank LM, Wierckx N, Klebensberger J, Beckham GT (2018) Engineering *Pseudomonas putida* KT2440 for efficient ethylene glycol utilization. Metab Eng 48:197–207. https://doi.org/10.1016/j.ymben.2018.06.003

Fukumori F, Hirayama H, Takami H, Inoue A, Horikoshi K (1998) Isolation and transposon mutagenesis of a *Pseudomonas putida* KT2442 toluene-resistant variant: involvement of an efflux system in solvent resistance. Extremophiles 2:395–400

Gibson DG, Young L, Chuang R-Y, Venter JC, Hutchison CA, Smith HO (2009) Enzymatic assembly of DNA molecules up to several

hundred kilobases. Nat Methods 6:343–345. https://doi.org/10.1038/nmeth.1318

Gotoh N, Tsujimoto H, Poole K, Yamagishi JI, Nishino T (1995) The outer membrane protein OprM of *Pseudomonas aeruginosa* is encoded by *oprK* of the *mexA-mexB-oprK* multidrug resistance operon. Antimicrob Agents Chemother 39:2567–2569. https://doi.org/10.1128/AAC.39.11.2567

Habermehl G, Hammann PE, Krebs HC, Ternes W (2008) Naturstoffchemie, 3. Springer, Berlin Heidelberg, Berlin, Heidelberg

Heipieper HJ, Meinhardt F, Segura A (2003) The *cis-trans* isomerase of unsaturated fatty acids in *Pseudomonas* and *Vibrio*: biochemistry, molecular biology and physiological function of a unique stress adaptive mechanism. FEMS Microbiol Lett 229:1–7. https://doi.org/10.1016/S0378-1097(03)00792-4

Inoue A, Horikoshi K (1991) Estimation of solvent-tolerance of bacteria by the solvent parameter log P. J Ferment Bioeng 71:194–196. https://doi.org/10.1016/0922-338X(91)90109-T

Inoue A, Horikoshi K (1989) A *Pseudomonas* thrives in high concentrations of toluene. Nature 338:264–266. https://doi.org/10.1038/338264a0

Inoue H, Nojima H, Okayama H (1990) High efficiency transformation of *Escherichia coli* with plasmids. Gene 96:23–28. https://doi.org/10.1016/0378-1119(90)90336-p

Isken S, de Bont JA (1998) Bacteria tolerant to organic solvents. Extremophiles 2:229–238. https://doi.org/10.1007/s007920050065

Isken S, de Bont JA (1996) Active efflux of toluene in a solvent-resistant bacterium. J Bacteriol 178:6056–6058. https://doi.org/10.1128/jb.178.20.6056-6058.1996

Isken S, Derks A, Wolffs PF, de Bont JA (1999) Effect of organic solvents on the yield of solvent-tolerant *Pseudomonas putida* S12. Appl Environ Microbiol 65:2631–2635

Kabelitz N, Santos PM, Heipieper HJ (2003) Effect of aliphatic alcohols on growth and degree of saturation of membrane lipids in *Acinetobacter calcoaceticus*. FEMS Microbiol Lett 220:223–227. https://doi.org/10.1016/S0378-1097(03)00103-4

Kieboom J, Dennis JJ, de Bont JA, Zylstra GJ (1998) Identification and molecular characterization of an efflux pump involved in *Pseudomonas putida* S12 solvent tolerance. J Biol Chem 273:85–91. https://doi.org/10.1074/jbc.273.1.85

King EO, Ward MK, Raney DE (1954) Two simple media for the demonstration of pyocyanin and fluorescin. J Lab Clin Med 44:301–307

Klebensberger J, Lautenschlager K, Bressler D, Wingender J, Philipp B (2007) Detergent-induced cell aggregation in subpopulations of *Pseudomonas aeruginosa* as a preadaptive survival strategy. Environ Microbiol 9:2247–2259. https://doi.org/10.1111/j.1462-2920.2007.01339.x

Krell T, Terán W, Mayorga OL, Rivas G, Jiménez M, Daniels C, Molina-Henares A-J, Martínez-Bueno M, Gallegos M-T, Ramos J-L (2007) Optimization of the palindromic order of the TtgR operator enhances binding cooperativity. J Mol Biol 369:1188–1199. https://doi.org/10.1016/j.jmb.2007.04.025

Lampe DJ, Akerley BJ, Rubin EJ, Mekalanos JJ, Robertson HM (1999) Hyperactive transposase mutants of the *Himar1 mariner* transposon. Proc Natl Acad Sci 96:11428–11433. https://doi.org/10.1073/pnas.96.20.11428

Li XZ, Klebensberger J, Rosche B (2010) Effect of *gcl*, *glcB*, and *aceA* disruption on glyoxylate conversion by *Pseudomonas putida* JM37. J Microbiol Biotechnol 20:1006–1010. https://doi.org/10.4014/jmb.0912.12005

Mars AE, Gorissen JPL, van den Beld I, Eggink G (2001) Bioconversion of limonene to increased concentrations of perillic acid by *Pseudomonas putida* GS1 in a fed-batch reactor. Appl Microbiol Biotechnol 56:101–107. https://doi.org/10.1007/s002530100625

Martínez-García E, de Lorenzo V (2011) Engineering multiple genomic deletions in Gram-negative bacteria: analysis of the multi-resistant antibiotic profile of *Pseudomonas putida* KT2440. Environ Microbiol 13:2702–2716. https://doi.org/10.1111/j.1462-2920.2011.02538.x

Mi J, Becher D, Lubuta P, Dany S, Tusch K, Schewe H, Buchhaupt M, Schrader J (2014) *De novo* production of the monoterpenoid geranic acid by metabolically engineered *Pseudomonas putida*. Microb Cell Factories 13:1–11. https://doi.org/10.1186/s12934-014-0170-8

Mi J, Schewe H, Buchhaupt M, Holtmann D, Schrader J (2016) Efficient hydroxylation of 1,8-cineole with monoterpenoid-resistant recombinant *Pseudomonas putida* GS1. World J Microbiol Biotechnol 32:112. https://doi.org/10.1007/s11274-016-2071-y

Mikkers H, Allen J, Knipscheer P, Romeyn L, Hart A, Vink E, Berns A (2002) High-throughput retroviral tagging to identify components of specific signaling pathways in cancer. Nat Genet 32:153–159. https://doi.org/10.1038/ng950

Mosqueda G, Ramos J-L (2000) A set of genes encoding a second toluene efflux system in *Pseudomonas putida* DOT-T1E is linked to the tod genes for toluene metabolism. J Bacteriol 182:937–943. https://doi.org/10.1128/JB.182.4.937-943.2000

Nelson KE, Weinel C, Paulsen IT, Dodson RJ, Hilbert H, Martins dos Santos VAP, Fouts DE, Gill SR, Pop M, Holmes M, Brinkac L, Beanan M, DeBoy RT, Daugherty S, Kolonay J, Madupu R, Nelson W, White O, Peterson J, Khouri H, Hance I, Lee PC, Holtzapple E, Scanlan D, Tran K, Moazzez A, Utterback T, Rizzo M, Lee K, Kosack D, Moestl D, Wedler H, Lauber J, Stjepandic D, Hoheisel J, Straetz M, Heim S, Kiewitz C, Eisen J, Timmis KN, Düsterhöft A, Tümmler B, Fraser CM (2002) Complete genome sequence and comparative analysis of the metabolically versatile *Pseudomonas putida* KT2440. Environ Microbiol 4:799–808. https://doi.org/10.1046/j.1462-2920.2002.00366.x

Otto M, Wynands B, Drepper T, Jaeger K-E, Thies S, Loeschcke A, Blank LM, Wierckx N (2019) Targeting 16S rDNA for stable recombinant gene expression in *Pseudomonas*. ACS Synth Biol 8:1901–1912. https://doi.org/10.1021/acssynbio.9b00195

Papadopoulos CJ, Carson CF, Chang BJ, Riley TV (2008) Role of the MexAB-OprM efflux pump of *Pseudomonas aeruginosa* in tolerance to tea tree (*Melaleuca alternifolia*) oil and its monoterpene components terpinen-4-ol, 1,8-cineole, and a-terpineol. Appl Environ Microbiol 74:1932–1935. https://doi.org/10.1128/AEM.02334-07

Pinkart HC, White DC (1997) Phospholipid biosynthesis and solvent tolerance in *Pseudomonas putida* strains. J Bacteriol 179:4219–4226. https://doi.org/10.1128/jb.179.13.4219-4226.1997

Poole K, Gotoh N, Tsujimoto H, Zhao Q, Wada A, Yamasaki T, Neshat S, Yamagishi J, Li X-Z, Nishino T (1996) Overexpression of the *mexC-mexD-oprJ* efflux operon in *nfxB*-type multidrug-resistant strains of *Pseudomonas aeruginosa*. Mol Microbiol 21:713–725. https://doi.org/10.1046/j.1365-2958.1996.281397.x

Poole K, Krebes K, McNally C, Neshat S (1993) Multiple antibiotic resistance in *Pseudomonas aeruginosa*: evidence for involvement of an efflux operon. J Bacteriol 175:7363–7372. https://doi.org/10.1128/jb.175.22.7363-7372.1993

Ramos JL, Cuenca MS, Molina-Santiago C, Segura A, Duque E, omez-Garciá MR, Udaondo Z, Roca A (2015) Mechanisms of solvent resistance mediated by interplay of cellular factors in *Pseudomonas putida*. FEMS Microbiol Rev 39:555–566. https://doi.org/10.1093/femsre/fuv006

Ramos JL, Duque E, Gallegos M-T, Godoy P, Ramos-González MI, Rojas A, Terán W, Segura A (2002) Mechanisms of solvent tolerance in gram-negative bacteria. Annu Rev Microbiol 56:743–768. https://doi.org/10.1146/annurev.micro.56.012302.161038

Ramos JL, Duque E, Godoy P, Segura A (1998) Efflux pumps involved in toluene tolerance in *Pseudomonas putida* DOT-T1E. J Bacteriol 180:3323–3329

Ramos JL, Duque E, Rodríguez-Herva JJ, Godoy P, Haïdour A, Reyes F, Fernández-Barrero A (1997) Mechanisms for solvent tolerance in

bacteria. J Biol Chem 272:3887–3890. https://doi.org/10.1074/jbc.272.7.3887

Ramos JL, Martínez-Bueno M, Molina-Henares AJ, Terán W, Watanabe K, Zhang X, Trinidad Gallegos M, Brennan R, Tobes R (2005) The TetR family of transcriptional repressors. Microbiol Mol Biol Rev 69:326–356. https://doi.org/10.1128/MMBR.69.2.326

Rau MH, Calero P, Lennen RM, Long KS, Nielsen AT (2016) Genome-wide *Escherichia coli* stress response and improved tolerance towards industrially relevant chemicals. Microb Cell Factories 15:176. https://doi.org/10.1186/s12934-016-0577-5

Rodríguez-Herva JJ, García V, Hurtado A, Segura A, Ramos JL (2007) The *ttgGHI* solvent efflux pump operon of *Pseudomonas putida* DOT-T1E is located on a large self-transmissible plasmid. Environ Microbiol 9:1550–1561. https://doi.org/10.1111/j.1462-2920.2007.01276.x

Rojas A, Duque E, Mosqueda G, Golden G, Hurtado A, Ramos JL, Segura A (2001) Three efflux pumps are required to provide efficient tolerance to toluene in *Pseudomonas putida* DOT-T1E. J Bacteriol 183:3967–3973. https://doi.org/10.1128/JB.183.13.3967-3973.2001

Rojas A, Segura A, Guazzaroni ME, Terán W, Hurtado A, Gallegos MT, Ramos JL (2003) *In vivo* and *In vitro* evidence that TtgV is the specific regulator of the TtgGHI multidrug and solvent efflux pump of *Pseudomonas putida*. J Bacteriol 185:4755–4763. https://doi.org/10.1128/JB.185.16.4755-4763.2003

Schrader J (2010) Mikrobielle Oxidation von Monoterpenen. BioSpektrum 16:555–557

Schrader J, Bohlmann J (eds) (2015) Biotechnology of isoprenoids. Springer International Publishing, Cham

Segura A, Rojas A, Hurtado A, Huertas M-J, Ramos JL (2003) Comparative genomic analysis of solvent extrusion pumps in *Pseudomonas* strains exhibiting different degrees of solvent tolerance. Extremophiles 7:371–376. https://doi.org/10.1007/s00792-003-0331-x

Shah AA, Wang C, Chung Y-R, Kim J-Y, Choi E-S, Kim S-W (2013) Enhancement of geraniol resistance of *Escherichia coli* by MarA overexpression. J Biosci Bioeng 115:253–258. https://doi.org/10.1016/j.jbiosc.2012.10.009

Sikkema J, de Bont JA, Poolman B (1994) Interactions of cyclic hydrocarbons with biological membranes. J Biol Chem 269:8022–8028

Silby MW, Winstanley C, Godfrey SAC, Levy SB, Jackson RW (2011) *Pseudomonas* genomes: diverse and adaptable. FEMS Microbiol Rev 35:652–680. https://doi.org/10.1111/j.1574-6976.2011.00269.x

Speelmans G, Bijlsma A, Eggink G (1998) Limonene bioconversion to high concentrations of a single and stable product, perillic acid, by a solvent-resistant *Pseudomonas putida* strain. Appl Microbiol Biotechnol 50:538–544. https://doi.org/10.1007/s002530051331

Terán W, Felipe A, Fillet S, Guazzaroni M-E, Krell T, Ruiz R, Ramos JL, Gallegos M-T (2007) Complexity in efflux pump control: cross-regulation by the paralogues TtgV and TtgT. Mol Microbiol 66:1416–1428. https://doi.org/10.1111/j.1365-2958.2007.06004.x

Terán W, Felipe A, Segura A, Rojas A, Ramos J-L, Gallegos M-T (2003) Antibiotic-dependent induction of *Pseudomonas putida* DOT-T1E TtgABC efflux pump is mediated by the drug binding repressor TtgR. Antimicrob Agents Chemother 47:3067–3072. https://doi.org/10.1128/AAC.47.10.3067-3072.2003

Timmis KN (2002) *Pseudomonas putida*: a cosmopolitan opportunist par excellence. Environ Microbiol 4:779–781. https://doi.org/10.1046/j.1462-2920.2002.00365.x

Seemann T (2014) Prokka: rapid prokaryotic genome annotation. Bioinformatics 30:2068–2069

Trombetta D, Castelli F, Sarpietro MG, Venuti V, Cristani M, Daniele C, Saija A, Mazzanti G, Bisignano G, Grazia M (2005) Mechanisms of antibacterial action of three monoterpenes. J Antimicrob Agents Chemother 49:2474–2478. https://doi.org/10.1128/AAC.49.6.2474

Udaondo Z, Duque E, Fernández M, Molina L, de la Torre J, Bernal P, Niqui J-L, Pini C, Roca A, Matilla MA, Antonia Molina-Henares M, Silva-Jiménez H, Navarro-Avilés G, Busch A, Lacal J, Krell T, Segura A, Ramos J-L (2012) Analysis of solvent tolerance in *Pseudomonas putida* DOT-T1E based on its genome sequence and a collection of mutants. FEBS Lett 586:2932–2938. https://doi.org/10.1016/j.febslet.2012.07.031

Uribe S, Ramirez J, Peña A (1985) Effects of β-pinene on yeast membrane functions. J Bacteriol 161:1195–1200

van Beilen JB, Holtackers R, Lüscher D, Bauer U, Witholt B, Duetz WA (2005) Biocatalytic production of perillyl alcohol from limonene by using a novel *Mycobacterium* sp. cytochrome P450 alkane hydroxylase expressed in *Pseudomonas putida*. Appl Environ Microbiol 71:1737–1744. https://doi.org/10.1128/AEM.71.4.1737-1744.2005

Vidal-Aroca F, Meng A, Minz T, Page MGP, Dreier J (2009) Use of resazurin to detect mefloquine as an efflux-pump inhibitor in *Pseudomonas aeruginosa* and *Escherichia coli*. J Microbiol Methods 79:232–237. https://doi.org/10.1016/j.mimet.2009.09.021

Wang Q, Nomura CT (2010) Monitoring differences in gene expression levels and polyhydroxyalkanoate (PHA) production in *Pseudomonas putida* KT2440 grown on different carbon sources. J Biosci Bioeng 110:653–659. https://doi.org/10.1016/j.jbiosc.2010.08.001

Wang Y, Lim L, DiGuistini S, Robertson G, Bohlmann J, Breuil C (2013) A specialized ABC efflux transporter GcABC-G1 confers monoterpene resistance to *Grosmannia clavigera*, a bark beetle-associated fungal pathogen of pine trees. New Phytol 197:886–898. https://doi.org/10.1111/nph.12063

Weidner U, Geier S, Ptock A, Friedrich T, Leif H, Weiss H (1993) The gene locus of the proton-translocating NADH:ubiquinone oxidoreductase in *Escherichia coli*. J Mol Biol 233:109–122. https://doi.org/10.1006/jmbi.1993.1488

Wijte D, van Baar BLM, Heck AJR, Altelaar AFM (2011) Probing the proteome response to toluene exposure in the solvent tolerant *Pseudomonas putida* S12. J Proteome Res 10:394–403. https://doi.org/10.1021/pr100401n

Wu X, Monchy S, Taghavi S, Zhu W, Ramos J, van der Lelie D (2011) Comparative genomics and functional analysis of niche-specific adaptation in *Pseudomonas putida*. FEMS Microbiol Rev 35:299–323. https://doi.org/10.1111/j.1574-6976.2010.00249.x

Journal: Applied Microbiology and Biotechnology

SUPPLEMENTARY MATERIAL

Investigation of monoterpenoid resistance mechanisms in *Pseudomonas putida* and their consequences for biotransformations

Florence Miramella Schempp[1,2], Katharina Elisabeth Hofmann[1], Jia Mi[1], Ferdinand Kirchner[1], Annika Meffert[1], Hendrik Schewe[1], Jens Schrader[1], Markus Buchhaupt[1#]

[1]*DECHEMA-Forschungsinstitut, Industrial Biotechnology, Theodor-Heuss-Allee 25, 60486 Frankfurt am Main, Germany*

[2]*Faculty Biological Sciences, Goethe University Frankfurt, Max-von-Laue-Str. 9, 60438 Frankfurt am Main, Germany*

[#]Address correspondence to Markus Buchhaupt. Phone: +49-69-7564-629, Fax: +49-69-7564-388, e-mail: markus.buchhaupt@dechema.de.

Electronic supplementary material as Online Resource

Table S1. Bacterial strains, plasmids and oligonucleotides used in this study.

Table S2. Identified mutations in the strains TR, GR, GAR, VR1 and VR2.

Table S3. Identified Ttg efflux pump proteins in *P. putida* GS1 and comparison with homologues in *P. putida* strains DOT-T1E, KT2440 and S12.

Table S4. Summary of genome sequencing results and detected mutations.

Fig. S1 – S32. Further results of monoterpenoid tolerance assays.

Supplementary tables

Table S1. Bacterial strains, plasmids and oligonucleotides/PCR primers used in this study.

Strains	**Description**	**Reference**
P. putida GS1	alias DSM 12264, wild type *P. putida* isolated from sludge of wastewater treatment system in the Netherlands	DSMZ, Braunschweig, Germany, (Speelmans et al. 1998)
P. putida GS1 CR	*ttgR*::Tn, Tet^R, mutant selected in the presence of 60 mM 1,8-cineole	this work
P. putida GS1 GR	*ttgT*::Tn, Tet^R, mutant selected in the presence of 65 mM geraniol	this work
P. putida GS1 GAR	Δ41 nucleotides of *ttgA*, mutant selected in the presence of 90 mM geranic acid	this work
P. putida GS1 VR1	see Table S2, Tet^R, mutant selected in the presence of 35 mM verbenone	this work
P. putida GS1 VR2	See Table S2, Tet^R, mutant selected in the presence of 35 mM verbenone	this work
P. putida GS1 TR	Δ10 nucleotides of *ttgABC*-5'UTR and -35 region of *ttgR* promoter, Tet^R, mutant selected in the presence of 35 mM α-terpineol	this work
P. putida GS1 Δ*ttgR*	Δ*ttgR*	this work
P. putida GS1 Δ*ttgT*	Δ*ttgT*	this work
P. putida GS1 $\Delta 10nt_{ttgABC\text{-}5'UTR}$	Δ10 nucleotides of *ttgABC*-5'UTR and -35 region of *ttgR* promoter	this work
E. coli S17-1 λpir	TpR SmR *recA*, *thi, pro, hsdR*-M+RP4: 2-*Tc:Mu: Km Tn7 λpir*	(Simon et al. 1983)
E. coli DH5α	*fhuA2* Δ(*argF-lacZ*)U169 *phoA glnV44* Φ80 Δ(*lacZ*)M15 *gyrA96 recA1 relA1 endA1 thi-1 hsdR17*	(Hanahan 1985; Grant et al. 1990)
Plasmids		
pALMAR-3	plasmid harboring a mariner transposon used for transposon mutagenesis, Tet^R	kindly provided by Jenal group, Uni Basel (Klebensberger et al. 2007)
pMiS4	expression plasmid derived from pBBR1MCS-2; elements of the rhamnose expression system: promoter rhaPBAD and activator genes *rhaR* and *rhaS*; *mob*, pBBR1 *rep*G159S, MCS, Km^R,	(Mi et al. 2016)

pMiS4-eGFP	expression plasmid derived from pBBR1MCS-2; elements of the rhamnose expression system: promoter rhaPBAD and activator genes *rhaR* and *rhaS*; *mob*, pBBR1 *rep*G159S, eGFP, Km^R,	(Mi et al. 2016)
pMiS4-*ttgR*	expression plasmid derived from pBBR1MCS-2; mob, pBBR1 *rep*G159S, *ttgR* with native promoter region, Km^R,	this work
pMiS4-*ttgT*	expression plasmid derived from pBBR1MCS-2; mob, pBBR1 *rep*G159S, *ttgT* with native promoter region, Km^R,	this work
pEMG	*ori*R6K, *lacZα* with two flanking I-SceI sites, Km^R	(Martínez-García and de Lorenzo 2011)
pEMG-Δ*ttgR*	*ori*R6K, *lacZα* with two flanking I-SceI sites, bearing a 1.6 kb insert for deletion *ttgR* gene, Km^R	this work
pEMG-Δ*ttgT*	*ori*R6K, *lacZα* with two flanking I-SceI sites, bearing a 1.6 kb insert for deletion *ttgT* gene, Km^R	this work
pEMG-Δ10nt$_{ttgABC}$	*ori*R6K, *lacZα* with two flanking I-SceI sites, bearing a 1.6 kb insert for deletion of 10 nucleotides in *ttgABC*-5'-UTR, Km^R	this work
pSW-2	*ori*RK2, *xylS*, Pm→I-SceI (transcriptional fusion of I-SceI to *Pm*), Gm^R	(Martínez-García and de Lorenzo 2011)
Oligonucleotides/PCR primers		**Purpose**
P1	ATCCTTAACAAAGTGGGCAGTACAACCTCATCTGGCC	Cloning in pEMG (pEMG-Δ*ttgR*)
P2	AAGCTTGCATGCCTGCAGGTCGACTCTAGAGGATCC GCCATTGCTCACCAGCGC	
P3	ACGGCCAGTATAGGGATAACAGGGTAATCTGAATTCC GCTGCTGCCGCTCAGCC	
P4	TGAGGTTGTACTGCCCACTTTGTTAAGGATTGTGAGG GAG	
P5	AGTATAGGGATAACAGGGTAATCTGAATTCCTGCGCT TGCCCATTGGTC	Cloning in pEMG (pEMG-Δ*ttgT*)
P6	GCAAAAGTCCTCTAAACCGTTTCCTTCTGATCCAGG	
P7	TCAGAAGGAAACGGTTTAGAGGACTTTTGCTCGGC	
P8	GCATGCCTGCAGGTCGACTCTAGAGGATCCAGACCG CCTATTTATCTGCCTGG	
P9	AGTATAGGGATAACAGGGTAATCTGAATTCTGTCATTT GCGCAGAGCCG	Cloning in pEMG (pEMG-Δ10nt$_{ttgABC}$)
P10	AATGCTATCCGGTGGTGCTAAGGAATATACTTACATT CATGG	

P11	GTATATTCCTTAGCACCACCGGATAGCATTTTTTCCAG	
P12	GCATGCCTGCAGGTCGACTCTAGAGGATCCGCTTGA ACAGGCTGCCGTC	
P13	TTTTCAGGAAATGCGGTGAGCATCACATCAGAGGATC CTCGGGTCGCTG	Cloning of *ttgR* gene in pMiS4 backbone
P14	GGTAGTCAATAAACCGGTAAGCTTGGATCCTCATTTG CGCAGAGCCGG	
P15	TTTTCAGGAAATGCGGTGAGCATCACATCAACCAGAT GGCTGCTAGCGG	Cloning of *ttgT* gene in pMiS4 backbone
P16	GGTAGTCAATAAACCGGTAAGCTTGGATCCTCAACCC GCAAACTCCCGAG	
P17	CGAATCGTAACCGTTCGTACGAGAATTCGTACGAGAA TCGCTGTCCTCTCCAACGAGCCAAGA	Splinkerette PCR
P18	GATCTCTTGGCTCGTTTTTTTTTGCAAAAA	
P19	CGAATCGTAACCGTTCGTACGAGAA	
P20	CAACCCTTGGCAGAACATATCC	
P21	TCGTACGAGAATCGCTGTCCTCTCC	
P22	GTCCGCCATCTCCAGCAG	
P23	AGGCATTCGTGAAGTCATGG	qPCR, amplification of *rpoD* gene (Franden et al. 2018)
P24	ATGTAACCGCTGAGAACGTC	
P25	GCTCAAGCGCAGCATATC	qPCR, amplification of *ttgR* gene
P26	CCATGTTTGCCTATGTCG	
P27	CAGTTGTATCAGATCGACCCTG	qPCR, amplification of *ttgA* gene
P28	CAGTTGCTTGTAACGTTCGG	
P29	GTATTCCCGTATGACACCACC	qPCR, amplification of *ttgB* gene
P30	GTACATCACCAGGAACACCAG	
P31	GAAGACGATCAAGTCCGGTG	qPCR, amplification of *ttgT* gene
P32	GGATACCGAGTAATGCCCAAG	
P33	GACAAAACCGGCAAGATGAC	qPCR, amplification of *ttgE* gene
P34	AGCCAAACAAGAGGAAGTCG	

Table S2. Identified mutations in the strains TR, GR, GAR, VR1 and VR2. SNE: single nucleotide exchange, nt: nucleotides.

Strain	Type of mutation / Protein effect		Gene or intergenic region / annotated function	
TR	Deletion (10 nt, directly after P_{ttgABC} +1)		Intergenic region between *ttgABC* and *ttgR*	
	SNE (transversion)	Substitution	*eryA*	Erythronolide synthase, modules 3 and 4
GR	transposon insertion (40 nt downstream of start codon)		*ttgT*	Transcriptional regulator
GAR	Deletion (1x T, 2902 nt downstream of start codon)	Frame Shift	*pleC*	Non-motile and phage-resistance protein (PleC)
	Deletion (41 nt, 109 nt downstream of start codon)	Frame Shift	*ttgA*	Efflux system subunit (TtgA)
VR1	SNE (transition)	None	*bluB*	5,6-dimethylbenzimidazole synthase
	Deletion (16 nt, 1243 nt downstream of start codon)	Frame Shift	*mutS*	DNA mismatch repair protein (MutS)
	SNE (transition)	Substitution	*ispD*	2-C-methyl-D-erythritol 4-phosphate cytidylyltransferase
	SNE (transition)	None	*cdsA*	Phosphatidate cytidylyltransferase
	SNE (transition)	None	*kgtP_1*	Alpha-ketoglutarate permease
	SNE (transition)	Substitution	*purP_1*	putative adenine permease (PurP)
	SNE (transition)	None	*betB_1*	NAD/NADP-dependent betaine aldehyde dehydrogenase
	SNE (transition)	None	*ybhF_1*	putative ABC transporter ATP-binding protein (YbhF)
	SNE (transition)	Substitution	*tmoS*	Sensor histidine kinase (TmoS)
	SNE (transition)	None	*fccB*	Sulfide dehydrogenase (flavocytochrome c) flavoprotein chain precursor
	SNE (transition)	Substitution	Fatty acid desaturase	
	SNE (transition)	Substitution	*betT_2*	High-affinity choline transport protein
	SNE (transition)	Substitution	*envZ_1*	Osmolarity sensor protein (EnvZ)
	SNE (transition)	Substitution	*mcpS_4*	Methyl-accepting chemotaxis protein (McpS)
	SNE (transition)	Substitution	*dsbD_1*	Thiol:disulfide interchange protein precursor (DsbD)
	SNE (transition)	Substitution	*dppA_4*	Periplasmic dipeptide transport protein precursor
	SNE (transition)		Intergenic region between *mprF* and tRNA-Methionine	
	SNE (transition)	Substitution	Glutamine amidotransferases class-II	
	SNE (transition)	Substitution	*rssA_1*	NTE family protein (RssA)
	SNE (transition)	Substitution	*ydjA*	Putative NAD(P)H nitroreductase (YdjA)
	SNE (transition)	Substitution	*fliC*	B-type flagellin
	SNE (transition)	Substitution	*rutR_2*	HTH-type transcriptional regulator (RutR)
	SNE (transition)	Substitution	*guaD*	Guanine deaminase
	SNE (transition)	Substitution	*lgrB_2*	Linear gramicidin synthase subunit B
	SNE (transition)	Substitution	*adiA*	Biodegradative arginine decarboxylase
	SNE (transition)	Substitution	*nuoB*	NADH-quinone oxidoreductase subunit B

	SNE (transition)	None	*gntZ*	6-phosphogluconate dehydrogenase, NAD(+)-dependent, decarboxylating
	SNE (transition)	Substitution	*alkB_1*	Alkane 1-monooxygenase
	SNE (transition)		Intergenic region between *ssuA2* and *ssuA3*	
	SNE (transition)	Substitution	Hypothetical protein	
	SNE (transition)	None	*atzE*	Biuret hydrolase
	SNE (transition)	Substitution	*puuC_2*	Aldehyde dehydrogenase (PuuC)
	SNE (transition)	Substitution	*mcpS*	Methyl-accepting chemotaxis protein (McpS)
VR2	SNE (transition)	Substitution	*actP_1*	Cation/acetate symporter (ActP)
	SNE (transition)	Substitution	*serB_1*	Phosphoserine phosphatase (SerB_1)
	SNE (transition, 2842 nt downstream of start codon)	Substitution	*pleC*	Non-motile and phage-resistance protein (PleC)
	SNE (transition)	None	*cmpR_2*	HTH-type transcriptional activator (CmpR)
	SNE (transition)	Substitution	*rapA_1*	RNA polymerase-associated protein (RapA)
	SNE (transversion)	Substitution	*mutL*	DNA mismatch repair protein (MutL)
	SNE (transition)	Substitution	*dbpA*	ATP-dependent RNA helicase (DbpA)
	SNE (transition)	Substitution	*gltB*	Glutamate synthase [NADPH] large chain precursor (GltB)
	SNE (transition)		Intergenic region between hypothetical protein and *XpsE* (Type II secretion system protein E)	
	SNE (transversion)	Substitution	*exbB_1*	Biopolymer transport protein (ExbB)
	SNE (transition)		Intergenic region between *alkT* (Rubredoxin-NAD(+) reductase) and *hupB* (DNA-binding protein HU-beta)	
	SNE (transition)	Substitution	*pstC_1*	Phosphate transport system permease protein (PstC)
	SNE (transition)	Substitution	*soxC_2*	Dibenzothiophene desulfurization enzyme C (SoxC)
	SNE (transition)	Substitution	*dinF*	DNA-damage-inducible protein F
	SNE (transversion)		Intergenic region between *yigZ* and *csgA*	
	SNE (transition)	Substitution	*fdx_2*	2Fe-2S ferredoxin
	SNE (transition)	Substitution	*epsE_1*	Type II secretion system protein E
	SNE (transition)	Substitution	hypothetical protein	
	Insertion (tandem repeat – 1x G, 433 nt downstream of start codon)	Frame Shift	*nuoG*	NADH-quinone oxidoreductase subunit G
	SNE (transition)		tRNA-Glycine	
	SNE (transition)	Substitution	*proP_5*	Proline/betaine transporter
	SNE (transition)	Substitution	hypothetical protein	
	SNE (transition)	None	*ureC*	Urease subunit alpha
	SNE (transition)	Substitution	*pobB*	Phenoxybenzoate dioxygenase subunit beta
	Deletion (tandem repeat – 1x C, 1035 nt downstream of start codon)	Frame Shift	*bedA*	Benzene 1,2-dioxygenase system ferredoxin-NAD(+) reductase subunit
	SNE (transition)	Substitution	*atoE*	Short-chain fatty acids transporter
	SNE (transition)		Intergenic region between *dmlR* (HTH-type transcriptional regulator) and NADP-dependent 7-alpha-hydroxysteroid dehydrogenase	
	SNE (transition)	Substitution	Acetyltransferase (GNAT) family protein	

	SNE (transition)	None	*ipaH* (putative E3 ubiquitin-protein ligase ipaH4.5)	
	SNE (transition)	Substitution	*hndC*	NADP-reducing hydrogenase subunit (HndC)
	SNE (transition)	Substitution	Hypothetical protein	
	SNE (transition)	None	Hypothetical protein	

Table S3. Identification of Ttg efflux pump proteins in *P. putida* GS1 and comparison with homologues in *P. putida* strains DOT-T1E, KT2440 and S12. Protein identity in %. Pairwise % identity was determined using the software G*eneious* (Biomatters Ltd., Auckland, New Zealand) with *Pairwise alignment* function and standard settings.

GS1 protein	Identity to DOT-T1E	Identity to KT2440	Identity to S12 Srp proteins	
TtgR	99.5	99	SrpS	< 10
TtgA	99.5	99.7	SrpA	55.1
TtgB	100	99.8	SrpB	62.9
TtgC	100	99.8	SrpC	56.4
TtgT	100	--	SrpS	62.5
TtgD	99.7	--	SrpA	73.3
TtgE	100	--	SrpB	85.0
TtgF	99.8	--	SrpC	59.6

Table S4. Summary of genome sequencing results and detected mutations. SNE: single nucleotide exchange. [a]Including areas annotated as "hypothetical protein".

Strain (*P. putida* GS1)	**Total number of aligned Illumina sequence reads** [Reads]	**Reference genome coverage** [%]	**Average cover per base** [Reads ± standard deviation]	**Total number of mutations**	**Number of SNEs**	**Number of deletions/ insertions**	**Coding regions**	**Non-coding regions** [a]
GR	34,375,723	99.99	213.9 ± 44.5	1	0	1 (transposon insertion)	1	0
TR	30,613,901	99.99	190.5 ± 36.7	2	1	1	1	1
GAR	14,014,168	99.99	154.8 ± 32.6	2	0	2	2	0
VR1	34,341,592	99.99	213.6 ± 39.6	33	32	1	30	3
VR2	48,824,571	99.99	303.9 ± 50.3	32	30	2	24	8

Supplementary figures

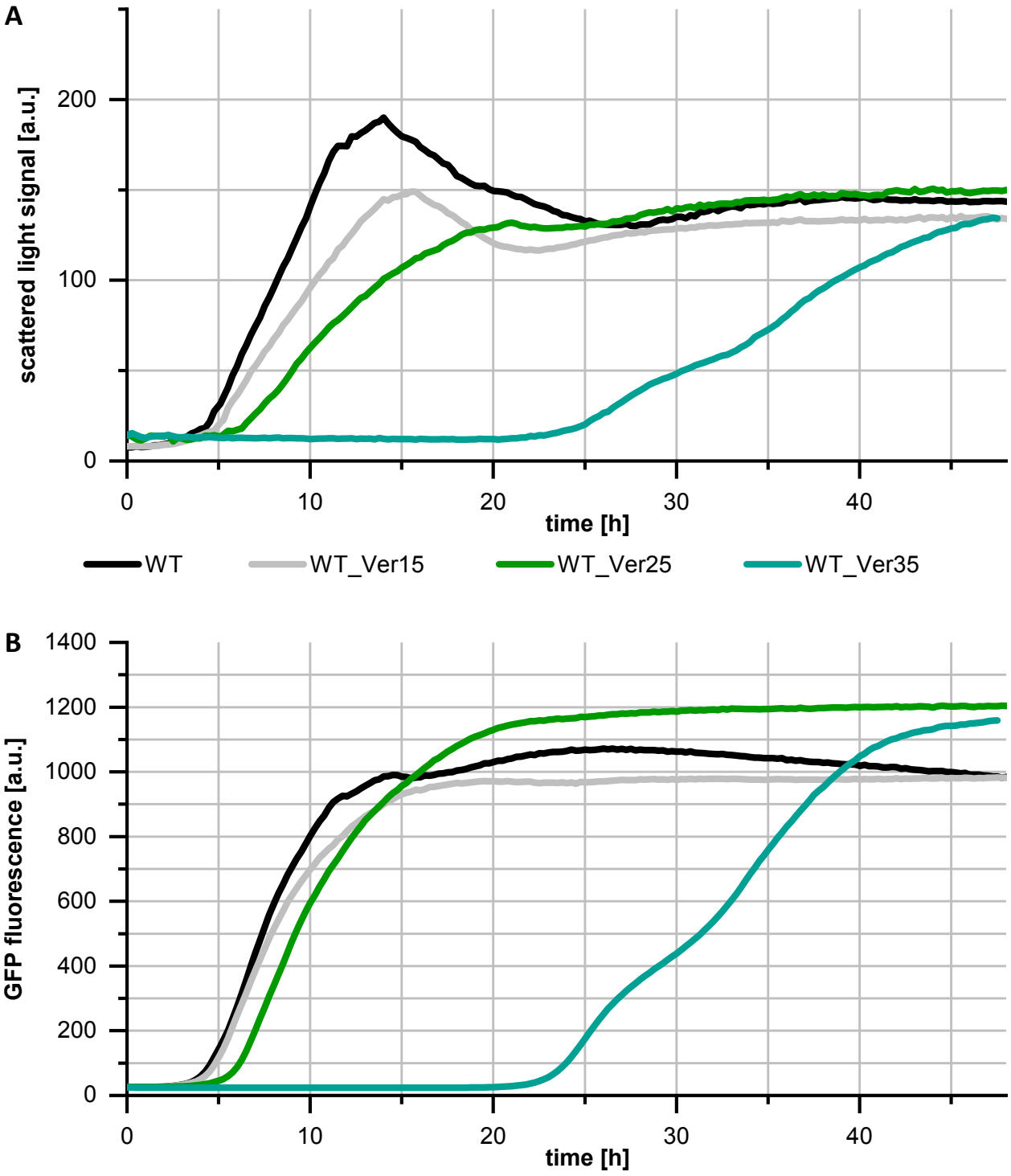

Figure S1. Growth of *P. putida* GS1 WT without and in the presence of different verbenone concentrations (15, 25 and 35 mM). Tolerance assays were conducted in a microbioreactor system over 48 h. Biomass formation was monitored every 10 – 15 minutes via (A) scattered light signal intensity (absorbance at 620 nm) and (B) GFP fluorescence signal intensity (excitation filter: 488 nm; emission filter: 520 nm). The data points represent the mean values of three biological replicas. For variations between the replicas of each strain see Figure S17.

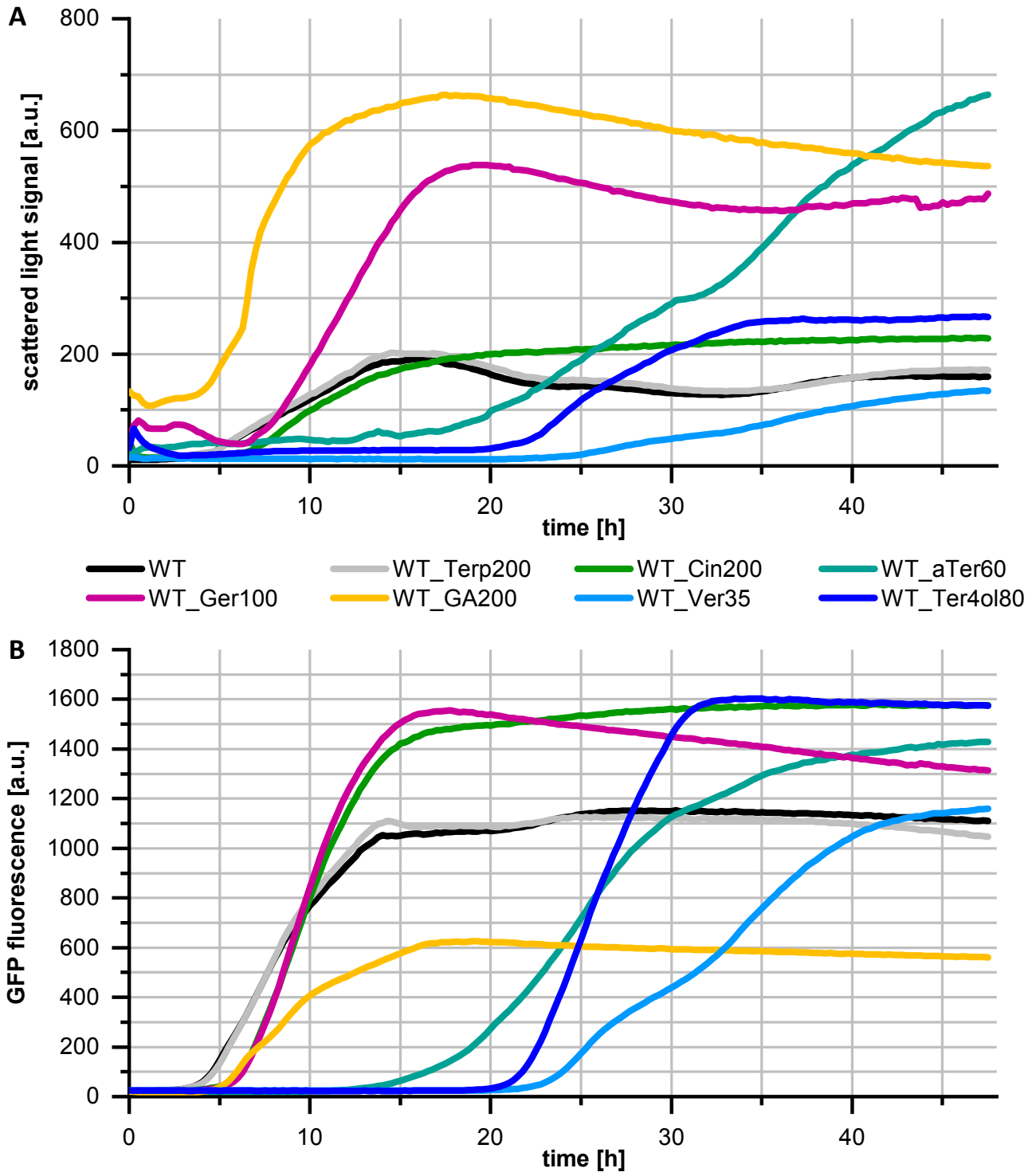

Figure S2. Growth of *P. putida* GS1 (WT) + pMiS4-eGFP without and in the presence of different monoterpenes and monoterpenoids. Terp200: γ-terpinene (200 mM), Cin200: 1,8-cineole (200 mM), aTer60: α-terpineol (60 mM), Ger100: geraniol (100 mM), GA200: geranic acid (200 mM), Ver35: verbenone (35 mM), Ter4ol80: terpinen-4-ol (80 mM). Tolerance assays were conducted in a microbioreactor system over 48 h. Biomass formation was monitored every 10 – 15 minutes via (A) scattered light signal intensity (absorbance at 620 nm) and (B) GFP fluorescence signal intensity (excitation filter: 488 nm; emission filter: 520 nm). The data points represent the mean values of three biological replicas. For variations between the replicas of each strain see Figure S18.

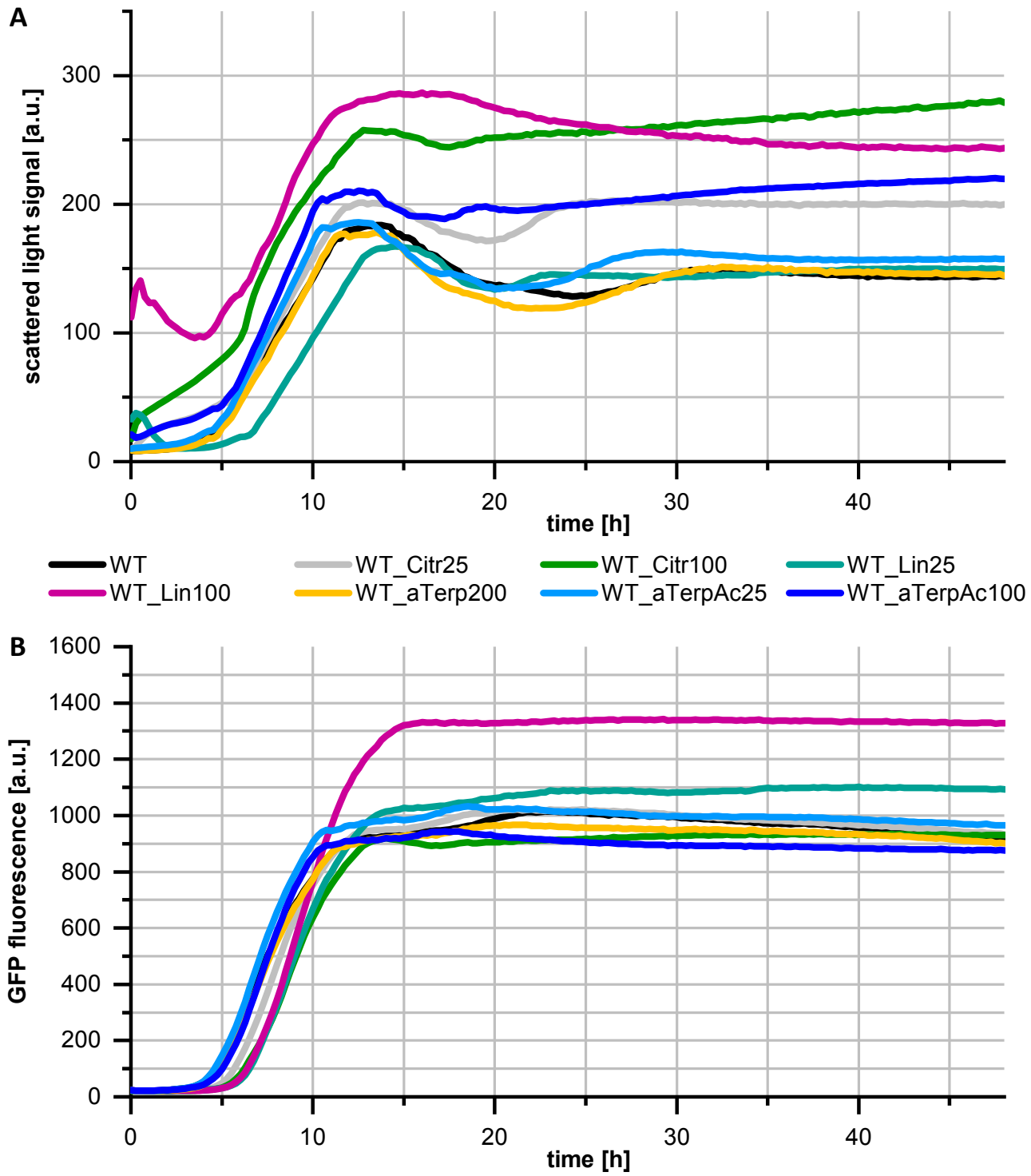

Figure S3. Growth of *P. putida* GS1 (WT) + pMiS4-eGFP without and in the presence of different monoterpenes and monoterpenoids. Citr25/100: citral (25/100 mM), Lin25/100: linalool (25/100 mM), aTerp200: α-terpinene (200 mM), aTerpAc25/100: α-terpinyl acetate (25/100 mM). Tolerance assays were conducted in a microbioreactor system over 48 h. Biomass formation was monitored every 10 – 15 minutes via (A) scattered light signal intensity (absorbance at 620 nm) and (B) GFP fluorescence signal intensity (excitation filter: 488 nm; emission filter: 520 nm). The data points represent the mean values of two or three biological replicas. For variations between the replicas of each strain see Figure S19.

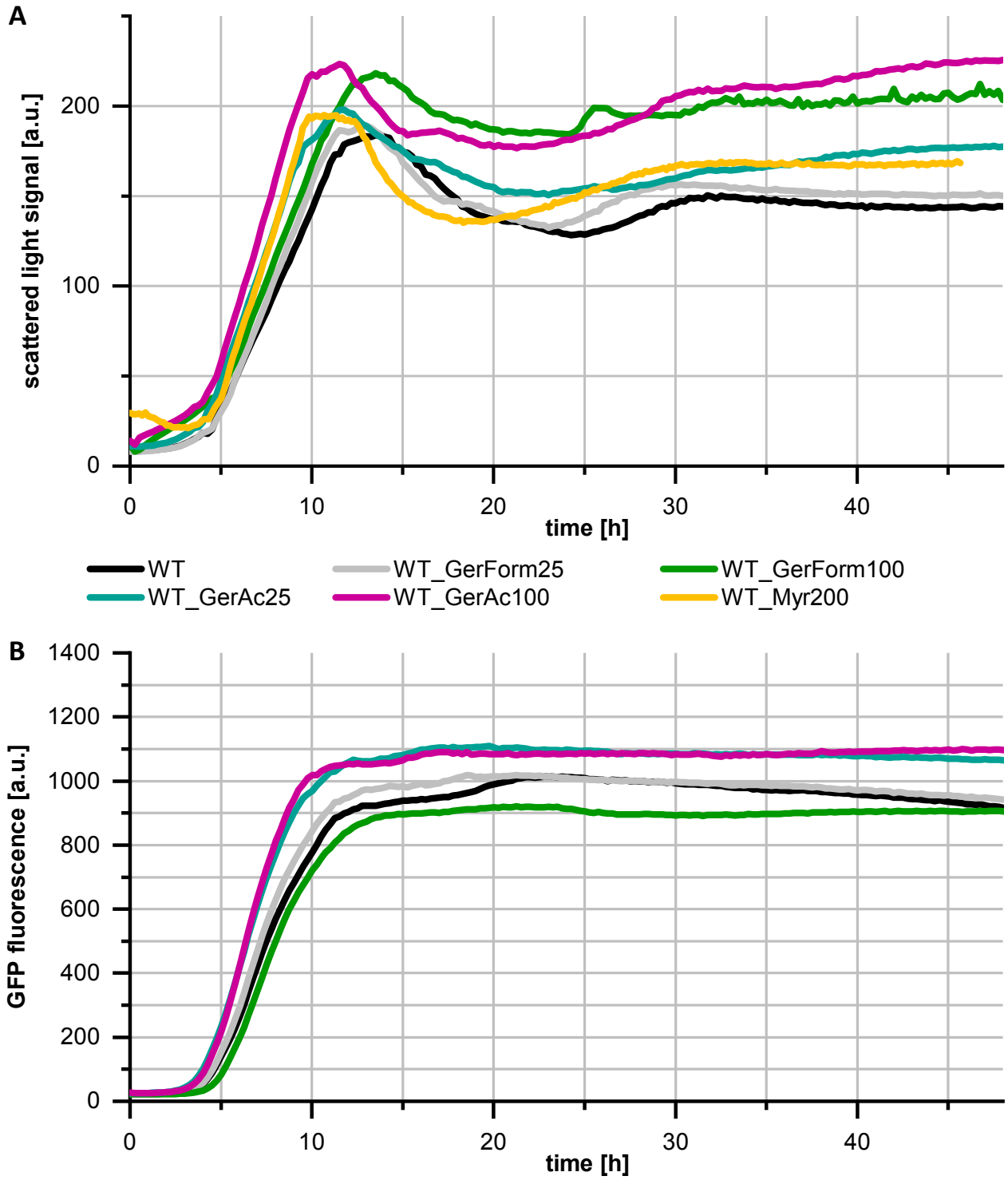

Figure S4. Growth of *P. putida* GS1 (WT) + pMiS4-eGFP without and in the presence of different monoterpenes and monoterpenoids. GerForm25/100: geranyl formate (25/100 mM), GerAc25/100: geranyl acetate (25/100 mM), Myr200: Myrcene (200 mM). Tolerance assays were conducted in a microbioreactor system over 48 h. Biomass formation was monitored every 10 – 15 minutes via (A) scattered light signal intensity (absorbance at 620 nm) and (B) GFP fluorescence signal intensity (excitation filter: 488 nm; emission filter: 520 nm). The data points represent the mean values of two or three biological replicas. For variations between the replicas of each strain see Figure S20.

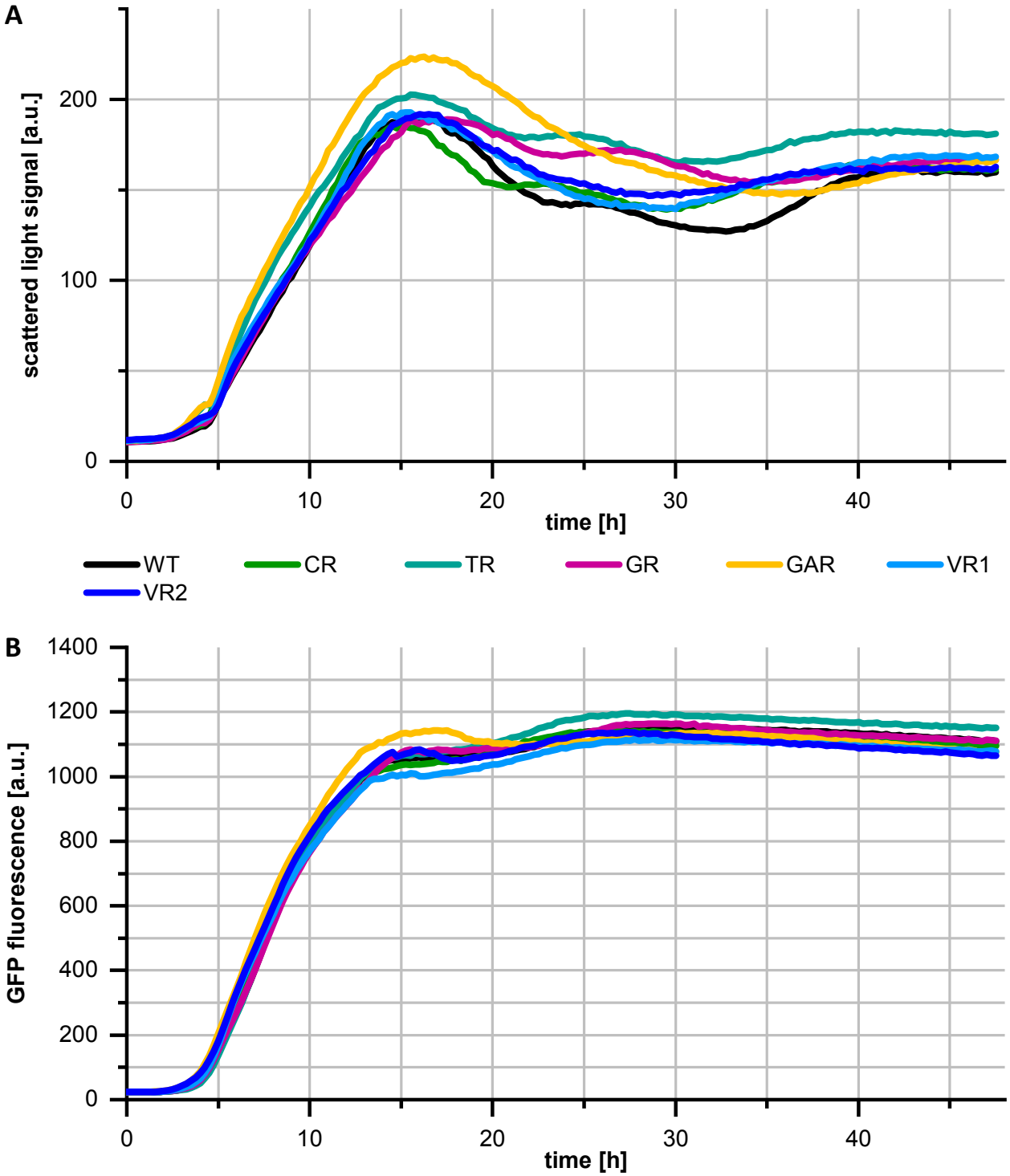

Figure S5. Growth of *P. putida* GS1 WT and mutants + pMiS4-eGFP without monoterpene or monoterpenoid. Tolerance assays were conducted in a microbioreactor system over 48 h. Biomass formation was monitored every 10 - 15 minutes via (A) scattered light signal intensity (absorbance at 620 nm) and (B) GFP fluorescence signal intensity (excitation filter: 488 nm; emission filter: 520 nm). The data points represent the mean values of three biological replicas. For variations between the replicas of each strain see Figure S21.

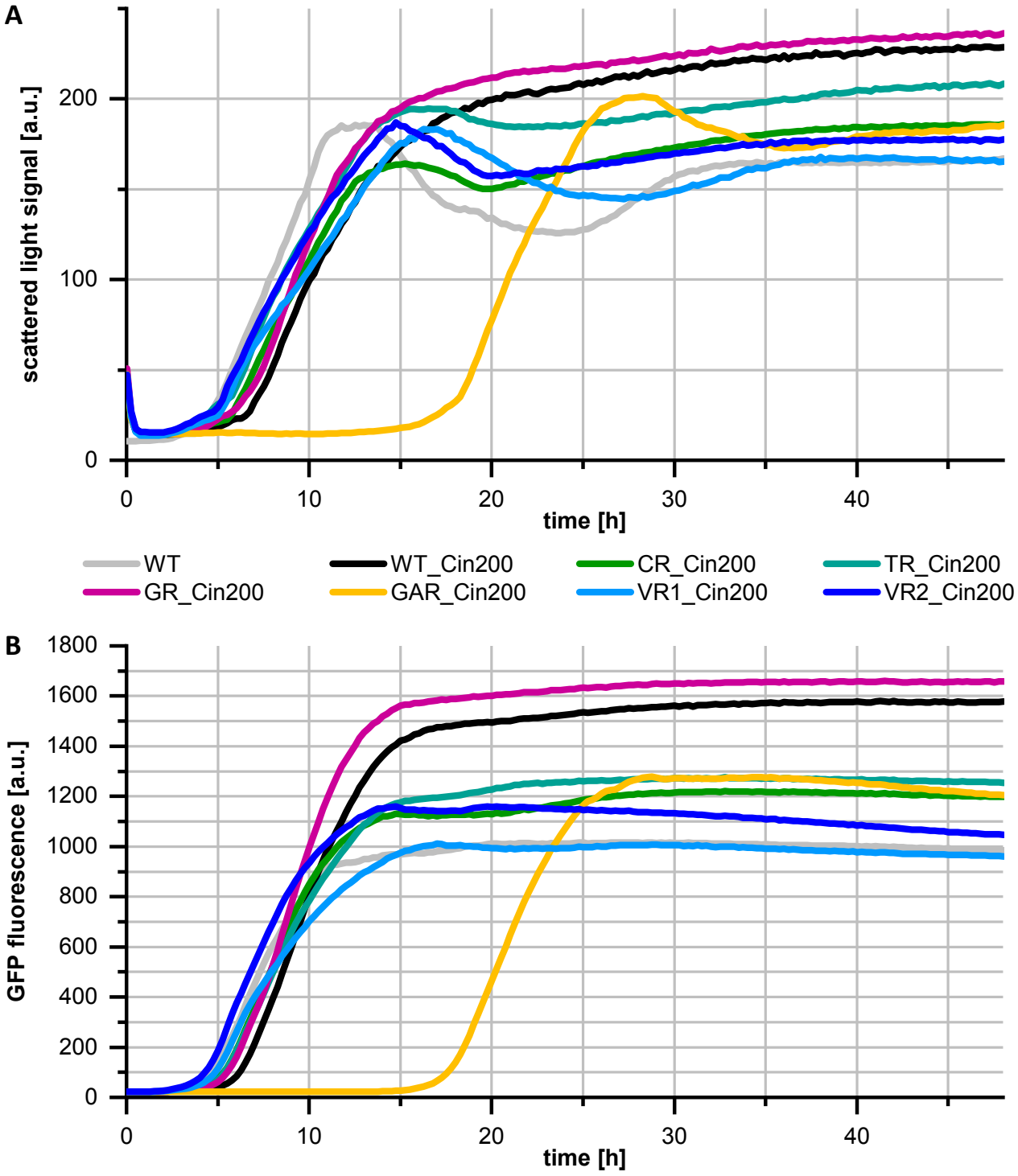

Figure S6. Growth of *P. putida* GS1 WT and mutants + pMiS4-eGFP without and in the presence of 200 mM 1,8-cineole. Tolerance assays were conducted in a microbioreactor system over 48 h. Biomass formation was monitored every 10 - 15 minutes via (A) scattered light signal intensity (absorbance at 620 nm) and (B) GFP fluorescence signal intensity (excitation filter: 488 nm; emission filter: 520 nm). The data points represent the mean values of three biological replicas. For variations between the replicas of each strain see Figure S22.

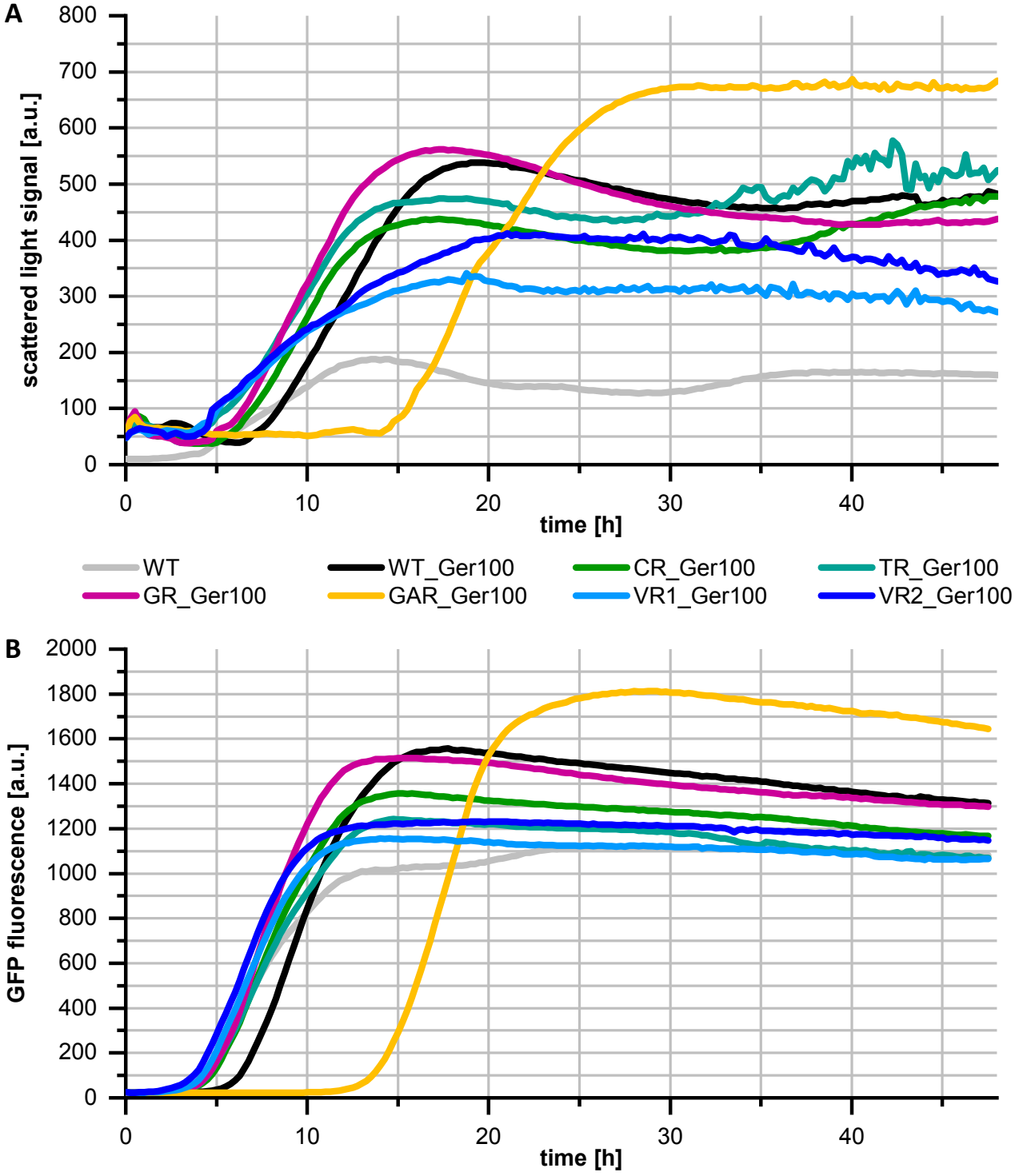

Figure S7. Growth of *P. putida* GS1 WT and mutants + pMiS4-eGFP without and in the presence of 100 mM geraniol. Tolerance assays were conducted in a microbioreactor system over 48 h. Biomass formation was monitored every 10 - 15 minutes via (A) scattered light signal intensity (absorbance at 620 nm) and (B) GFP fluorescence signal intensity (excitation filter: 488 nm; emission filter: 520 nm). The data points represent the mean values of three biological replicas. For variations between the replicas of each strain see Figure S23.

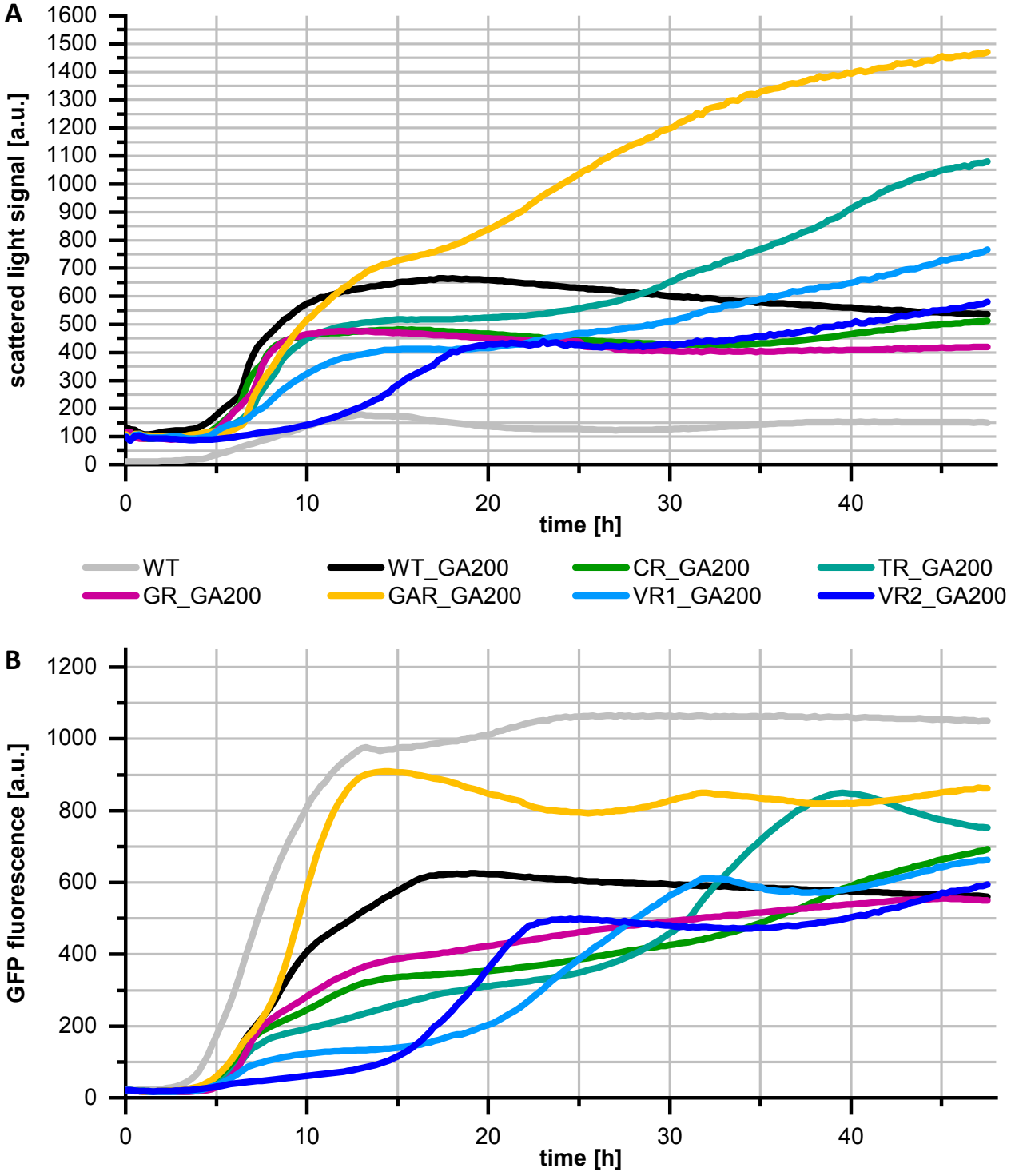

Figure S8. Growth of *P. putida* GS1 WT and mutants + pMiS4-eGFP without and in the presence of 200 mM geranic acid. Tolerance assays were conducted in a microbioreactor system over 48 h. Biomass formation was monitored every 10 - 15 minutes via (A) scattered light signal intensity (absorbance at 620 nm) and (B) GFP fluorescence signal intensity (excitation filter: 488 nm; emission filter: 520 nm). The data points represent the mean values of three biological replicas. For variations between the replicas of each strain see Figure S24.

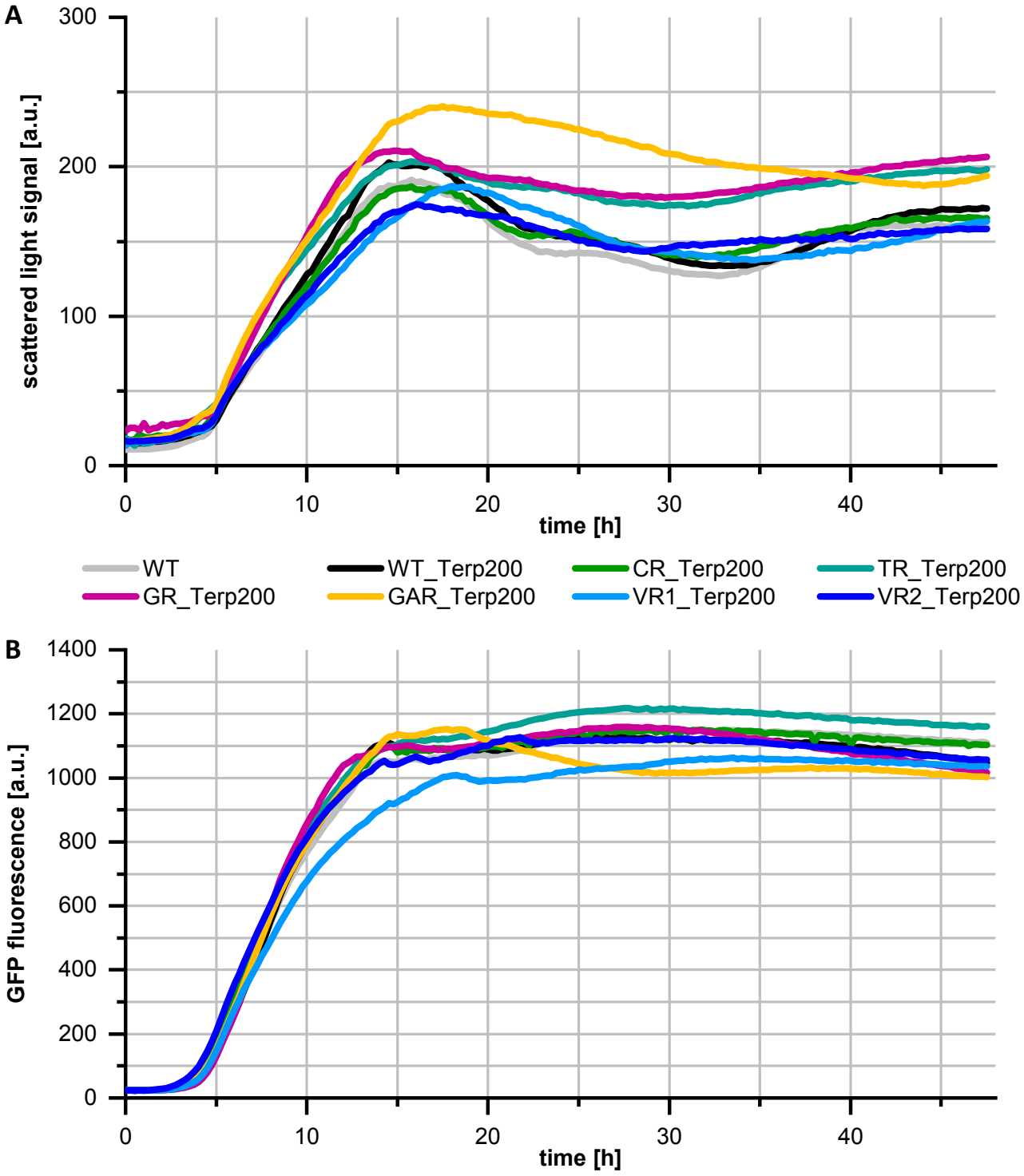

Figure S9. Growth of *P. putida* GS1 WT and mutants + pMiS4-eGFP without and in the presence of 200 mM γ-terpinene. Tolerance assays were conducted in a microbioreactor system over 48 h. Biomass formation was monitored every 10 - 15 minutes via (A) scattered light signal intensity (absorbance at 620 nm) and (B) GFP fluorescence signal intensity (excitation filter: 488 nm; emission filter: 520 nm). The data points represent the mean values of three biological replicas. For variations between the replicas of each strain see Figure S25.

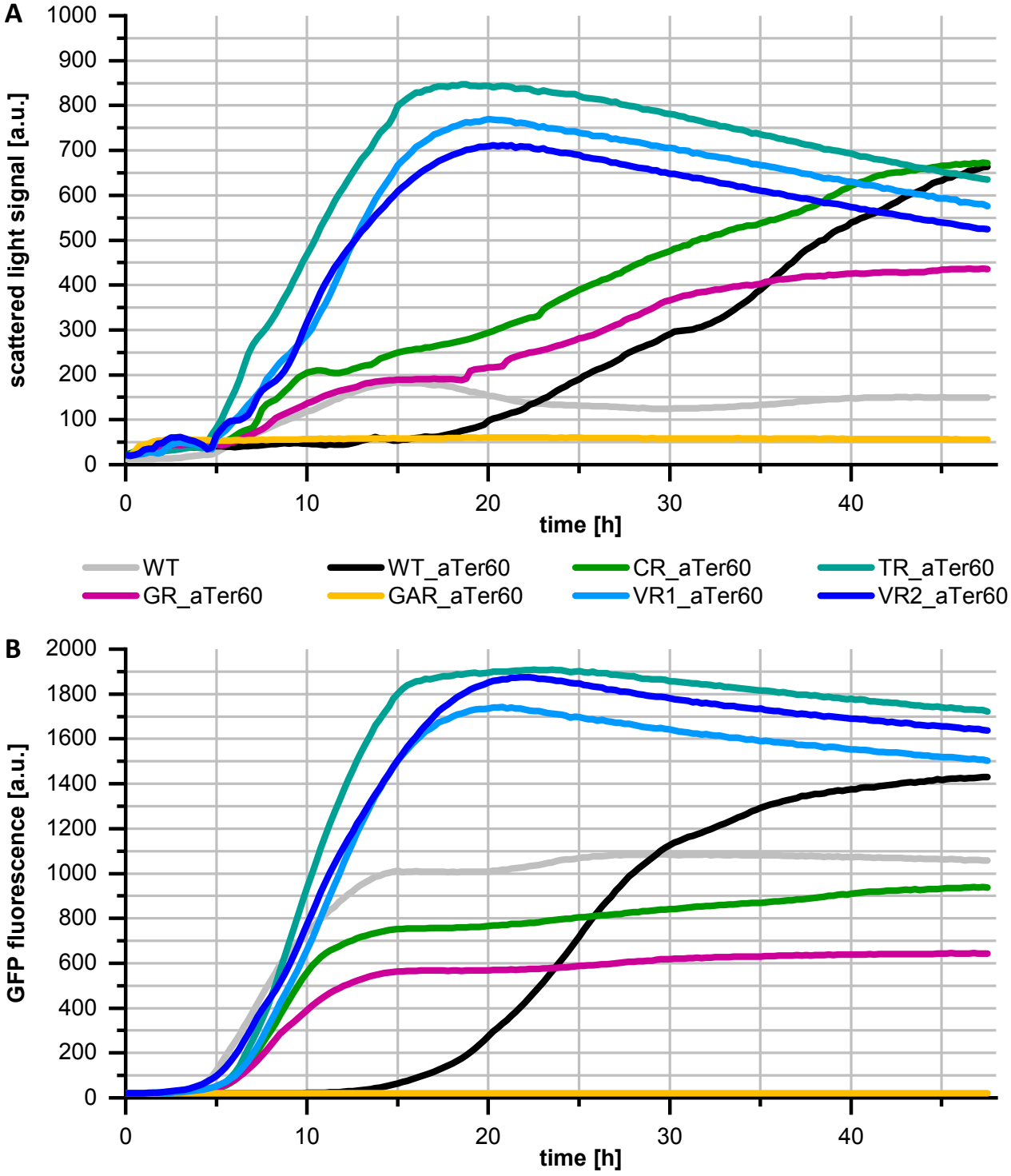

Figure S10. Growth of *P. putida* GS1 WT and mutants + pMiS4-eGFP without and in the presence of 60 mM α-terpineol. Tolerance assays were conducted in a microbioreactor system over 48 h. Biomass formation was monitored every 10 - 15 minutes via (A) scattered light signal intensity (absorbance at 620 nm) and (B) GFP fluorescence signal intensity (excitation filter: 488 nm; emission filter: 520 nm). The data points represent the mean values of two (VR1) or three biological replicas. For variations between the replicas of each strain see Figure S26.

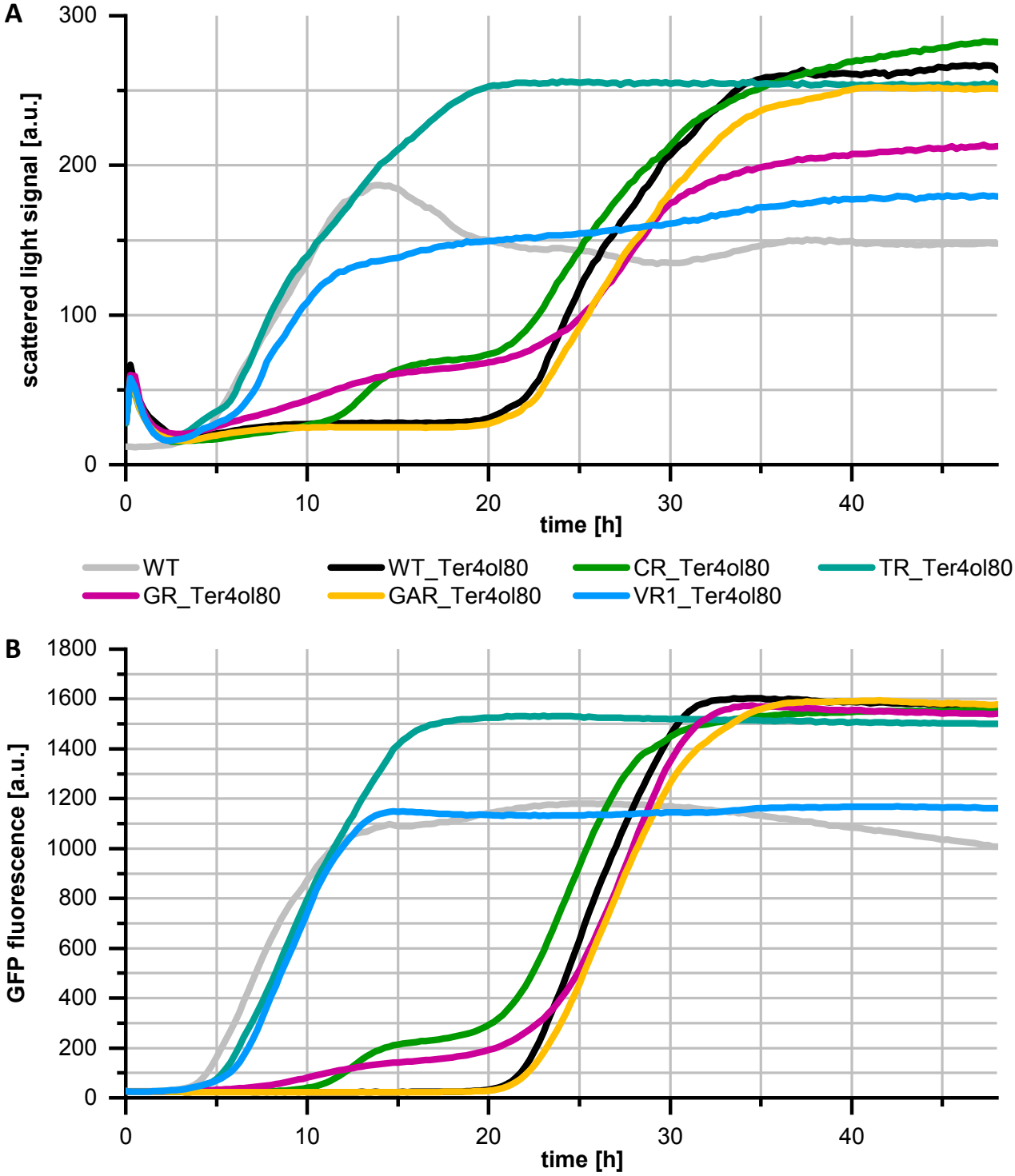

Figure S11. Growth of *P. putida* GS1 WT and mutants + pMiS4e-GFP without and in the presence of 80 mM terpinen-4-ol. Tolerance assays were conducted in a microbioreactor system over 48 h. Biomass formation was monitored every 10 - 15 minutes via (A) scattered light signal intensity (absorbance at 620 nm) and (B) GFP fluorescence signal intensity (excitation filter: 488 nm; emission filter: 520 nm). The data points represent the mean values of two or three biological replicas. For variations between the replicas of each strain see Figure S27.

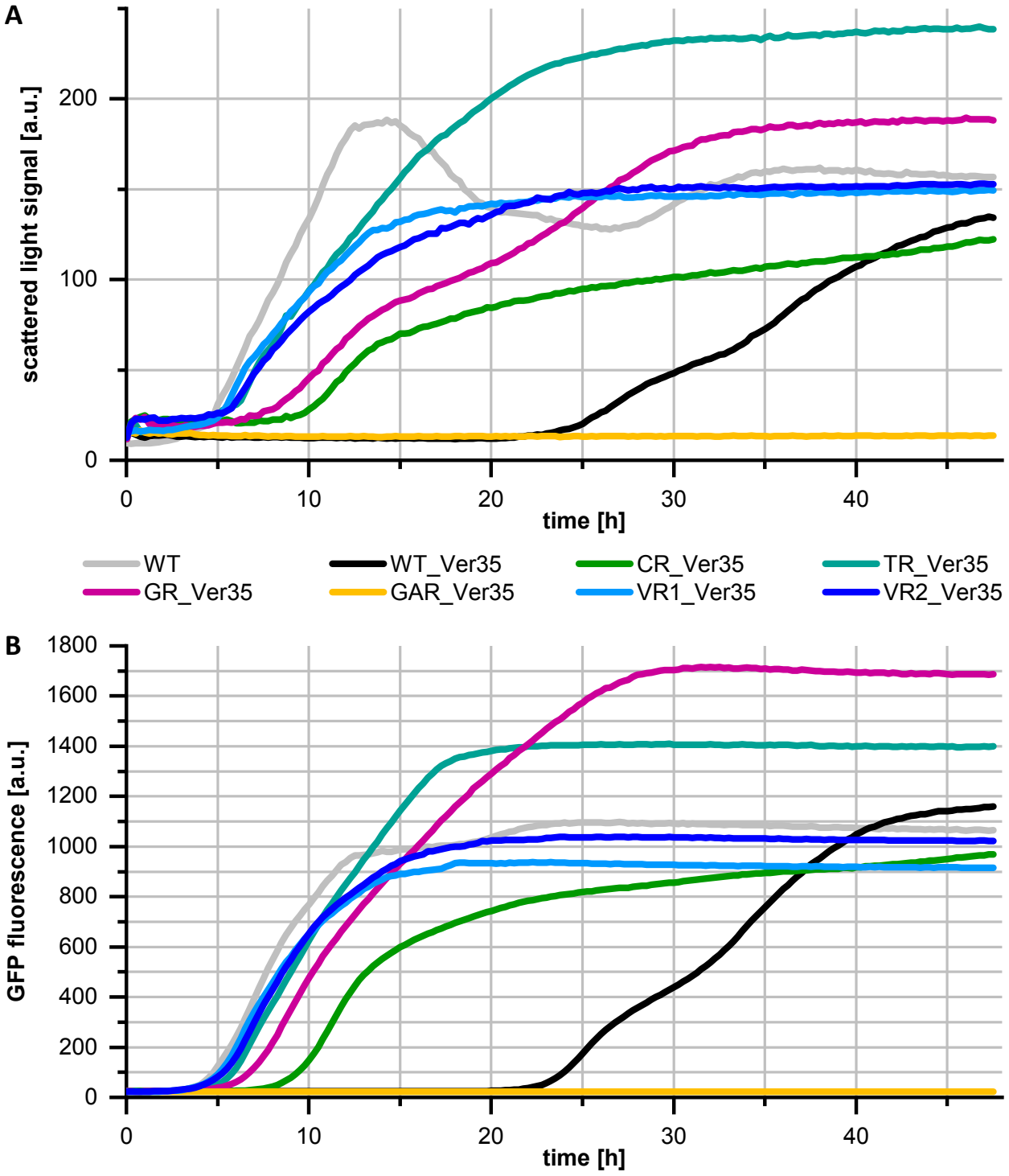

Figure S12. Growth of *P. putida* GS1 WT and mutants + pMiS4-eGFP without and in the presence of 35 mM verbenone. Tolerance assays were conducted in a microbioreactor system over 48 h. Biomass formation was monitored every 10 - 15 minutes via (A) scattered light signal intensity (absorbance at 620 nm) and (B) GFP fluorescence signal intensity (excitation filter: 488 nm; emission filter: 520 nm). The data points represent the mean values of two or three biological replicas. For variations between the replicas of each strain see Figure S28.

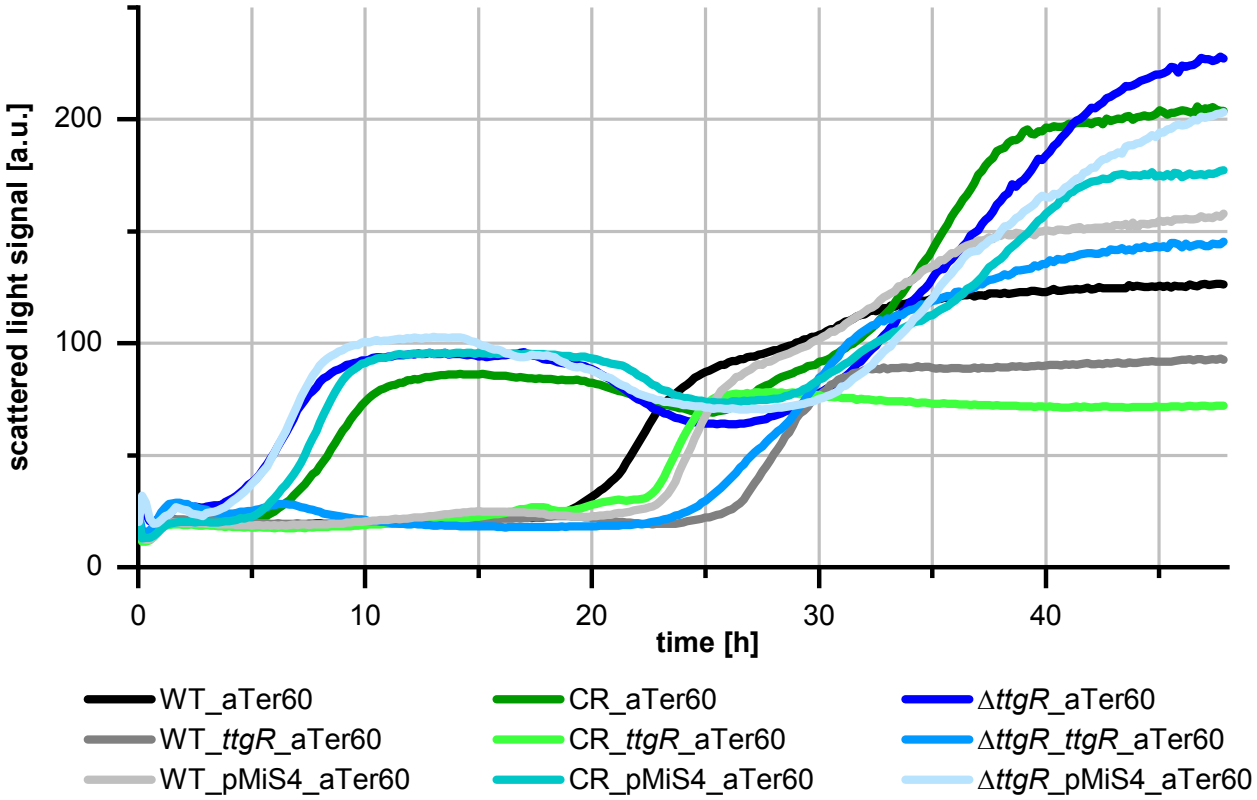

Figure S13. Verification of *ttgR* involvement in α-terpineol-hypertolerance phenotype by deletion and complementation. Growth curves of cultures with 60 mM α-terpineol are shown. pMiS4 = strains contain the pMiS4 empty plasmid, *_ttgR_* = strains contain the pMiS4-*ttgR* vector. Tolerance assays were conducted in a microbioreactor system over 48 h. Biomass formation was monitored every 10 - 15 minutes via (A) scattered light signal intensity (absorbance at 620 nm) and (B) GFP fluorescence signal intensity (excitation filter: 488 nm; emission filter: 520 nm). The data points represent the mean values of three biological replicas. For variations between the replicas of each strain see Figure S30.

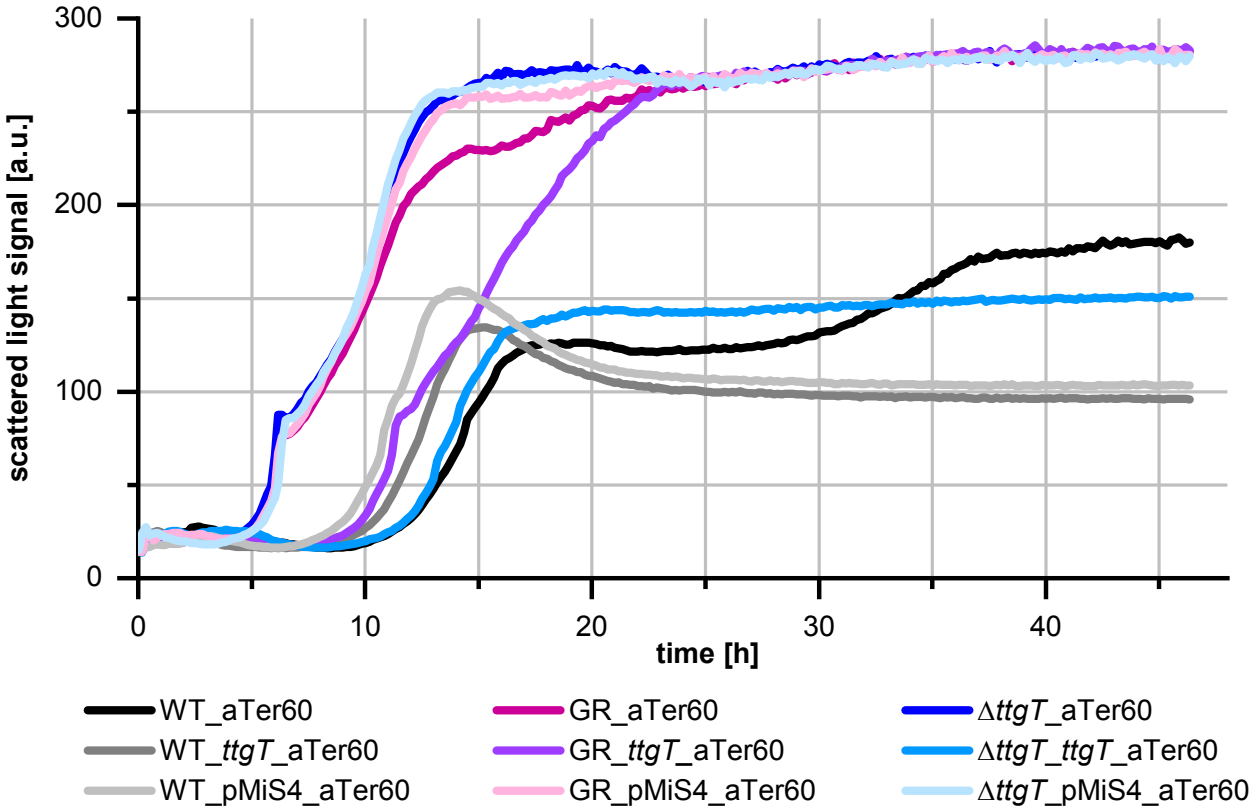

Figure S14. Verification of *ttgT* involvement in α-terpineol-hypertolerance phenotype by deletion and complementation. Growth curves of cultures with 60 mM α-terpineol are shown. pMiS4 = strains contain the pMiS4 empty plasmid, *_ttgT_* = strains contain the pMiS4-*ttgT* vector. Tolerance assays were conducted in a microbioreactor system over 48 h. Biomass formation was monitored every 10 - 15 minutes via (A) scattered light signal intensity (absorbance at 620 nm) and (B) GFP fluorescence signal intensity (excitation filter: 488 nm; emission filter: 520 nm). The data points represent the mean values of three biological replicas. For variations between the replicas of each strain see Figure S31.

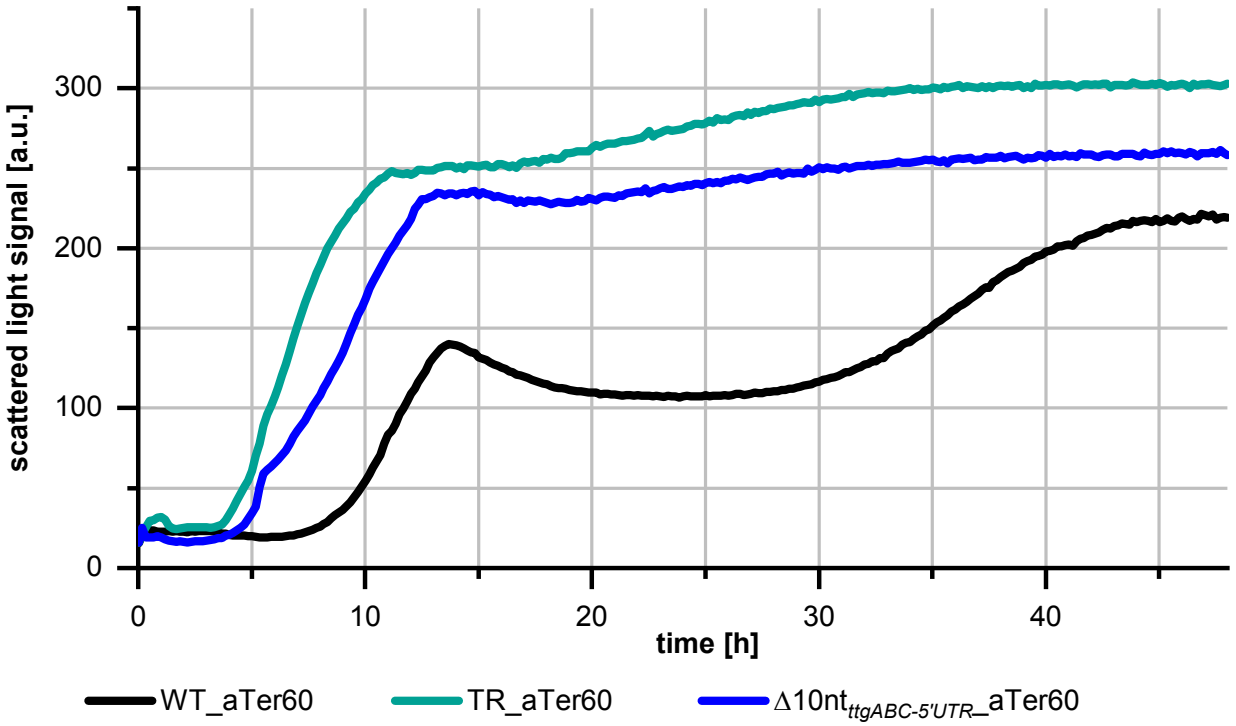

Figure S15. Verification of Δ10nt$_{ttgABC\text{-}5'UTR}$ involvement in α-terpineol-hypertolerance phenotype by deletion. Growth curves of cultures with 60 mM α-terpineol are shown. Tolerance assays were conducted in a microbioreactor system over 48 h. Biomass formation was monitored every 10 - 15 minutes via (A) scattered light signal intensity (absorbance at 620 nm) and (B) GFP fluorescence signal intensity (excitation filter: 488 nm; emission filter: 520 nm). The data points represent the mean values of three biological replicas. For variations between the replicas of each strain see Figure S32.

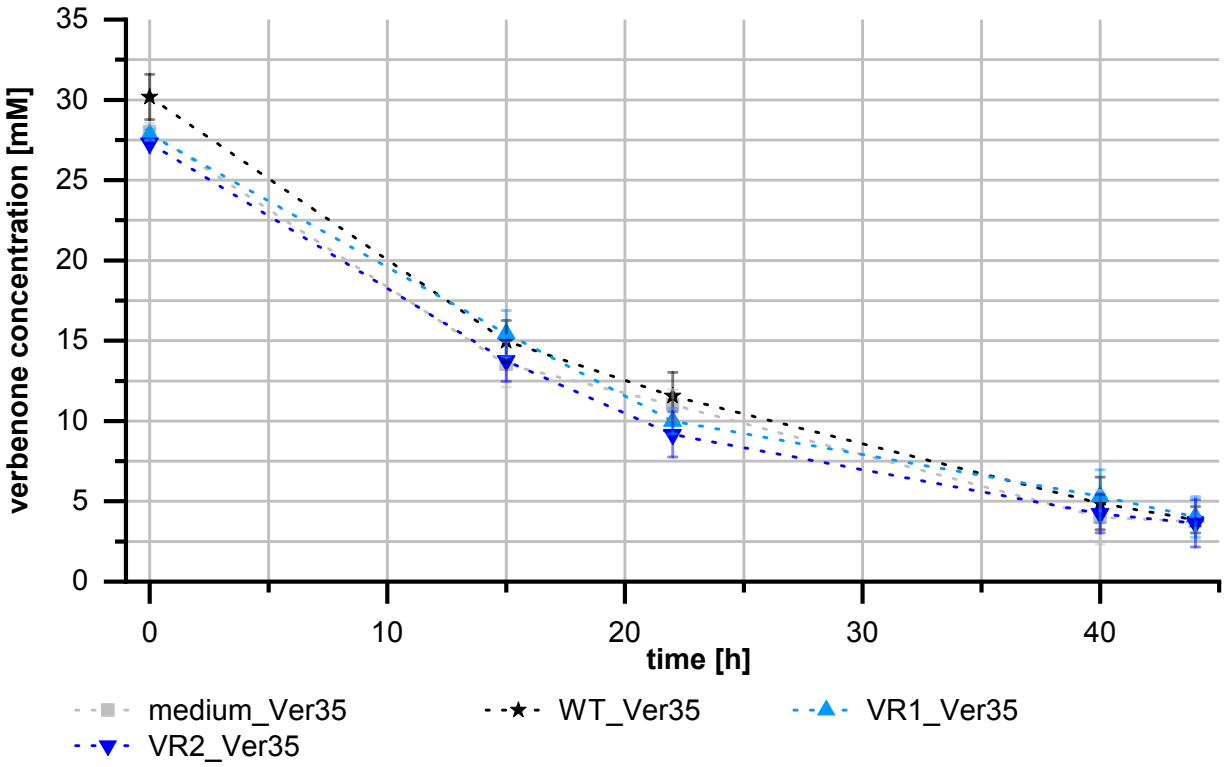

Figure S16. Determination of verbenone concentration in culture medium (WT, VR1, VR2) or in culture free medium (medium) over time. *P.* putida strains were grown in a microbioreactor system over 44 h with initial addition of 35 mM verbenone. To determine verbenone concentration, samples were taken at time points t = 0, 15, 22, 40, 44 h and analyzed via GC-MS. The data points represent the mean values and standard deviations of three biological replicas.

Supplementary note 1

The growth curve figures Fig. 2, Fig. 3 and Fig. 5 as well as Figure S1 - Figure S15 show mean values from cultivations of three biological replicates. To show the variations within the experiments, Figure S17 - Figure S32 present the corresponding individual growth curves.

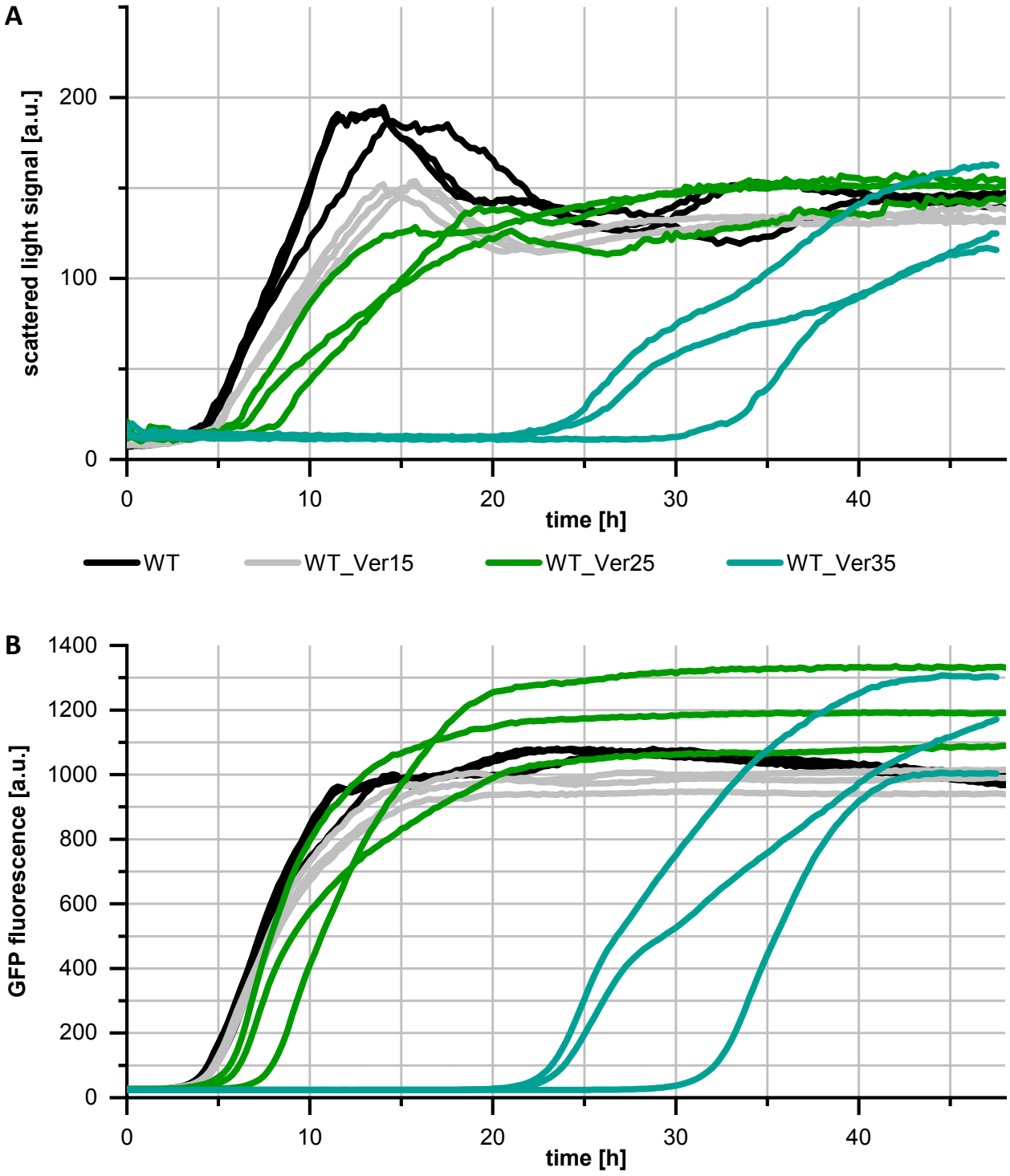

Figure S17. Growth of different *P. putida* GS1 WT cultures without and in the presence of different verbenone concentrations (15, 25 and 35 mM). Tolerance assays were conducted in a microbioreactor system over 48 h. Biomass formation was monitored every 10 - 15 minutes via (A) scattered light signal intensity (absorbance at 620 nm) and (B) GFP fluorescence signal intensity (excitation filter: 488 nm; emission filter: 520 nm).

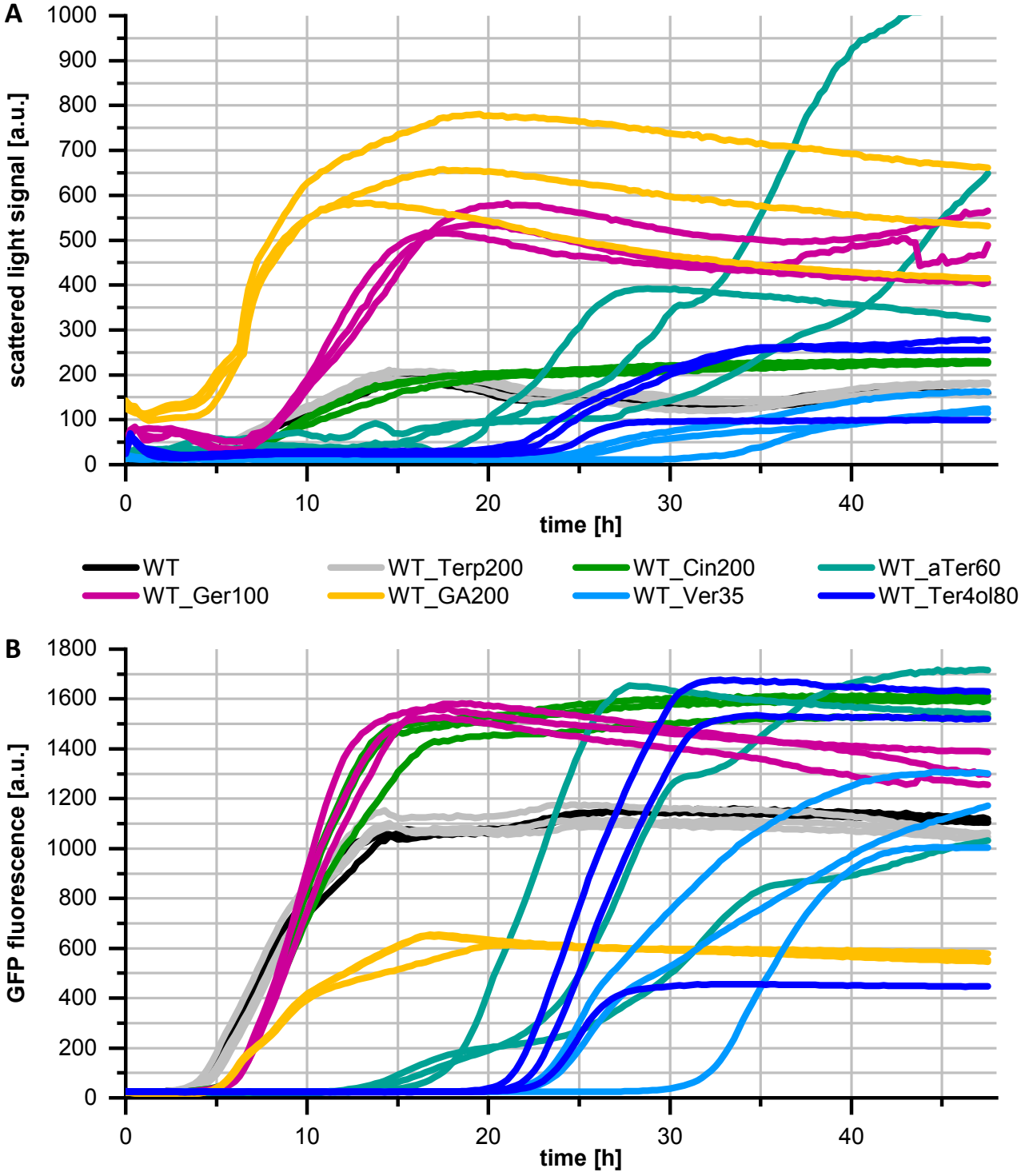

Figure S18. Growth of three different *P. putida* GS1 (WT) + pMiS4-eGFP cultures without and in the presence of different monoterpenes and monoterpenoids. Terp200: γ-terpinene (200 mM), Cin200: 1,8-cineole (200 mM), aTer60: α-terpineol (60 mM), Ger100: geraniol (100 mM), GA200: geranic acid (200 mM), Ver35: verbenone (35 mM), Ter4ol80: terpinen-4-ol (80 mM). Tolerance assays were conducted in a microbioreactor system over 48 h. Biomass formation was monitored every 10 - 15 minutes via (A) scattered light signal intensity (absorbance at 620 nm) and (B) GFP fluorescence signal intensity (excitation filter: 488 nm; emission filter: 520 nm).

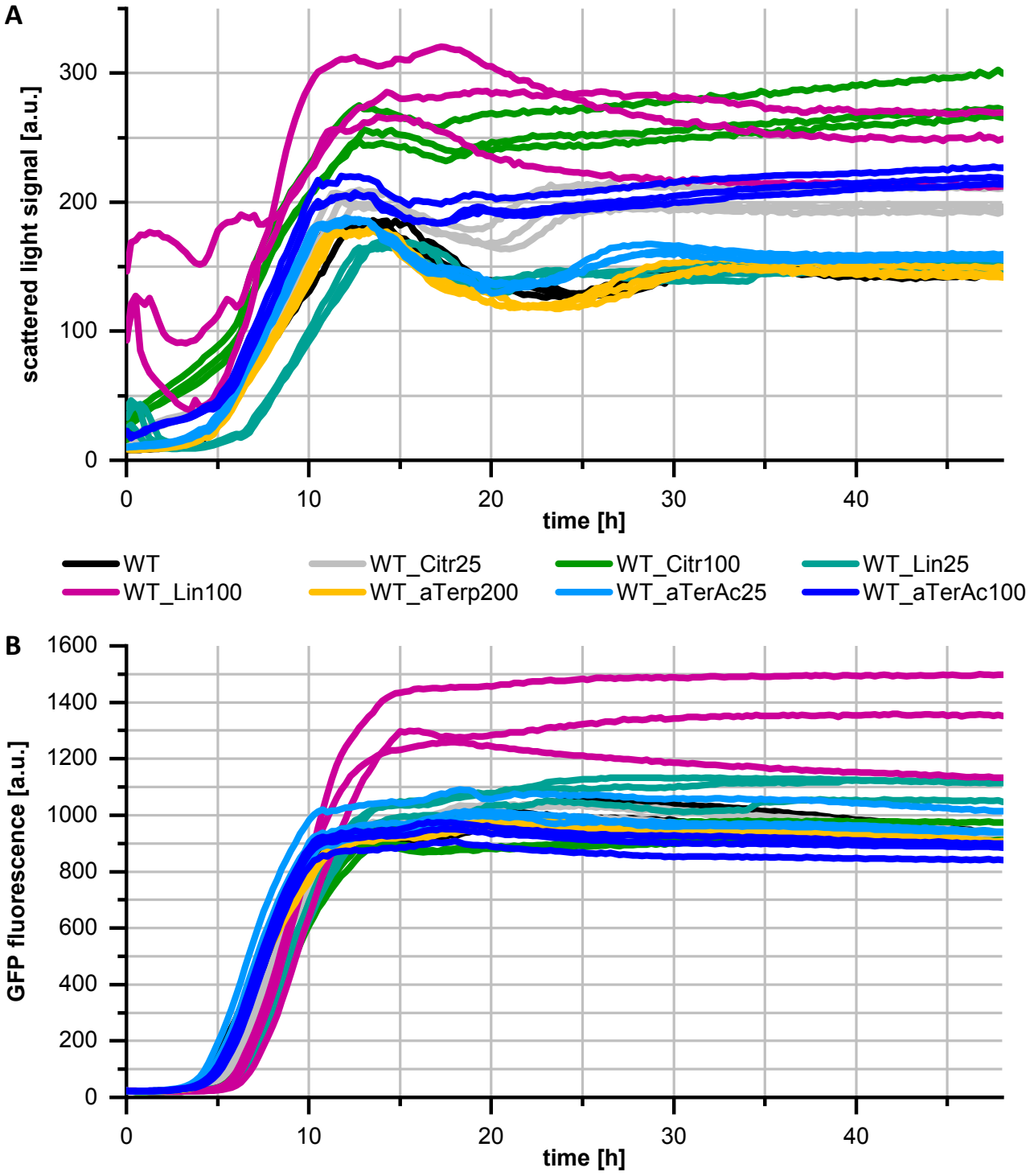

Figure S19. Growth of three different *P. putida* GS1 (WT) + pMiS4-eGFP cultures without and in the presence of different monoterpenes and monoterpenoids. Citr25/100: citral (25/100 mM), Lin25/100: linalool (25/100 mM), aTerp200: α-terpinene (200 mM), aTerpAc25/100: α-terpinyl acetate (25/100 mM). Tolerance assays were conducted in a microbioreactor system over 48 h. Biomass formation was monitored every 10 - 15 minutes via (A) scattered light signal intensity (absorbance at 620 nm) and (B) GFP fluorescence signal intensity (excitation filter: 488 nm; emission filter: 520 nm).

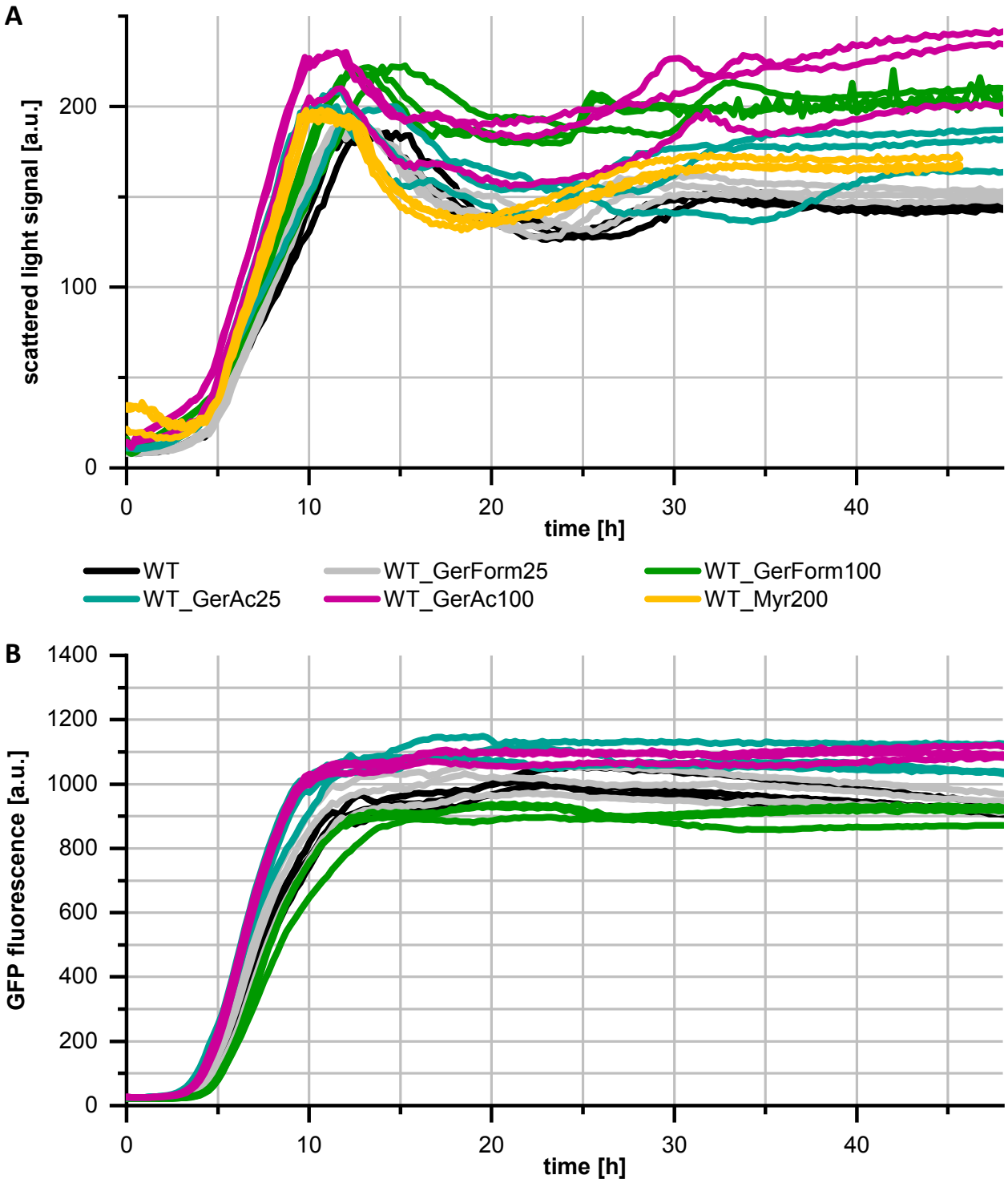

Figure S20. Growth of three different *P. putida* GS1 (WT) + pMiS4-eGFP cultures without and in the presence of different monoterpenes and monoterpenoids. GerForm25/100: geranyl formate (25/100 mM), GerAc25/100: geranyl acetate (25/100 mM), Myr200: Myrcene (200 mM). Tolerance assays were conducted in a microbioreactor system over 48 h. Biomass formation was monitored every 10 - 15 minutes via (A) scattered light signal intensity (absorbance at 620 nm) and (B) GFP fluorescence signal intensity (excitation filter: 488 nm; emission filter: 520 nm).

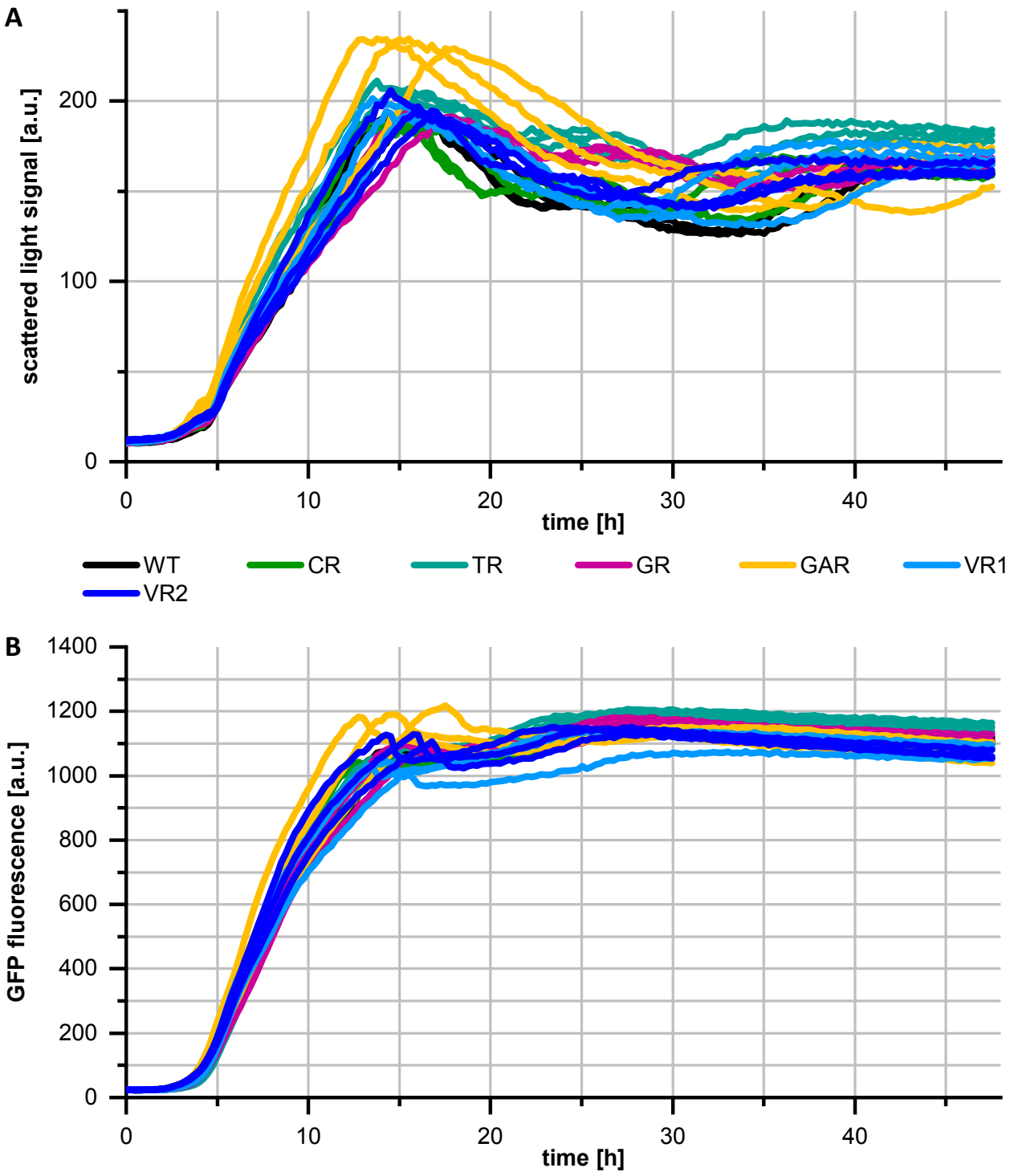

Figure S21. Growth of three different cultures of *P. putida* GS1 WT and mutants + pMiS4-eGFP without monoterpene or monoterpenoid. Tolerance assays were conducted in a microbioreactor system over 48 h. Biomass formation was monitored every 10 - 15 minutes via (A) scattered light signal intensity (absorbance at 620 nm) and (B) GFP fluorescence signal intensity (excitation filter: 488 nm; emission filter: 520 nm).

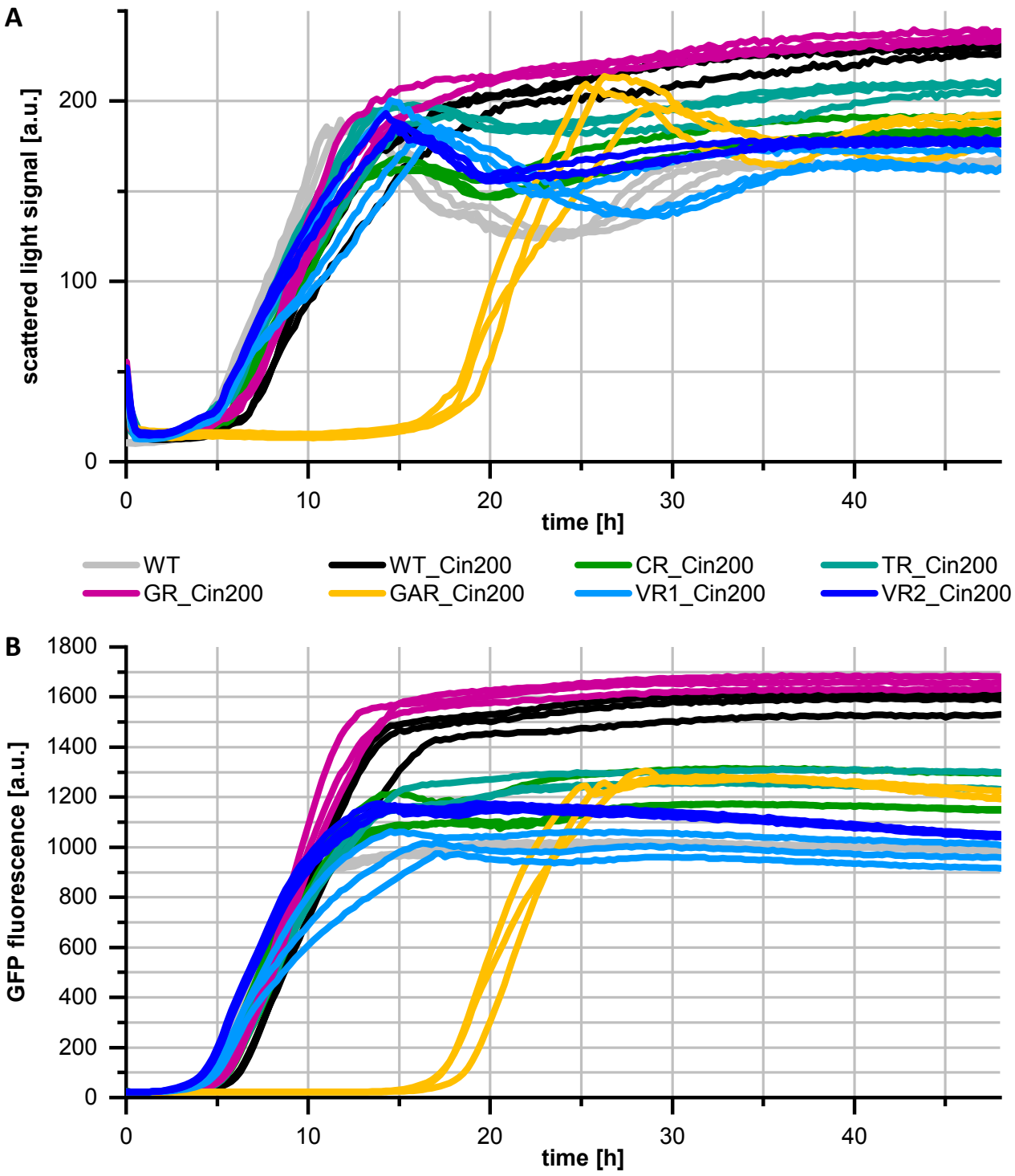

Figure S22. Growth of three different cultures of *P. putida* GS1 WT and mutants + pMiS4-eGFP without and in the presence of 200 mM 1,8-cineole. Tolerance assays were conducted in a microbioreactor system over 48 h. Biomass formation was monitored every 10 - 15 minutes via (A) scattered light signal intensity (absorbance at 620 nm) and (B) GFP fluorescence signal intensity (excitation filter: 488 nm; emission filter: 520 nm).

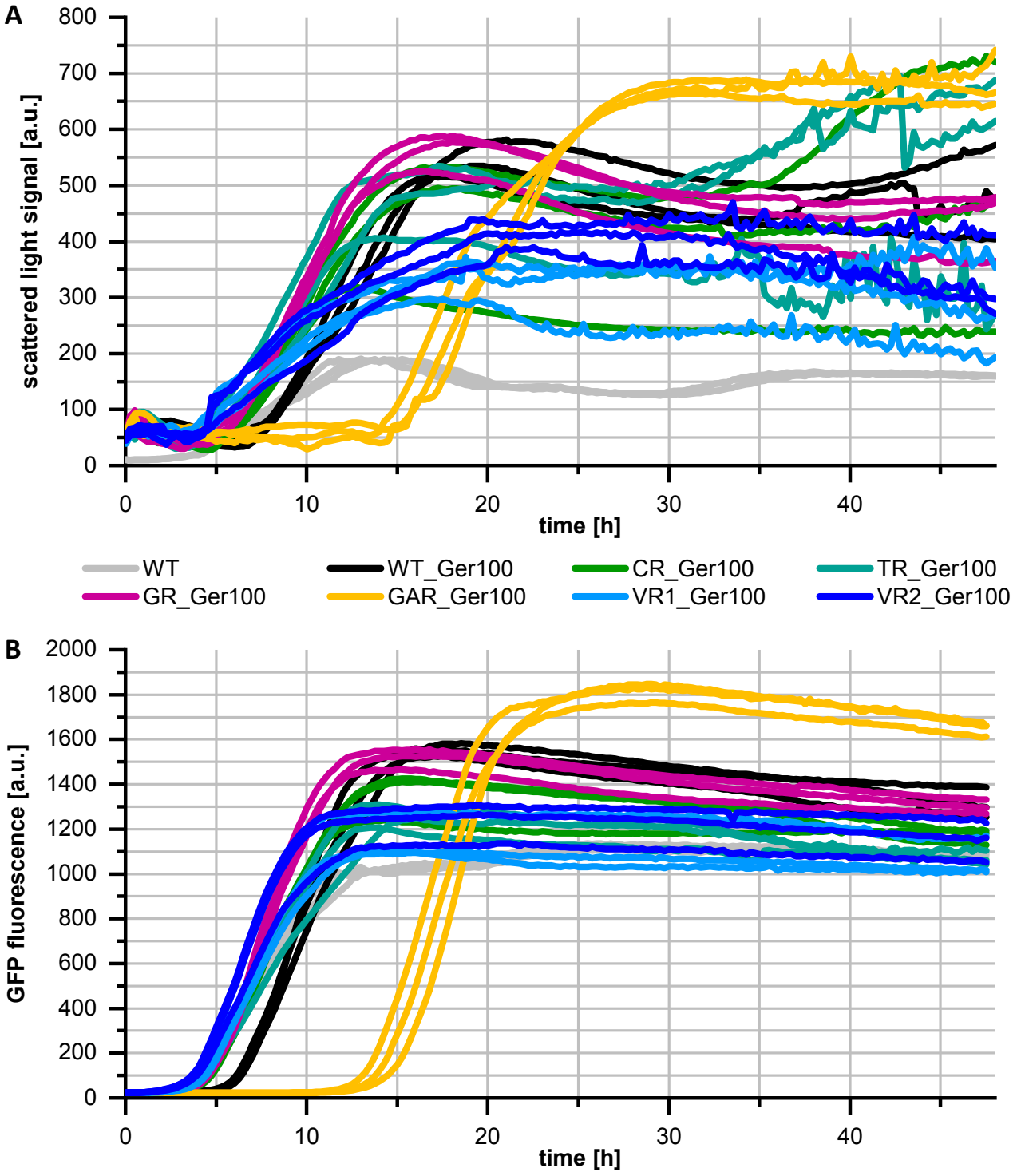

Figure S23. Growth of three different cultures of *P. putida* GS1 WT and mutants + pMiS4-eGFP without and in the presence of 100 mM geraniol. Tolerance assays were conducted in a microbioreactor system over 48 h. Biomass formation was monitored every 10 - 15 minutes via (A) scattered light signal intensity (absorbance at 620 nm) and (B) GFP fluorescence signal intensity (excitation filter: 488 nm; emission filter: 520 nm).

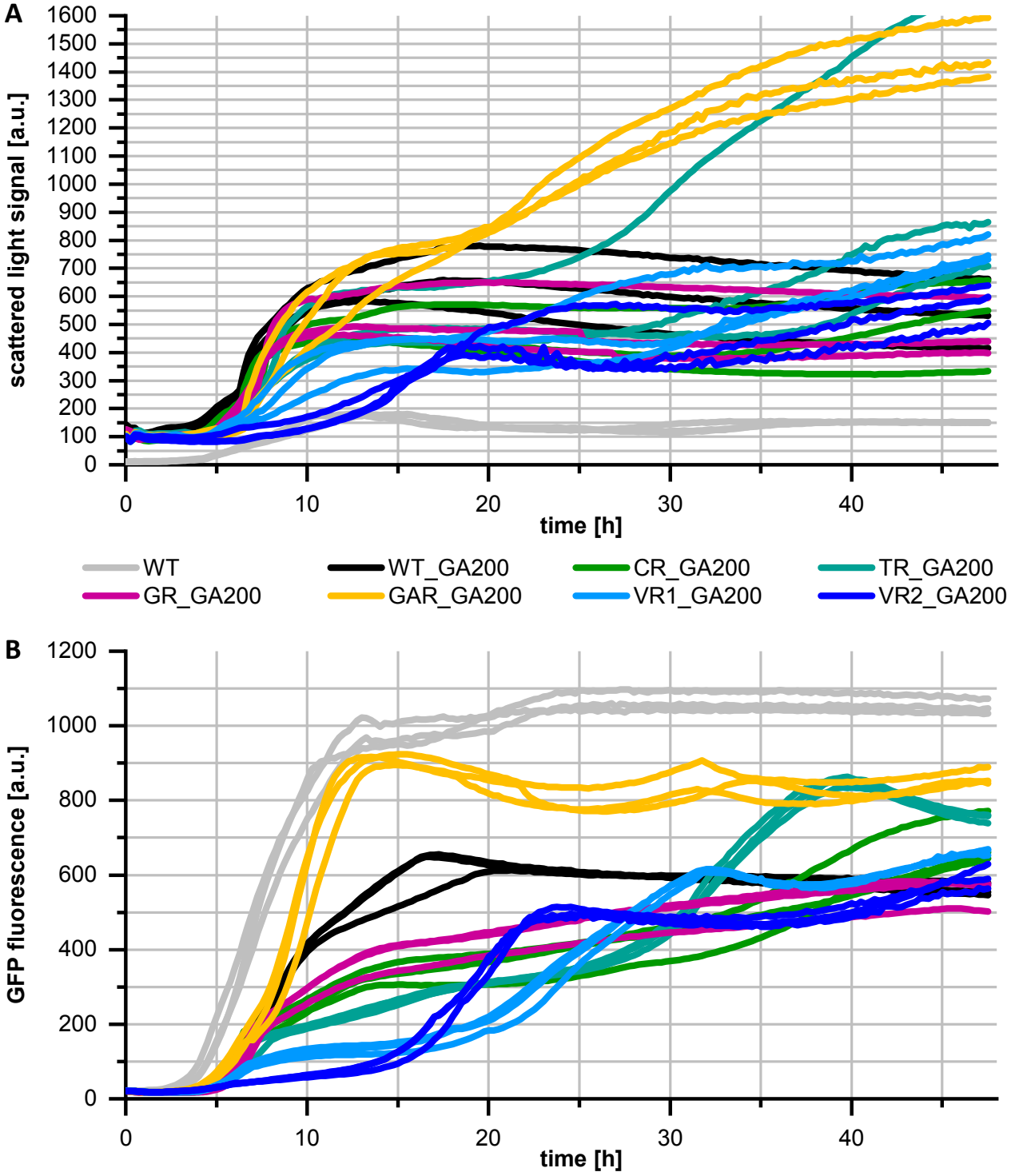

Figure S24. Growth of three different cultures of *P. putida* GS1 WT and mutants + pMiS4-eGFP without and in the presence of 200 mM geranic acid. Tolerance assays were conducted in a microbioreactor system over 48 h. Biomass formation was monitored every 10 - 15 minutes via (A) scattered light signal intensity (absorbance at 620 nm) and (B) GFP fluorescence signal intensity (excitation filter: 488 nm; emission filter: 520 nm).

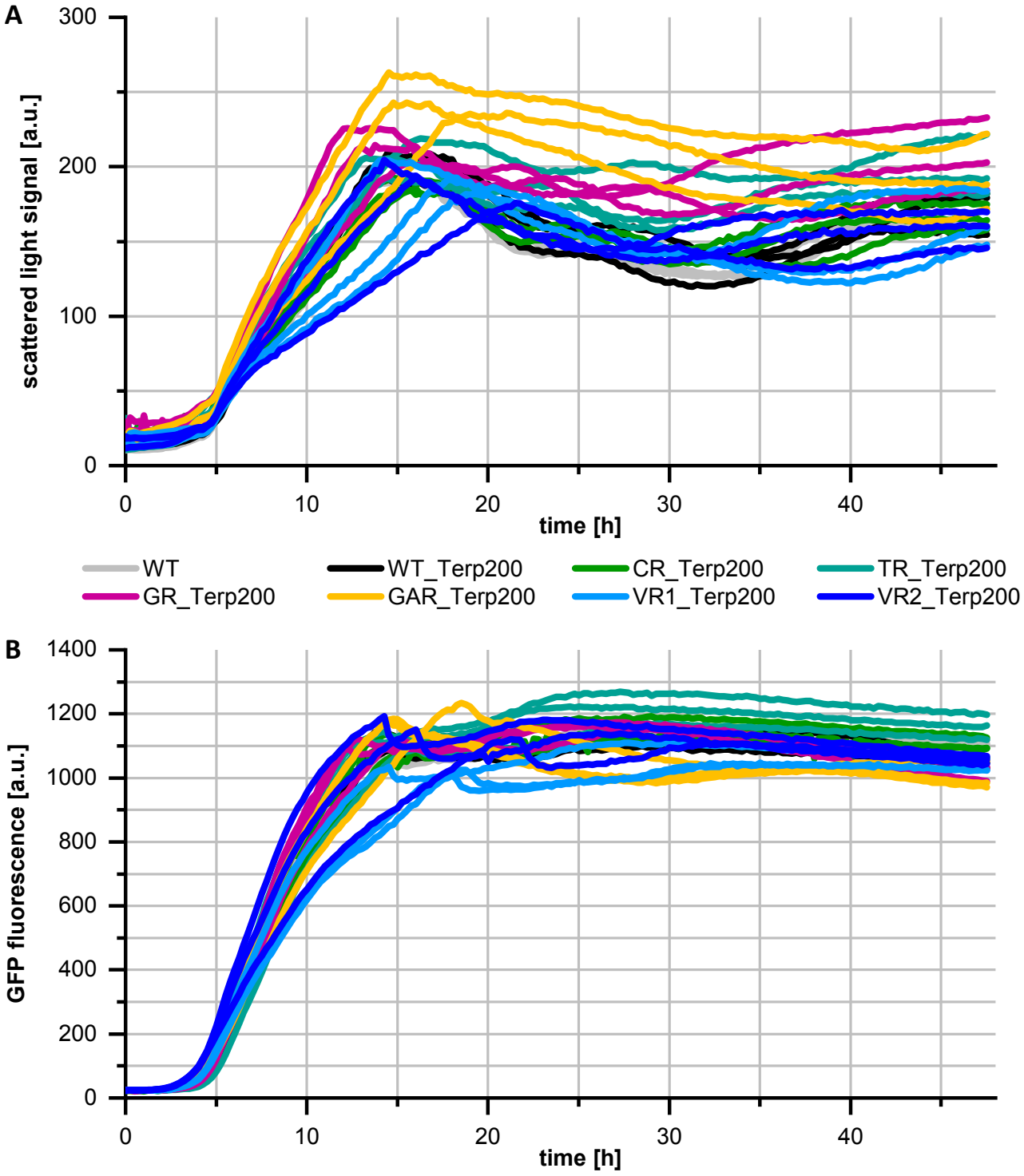

Figure S25. Growth of three different cultures of *P. putida* GS1 WT and mutants + pMiS4-eGFP without and in the presence of 200 mM γ-terpinene. Tolerance assays were conducted in a microbioreactor system over 48 h. Biomass formation was monitored every 10 - 15 minutes via (A) scattered light signal intensity (absorbance at 620 nm) and (B) GFP fluorescence signal intensity (excitation filter: 488 nm; emission filter: 520 nm).

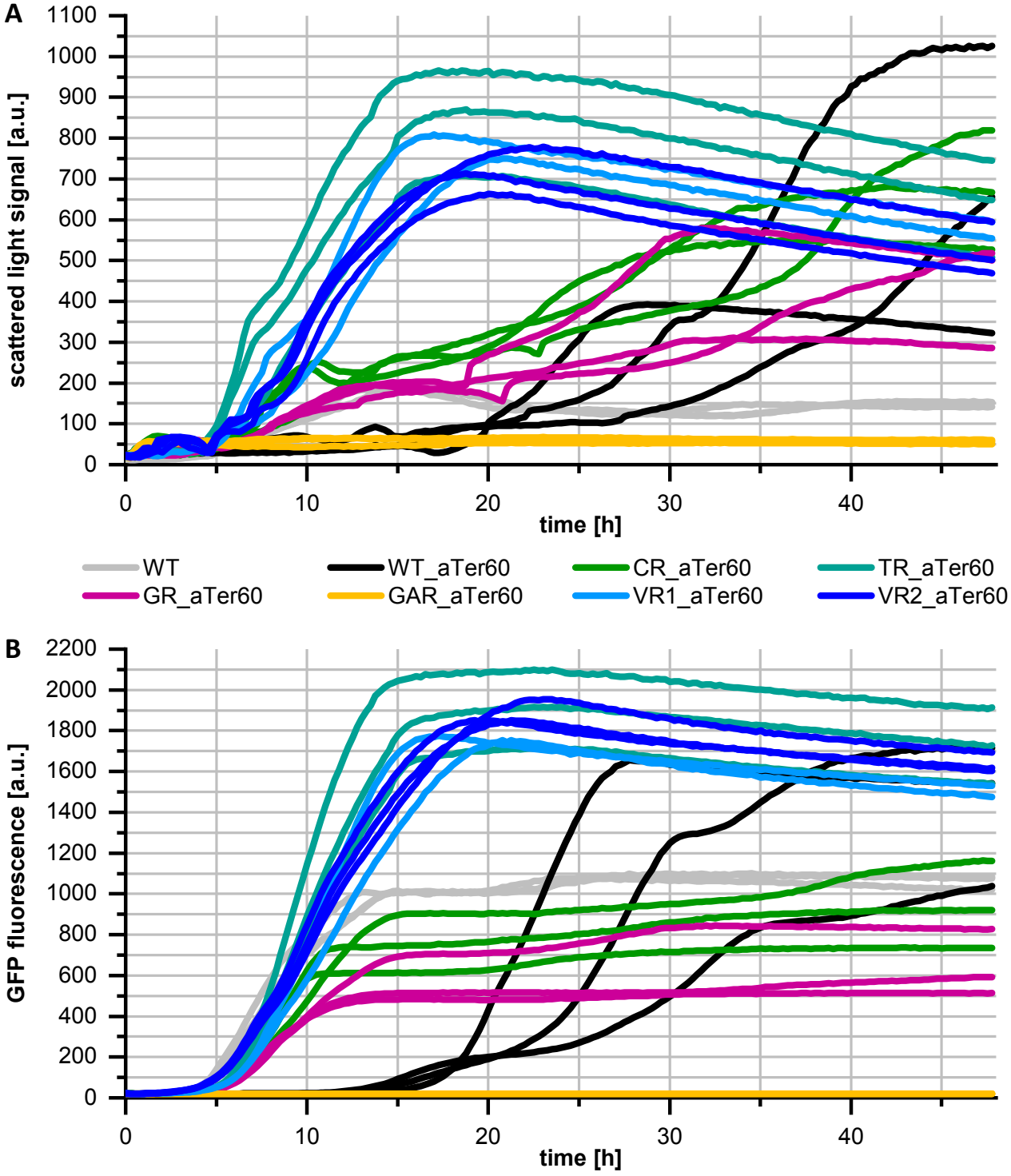

Figure S26. Growth of two (VR1) or three different cultures of *P. putida* GS1 WT and mutants + pMiS4-eGFP without and in the presence of 60 mM α-terpineol. Tolerance assays were conducted in a microbioreactor system over 48 h. Biomass formation was monitored every 10 - 15 minutes via (A) scattered light signal intensity (absorbance at 620 nm) and (B) GFP fluorescence signal intensity (excitation filter: 488 nm; emission filter: 520 nm).

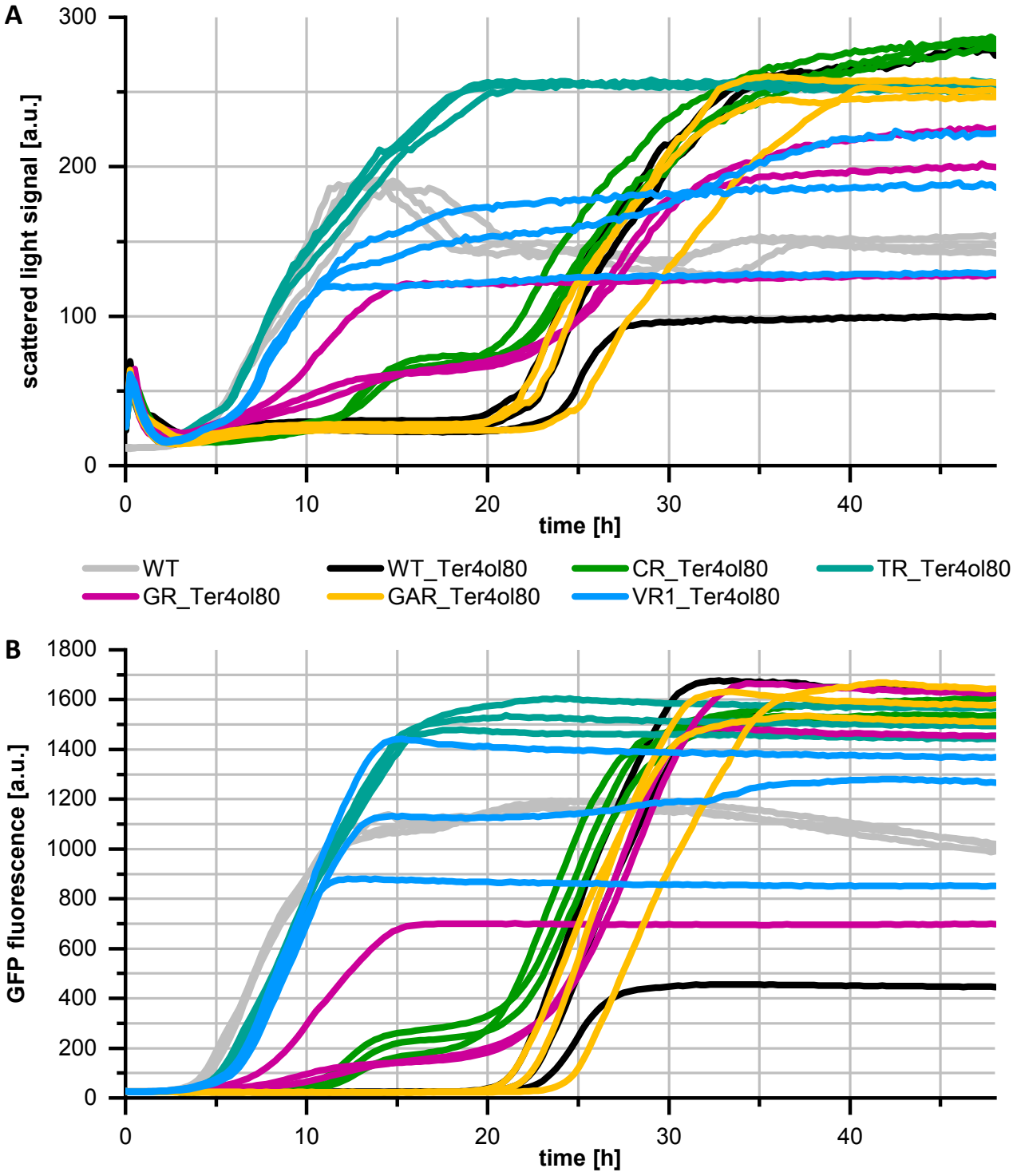

Figure S27. Growth of three different cultures of *P. putida* GS1 WT and mutants + pMiS4-eGFP without and in the presence of 80 mM terpinen-4-ol. Tolerance assays were conducted in a microbioreactor system over 48 h. Biomass formation was monitored every 10 - 15 minutes via (A) scattered light signal intensity (absorbance at 620 nm) and (B) GFP fluorescence signal intensity (excitation filter: 488 nm; emission filter: 520 nm).

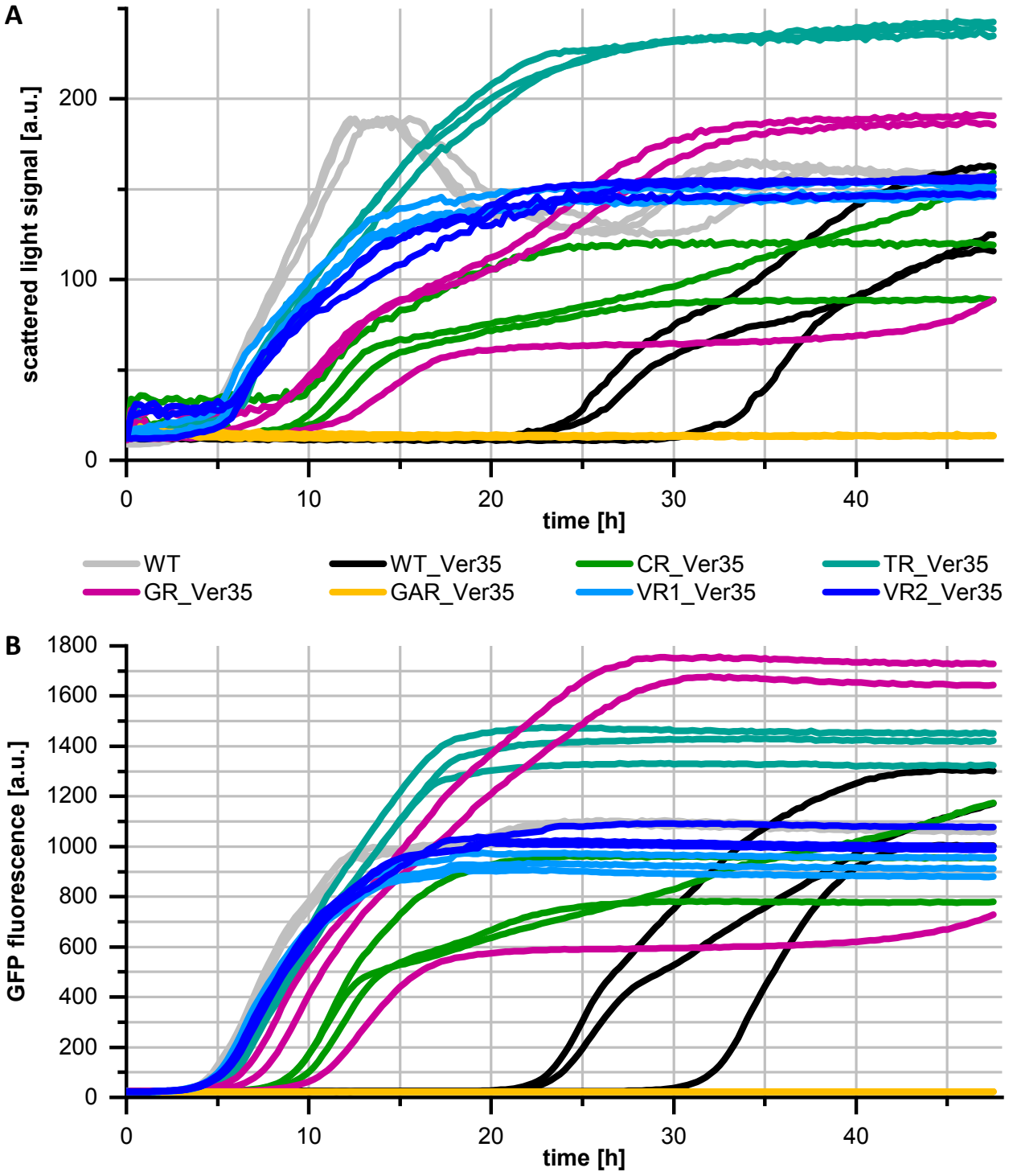

Figure S28. Growth of three different cultures of *P. putida* GS1 WT and mutants + pMiS4-eGFP without and in the presence of 35 mM verbenone. Tolerance assays were conducted in a microbioreactor system over 48 h. Biomass formation was monitored every 10 - 15 minutes via (A) scattered light signal intensity (absorbance at 620 nm) and (B) GFP fluorescence signal intensity (excitation filter: 488 nm; emission filter: 520 nm).

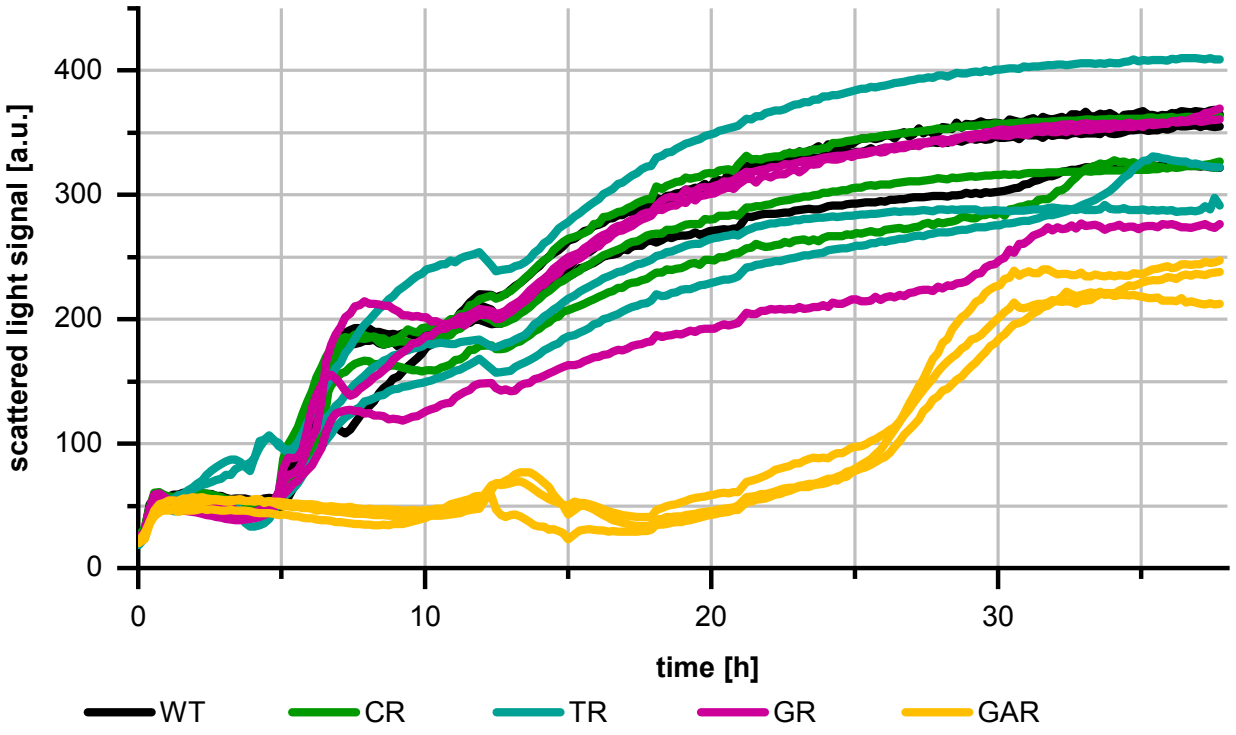

Figure S29. Growth of three different cultures of *P. putida* GS1 WT and mutants (CR, TR, GAR) in a geraniol to geranic acid biotransformation. The experiment was conducted in a microbioreactor system over 38 h. To determine geranic acid concentration samples were taken at time points t = 0, 12, 21 and 38 h and analyzed via HPLC-MS. Biomass formation was monitored every 10 - 15 minutes via scattered light signal intensity (absorbance at 620 nm).

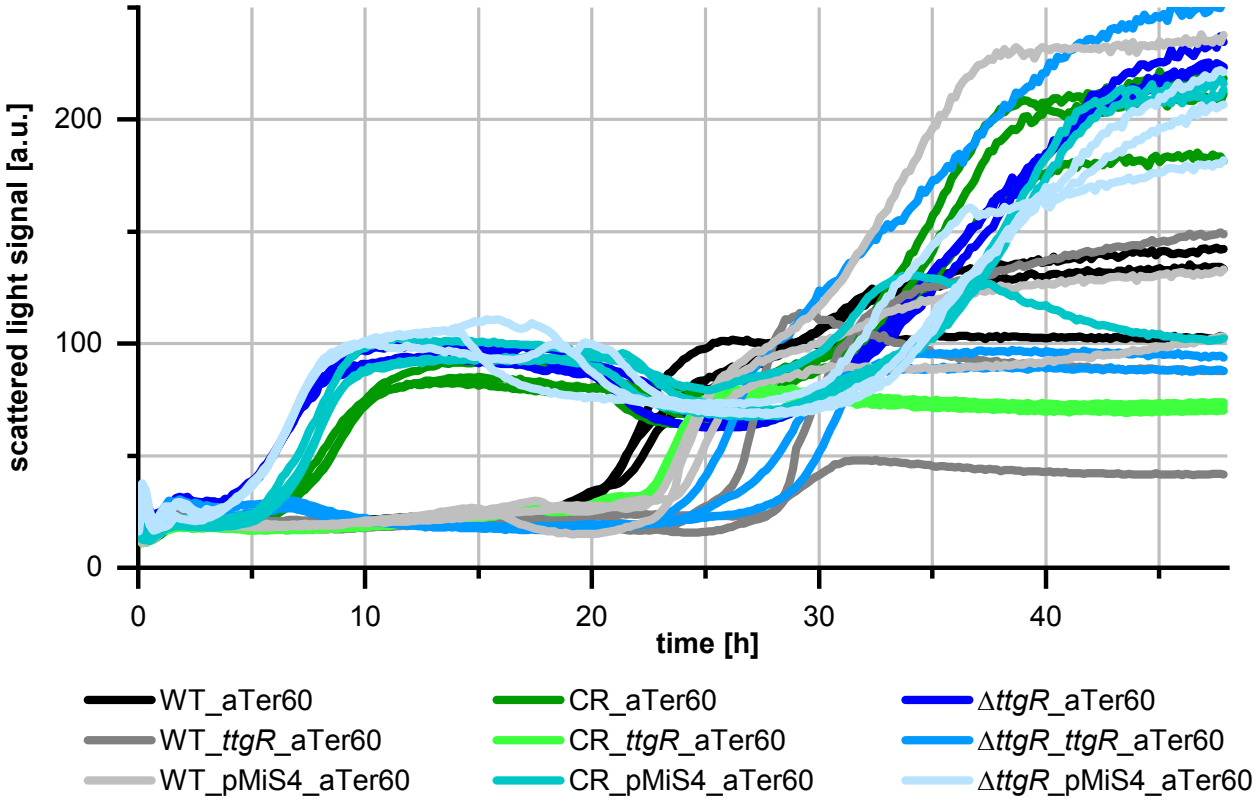

Figure S30. Verification of *ttgR* involvement in α-terpineol-hypertolerance phenotype by deletion and complementation. Growth curves of three individual cultures with 60 mM α-terpineol are shown. pMiS4 = strains contain the pMiS4 empty plasmid, *_ttgR_* = strains contain the pMiS4-*ttgR* vector. Tolerance assays were conducted in a microbioreactor system over 48 h. Biomass formation was monitored every 10 - 15 minutes via (A) scattered light signal intensity (absorbance at 620 nm) and (B) GFP fluorescence signal intensity (excitation filter: 488 nm; emission filter: 520 nm).

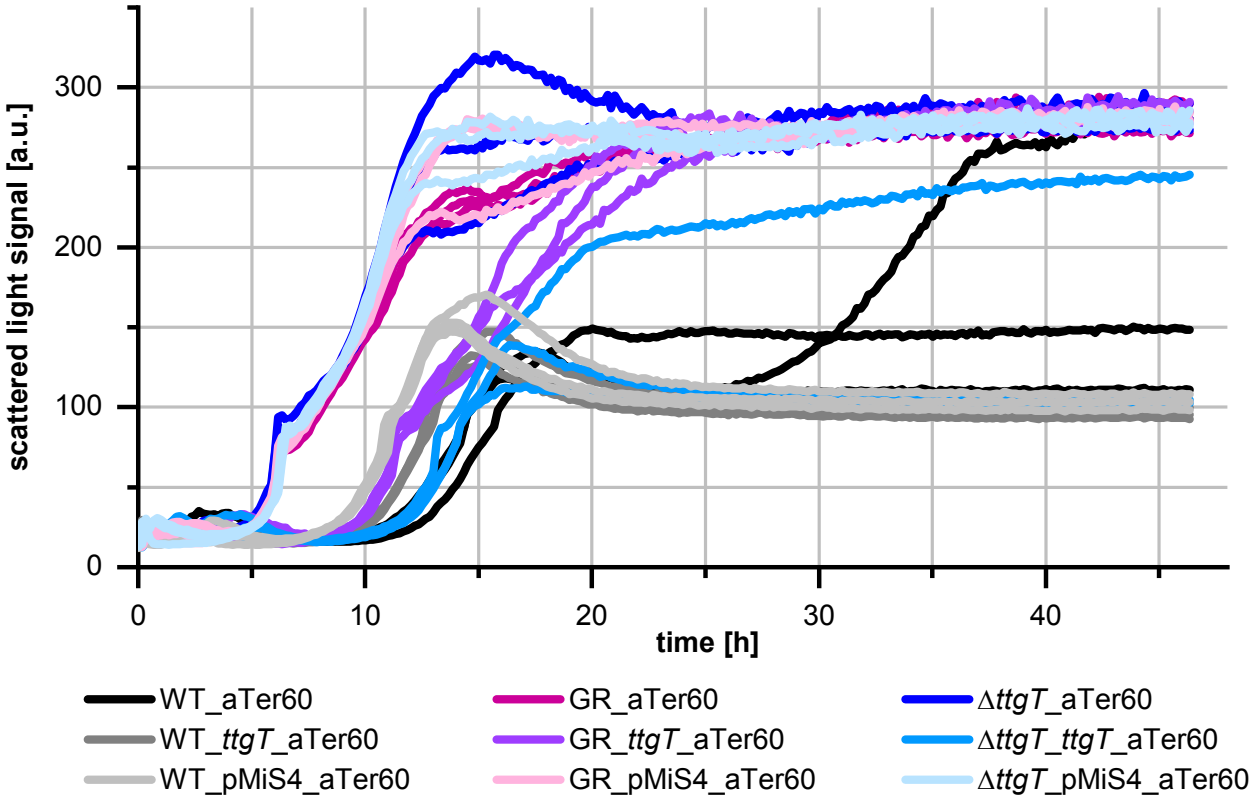

Figure S31. Verification of *ttgT* involvement in α-terpineol-hypertolerance phenotype by deletion and complementation. Growth curves of three individual cultures with 60 mM α-terpineol are shown. pMiS4 = strains contain the pMiS4 empty plasmid, *_ttgT_* = strains contain the pMiS4-*ttgT* vector. Tolerance assays were conducted in a microbioreactor system over 48 h. Biomass formation was monitored every 10 - 15 minutes via (A) scattered light signal intensity (absorbance at 620 nm) and (B) GFP fluorescence signal intensity (excitation filter: 488 nm; emission filter: 520 nm).

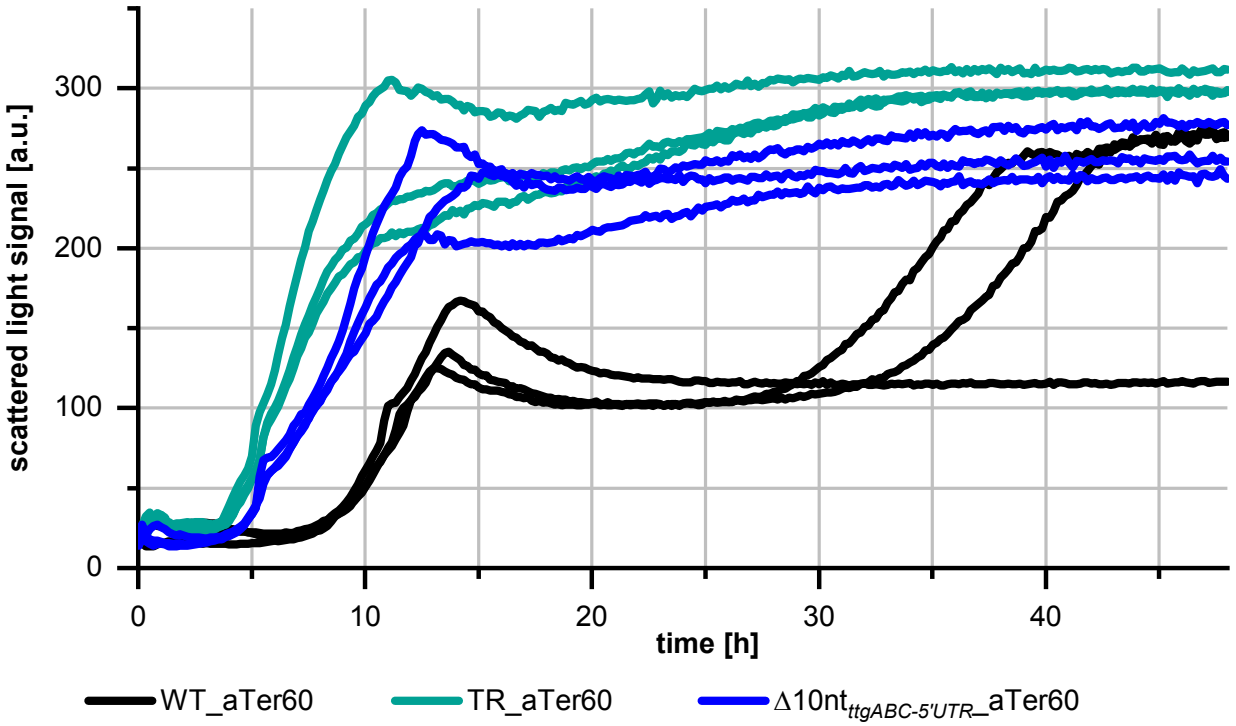

Figure S32. Verification of Δ10nt$_{ttgABC\text{-}5'UTR}$ involvement in α-terpineol-hypertolerance phenotype by deletion. Growth curves of three individual cultures with 60 mM α-terpineol are shown. Tolerance assays were conducted in a microbioreactor system over 48 h. Biomass formation was monitored every 10 - 15 minutes via (A) scattered light signal intensity (absorbance at 620 nm) and (B) GFP fluorescence signal intensity (excitation filter: 488 nm; emission filter: 520 nm).

References – Supplementary material

Franden MA, Jayakody LN, Li WJ, Wagner NJ, Cleveland NS, Michener WE, Hauer B, Blank LM, Wierckx N, Klebensberger J, Beckham GT (2018) Engineering *Pseudomonas putida* KT2440 for efficient ethylene glycol utilization. Metab Eng 48:197–207. https://doi.org/10.1016/j.ymben.2018.06.003

Grant SG, Jessee J, Bloom FR, Hanahan D (1990) Differential plasmid rescue from transgenic mouse DNAs into *Escherichia coli* methylation-restriction mutants. Proc Natl Acad Sci 87:4645–4649 . https://doi.org/10.1073/pnas.87.12.4645

Hanahan D (1985) Techniques for transformation of *E. coli*. In: Glover DM (ed) DNA cloning: a practical approach, 3. IRL Press, Oxford, United Kingdom, United Kingdom, pp 109–135

Klebensberger J, Lautenschlager K, Bressler D, Wingender J, Philipp B (2007) Detergent-induced cell aggregation in subpopulations of *Pseudomonas aeruginosa* as a preadaptive survival strategy. Environ Microbiol 9:2247–2259. https://doi.org/10.1111/j.1462-2920.2007.01339.x

Martínez-García E, de Lorenzo V (2011) Engineering multiple genomic deletions in Gram-negative bacteria: analysis of the multi-resistant antibiotic profile of *Pseudomonas putida* KT2440. Environ Microbiol 13:2702–2716. https://doi.org/10.1111/j.1462-2920.2011.02538.x

Mi J, Sydow A, Schempp F, Becher D, Schewe H, Schrader J, Buchhaupt M (2016) Investigation of plasmid-induced growth defect in *Pseudomonas putida*. J Biotechnol 231:167–173. https://doi.org/10.1016/j.jbiotec.2016.06.001

Simon R, Priefer U, Pühler A (1983) A broad host range mobilization system for in vivo genetic engineering: Transposon mutagenesis in Gram-negative bacteria. Bio/Technology 1:784–791. https://doi.org/10.1038/nbt1183-784

Speelmans G, Bijlsma A, Eggink G (1998) Limonene bioconversion to high concentrations of a single and stable product, perillic acid, by a solvent-resistant *Pseudomonas putida* strain. Appl Microbiol Biotechnol 50:538–544. https://doi.org/10.1007/s002530051331

Chapter 5 - Tolerance of *Pseudomonas putida* GS1 towards limonene and isopiperitenol and transfer of tolerance improvement to *P. putida* KT2440

Florence M. Schempp

Status: unpublished

Introduction:

As demonstrated in Chapter 4, the solvent-tolerant *P. putida* strain GS1 also exhibits high levels of tolerance towards various monoterpenes and monoterpenoids. This natural tolerance could be further improved by certain mutations that cause increased efflux activity.

In the following, it should be examined whether these mutations also contribute to an increased tolerance of the strain towards the reactant and intermediate product of the intended model process, (+)-limonene and (+)-*trans*-isopiperitenol.

Since most *P. putida* strains are classified in risk group 2 (R2) in Germany, they are not ideal microbes for industrial production processes. The only exception is *P. putida* KT2440, classified as biosafety level 1 organism,[132,135] which makes it a suitable choice as a host organism for the development of a cell factory. As a result, in recent years attempts have been made to streamline the genome of this bacterium in order to aid process optimization. These efforts have resulted, amongst others, in KT2440 derivatives called EM42 and EM383 which are missing around 300 genes (4.3 % of the entire genome), including the whole flagellar system. This is supposed to enhance desirable traits and eliminate problems such as ATP/NAD(P)H availability or genetic instability.[199]

While classified as an R1 organism, the drawback of *P. putida* KT2440 is that this strain is, in general, less solvent-tolerant than other *P. putida* subspecies.[200] Therefore, in the following it was to be investigated whether *P. putida* KT2440 and its derivative EM42 are also less tolerant towards monoterpenes and monoterpenoids than, for instance, the solvent-tolerant *P. putida* GS1. If this were the case, attempts would then be made to transfer favorable mutations for monoterpenoid tolerance from the studies with *P. putida* GS1 to these strains, in order to improve monoterpenoid tolerance of the intended cell factory host organism.

In addition, it should be investigated whether the different *P. putida* strains are able to metabolize *trans*-isopiperitenol, in order to eliminate possible side reactions of the later model process. While it is described in literature that *P. putida* GS1 can natively transform limonene

into perillic acid,[133] for *P. putida* KT2440 neither conversion, nor biodegradation, of limonene could be observed in previous experiments (K. Tusch, unpublished data[201]).

Materials and Methods:

Pseudomonas putida KT2440 was obtained from DSMZ (Deutsche Sammlung von Mikroorganismen und Zellkulturen, DSM No.: 6125), and the KT2440-derviative EM42 from Martínez-García and colleagues.[199] For further information to *P. putida* GS1 wild type (WT) and mutants see Chapter 4. Cultivation of microbes, transformation, toxicity assays and genome deletions in *P. putida* were conducted according to Chapter 4. In this way the mutant strains KT2440_Δ*ttgR*, KT2440_Δ10nt$_{ttgABC}$, EM42_Δ*ttgR* and EM42_Δ10nt$_{ttgABC}$ were constructed.

For toxicity assays 200 mM (+)-limonene (purity ≥ 99 %) or 6.25 – 200 mM (+)-isopiperitenol (2:1-mixture of *trans* and *cis)* were used. Both chemicals were received from the company SYMRISE.

For the (+)-limonene biotransformation experiments with *P. putida* GS1 wild type and mutants (see Chapter 4), strains were transformed with the empty pMiS1 plasmid[137] or with the pMiS1 plasmid containing a variant of the bacterial CYP enzyme P450cam (*camC,* P450cam_Y96F_V247L_C334A),[101,202] together with putidaredoxin reductase (PdR, *camA)* and putidaredoxin (Pd, *camB*) which are required for CYP functionality (CYP class I system) (H. Schewe, unpublished data). From each strain, two individual transformants were tested. Overnight cultures in TB medium were diluted 1:100 with 10 mL TB medium supplemented with kanamycin (75 µg mL^{-1}) in 100 ml shake flasks and cultivated at 30 °C and 180 rpm (orbit: 2.5 cm) until an OD_{600} of around 0.7 had been reached. Gene expression was then induced by the addition of 0.2 % (w/v) L-rhamnose. The cultures were incubated for a further 21 h at 30 °C and 180 rpm (orbit: 2.5 cm). Afterwards, cells were harvested by centrifugation (3,220 x g, 10 min) and resuspended in 2 mL TB medium, supplemented with kanamycin (75 µg mL^{-1}) and L-rhamnose (0.2 % w/v). OD_{600} values of each culture were measured and concentrated cell suspensions were transferred back into the shake flasks. To each concentrated culture, 40 µL (+)-limonene were added (final concentration ca. 125 mM) and the cell suspensions were incubated for 24 h at 30 °C and 180 rpm (orbit: 2.5 cm). As a negative control, TB medium without cells was used. Samples of 150 µl were then taken and extracted with the same volume of MTBE (methyl *tert*-butyl ether) containing 100 µM 3-carene as an internal standard. After phase separation by centrifugation for 15 min at 16,000 x g, the organic layers were analyzed

via GC-MS. For this purpose, a GCMS-QP2010 SE (Shimadzu) system containing a DB-5 column (30 m x 0.25 mm x 0.25 µm, Agilent Technologies, Inc.) was used. Measurements were conducted as follows: helium as the carrier gas, split ratio of 10, injections at 270 °C, column flow of 0.7 mL min^{-1} and a linear velocity of 30 cm s^{-1}. The column temperature was programmed as follows: 60 °C, with 9 °C per min up to 175 °C followed by 30 °C per min up to 300 °C.

To detect putative metabolization products of *trans*-isopiperitenol with the different *P. putida* strains, overnight cultures grown in TB medium were used to inoculate fresh TB medium to an OD_{600} of 0.1. The bacteria cultures were divided into 1.5 mL aliquots in 48-well Flowerplates® (m2p-labs GmbH, Baesweiler, Germany) and isopiperitenol (2:1-mixture of *trans* and *cis)* was added directly after inoculation to yield a final concentration of 12.5 mM. As a negative control, TB medium without cells was used. The Flowerplates® were incubated for 40 h at 30 °C in a microbioreactor system (BioLector®, m2p-labs GmbH, Baesweiler, Germany) at 1000 rpm covered by a gas-permeable sealing foil with evaporation reduction layer. All strains were tested in triplicate, distributed randomly on the plate. Samples of 180 µL were taken at time points t = 0, 15, 20, 40 h. To the samples, 20 µL of 1 M H_2SO_4 were added and analytes were extracted using 200 µL ethyl acetate containing 1 mM decane as an internal standard. Samples were centrifuged (2 min, 16,000 x g) and the organic phase was analyzed by a GC-17A QP5050A system (Shimadzu) with a VB-5 column (30 m x 0.25 mm x 0.25 µm, ValcoBond®, Valco Instruments Co. Inc. and VICI AG). Measurements were conducted as follows: helium as the carrier gas, split ratio of 100, injection at 250 °C with a sample volume of 3 µL, a column flow of 1.2 mL min^{-1} and a linear velocity of 39.9 cm s^{-1}. The column temperature was programmed as follows: 60 °C for 3 min, then with 5 °C per min up to 150 °C followed by 3 min at 150 °C.

In all GC-MS analyses, *trans*- and *cis*-isopiperitenol were identified by the comparison of retention times and mass spectra with those of chemically synthesized reference substances. Isopiperitenone was identified by comparison of the mass spectrum to those of the NIST mass spectral library (v14). Identity was assumed if the similarity index was equal to, or higher than, 90 %. Absolute concentrations of *trans*- and *cis*-isopiperitenol were calculated from chromatogram peak areas by comparison to calibration curves prepared by measuring a dilution series of isopiperitenol reference substance with known concentrations.

Results and discussion:

The effects of (+)-limonene and isopiperitenol on the growth of *P. putida* GS1, KT2440 and EM42 were investigated by comparing characteristics of the growth curves from microbioreactor cultivations under the influence of exogenously added substances. Biomass formation was monitored via scattered light signal and GFP fluorescence measurements. The GFP signal was used as a control to ensure that the addition of the chemicals did not interfere with the scattered light measurement. Previous experiments had confirmed that GFP gene expression does not influence the growth of *P. putida* (see Chapter 4).

Analysis of the resulting data showed that isopiperitenol has a concentration dependent effect on the growth of *P. putida* GS1 wild type (Figure 11). While concentrations between 6.25 and 25 mM isopiperitenol caused a prolongation of the lag phase to a different extent, the GS1 WT strain was not able to grow in the presence of 50 mM isopiperitenol and higher. In comparison to the tested monoterpenoids in Chapter 4, growth inhibition was found to be even more pronounced with isopiperitenol than with verbenone, α-terpineol and terpinen-4-ol.

Tolerance assays with the *P. putida* GS1 mutants (for a detailed description of the mutant strains see Chapter 4) revealed improved tolerance of the mutants CR, TR, GR, VR1 and VR2 when compared to the wild-type strain under cultivation with 25 mM isopiperitenol (Figure 12).

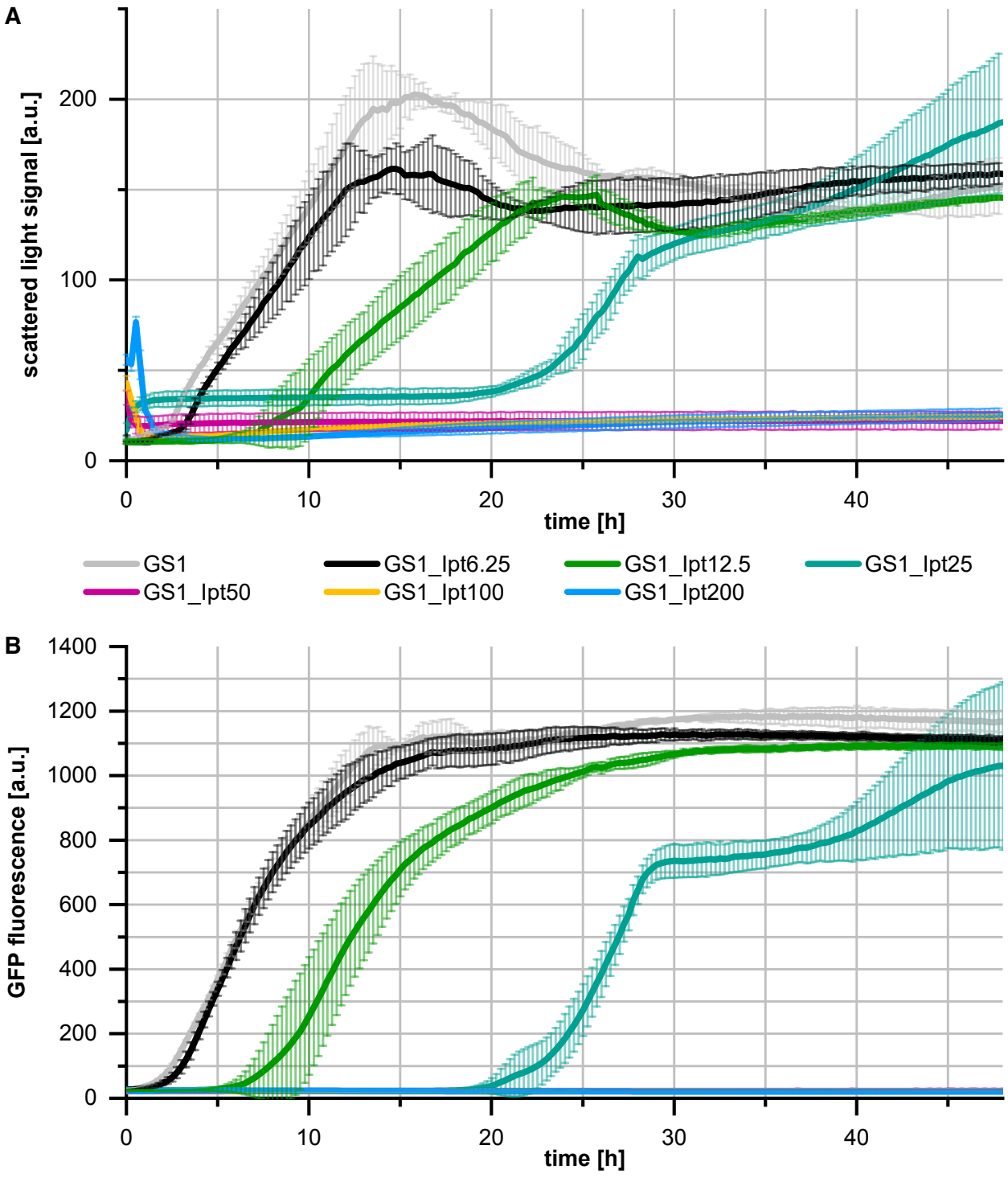

Figure 11: Growth of *P. putida* GS1 WT + pMiS4-eGFP in the presence of different isopiperitenol concentrations (Ipt, 0 - 200 mM). Tolerance assays were conducted in a microbioreactor system over 48 h. Biomass formation was monitored every 10 - 15 minutes via (A) scattered light signal intensity (absorbance at 620 nm) and (B) GFP fluorescence signal intensity (excitation filter: 488 nm; emission filter: 520 nm). The data points and error bars represent the mean values and standard deviations of three biological replicates (n = 3).

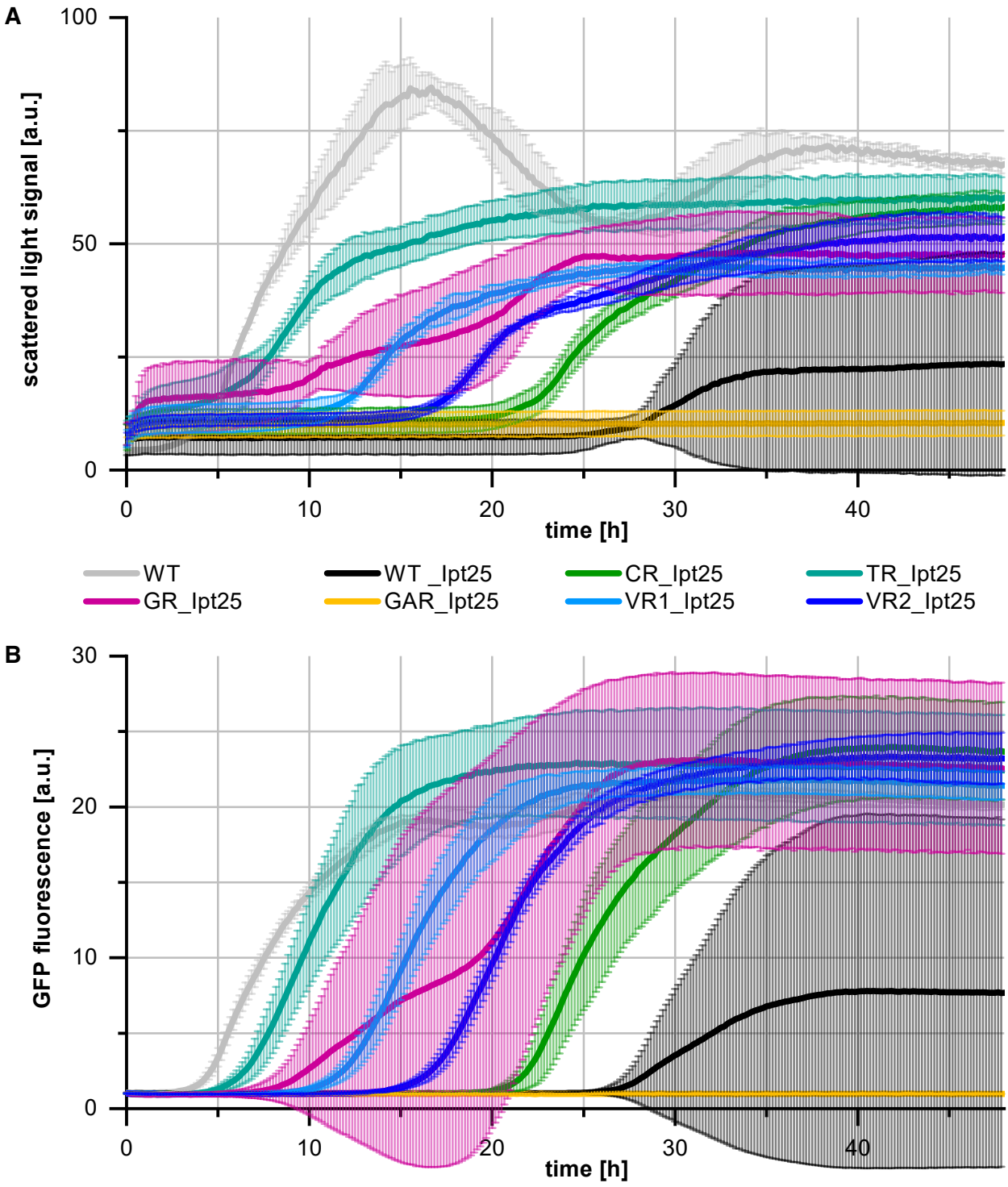

Figure 12: Growth of *P. putida* GS1 WT and mutants + pMiS4-eGFP without and in the presence of 25 mM isopiperitenol (Ipt). For a detailed description of the mutant strains see Chapter 4. Tolerance assays were conducted in a microbioreactor system over 48 h. Biomass formation was monitored every 10 – 15 minutes via (A) scattered light signal intensity (absorbance at 620 nm) and (B) GFP fluorescence signal intensity (excitation filter: 488 nm; emission filter: 520 nm). The data points and error bars represent the mean values and standard deviations of three biological replicates (n = 3).

Since it had been observed in previous experiments (see Chapter 4) that altered efflux activity affects significantly geraniol to geranic acid biotransformation, this potential effect should also be investigated for a (+)-limonene into (+)-*trans*-isopiperitenol conversion. For this purpose, a pMiS1 vector was used encoding a variant of the bacterial CYP enzyme P450cam (P450cam_Y96F_V247L_C334A)[101,202] together with two enzymes required for its functionality (putidaredoxin (Pd) and putidaredoxin reductase (PdR)) (H. Schewe, unpublished data). It has been described that this enzyme variant can convert externally added limonene into *trans*-isopiperitenol and other side products.[101,102] The enzymes were expressed in *P. putida* GS1 wild type and mutants and a (+)-limonene biotransformation experiment was conducted. In comparison to the geraniol-geranic acid bioconversion experiment in Chapter 4, in this case biotransformation was performed with resting cells (stationary growth phase) and an endpoint determination of *trans*-isopiperitenol concentration was conducted. While the amounts of *trans*-isopiperitenol achieved were still moderate, no significant difference between the WT and the mutants CR, TR and GR could be observed after 24 h (Figure 13). However, with the GAR mutant, which has a reduced efflux activity and showed the highest sensitivity towards isopiperitenol in the toxicity assays, *trans*-isopiperitenol production was clearly reduced. These results indicate that the overexpression of the Ttg efflux pumps, as present in the mutants TR, CR and GR, can be employed for the development of a whole-cell biocatalyst for limonene-to-isopiperitenol biotransformation without reducing production, at least when using resting cells. It should be noted, however, that when conducting a growth-coupled process, such as geranic acid production (see Chapter 4), an increased efflux activity could have a different effect. In addition, while for the (+)-limonene conversion experiment no difference between the wild type and the efflux pump overexpression strains, TR, CR and GR, could be detected, as soon as *trans*-isopiperitenol titers reach a toxic level for *P. putida,* e.g. by process optimization, the mutant strains could have an advantage and show their full potential. Why in this experiment the GAR mutant produced less *trans*-isopiperitenol than the other tested strains can only be speculated. Due to the reduced efflux activity, the mutant's tolerance towards limonene might be impaired, causing a damage of the GAR cells by the used limonene amount of around 125 mM. In comparison, in toxicity assays with the GS1 wild type 200 mM (+)-limonene did not affect growth (see Figure 16). Although biotransformation processes with resting cells do not require cell growth, a certain level of cell metabolism is still necessary to provide, for example, the NADPH cofactors essential for the CYP reaction. Apart from this, on the basis of the conducted experiments it cannot be excluded that the GAR mutant strain would show a better conversion if, for instance, the reactant (+)-limonene would be added in lower concentrations, or if the process time would be increased, as observed for geranic acid production (see Chapter 4).

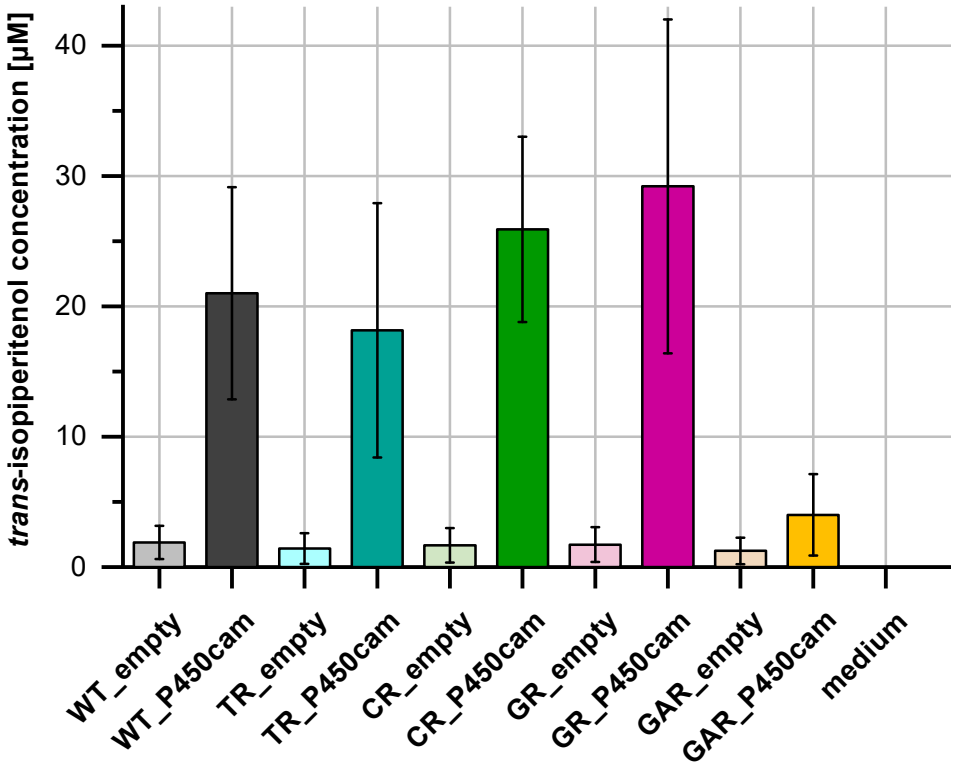

Figure 13: *trans*-Isopiperitenol concentrations achieved in (+)-limonene biotransformation experiment with *P. putida* GS1 WT and mutants after 24 h. WT: *P. putida* GS1 wild type; TR, CR, GR, GAR: *P. putida* GS1 mutant strains (see Chapter 4); medium: TB medium without cells. empty: pMiS1 expression vector without gene in MCS; P450cam: pMiS1 harboring genes of P450cam variant (P450cam_Y96F_V247L_C334A, *camC*), putidaredoxin reductase (PdR, *camA*) and putidaredoxin (Pd, *camB*) (CYP class I system). *trans*-Isopiperitenol peak areas achieved from GC-MS analysis were normalized to the peak area of the internal standard (3-carene) and the number of cells at the beginning of the biotransformation experiment corresponding to 1 OD_{600} unit. Resulting peak areas were compared to a calibration curve of *trans*-isopiperitenol to determine absolute concentrations. The data points and error bars represent the mean values and standard deviations of two biological replicates (n = 2).

When isopiperitenol tolerance was tested for the potential production hosts, *P. putida* KT2440 and its EM42 derivative, it was observed that KT2440 has a similar tolerance as GS1 WT, while EM42 is more sensitive (Figure 14).

Because (+)-*trans*-isopiperitenol is the intermediate product of the intended model process, it was then investigated if the different *P. putida* strains, GS1 WT and mutant TR, KT2440 WT and EM42 WT, are able to metabolize *trans*-isopiperitenol. GC-MS analysis revealed that the *trans*-isopiperitenol concentration decreased in the bacteria cultures over time with the same rate as in the medium control without cells (Figure 15 A). This was probably due to evaporation; no degradation or bioconversion of *trans*-isopiperitenol appeared to take place, neither with the different *P. putida* wild-type strains, nor with the efflux pump overexpression mutant TR.

As the isopiperitenol used in the assay was not pure *trans*-isomer, but a 2:1-mixture of *trans* and *cis*, *cis*-isopiperitenol could also be detected in the samples. Up until 20 h, the *cis*-isopiperitenol concentration also decreased in the bacteria cultures with the same rate as in the medium control; between 20 and 40 h the *cis*-concentration fell below the detection limit in the cultures with cells, but not in the medium control (Figure 15 B). Instead, a new peak appeared in the samples with bacteria cells which could be identified as isopiperitenone. Since the isopiperitenone peak reached similar amounts as the remaining *cis*-isopiperitenol in the medium control, it is assumed that the different *P. putida* strains oxidize *cis*-isopiperitenol to the corresponding ketone. However, since the intended intermediate product of the model process is (+)-*trans*- and not *cis*-isopiperitenol, this observation is not relevant for the further development of a production strain in the context of this thesis project.

Toxicity assays with (+)-limonene showed that even concentrations of 200 mM appeared not to influence the growth of the different *P. putida* strains, GS1, KT2440 and EM42 (Figure 16).

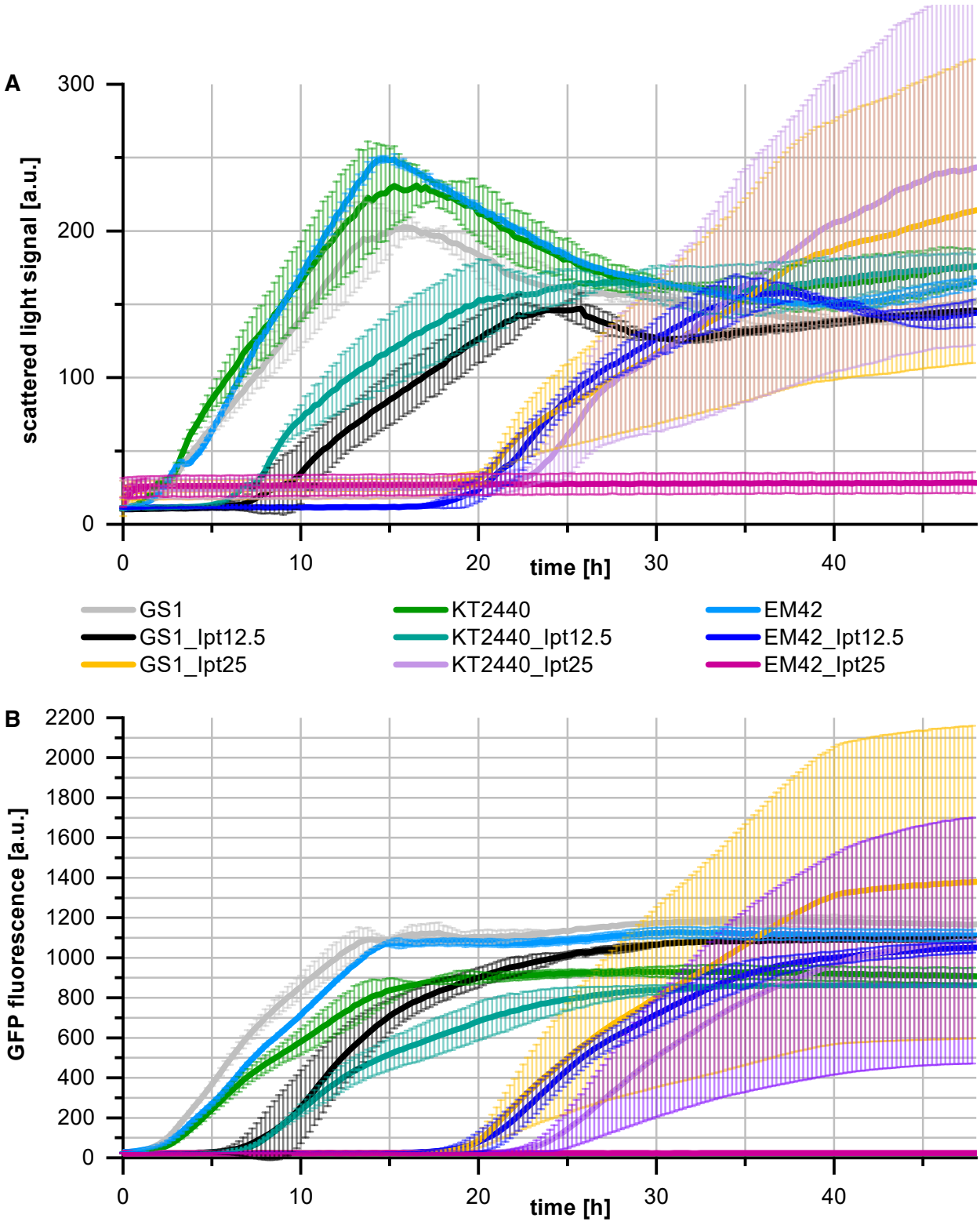

Figure 14: Growth of *P. putida* GS1 WT, KT2440 WT and EM42 WT + pMiS4-eGFP in the presence of different isopiperitenol concentrations (Ipt, 0 - 25 mM). Tolerance assays were conducted in a microbioreactor system over 48 h. Biomass formation was monitored every 10 - 15 minutes via (A) scattered light signal intensity (absorbance at 620 nm) and (B) GFP fluorescence signal intensity (excitation filter: 488 nm; emission filter: 520 nm). The data points and error bars represent the mean values and standard deviations of three biological replicates (n = 3).

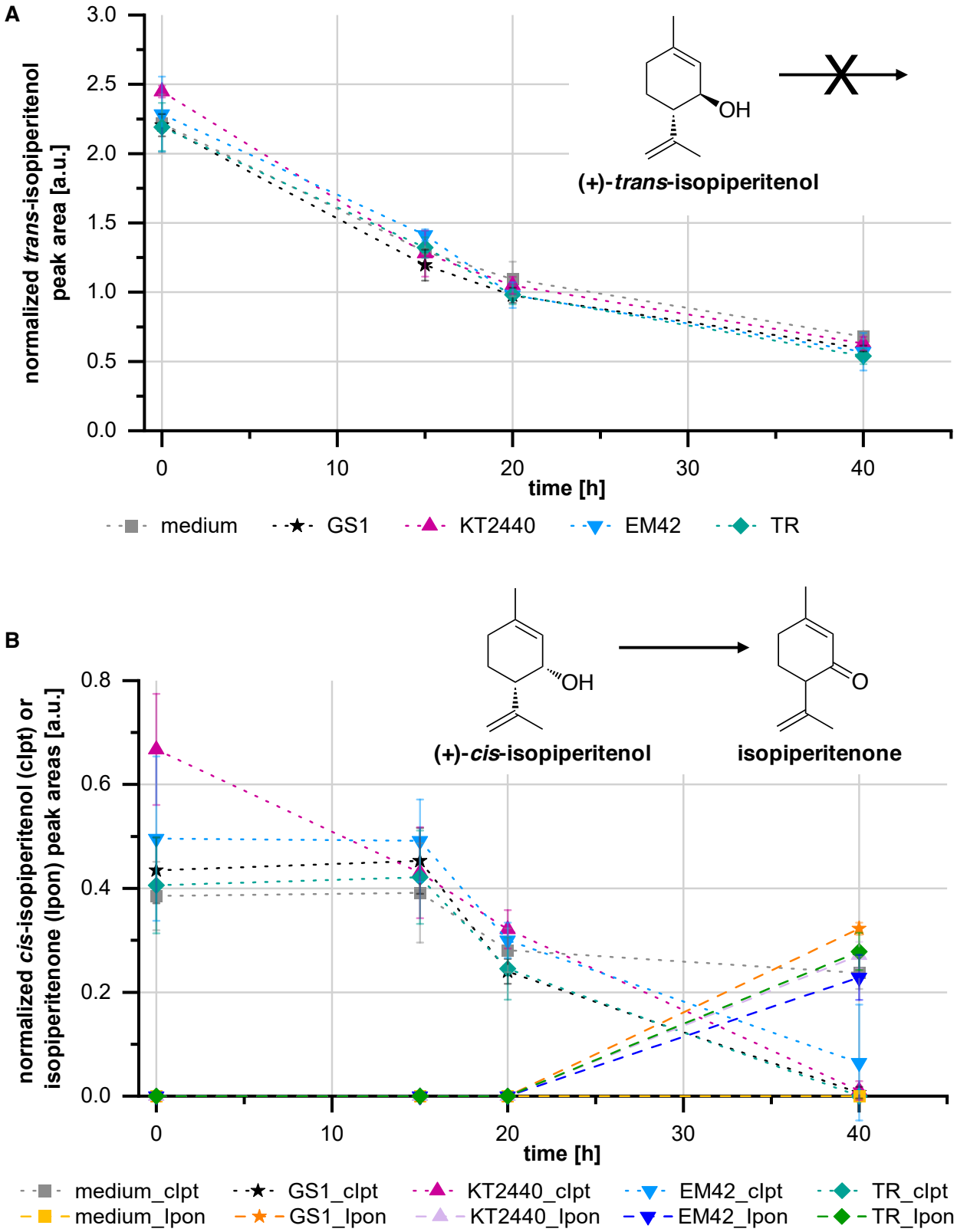

Figure 15: Determination of *trans*- and *cis*-isopiperitenol as well as isopiperitenone amounts in cultures of *P. putida* GS1 WT, GS1 mutant TR, KT2440 WT and EM42 WT or in cell-free medium (medium) over time. The cells and the cell-free medium were cultivated in a microbioreactor system over 40 h. At inoculation, 12.5 mM isopiperitenol (2:1-mixture of *trans* and *cis*) were added. To determine *trans*- and *cis*-isopiperitenol and isopiperitenone concentrations, samples were taken at time points t = 0, 15, 20 and 40 h and analyzed via GC-MS. Peak areas of (A) *trans*-isopiperitenol, as well as (B) *cis*-isopiperitenol (_clpt) and isopiperitenone (_Ipon) were normalized to the peak area of the internal standard (decane). The data points and error bars represent the mean values and standard deviations of three biological replicates (n = 3).

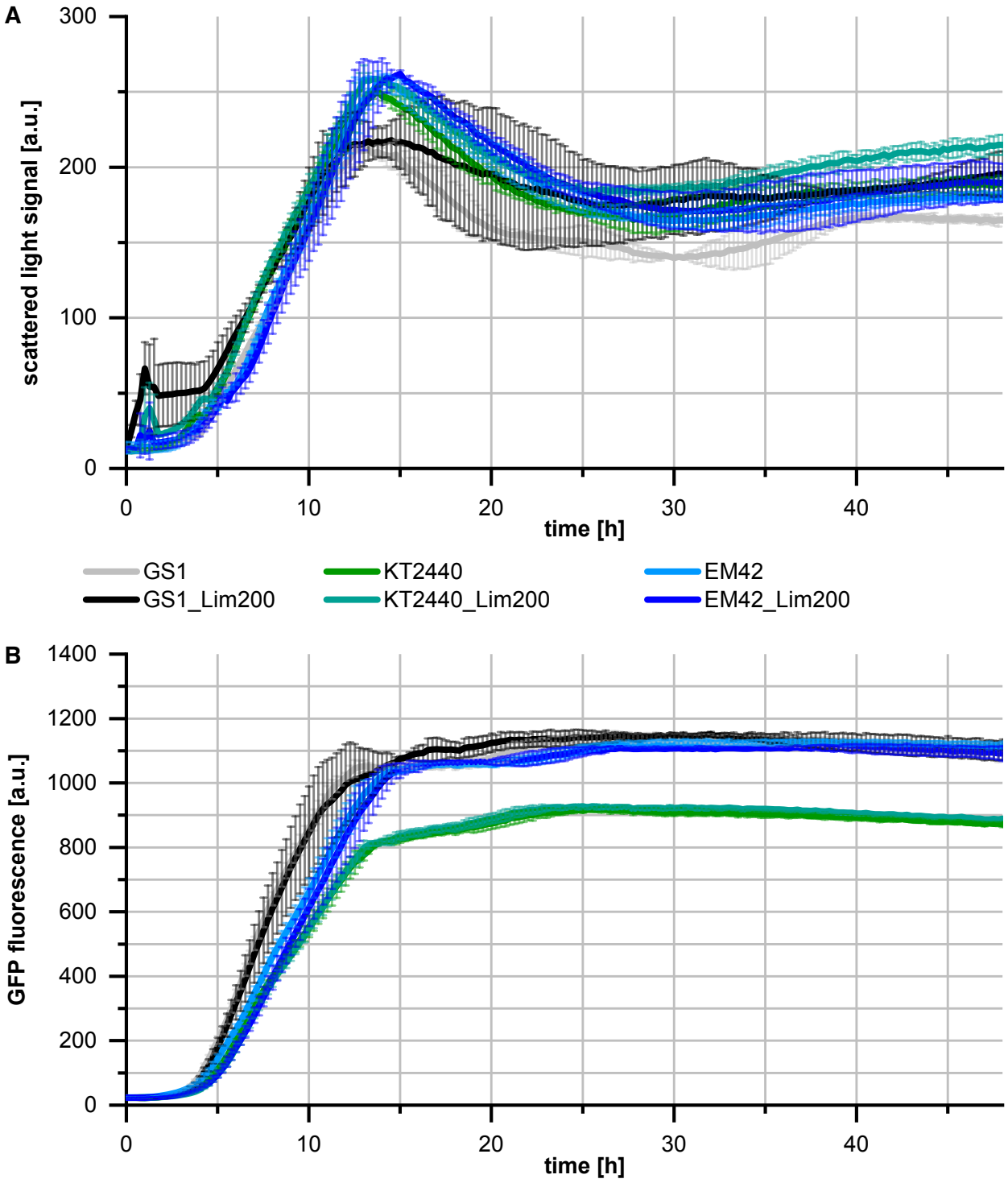

Figure 16: Growth of *P. putida* GS1 WT, KT2440 WT and EM42 WT + pMiS4-eGFP without and in the presence of 200 mM (+)-limonene (Lim). Tolerance assays were conducted in a microbioreactor system over 48 h. Biomass formation was monitored every 10 - 15 minutes via (A) scattered light signal intensity (absorbance at 620 nm) and (B) GFP fluorescence signal intensity (excitation filter: 488 nm; emission filter: 520 nm). The data points and error bars represent the mean values and standard deviations of three biological replicates (n = 3).

Taking into consideration the results of former experiments (K. Tusch, unpublished data[201]) and those described in this thesis, neither (+)-limonene nor (+)-*trans*-isopiperitenol appear to be metabolized by *P. putida* KT2440, the intended production organism of this dissertation project. Thus, the elimination of native metabolic reactions decreasing the reactant or product concentration was not necessary for the development of the cell factory basis.

However, while (+)-limonene was not toxic to any of the tested strains in concentrations up to 200 mM (highest concentration tested), isopiperitenol impaired the growth of the *P. putida* WT strains. Nevertheless, some of the tested *P. putida* GS1 mutants seemed to be more tolerant towards this compound.

Therefore, the beneficial mutations of the two mutants, TR and CR, were transferred to the different *P. putida* wild types, GS1, KT2440 and EM42; toxicity assays with 12.5 and 25 mM isopiperitenol were then conducted. The experiments revealed that with the deletion of the *ttgR* gene, which encodes the repressor of the TtgABC efflux system, a reduction of the lag phase time could be achieved for all strains (Figure 17). This effect was even more pronounced when the mutation of the TR mutant was reconstructed in the different *P. putida* strains. The results showed, however, that the EM42 mutants, similar to the EM42 WT, were significantly less tolerant towards isopiperitenol than the corresponding other strains (Figure 17).

The increased isopiperitenol tolerance qualifies the mutant *P. putida* KT2440_Δ10nt$_{ttgABC}$ as suitable basis for the further development of a cell factory for *trans*-isopiperitenol production.

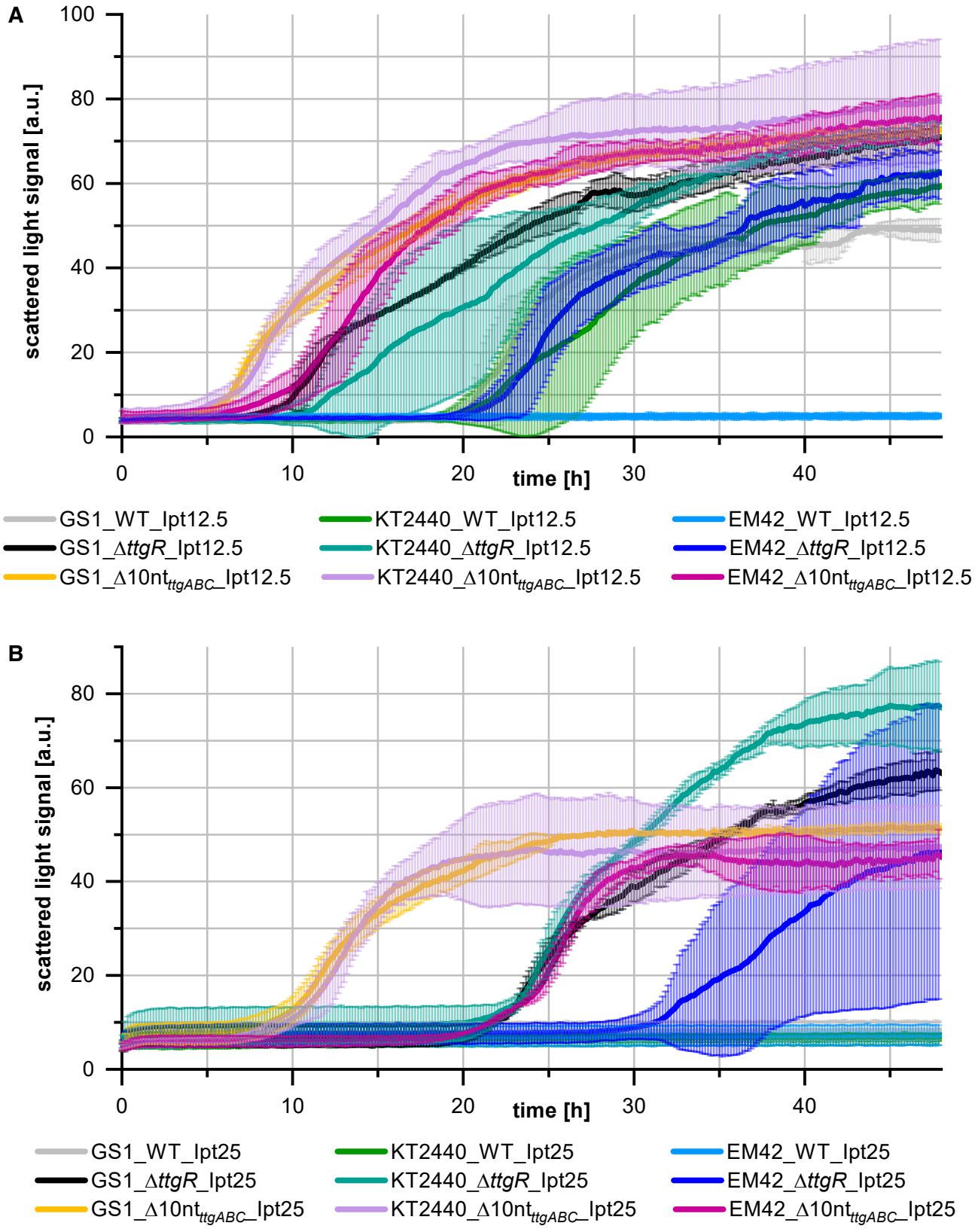

Figure 17: Growth of different *P. putida* strains in the presence of (A) 12.5 or (B) 25 mM isopiperitenol (lpt). Δ*ttgR*: genome deletion of *ttgR* gene. $\Delta 10nt_{ttgABC}$: deletion of 10 nucleotides in the 5'-UTR of *ttgABC* mRNA (directly after P_{ttgABC} +1) and of the -35 region of P_{ttgR}, similar to the mutation in the *P. putida* GS1 mutant TR (for more details on the location of mutation see Chapter 4). Tolerance assays were conducted in a microbioreactor system over 48 h. Biomass formation was monitored every 10 - 15 minutes via scattered light signal intensity (absorbance at 620 nm). The data points and error bars represent the mean values and standard deviations of two or three biological replicates.

Chapter 6 – Investigation of plasmid-induced growth defect in *Pseudomonas putida*

Jia Mi, Anne Sydow, Florence Schempp, Daniela Becher, Hendrik Schewe, Jens Schrader, Markus Buchhaupt

Journal of Biotechnology, 2016, 231, 167-173
DOI: 10.1016/j.jbiotec.2016.06.001

Type: research article
Status: published

Summary:
Genetic engineering of bacteria often relies on the use of plasmids. To effectively express genes heterologously in bacterial hosts, plasmids must not interfere with cellular functions. However, despite their widespread use for physiological studies and for the design and optimization of industrial production strains, only limited information on plasmid-induced growth defects is available for various replicons and organisms.
In the following chapter, the identification and characterization of such a phenomenon for *Pseudomonas putida* transformants carrying the pBBR1-derived plasmid pMiS1 is presented. The plasmid-induced growth defect could be eliminated by the introduction of a mutation in the plasmid-coded *rep* gene (encoding the replication initiation protein), allowing construction of the non-toxic variant pMiS4.
With pMiS4 a pBBR1 replicon variant for gene expression in *P. putida* is provided, which does not affect bacterial growth.

Declaration of author contributions to the publication:

Investigation of plasmid-induced growth defect in *Pseudomonas putida*

Status: published
Name of journal: Journal of Biotechnology

Contributing authors: J. Mi, A. Sydow, **F. Schempp** (Doctoral candidate), D. Becher, H. Schewe, J. Schrader, M. Buchhaupt

What are the contributions of the doctoral candidate and his co-authors?

(1) Concept and design		
J. Mi	50 %	
M. Buchhaupt	50 %	

(2) Conducting tests and experiments		
J. Mi	65 %	growth experiments, cloning experiments, plasmid copy number determinations, expression experiments with *gfp*
A. Sydow	20 %	*Evolutionary Engineering* experiments
F. Schempp	**10 %**	**growth experiments, cloning experiments**
D. Becher	5 %	cloning experiments

(3) Compilation of data sets and figures		
J. Mi	85 %	data collection and preparation of figures of growth experiments, plasmid copy number determinations and expression experiments with *gfp*
A. Sydow	5 %	data collection and creation of summary table of the *Evolutionary Engineering* experiment
F. Schempp	**10 %**	**data collection and preparation of figures of the growth experiments, plasmid maps**

(4) Analysis and interpretation of data		
J. Mi	50 %	analysis and interpretation of data, statistical analysis
A. Sydow	10 %	analysis of data
F. Schempp	**10 %**	**analysis of data**
H. Schewe	10 %	analysis of data
M. Buchhaupt	20 %	analysis and interpretation of data

(5) Drafting of manuscript	
J. Mi	50 %
A. Sydow	5 %
F. Schempp	**5 %**
J. Schrader	10 %
M. Buchhaupt	30 %

Journal of Biotechnology 231 (2016) 167–173

Contents lists available at ScienceDirect

Journal of Biotechnology

journal homepage: www.elsevier.com/locate/jbiotec

Investigation of plasmid-induced growth defect in *Pseudomonas putida*

Jia Mi, Anne Sydow, Florence Schempp, Daniela Becher, Hendrik Schewe, Jens Schrader, Markus Buchhaupt*

DECHEMA Research Institute, Frankfurt am Main, Germany

ARTICLE INFO

Article history:
Received 15 September 2015
Received in revised form 3 February 2016
Accepted 6 June 2016
Available online 7 June 2016

Keywords:
Plasmid induced growth defect
Metabolic burden
Pseudomonas putida
Plasmid copy number
pBBR1 replicon
Rep
Kan^R

ABSTRACT

Genetic engineering in bacteria mainly relies on the use of plasmids. But despite their pervasive use for physiological studies as well as for the design and optimization of industrially used production strains, only limited information about plasmid induced growth defects is available for different replicons and organisms. Here, we present the identification and characterization of such a phenomenon for *Pseudomonas putida* transformants carrying the pBBR1-derived plasmid pMiS1. We identified the kanamycin resistance gene and the transcription factor encoding *rhaR* gene to be causal for the growth defect in *P. putida*. In contrast, this effect was not observed in *Escherichia coli*. The plasmid-induced growth defect was eliminated after introduction of a mutation in the plasmid-encoded *rep* gene, thus enabling construction of the non-toxic variant pMiS4. GFP reporters construct analyses and qPCR experiments revealed a distinctly lowered plasmid copy number for pMiS4, which is probably the reason for alleviation of the growth defect by this mutation. Our work expands the knowledge about plasmid-induced growth defects and provides a useful low-copy pBBR1 replicon variant.

1. Introduction

In recent years, there has been an increasing interest in engineering *Pseudomonas putida* for the production of various chemicals and natural products, either by de novo synthesis or by bioconversion of precursor molecules (Poblete-Castro et al., 2012; Loeschcke and Thies, 2015; Mi et al., 2014; Cornelissen et al., 2013). Among the reasons are the fast growth of *P. putida*, its ease of genetic manipulation, its simple nutrient requirements and especially its pronounced ability to cope with toxic and hydrophobic substances. This solvent tolerance makes *P. putida*, for instance, an interesting microbe for the bioconversion of otherwise toxic monoterpenes such as limonene (Mirata et al., 2009). Numerous genetic tools have been invented and optimized in order to enable physiological studies and metabolic engineering in *P. putida* (Martínez-García and de Lorenzo, 2011; Martínez-García et al., 2014; Graf and Altenbuchner, 2011; Hoffmann and Altenbuchner, 2015).

Plasmid maintenance in microbes has often been described to burden the cells, most obviously resulting in a reduction of growth rate (Bailey et al., 1986). Different mechanisms for this effect have been described and discussed. First of all, a highly overexpressed protein encoded on the plasmid might interfere with cellular processes, e.g. by an enzyme acitivity or structural properties. Although they are usually expressed at moderate levels, this also applies to the antibiotic resistance proteins, for which the membrane integrity changes induced by the tetracycline resistance protein are a well known example (e.g. Hong et al., 2014; Lee and Edlin, 1985). Mechanisms like plasmid-induced growth defects have also entered the theoretical field of synthetic biology, where such feedback effects of an implemented module on the upstream machinery are described with the term retroactivity (Del Vecchio, 2015).

In accordance with the fact, that replication and maintenance of the introduced plasmid require carbon and energy sources, the extent of growth or viability defects has been shown to correlate with plasmid size (Cheah et al., 1987; Khosravi et al., 1990; Ryan et al., 1989) and copy number (Seo and Bailey, 1985; Birnbaum and Bailey, 1991). However, the respective causal chain needs to be examined in more depth, as stochiometric analyses showed that the energy costs for plasmid maintenance without high expression of recombinant proteins are negligible (da Silva and Bailey, 1986). As alternative explanation for the primary result of plasmid presence and maintenance, several groups detected stress-induced changes in the regulatory status of the cell (Diaz Ricci and Hernández, 2000; Ow et al., 2009, 2006). Omics studies in this field furthermore demonstrated that the overall cellular changes are highly diverse

* Corresponding author at: DECHEMA-Forschungsinstitut, Biochemical Engineering, Theodor-Heuss-Allee 25, D-60486 Frankfurt, Germany.
E-mail address: buchhaupt@dechema.de (M. Buchhaupt).

http://dx.doi.org/10.1016/j.jbiotec.2016.06.001
0168-1656/

(Hong et al., 2014; Ow et al., 2006), thereby complicating the identification of causal connections between primary plasmid-induced cellular changes and the phenotype of growth rate reduction. Using metabolomics, a plasmid-induced growth defect in *Methylobacterium extorquens* could be shown to be the result of reduced activity of an essential cobalamin-requiring enzyme, which was most probably the result of stress-induced downregulation of a cobalt import protein (Kiefer et al., 2009).

Regarding the design of plasmids with reduced impact on cell fitness, a recent publication demonstrates the use of a genome-integrated GFP reporter construct to assess changes in the so-called gene expression capacity of cells after introduction of plasmids (Ceroni et al., 2015). This approach was successfully applied to identify highly efficient expression vectors by modulating the copy number, the promoter and the ribosomal binding site.

Within this study, we demonstrate that introduction of the plasmid pMiS1 (Mi et al., 2014) adversely affects cell growth of *P. putida*. pMiS1 was derived from pBBR1MCS-2, a derivative of the medium-copy pBBR1 plasmid isolated from *Bordetella bronchiseptica* S87 (Kovach et al., 1995; Antoine and Locht, 1992). It carries the tightly regulated *L*-rhamnose-inducible $rhaP_{BAD}$ promoter and the two activator genes *rhaS* and *rhaR* of *E. coli*, which constitute an efficient induction system in *P. putida* (Jeske and Altenbuchner, 2010). Besides their frequent use for episomal expression in *P. putida* (Jeske and Altenbuchner, 2010; Lieder et al., 2015; Escapa et al., 2013; Wang et al., 2011; Nikel and de Lorenzo, 2014), plasmids derived from the pBBR1 replicon are also stably maintained in many other Gram-negative bacteria (Kovach et al., 1995; Antoine and Locht, 1992) and no plasmid incompatibility with plasmids of other broad-host-range Inc families (like IncP, IncQ or IncW) has been reported (Antoine and Locht, 1992). In the second part of this work, we present a new variant of the pBBR1 replicon with reduced copy number for episomal expression experiments in *P. putida* without causing a growth defect. It represents a plasmid useful for physiological studies and biotechnological applications.

2. Material and methods

2.1. Plasmids, bacterial strains, growth conditions and GFP quantification

Plasmids pBBR1MCS-2, -3 and -5 (Kovach et al., 1995) were purchased from CBS. The construction of pMiS1 was previously reported (Mi et al., 2014). The *gfp* gene was amplified via PCR using pJeM1 (Jeske and Altenbuchner, 2010) as the template and primer 1 (5'-GATCGGTACCATGACCATGATTACGCATC-3′) and primer 2 (5'-GATCCTCGAGTTACTTGTACAGCTCGTCC-3') and cloned into pMiS1 via *Kpn*I and *Xho*I to give pMiS1-gfp. The *rep* gene mutation leading to the G159S exchange was introduced into pMiS1 and pMiS1-gfp by exchange of a part of the *rep* gene with the mutation-containing part from plasmid C-F2 (see Table 1) via *Psh*AI and *Eco*47III to give pMiS4 and pMiS4-gfp, respectively. Plasmids pMiS1-deltarhaR, pMiS1-deltarhaS and pMiS1-deltaMCSrhaBADp were constructed by amplifying pMiS1 without the respective parts via PCR and subsequent Gibson isothermal assembly (Gibson et al., 2009). For construction of pMiS1-deltarhaR primer 3 (5′-CTTAATGAATTACAACAG-TTTTTATGCATTATTGCAGAAAGC CATCCCGTC-3′) and 4 (5′-TTTCTGCAATAATGCATAAAAACTGTTGTAATTCATTA AGCATTCTGCCGAC-3′), for pMiS1-deltarhaS primer 5 (5′-GCGTTATTGCAGAAAG CCATACTGGCCTCCTGATGTCGTC-3′) and 6 (5′-GACGACATCAGGAGGCCAGTA TGGCTTTCTGCAATAACGCG-3′) and for pMiS1-deltaMCSrhaBADp primer 7 (5′-CGGAAAAAAATCCACACTAT-GTAATACGGTCATACCGGTT-TATTGACTACCGGAAGC-3′) and 8 (5′-AACCGGTATGACCGTA-TTACATAGTGTGGATTTTTTTCCGTCTG GTAACGCGTC-3′) were used. A schematic overview of all plasmids with their relevant elements is given in Fig. 1.

Escherichia coli NEB 5-alpha was purchased from NEB GmbH, *P. putida* GS1 alias DSM 12264 (Speelmans et al., 1998) and KT2440 (Nelson et al., 2002) were purchased from DSMZ. *P. putida* (30 °C) and *E. coli* (37 °C) overnight cultures grown in TB (>14 h, 180 rpm) were used to inoculate TB or E2 (10% LB) main cultures to an OD_{600} of 0.1. E2 medium consists of 4.6 g glycerol, 2.4 g Na_2HPO_4, 0.91 g NH_4Cl, 5.7 g K_2HPO_4, 3.7 g KH_2PO_4 per liter supplemented with 10 mL of 100 mM $MgSO_4 \cdot 7H_2O$, 20 mL 5x LB stock solution and 1 mL micro elements stock solution consisting of 2.78 g $FeSO_4 \cdot 7H_2O$, 1.98 g $MnCl_2 \cdot 4H_2O$, 2.81 g $CoSO_4 \cdot 7H_2O$, 1.47 g $CaCl_2 \cdot 2H_2O$, 0.17 g $CuCl_2 \cdot 2H_2O$, 0.29 g $ZnSO_4 \cdot 7H_2O$ per liter of 1 M HCl. Cell cultivation was performed in a microbioreactor system (BioLector®) at 1000 rpm using 1.5 mL culture volume in 48-well Flowerplates® (m2p-labs GmbH) covered by gas-permeable sealing foil. *E. coli* was cultivated at 37 °C and *P. putida* at 30 °C. Biomass formation was monitored via scattered light at 620 nm. Most growth comparison experiments in Flowerplates® were done in triplicates each derived from one preculture. In case of experiments shown in Fig. 3(a)–(h) three different transformants were used to prepare separate precultures to inoculate the three cultures. Culture samples were randomly distributed in the plate. Antibiotics were added to final concentration of 30 μg/mL (kanamycin), 20 μg/mL (tetracycline) and 25 μg/mL (gentamicin), if required. For induction of GFP expression, *L*-rhamnose was added to a final concentration of 0.2% (w/v) directly after inoculation. GFP fluorescence was monitored using an excitation filter of 488 nm and an emission filter of 520 nm.

2.2. Determination of relative plasmid copy numbers (PCN)

Three precultures were inoculated for each tested strain and the main cultures were shaken in 48-well Flowerplates® as described above. For DNA template preparation, 1 mL cell culture was harvested during the growth phase (~8 h after inoculation) and prepared using the QIAamp DNA Mini kit (Qiagen) according to manufacturer's instructions. Extracted template DNA was diluted to 100 ng/μL with ddH_2O. Primer 3 (5'-CTTGTCGATCAGGATGATC-3') and primer 4 (5′-GTCACGACGAGATCCTC-3′) targeting 107 bp of the kanamycin resistance marker gene *kmR* (target) were used as plasmid-specific primers and primer 5 (5′-CCATCCTGCGCAACAAGG-3′) and primer 6 (5′-CTGGTCTTCTTCTGGCAG-3′) targeting 110 bp of the TtgABC multidrug efflux pump subunit gene *ttgB* (reference) were used as reference primers amplifying a DNA region of the chromosome. Real-time qPCR was performed in a PikoReal™ System (Thermo Scientific) using Luminaris Color HiGreen qPCR Master Mix (Life Technologies) according to manufacturers' instructions. Amplification specificities were confirmed by melting curve and gel electrophoresis analysis. Amplification efficiencies (E) were calculated according to the equation $E = 10^{-1/slope}$ (Lee et al., 2006). For calculation of the relative PCN, $\Delta\Delta C_T$ method is used (relative amount of target $= 2^{-\Delta\Delta C_T}$, (Livak and Schmittgen, 2001)), since the amplification efficiency for target and reference were found to be approximately equal. Each DNA sample was analyzed in triplicate.

3. Results

3.1. Observation of plasmid-induced growth defect in P. putida

In the context of studies on changes in the *P. putida* terpene resistance upon episomal overexpression of certain genes, we iden-

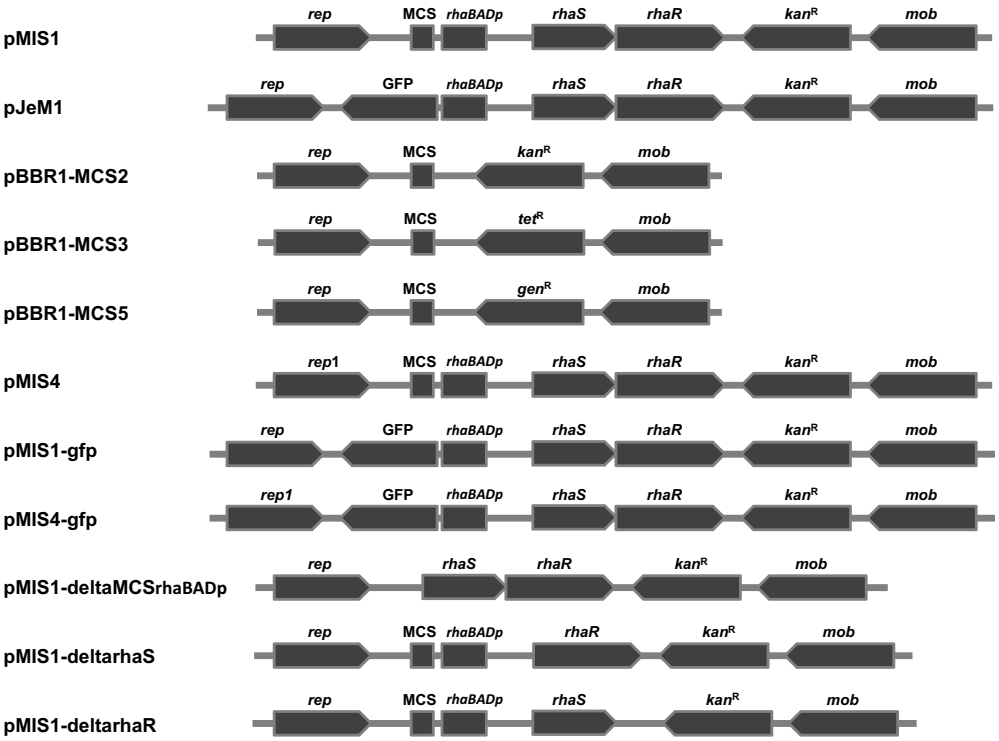

Fig. 1. Scheme of the relevant elements contained in the vectors used in this work. *rep1* encodes the G159S variant of the Rep protein. Vectors pJeM1 and pMiS1-gfp are nearly identical. Both contain a GFP gene encoding the fluorescent protein with an N-terminal 6xHis tag under control of the rhaBAD promoter. They only differ in the 25 nucleotides (pJeM1) or 48 nucleotides (pMiS1-gfp) between the rhaBAD promoter and the GFP start codon and in addition in a short region between the GFP stop codon and the *Hin*dIII site that encompasses 2 nucleotides in pJeM1 or 18 nucleotides in pMiS1-gfp.

tified a plasmid-induced growth defect. A comparison of the growth kinetics of *P. putida* GS1 without plasmid or with plasmid pMiS1, each in the presence or in the absence of 150 mM limonene is shown in Fig. 2. This example shows clear increases of the lag phase for the transformant harboring the plasmid in media without and with limonene.

3.2. Determination of growth defects in P. putida caused by different plasmids

The impairment of *P. putida* GS1 cell growth was induced by the plasmid pMiS1, which is a pBBR1MCS-2 derivative, in which *lacZ* and the lac promoter were substituted by an operon including *rhaS* and *rhaR* under control of *rha* promoter. First, we introduced various different pBBR1-based plasmids containing the kanamycin (pBBR1MCS-2), tetracycline (pBBR1MCS-3) or gentamicin (pBBR1MCS-5) resistance cassettes (Kovach et al., 1995; Antoine and Locht, 1992) into *P. putida* GS1 to compare their impact on cell growth (Fig. 3a–d). As shown in Fig. 3, cell growth of pBBR1MCS-3-carrying *P. putida* GS1 (c) was even more seriously impaired than growth of cells containing pMiS1 (a). For pBBR1MCS-2-containing cells the growth defect was clearly reduced compared to cells harboring pMiS1 (b) and in case of pBBR1MCS-5 an effect is hardly detectable.

To investigate the impact of components of the rhamnose induction system on cell growth, plasmids pJeM1 (the parental vector of pMiS1 also containing kan^R and the rhamnose induction system) as well as pMiS1 derivatives lacking the MCS and the rhamnose-inducible promoter (pMiS1-deltaMCSrhaBADp), the *rhaS* gene (pMiS1-deltarhaS) or the *rhaR* gene (pMiS1-deltarhaR)

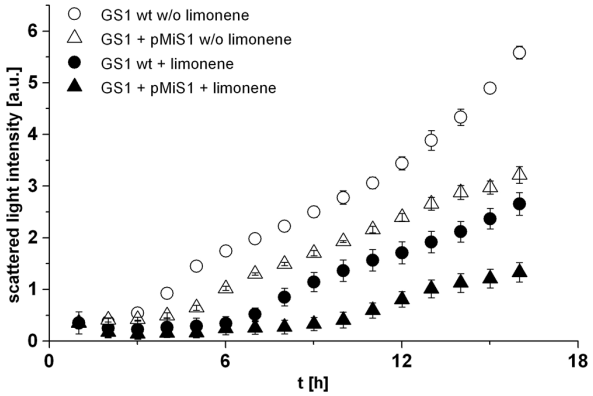

Fig. 2. Cell growth of plasmid-free (circles) and pMiS1-harboring (triangles) *P. putida* GS1 in E2 (10% LB) minimal medium without (open) and with (closed) 150 mM limonene. For cultures with plasmid-containing cells, 30 μg/mL kanamycin was added. The average of triplicates and corresponding standard deviations are shown.

were introduced into *P. putida* GS1. pJeM1 as well as pMiS1-deltaMCSrhaBADp and pMiS1-deltarhaS induced a growth defect similar to that of pMiS1, whereas the impact of pMiS1-deltarhaR on growth was clearly smaller.

Plasmids pMiS1, pBBR1MCS-2, pBBR1MCS-3 and pBBR1MCS-5 were also introduced into *P. putida* KT2440 cells and growth defects similar to that observed with respective *P. putida* GS1 transformants

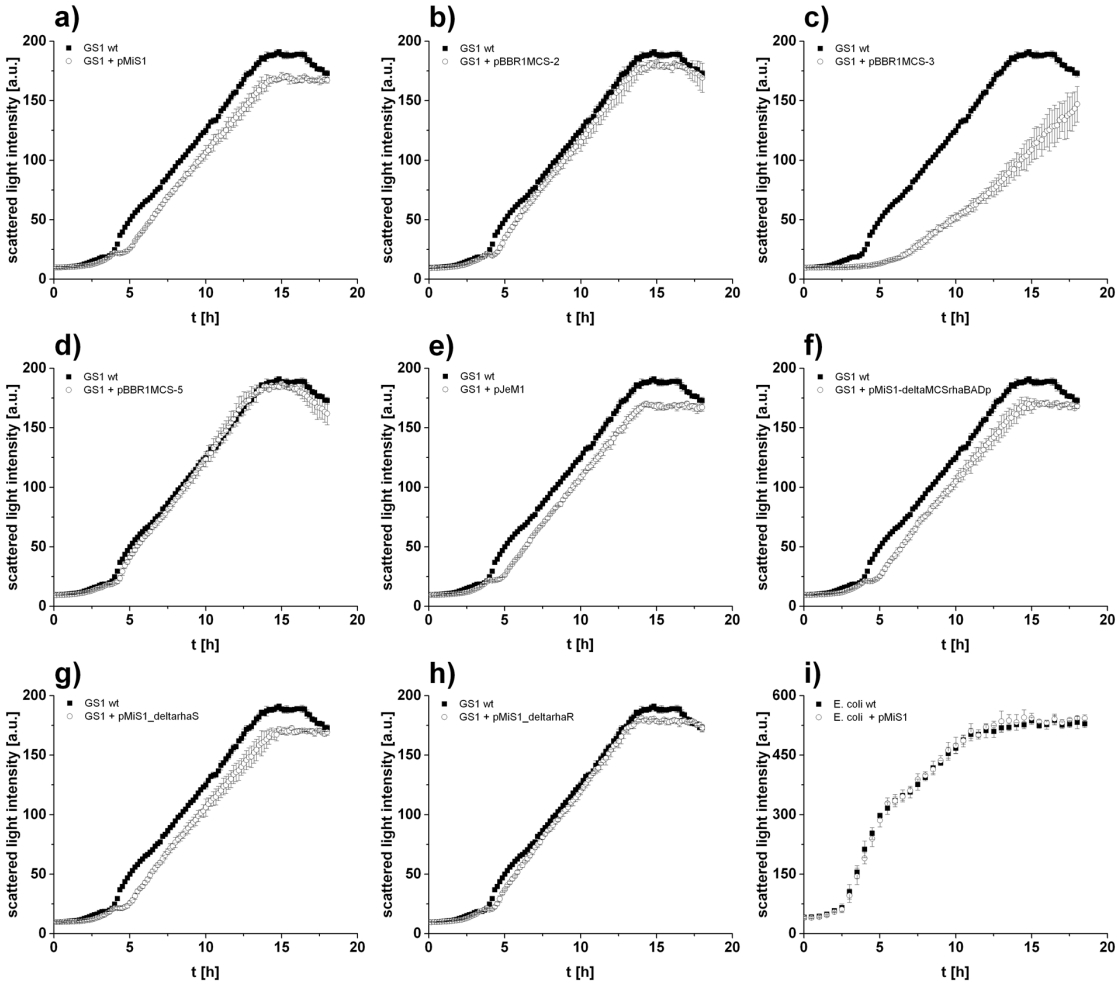

Fig. 3. Comparison of cell growth of *P. putida* GS1 without plasmid and transformants containing one of the pBBR1-derived plasmids pMiS1 (a), pBBR1MCS-2 (b), pBBR1MCS-3 (c), pBBR1MCS-5 (d), pJeM1 (e), pMiS1-deltaMCSrhaBADp (f), pMiS1-deltarhaS (g) or pMiS1-deltarhaR (h) and comparison of cell growth of plasmid-free and pMiS1-carrying *E. coli* NEB 5-alpha (i). Cells were cultivated in TB medium (supplemented with corresponding antibiotics, if required). The average of triplicates and corresponding standard deviations are shown.

were measured (data not shown). *E. coli* carrying pMiS1 was not affected in cell growth (e).

3.3. Identification of rep gene mutation in strains selected for faster growth

In the context of improving the limonene biotransformation capability of *P. putida* GS1 by using mutant enzymes, we performed evolutionary engineering experiments with randomly mutagenized pBBR1-based plasmids (unpublished work). We thereby found a number of plasmid-carrying isolates showing faster growth compared to *P. putida* GS1 containing the original plasmid. Plasmid sequencing revealed a mutation in the *rep* gene in many cases (Table 1). In plasmid C-H5, the *rep* gene mutation results in a premature stop codon, leading to a deduced Rep protein of only 185 amino acids, whereas the full-length protein should consist of 221 amino acids. In three independent clones, the mutation led to an amino acid change at position 159.

Table 1
Rep amino acid exchanges deduced from mutations found in pBBR1-based plasmids of *P. putida* GS1 strains evolved for faster growth.

Plasmid construct	Rep amino acid change
A-F1	G159S
B-D1	G159D
B-D5	P178L
B-E1	P165L
B-F3	E153K
C-F2	G159S
C-H1	P157S
C-H5	W186X

3.4. Rep G159S is causal for reduction of the plasmid-induced growth defect

To validate that mutation of the *rep* gene is responsible for the reduction of the observed growth defect, the mutation causing the Rep G159S exchange was introduced into pMiS1. The resulting plasmid was designated as pMiS4 and transformed into *P. putida* GS1 and *P. putida* KT2440. KT2440 was investigated additionally, as this strain is the model laboratory strain used in the majority of physiological studies with *P. putida*. Cell growth of the resulting transformants was compared to that of the corresponding plasmid-free strains and the pMiS1-harboring transformants, respectively (Fig. 4). For all transformants harboring the *rep* mutant-containing plasmid pMiS4, a plasmid-induced growth defect was not detectable.

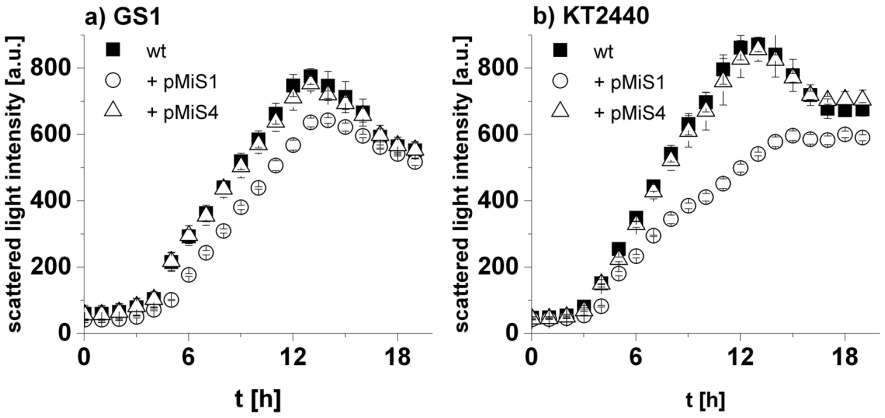

Fig. 4. Impact of pMiS1 and pMiS4 on *P. putida* cell growth. Cell growth of *P. putida* GS1 (a) and KT2440 (b) cells harboring no plasmid (*closed squares*), pMiS1 (*open circle*) or pMiS4 (*open triangles*) was monitored. Cells were cultivated in TB medium (supplemented with 30 μg/mL kanamycin, if required). The average of triplicates and corresponding standard deviations are shown.

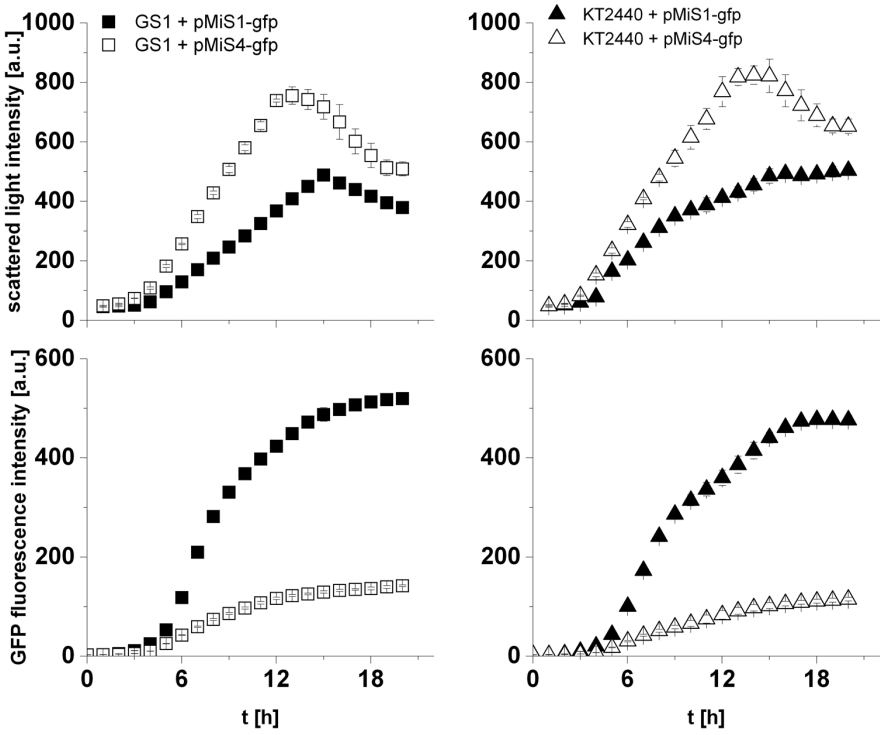

Fig. 5. Quantification of heterologous gene expression using pMiS1 and pMiS4 in *P. putida* GS1 and KT2440. *P. putida* GS1 (squares) and KT2440 (triangles) cells transformed with pMiS1 or pMiS4 were cultivated in TB medium (supplemented with 30 μg/mL kanamycin). Biomass formation via scattered light intensity (upper part) and GFP fluorescence (lower part) are shown for cells carrying pMiS1-gfp (closed) or pMiS4-gfp (open). The average of triplicates and corresponding standard deviations are shown.

3.5. Detection of strongly reduced copy number for the rep *mutant-containing plasmid pMiS4*

As we suggested the lack of plasmid toxicity of pMiS4 to be the result of a decreased PCN (plasmid copy number), we first determined the efficiency of heterologous *gfp* expression using pMiS1 and pMiS4. Fig. 5 shows relative biomass formation and GFP fluorescence of *P. putida* GS1 and KT2440 transformed with pMiS1-gfp and pMiS4-gfp. For both strains, growth rates were clearly higher with pMiS4-gfp than with pMiS1-gfp. On the other hand, GFP fluorescence was distinctly lower in both strains carrying the pMiS4-derived expression vector, providing evidence for a PCN reduction caused by the *rep* mutation in pMiS4. Indeed, real-time qPCR revealed a strong reduction of the relative PCN of pMiS4 to values of about 25% for both *P. putida* GS1 and KT2440 (Fig. 6).

4. Discussion

During episomal expression experiments in *P. putida*, we observed a distinct growth defect induced by the pBBR1MCS-2 derivative pMiS1, which was not detected in *E. coli*. The presence of expression vectors and the addition of solvents like limonene to the medium caused additive growth defects, making interpreta-

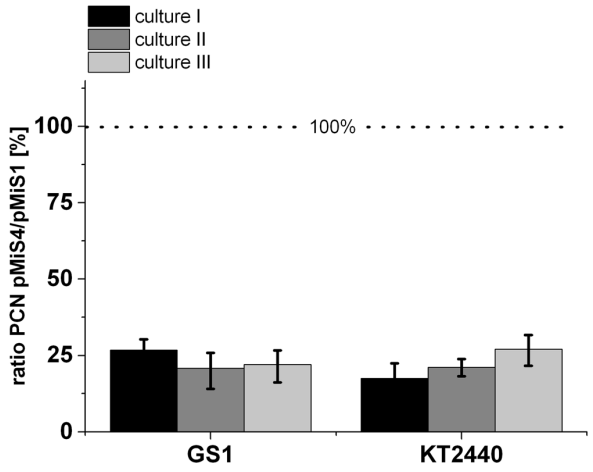

Fig. 6. Ratio of relative PCN of pMiS4 to pMiS1 in *P. putida* GS1 and KT2440. The average of three independent cultures with three technical replicates and error bars indicating standard deviations are shown.

tion of growth comparison datasets complicated. *P. putida* GS1 and KT2440 growth experiments in complex medium with the original pBBR1MCS plasmids containing the kanamycin, tetracycline or gentamicin resistance cassettes (Kovach et al., 1995), respectively, demonstrated different impacts depending on the resistance marker. Whereas no or only a very small growth impairment was observed for pBBR1MCS-5 (gentamicin resistance), pBBR1MCS-3 (tetracycline resistance) distinctly affected cell growth of *P. putida*. This growth deficiency is thus caused by the tetracycline resistance gene (McNicholas et al., 1992) that has already been shown to cause a fitness decrease in *E. coli* (Lee and Edlin, 1985). pBBR1MCS-2 (kanamycin resistance) also induced a small growth defect, which together with the data from pBBR1MCS-5 demonstrates the presence of the kanamycin resistance gene to be in part responsible for the growth impairment observed with pMiS1. The possibility of a growth-affecting action of kanamycin itself can be excluded as cells containing the low copy variant pMiS4 are not affected by the antibiotic. Furthermore, tests with plasmids harboring only parts of the rhamnose induction system clearly showed that the presence of the *rhaR* gene also contributes to the growth defect induced by pMiS1 and pJeM1. Therefore we conclude the synthesis of the proteins encoded by kan^R and *rhaR* and/or their possible interference with cellular functions to be causal for the pMiS1-induced growth defect.

In a different context, we identified pMiS1 variants in evolutionary engineering experiments that do not confer a burden to *P. putida*. Sequencing of obtained pMiS1 variants revealed a single mutation of the *rep* gene (Table 1). All identified mutations in *rep* occurred in the last third of the gene, suggesting that mutations in this part do not destroy overall functionality. In 6 of all 8 variants identified, a glycine or proline was substituted. These two amino acids are typically responsible for turns and loops in polypeptides (Richardson, 1981; Krieger et al., 2005); hence, substitution at this position very likely considerably changes conformation and folding of the polypeptide. Besides, the amino acid glycine at position 159 was exchanged in three cases, two times into serine and one time into aspartate, suggesting that this is a key position for functional alterations of Rep leading to elimination of the growth defect. The underlying mechanism is yet unknown, since the replication mechanism of pBBR1-based plasmids is not elucidated so far. However, as mutations of the *rep* gene in pBBR1 leading to a 3–7 fold increase of the PCN were previously identified by Tao and coworkers, the corresponding protein is obviously involved in control of the PCN (Tao et al., 2005).

To verify the amino acid exchange at position 159 to be solely responsible for elimination of the growth defect, we introduced the corresponding mutation into the *rep* gene of pMiS1. As expected, *P. putida* GS1 and KT2440 (Fig. 4) transformed with the resulting plasmid pMiS4, did not exhibit the growth defect found for pMiS1. First evidence for a reduction of the PCN of pMiS4 in comparison to pMiS1 was provided by the strongly decreased GFP content of pMiS4-gfp-containing cells in comparison to cells carrying pMiS1-gfp (Fig. 5). qPCR analyses confirmed the assumed PCN reduction of pMiS4, which was found to be approximately one fourth of the PCN of pMiS1 (Fig. 6). It is likely that this PCN decrease is causal for reduction of the plasmid toxicity, as it has been shown for *E. coli* that cell growth is gradually decreasing with increasing PCN (Seo and Bailey, 1985). The most obvious hypothesis for the elimination of the growth defect by the copy number-lowering *rep* mutation is a reduction of the resources necessary for synthesis of Kan^R and RhaR or a decrease of possible cellular interferences caused by the respective proteins.

The *rep* gene variant described in the present work represents a new useful module for pBBR1-derived plasmids with a distinctly lowered PCN. Since it is known that low-copy plasmids can perform just as well or even better than high-copy plasmids for metabolic engineering (Jones et al., 2000), pMiS4 can be considered as a useful plasmid for biotechnological purposes and physiological studies in *Pseudomonas* and possibly also other Gram-negative bacteria.

Competing interests

The authors declare that they have no competing interests.

Authors' contributions

JM and FS performed the growth experiments. JM performed the qPCRs and the statistical analysis and drafted the manuscript. JM and MB analyzed the data and interpreted the results. AS and HS performed the evolutionary engineering experiments. JM, FS and DB carried out plasmid construction. MB and JS critically revised the manuscript. All authors read and approved the final manuscript.

References

Antoine, R., Locht, C., 1992. Isolation and molecular characterization of a novel broad-host-range plasmid from *Bordetella bronchiseptica* with sequence similarities to plasmids from gram-positive organisms. Mol. Microbiol. 6 (13), 1785–1799, http://dx.doi.org/10.1111/j.1365-2958.1992.tb01351.x (PubMed PMID: 1321324).

Bailey, J.E., Da Silva, N.A., Peretti, S.W., Seo, J.H., Srienc, F., 1986. Studies of host-plasmid interactions in recombinant microorganisms. Ann. N. Y. Acad. Sci. 469, 194–211, http://dx.doi.org/10.1111/j.1749-6632.1986.tb26498.x (PubMed PMID: 3524397).

Birnbaum, S., Bailey, J.E., 1991. Plasmid presence changes the relative levels of many host cell proteins and ribosome components in recombinant *Escherichia coli*. Biotechnol. Bioeng. 37 (8), 736–745, http://dx.doi.org/10.1002/bit.260370808 (PubMed PMID: 18600670).

Ceroni, F., Algar, R., Stan, G.B., Ellis, T., 2015. Quantifying cellular capacity identifies gene expression designs with reduced burden. Nat. Methods 12 (5), 415–418, http://dx.doi.org/10.1038/nmeth.3339, Epub 2015/04/08; PubMed PMID: 25849635.

Cheah, U.E., Weigand, W.A., Stark, B.C., 1987. Effects of recombinant plasmid size on cellular processes in *Escherichia coli*. Plasmid 18 (2), 127–134, http://dx.doi.org/10.1016/0147-619X(87)90040-0 (PubMed PMID: 3324124).

Cornelissen, S., Julsing, M.K., Volmer, J., Riechert, O., Schmid, A., Bühler, B., 2013. Whole-cell-based CYP153A6-catalyzed (S)-limonene hydroxylation efficiency depends on host background and profits from monoterpene uptake via AlkL. Biotechnol. Bioeng. 110 (5), 1282–1292, http://dx.doi.org/10.1002/bit.24801 (PubMed PMID: 23239244).

Del Vecchio, D., 2015. Modularity, context-dependence, and insulation in engineered biological circuits. Trends Biotechnol. 33 (2), 111–119, http://dx.doi.org/10.1016/j.tibtech.2014.11.009 (PubMed PMID: 25544476).

Diaz Ricci, J.C., Hernández, M.E., 2000. Plasmid effects on *Escherichia coli* metabolism. Crit. Rev. Biotechnol. 20 (2), 79–108, http://dx.doi.org/10.1080/07388550008984167 (PubMed PMID: 10890453).
Escapa, I.F., del Cerro, C., García, J.L., Prieto, M.A., 2013. The role of GlpR repressor in *Pseudomonas putida* KT2440 growth and PHA production from glycerol. Environ. Microbiol. 15 (1), 93–110, http://dx.doi.org/10.1111/j.1462-2920.2012.02790.x (PubMed PMID: 22646161).
Gibson, D.G., Young, L., Chuang, R.Y., Venter, J.C., Hutchison, C.A., 2009. 3rd, Smith HO. Enzymatic assembly of DNA molecules up to several hundred kilobases. Nat. Methods 6 (5), 343–345, http://dx.doi.org/10.1038/nmeth.1318, Epub 2009/04/14; PubMed PMID: 19363495.
Graf, N., Altenbuchner, J., 2011. Development of a method for markerless gene deletion in *Pseudomonas putida*. Appl. Environ. Microbiol. 77 (15), 5549–5552, http://dx.doi.org/10.1128/AEM.05055-11 (PubMed PMID: 21666018; PubMed Central PMCID: PMCPMC3147467).
Hoffmann, J., Altenbuchner, J., 2015. Functional characterization of the mannitol promoter of *Pseudomonas fluorescens* DSM 50106 and its application for a mannitol-inducible expression system for *Pseudomonas putida* KT2440. PLoS One 10 (7), e0133248, http://dx.doi.org/10.1371/journal.pone.0133248 (PubMed PMID: PMC4514859).
Hong, H., Jung, J., Park, W., 2014. Plasmid-encoded tetracycline efflux pump protein alters bacterial stress responses and ecological fitness of *Acinetobacter oleivorans*. PLoS One. 9 (9), e107716, http://dx.doi.org/10.1371/journal.pone.0107716 (PubMed PMID: 25229538; PubMed Central PMCID: PMC4167995).
Jeske, M., Altenbuchner, J., 2010. The Escherichia coli rhamnose promoter rhaP(BAD) is in *Pseudomonas putida* KT2440 independent of Crp-cAMP activation. Appl. Microbiol. Biotechnol. 85 (6), 1923–1933, http://dx.doi.org/10.1007/s00253-009-2245-8 (PubMed PMID: 19789867).
Jones, K.L., Kim, S.W., Keasling, J.D., 2000. Low-copy plasmids can perform as well as or better than high-copy plasmids for metabolic engineering of bacteria. Metab. Eng. 2 (4), 328–338, http://dx.doi.org/10.1006/mben.2000.0161 (PubMed PMID: 11120644).
Khosravi, M., Ryan, W., Webster, D.A., Stark, B.C., 1990. Variation of oxygen requirement with plasmid size in recombinant *Escherichia coli*. Plasmid 23 (2), 138–143, http://dx.doi.org/10.1016/0147-619X(90)90032-8 (PubMed PMID: 2194228).
Kiefer, P., Buchhaupt, M., Christen, P., Kaup, B., Schrader, J., Vorholt, J.A., 2009. Metabolite profiling uncovers plasmid-induced cobalt limitation under methylotrophic growth conditions. PLoS One 4 (11), e7831, http://dx.doi.org/10.1371/journal.pone.0007831 (PubMed PMID: 19915676; PubMed Central PMCID: PMCPMC2773004).
Kovach, M.E., Elzer, P.H., Hill, D.S., Robertson, G.T., Farris, M.A., Roop, R.M., et al., 1995. Four new derivatives of the broad-host-range cloning vector pBBR1MCS, carrying different antibiotic-resistance cassettes. Gene 166 (1), 175–176 (PubMed PMID: 8529885).
Krieger, F., Möglich, A., Kiefhaber, T., 2005. Effect of proline and glycine residues on dynamics and barriers of loop formation in polypeptide chains. J. Am. Chem. Soc. 127 (10), 3346–3352, http://dx.doi.org/10.1021/ja042798i (PubMed PMID: 15755151).
Lee, S.W., Edlin, G., 1985. Expression of tetracycline resistance in pBR322 derivatives reduces the reproductive fitness of plasmid-containing *Escherichia coli*. Gene 39 (2–3), 173–180, http://dx.doi.org/10.1016/0378-1119(85)90311-7 (PubMed PMID: 3005111).
Lee, C., Kim, J., Shin, S.G., Hwang, S., 2006. Absolute and relative QPCR quantification of plasmid copy number in *Escherichia coli*. J. Biotechnol. 123 (3), 273–280, http://dx.doi.org/10.1016/j.jbiotec.2005.11.014 (PubMed PMID: 16388869).
Lieder, S., Nikel, P.I., de Lorenzo, V., Takors, R., 2015. Genome reduction boosts heterologous gene expression in *Pseudomonas putida*. Microb. Cell Fact. 14, 23, http://dx.doi.org/10.1186/s12934-015-0207-7 (PubMed PMID: 25890048; PubMed Central PMCID: PMCPMC4352270).
Livak, K.J., Schmittgen, T.D., 2001. Analysis of relative gene expression data using real-time quantitative PCR and the 2(-Delta Delta C(T)) Method. Methods 25 (4), 402–408, http://dx.doi.org/10.1006/meth.2001.1262 (PubMed PMID: 11846609).
Loeschcke, A., Thies, S., 2015. *Pseudomonas putida*-a versatile host for the production of natural products. Appl. Microbiol. Biotechnol., http://dx.doi.org/10.1007/s00253-015-6745-4 (PubMed PMID: 26099332).
Martínez-García, E., de Lorenzo, V., 2011. Engineering multiple genomic deletions in Gram-negative bacteria: analysis of the multi-resistant antibiotic profile of *Pseudomonas putida* KT2440. Environ. Microbiol. 13 (10), 2702–2716, http://dx.doi.org/10.1111/j.1462-2920.2011.02538.x (PubMed PMID: 21883790).
Martínez-García, E., Nikel, P.I., Aparicio, T., de Lorenzo, V., 2014. Pseudomonas 2.0: genetic upgrading of *P. putida* KT2440 as an enhanced host for heterologous gene expression. Microb. Cell Fact. 13, 159, http://dx.doi.org/10.1186/s12934-014-0159-3 (PubMed PMID: 25384394; PubMed Central PMCID: PMCPMC4230525).
McNicholas, P., Chopra, I., Rothstein, D.M., 1992. Genetic analysis of the tetA(C) gene on plasmid pBR322. J. Bacteriol. 174 (24), 7926–7933 (PubMed PMID: 1459940; PubMed Central PMCID: PMCPM C207527).
Mi, J., Becher, D., Lubuta, P., Dany, S., Tusch, K., Schewe, H., et al., 2014. De novo production of the monoterpenoid geranic acid by metabolically engineered *Pseudomonas putida*. Microb. Cell Fact. 13 (1), 170, http://dx.doi.org/10.1186/s12934-014-0170-8 (PubMed PMID: 25471523; PubMed Central PMCID: PMCPMC4266966).
Mirata, M.A., Heerd, D., Schrader, J., 2009. Integrated bioprocess for the oxidation of limonene to perillic acid with *Pseudomonas putida* DSM 12264. Process Biochem. 44 (7), 764–771, http://dx.doi.org/10.1016/j.procbio.2009.03.013.
Nelson, K.E., Weinel, C., Paulsen, I.T., Dodson, R.J., Hilbert, H., 2002. Martins dos Santos VA, et al Complete genome sequence and comparative analysis of the metabolically versatile *Pseudomonas putida* KT2440. Environ. Microbiol. 4 (12), 799–808, http://dx.doi.org/10.1046/j.1462-2920.2002.00366.x (PubMed PMID: 12534463).
Nikel, P.I., de Lorenzo, V., 2014. Robustness of *Pseudomonas putida* KT2440 as a host for ethanol biosynthesis. N. Biotechnol. 31 (6), 562–571, http://dx.doi.org/10.1016/j.nbt.2014.02.006 (PubMed PMID: 24572656).
Ow, D.S., Nissom, P.M., Philp, R., Oh, S.K.-W., Yap, M.G.-S., 2006. Global transcriptional analysis of metabolic burden due to plasmid maintenance in *Escherichia coli* DH5α during batch fermentation. Enzyme Microb. Technol. 39 (3), 391–398, http://dx.doi.org/10.1016/j.enzmictec.2005.11.048.
Ow, D.S., Lee, D.Y., Yap, M.G., Oh, S.K., 2009. Identification of cellular objective for elucidating the physiological state of plasmid-bearing *Escherichia coli* using genome-scale in silico analysis. Biotechnol. Prog. 25 (1), 61–67, http://dx.doi.org/10.1002/btpr.51 (PubMed PMID: 19224555).
Poblete-Castro, I., Becker, J., Dohnt, K., dos Santos, V.M., Wittmann, C., 2012. Industrial biotechnology of *Pseudomonas putida* and related species. Appl. Microbiol. Biotechnol. 93 (6), 2279–2290, http://dx.doi.org/10.1007/s00253-012-3928-0 (PubMed PMID: 22350258).
Richardson, J.S., 1981. The anatomy and taxonomy of protein structure. In: Anfinsen JTEaFMR, C.B. (Ed.), Adv Protein Chem, vol. 34. Academic Press, pp. 167–339.
Ryan, W., Parulekar, S.J., Stark, B.C., 1989. Expression of beta-lactamase by recombinant *Escherichia coli* strains containing plasmids of different sizes-effects of pH, phosphate, and dissolved oxygen. Biotechnol. Bioeng. 34 (3), 309–319, http://dx.doi.org/10.1002/bit.260340306 (PubMed PMID: 18588109).
Seo, J.H., Bailey, J.E., 1985. Effects of recombinant plasmid content on growth properties and cloned gene product formation in *Escherichia coli*. Biotechnol. Bioeng. 27 (12), 1668–1674, http://dx.doi.org/10.1002/bit.260271207 (PubMed PMID: 18553628).
Speelmans, G., Bijlsma, A., Eggink, G., 1998. Limonene bioconversion to high concentrations of a single and stable product, perillic acid, by a solvent-resistant *Pseudomonas putida* strain. Appl. Microbiol. Biotechnol. 50 (5), 538–544, http://dx.doi.org/10.1007/s002530051331.
Tao, L., Jackson, R.E., Cheng, Q., 2005. Directed evolution of copy number of a broad host range plasmid for metabolic engineering. Metab. Eng. 7 (1), 10–17, http://dx.doi.org/10.1016/j.ymben.2004.05.006 (PubMed PMID: 15721806).
Wang, H.H., Zhou, X.R., Liu, Q., Chen, G.Q., 2011. Biosynthesis of polyhydroxyalkanoate homopolymers by *Pseudomonas putida*. Appl. Microbiol. Biotechnol. 89 (5), 1497–1507, http://dx.doi.org/10.1007/s00253-010-2964-x (PubMed PMID: 21046374).
da Silva, N.A., Bailey, J.E., 1986. Theoretical growth yield estimates for recombinant cells. Biotechnol. Bioeng. 28 (5), 741–746, http://dx.doi.org/10.1002/bit.260280514 (PubMed PMID: 18555386).

Chapter 7 – Sequence analysis and expression of fungal limonene-3-hydroxylase enzymes in prokaryotic host

Florence M. Schempp

Status: unpublished

Introduction:

After fungal limonene-3-hydroxylase (L3H) enzymes were identified, one from *A. pullulans* and one from *H. carpetanum* (see Chapter 3), and the monoterpenoid tolerance of the intended production organism *P. putida* KT2440 was increased (see Chapter 5), the next step was to combine both components. For this purpose, first of all, the protein structure of the identified limonene-3-hydroxylase enzyme from *A. pullulans,* L3H.Ap, was analyzed. Afterwards different variants of the L3H.Ap gene, as well as of potentially compatible CYP reductase enzymes were designed, in order to aid protein expression, and heterologous expression in *E. coli* was investigated.

As described in Chapter 1, cytochrome P450 monooxygenase systems can be classified into different groups, depending on the composition and arrangement of their redox chain. While bacterial forms are often soluble in the cytoplasm, fungal CYP enzymes belong mostly to class II: integral proteins of the endoplasmic reticulum (ER) that require an additional reductase for their function.[93] The targeting of the proteins into the ER membrane is a co-translational process. For this, the proteins possess signal sequences, which can be recognized at the ribosome.[203] In addition to this N-terminal signal sequence, the CYP genes usually encode a hydrophobic helix as transmembrane domain (TMD) anchoring the protein into the ER membrane. Thereby, most of the protein is located on the cytosolic face of the ER membrane.[77] N-terminal signal and anchor sequence together function as an ER retention signal.[204–206]

Since prokaryotic cells lack ERs and other organelles, expression of eukaryotic membrane proteins in prokaryotic hosts involves some challenges, such as low gene expression and protein activity or the formation of insoluble protein aggregates (inclusion bodies). Due to the relevance of CYP enzymes for the development of biotechnological processes, several attempts have been made to overcome these difficulties, reviewed, for example, by Jana and Deb (2005)[207] or Gillam *et al.* (2008).[86] Such strategies include codon optimization of the respective genes and variation or truncation of the N-terminal sequence.[88,104]

Materials and Methods:

Chemicals and media

All chemicals were purchased from Sigma-Aldrich (Taufkirchen, Germany), Carl-Roth (Karlsruhe, Germany) or Merck Millipore (Darmstadt, Germany).

For cultivation of *E. coli,* the following media were used:

- lysogeny broth (LB, tryptone 10 g L^{-1}, yeast extract 5 g L^{-1}, NaCl 10 g L^{-1})
- terrific broth (TB, tryptone 12 g L^{-1}, yeast extract 24 g L^{-1}, glycerol 5 g L^{-1}, potassium phosphate buffer 89 mM (KH_2PO_4/K_2HPO_4, pH 7.5))
- ZYP-5052 autoinduction medium[208] (AI, tryptone 10 g L^{-1}, yeast extract 5 g L^{-1}, glycerol 5 g L^{-1}, glucose 0.5 g L^{-1}, α-lactose 2 g L^{-1}, $(NH_4)_2SO_4$ 3.3 g L^{-1}, KH_2PO_4 6.8 g L^{-1}, Na_2HPO_4 7.1 g L^{-1})

For solid media 17 g L^{-1} agar-agar were added. Antibiotics and other supplements were used at the following concentrations, if required: chloramphenicol (Cm) 30 µg mL^{-1}, ampicillin (Amp) 100 µg mL^{-1}, spectinomycin/streptomycin (Spec/Strep) 50 µg mL^{-1}, kanamycin (Kan) 50 µg mL^{-1}, isopropyl-β-D-thiogalactopyranoside (IPTG) 0.1 - 1 mM, 5-aminolevulinic acid (5-ALA) 75 µg mL^{-1}, thiamine HCl 1 mM, L-arabinose 50 mg mL^{-1}, tetracycline (Tet) 5 ng mL^{-1}, L-(+)-rhamnose 100 - 2000 µM.

Strains, plasmids and transformation

All strains and plasmids used in this study are listed in Table 1. The pCDFDuet™-1 and pETDuet™-1 expression plasmids were either purchased from the company BioCat GmbH (Heidelberg, Germany) or constructed using PCR amplification and Gibson isothermal assembly cloning.[209,210] Transformation of *E. coli* cells with the respective plasmids was carried out by electroporation or with chemically competent cells according to the manufacturer's instructions. Plasmid storage, propagation and isolation was performed using *E. coli* NEB® 5-alpha and the *GeneJET Plasmid Miniprep Kit* (Thermo Fisher Scientific Inc.).

Table 1: Bacterial strains and plasmids used in this study.
[a]in constructs of L3H.Ap, Red.Ap, PM17 and ATR1 with TMD, as second codon the base pairs for alanine were inserted in the gene sequence.[104] [b]altered N-terminus: replacement of native sequence with N-terminus of CYP51144C1.[211]

Strains	**Genotype**	**Reference**
E. coli NEB® 5-alpha	*fhuA2* α(*argF-lacZ*)*U169 phoA glnV44* ϕ*80* Δ(l*acZ*)*M15 gyrA96 recA1 relA1 endA1 thi-1 hsdR17*	New England BioLabs Inc.
E. coli BL21(DE3)	*fhuA2 [lon] ompT gal* (λ *DE3*) [*dcm*] Δ*hsdS* λ *DE3* = *sBamHIo* Δ*EcoRI-B int::*(*lacI::PlacUV5::T7 gene1*) *i21* Δ*nin5*	New England BioLabs Inc.
E. coli Lemo21(DE3)	*fhuA2 [lon] ompT gal* (λ *DE3*) [*dcm*] Δ*hsdS/* pLemo(Cm^R) λ *DE3* = *sBamHIo* Δ*EcoRI-B int::*(*lacI::PlacUV5::T7 gene1*) *i21* Δ*nin5* pLemo = pACYC184-*PrhaBAD-lysY*, Cm^R	New England BioLabs Inc.
E. coli ArcticExpress(DE3)	*E. coli* B F^- *ompT hsdS*(r_B^- m_B^-) *dcm*$^+$ Tet^R *gal* λ(DE3) *endA* Hte, *cpn10_cpn60*_$Gent^R$ expression plasmid	Agilent Technologies, Inc.
Plasmids	**Description**	**Reference**
pG-KJE8	expression of chaperones DnaK, DnaJ, GrpE, GroES, GroEL; promoter: *araB, Pzt-1*; inductor: L-arabinose, tetracycline; Cm^R	TaKaRa Bio Inc.
pGro7	expression of chaperones GroES, GroEL; promoter: *araB*; inductor: L-arabinose; Cm^R	TaKaRa Bio Inc.
pKJE7	expression of chaperones DnaK, DnaJ, GrpE; promoter: *araB;* inductor: L-arabinose; Cm^R	TaKaRa Bio Inc.
pG-Tf2	expression of chaperones GroES, GroEL, Tig; promoter: *Pzt-1*; inductor: tetracycline; Cm^R	TaKaRa Bio Inc.
pTf16	expression of chaperone Tig; promoter: *araB*; inductor: L-arabinose; Cm^R	TaKaRa Bio Inc.
pETDuet™-1	ColE1 (pBR322); promoter: T7*lac*; inductor: IPTG; Amp^R	Novagen®
pCDFDuet™-1	CloDF13; promoter: T7*lac*; inductor: IPTG; $Spec^R$	Novagen®
pCDF_Sfp	pCDF plasmid containing phosphopantetheinyl transferase gene (*sfp*) of *Bacillus subtilis*; $Spec^R$	Prof. Turner, University of Manchester, United Kingdom
pET24_P450cam_Pd_PdR	pET24 encoding a variant of the CYP enzyme P450cam of *P. putida* (*camC*; mutations: Y96F, V247L,[101] C334A[202]), putidaredoxin reductase (PdR, *camA*) and putidaredoxin (Pd, *camB*)*;* Kan^R	H. Schewe, unpublished data
pCDF_Red.Ap	pCDFDuet™-1 encoding putative CYP reductase enzyme of *A. pullulans*; $Spec^R$	this work
pCDF_Red.Ap_N-var	pCDFDuet™-1 encoding putative CYP reductase enzyme of *A. pullulans* with altered N-terminus[a,b]; $Spec^R$	this work
pCDF_Red.Ap-His	pCDFDuet™-1 encoding putative CYP reductase enzyme of *A. pullulans* with truncated N-terminus and addition of 6xHis-tag; $Spec^R$	this work

pCDF_Red.Ap.co	pCDFDuet™-1 encoding putative CYP reductase enzyme of *A. pullulans*, codon-optimized for *E. coli*; $Spec^R$	this work
pCDF_Red.Ap.co_N-var	pCDFDuet™-1 encoding putative CYP reductase enzyme of *A. pullulans* with altered N-terminus[a,b], codon-optimized for *E. coli*; $Spec^R$	this work
pCDF_Red.Ap.co-His	pCDFDuet™-1 encoding putative CYP reductase enzyme of *A. pullulans* with truncated N-terminus and addition of 6xHis-tag, codon-optimized for *E. coli*; $Spec^R$	this work
pCDF_ATR1.co	pCDFDuet™-1 encoding CYP reductase enzyme ATR1 of *A. thaliana* (NCBI: NP_194183.1)[a],[212,213] codon-optimized for *E. coli*; $Spec^R$	this work
pCDF_ATR1.co_N-var	pCDFDuet™-1 encoding CYP reductase enzyme ATR1 of *A. thaliana* (NCBI: NP_194183.1),[212,213] with altered N-terminus[a,b], codon-optimized for *E. coli*; $Spec^R$	this work
pET_L3H.Ap	pETDuet™-1 encoding L3H enzyme CYP65AH1 of *A. pullulans*[a]; Amp^R	this work
pET_L3H.Ap_N-var	pETDuet™-1 encoding L3H enzyme CYP65AH1 of *A. pullulans* with altered N-terminus[a,b]; Amp^R	this work
pET_L3H.Ap-His	pETDuet™-1 encoding L3H enzyme CYP65AH1 of *A. pullulans* with truncated N-terminus and addition of 6xHis-tag; Amp^R	this work
pET_L3H.Ap.co	pETDuet™-1 encoding L3H enzyme CYP65AH1 of *A. pullulans*[a], codon-optimized for *E. coli*; Amp^R	this work
pET_L3H.Ap.co_N-var	pETDuet™-1 encoding L3H enzyme CYP65AH1 of *A. pullulans* with altered N-terminus[a,b], codon-optimized for *E. coli;* Amp^R	this work
pET_L3H.Ap.co-His	pETDuet™-1 encoding L3H enzyme CYP65AH1 of *A. pullulans* with truncated N-terminus and addition of 6xHis-tag, codon-optimized for *E. coli*; Amp^R	this work
pET_PM17.co	pETDuet™-1 encoding L3H enzyme PM17 of *Mentha* x *piperita* (NCBI: AAD44151.1)[a],[58] codon-optimized for *E. coli*; Amp^R	this work
pET_PM17.co_N-var	pETDuet™-1 encoding L3H enzyme PM17 of *Mentha* x *piperita* (NCBI: AAD44151.1)[58] with altered N-terminus[a,b], codon-optimized for *E. coli*; Amp^R	this work

Cytochrome P450 reductase activity assay

Cultures of *E. coli* cells harboring different pCDF plasmids were inoculated 1:100 (v/v) from pre-cultures in 10 mL TB medium supplemented with spectinomycin and cultivated in 100 mL shake flasks at 180 rpm (orbit: 2.5 cm) and 37 °C until mid-exponential phase (OD_{600} = 0.6 - 1.1). Gene expression was induced with 0.2 mM IPTG and the cells were cultivated further at 25 °C for around 20 h. Cell suspensions (7 mL each) were cooled on ice for 1 h and

afterwards the cells were harvested by centrifugation (5,285 x g, 10 min, 4 °C). Cells were then resuspended in potassium phosphate buffer (100 mM, pH 7.4, 6 mL each). Cell disruption was performed using ultrasound (5 mm peak; program: 1 s pulse, 2 s break, total 6 min). The reductase assay was conducted according to a protocol from Guengerich *et al.* (2009).[214] Experiments were performed with biological triplicates.

Limonene biotransformation experiment with *E. coli*

For biotransformation experiments, *E. coli* BL21(DE3) strains expressing different CYP and reductase variants were cultivated in shake flasks in 10 mL TB medium each with appropriate antibiotics and supplemented with 5-aminolevulinic acid and thiamine HCl, to aid heme biosynthesis. After an OD_{600} of around 2 was reached, gene expression was induced with 0.1 mM IPTG. After 18 h of growth phase (25 °C, 110 rpm (orbit: 2.5 cm)), the cells were harvested (3,214 x g, 10 min, 4 °C) and concentrated by a factor of 5 by resuspending the cells in 2 mL TB medium (with appropriate antibiotics) containing glucose (10.9 g L^{-1}) and IPTG (0.1 mM). Concentrated cell suspensions were transferred back into the shake flasks and (+)-limonene was added two times (t = 0 and 24 h, final concentration: 25.2 g L^{-1}, 185 mM). Biotransformation experiments were incubated for 45 h at 30 °C and 200 rpm (orbit: 2.5 cm). Experiments were performed with biological triplicates. At different time points samples of 150 µL (t = 0, 24 h) or 700 µL (45 h) were taken and extracted with MTBE containing 100 mg L^{-1} 3-carene as an internal standard. After phase separation by centrifugation for 15 min at 16,000 x g, the organic layers were analyzed via GC-MS. For this purpose, a GCMS-QP2010 SE (Shimadzu) system containing a DB-5 column (30 m x 0.25 mm x 0.25 µm, Agilent Technologies, Inc.) was used. Measurements were conducted as follows: helium as the carrier gas, split ratio of 0.5 - 10, injections at 270 °C, column flow of 0.7 mL min^{-1} and a linear velocity of 30 cm s^{-1}. The column temperature was programmed as follows: 60 °C, with 10 °C per min up to 130 °C, followed by 30 °C per min up to 300 °C. Limonene and *trans*-isopiperitenol were identified by the comparison of retention times and mass spectra with those of chemically synthesized reference substances.

Heterologous gene expression in *E. coli* and evaluation via SDS-PAGE

For heterologous expression of CYP and reductase variants, different *E. coli* strains were transformed with combinations of pET and pCDF plasmids, which are listed in Table 1. Of the respective *E. coli* strains pre-cultures were cultivated in TB medium with appropriate antibiotics at 37 °C overnight. Afterwards fresh cultures were inoculated 1:100 (v/v) from pre-cultures in different media with respective antibiotics, 5-ALA and thiamine HCl in shake flasks (EF) or deep well plates (DW). Cultures were grown at 180 rpm (EF) or 800 rpm (DW) and 30 °C until

mid-exponential phase (ca. 3 h). If induction of gene expression was required, IPTG, L-arabinose, rhamnose or tetracycline were added and the cells were further cultivated at different temperatures. Conditions used for heterologous gene expression are summarized in Table 2.

Expression was evaluated via SDS-PAGE. For this, cell disruption was carried out with the *BugBuster® Master Mix* (Merck Millipore) according to the manufacturer's instructions. For SDS-PAGE *Mini-PROTEAN TGX Precast Gel*s (8-16 %, 10-well or Any kD™, 15-well) were purchased from Bio-Rad Laboratories, Inc. and used according to manufacturer's instructions. As size standard *PageRuler™ Unstained Protein Ladder* (Thermo Fisher Scientific Inc.) was used. Gel staining was carried out with Coomassie Brilliant Blue staining solution (ammonium sulphate 170 g L^{-1}, phosphoric acid (85 %) 30 mL L^{-1}, methanol 340 mL L^{-1}, Coomassie Brilliant Blue 0.35 mg L^{-1}).

Table 2: Conditions used for heterologous gene expression in different *E. coli* strains. TB: terrific broth medium, AI: ZYP-5052 autoinduction medium, IPTG: isopropyl-β-D-thiogalactopyranoside, EF: (Erlenmeyer) shake flasks, DW: deep well plates.

***E. coli* strain**	**medium**	**induction type**	**expression temperature [°C]**	**expression duration [h]**	**cultivation vessel**
BL21(DE3)	TB	without induction	16	72	EF
	TB	IPTG	25	20	EF, DW
	TB	without induction	25	20	EF, DW
	AI	autoinduction	16	72	EF
	AI	autoinduction	25	20	EF, DW
BL21(DE3) + chaperone plasmids	TB	without IPTG induction (tetracycline, arabinose)	25	20	DW
	TB	IPTG (tetracycline, arabinose)	25	20	DW
	AI	autoinduction (tetracycline, arabinose)	25	20	DW

Lemo21(DE3)	TB	without induction	11	68	DW
	TB	IPTG	11	68	DW
	AI	autoinduction	11	68	DW
	TB	without induction	25	20	DW
	TB	IPTG, rhamnose: 0 - 2000 µM	25	20	DW
	AI	autoinduction, rhamnose: 0 - 2000 µM	25	20	DW
ArcticExpress(DE3)	TB	without induction	11	68	DW
	TB	IPTG	11	68	DW
	AI	autoinduction	11	68	DW
	TB	without induction	25	20	DW
	TB	IPTG	25	20	DW
	AI	autoinduction	25	20	DW

Results and discussion:

L3H.Ap sequence analysis shows typical features of class II CYP proteins

After initial characterization of limonene-3-hydroxylase L3H.Ap (CYP65AH1.Ap) of *A. pullulans* in yeasts (see Chapter 3), the enzyme was to be further investigated.

In total, the protein L3H.Ap has a size of 57.7 kDa with 502 amino acids (aa). First of all, the sequence of the protein was analyzed for specific sequence features, topologies, domains and functional sites. Various online tools are available for this purpose, e.g. *prosite* (https://prosite.expasy.org), *Phobius* (http://phobius.sbc.su.se) and *Protter* (http://wlab.ethz.ch/protter/start/). In this way, in the protein sequence of L3H.Ap an N-terminal transmembrane domain (TMD) (aa 12 - 30, blue) behind a short amino acid sequence (aa 1 - 11, green) could be identified (Figure 18 A - C). In addition, the sequence contains a heme binding site (aa 433 - 442, red), a conserved motif of CYP enzymes.[77] The main part of the protein (aa 31 - 502) is probably located on the cytosolic face of the ER membrane, because there are more positively charged amino acids on the C-terminal site of the TMD as on the N-terminal site.[215] Such an orientation, where the major part of the enzyme including the catalytic domain extends into the cytosol, is described for most CYP enzymes anchored in the ER membrane, because it facilitates the interaction with the electron donors.[216,217] Due to the presence of a TMD, it can be assumed that the enzyme L3H.Ap belongs to the CYP class II, the most abundant CYP class in the fungal kingdom.[93]

In comparison to other potential CYP enzymes of *A. pullulans* and *H. carpetanum,* L3H.Ap has the highest protein identity to CYP65Z1 of *A. pullulans* and CYP65AH1 of *H. carpetanum* (L3H.Hc) with 53 % and 52 %, respectively. While CYP65Z1 showed no L3H activity under the tested conditions, L3H.Hc expression led to *trans*-isopiperitenol production in the presence of limonene (see Chapter 3). According to the online tools *prosite, Phobius* and *Protter*, L3H.Hc has protein sequence features (TMD, heme binding motif, major part extends into cytosol) similar to L3H.Ap.

A

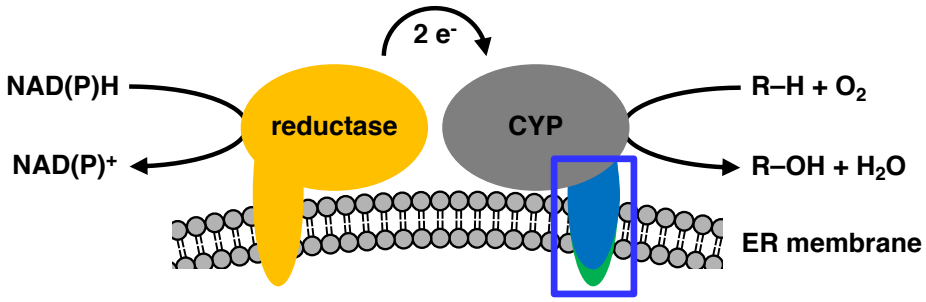

B

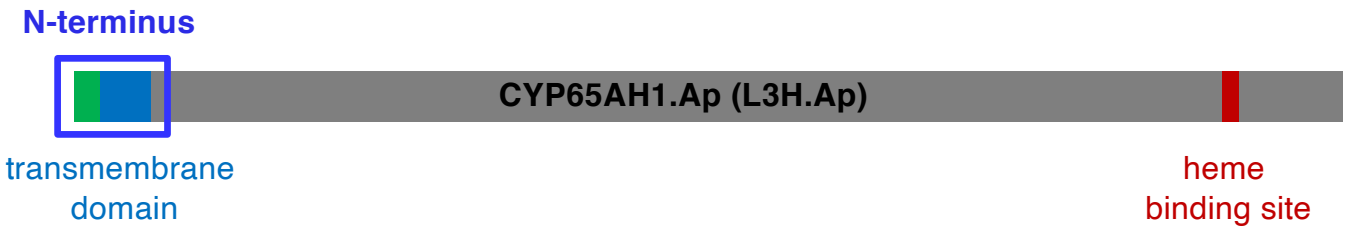

C

CYP65AH1.Ap (L3H.Ap)

MFSEQITKAAGYLLTGVVLYSTSIVFYNLYINPVSKYPGSWLYTSTPFPRLWLYISG
REPFVVLDMHKRYGPIVRIAPNELSFIDQQAWKDIYGHKNNNPKDPTFYPFAPDTK
NSLILANDEDHHRMRKMFLPAFSARALRDQNDMLNHYVRKLVEALKEKQKNGEKV
DLVKFYNFTTFDVIADLCFGESLGLLEKQEYTPWLQGIFDQIFLACSSRTIQYFPLL
WMVVQKFMPKSLTDAANASFKHSSDRVDKRLAMDTDRPDIFGLVLKHKDGANMS
RQMMYSNADLLMIAGTETTATMLSGLTYNLLRNPGPMKRLTAEIRERFASEDDITID
ELPRLPYLTACIEEGLRTYPSVAEGVRRKTKPGTATEICGQWIPPNVGVSVPHYAA
YHSEYNFVEPDSFIPERWLAEGIDGHDPRFAADKKSAMNPFSTGPRNCIGMNLAY
HEMRLIIAHLLWNFDLEADGVPRDWLKQEVHVVWDKKPLMVGFRHRSKVTFETTT

D

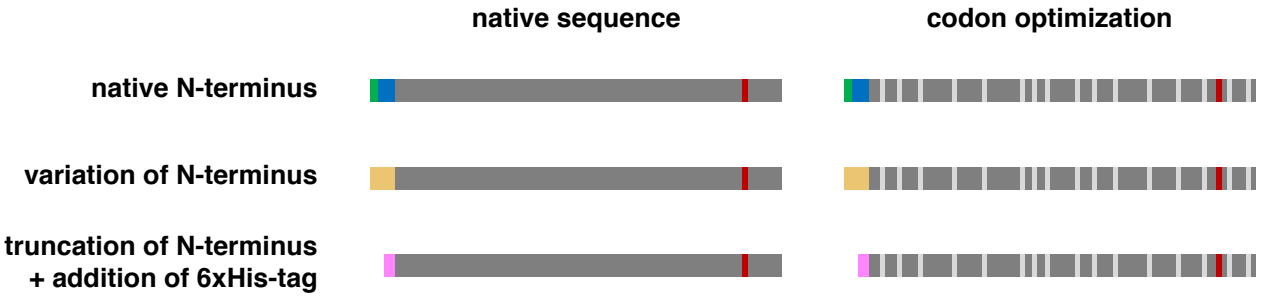

Figure 18: Sequence analysis of L3H.Ap of *A. pullulans* and overview of variants designed for heterologous gene expression in *E. coli*. (A) Schematic illustration of a class II cytochrome P450 redox system. (B) and (C) Result of sequence analysis of CYP65AH1 (L3H.Ap) of *A. pullulans* conducted by different online tools. Green: N-terminal sequence, blue: predicted transmembrane domain, red: predicted heme binding site. (D) Schematic overview of variants designed for heterologous gene expression of L3H.Ap in *E. coli*.

Heterologous expression of L3H.Ap in *E. coli*

In order to integrate the protein L3H.Ap into the prepared *P. putida* production organism, first of all, heterologous gene expression in the most commonly used bacterial host organism *E. coli* was tested. *E. coli* was chosen for the initial test, because it is a bacterium, just as *P. putida*, has natively no CYP enzymes encoded in the genome,[218] and is, together with *S. cerevisiae,* the best-established host for terpenoid production so far.[1]

Since eukaryotic membrane-anchored proteins are often difficult to express in prokaryotic hosts, constructs with different modifications were created, based on different publications.[88,186,211,219] The gene of L3H.Ap was employed either in its native form or codon-optimized (.co) for *E. coli*. In addition, the sequence encoding the N-terminus was varied (_N-var)[211] or replaced by the codons for a 6xHis-tag (-His) (Figure 18 D). Furthermore, as second codon the base pairs for alanine were inserted into the gene sequence, because it is described to enhance expression of eukaryotic CYP proteins in bacterial systems; codons that can prevent secondary structures near the initiation site are supposed to render it more accessible to translation by ribosomes.[104] The different L3H.Ap gene variants were constructed into the pETDuet™-1 vector backbone. Furthermore, different versions of the limonene-3-hydroxylase of *Mentha* x *piperita*, PM17,[58,186] were created to compare the plant enzyme with the fungal one.

To provide electrons for the CYP reactions, the putative CYP reductase enzyme of *A. pullulans* (Red.Ap, for more information see Chapter 3), as well as the cytochrome P450 reductase of *A. thaliana*, ATR1,[212,213] were to be expressed together with the L3H.Ap and PM17 variants. ATR1 has been described in literature to be active in *E. coli*.[220,221] Different variants of the reductase genes were constructed in the pCDFDuet™-1 plasmid.

As a kind of positive control, a variant of the bacterial CYP enzyme P450cam (P450cam_Y96F_V247L[101]_C334A[202]) was used, which was integrated in the pET24 vector together with two enzymes required for its functionality (putidaredoxin (Pd) and putidaredoxin reductase (PdR)). Previous experiments had already shown that *E. coli* BL21(DE3) expressing these enzymes is able to transform externally added (+)-limonene into *trans*-isopiperitenol and several side products (H. Schewe, unpublished data).

To first of all test the functional expression of the reductase enzymes, a reductase assay was conducted, following a protocol published by Guengerich *et al*. in 2009.[214] As electron acceptor cytochrome c was used (Figure 19 A) and the cytochrome c reduction rate was measured over time. As a negative control, the pCDF plasmid encoding a control protein (Sfp: phosphopantetheinyl transferase of *Bacillus subtilis*, involved in fatty acid biosynthesis) was employed to get a value of the *E. coli* background.

The experiments with cell lysate of *E. coli* BL21(DE3) strains, harboring the different reductase expression plasmids, showed that, compared to the *E. coli* background (Sfp) and the assay buffer with cytochrome c and NADPH but without cell lysate (without), the different versions of the putative CYP reductase gene of *A. pullulans* (Red) showed a reductase activity when NADPH was added as a cofactor (Figure 19 B). The highest activity was observed for the variant with a truncated N-terminus and the addition of a 6xHis-tag (Red-His). This result is in accordance with previous observations; it has been described that N-terminal deletions have proven successful for expression of membrane-bound eukaryotic enzymes in *E. coli* in many cases, including CYPs and CYP reductases.[88,104,222]

With both variants of the CYP reductase of *A. thaliana,* ATR1, codon-optimized for *E. coli* (ATR1.co and ATR1.co_N-Var), no activity compared to the *E. coli* background could be observed (Figure 19 B), although an activity of this protein in *E. coli* has been reported before.[220,221] However, it could be worth testing if with the native gene sequence or a truncation of the N-terminus better activities can be achieved. At least for the putative CYP reductase of *A. pullulans,* the best results were obtained with the non-codon-optimized gene sequence and the N-terminus-truncated variants.

With NADH as a cofactor, no reductase activity could be detected (Figure 19 B, right side). This was already expected, because for most CYP reductase enzymes and other components of CYP redox systems NADPH seems to be the preferred reductant. However, for some redox chain elements also activity with NADH has been described in literature.[75,223]

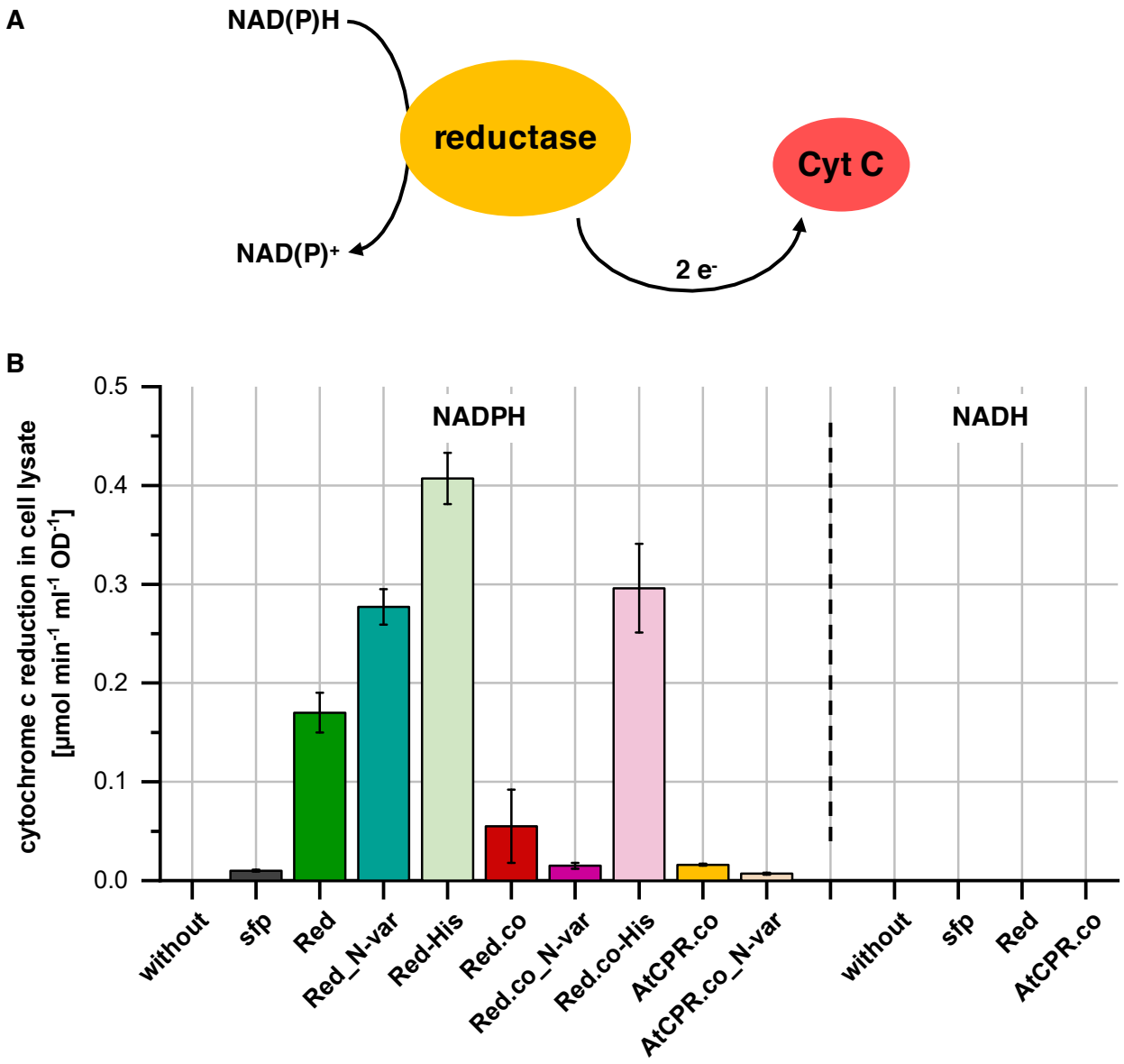

Figure 19: NAD(P)H-cytochrome c reduction assay. As electron acceptor cytochrome c was used (A). Reductase activity in cell lysate of *E. coli* strains, harboring different reductase expression plasmids (pCDF backbone), was measured with NADPH or NADP as cofactor (B). without: assay mix without cell lysate; Sfp: negative control, pCDF plasmid with *sfp* gene (phosphopantetheinyl transferase of *Bacillus subtilis*); Red: native sequence of putative CYP reductase gene of *A. pullulans*; Red_N-var: putative CYP reductase gene of *A. pullulans* with altered N-terminus; Red-His: putative CYP reductase gene of *A. pullulans* with truncated N-terminus and addition of 6xHis-tag; Red.co: putative CYP reductase gene of *A. pullulans* codon-optimized for *E. coli;* Red.co_N-var: putative CYP reductase gene of *A. pullulans* codon-optimized for *E. coli* with altered N-terminus, Red.co-His: putative CYP reductase gene of *A. pullulans* codon-optimized for *E. coli* with truncated N-terminus and addition of 6xHis-tag; ATR1.co: CYP reductase gene ATR1 of *A. thaliana* codon-optimized for *E. coli*; ATR1.co_N-var: CYP reductase gene ATR1 of *A. thaliana* codon-optimized for *E. coli* with altered N-terminus. The data points and error bars represent the mean values and standard deviations of three biological replicates (n = 3).

Once the functionality of the reductase enzyme of *A. pullulans* in *E. coli* could be confirmed, the strains were transformed with the different CYP expression plasmids (pET backbone, see Table 1) and a (+)-limonene biotransformation experiment was conducted. For the experiment, strains with combinations of different CYP enzyme and CYP reductase variants were used. As a negative control, an *E. coli* strain harboring the pCDF_Sfp plasmid and the pETDuet™-1 empty vector was employed. As a positive control for CYP activity in *E. coli*, the pET24 vector with a P450cam variant (H. Schewe, unpublished data) was used. GC-MS measurements showed that only with the bacterial P450cam variant *trans*-isopiperitenol production could be obtained. In the samples with L3H.Ap or PM17 also small *trans*-isopiperitenol peaks could be detected, but the amounts obtained differed only slightly or not at all from the values of the negative control with the empty plasmid backbone (data not shown).

To further investigate if the genes are expressed in the *E. coli* BL21(DE3) cells in a functional form, protein expression was analyzed via SDS-PAGE. While the majority of the expressed P450cam variant could be found in the soluble fraction of the cell lysate, the L3H and reductase enzymes from *A. pullulans, M.* x *piperita* and *A. thaliana* were mainly, if not completely, detectable in the insoluble/pellet fraction (Figure 20 A), probably as inclusion bodies. This could explain the lack of activity in the biotransformation experiment. However, based on the SDS-PAGE results, it cannot be excluded that the proteins are found in the insoluble pellet fraction, because they are anchored in the bacterial cell membrane.[88,104,219]

For the optimization of heterologous gene expression in *E. coli* several strategies are described, reviewed in many publications.[88,104,207,224,225] These include parameters such as the choice of a suitable host strain, promoter, transcription strength, codon usage, culture media supplements, incubation temperature and other growth conditions. However, heterologous expression of CYP genes in *E. coli* remains a trail-and-error process.[219,225]

Both plasmids, pETDuet™-1 and pCDFDuet™-1, contain the T7 promoter and the *lac* operator. Gene expression can be induced by IPTG (isopropyl-β-D-thiogalactoside) addition. T7 is a strong, leaky promoter,[207,226] which leads to a high level of gene expression. If the proteins accumulate to fast, it can result in the formation of inclusion bodies.[88] To slow down the expression rate, alteration of expression temperature and cultivation without IPTG induction or with autoinduction medium was investigated. SDS-PAGE analysis showed that without IPTG induction and with autoinduction medium, as well as with lower cultivation temperatures proteins are still expressed, but in a smaller quantity than with IPTG induction. However, expressed proteins remained mostly or completely in the insoluble fraction and no improvement in regard to solubility could be obtained in this way (data not shown).

In a further attempt, expression in *E. coli* strains with additional features was investigated. These features included the expression of chaperone plasmids (TaKaRa Chaperone plasmid set) in *E. coli* BL21(DE3) as well as the use of specific *E. coli* strains. *E. coil* ArcticExpress(DE3) (Agilent Technologies, Inc.) contains a chaperone plasmid and is optimized for gene expression at low temperatures. *E. coli* Lemo21(DE3) (New England BioLabs Inc.) contains the Lemo System™ and allows a more tunable T7 expression.[227,228] In addition, supplementation of the cultivation medium with thiamin HCl and 5-aminolevulinic acid (5-ALA) was investigated. 5-ALA is a heme-precursor and has been shown to be beneficial for expression of active CYPs, because the incorporation of the heme group into the active center of the enzyme is one of the major challenges.[88] However, all these attempts to obtain the proteins of *A. pullulans, M.* x *piperita* and *A. thaliana* in a soluble form in *E. coli* were unsuccessful. Figure 20 B shows exemplarily the SDS-PAGE analysis of the heterologous gene expression experiments with *E. coli* Lemo21(DE3).

As indicated before, based on the SDS-PAGE analyses performed, it cannot be excluded that the proteins are anchored in the bacterial cell membrane via their N-termini and are therefore not found in the soluble fraction of the cell lysate. However, for the variants with truncated N-terminus and the addition of a 6xHis-tag soluble expression should be possible.

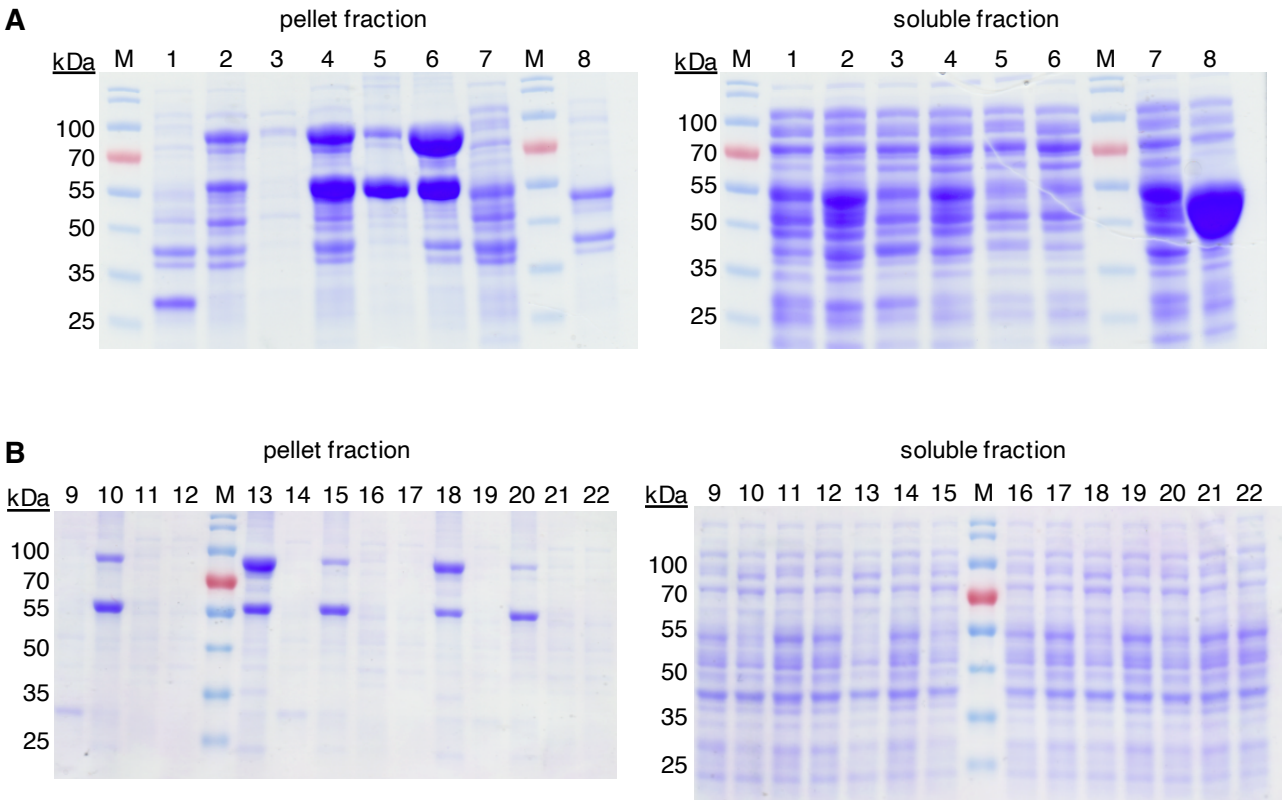

Figure 20: SDS-PAGE analyses of heterologous gene expression of CYP and CYP reductase variants in different *E. coli* strains. The different gene variants were expressed from the pETDuet™-1 or the pCDFDuet™-1 plasmid backbone. As size standard (M) the *PageRuler™ Unstained Protein Ladder* (Thermo Fisher Scientific Inc.) was used. Expected protein sizes: L3H.Ap: 58 kDa, Red.Ap: 77 kDa, PM17: 58 kDa, ATR1: 77 kDa, P450cam variant: 47 kDa. Left: unsoluble/pellet fraction, right: cleared cell lysate/soluble fraction. (A) Expression in *E. coli* BL21(DE3) cells, TB medium, induction with 0.1 mM IPTG. 1: pCDF_sfp pETDuet™-1 (negative control), 2: pCDF_Red.Ap pET_L3H.Ap, 3: pCDF_Red.Ap_N-var pET_L3H.Ap_N-var, 4: pCDF_Red.Ap-His pET_L3H.Ap-His, 5: pCDF_Red.Ap.co pET_L3H.Ap.co, 6: pCDF_Red.Ap.co-His pET_L3H.Ap.co-His, 7: pCDF_ATR1.co pET_PM17.co, 8: pCDF_Red.Ap_N-var pET24_P450cam_Pd_PdR. (B) Expression in *E. coli* Lemo21(DE3) cells, autoinduction medium, with 100 (9 – 13), 200 (14 – 18) or 500 µM (19 – 22) L-rhamnose. 9/14/19: pCDF_sfp pETDuet™-1 (negative control), 10/15/20: pCDF_Red.Ap-His pET_L3H.Ap-His, 11/16/21: pCDF_Red.Ap.co pET_L3H.Ap.co, 12/17/22: pCDF_Red.Ap.co_N-var pET_L3H.Ap.co_N-var, 13/18: pCDF_Red.Ap.co-His pET_L3H.Ap.co-His.

Despite various attempts, so far, it was not possible to express L3H.Ap in a functional form in *E. coli.* However, although no soluble expression of the reductase enzymes could be detected by SDS-PAGE either, the reductase assay performed showed reductase activity of at least some protein variants.

A further approach to obtain the expression of functional CYPs could be to fuse protein-solubility-promoting tags, such as GST (glutathione S-transferase) or MBP (maltose binding protein),[225] to the proteins of interest. In addition, if the proteins are present in the *E. coli* cells as inclusion bodies, refolding of these protein aggregates could be investigated. For this purpose, several approaches have been described in literature, for instance, by Singh and

Panda (2005)[229] or Basu *et al.* (2011).[230] Furthermore, other *E. coli* strains could be tested as host organisms, such as *E. coli* Origami (Novagen®), C41(DE3) or C43(DE3).[231] The latter two were developed for the expression of toxic and membrane proteins.[231,232] Also the use of a low-copy plasmid to obtain a low expression level could lead to expression in a functional form.[233] In addition, supplementation of the cultivation medium with hemin to increase the supply of the CYP cofactor heme could be tested.[234,235] In order to enable the activity of the CYP enzymes, it must be further investigated, whether the enzymes have the complete redox chain at their disposal that they need for their function. Apart from a suitable CYP reductase enzyme, further modules might also be required for efficient functionality such as cytochrome b_5.[236–238] With regard to the optimization of electron supply, a fusion between reductase and CYP[239] or an adjusted ratio between CYP and CYP reductase expression[233] could also improve activity.

Chapter 8 – Concluding discussion and outlook

The following chapter gives an overall discussion about this work and an outlook. For a detailed discussion of each part of this thesis and its specific role in the respective research area, please also see the discussion sections of the corresponding chapters/publications/ manuscript.

The aim of this thesis was to develop the basis for a microbial cell factory for monoterpenoid production. In particular, the conversion of (+)-limonene into (+)-*trans*-isopiperitenol should be realized. For this purpose, two components, a suitable enzyme as "production machinery" and a modified bacterium strain as the "production facility", were to be developed separately and then combined within one microorganism.

As machinery, two enzymes for the hydroxylation of (+)-limonene to (+)-*trans*-isopiperitenol with high regio- and stereoselectivity on carbon atom 3 from the fungi *A. pullulans* (L3H.Ap) and *H. carpetanum* (L3H.Hc) could be identified, and successfully expressed in *P. pastoris* (see Chapter 3). Even if the selectivity of the fungal enzymes is not yet as high as that of the PM17 enzyme from peppermint (90 % vs. 100 % regioselectivity), it provides a solid basis for further optimization, for example by means of protein engineering. Compared to the bacterial CYP variants, the fungal enzymes are already much more specific.[102]

As a production facility (host organism), a *P. putida* strain with improved tolerance towards isopiperitenol could be developed (see Chapters 4 and 5). *P. putida* KT2440_Δ10nt$_{ttgABC}$ overexpresses the TtgABC efflux system and is now able to grow relatively well with up to 25 mM isopiperitenol, corresponding to around 4 g L^{-1} cell suspension.

Despite several attempts to heterologously express L3H.Ap in *E. coli*, no functional expression in the prokaryotic host could be obtained (see Chapter 7). Due to these results, expression of the CYP gene in the prepared *P. putida* production organism KT2440_Δ10nt$_{ttgABC}$ has not, as yet, been tested.

<u>Further steps to develop the fungal L3H enzyme towards biotechnological applications</u>

Apart from the optimization parameters evaluated so far (codon-optimization, variation of N-terminal sequence, variation of expression strain and cultivation conditions), there are many more adjustments that could be performed in order to obtain a functional protein version of L3H.Ap in *E. coli.* Such strategies to improve heterologous gene expression are summarized in numerous review articles.[60,88,95,104,225,240] Additionally, expression directly in the intended production strain *P. putida* could be investigated as heterologous expression efficiency can vary greatly between different host organisms.[1,97,241–243] For expression in *P. putida,* the described pMiS4 plasmid could be used (see Chapter 6). However, while in contrast to the

parental plasmid pMiS1, the pMiS4 vector does not affect cell growth, it is a low-copy plasmid. Whether this is of advantage for the functional expression of the genes needs to be investigated. It has already been shown that low-copy plasmids can perform as well as or better than high-copy plasmids for metabolic engineering of bacteria.[233,244] However, it usually also results in lower amounts of target protein in the whole-cell biocatalyst, as shown for *gfp* expression with the pMiS1 and the pMiS4 plasmid (see Chapter 6).

If functional expression of the genes of interest can be obtained in *P. putida*, integration of the respective genes into the genome should be considered for long-term stable expression. For this purpose, different methods have been established in the last few years.[117,122,245]

Furthermore, the use of the L3H.Ap enzyme by expression in the yeasts *S. cerevisiae* and *P. pastoris* could be considered, if the reactant and product toxicity is reduced by appropriate methods. Compared to *P. putida*, yeasts such as *S. cerevisiae* seem to be much less tolerant towards monoterpenoids.[137] A reduction of the toxic effect of monoterpenes and monoterpenoids could possibly be achieved by bioprocess engineering including strategies such as *in situ* product removal.[246] Another possibility would be the transfer of monoterpenoid resistance mechanisms to yeast. It has already been shown that the heterologous expression of an efflux system of the fungus *Grosmannia clavigera* in *S. cerevisiae* increases tolerance towards some monoterpenes, including limonene, pinene and 3-carene.[247] Also evolutionary adaptation of the yeast strains to the bioprocess reactant and product could improve cell fitness, as demonstrated for limonene.[248]

In order to increase functional expression of L3H.Ap in *S. cerevisiae* and *P. pastoris* to obtain higher product titers, different strategies could be applied, including N-terminal modifications and CYP reductase overexpression.[88] In addition, studies have shown that alteration of cultivation conditions, such as the carbon source provided or supplementation of the cultivation medium with required cofactor precursors can also positively influence the performance of CYP enzymes in yeast.[234,235]

While L3H.Ap already demonstrates 100 % stereospecificity, regioselectivity can still be improved, because apart from *trans*-isopiperitenol, *p*-1,8-menthadien-4-ol is formed as a by-product (< 10 %). In *p*-1,8-menthadien-4-ol the hydroxy group is attached to carbon atom 4 instead of 3 (see Chapter 3). To further increase the regioselectivity of the fungal enzyme, protein engineering strategies could be applied. Such methods include, for instance, the identification of the amino acids responsible for substrate conversion in the active center of the enzyme and the subsequent generation of a mutant library.[100,249–251]

Apart from the fact that (+)-*trans*-isopiperitenol is required for the intended (-)-menthol production process, it might also be worthwhile to further identify the flavor and fragrance properties of the by-product and its derivatives. *p*-1,8-Menthadien-4-ol is also referred to as

limonene-4-ol, which is an intermediate of terpinen-4-ol synthesis.[252] Terpinen-4-ol as well as limonene-4-ol are used in industrial applications as synthetic perfume and flavoring substances.[253] To ensure supply, patents for synthetic limonene-4-ol production have been filed.[252,253] Furthermore, it has been shown for other natural flavor and fragrance substances that by-products can contribute decisively to the overall aroma. An example for this is patchouli essential oil.[98,254,255]

Implementation of the second reaction step of the two-step menthol synthesis

If the efficient production of (+)-*trans*-isopiperitenol with *P. putida* or yeast can be achieved, a further step would be the implementation of the second reaction of the intended process towards (-)-menthol production. For the conversion of (+)-*trans*-isopiperitenol into (-)-menthol, two double bonds in the molecular structure of (+)-*trans*-isopiperitenol, one in the ring structure (between carbon atom 1 and 2) and one in the aliphatic residue (between carbon atom 8 and 9), have to be hydrogenated. This could be achieved either by further optimization of chemical hydrogenation strategies[190,256,257] or by the investigation of enzymes that can catalyze the intended hydrogenation reactions. In literature, organisms and enzymes, such as enoate reductases, have already been described that, for instance, can convert carvone into dihydrocarvone by hydrogenation of the double bond in the ring.[189,258–264] Such enzymes are, for example, XenB from *Pseudomonas* sp.[265] or OYE1 (old yellow enzyme 1) from *Saccharomyces pastorianus*.[266] A double bond at the same position as in carvone can be found in the molecular structure of *trans*-isopiperitenol (between carbon atom 1 and 2). If a carbonyl group is required for substrate recognition, it could be introduced by a suitable alcohol dehydrogenase enzyme via oxidation of the hydroxy group, and then reduced again after hydrogenation by the same enzyme.[267,268] Apart from these examples, several other enzymes with hydrogenation abilities have been reported.[260-268] Whether these enzymes are also able to catalyze the two hydrogenation reactions from (+)-*trans*-isopiperitenol to (-)-menthol would have to be investigated. The advantage of a complete biotechnological conversion of (+)-limonene into (-)-menthol, compared to a chemical hydrogenation as second step, would be that according to U.S. and European Union (EU) flavor regulations, aroma compounds that have been produced from natural raw materials with the use of microorganisms or isolated enzymes can be labeled as “natural”, if these substances are known to exist in nature.[3,41]

Implementation of a *de novo* synthesis

A further step towards an economic biotechnological process for (-)-menthol production would be the development of a *de novo* synthesis, starting from simple carbon sources such as glycerol. For this, the production of the monoterpene(oid) precursors IPP and DMAPP, as well

as GPP, would have to be optimized to redirect cell metabolism to terpene synthesis (see Chapter 2). In addition, a suitable terpene synthase would have to be integrated into the cell factory, to transform the general monoterpene(oid) precursor GPP into (+)-limonene. For this purpose, several terpene synthases have been described in literature,[277] including (+)-limonene synthase from citrus (*Citrus limon*) and caraway (*Carum carvi*).[71,278] Compared to a biotransformation with externally added reactant, *de novo* synthesis has the advantage that limonene is produced inside the cells, avoiding limitations due to poor limonene import.[279] Over the last decades, many efforts have been made to optimize the *de novo* synthesis of terpenes and terpenoids in microorganisms and to obtain high production titers, rates and yields (TRYs).[1,43,98,280] However, it has been shown that this cannot be achieved by simply overexpressing the genes encoding the proteins involved, such as the enzymes of the MEP and MVA pathway, or by redirecting the flux towards the synthesis of specific terpene(oid)s. Rather, the metabolic flux has to be harmonized with cell growth to achieve maximum overall production.[1,43] This has to do, among other things, with the fact that terpenes are needed for the synthesis of essential cell components.[6] Furthermore, the toxicity of intermediates and feedback inhibition can also reduce the productivity of the metabolic pathways involved in terpene synthesis.[43] Such limitations can be overcome, or at least reduced, by the introduction of optimized or alternative enzymes and entire artificial pathways,[43,98,281] or the use of dynamic regulators.[282–284] In addition, the implementation of enzymes with increased catalytic activities could improve terpene(oid) production. Since terpenes and terpenoids are usually produced in low concentrations in living cells, it can be expected that the enzymes of the terpene metabolic pathways are probably not designed to efficiently redirect the central metabolism towards terpene(oid) production.[43] Furthermore, apart from enzyme optimization and balancing, also incorporation of efflux pumps to transport the end products out of the cells, or any other kind of product removal could be efficient to increase the flux through the desired pathway.[43,285,286] Despite various strategies, only a few terpenes and their derivatives, in particular sesquiterpene(oid)s, can currently be produced *de novo* somewhere near the theoretical yield. Especially monoterpenes and monoterpenoids are far away from it.[43] One reason for this is probably the low availability of the monoterpene(oid) precursor GPP in microbial cells, compared to the sesquiterpene precursor farnesyl diphosphate (FPP), because in microorganisms most of GPP is efficiently further converted to FPP.[1,43,287] This can be circumvented, for example, by heterologous expression of suitable GPP synthase (GPPS) proteins or by engineering native FPP synthases to produce GPP preferentially.[1] It has been shown, for instance, that overexpression of GPPS in *E. coli* can increase geraniol production by 6-fold.[288]

Besides GPPS, also terpene synthases are often a bottleneck in monoterpene and monoterpenoid production as demonstrated for limonene synthesis by Alonso-Gutierrez and colleagues (2015)[289] and for geraniol production by Jiang *et al.* (2017).[290]

The raw material limonene

In addition to be used as substrate for biotransformation processes, (+)-limonene has a wide variety of applications, including its use as a flavor and fragrance compound, as solvent or as feedstock for fine chemical production.[291–293] In order to become more independent from plant-based production, many efforts have already been made in recent years to biosynthesize limonene;[188,278–280,291,294–296] these approaches could also be taken into account for the development of a *de novo* process for (-)-menthol production. However, a techno-economic analysis of microbial limonene production, recently conducted by Sun and colleagues (2020), indicates that "Given the current state of technology, a 20-fold improvement in productivity would be necessary", "[…] for the process to be economically viable".[292] But research is ongoing and higher titers and space-time yields are regularly published.[42]

The implementation of the necessary steps towards a *de novo* process for (+)-limonene production has become even more important in the last few years. While in previous times (+)-limonene was traded as a kind of waste by-product from the production of orange juice[53,293] with a value of around 0.4 US$ per kg fifteen years ago, the market price of limonene had increased tremendously with 3 - 4 US$ per kg in 2011, to up to around 9 - 10 US$ per kg by 2018, accompanied by strong fluctuations.[41,293] In a recent publication from 2020, even a range of the market price from 7 to 20 US$ per kg is indicated.[292] This price increase of limonene was caused, among others, by a drastic reduction in the citrus fruit harvest in Brazil and Florida,[297,298] since limonene is currently mainly extracted from citrus peels.[291,293] Reasons for these poor harvests included the strong hurricanes in Florida in recent years and that important citrus production areas in Brazil and the USA have been infested by the bacterial disease Huanglongbing (HLB) ("citrus greening disease").[293-295]

Compared to limonene, carbon sources such as glycerol or glucose are relatively cheap, with prices of around 0.115 US$ per kg for crude glycerol (80 % pure) and 0.4 - 0.6 US$ per kg for glucose.[292] While glucose can be extracted from sugar cane, fruits, vegetables or grains,[302] glycerol is a by-product of biodiesel and bioethanol production.[303,304] However, for the future, it would be even more socially acceptable if the cell factories could utilize sugars and waste streams that cannot be used for human food production. Such carbon sources could be, for instance, (ligno-)cellulosic biomass from e.g. corn plant or cereal straw,[305–307] which is, in addition, very cheap (30 – 45 US$ per dry ton, as of 2007).[308] With regard to this, using

pseudomonads as microbial cell factories has the advantage that they are able to assimilate a variety of feedstocks, either natively or engineered to do so.[107,109,112,309–314]

Further economic considerations for the use of the fungal L3H enzyme

In addition to the development of a *de novo* process, the production titer of the conversion of (+)-limonene with the fungal enzyme L3H.Ap would have to be considerably improved, since an output of ca. 45 - 90 mg (+)-*trans*-isopiperitenol per liter concentrated yeast cell suspension (300 - 600 µM) is still far too low to form an economic industrial process; this is mainly because the prices for flavors and fragrances are relatively low compared to high-value chemicals, such as drugs and medical ingredients. In 2012, the market price per kg (-)-menthol was around 30 - 60 US$,[279] regardless of whether it was chemically produced or extracted from plants. In addition, the menthol price has been subject to strong fluctuations in the past.[315] Therefore, even if a complete biotechnological production route from glycerol to (-)-menthol were available, it is questionable whether the companies would implement it. The acquisition of new manufacturing equipment is expensive and, unless consumers are willing to pay more for non-chemically synthesized menthol in their toothpaste, it is not profitable for companies to invest in this.

However, even though such a biotechnological production route for (-)-menthol might never be profitable, parts of this thesis could still be used for the synthesis of other fine and specialty chemicals. The experiments have shown that, apart from the limonene-3-hydroxylase activity, the fungal enzyme L3H.Ap is also able to transform other substrates, for instance α- and β-pinene, into specific products. If this path is investigated further, it may be possible to identify other, more valuable products for which the profit margin would be higher compared to menthol due to a higher selling price. The substances α- and β-pinene can be found in high concentrations in turpentine oil, a paper and pulp industry waste, and are, therefore, available in bulk at a low price.[185,316] The potential products of α-pinene conversion, verbenol and verbenone, are natural insect pheromones and have a high application potential as environmentally friendly pesticides, for example as “BeetleBlock - Verbenone as a treatment against pine beetles”.[317] Furthermore, verbenone also serves as a synthesis building block for taxol (a cancer drug) and taxol analogues[318] and, in addition, is a character impact compound of rosemary oil.[53]

Further potential applications of the insights on monoterpene(oid) tolerance

Based on the identified monoterpenoid resistance mechanisms of *P. putida* and the findings from the toxicity assays with verbenone and other monoterpenoids (see Chapter 4), it is likely that the modified *P. putida* strain KT2440_Δ10nt$_{ttgABC}$ is not only highly tolerant towards

isopiperitenol, but also towards other hydroxylated monoterpenes such as verbenol. With regard to this, even if heterologous expression of the fungal L3H enzyme in *P. putida* fails, the production facility, i.e. the strain with high monoterpenoid tolerance potential, could still be used for the biotechnological production of other monoterpenoids. Due to its modular architecture, terpenoid biosynthesis is especially well suited for the microbial cell factory concept; in theory, a platform host engineered for high tolerance towards several monoterpenoids and for a high flux towards the central C_5 prenyl diphosphate precursors and GPP, enables the production of a broad range of target monoterpenoids just by varying the pathway modules converting GPP to the product of interest. Such pathway modules could be, for example, oxidizing enzymes.[44,98,277,319] In literature, several bacterial CYP enzymes have been described which can be easily expressed in prokaryotes with high activities and which oxidize monoterpene hydrocarbons with high selectivity.[97,102,138,320–322]

However, as the experiments within this thesis also demonstrated, while the developed tolerance-improved *P. putida* strain, utilizing Ttg efflux pump overexpression, could presumably be used for the production of most monoterpene alcohols, for some products, such as geranic acid, host organisms with other tolerance phenotypes would be necessary (see Chapter 4). For geranic acid production, it would probably be more favorable to create a *P. putida* KT2440 strain with a deletion of the Ttg efflux pump systems. In this case, a suitable process solution for the biotransformation would have to be implemented, in order to keep the toxic effect of the reactant geraniol on this efflux-deficient production strain as low as possible. One option would be, for example, a gradual addition of the reactant over time to maintain the concentration in the medium below a critical value. This could be realized by the addition of a solvent layer (second distinct organic phase) to achieve a controlled substrate release from the organic to the aqueous phase.[323,324] For such an approach, however, it must first be determined whether such an efflux-deficient *P. putida* mutant can still tolerate the solvents used previously for this purpose.[246,325,326] A separation of growth and production phase[320-322] cannot be applied in this case, as the oxidation of geraniol to geranic acid seems to be a growth-coupled process (F.M. Schempp, unpublished data).

The experiments within this thesis also showed that cytotoxicity is not a general characteristic of all monoterpenes and monoterpenoids as stated in publications on biotechnological production of these substances.[1] Instead, at least in regard to *Pseudomonas putida,* the level of toxicity highly depends on the molecular structure and functional groups, both related to the $\log P_{ow}$ value. While the monoterpenoids inhibited the growth of the *P. putida* strains to varying degrees, the addition of monoterpene hydrocarbons, such as limonene or terpinene in amounts of up to 200 mM (around 27 g L^{-1}) had no effect (see Chapters 4 and 5). This amount is far above the titers which can currently be produced *de novo* with microorganisms,[43]

allowing even the use of *P. putida* wild-type strains for the production of hydrocarbons without the need to strengthen resistance mechanisms; but as soon as yields increase, export pumps could play a more important role. And while the output of *de novo* production is still quite low, the product titers reached by single- or few-step biotransformation processes to obtain, for instance, oxyfunctionalized monoterpenes are in completely different dimensions.[137,138,321,330] In addition, it has been demonstrated for *E. coli* that efflux pump expression can increase, for example, limonene production, even if the titers are not yet toxic to the cells.[285] In this case, limonene export may help to alleviate product inhibition of metabolic pathway enzymes and thereby improve production.[285] Furthermore, the ability to tolerate a level of 200 mM externally added limonene only applies specifically to some microbes, e.g. *Pseudomonas* strains. For other organisms, such as *E. coli*, the tolerance limits are much lower. With limonene an effect on the growth of *E. coli* could already be observed at a amount of 12 mM (1.6 g L^{-1}) (F.M. Schempp, unpublished data). For *S. cerevisiae,* the minimal inhibitory concentration (MIC) values are even lower (0.44 mM, 60 mg L^{-1}).[331] If, nevertheless, a production with *E. coli* is desired, a transfer of the monoterpenoid resistance-mediating efflux pump genes, described in this thesis, to *E. coli* production strains could be considered. It has already been reported that solvent tolerance mechanisms could be successfully transferred from *P. putida* to *E. coli* and other bacteria, including solvent-sensitive pseudomonads.[175,285,332]

Apart from the presented monoterpenoid resistance mechanisms, another option to overcome cytotoxicity could be to use cell-free biosynthesis and thereby completely decouple cell growth from production.[43] In such a self-sustainable *in vitro* system with 27 purified enzymes, a limonene titer of 12.5 g L^{-1} could be reached after 7 days. In addition, in the same system also pinene as well as sabinene could be produced.[333] However, those systems still have their own challenges, such as producing at low-cost and large scale.[334]

Biological function of L3H enzymes in fungi

Besides the development of a whole-cell biocatalyst, the results in this thesis on fungal L3H enzymes raise the interesting question as to why different fungi possess enzymes that can specifically hydroxylate certain monoterpenes, such as limonene or pinene. It is described that CYP enzymes can contribute to detoxification of plant defense compounds (phytoalexins) or to degradation and utilization of substances as carbon source.[93,335,336] However, in toxicity assays with *A. pullulans*, growth of the fungus was more inhibited by externally added isopiperitenol than with limonene (E. Biewirth, unpublished data). These results contradict the hypothesis that the hydroxylation reaction leads to detoxification. Nevertheless, this finding under laboratory conditions does not exclude that the tested substances do not affect the fungus differently under changing environmental conditions. Furthermore, it is also

conceivable that the natural substrate of the fungal L3H enzymes is actually a totally different one and that they can only by chance also accept limonene and pinene as substrates. Moreover, even if the hydroxylated form of the natural substrate would be more toxic than the reactant, it cannot be ruled out that there are no other enzymatic reactions in the metabolism of the fungi that would cause a rapid, further degradation of the intermediate product into a non-toxic end product. The data obtained in this thesis so far only show that *A. pullulans* and other fungi are apparently not able to further transform or degrade *trans*-isopiperitenol under the conditions tested (see Chapter 3).

Brief excursion on further aspects to consider when discussing the transition from conventional to biotechnological production

For scientists in the advancing field of biotechnology, future advantages of bio-production and its potential to contribute to societal challenges are obvious and are often listed in publication and lecture introduction:

- sustainable and environmentally-friendly production (e.g. preventing negative impacts on biodiversity and the consumption of limited and rare natural resources, avoiding the use of chemicals in agriculture),
- higher reliability and price stability compared to natural agriculture-based sources (avoiding seasonal variations, quality and price fluctuations, geopolitical issues, security of supply),
- usage of renewable resources and waste streams (detachment from an economy based on fossil resources),
- running under mild process conditions,
- elevated regio- and stereoselectivity, and
- the possibility of manufacturing products considered as “natural”,

are to name just a few.[1,43,47,98,185] However, it remains to be seen whether biotechnology can actually fulfill these expectations.

In addition to all the promises made to promote biotechnological research projects, there are a number of other aspects that need to be considered when debating the consequences of a transition from conventional to the biosynthetic/biotechnological production of fine chemicals such as flavor and fragrance compounds. These topics were recently discussed in detail by Ribeiro and Shapira (2019) with regard to menthol.[47] Among them are societal aspects as well as public perception, market preference and regulatory aspects, such as risk assessment and labeling.[47,337]

Menthol is a ubiquitous compound that most people encounter in their everyday lives. Therefore, when discussing the replacement of agricultural production by biotechnology, the

aspect of public perception and market acceptability has to be considered. This alone might determine the success or failure of biotechnologically-produced products.[47] Nevertheless, far too little has been done, as yet, to communicate the potential benefits of biotechnological production with genetically modified organisms (GMOs) to the public. On the contrary, with increasing development in the field of biotechnology, the population's fear of products manufactured in this way is growing.[337] This is reflected in our everyday lives, for instance, in the fact that the label "GMO-free" or "without genetic engineering" has presently become a label which stands for quality of food products; up to now, more than 12,000 products display such a label in German supermarkets.[338] In addition, the term "gene free", especially for milk, is widespread. The use of the word “gene” here is a misleading shortening of the term “genetic engineering”, since all foods produced from living organisms contain their genes.[339] Another example for the poor image of fabrication with genetically modified organisms is that companies which already use biotechnology to produce flavor and fragrance compounds, for instance Evolva or Isobionics,[98] do not communicate this openly but use phrases such as “manufactured by […] fermentation technology (‘Similar to brewing beer’)”[340] or by publishing explanation videos to link their production strategies to baking with yeast.[341,342] These developments show that in addition to the many efforts carried out in research laboratories in order to make biotechnological production suitable for the future, there is also an urgent need to improve the image of genetic engineering to the public.

Apart from menthol, there are many other products for which biotechnological production processes are under development or are already marketed to replace plant-extracted or chemically-synthesized substances such as patchouli, orange, grapefruit and rose fragrance or vanilla.[47,98,341] Although at the moment these biotechnologically-produced products can be labeled as “natural”,[41] it is uncertain as to how these will be treated by labeling legislation, for example, in the USA and the EU in the future.[341] This legislation, in addition, will probably also influence public perception in different ways.

In order to actively work on improving public acceptance, information campaigns and education of the population are required. The public needs to understand how exactly biotechnological production can positively contribute to each individual's everyday life and the fear of the new technological possibilities has to be overcome.[337,341] In this regard, it may be beneficial to advertise intensely the areas where biotechnology, and in particular genetic engineering, is already contributing to everyday life, other than the food industry. Many people are unaware that it is already used for the production of a wide range of products, including pharmaceuticals;[308] an important example of this is the hormone insulin, which has been produced using genetically modified organisms for more than 25 years and has made life much easier for over 300 million insulin-dependent diabetics worldwide.[183] In total, more than 100

pharmaceutical substances manufactured with genetic engineering methods have now been approved in Europe with five to ten new products being added every year.[343]

These examples show that the responsible development of biotechnological production processes not only includes the scientific component, but also other aspects, such as how consumers experience the uncertainty of new technologies in their everyday practice.[47] In addition, as long as the costs of fossil fuels and feedstock for key chemicals do not exceed their respective critical thresholds, it will be difficult for industrial biotechnology and its products to become competitive, especially in the sectors of fuels and bulk-chemicals.[344]

In the end, the future marketability of biotechnology will depend on factors such as price developments and availability of fossil raw materials, price competitiveness of biotechnological processes, as well as future restrictions and regulations created by politics, society and global developments.

Conclusion

Scientists have proven the feasibility of some routes to biotechnological (-)-menthol production on a laboratory scale by biotransformation as a proof-of-concept.[59,345] However, the development of such processes, especially as *de novo* synthesis, is still in its infancy and new innovative ways around the bottlenecks, faced by these production pathways, have yet to be found in order to translate laboratory research into successful commercial manufacturing. This has also been stated as such in a recently published review article by Moser and Pichler (2019): “In contrast to the […] described biosynthesis of terpenoid backbones, further modifications of the hydrocarbons, as for example the conversion of limonene to menthol catalyzed by an enzyme cascade involving CYP450s from *Mentha spp.*, still remain a major challenge in microbial hosts. To our knowledge, no *de novo* biosynthesis of menthol from simple carbon source has been described, yet.”[1]

Within this thesis, another step towards a potential biotechnological production of (-)-menthol and other monoterpenoids could be demonstrated. However, there is still a long way to go to reach biotechnological monoterpenoid production on an industrial scale, both on a scientific and a societal level.

References – Chapters 1, 5, 7 and 8

For references of Chapters 2 - 4 and 6 see respective chapter.

1. Moser S, Pichler H. **2019**. Identifying and engineering the ideal microbial terpenoid production host. *Appl Microbiol Biotechnol* **103** 5501–5516.
2. Dickschat JS. **2019**. Terpenes. *Beilstein J Org Chem* **15** 2966–2967.
3. **2007**. Flavours and Fragrances. Springer-Verlag, Berlin, Heidelberg.
4. Schrader J. **2010**. Mikrobielle Oxidation von Monoterpenen. *BioSpektrum* **16** 555–557.
5. Dudareva N, Klempien A, Muhlemann JK, Kaplan I. **2013**. Biosynthesis, function and metabolic engineering of plant volatile organic compounds. *New Phytol* **198** 16–32.
6. **2015**. Biotechnology of Isoprenoids. Springer International Publishing, Cham.
7. de Carvalho CCCR, da Fonseca MMR. **2006**. Biotransformation of terpenes. *Biotechnol Adv* **24** 134–142.
8. Ruzicka L. **1953**. The isoprene rule and the biogenesis of terpenic compounds. *Experientia* **9** 357–367.
9. Miziorko HM. **2011**. Enzymes of the mevalonate pathway of isoprenoid biosynthesis. *Arch Biochem Biophys* **505** 131–143.
10. Frank A, Groll M. **2017**. The Methylerythritol Phosphate Pathway to Isoprenoids. *Chem Rev* **117** 5675–5703.
11. Dellas N, Thomas ST, Manning G, Noel JP. **2013**. Discovery of a metabolic alternative to the classical mevalonate pathway. *Elife* **2** e00672.
12. Vinokur JM, Korman TP, Cao Z, Bowie JU. **2014**. Evidence of a Novel Mevalonate Pathway in Archaea. *Biochemistry* **53** 4161–4168.
13. Kschowak MJ, Wortmann H, Dickschat JS, Schrader J, Buchhaupt M. **2018**. Heterologous expression of 2-methylisoborneol / 2-methylenebornane biosynthesis genes in *Escherichia coli* yields novel C11-terpenes. *PLoS One* **13** 1–15.
14. Drummond L, Kschowak MJ, Breitenbach J, Wolff H, Shi YM, Schrader J, Bode HB, Sandmann G, Buchhaupt M. **2019**. Expanding the Isoprenoid Building Block Repertoire with an IPP Methyltransferase from *Streptomyces monomycini*. *ACS Synth Biol* **8** 1303–1313.
15. Ignea C, Pontini M, Motawia MS, Maffei ME, Makris AM, Kampranis SC. **2018**. Synthesis of 11-carbon terpenoids in yeast using protein and metabolic engineering. *Nat Chem Biol* **14** 1090–1098.
16. Rudolf JD, Chang C-Y. **2020**. Terpene synthases in disguise: enzymology, structure, and opportunities of non-canonical terpene synthases. *Nat Prod Rep* **37** 425–463.
17. Eiben CB, De Rond T, Bloszies C, Gin J, Chiniquy J, Baidoo EEK, Petzold CJ, Hillson NJ, Fiehn O, Keasling JD. **2019**. Mevalonate Pathway Promiscuity Enables Noncanonical Terpene Production. *ACS Synth Biol* **8** 2238–2247.
18. Habermehl G, Hammann PE, Krebs HC, Ternes W. **2008**. Naturstoffchemie. 3., vollständig überarbeitete und erweiterte Auflage. Springer, Berlin, Heidelberg.
19. Janocha S, Schmitz D, Bernhardt R. **2015**. Terpene Hydroxylation with Microbial Cytochrome P450 Monooxygenases. *Adv Biochem Eng Biotechnol* **148** 215–250.
20. Breitmaier E. **2005**. Terpene. 2. Auflage. WILEY-VCH Verlag GmbH & Co. KGaA, Weinheim.
21. Charlwood BV, Charlwood KA. **1991**. Monoterpenes, p. 43–98. *In* Charlwood BV, Banthorpe DV (eds.), Terpenoids. Academic Press, London.
22. Gershenzon J, McConkey ME, Croteau RB. **2000**. Regulation of monoterpene accumulation in leaves of peppermint. *Plant Physiol* **122** 205–213.
23. Langenheim JH. **1994**. Higher plant terpenoids: A phytocentric overview of their ecological roles. *J Chem Ecol* **20** 1223–1280.
24. Nahrstedt A. **1982**. Strukturelle Beziehungen zwischen pflanzlichen und tierischen Sekundärstoffen. *Planta Med* **44** 2–14.
25. Helfrich EJN, Lin GM, Voigt CA, Clardy J. **2019**. Bacterial terpene biosynthesis: Challenges and opportunities for pathway engineering. *Beilstein J Org Chem* **15** 2889–2906.
26. Macías-Rubalcava ML, Hernández-Bautista BE, Oropeza F, Duarte G, González MC, Glenn AE, Hanlin RT, Anaya AL. **2010**. Allelochemical Effects of Volatile Compounds and Organic Extracts from *Muscodor yucatanensis*, a Tropical Endophytic Fungus from *Bursera simaruba*. *J Chem Ecol* **36** 1122–1131.
27. Fiers M, Lognay G, Fauconnier M-L, Jijakli MH. **2013**. Volatile Compound-Mediated Interactions between Barley and Pathogenic Fungi in the Soil. *PLoS One* **8** e66805.
28. Dickschat JS. **2016**. Bacterial terpene cyclases. *Nat Prod Rep* **33** 87–110.
29. Nakano C, Kim H, Ohnishi Y. **2011**. Identification of the First Bacterial Monoterpene Cyclase, a 1,8-Cineole Synthase, that Catalyzes the Direct Conversion of Geranyl Diphosphate. *ChemBioChem* **12** 1988–1991.
30. Nakano C, Kim H-K, Ohnishi Y. **2011**. Identification and Characterization of the Linalool/Nerolidol Synthase from *Streptomyces clavuligerus*. *ChemBioChem* **12** 2403–2407.
31. Dickschat JS, Nawrath T, Thiel V, Kunze B, Müller R, Schulz S. **2007**. Biosynthesis of the Off-Flavor 2-Methylisoborneol by the Myxobacterium *Nannocystis exedens*. *Angew Chemie Int Ed* **46** 8287–8290.
32. Wang C-M, Cane DE. **2008**. Biochemistry and Molecular Genetics of the Biosynthesis of the Earthy Odorant Methylisoborneol in *Streptomyces coelicolor*. *J Am Chem Soc* **130** 8908–8909.

33. Yassaa N, Peeken I, Zöllner E, Bluhm K, Arnold S, Spracklen D, Williams J. **2008**. Evidence for marine production of monoterpenes. *Environ Chem* **5** 391–401.
34. Gould MN. **1997**. Cancer chemoprevention and therapy by monoterpenes. *Environ Health Perspect* **105** 977–979.
35. Schrader J, Berger RG. **2001**. Biotechnological Production of Terpenoid Flavor and Fragrance Compounds, p. 373–422. *In* Rehm H-J, Reed G (eds.), Biotechnology Set. VCH Verlagsgesellschaft mbH, Weinheim.
36. Zhang N, Yao L. **2019**. Anxiolytic Effect of Essential Oils and Their Constituents: A Review. *J Agric Food Chem* **67** 13790–13808.
37. Bhatti HN, Khan SS, Khan A, Rani M, Ahmad VU, Choudhary MI. **2014**. Biotransformation of monoterpenoids and their antimicrobial activities. *Phytomedicine* **21** 1597–1626.
38. Dunlop MJ. **2011**. Engineering microbes for tolerance to next-generation biofuels. *Biotechnol Biofuels* **4** 32.
39. Tomko TA, Dunlop MJ. **2015**. Engineering improved bio-jet fuel tolerance in *Escherichia coli* using a transgenic library from the hydrocarbon-degrader *Marinobacter aquaeolei*. *Biotechnol Biofuels* **8** 165.
40. George KW, Alonso-Gutierrez J, Keasling JD, Lee TS. **2015**. Isoprenoid Drugs, Biofuels, and Chemicals - Artemisinin, Farnesene, and Beyond. *Adv Biochem Eng Biotechnol* **148** 355–389.
41. Braga A, Guerreiro C, Belo I. **2018**. Generation of Flavors and Fragrances Through Biotransformation and De Novo Synthesis. *Food Bioprocess Technol* **11** 2217–2228.
42. Rolf J, Julsing MK, Rosenthal K, Lütz S. **2020**. A Gram-Scale Limonene Production Process with Engineered *Escherichia coli*. *Molecules* **25** 1881.
43. Chen X, Zhang C, Lindley ND. **2020**. Metabolic Engineering Strategies for Sustainable Terpenoid Flavor and Fragrance Synthesis. *J Agric Food Chem* acs.jafc.9b06203.
44. Zhang L, Xiao W-H, Wang Y, Yao M-D, Jiang G-Z, Zeng B-X, Zhang R-S, Yuan Y-J. **2017**. Chassis and key enzymes engineering for monoterpenes production. *Biotechnol Adv* **35** 1022–1031.
45. Trombetta D, Castelli F, Sarpietro MG, Venuti V, Cristani M, Daniele C, Saija A, Mazzanti G, Bisignano G, Grazia M. **2005**. Mechanisms of antibacterial action of three monoterpenes. *Antimicrob Agents Chemother* **49** 2474–2478.
46. Ramos JL, Cuenca MS, Molina-Santiago C, Segura A, Duque E, Ǵomez-Garciá MR, Udaondo Z, Roca A. **2015**. Mechanisms of solvent resistance mediated by interplay of cellular factors in *Pseudomonas putida*. *FEMS Microbiol Rev* **39** 555–566.
47. Ribeiro B, Shapira P. **2019**. Anticipating governance challenges in synthetic biology: Insights from biosynthetic menthol. *Technol Forecast Soc Change* **139** 311–320.
48. Kamatou GPP, Vermaak I, Viljoen AM, Lawrence BM. **2013**. Menthol: A simple monoterpene with remarkable biological properties. *Phytochemistry* **96** 15–25.
49. Surburg H, Panten J. **2006**. Common Fragrance and Flavor Materials. Preparation, Properties and Uses. 5th Ed. WILEY-VCH Verlag GmbH & Co. KGaA, Weinheim.
50. Galeotti N, Di Cesare Mannelli L, Mazzanti G, Bartolini A, Ghelardini C. **2002**. Menthol: A natural analgesic compound. *Neurosci Lett* **322** 145–148.
51. Souza MAA, Lemos MJ, Brito DMC, Fernandes MS, Castro RN, Souza SR. **2014**. Production and Quality of Menthol Mint Essential Oil and Antifungal and Antigerminative Activity. *Am J Plant Sci* **5** 3311–3318.
52. Verma RS, Rahman L, Verma RK, Chauhan A, Yadav AK, Singh A. **2010**. Essential Oil Composition of Menthol Mint (*Mentha arvensis*) and Peppermint (*Mentha piperita*) Cultivars at Different Stages of Plant Growth from Kumaon Region of Western Himalaya. *Open Access J Med Aromat Plants* **1** 13–18.
53. Surburg H, Panten J. **2016**. Common Fragrance and Flavor Materials. Preparation, Properties and Uses. 6th Ed. Wiley-VCH Verlag GmbH & Co. KGaA, Weinheim.
54. Gershenzon J, Maffei M, Croteau R. **1989**. Biochemical and histochemical localization of monoterpene biosynthesis in the glandular trichomes of spearmint (*Mentha spicata*). *Plant Physiol* **89** 1351–1357.
55. McCaskill D, Gershenzon J, Croteau R. **1992**. Morphology and monoterpene biosynthetic capabilities of secretory cell clusters isolated from glandular trichomes of peppermint (*Mentha piperita* L.). *Planta* **187** 445–454.
56. Croteau RB, Davis EM, Ringer KL, Wildung MR. **2005**. (–)-Menthol biosynthesis and molecular genetics. *Naturwissenschaften* **92** 562–577.
57. Lange BM, Turner GW. **2013**. Terpenoid biosynthesis in trichomes — current status and future opportunities. *Plant Biotechnol J* **11** 2–22.
58. Lupien S, Karp F, Wildung M, Croteau R. **1999**. Regiospecific cytochrome P450 limonene hydroxylases from mint (*Mentha*) species: cDNA isolation, characterization, and functional expression of (-)-4S-limonene-3-hydroxylase and (-)-4S-limonene-6-hydroxylase. *Arch Biochem Biophys* **368** 181–192.
59. Toogood HS, Cheallaigh AN, Tait S, Mansell DJ, Jervis A, Lygidakis A, Humphreys L, Takano E, Gardiner JM, Scrutton NS. **2015**. Enzymatic Menthol Production: One-Pot Approach Using Engineered *Escherichia coli*. *ACS Synth Biol* **4** 1112–1123.
60. Kirby J, Keasling JD. **2009**. Biosynthesis of Plant Isoprenoids: Perspectives for Microbial Engineering. *Annu Rev Plant Biol* **60** 335–355.
61. Eccles R. **1994**. Menthol and Related Cooling Compounds. *J Pharm Pharmacol* **46** 618–630.
62. A. Farco J, Grundmann O. **2012**. Menthol – Pharmacology of an Important Naturally Medicinal "Cool." *Mini-Reviews Med Chem* **13** 124–131.
63. Hensel H, Zotterman Y. **1951**. The Effect of Menthol on the Thermoreceptors. *Acta Physiol Scand* **24** 27–34.

64. Patel T, Ishiuji Y, Yosipovitch G. **2007**. Menthol: A refreshing look at this ancient compound. *J Am Acad Dermatol* **57** 873–878.
65. Galeotti N, Ghelardini C, Di Cesare Mannelli L, Mazzanti G, Baghiroli L, Bartolini A. **2001**. Local Anaesthetic Activity of (+)- and (-)-Menthol. *Planta Med* **67** 174–176.
66. Freires IA, Denny C, Benso B, de Alencar SM, Rosalen PL. **2015**. Antibacterial activity of essential oils and their isolated constituents against cariogenic bacteria: A systematic review. *Molecules* **20** 7329–7358.
67. Watt EE, Betts BA, Kotey FO, Humbert DJ, Griffith TN, Kelly EW, Veneskey KC, Gill N, Rowan KC, Jenkins A, Hall AC. **2008**. Menthol shares general anesthetic activity and sites of action on the GABAA receptor with the intravenous agent, propofol. *Eur J Pharmacol* **590** 120–126.
68. Juergens UR, Stöber M, Vetter H. **1998**. The anti-inflammatory activity of L-menthol compared to mint oil in human monocytes in vitro: a novel perspective for its therapeutic use in inflammatory diseases. *Eur J Med Res* **3** 539–45.
69. Al-Bayati FA. **2009**. Isolation and identification of antimicrobial compound from *Mentha longifolia* L. leaves grown wild in Iraq. *Ann Clin Microbiol Antimicrob* **8** 20.
70. Schäfer B. **2013**. Menthol. *Chemie unserer Zeit* **47** 174–182.
71. Lange BM. **2015**. Biosynthesis and Biotechnology of High-Value *p*-Menthane Monoterpenes, Including Menthol, Carvone, and Limonene. *Adv Biochem Eng Biotechnol* **148** 319–353.
72. Lawrence BM. **2013**. The Story of India's Mint Oils and Menthol. *Perfum Flavorist* **38** 26–35.
73. Sell CS. **2003**. A Fragrant Introduction to Terpenoid Chemistry. Royal Society of Chemistry, Cambridge.
74. Urlacher VB, Girhard M. **2012**. Cytochrome P450 monooxygenases: an update on perspectives for synthetic application. *Trends Biotechnol* **30** 26–36.
75. Lamb DC, Waterman MR. **2013**. Unusual properties of the cytochrome P450 superfamily. *Phil Trans R Soc B* **368** 20120434.
76. Denisov IG, Makris TM, Sligar SG, Schlichting I. **2005**. Structure and chemistry of cytochrome P450. *Chem Rev* **105** 2253–2277.
77. Chapple C. **1998**. Molecular-Genetic Analysis of Plant Cytochrome P450-Dependent Monooxygenases. *Annu Rev Plant Physiol Plant Mol Biol* **49** 311–343.
78. Pateraki I, Heskes AM, Hamberger B. **2015**. Cytochromes P450 for Terpene Functionalisation and Metabolic Engineering. *Adv Biochem Eng Biotechnol* **148** 107–139.
79. Mizutani M, Sato F. **2011**. Unusual P450 reactions in plant secondary metabolism. *Arch Biochem Biophys* **507** 194–203.
80. Bernhardt R. **2006**. Cytochromes P450 as versatile biocatalysts. *J Biotechnol* **124** 128–145.
81. Guengerich FP, Munro AW. **2013**. Unusual cytochrome P450 enzymes and reactions. *J Biol Chem* **288** 17065–17073.
82. Isin EM, Guengerich FP. **2007**. Complex reactions catalyzed by cytochrome P450 enzymes. *Biochim Biophys Acta* **1770** 314–329.
83. Sono M, Roach MP, Coulter ED, Dawson JH. **1996**. Heme-Containing Oxygenases. *Chem Rev* **96** 2841–2888.
84. Nelson DR. **2009**. The cytochrome p450 homepage. *Hum Genomics* **4** 59–65.
85. Sirim D, Wagner F, Lisitsa A, Pleiss J. **2009**. The Cytochrome P450 Engineering Database: integration of biochemical properties. *BMC Biochem* **10** 27.
86. Gillam EMJ. **2008**. Engineering Cytochrome P450 Enzymes. *Chem Res Toxicol* **21** 220–231.
87. Guengerich FP, Tang Z, Cheng Q, Salamanca-Pinzón SG. **2011**. Approaches to deorphanization of human and microbial cytochrome P450 enzymes. *Biochim Biophys Acta* **1814** 139–145.
88. Hausjell J, Halbwirth H, Spadiut O. **2018**. Recombinant production of eukaryotic cytochrome P450s in microbial cell factories. *Biosci Rep* **38** BSR20171290.
89. Hannemann F, Bichet A, Ewen KM, Bernhardt R. **2007**. Cytochrome P450 systems—biological variations of electron transport chains. *Biochim Biophys Acta* **1770** 330–344.
90. Tanaka Y, Brugliera F. **2013**. Flower colour and cytochromes P450. *Phil Trans R Soc B* **368** 20120432.
91. Hasler JA, Estabrook R, Murray M, Pikuleva I, Waterman M, Capdevila J, Holla V, Helvig C, Falck JR, Farrell G, Kaminsky LS, Spivack SD, Boitier E, Beaune P. **1999**. Human cytochromes P450. *Mol Aspects Med* **20** 1–137.
92. Sadeghi SJ, Gilardi G. **2013**. Chimeric P450 enzymes: Activity of artificial redox fusions driven by different reductases for biotechnological applications. *Biotechnol Appl Biochem* **60** 102–110.
93. Črešnar B, Petrič Š. **2011**. Cytochrome P450 enzymes in the fungal kingdom. *Biochim Biophys Acta* **1814** 29–35.
94. Hasemann CA, Kurumbail RG, Boddupalli SS, Peterson JA, Deisenhofer J. **1995**. Structure and function of cytochromes P450: a comparative analysis of three crystal structures. *Structure* **3** 41–62.
95. Renault H, Bassard J-E, Hamberger B, Werck-Reichhart D. **2014**. Cytochrome P450-mediated metabolic engineering: current progress and future challenges. *Curr Opin Plant Biol* **19** 27–34.
96. Jung ST, Lauchli R, Arnold FH. **2011**. Cytochrome P450: taming a wild type enzyme. *Curr Opin Biotechnol* **22** 809–817.
97. Bernhardt R, Urlacher VB. **2014**. Cytochromes P450 as promising catalysts for biotechnological application: chances and limitations. *Appl Microbiol Biotechnol* **98** 6185–6203.
98. Schempp FM, Drummond L, Buchhaupt M, Schrader J. **2018**. Microbial Cell Factories for the Production of Terpenoid Flavor and Fragrance Compounds. *J Agric Food Chem* **66** 2247–2258.

99. Chang MCY, Keasling JD. **2006**. Production of isoprenoid pharmaceuticals by engineered microbes. *Nat Chem Biol* **2** 674–681.
100. Seifert A, Antonovici M, Hauer B, Pleiss J. **2011**. An Efficient Route to Selective Bio-oxidation Catalysts: an Iterative Approach Comprising Modeling, Diversification, and Screening, Based on CYP102A1. *ChemBioChem* **12** 1346–1351.
101. Bell SG, Sowden RJ, Wong L-L. **2001**. Engineering the haem monooxygenase cytochrome P450cam for monoterpene oxidation. *Chem Commun* 635–636.
102. Hernandez-Ortega A, Vinaixa M, Zebec Z, Takano E, Scrutton NS. **2018**. A Toolbox for Diverse Oxyfunctionalisation of Monoterpenes. *Sci Rep* **8** 14396.
103. Girvan HM, Munro AW. **2016**. Applications of microbial cytochrome P450 enzymes in biotechnology and synthetic biology. *Curr Opin Chem Biol* **31** 136–145.
104. Zelasko S, Palaria A, Das A. **2013**. Optimizations to achieve high-level expression of cytochrome P450 proteins using *Escherichia coli* expression systems. *Protein Expr Purif* **92** 77–87.
105. Silby MW, Winstanley C, Godfrey SAC, Levy SB, Jackson RW. **2011**. *Pseudomonas* genomes: diverse and adaptable. *FEMS Microbiol Rev* **35** 652–680.
106. Nelson KE, Weinel C, Paulsen IT, Dodson RJ, Hilbert H, Martins dos Santos VAP, Fouts DE, Gill SR, Pop M, Holmes M, Brinkac L, Beanan M, DeBoy RT, Daugherty S, Kolonay J, Madupu R, Nelson W, White O, Peterson J, Khouri H, Hance I, Lee PC, Holtzapple E, Scanlan D, Tran K, Moazzez A, Utterback T, Rizzo M, Lee K, Kosack D, Moestl D, Wedler H, Lauber J, Stjepandic D, Hoheisel J, Straetz M, Heim S, Kiewitz C, Eisen J, Timmis KN, Düsterhöft A, Tümmler B, Fraser CM. **2002**. Complete genome sequence and comparative analysis of the metabolically versatile *Pseudomonas putida* KT2440. *Environ Microbiol* **4** 799–808.
107. Wu X, Monchy S, Taghavi S, Zhu W, Ramos J, van der Lelie D. **2011**. Comparative genomics and functional analysis of niche-specific adaptation in *Pseudomonas putida*. *FEMS Microbiol Rev* **35** 299–323.
108. Timmis KN. **2002**. *Pseudomonas putida*: a cosmopolitan opportunist par excellence. *Environ Microbiol* **4** 779–781.
109. Poblete-Castro I, Becker J, Dohnt K, dos Santos VM, Wittmann C. **2012**. Industrial biotechnology of *Pseudomonas putida* and related species. *Appl Microbiol Biotechnol* **93** 2279–2290.
110. Martins dos Santos VAP, Heim S, Moore ERB, Strätz M, Timmis KN. **2004**. Insights into the genomic basis of niche specificity of *Pseudomonas putida* KT2440. *Environ Microbiol* **6** 1264–1286.
111. Molina L, Duque E, Gómez MJ, Krell T, Lacal J, García-Puente A, García V, Matilla MA, Ramos J-L, Segura A. **2011**. The pGRT1 plasmid of *Pseudomonas putida* DOT-T1E encodes functions relevant for survival under harsh conditions in the environment. *Environ Microbiol* **13** 2315–2327.
112. Belda E, van Heck RGA, Lopez-Sanchez MJ, Cruveiller S, Barbe V, Fraser C, Klenk H-P, Petersen J, Morgat A, Nikel PI, Vallenet D, Rouy Z, Sekowska A, Martins dos Santos VAP, de Lorenzo V, Danchin A, Médigue C. **2016**. The revisited genome of *Pseudomonas putida* KT2440 enlightens its value as a robust metabolic chassis. *Environ Microbiol* **18** 3403–3424.
113. Loeschcke A, Thies S. **2015**. *Pseudomonas putida*—a versatile host for the production of natural products. *Appl Microbiol Biotechnol* **99** 6197–6214.
114. Martínez-García E, de Lorenzo V. **2011**. Engineering multiple genomic deletions in Gram-negative bacteria: analysis of the multi-resistant antibiotic profile of *Pseudomonas putida* KT2440. *Environ Microbiol* **13** 2702–2716.
115. Aparicio T, de Lorenzo V, Martínez-García E. **2018**. CRISPR/Cas9-Based Counterselection Boosts Recombineering Efficiency in *Pseudomonas putida*. *Biotechnol J* **13** 1–10.
116. Mougiakos I, Mohanraju P, Bosma EF, Vrouwe V, Finger Bou M, Naduthodi MIS, Gussak A, Brinkman RBL, van Kranenburg R, van der Oost J. **2017**. Characterizing a thermostable Cas9 for bacterial genome editing and silencing. *Nat Commun* **8** 1647.
117. Sun J, Wang Q, Jiang Y, Wen Z, Yang L, Wu J, Yang S. **2018**. Genome editing and transcriptional repression in *Pseudomonas putida* KT2440 via the type II CRISPR system. *Microb Cell Fact* **17** 41.
118. Martínez-García E, Aparicio T, de Lorenzo V, Nikel PI. **2017**. Engineering Gram-Negative Microbial Cell Factories Using Transposon Vectors, p. 273–293. *In* Reeves A. (ed.), In Vitro Mutagenesis. Methods in Molecular Biology. Vol 1498. Humana Press, New York.
119. Brown WRA, Lee NCO, Xu Z, Smith MCM. **2011**. Serine recombinases as tools for genome engineering. *Methods* **53** 372–379.
120. Choi K-H, Kim K-J. **2009**. Applications of Transposon-Based Gene Delivery System in Bacteria. *J Microbiol Biotechnol* **19** 217–228.
121. Craig NL. **1991**. Tn7: a target site-specific transposon. *Mol Microbiol* **5** 2569–2573.
122. Zobel S, Benedetti I, Eisenbach L, de Lorenzo V, Wierckx N, Blank LM. **2015**. Tn7-Based Device for Calibrated Heterologous Gene Expression in *Pseudomonas putida*. *ACS Synth Biol* **4** 1341–1351.
123. Martínez-García E, Aparicio T, de Lorenzo V, Nikel PI. **2014**. New transposon tools tailored for metabolic engineering of Gram-negative microbial cell factories. *Front Bioeng Biotechnol* **2** 46.
124. Elmore JR, Furches A, Wolff GN, Gorday K, Guss AM. **2017**. Development of a high efficiency integration system and promoter library for rapid modification of *Pseudomonas putida* KT2440. *Metab Eng Commun* **5** 1–8.
125. Nikel PI, de Lorenzo V. **2013**. Implantation of unmarked regulatory and metabolic modules in Gram-negative bacteria with specialised mini-transposon delivery vectors. *J Biotechnol* **163** 143–154.

126. de Lorenzo V, Herrero M, Jakubzik U, Timmis KN. **1990**. Mini-Tn5 transposon derivatives for insertion mutagenesis, promoter probing, and chromosomal insertion of cloned DNA in Gram-negative eubacteria. *J Bacteriol* **172** 6568–6572.
127. Domröse A, Hage-Hülsmann J, Thies S, Weihmann R, Kruse L, Otto M, Wierckx N, Jaeger K-E, Drepper T, Loeschcke A. **2019**. *Pseudomonas putida* rDNA is a favored site for the expression of biosynthetic genes. *Sci Rep* **9** 7028.
128. Martínez-García E, Aparicio T, Goñi-Moreno A, Fraile S, de Lorenzo V. **2015**. SEVA 2.0: an update of the Standard European Vector Architecture for de-/re-construction of bacterial functionalities. *Nucleic Acids Res* **43** D1183–D1189.
129. Silva-Rocha R, Martínez-García E, Calles B, Chavarría M, Arce-Rodríguez A, de las Heras A, Páez-Espino AD, Durante-Rodríguez G, Kim J, Nikel PI, Platero R, de Lorenzo V. **2013**. The Standard European Vector Architecture (SEVA): a coherent platform for the analysis and deployment of complex prokaryotic phenotypes. *Nucleic Acids Res* **41** D666–D675.
130. Verhoef S, Ballerstedt H, Volkers RJM, de Winde JH, Ruijssenaars HJ. **2010**. Comparative transcriptomics and proteomics of *p*-hydroxybenzoate producing *Pseudomonas putida* S12: novel responses and implications for strain improvement. *Appl Microbiol Biotechnol* **87** 679–690.
131. Puchałka J, Oberhardt MA, Godinho M, Bielecka A, Regenhardt D, Timmis KN, Papin JA, Martins dos Santos VAP. **2008**. Genome-Scale Reconstruction and Analysis of the *Pseudomonas putida* KT2440 Metabolic Network Facilitates Applications in Biotechnology. *PLoS Comput Biol* **4** e1000210.
132. Kampers LFC, Volkers RJM, Martins dos Santos VAP. **2019**. *Pseudomonas putida* KT2440 is HV1 certified, not GRAS. *Microb Biotechnol* **12** 845–848.
133. Speelmans G, Bijlsma A, Eggink G. **1998**. Limonene bioconversion to high concentrations of a single and stable product, perillic acid, by a solvent-resistant *Pseudomonas putida* strain. *Appl Microbiol Biotechnol* **50** 538–544.
134. Yoshino Y, Kitazawa T, Kamimura M, Tatsuno K, Yotsuyanagi H, Ota Y. **2011**. *Pseudomonas putida* bacteremia in adult patients: five case reports and a review of the literature. *J Infect Chemother* **17** 278–282.
135. Bundesamt für Verbraucherschutz und Lebensmittelsicherheit. **2012**. Stellungnahme der ZKBS zur Risikobewertung von *Pseudomonas putida* als Spender- oder Empfängerorganismus für gentechnische Arbeiten gemäß § 5 Absatz 1 GenTSV (2. geänderte Fassung). *Az 6790-05-01-099*.
136. Mars AE, Gorissen JPL, van den Beld I, Eggink G. **2001**. Bioconversion of limonene to increased concentrations of perillic acid by *Pseudomonas putida* GS1 in a fed-batch reactor. *Appl Microbiol Biotechnol* **56** 101–107.
137. Mi J, Becher D, Lubuta P, Dany S, Tusch K, Schewe H, Buchhaupt M, Schrader J. **2014**. *De novo* production of the monoterpenoid geranic acid by metabolically engineered *Pseudomonas putida*. *Microb Cell Fact* **13** 170.
138. Mi J, Schewe H, Buchhaupt M, Holtmann D, Schrader J. **2016**. Efficient hydroxylation of 1,8-cineole with monoterpenoid-resistant recombinant *Pseudomonas putida* GS1. *World J Microbiol Biotechnol* **32** 112.
139. Sikkema J, de Bont JA, Poolman B. **1994**. Interactions of cyclic hydrocarbons with biological membranes. *J Biol Chem* **269** 8022–8028.
140. Ramos JL, Duque E, Gallegos M-T, Godoy P, Ramos-González MI, Rojas A, Terán W, Segura A. **2002**. Mechanisms of Solvent Tolerance in Gram-Negative Bacteria. *Annu Rev Microbiol* **56** 743–768.
141. Papadopoulos CJ, Carson CF, Chang BJ, Riley T V. **2008**. Role of the MexAB-OprM Efflux Pump of *Pseudomonas aeruginosa* in Tolerance to Tea Tree (*Melaleuca alternifolia*) Oil and Its Monoterpene Components Terpinen-4-ol, 1,8-Cineole, and alpha-Terpineol. *Appl Environ Microbiol* **74** 1932–1935.
142. de Bont JAM. **1998**. Solvent-tolerant bacteria in biocatalysis. *Trends Biotechnol* **16** 493–499.
143. Ramos JL, Duque E, Godoy P, Segura A. **1998**. Efflux pumps involved in toluene tolerance in *Pseudomonas putida* DOT-T1E. *J Bacteriol* **180** 3323–3329.
144. Sikkema J, de Bont JAM, Poolman B. **1995**. Mechanisms of membrane toxicity of hydrocarbons. *Microbiol Rev* **59** 201–222.
145. Heipieper HJ, Weber FJ, Sikkema J, Keweloh H, de Bont JAM. **1994**. Mechanisms of resistance of whole cells to toxic organic solvents. *Trends Biotechnol* **12** 409–415.
146. Domínguez-Cuevas P, González-Pastor J-E, Marqués S, Ramos J-L, de Lorenzo V. **2006**. Transcriptional Tradeoff between Metabolic and Stress-response Programs in *Pseudomonas putida* KT2440 Cells Exposed to Toluene. *J Biol Chem* **281** 11981–11991.
147. Inoue A, Horikoshi K. **1989**. A *Pseudomonas* thrives in high concentrations of toluene. *Nature* **338** 264–266.
148. Inoue A, Horikoshi K. **1991**. Estimation of solvent-tolerance of bacteria by the solvent parameter log P. *J Ferment Bioeng* **71** 194–196.
149. SciFinder database - https://sso.cas.org - 2019-12-04.
150. Udaondo Z, Duque E, Fernández M, Molina L, de la Torre J, Bernal P, Niqui J-L, Pini C, Roca A, Matilla MA, Antonia Molina-Henares M, Silva-Jiménez H, Navarro-Avilés G, Busch A, Lacal J, Krell T, Segura A, Ramos J-L. **2012**. Analysis of solvent tolerance in *Pseudomonas putida* DOT-T1E based on its genome sequence and a collection of mutants. *FEBS Lett* **586** 2932–2938.
151. Heipieper HJ, de Bont JAM. **1994**. Adaptation of *Pseudomonas putida* S12 to ethanol and toluene at the level of fatty acid composition of membranes. *Appl Environ Microbiol* **60** 4440–4444.

152. Heipieper HJ, Meinhardt F, Segura A. **2003**. The *cis-trans* isomerase of unsaturated fatty acids in *Pseudomonas* and *Vibrio*: Biochemistry, molecular biology and physiological function of a unique stress adaptive mechanism. *FEMS Microbiol Lett* **229** 1–7.
153. Bernal P, Segura A, Ramos JL. **2007**. Compensatory role of the *cis-trans*-isomerase and cardiolipin synthase in the membrane fluidity of *Pseudomonas putida* DOT-T1E. *Environ Microbiol* **9** 1658–1664.
154. Heipieper HJ, Neumann G, Cornelissen S, Meinhardt F. **2007**. Solvent-tolerant bacteria for biotransformations in two-phase fermentation systems. *Appl Microbiol Biotechnol* **74** 961–973.
155. Isken S, de Bont JAM. **1996**. Active efflux of toluene in a solvent-resistant bacterium. *J Bacteriol* **178** 6056–6058.
156. Ramos JL, Duque E, Rodríguez-Herva JJ, Godoy P, Haïdour A, Reyes F, Fernández-Barrero A. **1997**. Mechanisms for solvent tolerance in bacteria. *J Biol Chem* **272** 3887–3890.
157. Isken S, de Bont JAM. **1998**. Bacteria tolerant to organic solvents. *Extremophiles* **2** 229–238.
158. Wijte D, van Baar BLM, Heck AJR, Altelaar AFM. **2011**. Probing the Proteome Response to Toluene Exposure in the Solvent Tolerant *Pseudomonas putida* S12. *J Proteome Res* **10** 394–403.
159. Isken S, Derks A, Wolffs PF, de Bont JAM. **1999**. Effect of organic solvents on the yield of solvent-tolerant *Pseudomonas putida* S12. *Appl Environ Microbiol* **65** 2631–2635.
160. Segura A, Godoy P, van Dillewijn P, Hurtado A, Arroyo N, Santacruz S, Ramos JL. **2005**. Proteomic analysis reveals the participation of energy- and stress-related proteins in the response of *Pseudomonas putida* DOT-T1E to toluene. *J Bacteriol* **187** 5937–5945.
161. Rojas A, Segura A, Guazzaroni ME, Terán W, Hurtado A, Gallegos MT, Ramos JL. **2003**. In vivo and In vitro evidence that TtgV is the specific regulator of the TtgGHI multidrug and solvent efflux pump of *Pseudomonas putida*. *J Bacteriol* **185** 4755–4763.
162. Poole K. **2001**. Multidrug resistance in Gram-negative bacteria. *Curr Opin Microbiol* **4** 500–508.
163. Martinez JL, Sánchez MB, Martínez-Solano L, Hernandez A, Garmendia L, Fajardo A, Alvarez-Ortega C. **2009**. Functional role of bacterial multidrug efflux pumps in microbial natural ecosystems. *FEMS Microbiol Rev* **33** 430–449.
164. Kim K, Lee S, Lee K, Lim D. **1998**. Isolation and characterization of toluene-sensitive mutants from the toluene-resistant bacterium *Pseudomonas putida* GM73. *J Bacteriol* **180** 3692–3696.
165. Duque E, Segura A, Mosqueda G, Ramos JL. **2001**. Global and cognate regulators control the expression of the organic solvent efflux pumps TtgABC and TtgDEF of *Pseudomonas putida*. *Mol Microbiol* **39** 1100–1106.
166. Mosqueda G, Ramos J-L. **2000**. A Set of Genes Encoding a Second Toluene Efflux System in *Pseudomonas putida* DOT-T1E Is Linked to the *tod* Genes for Toluene Metabolism. *J Bacteriol* **182** 937–943.
167. Rodríguez-Herva JJ, García V, Hurtado A, Segura A, Ramos JL. **2007**. The *ttgGHI* solvent efflux pump operon of *Pseudomonas putida* DOT-T1E is located on a large self-transmissible plasmid. *Environ Microbiol* **9** 1550–1561.
168. Terán W, Krell T, Ramos JL, Gallegos MT. **2006**. Effector-repressor interactions, binding of a single effector molecule to the operator-bound TtgR homodimer mediates derepression. *J Biol Chem* **281** 7102–7109.
169. Terán W, Felipe A, Segura A, Rojas A, Ramos J-L, Gallegos M-T. **2003**. Antibiotic-Dependent Induction of *Pseudomonas putida* DOT-T1E TtgABC Efflux Pump Is Mediated by the Drug Binding Repressor TtgR. *Antimicrob Agents Chemother* **47** 3067–3072.
170. Rojas A, Duque E, Mosqueda G, Golden G, Hurtado A, Ramos JL, Segura A. **2001**. Three Efflux Pumps Are Required To Provide Efficient Tolerance to Toluene in *Pseudomonas putida* DOT-T1E. *J Bacteriol* **183** 3967–3973.
171. Terán W, Felipe A, Fillet S, Guazzaroni M-E, Krell T, Ruiz R, Ramos JL, Gallegos M-T. **2007**. Complexity in efflux pump control: cross-regulation by the paralogues TtgV and TtgT. *Mol Microbiol* **66** 1416–1428.
172. Krell T, Terán W, Mayorga OL, Rivas G, Jiménez M, Daniels C, Molina-Henares A-J, Martínez-Bueno M, Gallegos M-T, Ramos J-L. **2007**. Optimization of the Palindromic Order of the TtgR Operator Enhances Binding Cooperativity. *J Mol Biol* **369** 1188–1199.
173. Wagner S, Baars L, Ytterberg AJ, Klussmeier A, Wagner CS, Nord O, Nygren P-Å, van Wijk KJ, de Gier J-W. **2007**. Consequences of Membrane Protein Overexpression in *Escherichia coli*. *Mol Cell Proteomics* **6** 1527–1550.
174. Fillet S, Vélez M, Lu D, Zhang X, Gallegos M-T, Ramos JL. **2009**. TtgV represses two different promoters by recognizing different sequences. *J Bacteriol* **191** 1901–1909.
175. Kieboom J, Dennis JJ, de Bont JAM, Zylstra GJ. **1998**. Identification and molecular characterization of an efflux pump involved in *Pseudomonas putida* S12 solvent tolerance. *J Biol Chem* **273** 85–91.
176. Wery J, Hidayat B, Kieboom J, de Bont JAM. **2001**. An insertion sequence prepares *Pseudomonas putida* S12 for severe solvent stress. *J Biol Chem* **276** 5700–5706.
177. Kieboom J, Dennis JJ, Zylstra GJ, de Bont JAM. **1998**. Active efflux of organic solvents by *Pseudomonas putida* S12 is induced by solvents. *J Bacteriol* **180** 6769–6772.
178. Poole K, Krebes K, McNally C, Neshat S. **1993**. Multiple antibiotic resistance in *Pseudomonas aeruginosa*: evidence for involvement of an efflux operon. *J Bacteriol* **175** 7363–7372.
179. Gotoh N, Tsujimoto H, Poole K, Yamagishi JI, Nishino T. **1995**. The outer membrane protein OprM of *Pseudomonas aeruginosa* is encoded by *oprK* of the *mexA-mexB-oprK* multidrug resistance operon. *Antimicrob Agents Chemother* **39** 2567–2569.

180. Poole K, Gotoh N, Tsujimoto H, Zhao Q, Wada A, Yamasaki T, Neshat S, Yamagishi J, Li X-Z, Nishino T. **1996**. Overexpression of the *mexC-mexD-oprJ* efflux operon in *nfxB*-type multidrug-resistant strains of *Pseudomonas aeruginosa*. *Mol Microbiol* **21** 713–725.
181. Poole K, Srikumar R. **2001**. Multidrug Efflux in *Pseudomonas aeruginosa*: Components, Mechanisms and Clinical Significance. *Curr Top Med Chem* **1** 59–71.
182. Roca A, Rodríguez-Herva JJ, Duque E, Ramos JL. **2008**. Physiological responses of *Pseudomonas putida* to formaldehyde during detoxification. *Microb Biotechnol* **1** 158–169.
183. **2010**. Insulin - Hormon aus Bakterien, Hefen und Pflanzen. *Pharm Ztg*.
184. Bagdasarian M, Lurz R, Rückert B, Franklin FCH, Bagdasarian MM, Frey J, Timmis KN. **1981**. Specific-purpose plasmid cloning vectors II. Broad host range, high copy number, RSF 1010-derived vectors, and a host-vector system for gene cloning in *Pseudomonas*. *Gene* **16** 237–247.
185. Bicas JL, Dionísio AP, Pastore GM. **2009**. Bio-oxidation of Terpenes: An Approach for the Flavor Industry. *Chem Rev* **109** 4518–4531.
186. Haudenschild C, Schalk M, Karp F, Croteau R. **2000**. Functional expression of regiospecific cytochrome P450 limonene hydroxylases from mint (*Mentha* spp.) in *Escherichia coli* and *Saccharomyces cerevisiae*. *Arch Biochem Biophys* **379** 127–136.
187. Emmerstorfer A, Wimmer-Teubenbacher M, Wriessnegger T, Leitner E, Müller M, Kaluzna I, Schürmann M, Mink D, Zellnig G, Schwab H, Pichler H. **2015**. Over-expression of ICE2 stabilizes cytochrome P450 reductase in *Saccharomyces cerevisiae* and *Pichia pastoris*. *Biotechnol J* **10** 623–635.
188. Duetz WA, Bouwmeester H, Beilen JB, Witholt B. **2003**. Biotransformation of limonene by bacteria, fungi, yeasts, and plants. *Appl Microbiol Biotechnol* **61** 269–277.
189. Balcerzak L, Lipok J, Strub D, Lochyński S. **2014**. Biotransformations of monoterpenes by photoautotrophic micro-organisms. *J Appl Microbiol* **117** 1523–1536.
190. van Dyk MS, van Rensburg E, Moleleki N. **1998**. Hydroxylation of (+)limonene, (–)alpha-pinene and (–)beta-pinene by a *Hormonema* sp. *Biotechnol Lett* **20** 431–436.
191. Webb TA, Mundt JO. **1978**. Molds on vegetables at the time of harvest. *Appl Environ Microbiol* **35** 655–658.
192. Chi Z, Wang F, Chi Z, Yue L, Liu G, Zhang T. **2009**. Bioproducts from *Aureobasidium pullulans*, a biotechnologically important yeast. *Appl Microbiol Biotechnol* **82** 793–804.
193. Andrews JH, Spear RN, Nordheim EV. **2002**. Population biology of *Aureobasidium pullulans* on apple leaf surfaces. *Can J Microbiol* **48** 500–513.
194. Rajeeva G, Ranjan S, Monika G, Manogya KG. **2010**. *Aureobasidium pullulans*, an economically important polymorphic yeast with special reference to pullulan. *African J Biotechnol* **9** 7989–7997.
195. Ferreira-Pinto MM, Moura-Guedes MC, Barreiro MG, Pais I, Santos MR, Silva MJ. **2006**. *Aureobasidium pullulans* as a biocontrol agent of blue mold in “Rocha” pear. *Commun Agric Appl Biol Sci* **71** 973–978.
196. Sorge-Röder I. **2012**. Erdbeergenuss ohne chemische Belastung: Hefepilz schützt vor Graufäule. *BioLAGO (© BIOPRO Baden-Württemberg GmbH)*.
197. Deshpande MS, Rale VB, Lynch JM. **1992**. *Aureobasidium pullulans* in applied microbiology: A status report. *Enzyme Microb Technol* **14** 514–527.
198. Rishi V, Sandhu AK, Kaur A, Kaur J, Sharma S, Soni SK. **2020**. Utilization of kitchen waste for production of pullulan to develop biodegradable plastic. *Appl Microbiol Biotechnol* **104** 1307–1317.
199. Martínez-García E, Nikel PI, Aparicio T, de Lorenzo V. **2014**. *Pseudomonas* 2.0: genetic upgrading of *P. putida* KT2440 as an enhanced host for heterologous gene expression. *Microb Cell Fact* **13** 159.
200. Segura A, Rojas A, Hurtado A, Huertas M-J, Ramos JL. **2003**. Comparative genomic analysis of solvent extrusion pumps in *Pseudomonas* strains exhibiting different degrees of solvent tolerance. *Extremophiles* **7** 371–376.
201. Tusch K. **2013**. Biotransformation von Monoterpenen mit *Pseudomonas putida*. Masterarbeit. Goethe-Universität Frankfurt am Main.
202. Nickerson DP, Wong LL. **1997**. The dimerization of *Pseudomonas putida* cytochrome $P450_{cam}$: practical consequences and engineering of a monomeric enzyme. *Protein Eng* **10** 1357–1361.
203. Nyathi Y, Wilkinson BM, Pool MR. **2013**. Co-translational targeting and translocation of proteins to the endoplasmic reticulum. *Biochim Biophys Acta* **1833** 2392–2402.
204. Szczesna-Skorupa E, Ahn K, Chen CD, Doray B, Kemper B. **1995**. The cytoplasmic and N-terminal transmembrane domains of cytochrome P450 contain independent signals for retention in the endoplasmic reticulum. *J Biol Chem* **270** 24327–24333.
205. Letourneur F, Cosson P. **1998**. Targeting to the endoplasmic reticulum in yeast cells by determinants present in transmembrane domains. *J Biol Chem* **273** 33273–33278.
206. Monk BC, Tomasiak TM, Keniya MV, Huschmann FU, Tyndall JDA, O’Connell III JD, Cannon RD, McDonald JG, Rodriguez A, Finer-Moore JS, Stroud RM. **2014**. Architecture of a single membrane spanning cytochrome P450 suggests constraints that orient the catalytic domain relative to a bilayer. *Proc Natl Acad Sci* **111** 3865–3870.
207. Jana S, Deb JK. **2005**. Strategies for efficient production of heterologous proteins in *Escherichia coli*. *Appl Microbiol Biotechnol* **67** 289–298.
208. Studier FW. **2005**. Protein production by auto-induction in high density shaking cultures. *Protein Expr Purif* **41** 207–234.

209. Gibson DG, Young L, Chuang R-Y, Venter JC, Hutchison CA, Smith HO. **2009**. Enzymatic assembly of DNA molecules up to several hundred kilobases. *Nat Methods* **6** 343–345.
210. Inoue H, Nojima H, Okayama H. **1990**. High efficiency transformation of *Escherichia coli* with plasmids. *Gene* **96** 23–28.
211. Ichinose H, Wariishi H. **2013**. High-level heterologous expression of fungal cytochrome P450s in *Escherichia coli*. *Biochem Biophys Res Commun* **438** 289–294.
212. Mizutani M, Ohta D. **1998**. Two Isoforms of NADPH:Cytochrome P450 Reductase in *Arabidopsis thaliana*. *Plant Physiol* **116** 357–367.
213. Urban P, Mignotte C, Kazmaier M, Delorme F, Pompon D. **1997**. Cloning, yeast expression, and characterization of the coupling of two distantly related *Arabidopsis thaliana* NADPH-cytochrome P450 reductases with P450 CYP73A5. *J Biol Chem* **272** 19176–19186.
214. Guengerich FP, Martin MV, Sohl CD, Cheng Q. **2009**. Measurement of cytochrome P450 and NADPH–cytochrome P450 reductase. *Nat Protoc* **4** 1245–1251.
215. Alberts B, Johnson A, Lewis J, Raff M, Roberts K, Walter P. **2002**. Molecular biology of the cell. 4th ed. Garland Science, New York.
216. Guo J, Thiess S, Johansson I, Mkrtchian S, Ingelman-Sundberg M. **2016**. Membrane topology and search for potential redox partners of colon cancer-specific cytochrome P450 2W1. *FEBS Lett* **590** 330–339.
217. Black SD. **1992**. Membrane topology of the mammalian P450 cytochromes. *FASEB J* **6** 680–685.
218. Werck-Reichhart D, Feyereisen R. **2000**. Cytochromes P450: a success story. *Genome Biol* **1** reviews3003.1–reviews3003.9.
219. Ichinose H, Hatakeyama M, Yamauchi Y. **2015**. Sequence modifications and heterologous expression of eukaryotic cytochromes P450 in *Escherichia coli*. *J Biosci Bioeng* **120** 268–274.
220. Mao H, Shen Q, Wang Q. **2017**. CYP701A26 is characterized as an *ent*-kaurene oxidase with putative involvement in maize gibberellin biosynthesis. *Biotechnol Lett* **39** 1709–1716.
221. Mao H, Liu J, Ren F, Peters RJ, Wang Q. **2016**. Characterization of CYP71Z18 indicates a role in maize zealexin biosynthesis. *Phytochemistry* **121** 4–10.
222. Ge F, Cheng S, Jiang A, Ren Y, Chen G, Li W. **2018**. Cloning, heterologous expression, and activity analysis of NADPH-cytochrome P450 reductase from the Chinese white rabbit. *Biotechnol Biotechnol Equip* **32** 163–170.
223. Porter TD. **2002**. The roles of cytochrome b5 in cytochrome P450 reactions. *J Biochem Mol Toxicol* **16** 311–316.
224. Marschall L, Sagmeister P, Herwig C. **2017**. Tunable recombinant protein expression in *E. coli*: promoter systems and genetic constraints. *Appl Microbiol Biotechnol* **101** 501–512.
225. Rosano GL, Ceccarelli EA. **2014**. Recombinant protein expression in *Escherichia coli*: advances and challenges. *Front Microbiol* **5** 172.
226. Deuschle U, Kammerer W, Gentz R, Bujard H. **1986**. Promoters of *Escherichia coli*: a hierarchy of *in vivo* strength indicates alternate structures. *EMBO J* **5** 2987–2994.
227. Zhang X, Studier FW. **1997**. Mechanism of inhibition of bacteriophage T7 RNA polymerase by T7 lysozyme. *J Mol Biol* **269** 10–27.
228. Wagner S, Klepsch MM, Schlegel S, Appel A, Draheim R, Tarry M, Hogbom M, van Wijk KJ, Slotboom DJ, Persson JO, de Gier J-W. **2008**. Tuning *Escherichia coli* for membrane protein overexpression. *Proc Natl Acad Sci* **105** 14371–14376.
229. Singh SM, Panda AK. **2005**. Solubilization and refolding of bacterial inclusion body proteins. *J Biosci Bioeng* **99** 303–310.
230. Basu A, Li X, Leong SSJ. **2011**. Refolding of proteins from inclusion bodies: rational design and recipes. *Appl Microbiol Biotechnol* **92** 241–251.
231. Miroux B, Walker JE. **1996**. Over-production of Proteins in *Escherichia coli*: Mutant Hosts that Allow Synthesis of some Membrane Proteins and Globular Proteins at High Levels. *J Mol Biol* **260** 289–298.
232. Dumon-Seignovert L, Cariot G, Vuillard L. **2004**. The toxicity of recombinant proteins in *Escherichia coli*: A comparison of overexpression in BL21(DE3), C41(DE3), and C43(DE3). *Protein Expr Purif* **37** 203–206.
233. Biggs BW, Lim CG, Sagliani K, Shankar S, Stephanopoulos G, De Mey M, Ajikumar PK. **2016**. Overcoming heterologous protein interdependency to optimize P450-mediated Taxol precursor synthesis in *Escherichia coli*. *Proc Natl Acad Sci* **113** 3209–3214.
234. Krainer FW, Capone S, Jäger M, Vogl T, Gerstmann M, Glieder A, Herwig C, Spadiut O. **2015**. Optimizing cofactor availability for the production of recombinant heme peroxidase in *Pichia pastoris*. *Microb Cell Fact* **14** 4.
235. Wernig F, Boles E, Oreb M. **2020**. *De novo* biosynthesis of 8-hydroxyoctanoic acid via a medium-chain length specific fatty acid synthase and cytochrome P450 in *Saccharomyces cerevisiae*. *Metab Eng Commun* **10** e00111.
236. Schenkman JB, Jansson I. **2003**. The many roles of cytochrome b5. *Pharmacol Ther* **97** 139–152.
237. Im S-C, Waskell L. **2011**. The interaction of microsomal cytochrome P450 2B4 with its redox partners, cytochrome P450 reductase and cytochrome b5. *Arch Biochem Biophys* **507** 144–153.
238. Ichinose H, Wariishi H. **2012**. Heterologous expression and mechanistic investigation of a fungal cytochrome P450 (CYP5150A2): Involvement of alternative redox partners. *Arch Biochem Biophys* **518** 8–15.

239. Schückel J, Rylott EL, Grogan G, Bruce NC. **2012**. A Gene-Fusion Approach to Enabling Plant Cytochromes P450 for Biocatalysis. *ChemBioChem* **13** 2758–2763.
240. Francis DM, Page R. **2010**. Strategies to Optimize Protein Expression in *E. coli*. *Curr Protoc Protein Sci* **61** 5.24.1-5.24.29.
241. Fernández FJ, Vega MC. **2016**. Choose a Suitable Expression Host: A Survey of Available Protein Production Platforms, p. 15–24. *In* Vega, MC (ed.), Advanced Technologies for Protein Complex Production and Characterization. Springer International Publishing, Cham.
242. Beekwilder J, van Houwelingen A, Cankar K, van Dijk ADJ, de Jong RM, Stoopen G, Bouwmeester H, Achkar J, Sonke T, Bosch D. **2014**. Valencene synthase from the heartwood of Nootka cypress (*Callitropsis nootkatensis*) for biotechnological production of valencene. *Plant Biotechnol J* **12** 174–182.
243. Loeschcke A, Dienst D, Wewer V, Hage-Hülsmann J, Dietsch M, Kranz-Finger S, Hüren V, Metzger S, Urlacher VB, Gigolashvili T, Kopriva S, Axmann IM, Drepper T, Jaeger K-E. **2017**. The photosynthetic bacteria *Rhodobacter capsulatus* and *Synechocystis* sp. PCC 6803 as new hosts for cyclic plant triterpene biosynthesis. *PLoS One* **12** e0189816.
244. Jones KL, Kim S-W, Keasling J. **2000**. Low-Copy Plasmids can Perform as Well as or Better Than High-Copy Plasmids for Metabolic Engineering of Bacteria. *Metab Eng* **2** 328–338.
245. Choi KR, Cho JS, Cho IJ, Park D, Lee SY. **2018**. Markerless gene knockout and integration to express heterologous biosynthetic gene clusters in *Pseudomonas putida*. *Metab Eng* **47** 463–474.
246. Schewe H, Mirata MA, Schrader J. **2015**. Bioprocess Engineering for Microbial Synthesis and Conversion of Isoprenoids. *Adv Biochem Eng Biotechnol* **148** 251–286.
247. Wang Y, Lim L, DiGuistini S, Robertson G, Bohlmann J, Breuil C. **2013**. A specialized ABC efflux transporter GcABC-G1 confers monoterpene resistance to *Grosmannia clavigera*, a bark beetle-associated fungal pathogen of pine trees. *New Phytol* **197** 886–898.
248. Brennan TCR, Williams TC, Schulz BL, Palfreyman RW, Krömer JO, Nielsen LK. **2015**. Evolutionary Engineering Improves Tolerance for Replacement Jet Fuels in *Saccharomyces cerevisiae*. *Appl Environ Microbiol* **81** 3316–3325.
249. Urlacher VB, Schmid RD. **2004**. Protein engineering of the cytochrome P450 monooxygenase from *Bacillus megaterium*. *Methods Enzymol* **388** 208–224.
250. Wong LL, Westlake ACG, Nickerson DP. **1997**. Protein engineering of cytochrome P450cam, p. 175–207. *In* Hill HAO, Sadler PJ, Thomson AJ (eds.), Metal Sites in Proteins and Models. Structure and Bonding. Vol 88. Springer, Berlin, Heidelberg.
251. Peters MW, Meinhold P, Glieder A, Arnold FH. **2003**. Regio- and Enantioselective Alkane Hydroxylation with Engineered Cytochromes P450 BM-3. *J Am Chem Soc* **125** 13442–13450.
252. Wolf B, Rack M, Benson S, Kraus H, Goetz R, Anan S, Rishinaradamangalam C. **2016**. A process for the preparation of limonene-4-ol. WO 2016/180614 AI.
253. Wolf B, Rack M, Benson S, Kraus H. **2017**. Process for preparing a mixture of terpene alcohols. WO 2017/144337 Al.
254. Leffingwell JC, Leffingwell D. **2015**. Biotechnology - Conquests and Challenges in Flavors & Fragrances. *Leffingwell Reports* **7** 1–11.
255. Deguerry F, Pastore L, Wu S, Clark A, Chappell J, Schalk M. **2006**. The diverse sesquiterpene profile of patchouli, *Pogostemon cablin*, is correlated with a limited number of sesquiterpene synthases. *Arch Biochem Biophys* **454** 123–136.
256. van Dyk MS, van Rensburg E, Rensburg IPB, Moleleki N. **1998**. Biotransformation of monoterpenoid ketones by yeasts and yeast-like fungi. *J Mol Catal B Enzym* **5** 149–154.
257. Bain JP, Hunt HG, Albert KE, Booth AB. **1953**. Conversion of verbenol to monocyclic and acyclic compounds. US2972632A.
258. Shimoda K, Kubota N, Hamada H, Kaji M, Hirata T. **2004**. Asymmetric reduction of enones with *Synechococcus* sp. PCC 7942. *Tetrahedron Asymmetry* **15** 1677–1679.
259. Goretti M, Ponzoni C, Caselli E, Marchigiani E, Cramarossa MR, Turchetti B, Buzzini P, Forti L. **2009**. Biotransformation of electron-poor alkenes by yeasts: Asymmetric reduction of (*4S*)-(+)-carvone by yeast enoate reductases. *Enzyme Microb Technol* **45** 463–468.
260. dos Santos RAM, de Oliveira Souza F, Pilau EJ, Porto C, Gonçalves JE, de Oliveira AJB, Gonçalves RAC. **2018**. Biotransformation of (+)-carvone and (–)-carvone using human skin fungi: A green method of obtaining fragrances and flavours. *Biocatal Biotransformation* **36** 396–400.
261. Goretti M, Turchetti B, Cramarossa M, Forti L, Buzzini P. **2013**. Production of Flavours and Fragrances via Bioreduction of (4*R*)-(-)-Carvone and (1*R*)-(-)-Myrtenal by Non-Conventional Yeast Whole-Cells. *Molecules* **18** 5736–5748.
262. Gao X, Ren J, Wu Q, Zhu D. **2012**. Biochemical characterization and substrate profiling of a new NADH-dependent enoate reductase from *Lactobacillus casei*. *Enzyme Microb Technol* **51** 26–34.
263. Zhang H, Gao X, Ren J, Feng J, Zhang T, Wu Q, Zhu D. **2014**. Enzymatic hydrogenation of diverse activated alkenes. Identification of two *Bacillus* old yellow enzymes with broad substrate profiles. *J Mol Catal B Enzym* **105** 118–125.
264. Scholtissek A, Tischler D, Westphal AH, van Berkel WJH, Paul CE. **2017**. Old Yellow Enzyme-Catalysed Asymmetric Hydrogenation: Linking Family Roots with Improved Catalysis. *Catalysts* **7** 130.

265. Oberleitner N, Peters C, Muschiol J, Kadow M, Saß S, Bayer T, Schaaf P, Iqbal N, Rudroff F, Mihovilovic MD, Bornscheuer UT. **2013**. An Enzymatic Toolbox for Cascade Reactions: A Showcase for an In Vivo Redox Sequence in Asymmetric Synthesis. *ChemCatChem* **5** 3524–3528.
266. Toogood HS, Gardiner JM, Scrutton NS. **2010**. Biocatalytic Reductions and Chemical Versatility of the Old Yellow Enzyme Family of Flavoprotein Oxidoreductases. *ChemCatChem* **2** 892–914.
267. Oberleitner N, Peters C, Rudroff F, Bornscheuer UT, Mihovilovic MD. **2014**. *In vitro* characterization of an enzymatic redox cascade composed of an alcohol dehydrogenase, an enoate reductases and a Baeyer-Villiger monooxygenase. *J Biotechnol* **192** 393–399.
268. Milker S, Fink MJ, Oberleitner N, Ressmann AK, Bornscheuer UT, Mihovilovic MD, Rudroff F. **2017**. Kinetic Modeling of an Enzymatic Redox Cascade In Vivo Reveals Bottlenecks Caused by Cofactors. *ChemCatChem* **9** 3420–3427.
269. Joo JC, Khusnutdinova AN, Flick R, Kim T, Bornscheuer UT, Yakunin AF, Mahadevan R. **2017**. Alkene hydrogenation activity of enoate reductases for an environmentally benign biosynthesis of adipic acid. *Chem Sci* **8** 1406–1413.
270. Pesic M, Fernández-Fueyo E, Hollmann F. **2017**. Characterization of the Old Yellow Enzyme Homolog from *Bacillus subtilis* (YqjM). *ChemistrySelect* **2** 3866–3871.
271. Nestl BM, Hammer SC, Nebel BA, Hauer B. **2014**. New generation of biocatalysts for organic synthesis. *Angew Chem Int Ed Engl* **53** 3070–3095.
272. Brown G, Moody TS, Smyth M, Taylor SJC. **2018**. Almac: An Industrial Perspective of Ene Reductase (ERED) Biocatalysis, p. 229–256. *In* Biocatalysis: An Industrial Perspective. The Royal Society of Chemistry.
273. Swiderska MA, Stewart JD. **2006**. Stereoselective enone reductions by *Saccharomyces carlsbergensis* old yellow enzyme. *J Mol Catal B Enzym* **42** 52–54.
274. Williams RE, Bruce NC. **2002**. "New uses for an old enzyme" - The Old Yellow Enzyme family of flavoenzymes. *Microbiology* **148** 1607–1614.
275. Amato ED, Stewart JD. **2015**. Applications of protein engineering to members of the old yellow enzyme family. *Biotechnol Adv* **33** 624–631.
276. Durchschein K, Hall M, Faber K. **2013**. Unusual reactions mediated by FMN-dependent ene- and nitro-reductases. *Green Chem* **15** 1764–1772.
277. Leferink NGH, Jervis AJ, Zebec Z, Toogood HS, Hay S, Takano E, Scrutton NS. **2016**. A 'Plug and Play' Platform for the Production of Diverse Monoterpene Hydrocarbon Scaffolds in *Escherichia coli*. *ChemistrySelect* **1** 1893–1896.
278. Jongedijk E, Cankar K, Ranzijn J, van der Krol S, Bouwmeester H, Beekwilder J. **2015**. Capturing of the monoterpene olefin limonene produced in *Saccharomyces cerevisiae*. *Yeast* **32** 159–171.
279. Alonso-Gutierrez J, Chan R, Batth TS, Adams PD, Keasling JD, Petzold CJ, Lee TS. **2013**. Metabolic engineering of *Escherichia coli* for limonene and perillyl alcohol production. *Metab Eng* **19** 33–41.
280. Zebec Z, Wilkes J, Jervis AJ, Scrutton NS, Takano E, Breitling R. **2016**. Towards synthesis of monoterpenes and derivatives using synthetic biology. *Curr Opin Chem Biol* **34** 37–43.
281. Hernandez-Arranz S, Perez-Gil J, Marshall-Sabey D, Rodriguez-Concepcion M. **2019**. Engineering *Pseudomonas putida* for isoprenoid production by manipulating endogenous and shunt pathways supplying precursors. *Microb Cell Fact* **18** 152.
282. Farmer WR, Liao JC. **2000**. Improving lycopene production in *Escherichia coli* by engineering metabolic control. *Nat Biotechnol* **18** 533–537.
283. Dahl RH, Zhang F, Alonso-Gutierrez J, Baidoo E, Batth TS, Redding-Johanson AM, Petzold CJ, Mukhopadhyay A, Lee TS, Adams PD, Keasling JD. **2013**. Engineering dynamic pathway regulation using stress-response promoters. *Nat Biotechnol* **31** 1039–1046.
284. Shen H-J, Cheng B-Y, Zhang Y-M, Tang L, Li Z, Bu Y-F, Li X-R, Tian G-Q, Liu J-Z. **2016**. Dynamic control of the mevalonate pathway expression for improved zeaxanthin production in *Escherichia coli* and comparative proteome analysis. *Metab Eng* **38** 180–190.
285. Dunlop MJ, Dossani ZY, Szmidt HL, Chu HC, Lee TS, Keasling JD, Hadi MZ, Mukhopadhyay A. **2011**. Engineering microbial biofuel tolerance and export using efflux pumps. *Mol Syst Biol* **7** 487.
286. Zhang C, Chen X, Stephanopoulos G, Too H-P. **2016**. Efflux transporter engineering markedly improves amorphadiene production in *Escherichia coli. Biotechnol Bioeng* **113** 1755–1763.
287. Reiling KK, Yoshikuni Y, Martin VJJ, Newman J, Bohlmann J, Keasling JD. **2004**. Mono and Diterpene Production in *Escherichia coli*. *Biotechnol Bioeng* **87** 200–212.
288. Zhou J, Wang C, Yang L, Choi E-S, Kim S-W. **2015**. Geranyl diphosphate synthase: An important regulation point in balancing a recombinant monoterpene pathway in *Escherichia coli*. *Enzyme Microb Technol* **68** 50–55.
289. Alonso-Gutierrez J, Kim E-M, Batth TS, Cho N, Hu Q, Chan LJG, Petzold CJ, Hillson NJ, Adams PD, Keasling JD, Garcia Martin H, Lee TS. **2015**. Principal component analysis of proteomics (PCAP) as a tool to direct metabolic engineering. *Metab Eng* **28** 123–133.
290. Jiang G-Z, Yao M-D, Wang Y, Zhou L, Song T-Q, Liu H, Xiao W-H, Yuan Y-J. **2017**. Manipulation of GES and ERG20 for geraniol overproduction in *Saccharomyces cerevisiae*. *Metab Eng* **41** 57–66.
291. Jongedijk E, Cankar K, Buchhaupt M, Schrader J, Bouwmeester H, Beekwilder J. **2016**. Biotechnological production of limonene in microorganisms. *Appl Microbiol Biotechnol* **100** 2927–2938.

292. Sun C, Theodoropoulos C, Scrutton NS. **2020**. Techno-economic assessment of microbial limonene production. *Bioresour Technol* **300** 122666.
293. Ciriminna R, Lomeli-Rodriguez M, Demma Carà P, Lopez-Sanchez JA, Pagliaro M. **2014**. Limonene: a versatile chemical of the bioeconomy. *Chem Commun* **50** 15288–15296.
294. Cao X, Lv Y-B, Chen J, Imanaka T, Wei L-J, Hua Q. **2016**. Metabolic engineering of oleaginous yeast *Yarrowia lipolytica* for limonene overproduction. *Biotechnol Biofuels* **9** 214.
295. Willrodt C, David C, Cornelissen S, Bühler B, Julsing MK, Schmid A. **2014**. Engineering the productivity of recombinant *Escherichia coli* for limonene formation from glycerol in minimal media. *Biotechnol J* **9** 1000–1012.
296. Wu J, Cheng S, Cao J, Qiao J, Zhao G-R. **2019**. Systematic Optimization of Limonene Production in Engineered *Escherichia coli*. *J Agric Food Chem* **67** 7087–7097.
297. Hodges AW, Rahmani M, Stevens TJ, Spreen TH. **2014**. Economic Impacts of the Florida Citrus Industry in 2012-13. *University of Florida*.
298. Hodges AW, Spreen TH. **2012**. Economic impacts of Citrus greening (HLB) in Florida, 2006/07–2010/11. *University of Florida,* Document No. FE903.
299. Wang N, Trivedi P. **2013**. Citrus Huanglongbing: A Newly Relevant Disease Presents Unprecedented Challenges. *Phytopathology* **103** 652–665.
300. Gottwald TR, da Graça JV, Bassanezi RB. **2007**. Citrus Huanglongbing: The Pathogen and Its Impact. *Plant Heal Prog* **8**.
301. Gottwald TR. **2010**. Current Epidemiological Understanding of Citrus Huanglongbing. *Annu Rev Phytopathol* **48** 119–139.
302. Glucose - https://en.wikipedia.org/wiki/Glucose - 2020-01-26.
303. Monteiro MR, Kugelmeier CL, Pinheiro RS, Batalha MO, da Silva César A. **2018**. Glycerol from biodiesel production: Technological paths for sustainability. *Renew Sustain Energy Rev* **88** 109–122.
304. Atiyeh H, Duvnjak Z. **2001**. Study of the production of fructose and ethanol from sucrose media by *Saccharomyces cerevisiae*. *Appl Microbiol Biotechnol* **57** 407–411.
305. **2015**. Fuel Production from Non-Food Biomass. Apple Academic Press, New York.
306. Yabushita M. **2016**. A Study on Catalytic Conversion of Non-Food Biomass into Chemicals. Springer, Singapore.
307. Zhang C, Too H-P. **2019**. Revalorizing Lignocellulose for the Production of Natural Pharmaceuticals and Other High Value Bioproducts. *Curr Med Chem* **26** 2475–2484.
308. Lopes MSG. **2015**. Engineering biological systems toward a sustainable bioeconomy. *J Ind Microbiol Biotechnol* **42** 813–838.
309. Schutyser W, Renders T, Van den Bosch S, Koelewijn S-F, Beckham GT, Sels BF. **2018**. Chemicals from lignin: an interplay of lignocellulose fractionation, depolymerisation, and upgrading. *Chem Soc Rev* **47** 852–908.
310. Wackett LP. **2003**. *Pseudomonas putida* - a versatile biocatalyst. *Nat Biotechnol* **21** 136–138.
311. Kohlstedt M, Starck S, Barton N, Stolzenberger J, Selzer M, Mehlmann K, Schneider R, Pleissner D, Rinkel J, Dickschat JS, Venus J, van Duuren JBJH, Wittmann C. **2018**. From lignin to nylon: Cascaded chemical and biochemical conversion using metabolically engineered *Pseudomonas putida*. *Metab Eng* **47** 279–293.
312. Poblete-Castro I, Wittmann C, Nikel PI. **2020**. Biochemistry, genetics and biotechnology of glycerol utilization in *Pseudomonas* species. *Microb Biotechnol* **13** 32–53.
313. Nikel PI, Kim J, de Lorenzo V. **2014**. Metabolic and regulatory rearrangements underlying glycerol metabolism in *Pseudomonas putida* KT2440. *Environ Microbiol* **16** 239–254.
314. Li W-J, Narancic T, Kenny ST, Niehoff P-J, O'Connor K, Blank LM, Wierckx N. **2020**. Unraveling 1,4-Butanediol Metabolism in *Pseudomonas putida* KT2440. *Front Microbiol* **11** 382.
315. Clark GS. **2007**. Aroma Chemical Profile: Menthol. *Perfum Flavorist* **32** 38–47.
316. Vespermann KAC, Paulino BN, Barcelos MCS, Pessôa MG, Pastore GM, Molina G. **2017**. Biotransformation of α- and β-pinene into flavor compounds. *Appl Microbiol Biotechnol* **101** 1805–1817.
317. BeetleBlock-Verbenone - www.agbio-inc.com/beetleblock-verbenone.html - 2020-01-13.
318. Wender PA, Mucciaro TP. **1992**. A new and practical approach to the synthesis of taxol and taxol analogs: the pinene path. *J Am Chem Soc* **114** 5878–5879.
319. Srividya N, Lange I, Lange BM. **2016**. Generation and Functional Evaluation of Designer Monoterpene Synthases. *Methods Enzymol* **576** 147–165.
320. Lewis DFV, Wiseman A. **2005**. A selective review of bacterial forms of cytochrome P450 enzymes. *Enzyme Microb Technol* **36** 377–384.
321. Schewe H, Mirata MA, Holtmann D, Schrader J. **2011**. Biooxidation of monoterpenes with bacterial monooxygenases. *Process Biochem* **46** 1885–1899.
322. Girhard M, Machida K, Itoh M, Schmid RD, Arisawa A, Urlacher VB. **2009**. Regioselective biooxidation of (+)-valencene by recombinant *E. coli* expressing CYP109B1 from *Bacillus subtilis* in a two-liquid-phase system. *Microb Cell Fact* **8** 36.
323. Daugulis AJ. **2001**. Two-phase partitioning bioreactors: a new technology platform for destroying xenobiotics. *Trends Biotechnol* **19** 457–462.
324. Malinowski JJ. **2001**. Two-phase partitioning bioreactors in fermentation technology. *Biotechnol Adv* **19** 525–538.

325. Neumann G, Kabelitz N, Zehnsdorf A, Miltner A, Lippold H, Meyer D, Schmid A, Heipieper HJ. **2005**. Prediction of the Adaptability of *Pseudomonas putida* DOT-T1E to a Second Phase of a Solvent for Economically Sound Two-Phase Biotransformations. *Appl Environ Microbiol* **71** 6606–6612.
326. Vrionis HA, Kropinski AM, Daugulis AJ. **2002**. Enhancement of a two-phase partitioning bioreactor system by modification of the microbial catalyst: Demonstration of concept. *Biotechnol Bioeng* **79** 587–594.
327. Westfall PJ, Gardner TS. **2011**. Industrial fermentation of renewable diesel fuels. *Curr Opin Biotechnol* **22** 344–350.
328. Siedler S, Bringer S, Bott M. **2011**. Increased NADPH availability in *Escherichia coli*: improvement of the product per glucose ratio in reductive whole-cell biotransformation. *Appl Microbiol Biotechnol* **92** 929–937.
329. Julsing MK, Kuhn D, Schmid A, Bühler B. **2012**. Resting cells of recombinant *E. coli* show high epoxidation yields on energy source and high sensitivity to product inhibition. *Biotechnol Bioeng* **109** 1109–1119.
330. Mirata MA, Heerd D, Schrader J. **2009**. Integrated bioprocess for the oxidation of limonene to perillic acid with *Pseudomonas putida* DSM 12264. *Process Biochem* **44** 764–771.
331. Brennan TCR, Turner CD, Krömer JO, Nielsen LK. **2012**. Alleviating monoterpene toxicity using a two-phase extractive fermentation for the bioproduction of jet fuel mixtures in *Saccharomyces cerevisiae*. *Biotechnol Bioeng* **109** 2513–2522.
332. Janardhan Garikipati SVB, Peeples TL. **2015**. Solvent resistance pumps of *Pseudomonas putida* S12: Applications in 1-naphthol production and biocatalyst engineering. *J Biotechnol* **210** 91–99.
333. Korman TP, Opgenorth PH, Bowie JU. **2017**. A synthetic biochemistry platform for cell free production of monoterpenes from glucose. *Nat Commun* **8** 15526.
334. Hodgman CE, Jewett MC. **2012**. Cell-free synthetic biology: Thinking outside the cell. *Metab Eng* **14** 261–269.
335. Wang Y, Lim L, Madilao L, Lah L, Bohlmann J, Breuil C. **2014**. Gene Discovery for Enzymes Involved in Limonene Modification or Utilization by the Mountain Pine Beetle-Associated Pathogen *Grosmannia clavigera*. *Appl Environ Microbiol* **80** 4566–4576.
336. Hussain R, Ahmed M, Khan TA, Akhter Y. **2020**. Fungal P450 monooxygenases - the diversity in catalysis and their promising roles in biocontrol activity. *Appl Microbiol Biotechnol* **104** 989–999.
337. Meckin R, Balmer A. **2018**. Everyday Uncertainty Work: Making Sense of Biosynthetic Menthol. *Engag Sci Technol Soc* **4** 458.
338. https://label-online.de/label/ohne-gentechnik - 2019-12-02.
339. Kritik am Begriff „genfrei“ - https://de.wikipedia.org/wiki/Gentechnikfrei#Kritik_am_Begriff_„genfrei“ - 2020-01-20.
340. Isobionics - Nootkatone - www.isobionics.com/index-Nootkatone.html - 2017-01-22.
341. Waltz E. **2015**. Engineers of scent. *Nat Biotechnol* **33** 329–332.
342. Eve explains Evolva’s fermentation - www.youtube.com/watch?v=y96w21HkaHQ - 2020-02-29.
343. **2010**. Rekombinante Wirkstoffe in Europa. *Pharm Ztg*. - www.pharmazeutische-zeitung.de/ausgabe-372010/rekombinante-wirkstoffe-in-europa - 2020-01-14.
344. Lorenz P, Zinke H. **2005**. White biotechnology: differences in US and EU approaches? *Trends Biotechnol* **23** 570–574.
345. Currin A, Dunstan MS, Johannissen LO, Hollywood KA, Vinaixa M, Jervis AJ, Swainston N, Rattray NJW, Gardiner JM, Kell DB, Takano E, Toogood HS, Scrutton NS. **2018**. Engineering the “Missing Link” in Biosynthetic (–)-Menthol Production: Bacterial Isopulegone Isomerase. *ACS Catal* **8** 2012–2020.
346. Moss GP, Smith PAS, Tavernier D. **1995**. Glossary of class names of organic compounds and reactivity intermediates based on structure (IUPAC Recommendations 1995). *Pure Appl Chem* **67** 1307–1375.
347. **2009**. IUPAC. Compendium of Chemical Terminology. 2nd ed. Blackwell Scientific Publications, Oxford.

List of tables - Chapters 1, 5, 7 and 8

Tables of the publications and manuscript included in this thesis (Chapters 2 - 4 and 6) are not listed here.

List of figures - Chapters 1, 5, 7 and 8

Figures of the publications and manuscript included in this thesis (Chapters 2 - 4 and 6) are not listed here.

List of abbreviations

aa	amino acids
ABC transporter	ATP-binding cassette transporter
AI	autoinduction medium
Amp	ampicillin
Amp^R	ampicillin resistance gene or ampicillin-resistant
.Ap	of *A. pullulans*
A. pullulans	*Aureobasidium pullulans*
ATP	adenosine triphosphate
a.u.	arbitrary unit
BINAP	2,2'-bis(diphenylphosphino)-1,1'-binaphthyl
BLAST	basic local alignment search tool
BMDY	buffered complex glucose (= dextrose) medium
BMGY	buffered complex glycerol medium
BMMY	buffered complex methanol medium
bp	base pair(s)
C_5	molecular skeleton consisting of five carbon atoms
ca.	circa
CAS	Chemical Abstracts Service
CBS	Centraalbureau voor Schimmelcultures
cDNA	complementary DNA
Cfa	cyclopropane synthase
cm	centimeter
Cm	chloramphenicol
CMK	4-(cytidine 5-diphospho)-2-C-methyl-D-erythritol kinase
Cm^R	chloramphenicol resistance gene or chloramphenicol-resistant
CPA	cyclopropane fatty acid
CPR	cytochrome P450 reductase
CRISPR	clustered regularly interspaced short palindromic repeats
.co	codon-optimized for *E. coli*
CoA	coenzyme A
CR	*P. putida* mutant selected for increased resistance towards 1,8-cineole
C-terminal/-terminus	carboxyl-terminus or COOH-terminus, end of a protein or polypeptide terminated by a free carboxyl group (-COOH)
Cti	*cis-trans* isomerase

CYP	cytochrome P450 monooxygenase
cyt b_5	cytochrome b5
DCW	dry cell weight
DAD	diode array detector
DMAPP	dimethylallyl diphosphate
DECHEMA	Gesellschaft für Chemische Technik und Biotechnologie („Deutsche Gesellschaft für chemisches Apparatewesen“)
DMSO	dimethyl sulfoxide
DNA	deoxyribonucleic acid
DOI	digital object identifier (international standard for document identification)
DSMZ	German Collection of Microorganisms and Cell Cultures (Deutsche Sammlung von Mikroorganismen und Zellkulturen)
DW	deep well plates
DXP	1-deoxy-D-xylulose 5-phosphate
DXR	DXP reductoisomerase
DXS	DXP synthase
e^-	electron
ECF	extracytoplasmic function
E. coli	*Escherichia coli*
EDTA	ethylenediaminetetraacetic acid
EF	(Erlenmeyer) shake flasks
e.g.	*exempli gratia* = for example
ER	endoplasmic reticulum
et al.	et alii = and others
EtOAc	ethyl acetate
EU	European Union
F	Farad = SI unit of electrical capacity
$FADH_2$ / FAD	flavin adenine dinucleotide (reduced / oxidized)
Fdx	ferredoxin
FID	flame ionization detector
Fig.	Figure
FPP	farnesyl diphosphate
FW	forward primer
g	gram
G3P	D-glyceraldehyde 3-phosphate

GAR	*P. putida* mutant selected for a higher resistance towards geranic acid
GC-MS	gas chromatography with mass spectrometry coupling
gDNA	genomic DNA
Gent	gentamicin
$Gent^R$	gentamycin resistance gene or gentamycin-resistant
GFP / *gfp* / eGFP	green fluorescent protein / green fluorescent protein gene / enhanced green fluorescent protein
GGPP	geranylgeranyl diphosphate
GMO	genetically modified organism
GPP	geranyl diphosphate
GPPS	GPP synthase
GR	*P. putida* mutant selected for a higher resistance towards geraniol
GST	glutathione S-transferase
h	hour(s)
H^+	proton
H_2O / dH_2O / ddH_2O	water / deionized water / ultrapure water
H_2SO_4	sulfuric acid
.Hc	of *H. carpetanum*
H. carpetanum	*Hormonema carpetanum*
HCl	hydrogen chloride
HDR	4-hydroxy-3-methylbut-2-enyl diphosphate reductase
HDS	4-hydroxy-3-methylbut-2-enyl diphosphate synthase
Hepes	4-(2-hydroxyethyl)-1-piperazineethanesulfonic acid
-His	truncation of N-terminus and addition of 6xHis-tag
HLB	Huanglongbing (bacterial “citrus greening disease“)
HMG-CoA	3-hydroxy-3-methylglutaryl-CoA
HMGR	HMG-CoA reductase
HMGS	HMG-CoA synthase
HPLC	high-performance liquid chromatography
IclR	isocitrate lyase regulator
IDI	IPP isomerase
i.d.R.	in der Regel
IPD	*trans*-isopiperitenol dehydrogenase
IPI	*cis*-isopulegone isomerase
IPP	isopentenyl diphosphate
IPR	isopiperitenone reductase

IPTG	isopropyl-β-D-thiogalactopyranoside
ISPR	*in situ* product removal
K_2HPO_4	dipotassium hydrogenphosphate
KH_2PO_4	potassium dihydrogenphosphate
Kan	kanamycin
Kan^R	Kanamycin resistance gene or kanamycin-resistant
Kan^S	Kanamycin sensitive
kb	kilobase pair(s) (1 kb = 1,000 nucleotide pairs)
kDa	kilodalton (1 kDa = 1,000 Da)
kg	kilogram (1 kg = 1,000 g)
L / l	liter
L3H / L3H.Ap / L3H.Hc	limonene-3-hydroxylase enzyme / … of *A. pullulans* / … of *H. carpetanum*
LB	lysogeny broth medium
log	logarithm
LS	limonene synthase
M	molar (mol per L)
M	molecular weight or molar mass (g per mol)
M. (x *piperita*)	*Mentha* (x *piperita*)
Mbp	Mega base pair(s) (1 Mbp = 10^6 base pairs)
MBP	maltose binding protein
MCS	multiple cloning site
MCT	MEP cytidyltransferase
MDR	multidrug resistance (efflux pumps)
MDS	2-C-methyl-D-erythritol 2,4-cyclodiphosphate synthase
MEP	2-C-methyl-D-erythritol 4-phosphate or methylerythritol phosphate pathway
MFP	membrane fusion protein
mg	milligram
MIC	minimal inhibitory concentration
min	minute(s)
MK	mevalonate kinase
mL / ml	milliliter (1 mL = 10^{-3} L)
mm	millimeter (1 mm = 10^{-3} m)
mM	millimolar (1 mM = 10^{-3} M = 10^{-3} mol L^{-1})
MR	menthone reductase

mRNA	messenger ribonucleic acid
MTBE	methyl *tert*-butyl ether
MVA	mevalonate or mevalonate pathway
MVD	5-diphosphomevalonate decarboxylase
n	sample size (statistics), number of biological replicates
n/a	not applicable
_N-var	altered N-terminus sequence
NADH / NAD^+	nicotinamide adenine dinucleotide (reduced / oxidized)
NADPH / $NADP^+$	nicotinamide adenine dinucleotide phosphate (reduced / oxidized)
NaH_2PO_4	sodium dihydrogen phosphate
ng	nanogram (1 ng = 10^{-9} g)
NH_3	ammonia
NIST	National Institute of Standards and Technology
nm	nanometer (1 nm = 10^{-9} m)
N-terminal/-terminus	amino-terminus or NH_2-terminus, start of a protein or polypeptide, referring to the free amine group (-NH_2) located at the end of a polypeptide
OD_{600}	optical density at 600 nm
oligo(dT)	short, single-stranded oligonucleotide consisting only of deoxythymidine phosphate nucleotides
ori	origin of replication
OYE	old yellow enzyme
p	p-value = probability value (statistics)
P450	cytochrome P450 monooxygenase
P. aeruginosa	*Pseudomonas aeruginosa*
P. putida	*Pseudomonas putida*
PCN	plasmid copy number
PCR	polymerase chain reaction
PDH	pyruvate dehydrogenase
PEP	phosphoenolpyruvate
PHA	polyhydroxyalkanoate
PHB	polyhydroxybutyrate
PM2	CYP71D15 of *Mentha* x *piperita*
PM17	CYP71D13 of *Mentha* x *piperita*
PMF	proton motive force
PMK	5-phosphomevalonate kinase

PP_i	pyrophosphate or diphosphate
P_{ow}	partition coefficient between a 1:1-mixture of *n*-octanol and water
PR	pulegone reductase
PT	prenyltransferase(s)
P_{ttg}	promoter of *ttg* gene or operon
qPCR	quantitative PCR
R1 / R2	risk group 1 / 2
R5P	ribulose 5-phosphate
R&D	research and development
RBS	ribosome binding site
RNA	ribonucleic acid
RND	Resistance-Nodulation-Division (protein family of efflux pumps)
ROS	reactive oxygen species
rpm	revolutions per minute
rRNA	ribosomal ribonucleic acid
RT	room temperature
Rt	retention time
RV	reverse primer
s	second(s)
SC	synthetic complete medium
SDS-PAGE	sodium dodecyl sulfate polyacrylamide gel electrophoresis
SEVA	Standard European Vector Architecture (database)
SI	International System of Units
SMRT	single molecule real-time
SNE	single nucleotide exchange
SNP	single nucleotide polymorphism
SOB	super optimal broth medium
sp.	species
Spec / Strep	spectinomycin/streptomycin
$Spec^R$ / $Strep^R$	spectinomycin/streptomycin resistance gene or spectinomycin/streptomycin-resistant
sRNA	small regulating RNA
srp / Srp	solvent resistant pump gene / protein
t	time
T	thymidine nucleotide
T_A	annealing temperature

TAE	tris acetate EDTA buffer
TB	terrific broth medium
TCA	tricarboxylic acid (cycle)
Tet	tetracycline
Tet^R	tetracycline resistance gene or tetracycline-resistant
T_m	melting temperature
TMD	transmembrane domain
Tn	transposon
Tris	tris(hydroxymethyl) aminomethane
TRYs	production titers, rates and yields
ttg / Ttg	toluene tolerance gene / protein
TR	*P. putida* mutant selected for a higher resistance towards α-terpineol
tRNA	transfer ribonucleic acid
TRP	transient receptor potential
TRYs	production titers, rates and yields
TS	terpene synthase(s)
UTR	untranslated region
U.S. / USA	United States of America
US$	currency of the USA
UV	ultraviolet
V	volt = SI unit of electric potential difference (voltage)
v/v	volume per volume
vis	visible
v_{max}	maximum rate of reaction
VR	*P. putida* mutants selected for a higher resistance towards verbenone
vs.	versus
w/v	weight per volume
WT	wild type
X5P	xylulose 5-phosphate
YEP	yeast extract peptone medium
YM	yeast extract/malt extract medium
YPD(S)	yeast extract peptone medium with glucose (= dextrose) (and sorbitol)
Zeo	zeocin
+1 / -10 / -35	elements/regions of bacterial promoters; +1: transcription start, -10 and -35: recognition sequences for RNA polymerase
3MB	3-methyl benzoate

5’- / 3’-end	convention of naming ends of single-stranded DNA or RNA molecules according to carbon atom numbers in the nucleotide sugar-ring; 5’-end: carbon atom 5, usually a phosphate group is attached; 3’-end: carbon atom 3, is typically unmodified with ribose -OH substituent
5-ALA	5- or δ-aminolevulinic acid
6xHis-tag	polyhistidine-tag, amino acid motif in proteins consisting of six histidine (His) residues
%	percent
°C	degree Celsius
µL	microliter (1 µL = 10^{-6} L)
µM	micromolar (1 µM = 10^{-6} M = 10^{-6} mol L^{-1})
Ω	Ohm = SI unit of electrical resistance
x g	multiple of mean acceleration of gravity (“times gravity”) = unit of relative centrifugal force (RCF)
Δ	gene deletion
[ ]	concentration of a substance or physical unit